APPROVED FOR RELEASE: 2007/02/08: CIA-RDP82-00850R000200090053-2

OF OR

30 JUNE 1980 YE. B. VOLKOV, T. A. SYRITSYN AND G. YU. MAZIN BY 1 OF 4

APPROVED FOR RELEASE: 2007/02/08: CIA-RDP82-00850R000200090053-2

APPROVED FOR RELEASE: 2007/02/08: CIA-RDP82-00850R000200090053-2

FOR OFFICIAL USE ONLY

JPRS L/9167

30 June 1980

Translation

DYNAMICS OF ROCKET MOTOR SYSTEMS

By

Ye. B. Volkov, T.A. Syritsyn and G. Yu. Mazin

FBIS FOREIGN BROADCAST INFORMATION SERVICE

FOR OFFICIAL USE ONLY

APPROVED FOR RELEASE: 2007/02/08: CIA-RDP82-00850R000200090053-2

APPROVED FOR RELEASE: 2007/02/08: CIA-RDP82-00850R000200090053-2

NOTE

JPRS publications contain information primarily from foreign newspapers, periodicals and books, but also from news agency transmissions and broadcasts. Materials from foreign-language sources are translated; those from English-language sources are transcribed or reprinted, with the original phrasing and other characteristics retained.

Headlines, editorial reports, and material enclosed in brackets [] are supplied by JPRS. Processing indicators such as [Text] or [Excerpt] in the first line of each item, or following the last line of a brief, indicate how the original information was processed. Where no processing indicator is given, the information was summarized or extracted.

Unfamiliar names rendered phonetically or transliterated are enclosed in parentheses. Words or names preceded by a question mark and enclosed in parentheses were not clear in the original but have been supplied as appropriate in context. Other unattributed parenthetical notes within the body of an item originate with the source. Times within items are as given by source.

The contents of this publication in no way represent the policies, views or attitudes of the U.S. Government.

For further information on report content call (703) 351-2938 (economic); 3468 (political, sociological, military); 2726 (life sciences); 2725 (physical sciences).

COPYRIGHT LAWS AND REGULATIONS GOVERNING OWNERSHIP OF MATERIALS REPRODUCED HEREIN REQUIRE THAT DISSEMINATION OF THIS PUBLICATION BE RESTRICTED FOR OFFICIAL USE ONLY.

APPROVED FOR RELEASE: 2007/02/08: CIA-RDP82-00850R000200090053-2

APPROVED FOR RELEASE: 2007/02/08: CIA-RDP82-00850R000200090053-2

JPRS L/9167

30 June 1980

DYNAMICS OF ROCKET MOTOR SYSTEMS

Moscow STATIKA I DINAMIKA RAKETNYKH DVIGATEL'NYKH USTANOVOK V DVUKH KNIGAKH ("Statics and Dynamics of Rocket Motor Systems in Two Volumes") in Russian 1978 signed to press 15 Mar 78 pp 1-320

[Volume Two ("Dynamics") of book by Ye. B. Volkov, T.A. Syritsyn and G. Yu. Mazin, Mashinostroyeniye Publishers, 1550 copies; Volume One ("Statics") was published in JPRS L/8627, 21 August 1979, entitled "Statics of Rocket Motor Systems"]

CONTENTS

APPROVED FOR RELEASE: 2007/02/08: CIA-RDP82-00850R000200090053-2

APPROVED FOR RELEASE: 2007/02/08: CIA-RDP82-00850R000200090053-2

APPROVED FOR RELEASE: 2007/02/08: CIA-RDP82-00850R000200090053-2

APPROVED FOR RELEASE: 2007/02/08: CIA-RDP82-00850R000200090053-2

APPROVED FOR RELEASE: 2007/02/08: CIA-RDP82-00850R000200090053-2

APPROVED FOR RELEASE: 2007/02/08: CIA-RDP82-00850R000200090053-2

APPROVED FOR RELEASE: 2007/02/08: CIA-RDP82-00850R000200090053-2

APPROVED FOR RELEASE: 2007/02/08: CIA-RDP82-00850R000200090053-2

APPROVED FOR RELEASE: 2007/02/08: CIA-RDP82-00850R000200090053-2

APPROVED FOR RELEASE: 2007/02/08: CIA-RDP82-00850R000200090053-2

PUBLICATION DATA

English title	:	DYNAMICS OF ROCKET MOTOR SYSTEMS
Russian title	:	STATIKA I DINAMIKA RAKETNYKH DVIGATEL'NYKH USTANOVOK V DVUKH KNIGAKH
Author (s)	:	Ye. B. Volkov, T.A Syritsyn, G. Yu. Mazin
Editor (s)	:	
Publishing House	:	Mashinostroyeniye
Place of Publication	:	Moscow
Date of Publication	:	1978
Signed to press	:	15 Mar 78
Copies	:	1550
COPYRIGHT	:	Izdatel'stvo "Mashinostroyeniye", 1978

APPROVED FOR RELEASE: 2007/02/08: CIA-RDP82-00850R000200090053-2

APPROVED FOR RELEASE: 2007/02/08: CIA-RDP82-00850R000200090053-2

ANNOTATION

[Text] This book is written on the problems of the theory, engineering analysis and calculation of the dynamic characteristics of liquid and solid-fuel engines. Primary attention has been given to the low-frequency dynamics of the engines.

A discussion is presented of the methods of describing the dynamic characteristics of the units and the engines as a whole and also the sensitivity of the dynamic characteristics to external and internal disturbances.

A study is made of the wave processes in the pipelines, the compression and rarefaction wave propagation in complex lines. A static analysis of the engine dynamics is presented on a performance level. The methods of calculating the engine characteristics under transient conditions are given, and a detailed discussion is presented of the process of the ignition of solid fuel in the solid-propellant rocket engine.

This book is designed for scientific workers and specialists in the field of rocket engine building. It can be useful to teachers, postgraduates and students in the advanced courses at the higher technical schools in the corresponding specialties.

There are 32 tables, 151 figures and 52 references.

APPROVED FOR RELEASE: 2007/02/08: CIA-RDP82-00850R000200090053-2

APPROVED FOR RELEASE: 2007/02/08: CIA-RDP82-00850R000200090053-2

FOREWORD

The improvement of rocket engines caused by the solution of new problems in the field of rocket and space engineering is proceeding along the path of the further complication of the schematic and structural solutions and improvement of the parameters of the operating process.

The most complex from the point of view of the occurrence of the physical-chemical processes are the transient and nonsteady-state operating conditions of the rocket engines. At the same time the transient operating conditions basically determine the operating reliability and the operating stability of the engines. Therefore extremely great significance is attached to the investigation of the nonsteady state processes in the theory and practice of engine building.

At the present time there are a large number of papers in which the dynamics of rocket engines are investigated. B. F. Glikman, Ye. K. Moshkin, V. A. Makhin, M. S. Natanzon, and so on have made a significant contribution to the resolution of the problems of the dynamics of liquid-fuel rocket engines. Some of the problems of the ballistics of solid-fuel rocket engines and nonsteady state combustion of solid fuel have been investigated in the papers by R. Ye. Sorkin, Ya. M. Shapiro, B. V. Orlov, B. T. Yerokhin, B. A. Rayzberg, Ya. B. Zel'dovich, and so on.

However, scientific and practical experience in the field of dynamics, especially the dynamics of solid-fuel rocket engines, has been discussed and generalized clearly insufficiently. The available individual articles and monographs are basically on special problems.

This book is one of the first in which the problems of the dynamics of liquid-propellant and solid-propellant rocket engines and the interrelation of the operating processes in the engine systems are discussed from unique points of view in systematic form.

The liquid-fuel rocket engine is a dynamic system consisting of a branched network of gas and liquid lines connecting the engine power units.

The dynamic characteristics of the engine are determined to a great extent by the characteristics of the lines; therefore a great deal of significance

FOR OFFICIAL USE ONLY

APPROVED FOR RELEASE: 2007/02/08: CIA-RDP82-00850R000200090053-2

APPROVED FOR RELEASE: 2007/02/08: CIA-RDP82-00850R000200090053-2

is attached to the wave processes in the lines in this book. On the organizational level an effort is also made to discuss the most complex and the least investigated statistical analysis of engine operating dynamics.

The authors, understanding the complexity and the insufficient degree to which a number of the problems of nonsteady state processes in engines have been studied, have not set the goal of exhausting this topic. The book discusses the methods of analysis, and in some cases also synthesis, of the low-frequency dynamics of rocket engines.

Special attention has been given to theory. The experimental data on the dynamic characteristics known from the literature are called on when necessary to substantiate the mathematical models or to confirm the correctness of the theoretical conclusions.

The formulas and numerical values are presented in accordance with the International System of Units.

The bibliography at the end of the book is not a bibliography of the problem at large, but, with little exception, only a list of sources from which information was borrowed.

The authors express their appreciation to Candidate of Technical Sciences A. S. Kotelkin for the materials made available to write Chapter 3, and they express their appreciation in advance to the readers for critical remarks and suggestions which it is requested be sent to the following address: Moscow, B-78, 1-y Basmannyy per., 3, izdatel'stvo Mashinostroyeniye.

APPROVED FOR RELEASE: 2007/02/08: CIA-RDP82-00850R000200090053-2

APPROVED FOR RELEASE: 2007/02/08: CIA-RDP82-00850R000200090053-2

SECTION I. DYNAMIC CHARACTERISTICS OF LIQUID-FUEL ENGINES

The dynamic characteristics of an engine determine the interrelation of the working processes in the units under nonsteady-state operating conditions.

The nonsteady-state operating conditions of the engine include the conditions under which the parameters of the operating process are time functions, that is,

$$\{y_j\} = \text{var, where. } y_j(t) = p_к, \dot{m}, n \text{ and so on.}$$

The engine is characterized by several nonsteady-state operating conditions: the starting mode, the shutdown mode, the transient mode (switching of the thrust stages), and regulation of the parameters of the operating process. During the nonsteady-state modes, the structure of the engine is under significant mechanical, thermal and erosion load gradients which in the case of unfavorable combinations of parameters of the operating process and bearing capacity lead to emergencies and failures. Therefore the study of the behavior of the units and the engine as a whole under nonsteady-state conditions, that is, the investigation of the dynamic characteristics, is an extremely important problem of engine building theory.

The dynamic characteristics include the following:

The dynamic equations of the relations between the parameters of the operating process;

The time constants, the boost factors, the frequency and transient characteristics of the units and the engine as a whole;

The characteristics of the starting and shutdown process;

The quality and stability of the adjustment process;

The characteristics of the high-frequency and low-frequency vibrations.

APPROVED FOR RELEASE: 2007/02/08: CIA-RDP82-00850R000200090053-2

APPROVED FOR RELEASE: 2007/02/08: CIA-RDP82-00850R000200090053-2

The engine in which nonsteady-state processes take place is a complex dynamic system made up of a number of elements interconnected in a defined way.

The dynamic element of the engine is considered to be the assembly or element having the characteristic features of the operating process which can be described analytically.

The basic dynamic elements of the engine are the thrust chamber, the gas generator, the turbopump, the lines and the automation units. The dynamic characteristics of the engine are determined by the characteristics of the elements. Therefore initially an analysis is made of the dynamic characteristics of the individual elements and then, using special methods, closure of the characteristics of the elements is carried out, and the dynamic characteristics of the engine as a whole are investigated.

The initial material for analysis of the dynamic characteristics is a system of differential equations describing the nonsteady-state operating conditions of the units.

The set of differential equations of the units together with the compatibility conditions forms the dynamic mathematical model of the engine.

Depending on the specific problems of dynamic analysis, the type of equations of the units can be different. Thus, when analyzing the starting and shutdown processes, when the parameters of the operating process vary significantly with time, nonlinear differential equations are used, and computers are used to solve them.

For analysis of the transient processes when the parameters of the operating process vary insignificantly, and the dynamic processes are characterized by low frequencies, linear differential equations are used, that is, the linear model of the engine.

In subsequent chapters primary attention has been given to the low-frequency engine dynamics.

APPROVED FOR RELEASE: 2007/02/08: CIA-RDP82-00850R000200090053-2

APPROVED FOR RELEASE: 2007/02/08: CIA-RDP82-00850R000200090053-2

CHAPTER 1. DYNAMIC CHARACTERISTICS OF THE ENGINE UNITS

1.1. Thrust Chamber

1.1.1. Nonlinear Equations

Complex processes of preparing the fuel mix and conversion of this mix to the products of combustion take place in the thrust chamber. When investigating the dynamics of the chamber, the following processes are taken into account:

The accumulation of mass and variation of the internal energy of the gas in the half-closed volume of the chamber;

Combustion;

Escape of the combustion products from the chamber cavity;

All of the enumerated processes are interrelated in space and time, and their mathematical description is extremely difficult.

When investigating the low-frequency dynamics it is possible to make the following assumptions:

For gas formed in the combustion chamber volume, the equations of state and conservation of energy are valid;

The pressure waves are propagated in the chamber instantaneously, which makes it possible at each point in time to take the gas pressure identical for all points of the combustion chamber (from the injector head to the nozzle entrance);

The conversion of fuel to the products of combustion is characterized by the burn-up curve.

Since the conversion process is realized in the chambers in thousandths of seconds, this process is assumed to be inertialess for significant

APPROVED FOR RELEASE: 2007/02/08: CIA-RDP82-00850R000200090053-2

APPROVED FOR RELEASE: 2007/02/08: CIA-RDP82-00850R000200090053-2

simplification, that is, the fuel is converted instantaneously into the products of combustion.

Heat exchange of the products of combustion with the external environment does not occur.

Making the indicated assumptions, the nature of variation of the pressure in the combustion chamber $p_k(t)$ can be obtained by applying the laws of thermodynamics for a gas in a constant volume

$$du = \underset{(1)}{i_{обр}\dot{m}_{обр}dt} - \underset{(2)}{i_{ист}\dot{m}_{ист}dt}, \tag{1.1}$$

Key: 1. formed; 2. escaping

where du is the change in internal energy of the gas; i_{formed}; $i_{escaping}$ are the enthalpies, respectively, of the gas formed and the gas escaping from the chamber; $\dot{m}_{formed}$; $\dot{m}_{escaping}$ are the masses of the gas formed in the combustion zone and escaping through the nozzle, respectively.

When using the equation of state and the thermodynamic functions, the internal energy is determined as follows in terms of the chamber parameters:

$$\begin{gathered} u = c_v T_к M_к;\ \underset{(1)}{i_{обр}} = c_p T_{обр}; \\ \underset{(2)}{i_{ист}} = \frac{\varkappa}{\varkappa - 1} R;\quad c_v = \frac{1}{\varkappa - 1} R; \\ \varkappa = \frac{c_p}{c_v};\quad M_к = \frac{p_к V_к}{R T_к}, \end{gathered} \tag{1.2}$$

Key: 1. formed; 2. escaping

where M_k is the mass of the gas in the combustion chamber volume V_k; T_k is the average gas temperature; c_p, c_v are the heat capacitances of the gas; R is the gas constant.

After joint transformation of the equations (1.1) and (1.2) we obtain the equation of the rate of pressure variation in the combustion chamber which is the energy equation for a variable amount of gas in the chamber volume

$$\frac{dp_к(t)}{dt} = \frac{\varkappa}{V_к}\left[\underset{(1)}{RT_{обр}(t)\dot{m}_{обр}(t)} - \underset{(2)}{RT_{ист}(t)\dot{m}_{ист}(t)}\right]. \tag{1.3}$$

Key: 1. formed; 2. escaping

The combustion of the fuel components coming through the injectors into the combustion chamber is characterized by a conversion law or the burn-up curve $\psi(t)$ (Fig 1.1).

APPROVED FOR RELEASE: 2007/02/08: CIA-RDP82-00850R000200090053-2

APPROVED FOR RELEASE: 2007/02/08: CIA-RDP82-00850R000200090053-2

Considering the burn-up functions, the arrival of the formed gases is defined as follows:

$$\underset{(1)}{\dot{m}_{\text{обр}}(t)}=\int_0^{t_1+t_2}\dot{m}_{\Sigma}(t-\tau')\frac{d\psi(\tau')}{d\tau}d\tau',$$

Key: 1. formed

where t is the process time; τ' is the integration variable; t_1 is the fuel ignition time; t_2 is the burn-up time.

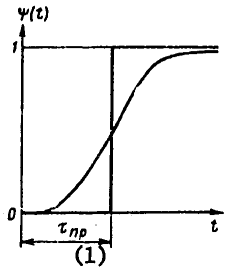

Figure 1.1. Fuel burn-up function

Key:
1. conv

The determination of the analytical function of the burn-up curve $\psi(t)$ presents significant difficulties. Therefore on the basis of the third assumption, the actual burn-up curve is replaced by a step function (see Fig 1.1), assuming that on expiration of the time τ_{conv} the fuel coming into the chamber is instantaneously converted to the products of combustion, that is,

$$\psi(t)=0 \text{ for } t\leqslant\tau_{\text{пр}},$$
$$\psi(t)=1 \text{ for } t\geqslant\tau_{\text{пр}}.$$
(1)

Key: 1. conv

Then the amount of burned fuel or gas formed $M_{formed}(t)$ in the interval 0-t will be defined as

$$\underset{(1)}{M_{\text{обр}}(t)}=\int_0^t\dot{m}_{\text{обр}}(t)\,dt=\int_0^{t-\tau_{\text{пр}}}[\underset{(2)}{\dot{m}_{\text{ок}}(t)}+\underset{(3)}{\dot{m}_{\text{т}}(t)}]\,dt, \qquad (1.4)$$

Key: 1. formed; 2. oxidant; 3. fuel

where $\dot{m}_{oxidant}(t)$, $\dot{m}_{fuel}(t)$ are the consumptions of the oxidizing agent and the combustible component of the fuel per second.

APPROVED FOR RELEASE: 2007/02/08: CIA-RDP82-00850R000200090053-2

APPROVED FOR RELEASE: 2007/02/08: CIA-RDP82-00850R000200090053-2

The upper integration limit $t-\tau_{conv}$ is taken because the fuel (the oxidant and the combustible component) entering into the chamber up to this time still has not burned as a result of the presence of the conversion delay τ_{conv}.

Differentiating equation (1.4) with respect to the integration limit, the gas formation rate is determined

$$\dot{m}^{(1)}_{\text{обр}}(t)=\left(1-\frac{d\tau_{\text{пр}}}{dt}\right)[\dot{m}^{(2)}_{\text{ок}}(t-\tau_{\text{пр}})+\dot{m}_{\text{г}}(t-\tau_{\text{пр}})]. \qquad (1.5)$$

Key: See (1.4). (3)

The conversion time depends on the quality of the mixture formation, the properties of the fuel components, the pressure in the gas chamber and other factors.

The basic factor determining the conversion time is the pressure in the combustion chamber. Accordingly, we have [20]

$$\tau_{\text{пр}}=\frac{A}{p_{\text{к}}^{\nu}}$$

and

$$\frac{d\tau_{\text{пр}}}{dt}=-\frac{A\nu}{p_{\text{к}}^{\nu+1}}\frac{dp_{\text{к}}}{dt}. \qquad (1.6)$$

The gas flow rate through the nozzle is defined by the function

$$\dot{m}_{\text{ист}}(t)=\frac{\varphi b(\varkappa)F_{\text{кр}}\overset{(1)}{p_{\text{к}}}(t)}{\sqrt{RT_{\text{ист}}(t)}}. \qquad (1.7)$$

Key: 1. cr

If we assume that the flow rate coefficient ϕ and the index of the adiabatic curve χ depend weakly on the pressure in the chamber, it is possible to set the complex $\phi bF_{cr}=c$, which is defined in terms of the chamber parameters in the steady state mode:

$$B=\varphi b(\varkappa)F_{\text{кр}}=\frac{\bar{\dot{m}}\sqrt{\overline{RT}_{\text{к}}}}{\bar{p}_{\text{к}}};\quad \bar{\dot{m}}=\bar{\dot{m}}_{\text{ок}}+\bar{\dot{m}}_{\text{г}}.$$

Considering the remarks that have been made, the flow rate through the nozzle will be defined as follows:

$$\dot{m}_{\text{ист}}(t)=B\frac{p_{\text{к}}(t)}{\sqrt{RT_{\text{ист}}(t)}}. \qquad (1.8)$$

(1)

Key: 1. escape

Substituting equations (1.5-1.8 and 1.6) in the initial (1.3), we obtain the nonlinear equation of the thrust chamber

APPROVED FOR RELEASE: 2007/02/08: CIA-RDP82-00850R000200090053-2

APPROVED FOR RELEASE: 2007/02/08: CIA-RDP82-00850R000200090053-2

$$\left[1-\frac{\varkappa}{V_к}RT_{обр}(t)\frac{Av}{p_к^{v+1}(t)}\dot{m}(t-\tau_{пр})\right]\frac{dp_к(t)}{dt}=$$
$$=\frac{\varkappa}{V_к}\{RT_{обр}(t)[\dot{m}_{ок}(t-\tau_{пр})+\dot{m}_г(t-\tau_{пр})]-B\sqrt{RT_{ист}(t)}\,p_к(t)\}. \quad (1.9)$$

Depending on the purpose of the investigation, equation (1.9) can be converted to the corresponding form.

Thus, for small variations of the value of τ_{conv}, which occurs during operation of the engine under steady-state conditions (p_k varies insignificantly), it is possible to assume that τ_{conv}=const and $d\tau_{conv}/dt=0$. In this case, which hereafter will be considered, equation (1.9) assumes the form

$$\frac{dp_к(t)}{dt}+\frac{\varkappa}{V_к}B\sqrt{RT_{ист}(t)}\,p_к(t)=$$
$$=\frac{\varkappa}{V_к}RT_{обр}(t)[\dot{m}_{ок}(t-\tau_{пр})+\dot{m}_г(t-\tau_{пр})]. \quad (1.10)$$

RT depends on the ratio of the fuel components K and the pressure in the combustion chamber. However, the last function can be neglected, especially at moderate pressures, and it is possible to set

$$RT_к=RT(K),$$

where

$$K=\frac{\dot{m}_{ок}}{\dot{m}_г}.$$

It is possible to define the analytical function RT=RT(K) by the results of the thermodynamic calculation of the combustion of specific fuel components for various values of K and p_k.

The following functional relation can be obtained by approximation of the calculations:

$$RT_к(K)=A_1+A_2K+A_3K^2,$$

where A_1, A_2, A_3 are the constant coefficients defined basically by the properties of the fuel components.

Since in the combustion chamber there is a period of conversion of the fuel components to combustion products τ_{conv} and a finite time that the gases stay in the combustion chamber τ_{stay} before the escape time ($\tau_{stay}\geq\tau_{conv}$), the following expressions are valid for the fitness of the gases:

APPROVED FOR RELEASE: 2007/02/08: CIA-RDP82-00850R000200090053-2

APPROVED FOR RELEASE: 2007/02/08: CIA-RDP82-00850R000200090053-2

$$RT^{(1)}_{\text{обр}}(t)=A_1+A_2K(t-\tau_{\text{пб}})+A_3K^2(t-\tau^{(3)}_{\text{пб}});$$
$$RT^{(2)}_{\text{ист}}(t)=A_1+A_2K(t-\tau_{\text{пр}})+A_3K^2(t-\tau_{\text{пр}}).\quad (1.11)$$
$$(4)$$

Key: 1. formed; 2. escape; 3. stay; 4. conv

Considering the equations (1.11) and the function $K(t)=\dot{m}_{ox}(t)/\dot{m}_{fuel}(t)$ the nonlinear equation of the thrust chamber is written in the following form:

$$\frac{dp_к(t)}{dt}+\frac{\varkappa}{V_к}B\left[A_1+A_2\frac{\dot{m}_{ок}(t-\tau_{\text{пр}})}{\dot{m}_г(t-\tau_{\text{пр}})}+A_3\frac{\dot{m}^2_{ок}(t-\tau_{\text{пр}})}{\dot{m}^2_г(t-\tau_{\text{пр}})}\right]^{0,5}p_к(t)=$$
$$=\frac{\varkappa}{V_к}\left[A_1+A_2\frac{\dot{m}_{ок}(t-\tau_{\text{пб}}-\tau_{\text{пр}})}{\dot{m}_г(t-\tau_{\text{пб}}-\tau_{\text{пр}})}+A_3\frac{\dot{m}^2_{ок}(t-\tau_{\text{пб}}-\tau_{\text{пр}})}{\dot{m}^2_г(t-\tau_{\text{пб}}-\tau_{\text{пр}})}\right]\times$$
$$\times[\dot{m}_{ок}(t-\tau_{\text{пр}})+\dot{m}_г(t-\tau_{\text{пр}})].\quad (1.12)$$

For the steady-state operating mode $p_k(t)=\text{const}$, $\dot{m}(t)=\text{const}$, from the equation (1.12) we obtain the static characteristic of the thrust chamber:

$$p_к=\frac{\bar{p}_к}{\bar{\dot{m}}\sqrt{\bar{R}\bar{T}_к}}\sqrt{RT_к}(\dot{m}_{ок}+\dot{m}_г).$$

Equation (1.12) is a nonlinear equation with variable coefficient; it is used for significant variation of the parameters of the operating process and, namely, for analysis and calculation of the start-up and shutdown of the engine.

1.1.2. Linearized Equation of the Chamber

For investigation of the engine dynamics in the vicinity of the steady-state operating conditions (adjustment, transient processes), it is possible to reduce equation (1.12) to the linear equation and represent it in linearized form in relative deviations.

If we introduce the relative deviations of the variables $\delta y(t)=(y(t)-\bar{y})/\bar{y}$, then from (1.12) we obtain

$$\frac{V_к\bar{p}_к}{\varkappa}\frac{d}{dt}\delta p_к(t)+\frac{\bar{\dot{m}}R\bar{T}_к}{\bar{p}_к}\delta p_к(t)=R\bar{T}_к[\bar{\dot{m}}_{ок}\delta\dot{m}_{ок}(t-\tau_{\text{пр}})+$$
$$+\bar{\dot{m}}_г\delta\dot{m}_г(t-\tau_{\text{пр}})]+\bar{\dot{m}}\left(\frac{\partial RT_к}{\partial K}\right)\bar{K}\delta K(t-\tau_{\text{пр}})-\frac{\bar{\dot{m}}}{2}\left(\frac{\partial RT_к}{\partial K}\right)\bar{K}\delta K\times$$
$$\times(t-\tau_{\text{пр}}-\tau_{\text{пб}}).$$

APPROVED FOR RELEASE: 2007/02/08: CIA-RDP82-00850R000200090053-2

APPROVED FOR RELEASE: 2007/02/08: CIA-RDP82-00850R000200090053-2

The last equation is divided by the coefficient for δp_k, and we obtain the linearized equation of the thrust chamber in the standard form

$$T_{к.з}\frac{d\delta p_к(t)}{dt}+\delta p_к(t)=K_{p_к,\dot{m}_{ок}}\delta\dot{m}_{ок}(t-\tau_{пр})+K_{p_к,\dot{m}_г}\delta\dot{m}_г(t-\tau_{пр})+ +K_{p_к,K}[2\delta K(t-\tau_{пр})-\delta K(t-\tau_{пр}-\tau_{пб})], \quad (1.13)$$

(1)

Key: 1. thrust chamber

where $T_{к.з}=\frac{V_к\bar{p}_к}{\varkappa\bar{m}R\bar{T}_к}$ is the time constant of the thrust chamber;

K_{p_k}, x are the pressure boosting coefficients in the combustion chamber with respect to the x-th input signal.

$$K_{p_к,\dot{m}_{ок}}=\frac{\bar{K}}{\bar{K}+1};\quad K_{p_к,\dot{m}_г}=\frac{1}{\bar{K}+1};$$
$$K_{p_к,K}=\frac{\bar{K}}{2\bar{R}\bar{T}_к}\operatorname{tg}\alpha_к;\quad \operatorname{tg}\alpha_к=\frac{\partial RT_к}{\partial K}.$$

The equation of the ratio of the fuel component

$$\delta K(t)=\delta\dot{m}_{ок}(t)-\delta\dot{m}_г(t). \quad (1.14)$$

(1) (2)

Key: 1. ox=oxidant; 2. fuel [combustible component]

The ratio of the fuel component in the thrust chamber is selected from the condition of obtaining the maximum specific thrust.

The maximum specific thrust is obtained for $RT_k=(RT_k)_{max}$; therefore the value of $\partial RT_k/\partial K$ for $\bar{K}=K$ defined by the tangent of the slope angle of the tangent to the curve $RT_k(K)$, is in practice equal to zero, and

$$K_{p_к,K}=0.$$

In this case the linear equation of the thrust chamber is simplified significantly and assumes the form

$$T_{к.з}\frac{d\delta p_к(t)}{dt}+\delta p_к(t)=K_{p_к,\dot{m}_{ок}}\delta\dot{m}_{ок}(t-\tau_{пр})+K_{p_к,\dot{m}_г}\delta\dot{m}_г(t-\tau_{пр}). \quad (1.15)$$

1.1.3. Dynamic Characteristics of the Thrust Chamber

The equation of the thrust chamber in the Laplace transformations has the form

$$(T_{к.з}s+1)\delta p_к(s)=e^{-s\tau_{пр}}[K_{p_к,\dot{m}_{ок}}\delta\dot{m}_{ок}(s)+K_{p_к,\dot{m}_г}\delta\dot{m}_г(s)], \quad (1.16)$$

(1)

Key: 1. thrust chamber

APPROVED FOR RELEASE: 2007/02/08: CIA-RDP82-00850R000200090053-2

APPROVED FOR RELEASE: 2007/02/08: CIA-RDP82-00850R000200090053-2

where $s=j\omega$ is the complex frequency.

The latter equation can be written in terms of the transfer function

$$\delta p_к(s)=e^{-s\tau_{пр}}(W_{p_к,\dot{m}_{ок}}\delta\dot{m}_{ок}+W_{p_к,\dot{m}_г}\delta\dot{m}_г), \tag{1.17}$$

where $W_{p_к,\dot{m}_i}=\frac{K_{p_к,\dot{m}_i}}{T_{к.д}s+1}$ is the transfer function of the pressure in the thrust chamber with respect to the i-th fuel component.

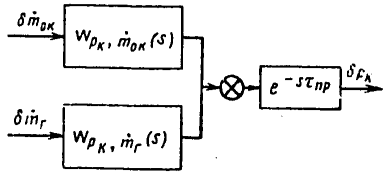

Figure 1.2. Structural diagram of the thrust chamber

The structural diagram of the chamber as a dynamic element constructed by equation (1.17) is shown in Fig 1.2.

Thus, with respect to its dynamic structure the thrust chamber is a set of inertial and delay elements.

The transient characteristic of the thrust chamber, that is, the variation of the output signal $\delta p_к(t)$ with step variation of the input signal $\delta m=h\cdot 1(t)$; h is the magnitude of the input disturbance; obtained by solving the equation (1.16), and it has the form

$$\delta p_к(t)=hK_{p_к,\dot{m}_i}\left(1-e^{-\frac{t-\tau_{пр}}{T_{к.д}}}\right). \tag{1.18}$$

The transient characteristic is illustrated in Fig 1.3.

The dynamic characteristics, in particular, the inertial properties of the chamber, are defined by the time constant

$$T_{к.т}=\frac{V_к\bar{p}_к}{\bar{m}_к\bar{R}\bar{T}_к}=\frac{1}{\varkappa}\tau_{пб}. \tag{1.19}$$

Key: (1) Thrust chamber

Consequently, the value of $T_{\text{thrust chamber}}$ is proportional to the time the gases stay in the chamber.

APPROVED FOR RELEASE: 2007/02/08: CIA-RDP82-00850R000200090053-2

APPROVED FOR RELEASE: 2007/02/08: CIA-RDP82-00850R000200090053-2

Since $\bar{\dot{m}} = \frac{\varphi b(\varkappa) F_{кр} \bar{p}_к}{V \overline{RT}_к}$, then $T_{\text{thrust chamber}} = a l_{\text{conv}}$,

where $a = (\varphi b(\varkappa) V \overline{RT}_к)^{-1}$; $l_{пр} = \frac{V_к}{F_{кр}}$ is the reduced length of the chamber.

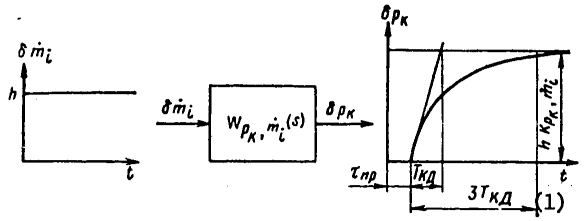

Figure 1.3. Transient characteristics of the thrust chamber

Key:
1. thrust chamber

For a=const the time constant is basically determined by the configuration of the chamber. With an increase in the chamber volume V_k or a decrease in the area of the critical cross section of the nozzle F_{cr} the inertia of the chamber increases (see Fig 1.4). The boost factors of the thrust chamber depend on the ratio of the fuel components. For $K=0$, $K_{p_k, \dot{m}_{ox}}=0$, $K_{p_k, \dot{m}_{fuel}}=1$; for $K=\infty$, $K_{p_k, \dot{m}_{ox}}=1$, $K_{p_k, \dot{m}_{fuel}}=0$ (Fig 1.5).

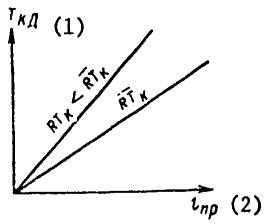

Figure 1.4. Time constant of the thrust chamber as a function of the reduced length and working capacity of the gas

Key:
1. thrust chamber
2. conv

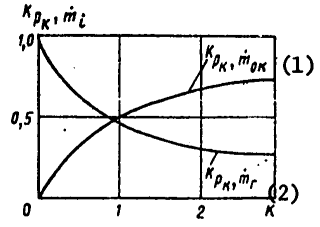

Figure 1.5. Boost factors as a function of the fuel component ratio

Key:
1. ox
2. fuel

For a conversion (delay) time constant τ_{conv}=const, the characteristic equation of the chamber $T_{\text{thrust chamber}} s+1=0$ has one negative root $s=-1/T_{\text{thrust chamber}}$, for $T_{\text{thrust chamber}}>0$; therefore the process in the chamber is stable.

APPROVED FOR RELEASE: 2007/02/08: CIA-RDP82-00850R000200090053-2

APPROVED FOR RELEASE: 2007/02/08: CIA-RDP82-00850R000200090053-2

However, in the general case the conversion time depends on the pressure in the thrust chamber, which in turn leads to a flexible positive feedback with respect to pressure in the chamber. With an increase in pressure in the chamber, the conversion time decreases, and additional gas formation is obtained; the so-called intrachamber instability can occur.

Let us determine the region of stability of the combustion chamber.

Considering the function $\tau_{conv}=A/P_k^{\nu}$, the dynamic equation is obtained for the thrust chamber (1.9).

After linearization of equation (1.9) the characteristic equation of the thrust chamber assumes the form

$$(T_{к.т}-\bar{\tau}_{пр}\cdot\nu)s+1=0, \tag{1.19a}$$

where $\bar{\tau}_{пр}=\frac{A}{\bar{p}_к^{\nu}}$.

The characteristic equation (1.19, a) has one root $s=\frac{-1}{T_{к.к}-\bar{\tau}_{пр}\cdot\nu}$, but its sign is determined by the ratio of the terms in the denominator.

For $\bar{\tau}_{conv}\cdot\nu>T_{\text{thrust chamber}}$ the root of the equation becomes positive, and the thrust chamber loses stability. The chamber is at the stability limit when the root of the characteristic equation s=0.

Thus, the condition of the stability limit is

$$\frac{\bar{\tau}_{пр}}{T_{к.к}}=\frac{1}{\nu}. \tag{1.20}$$

The satisfaction of the condition $T_{\text{thrust chamber}}>\bar{\tau}_{conv}\cdot\nu$ insures stability of the thrust chamber as a dynamic element.

1.2. Gas Generator

The operating processes of the gas generator are similar to the operating processes of the thrust chamber. Therefore when describing the dynamics of the gas generator it is possible to use equations obtained for the thrust chamber.

On the basis of equations (1.9), (1.11), (1.12), the corresponding equations are written for the gas generator:

The equation of the gas capacity of the gas generator

$$\frac{dp_{гг}^{(1)}(t)}{dt}=\frac{\varkappa'}{V_{гг}}\left[RT^{(2)}_{г.обр}(t)\left[\dot{m}'_{ок}(t-\tau'_{пр})+\dot{m}'_{г}(t-\tau'_{пр})\right]-RT^{(3)}_{г.ист}(t)\dot{m}_{г}(t)\right]. \tag{1.21}$$

(6) (4) (5)

Key: 1. gas generator; 2. gas formation; 3. gas escape; 4. conv; 5. fuel; 6. ox

APPROVED FOR RELEASE: 2007/02/08: CIA-RDP82-00850R000200090053-2

APPROVED FOR RELEASE: 2007/02/08: CIA-RDP82-00850R000200090053-2

The work capacity equations of the generator gas follow:

$$RT_{\text{г.общ}}(t)=f_1[K'(t-\tau'_{\text{пр}})];$$
$$RT_{\text{г.ист}}(t)=f_2[K'(t-\tau'_{\text{пб}}-\tau'_{\text{пр}})]. \quad (1) \qquad (1.22)$$

Key: 1. stay

The equation of the fuel component ratio is

$$K'(t)=\frac{\dot{m}'_{\text{ок}}(t)}{\dot{m}'_{\text{г}}(t)}. \qquad (1.23)$$

When determining the gas flow rate from the gas generator to the turbine $\dot{m}_T(t)$ it is necessary to consider the structural diagram of the engine and type of turbine used.

In the engines without afterburning of the generator gas, the generator gas escape is subcritical

$$\dot{m}_{\text{г}}=\frac{\bar{\dot{m}}_{\text{г}}\sqrt{\bar{R}\bar{T}_{\text{г}}}}{\bar{p}_{\text{гг}}}\frac{p_{\text{гг}}}{\sqrt{RT_{\text{г}}}}. \qquad (1.24)$$

In the engines with afterburning of the generator gas, jet turbines are used, and the generator gas escape takes place to the thrust chamber; in this case the subcritical escape conditions are insured:

$$\dot{m}_{\text{г}}=\frac{\dot{m}_{\text{г}}\sqrt{\bar{R}\bar{T}_{\text{г}}}p_{\text{гг}}}{\bar{p}_{\text{гг}}\sqrt{\left(\frac{\bar{p}_{1\text{т}}}{\bar{p}_{\text{гг}}}\right)^{\frac{2}{\varkappa}}-\left(\frac{\bar{p}_{1\text{т}}}{\bar{p}_{\text{гг}}}\right)^{\frac{\varkappa+1}{\varkappa}}}\sqrt{RT_{\text{г.ист}}}}\sqrt{\left(\frac{p_{1\text{т}}}{p_{\text{гг}}}\right)^{\frac{2}{\varkappa}}-\left(\frac{p_{1\text{т}}}{p_{\text{гг}}}\right)^{\frac{\varkappa+1}{\varkappa}}}, \qquad (1.25)$$

where p_{1T} is the generator gas pressure at the exit of the turbine guide vane.

Consequently, the gas generator is described by the system of equations (1.21-1.24) and (1.25).

As a result of linearization of the equations (1.21-1.24) for small deviations of the parameters, we obtain the linearized equation of the gas generator

$$T_{\text{гг}}\frac{d\delta p_{\text{гг}}(t)}{dt}+\delta p_{\text{гг}}(t)=\sum_{i_1=0,\text{г}}K_{p_{\text{гг}},\dot{m}'_i}\delta\dot{m}'_i(t-\tau'_{\text{пр}})+$$
$$+K_{p_{\text{гг}},K'}[2\delta K'(t-\tau'_{\text{пр}})-\delta K'(t-\tau'_{\text{пб}}-\tau'_{\text{пр}})]+K_{p_{\text{гг}},p_{1\text{т}}}\delta p_{1\text{т}}(t). \qquad (1.26)$$

APPROVED FOR RELEASE: 2007/02/08: CIA-RDP82-00850R000200090053-2

APPROVED FOR RELEASE: 2007/02/08: CIA-RDP82-00850R000200090053-2

In operator form

$$(T_{\Gamma\Gamma}s+1)\delta p_{\Gamma\Gamma}(s)=\sum_{i=0,\Gamma}K_{p_{\Gamma\Gamma},\dot{m}_i'}e^{-s\tau'_{\text{пр}}}\delta\dot{m}_i'(s)+$$
$$+K_{p_{\Gamma\Gamma},K'}e^{-s\tau'_{\text{пр}}}\left(2-e^{-s\tau'_{\text{пб}}}\right)\delta K'(s)+K_{p_{\Gamma\Gamma},p_{1\Gamma}}\delta p_{1\Gamma}(s), \qquad (1.27)$$

Key: (1) gas generator

where $T_{\Gamma\Gamma}=\dfrac{V_{\Gamma\Gamma}\bar{p}_{\Gamma\Gamma}}{\varkappa'\bar{R}\bar{T}_{\Gamma}\bar{\dot{m}}_{\Gamma}q_{\Gamma}}$ is the time constant of the gas generator;

$q_{\Gamma}=1-\dfrac{1}{2\varkappa'}\dfrac{2-(\varkappa'+1)\left(\bar{p}_{1\Gamma}/\bar{p}_{\Gamma\Gamma}\right)^{\frac{\varkappa'-1}{\varkappa}}}{1-\left(\bar{p}_{1\Gamma}/\bar{p}_{\Gamma\Gamma}\right)^{\frac{\varkappa'-1}{\varkappa}}}$ is the coefficient which depends on the escape conditions.

For the critical escape conditions when

$$p_{1\Gamma}/p_{\Gamma\Gamma}=\bar{p}_{1\Gamma}/\bar{p}_{\Gamma\Gamma}=\left(\frac{2}{\varkappa'+1}\right)^{\frac{\varkappa'}{\varkappa'-1}}=\text{const},\ q_{\Gamma}=1.$$

$K_{p_{\Gamma\Gamma},x}$ are the boost factors which are determined by the functions

$$K_{p_{\Gamma\Gamma},\dot{m}'_{\text{ок}}}=\frac{\bar{K}'}{q_{\Gamma}(\bar{K}'+1)};\quad K_{p_{\Gamma\Gamma},\dot{m}_{\Gamma}}=\frac{1}{q_{\Gamma}(\bar{K}'+1)};$$
$$K_{p_{\Gamma\Gamma},K'}=\frac{\bar{K}'}{2q_{\Gamma}\bar{R}\bar{T}_{\Gamma}}\operatorname{tg}\alpha_{\Gamma}.$$

$\operatorname{tg}\alpha_{\text{fuel}}$ is determined by the ratio of the fuel components.

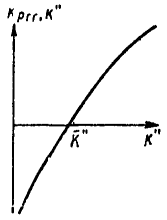

Figure 1.6. Boost factor of the gas generator as a function of the ratio of the fuel components

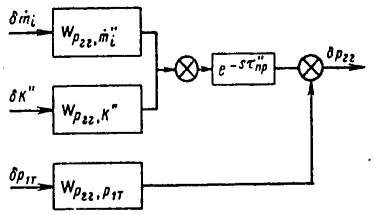

Figure 1.7. Structural diagram of the gas generator

The ratio of the fuel components fed to the gas generator differs sharply from stoichiometric. Therefore for a reducing gas generator $\operatorname{tg}\alpha_{\text{fuel}}>0$ and $K_{p_{\Gamma\Gamma},K'}>0$, and for the oxidizing gas generator, on the contrary, $\operatorname{tg}\alpha_{\text{fuel}}<0$ and $K_{p\text{gas generator}},K'<0$ (Fig 1.6)

$$K_{p_{\Gamma\Gamma},p_{1\Gamma}}=\frac{q_{\Gamma}-1}{q_{\Gamma}}.$$

APPROVED FOR RELEASE: 2007/02/08: CIA-RDP82-00850R000200090053-2

APPROVED FOR RELEASE: 2007/02/08: CIA-RDP82-00850R000200090053-2

For the critical escape mode of the gas generator gas $q_{fuel}=1$ and $\kappa_{p_{gas\ generator}}$, $p_{1T}=0$; in this case the equation of the gas generator becomes similar to the equation of the thrust chamber.

The structural diagram of the gas generator is shown in Fig 1.7.

The transfer functions which figure in the structural diagram are defined by the expressions

$$W_{p_{rr}, \dot{m}_l'}(s)=\frac{K_{p_{rr}, \dot{m}_l'}}{T_{rr}s+1}; \quad W_{p_{rr}, p_{1T}}(s)=\frac{K_{p_{rr}, p_{1T}}}{T_{rr}s+1};$$

$$W_{p_{rr}, K'}(s)=\frac{K_{p_{rr}, K'}\left(2-e^{-s\tau_{n6}'}\right)}{T_{rr}s+1}.$$

1.3. Hydraulic Channels

1.3.1. Nonlinear Equations

The liquid-fuel rocket engine assemblies (pumps, chambers, turbines, gas generators) are connected to each other by hydraulic and gas lines; the assemblies themselves have channels with liquid and gas flow. Therefore the basic steps in the operating processes defining the engine characteristics take place in the flow sections (channels) of the units.

The analysis of the dynamics of the hydraulic channels is performed using the equations of hydromechanics which are compiled on the basis of the laws of conservation of mass, momentum and energy.

If the movement of the liquid or gas takes place through the channel without heat exchange with the external environment, then it is sufficient to use the mass conservation law (the continuity equation), the law of conservation of momentum (the equation of motion) and the equation of state.

If the movement of the gas with supply or removal of heat is considered, it is necessary to add the equation of conservation of energy.

In addition to what has been indicated, when investigating the fluctuations of the channels it is necessary to consider the distributed nature of the parameters, that is, the finite propagation time of the disturbances, and this process is described by the wave equations.

Thus, in the general case the movement of a liquid or gas in the channels is described by the partial differential equations.

For analysis of the dynamic characteristics of the channels of liquid-fuel rocket engines, especially in the low frequency and vibration amplitude region it is possible to make the following assumptions:

APPROVED FOR RELEASE: 2007/02/08: CIA-RDP82-00850R000200090053-2

APPROVED FOR RELEASE: 2007/02/08: CIA-RDP82-00850R000200090053-2

The heat exchange with the external environment is absent;

The viscosity of the liquid is taken into account only in the local hydraulic drags;

The motion of the liquid is uniform, that is, all of the parameters (velocity, pressure) at different points of the transverse cross section of the line are identical;

The liquid is incompressible;

The distribution of the parameters is absent.

Considering the assumptions, the motion of an incompressible liquid in a cylindrical line is described by the equation of the pulses taking into account the inertia of the column of liquid, the pressure force at the ends of the line, the force of the hydraulic drag and external forces.

$$F_T(p_1-p_2)=m\frac{dv_{ж}}{dt}+I_x+\varepsilon\frac{l}{d}\frac{\varrho v_{ж}^2}{2}F_T, \tag{1.28}$$

where ε is the friction coefficient; m is the mass of the liquid; v is the liquid velocity; $v=\dot{m}/\rho F_T$.

Using the last equations, equation (1.28) for a section of the main is reduced to the form

$$\frac{l_l}{F_{Tl}}\frac{d\dot{m}}{dt}=p_1-p_2+\frac{\dot{m}^2}{\varrho}\xi_l+p_x, \tag{1.29}$$

where ξ is the hydraulic drag coefficient of the line; p_x is the additional pressure gradient occurring as a result of the effect of gravitational forces and g-loads.

The equation of motion (1.29) for individual sections of the line can be combined into one equation. The liquid flow rate for all sections is identical; the losses to friction and local drag and losses to inertia of the liquid are summed, that is,

$$\sum\frac{l_l}{F_{Tl}}\frac{d\dot{m}}{dt}=\underset{(1)}{p_{вх}}-\underset{(2)}{p_{вых}}+(\xi+\xi_M)\frac{\dot{m}^2}{\varrho}+p_x, \tag{1.30}$$

Key: inp; 2. out

where $\sum\frac{l_l}{F_{Tl}}=R'$ -- the coefficient of inertial resistance of the line determines its inertial properties; ξ is the total hydraulic friction drag; ξ_M is the coefficient of total local losses.

APPROVED FOR RELEASE: 2007/02/08: CIA-RDP82-00850R000200090053-2

APPROVED FOR RELEASE: 2007/02/08: CIA-RDP82-00850R000200090053-2

Thus, without considering the compressibility, the equation of motion of the liquid in the line has the form

$$R' \frac{dm}{dt} + \frac{(\xi + \xi_м)\dot{m}^2}{\varrho} = \underset{(1)}{p_{вх}} - \underset{(2)}{p_{вых}} + p_x. \qquad (1.31)$$

Key: 1. inp; 2. out

Let us consider the peculiarities of the equation of motion for the intake and delivery lines.

The delivery lines are the lines connecting the TNA [turbine pump assembly] pumps to the thrust chamber and the gas generator together with the injectors.

For the delivery lines the gravitational forces and g-loads can be neglected, that is, $p_x=0$.

The pressure at the entrance to the line is the pressure after the pumps, that is, $p_{inp}(t)=p_{del}(t)$. The pressure at the output of the line is the pressure in the thrust chamber (gas generator)

$$\overset{(1)}{p_{вых}}(t) = p_к(t);\ p_{вых}(t) = \overset{(2)}{p_{гг}}(t).$$

Key: 1. out; 2. gas generator

Thus, the equations of motion of the fuel components through the lines connecting the pumps to the thrust chamber or the gas generator have the form

$$R'_{M,l} \frac{d\dot{m}_l(t)}{dt} + \frac{\xi_l \dot{m}_l^2(t)}{\varrho_l} = p_{нl}(t) - p_j(t), \qquad (1.32)$$

where i=ox, fuel; j=k, gas generator.

For the steady-state operating conditions

$$\dot{m}(t) = \bar{\dot{m}};\ \frac{d\dot{m}(t)}{dt} = 0 \text{ and } \frac{\xi}{\varrho}\bar{\dot{m}}^2 = \bar{p}_1 - \bar{p}_2,$$

that is, the known static equation of the line is obtained.

Since the delivery lines feed the fuel components to the thrust chamber or the gas generator, the input variables of the lines are the pressures after the pumps and the hydraulic drags, and the output variables are the mass flow rates of the fuel components.

For the intake lines connecting the tanks to the pumps the value of p_x cannot be neglected, and it is defined by the pressure of the column of liquid above the pumps and the axial g-load.

APPROVED FOR RELEASE: 2007/02/08: CIA-RDP82-00850R000200090053-2

APPROVED FOR RELEASE: 2007/02/08: CIA-RDP82-00850R000200090053-2

$$p_x(t)=gQl_M\left[\sin\theta+\frac{j_x(t)}{g}\right],$$

where ℓ_M is the length of the line (from the pump to the fuel surface in the tank); θ is the pitch angle; j_X is the projection of the rocket acceleration on the direction of the line.

The intake line determines the pressure at the entrance to the pump:

$$p_{вх}(t)=p_б(t)+\frac{\xi}{Q}\dot{m}^2(t)-R'\frac{d\dot{m}(t)}{dt}+gQl_M\left[\sin\theta+\frac{j_x(t)}{g}\right]. \qquad (1.33)$$

1.3.2. Linear Equations

For the delivery line

$$T_M\frac{d\dot{m}(t)}{dt}+\delta\dot{m}_l(t)=K_{\dot{m},p_н}\delta p_н(t)-K_{\dot{m},p_j}\delta p_j(t)-k_{\dot{m},\xi}\delta\xi(t), \qquad (1.34)$$

where $T_M=\frac{Q}{2\dot{m}}\left(\frac{R'}{\xi}\right)$ is the time constant of the line; $K_{\dot{m},x}$ are the boost factors

$$K_{\dot{m},p_н}=\frac{\pi_н}{2(\pi_н-1)};\quad K_{\dot{m},p_j}=\frac{1}{2(\pi_н-1)};$$

$$K_{\dot{m},\xi}=0{,}5;\quad \pi_н=\frac{\bar{p}_н}{\bar{p}_j};\quad j=к,\ гг.$$

For the intake line

$$\delta p_{вх}=K_{p_{вх},p_б}\delta p_б(t)-K_{p_{вх},\dot{m}}\left[\delta\dot{m}(t)+T_M\frac{d\dot{m}(t)}{dt}\right]+K_{p_{вх},p_x}\delta p_x(t), \qquad (1.35)$$

where

$$K_{p_{вх},p_б}=\pi_б;\quad K_{p_{вх},\dot{m}}=\frac{2\pi_б}{Q};$$

$$K_{p_{вх},p_x}=\frac{1}{\bar{p}_{вх}};\quad \pi_б=\frac{\bar{p}_б}{\bar{p}_{вх}}.$$

(1) (1)

Key: 1. input

The equation of the delivery line in the Laplace transforms is written in the form

$$(T_Ms+1)\delta\dot{m}(s)=K_{\dot{m},p_н}\delta p_н(s)-K_{\dot{m},p_j}\delta p_j(s)-K_{\dot{m},\xi}\delta\xi(s), \qquad (1.36)$$

APPROVED FOR RELEASE: 2007/02/08: CIA-RDP82-00850R000200090053-2

APPROVED FOR RELEASE: 2007/02/08: CIA-RDP82-00850R000200090053-2

or $$\delta\dot{m}(s)=W_{\dot{m},p_н}\delta p_н(s)-W_{\dot{m},p_j}\delta p_j(s)-W_{\dot{m},\xi}\delta\xi(s),$$

where $W_{\dot{m},x}(s)$ are the operator transfer functions;

$$W_{\dot{m},x}=\frac{K_{\dot{m},x}}{T_M s+1},\quad x=\overline{p_н, p_к, p_{гг}, \xi}.$$

The structural diagram of the delivery line is shown in Fig 1.8.

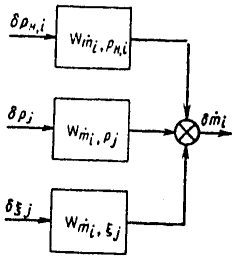

Figure 1.8. Structural diagram of the delivery line

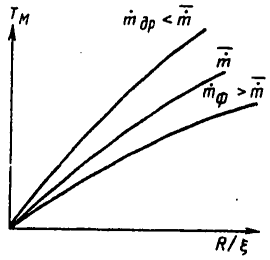

Figure 1.9. Function $T_M=T_M(R/\zeta)$

Thus, the delivery line is a set of inertial elements. The dynamic characteristics of the line are determined by the time constant and the boost factors.

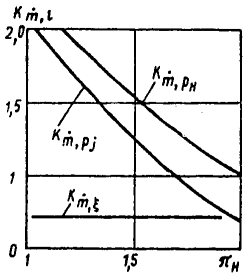

Figure 1.10. Boost factors of the line as a function of pressure gradient

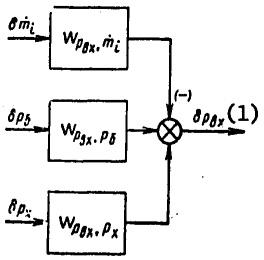

Figure 1.11. Structural diagram of the intake line
Key:
1. input

APPROVED FOR RELEASE: 2007/02/08: CIA-RDP82-00850R000200090053-2

APPROVED FOR RELEASE: 2007/02/08: CIA-RDP82-00850R000200090053-2

The time constant of the line depends on the length, the pressure gradient in the line and the mass flow rate. With an increase in the pressure gradient and the length of the line, the time constant increases, and the boost factor decreases, Fig 1.9, Fig 1.10.

The equation of the intake line

$$\delta p_{вх}(s)=K_{p_{вх},\,p_б}\delta p_б(s)-K_{p_{вх},\,\dot{m}}(1+T_M s)\delta\dot{m}(s)+K_{p_{вх},\,p_x}\delta p_x(s). \qquad (1.37)$$

The structural diagram is shown in Fig 1.11.

The intake line is a set of inertial and forcing elements.

1.3.3. Consideration of the Compressibility of the Liquid and the Elasticity of the Walls

In certain cases, the condition ρ=const, and the equality of the flow rates at the input and output from the lines are not observed. Violation of the indicated conditions occurs in long thin-walled lines and in lines with elastic sections.

In this case the equation (1.31) will contain three unknowns $\dot{m}$, p, ρ and for closure of the system it is necessary to add additional equations, the equations of the capacity and the equivalent state for the liquid density.

The equation of the line capacity

$$\frac{dm}{dt}=\dot{m}_1-\dot{m}_2, \qquad (1.38)$$

where m is the mass of liquid in the line; $\dot{m}_1$, $\dot{m}_2$ is the flow rate of the liquid at the entrance and exit of the line, respectively.

The equation of state for the motion of an isothermal drop liquid is written in the form of Hook's law

$$\underset{(1)}{\rho}=\underset{(1)}{\rho_{ср}}\left(1+\frac{p-p_{ср}}{\underset{(2)}{K_{ж}}}\right), \qquad (1.39)$$

Key: 1. mean; 2. liquid

where ρ_{mean} is the liquid density for mean pressure

$$p_{ср}=\frac{p_1+p_2}{2};$$

K_{liquid} is the coefficient which depends on the elasticity of bulk of the liquid and the pliability of the line walls.

From the equation of the propagation rate of sound (the formula of N. Ye. Zhukovskiy)

APPROVED FOR RELEASE: 2007/02/08: CIA-RDP82-00850R000200090053-2

APPROVED FOR RELEASE: 2007/02/08: CIA-RDP82-00850R000200090053-2

$$K_{ж}=\frac{K'_{ж}}{1-\chi\frac{K'_{ж}}{E}}, \qquad (1.40)$$

(1)

Key: 1. liquid

where K'_{liquid} is the modulus of the elasticity of bulk of the liquid without considering the pliability of the walls; E is the modulus of elasticity of the wall material; χ is the parameter which depends on the shape of the tube which is defined as follows.

The values of the modulus K_{liquid}' are presented in Table 1.1 for certain fuel components.

Table 1.1

Fuel component	$K'_{liquid}\cdot10^{-5}$, newtons/m^2	Fuel component	$K'_{liquid}\cdot10^{-5}$, newtons/m^2
Nitrogen tetroxide	31577	Kerosene	11830
NDMG	18397	Ethyl alcohol	8918
Hydrogen (liquid)	4419	Tetranitromethane	17315
Oxygen (liquid)	9296	Water	21360

Assuming that the line wall material operates in the elastic deformation region, it is possible to write

$$\frac{d-d_0}{d_0}=\frac{\chi}{2}\frac{p-p_0}{E}. \qquad (1.41)$$

The increase in force trying to rupture the tube on variation of the pressure by the amount $\Delta p=p-p_0$ is $dl\Delta p$. Consequently, the increase in the tensile stress in the longitudinal cross section of the wall

$$\Delta\sigma=\frac{dl\Delta p}{2l\delta}=\frac{\Delta pd}{2\delta}.$$

The relative elongation according to Hook's law

$$\frac{\Delta d}{d}=\frac{\Delta\sigma}{E}=\frac{d}{2\delta}\left(\frac{p-p_0}{E}\right). \qquad (1.42)$$

Comparing the equations (1.41) and (1.42), we obtain

$$\chi=\frac{d}{\delta}.$$

For tubes of great thickness, there are more complex functions for [10]

APPROVED FOR RELEASE: 2007/02/08: CIA-RDP82-00850R000200090053-2

APPROVED FOR RELEASE: 2007/02/08: CIA-RDP82-00850R000200090053-2

$$\chi=2\mu+\frac{d+2\delta+\frac{2\delta^2}{d}}{d+2\frac{\delta^2}{d}}. \tag{1.43}$$

The flow rates at the entrance and exit of the lines are found from the equations of hydraulic drags of the ends of the investigated section

$$\begin{aligned}\dot{m}_1&=\mu F_1\sqrt{2\varrho(p_{\text{н}1}-p_1)};\\ \dot{m}_2&=\mu F_2\sqrt{2\varrho(p_2-p_{\text{н}2})},\end{aligned} \tag{1.44}$$

where μF_1, μF_2 are the effective through cross sections of the local drags at the boundaries of the line sections.

When considering the compressibility of the liquid, the average flow rate is substituted in the equation of motion (1.31):

$$\dot{m}=\frac{\dot{m}_1+\dot{m}_2}{2}. \tag{1.45}$$

After substitution of ρ from expression (1.39) in equation (1.38) and proceeding to the equation in small deviations, we obtain

$$T_M\frac{d\delta p_{\text{ср}}^{(1)}}{dt}=\delta\dot{m}_1-\delta\dot{m}_2, \tag{1.46}$$

Key: mean

where $T_M=\frac{F_T l\rho_{\text{ср}}\varrho_{\text{ср}}}{\bar{m}K'_{\text{ж}}}$ is the time constant (capacitive) of the section of the line;

$$\begin{aligned}\delta\dot{m}_1&=\mu F_1\sqrt{\frac{\bar{p}_{\text{н}1}}{\Delta\bar{p}_1}\delta p_{\text{н}1}-\frac{\bar{p}_1}{\Delta\bar{p}_1}\delta p_1};\\ \delta\dot{m}_2&=\mu F_2\sqrt{\frac{\bar{p}_2}{\Delta\bar{p}_2}\delta p_2-\frac{\bar{p}_{\text{н}2}}{\Delta\bar{p}_2}\delta p_{\text{н}2}},\end{aligned} \tag{1.47}$$

where $\bar{p}_{H1}$ and $\bar{p}_{H2}$ are the pressures in the capacitive sections of the lines (adjacent units) in the rated operating mode; Δp_1, Δp_2 are the pressure gradients in the hydraulic drags at the boundaries of the adjacent sections in the rated mode.

When it is necessary to consider the compressibility, equations (1.31), (1.46), (1.47) are solved with respect to δp_1, δp_2, $\delta\dot{m}_1$, $\delta\dot{m}_2$ of each section of the line.

1.4. Gas Reservoirs

Let us consider the process of pressurizing with gases forcing out the fuel components, Fig 1.12.

APPROVED FOR RELEASE: 2007/02/08: CIA-RDP82-00850R000200090053-2

APPROVED FOR RELEASE: 2007/02/08: CIA-RDP82-00850R000200090053-2

The mass of the gas in the reservoir is defined by the function

$$\overset{(1)}{m_r} = pRT_rV_r. \tag{1.48}$$

Key: 1. gas

If we neglect the heat exchange and the choke effect and use the mass balance equation $dm_g = \dot{m}_g dt$, then considering the function (1.48) we have

$$V_rRT_r\frac{dp}{dt} + pRT_r\frac{dV_r}{dt} = \dot{m}_r. \tag{1.49}$$

The variation of the gas volume in the reservoir

$$\frac{dV_r}{dt} = -\frac{dV_ж}{dt} = \frac{\dot{m}_ж}{\varrho_ж(1)}. \tag{1.50}$$

Key: 1. liquid

The arrival of gas in the reservoir is determined by the pressure gradient and the flow conditions in the choking cross section F_g.

In the case of subcritical conditions

$$\dot{m}_r = F_r\sqrt{\frac{2\varkappa p_б^2}{RT_r(\varkappa-1)}\left[\left(\frac{p}{p_б}\right)^{\frac{2}{\varkappa}} - \left(\frac{p}{p_б}\right)^{\frac{\varkappa+1}{\varkappa}}\right]}, \tag{1.51}$$

for critical conditions

$$\dot{m}_r = F_r\sqrt{\varkappa\left(\frac{2}{\varkappa+1}\right)^{\frac{\varkappa+1}{\varkappa-1}}\frac{p_б^2}{RT_1}}. \tag{1.52}$$

The liquid (component) flow rate from the tank

$$\overset{(1)}{\dot{m}_ж} = F_ж\sqrt{2\varrho(p-p_{ар})}.(2) \tag{1.53}$$

Key: 1. liquid; 2. choke

After substitution of equation (1.50) in the initial equation (1.49), we obtain the equation of the gas tank

$$V_rRT_r\frac{dp}{dt} = \dot{m}_r - \frac{\varrho_r}{\varrho_ж}\dot{m}_ж, \tag{1.54}$$

where $\dot{m}_g$ and $\dot{m}_{liquid}$ are defined by the functions (1.51)-(1.53).

APPROVED FOR RELEASE: 2007/02/08: CIA-RDP82-00850R000200090053-2

APPROVED FOR RELEASE: 2007/02/08: CIA-RDP82-00850R000200090053-2

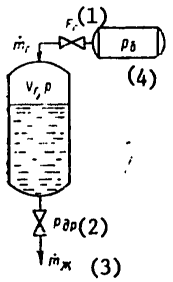

Figure 1.12. Diagram of the gas reservoir

Key:
1. gas
2. choke
3. liquid
4. tank

The last equation in linearized form is written as follows:

$$\frac{V_г \overline{RT}_г \bar{p}}{\dot{\bar{m}}_г} \frac{d\delta p}{dt} = \delta\dot{m}_г - \delta\dot{m}_ж. \tag{1.55}$$

Here we have in mind that in the steady-state mode

$$\frac{\dot{m}_ж}{\varrho_ж} = \frac{\dot{m}_г}{\varrho_г}.$$

From equation (1.51) we have

$$\delta\dot{m}_г = \delta F_г - 0{,}5\delta RT_г + (1+\alpha)\delta p_б + \alpha\delta p \tag{1.56}$$

or from (1.52)

$$\delta\dot{m}_г = \delta F_г - 0{,}5\delta RT_г + \delta p_б.$$

From the equation (1.53)

$$\delta\dot{m}_ж = \delta F_ж + \frac{1}{2(1-\pi_{кр})} \cdot \delta p - \frac{1}{2\left(\frac{1}{\pi_{кр}} - 1\right)} \delta p_{кр},$$

where

$$\pi_{кр} = \frac{p_{кр}}{p}; \quad \alpha = \frac{2\pi_б^{\frac{2}{\varkappa}} - (\varkappa+1)\pi_б^{\frac{\varkappa+1}{\varkappa}}}{2\varkappa\left(\pi_б^{\frac{2}{\varkappa}} - \pi_б^{\frac{\varkappa+1}{\varkappa}}\right)}; \quad \pi_б = \frac{p}{p_б}.$$

For the critical flow conditions $\alpha=0$. Substituting the last relations in equation (1.55), we obtain

$$T_э \frac{dp(t)}{dt} + \delta p(t) = K_{p, F_г}\delta F_г(t) - K_{p, F_ж}\delta F_ж(t) - K_{p, RT_г}\delta RT_г(t) + K_{p, p_б}\delta p_б(t) + K_{p, p_{кр}}\delta p_{кр}(t),$$

or

$$(T_э s + 1)\delta p(s) = \sum K_{p, x}\delta x(s), \tag{1.57}$$

APPROVED FOR RELEASE: 2007/02/08: CIA-RDP82-00850R000200090053-2

APPROVED FOR RELEASE: 2007/02/08: CIA-RDP82-00850R000200090053-2

where

$$\delta x=\overline{\delta F_{\text{г}},\ \delta F_{\text{ж}},\ \delta RT_{\text{г}},\ \delta p_{\text{б}}},$$

$$T_{\text{e}}=\frac{2V_{\text{г}}\bar{p}R\bar{T}_{\text{г}}(1-\pi_{\text{др}})}{\bar{m}_{\text{г}}}.$$

For critical flow let us substitute $\dot{m}_{\text{g}}$ in T_{e} -- we obtain

$$T_{\text{e}}=2\frac{V_{\text{г}}}{F_{\text{г}}}\pi_{\text{б}}(1-\pi_{\text{др}})b,$$

$$b=\frac{\sqrt{RT_{\text{г}}}}{\varkappa\left(\frac{2}{\varkappa+1}\right)^{\frac{\varkappa-1}{\varkappa+1}}}.$$

Thus, the gas reservoir is an inertial element with significant time constant which depends on the pressure gradient on the hydraulic drags. With a decrease in hydraulic drag of the fuel component lines $\pi_{\text{choke}}\to 1$, the time constant decreases.

The boost factors are also defined by the pressure gradient on the fuel component choke (line):

$$K_{p,\,F_{\text{г}}}=K_{p,\,F_{\text{ж}}}=K_{p,\,p_{\text{б}}}=2K_{p,\,RT}=2(1-\pi_{\text{др}});$$

$$K_{p,\,p_{\text{др}}}=\pi_{\text{др}}.$$

1.5. Pumps

1.5.1. Nonlinear Equation of the i-th Pump

The pump equation determines the relation between the pressure of the fuel component and the exit from the pump and the rpm, the flow rate, the pressure at the entrance and the geometric dimensions.

The laws of mechanics are used to derive the pump equation, neglecting the cavitation phenomena which are considered specially.

The calculated pump diagram is shown in Fig 1.13.

From the velocity triangle of the liquid on the blade of the impeller we have the expression:

$$c_u=u-w\cos\beta;\ c^2=u^2-2uw\cos\beta+w^2, \qquad (1.58)$$

where c, w are the absolute and relative velocities of the liquid in the channel between blades respectively; u is the angular velocity; c_u is the angular component of the absolute velocity.

APPROVED FOR RELEASE: 2007/02/08: CIA-RDP82-00850R000200090053-2

APPROVED FOR RELEASE: 2007/02/08: CIA-RDP82-00850R000200090053-2

The angular momentum of the liquid flowing through the channel between the blades is defined by the function

$$M_к=\int_{s_1}^{s_2} rc_u\varrho F ds=\int_{s_1}^{s_2} r(u-w\cos\beta)\varrho F ds, \tag{1.59}$$

where r is the radius of the element ds in the channel between blades; ρ is the liquid density; F is the total area of the channels between blades between the cross sections s_1 and s_2.

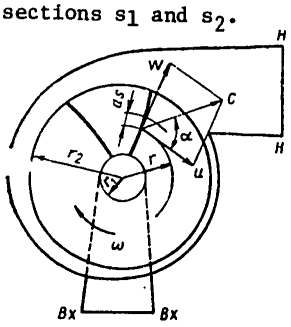

Figure 1.13. Calculated diagram of the pump

The torque applied to the impeller is defined as follows on the basis of the theorem of the variation of the momentum:

$$M=\frac{dM_к}{dt}=r(u-w\cos\beta)\varrho w|_2^1+ \\ +\int_{s_1}^{s_2} r\left(\frac{du}{dt}-\frac{dw}{dt}\cos\beta\right)\varrho F ds. \tag{1.60}$$

The first term of equation (1.60) is the static moment, and the second term is the dynamic component of the moment. The kinetic energy of the liquid in the impeller is

$$E=\iiint_V \frac{c^2}{2}dm=\frac{1}{2}\int_{s_1}^{s_2}(u^2-2uw\cos\beta+w^2)\varrho F ds.$$

The power as the derivative with respect to time of the kinetic energy, is defined by the function

$$N=\frac{dF}{dt}=\frac{1}{2}(u^2-2uw\cos\beta+w^2)|_1^2+ \\ +\int_{s_1}^{s_2}\left[u\frac{du}{dt}-\left(u\frac{dw}{dt}+w\frac{du}{dt}\right)\cos\beta+w\frac{dw}{dt}\right]\varrho F ds. \tag{1.61}$$

APPROVED FOR RELEASE: 2007/02/08: CIA-RDP82-00850R000200090053-2

APPROVED FOR RELEASE: 2007/02/08: CIA-RDP82-00850R000200090053-2

In the general case the total moment of the external forces is made up of the moment of the surface forces, the moment from the effect of the impeller on the isolated volume of liquid and the moments of the surface forces acting along the bounding surfaces s_1 and s_2 (at the entrance and exit of the impeller).

On the basis of what has been discussed and in accordance with the law of conservation of energy, it is possible to write the condition

$$N=M\omega+p_1F_1w_1-p_2F_2w_2, \tag{1.62}$$

where p_1, p_2 are the liquid pressure at the entrance and exit of the impeller; ω is the angular velocity of the impeller.

The liquid mass flow rate through the impeller is

$$\dot{m}=\varrho F w. \tag{1.63}$$

Inasmuch as

$$F_1w_1=F_2w_2=\frac{\dot{m}}{\varrho};\quad \omega=\frac{u}{r}\text{ and }\frac{u_1}{r_1}=\frac{u_2}{r_2}$$

after substitution of equations (1.60) and (1.63) in equation (1.62) we obtain the equation for the pressure difference at the entrance and exit of the impeller

$$p_2-p_1=\frac{\varrho}{2}\left[(u_2^2-w_2^2)-(u_1^2-w_1^2)\right]-\varrho\int_{s_1}^{s_2}\left(\frac{dw}{dt}-\frac{du}{dt}\cos\beta\right)ds. \tag{1.64}$$

By analogy with equation (1.64) let us write the equations for the pressure difference in the entrance and exit lines of the pump. Here it is necessary to consider the relations u=0, w=c. For the entrance line of the pump

$$p_1-p_{вх}=\frac{\varrho}{2}(c_{вх}^2-c_1^2)-\varrho\int_{s_{вх}}^{s_1}\frac{dc}{dt}ds. \quad (1)$$

Key: 1. entrance

If we consider that $c=\dot{m}/\rho F_{\text{entrance}}$, then the last equation is written in the form

$$p_1-p_{вх}=\frac{\varrho}{2}(c_{вх}^2-c_1^2)-\int_{s_{вх}}^{s_1}\frac{ds}{F}\frac{d\dot{m}}{dt}. \tag{1.65}$$

For the spiral casing and diffuser

$$p_н-p_2=\frac{\varrho}{2}(c_2^2-c_н^2)-\varrho\int_{s_2}^{s_н}\frac{dc}{dt}ds. \tag{1.66}$$

FOR OFFICIAL USE ONLY

APPROVED FOR RELEASE: 2007/02/08: CIA-RDP82-00850R000200090053-2

APPROVED FOR RELEASE: 2007/02/08: CIA-RDP82-00850R000200090053-2

Thus, the total pressure gradient created by the pump without considering the effect of the finite number of blades and travel losses is defined by the equation

$$p_н - p_{вх} = (p_н - p_2) + (p_2 - p_1) + (p_1 - p_{вх});$$

or

$$p_н - p_{вх} = \frac{\varrho}{2}\left[(c_2^2 - c_н^2) + (u_2^2 - w_2^2) - (u_1^2 - w_1^2) + (c_{вх}^2 - c_1^2)\right] -$$

$$- \varrho \int_{s_1}^{s_н} \frac{dc}{dt}\, ds - \varrho \int_{s_1}^{s_2} \left(\frac{dw}{dt} - \frac{du}{dt}\cos\beta\right) ds - \frac{d\dot{m}}{dt} \int_{s_{вх}}^{s_1} \frac{ds}{F}. \qquad (1.67)$$

In the steady-state operating mode (statistical characteristic)

$$\frac{dc}{dt} = \frac{dw}{dt} = \frac{d\dot{m}}{dt} = \frac{du}{dt} = 0,$$

the pressure gradient of the pump

$$(p_н - p_{вх})^*_{ст} = \frac{\varrho}{2}\left[(c_2^2 - c_н^2)^2 + (u_2^2 - w_2^2) - (u_1^2 - w_1^2) + (c_{вх}^2 - c_1^2)\right]. \qquad (1.68)$$

In equation (1.68) it is possible to proceed from the flow velocity to the geometric and the regime characteristics

$$c_j^2 = u_j^2 + w_j^2 - 2u_j w_j \cos\beta_j; \quad w_j \cos\beta_j = w_{ju} = \frac{w_{jz}}{\operatorname{tg}\beta_j};$$

$$w_{jz} = c_{jr} = \frac{\dot{m}}{\varrho F_j}; \quad F_j = \pi D_j b_j k_j;$$

$$k_j = 1 - \frac{z\delta_j}{\pi D_j \sin\beta_j}; \quad u_j = \frac{\pi D_j}{60} n; \quad c_н = \frac{\dot{m}}{\varrho F_н},$$

where j=1, 2 is the entrance and exit index of the impeller; n is the rpm of the impeller; D is the diameter of the impeller; b is the width of the impeller blade; δ is the blade thickness; z is the number of blades. The equation (1.68) is obtained without considering the reduction of the pressure gradient as a result of a finite number of blades and hydraulic losses in the flow section.

The pressure gradient defined by equation (1.68) is obtained under the assumption that the number of blades is infinite. In rotating circular gratings (finite number z) the angle of deflection of the flow does not coincide with the profile angle of the blades. This occurs as a result of the effect of the centrifugal forces of inertia occurring as a result of the curvature of the profile and the effect of the Coriolis forces of inertia. The greater the density of the gratings (the greater z), the less will be the difference in direction of the flow from the blade profile. The sparser the grating (the smaller z), the greater the deflection of the flow.

APPROVED FOR RELEASE: 2007/02/08: CIA-RDP82-00850R000200090053-2

APPROVED FOR RELEASE: 2007/02/08: CIA-RDP82-00850R000200090053-2

As a result, the pressure gradient of the pump with a finite number of blades $(p_{pump}-p_{inp})_{st}$ will be greater than $(p_{pump}-p_{inp})^{*}_{st}$ for $z=\infty$.

The ratio $(p_{pump}-p_{inp})_{st}/(p_{pump}-p_{inp})^{*}_{st}=q_{blade}$ is called the finite number of blades factor.

The value of q_{blade} depends on the number of blades, the ratio of D_1/D_2 and the angles of setting of the blades.

The analytical relation between q_{blade} and the indicated parameters is defined complexly. For the pumps used in the liquid-fuel rocket engines, $q_{blade}=0.75-0.9$.

In addition, the effective pressure gradient in the pump is less than that defined by formula (1.68) as a result of the pressure losses to overcome the hydraulic drag in the entrance tube, in the impeller and the diffuser. These losses can be approximately considered by the function

$$\Delta p_{\text{г}}=\frac{\xi}{Q}\dot{m}^2,$$

where ξ -- the coefficient of hydraulic losses -- is determined experimentally.

After considering the indicated losses and the transformations, the static characteristic (1.68) assumes the form

$$(p_{\text{н}}-p_{\text{вх}})_{\text{ст}}=AQn^2-Bn\dot{m}-c\dot{m}^2, \tag{1.69}$$

where

$$A=q_{\text{л}}\left(\frac{\pi}{60}\right)^2 D_2^2\left(1-\frac{D_1^2}{D_2^2}\right);$$

$$B=\frac{q_{\text{л}}}{60}\left(\frac{1}{b_2k_2\operatorname{tg}\beta_2}-\frac{1}{b_1k_1\operatorname{tg}\beta}\right);$$

$$C=\xi+0{,}5q_{\text{л}}\left(\frac{1}{F_{\text{н}}^2}-\frac{1}{F_{\text{вх}}^2}\right).$$

In order to determine the dynamic components of the pressure gradient during operation of the pump in the steady-state mode it is necessary to consider the dropped terms in the equation (1.67)

$$I_1=Q\int_{s_3}^{s_{\text{н}}}\frac{dc}{dt}ds=(D_{\text{с}}+D_{\text{л}})\frac{d\dot{m}}{dt}, \tag{1.70}$$

where

$$D_{\text{с}}=\int_{s_3}^{s_3}\frac{ds}{F}\simeq\frac{S_{\text{с}}}{F_{\text{сш}}};\quad D_{\text{л}}=\int_{s_3}^{s_{\text{н}}}\frac{ds}{F}=\frac{S_{\text{л}}}{F_{\text{л}}},$$

(1)

Key: 1. spiral casing

FOR OFFICIAL USE ONLY

APPROVED FOR RELEASE: 2007/02/08: CIA-RDP82-00850R000200090053-2

APPROVED FOR RELEASE: 2007/02/08: CIA-RDP82-00850R000200090053-2

S_c, S_d are the length of the midline of the spiral casing and the diffuser; F_{sp}, F_d are the average area of the through cross section of the spiral casing and the diffuser.

$$I_2=\varrho\int_{s_1}^{s_2}\left(\frac{dw}{dt}-\frac{du}{dt}\right)\cos\beta ds=\varrho\int_{s_1}^{s_2}\frac{dw}{dt}\cos\beta ds-\varrho\int_{s_1}^{s_2}\frac{du}{dt}\cos\beta ds.$$

If we make the substitution of variables

$$w=\frac{\dot m}{\varrho F\sin\beta};\quad u=\frac{\pi D_n}{60};\quad F=\pi Dbk,$$

then the last equation is rewritten in the form

$$I_2=D_к\frac{d\dot m}{dt}-E\frac{dn}{dt},\tag{1.71}$$

where

$$D_к=\int_{s_1}^{s_2}\frac{ds}{F\sin\beta};\quad E=\frac{\pi\varrho}{60}\int_{s_1}^{s_2}D\cos\beta ds.$$

These integrals can be defined by numerical integration with respect to sections of the midline or approximately

$$D_к=\int_{s_1}^{s_2}\frac{ds}{F\sin\beta}=\sum_{j=1}^{l}\frac{\Delta S_j}{F_j\sin\beta_j};$$

$$E=\frac{\pi\varrho}{60}\int_{s_1}^{s_2}D\cos\beta ds=\frac{\pi\varrho}{60}\sum_{j=1}^{l}D_j\cos\beta_j\Delta S_j,$$

where ℓ is the number of sections

$$I_3=D_п\frac{d\dot m}{dt},\tag{1.72}$$

where

$$D_п=\int_{s_{вх}}^{s_1}\frac{ds}{F_п}=\frac{s_п}{F_{п.ср}}.$$

After the substitution of the equations (1.70)-(1.72) in (1.67) we obtain the nonlinear equation of the pressure created by the pump in the steady-state operating mode

$$p_п(t)=p_{вх}(t)+A\varrho n^2(t)-Bn(t)\dot m(t)-c\dot m^2(t)-$$
$$-D\frac{d\dot m(t)}{dt}-E\frac{dn(t)}{dt};\quad D=D_c+D_л+D_к+D_п,\tag{1.73}$$

where the coefficients E and D depend on the geometric dimensions and the profile of the flow section of the pumps. With an increase in the overall dimensions of the pumps the coefficients E and D increase.

APPROVED FOR RELEASE: 2007/02/08: CIA-RDP82-00850R000200090053-2

APPROVED FOR RELEASE: 2007/02/08: CIA-RDP82-00850R000200090053-2

The coefficients E and D determine the inertial components of the head with respect to the flow rate and the rpm. The values of the coefficients E and D are much less than the values of the coefficients A, B, C; dn/dt and dṁ/dt are the input signals for the pump; they are given by the operation of the turbine and the lines.

The value of $p_H(t)$ is calculated when starting one of the engines [6], where dn/dt and dṁ/dt have maximum values.

In Fig 1.14 we have the results of the calculation which indicate that even in the start mode consideration of the dynamic components dn/dt and dṁ/dt has an insignificant effect on the accuracy of the calculation; therefore it is possible to neglect the last terms in equation (1.73).

The moment of the pump can be defined by the function (1.60) or by the theorem of the angular momentum with respect to the axis of rotation

$$M_н = \int_{F_2} (c_u r)_2 \, d\dot{m} - \int_{F_1} (c_u r)_1 \, d\dot{m} + \int_V \frac{d(c_u r)}{dt} dV + M_1, \qquad (1.74)$$

where F_1, F_2 are the bounding surfaces; $(c_u r)_1$ and $(c_u r)_2$ are the velocity moments at the entrance and exit of the impeller; M_1 is the moment of the tangential forces caused by liquid friction; this moment will be neglected hereafter; $\int_V \frac{d(c_u r)}{dt} dV$ is the variation of the angular momentum inside the flow section.

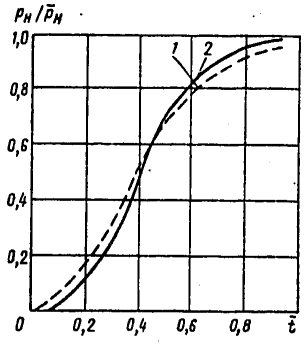

Figure 1.14. Effect of the inertial components on the pump head: 1 -- dn/dt=dṁ/dt=0; 2 -- considering dm/dt and dṁ/dt

Considering the nonsteady-state nature of the absolute motion in the impeller we find the mean mass value of the moment of the angular component of the velocity

$$\bar{c}_u r = \frac{\int_F (c_u r) \, d\dot{m}}{\dot{m}}. \qquad (1.75)$$

FOR OFFICIAL USE ONLY

APPROVED FOR RELEASE: 2007/02/08: CIA-RDP82-00850R000200090053-2

APPROVED FOR RELEASE: 2007/02/08: CIA-RDP82-00850R000200090053-2

Considering the function (1.75) the first two integrals in equation (1.74) assume the form

$$\int_{\dot{F}_2}(c_u r)_2\,d\dot{m}-\int_{\dot{F}_1}(c_u r_1)\,d\dot{m}=\dot{m}\left[(\overline{c_u r})_2-(\overline{c_u r})_1\right]. \tag{1.76}$$

The elementary volume of the flow section and the angular component of the velocity are defined as follows:

$$dV=2\pi r b dr,\quad c_u=u-\frac{\alpha}{r}\dot{m}, \tag{1.77}$$

where $$\alpha=\frac{1}{\pi b\varrho k\,\mathrm{tg}\,\beta}.$$

The geometric dimensions b and β depend on the radius, but without making large error these values will be assumed constant and equal to the mean values.

Since u=πDn/60 and dr/dt=0, considering the functions (1.77) the last integral equation (1.74) is defined as follows:

$$\int_{\dot{V}}\frac{d(c_u r)}{dt}dV=\frac{\pi^2}{30}b_{cp}\left(r_2^4-r_1^4\right)\frac{dn}{dt}-2\pi b_{cp}\alpha_{cp}\left(r_2^2-r_1^2\right)\frac{d\dot{m}}{dt}. \tag{1.78}$$

Substituting the functions (1.77-1.78) in the initial equation (1.74) we finally obtain

$$M_{\text{н}}=a_1 n\dot{m}-a_2\dot{m}^2+a_3\frac{dn}{dt}-a_4\frac{d\dot{m}}{dt}, \tag{1.79}$$

where $$a_1=\frac{\pi}{30}\left(r_2^2-r_1^2\right);\quad a_2=\alpha_2-\alpha_1;$$

$$a_3=\frac{\pi^2}{30}b_{cp}\left(r_2^4-r_1^4\right);\quad a_4=\frac{2}{\varrho k_{cp}\,\mathrm{tg}\,\beta_{cp}}.$$

The power intake by the pump is defined as the product of the moment times the rpm $N_H=M_H\omega$. In the equations (1.78-1.79) the coefficients a_1, a_2, a_3 and a_4 define the inertial components of the head and the moment with respect to the mass flow rate and rpm, and they depend on the configuration and the dimensions of the flow section of the pump, and with respect to magnitude they are appreciably less than the coefficient of the static components.

1.5.2. Linear Equation of Pumps

The linear equation of the pump is obtained from the function (1.73) after linearization in the vicinity of the steady-state conditions

$$\delta p_{\text{н}}(t)=K_{p_{\text{н}},n}\delta n(t)-K_{p_{\text{н}},\dot{m}}\delta\dot{m}(t)+K_{p_{\text{н}},p_{\text{вх}}}\delta p_{\text{вх}}(t), \tag{1.80}$$
(1)

Key: 1. inp

APPROVED FOR RELEASE: 2007/02/08: CIA-RDP82-00850R000200090053-2

APPROVED FOR RELEASE: 2007/02/08: CIA-RDP82-00850R000200090053-2

where $K_{p_{H,x}}$ are the boost factors;

$$K_{p_H, n}=\frac{2A\bar{Q}\bar{n}^2-B\bar{n}\bar{\dot{m}}}{\bar{p}_H};$$

$$K_{p_H, \dot{m}}=-\frac{B\bar{n}\bar{\dot{m}}+\frac{2\bar{c}\bar{\dot{m}}^2}{\bar{Q}}}{\bar{p}};\quad K_{p_H, p_{BX}}=\frac{\bar{p}_{BX}}{\bar{p}_H}.$$

In the vicinity of the steady-state mode the term $c\dot{m}^2/\rho$ defining the losses in the pump can be neglected. In this case

$$p_H=AQn^2-Bn\dot{m}. \tag{1.81}$$

The influence factors are approximately defined by the expressions

$$K_{p_H, n}=\frac{1}{1-\frac{B\bar{\dot{m}}}{A\bar{Q}\bar{n}}}+1;$$

since $\frac{B\bar{\dot{m}}}{A\bar{Q}\bar{n}}\ll 1$, then for approximate analysis it is possible to set $K_{pH^n}=2$.

$$K_{p_H, \dot{m}}=-\frac{1}{\frac{A\bar{Q}\bar{n}}{B\dot{m}}-1}.$$

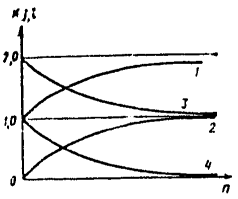

Figure 1.15. Boost factor of the pump as a function of the rpm:

1 – $K_{p_H, n}$; 2 – $K_{M,n}$; 3 – $K_{p_H, \dot{m}}$; 4 – $K_{M, \dot{m}}$

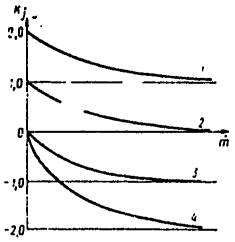

Figure 1.16. Boost factor of the pump as a function of flow rate:

1 – $K_{p_H, n}$; 2 – $K_{M,n}$; 3 – $K_{p_H, \dot{m}}$; 4 – $K_{M, \dot{m}}$

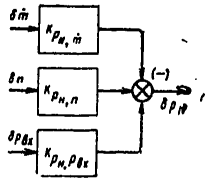

Figure 1.17. Structural diagram of the pump

APPROVED FOR RELEASE: 2007/02/08: CIA-RDP82-00850R000200090053-2

APPROVED FOR RELEASE: 2007/02/08: CIA-RDP82-00850R000200090053-2

The boost factors $K_{P_H,x}$ depend on the rpm and the flow rate. The equation of the moment of the pump has the form

$$\delta M_н(t)=K_{M_н,n}\delta n(t)-K_{M_н,\dot{m}}\delta\dot{m}(t), \tag{1.82}$$

where

$$K_{M_н,n}=\frac{1}{1-\frac{a_2\bar{m}}{a_1\bar{n}}};$$

$$K_{M_н,\dot{m}}=1-\frac{1}{\frac{a_1\bar{n}}{a_2\bar{m}}-1}.$$

The functions $K_{M_н,x}=f_1(n,\dot{m})$ and $K_{p_н,x}=f_2(n,\dot{m})$ are shown in Figures 1.15 and 1.16.

In the Laplace transforms, the pump equations are written in the form

$$\delta p_н(s)=K_{p_н,n}\delta n(s)+K_{p_н,p_{вх}}\delta p_{вх}(s)-K_{p_н,\dot{m}}\delta\dot{m}(s); \tag{1.83}$$
$$\delta M_н(s)=K_{M_н,n}\delta n(s)-K_{M_н,\dot{m}}\delta\dot{m}(s).$$

Thus, the pump is a set of booster elements, the structural diagram of which is presented in Fig 1.17.

1.5.3. Effect of Cavitation on the Pump Characteristic

In the volute centrifugal pumps, the cavitation phenomenon is observed which consists in the formation of a break in continuity of the flow of the moving liquid. The breaks in continuity of the flow (the cavitation cavities) occur in sections where a pressure drop below the saturated vapor pressure of the liquid occurs. The presence of dissolved and free gases in the liquid has a significant effect on the development of cavitation. They are released in the reduced pressure zones and lower the specific strength of the liquid.

Cavitation occurs in the pump with a pressure at its input significantly exceeding the saturated vapor pressure. This means that the region of minimum pressure is located inside the flow section and is connected with streamlining around the entrance edges of the blades.

In volute pumps the cavitation cavities occur on the outside diameter of the entrance edges of the blades.

APPROVED FOR RELEASE: 2007/02/08: CIA-RDP82-00850R000200090053-2

APPROVED FOR RELEASE: 2007/02/08: CIA-RDP82-00850R000200090053-2

The cavitation in the pump channels between blades is a flow of liquid with a set of moving cavities. The process of cavitation in the pumps is very complicated; therefore when investigating the dynamic characteristics, the actual process of movement of a two-phase medium is replaced by an idealized model of movement of a homogeneous liquid.

Significant studies of the cavitation phenomena in pumps have been performed by V. V. Pilipenko, M. S. Natanzon [11]. In accordance with the studies of the mentioned authors it is proposed that the saturation of the liquid with vapor phase takes place at the entrance to the pumps, and further movement of the medium in the flow section continues without variation of the vapor content of the mixture. On exiting from the pump instantaneous condensation of the vapor phase and a change in density in the medium are proposed; the appearance of vapor included in the liquid is accompanied by a sharp decrease in the speed of sound.

Therefore the changes in pressure and velocity of the flow at the exit from the pump are transmitted to its input with the speeds of sound equal to the differences of the undisturbed speeds of sound a_{10} and a_{20} and the speeds of movement of the media c_{10} and c_{20}.

The transmission time of these disturbances in the flow section of the pump is determined from the expression

$$\tau^* = \frac{l}{a_{20} - a_{10}},$$

where ℓ is the characteristic length of the flow section of the pump. For the pump, beginning with the nature of the cavitation flow of the liquid, the equation of the continuity of flow is written in the form

$$V_{\text{н}} \frac{d\rho}{dt} = \rho_{\text{ж}} [F_1 c_{\text{вх}}(t) - F_2 c_{\text{вых}}(t - \tau^*)], \qquad (1.84)$$

Key: 1. inp; 2. out (1) (2)

were c_{inp}, c_{out} are the flow velocities at the entrance and exit of the pump; F_1, F_2 are the areas of the through cross sections of the delivery and force mains connected to the pump; ρ is the average density of the vapor-liquid medium which is found by the expression

$$\rho = \frac{\rho_{\text{ж}}^{(1)} + \rho_{\text{п}}^{(2)} \vartheta(t)}{1 + \nu(t)}, \qquad (1.85)$$

Key: 1. liquid; 2. vapor

where ν is the ratio of the vapor and liquid volumes per unit mass of the vapor-liquid mixture.

In the first approximation the function $\nu(t)$ can be defined as follows:

APPROVED FOR RELEASE: 2007/02/08: CIA-RDP82-00850R000200090053-2

APPROVED FOR RELEASE: 2007/02/08: CIA-RDP82-00850R000200090053-2

$$\nu(t)=\nu^*\frac{h_{кр1}}{h_2(t)};$$

$$h_2(t)=\frac{p_1(t)}{\rho}+\frac{c_{вх}^2}{2},$$

where $h_{cr\ 1}$ is the minimum required energy of the flow in front of the entrance to the pump, insuring continuous operation of it; ν^* is the magnitude of the critical vapor content.

$$\nu^*=\frac{\rho_п a_п^2}{\rho_ж c^2}, \quad (1)$$

Key: 1. vapor; 2. liquid (2)

where $\rho_{vapor\ 1}$, a_{vapor} are the density and speed of sound of the vapor phase.

After linearization of equations (1.84 and 1.85) and representation of them in operator form we obtain

$$\begin{gathered} T_н sQ=K_1 c_{вх}-K_2 e^{-s\tau^*}c_{вых}; \\ Q=K_3\nu;\ \nu=K_4 h, \\ h_1=K_5 p_1+c_{вх}, \end{gathered} \quad (1.86)$$

where $T_н=V_н;\ K_1=F_1\rho_ж;\ K_2=F_2\rho_ж;\ K_3=\frac{\rho_п-\rho_ж}{(1+\nu)^2};$

$$K_4=-\frac{\nu^* h_{кр1}}{h_1^2};\quad K_5=\frac{1}{\rho}.$$

If we neglect the inertia of the pump caused by the vapor inclusions, which is admissible for the low-frequency range (0-20 hertz), we obtain the equation of cavitation

$$K_1 c_{вх}=K_2 e^{-s\tau^*}c_{вых}.$$

Without considering cavitation the pump equation has the form

$$\frac{p_1}{\rho_ж}+\frac{c_{вх}^2}{2}+H(p_1, c_2, n)=\frac{p_2}{\rho_ж}+\frac{c_{вых}^2}{2},$$

where $H(p_1, c_2, n)$ is the head created by the pump,

$$H=an^2-bnc_{вых}.$$

APPROVED FOR RELEASE: 2007/02/08: CIA-RDP82-00850R000200090053-2

APPROVED FOR RELEASE: 2007/02/08: CIA-RDP82-00850R000200090053-2

After linearization, equation (1.86) is written as follows:

$$K_5 p_1 + c_{вх} + K_6 n - K_7 c_{вых} = K_5 p_2 + c_{вых}. \qquad (1.87)$$

For analysis of the dynamic interrelation between the pump and the lines it is necessary to have boundary conditions which determine the conjugation of them.

The relations between the disturbances of the pressure and the disturbances of the velocity of the flow $Z=p(x,t)/c(x,t)$ which are called the boundary impedance, are taken as such boundary conditions. In the general case the impedance can be a complex number. In this case the real part of it characterizes the active resistance, and the imaginary part, the reactance, which occurs as a result of the presence on the ends of the liquid flow of concentrated elasticities (bellows, volumes of vapor-gas mixture).

The pump is installed at the output of the delivery main and the input of the force main. Therefore for investigation of the dynamic interrelations of the pumps with the mains, the boundary impedance of the entrance to the pump which determines the effect of the pump on the delivery main and the boundary impedance of the engine which is the boundary condition of the coupling of the pump to the force mains, must be determined.

Let us consider the effect of cavitation on the input impedance of the pump $Z_H=p_1(x)/c_{inp}(x)$.

Without considering cavitation Z_H' is determined from the equation

$$Z_н' = \frac{F_1}{F_2}\left(1 + Z_д + \frac{\partial H}{\partial c_{вых}} Q_ж\right) - Q_ж, \qquad (1.88)$$

where $Z_d=p_{out}(x)/c_{out}(x)$ is the input impedance of the pump, which is the load impedance from the engine on the pump. Thus, the impedance of the pump without cavitation is a real number; consequently the pump is an active resistance for the line and does not change its frequency characteristics.

The pump impedance considering cavitation is determined from the equation (1.86)

$$Z_н = \frac{F_1}{F_2}\left(\frac{\partial H}{\partial c_{вых}} Q_ж + Z_д + 1\right) e^{s\tau^*} - Q_ж.$$

If we carry out the substitution $s=j\omega$, then we obtain

$$Z_н = \frac{F_1}{F_2}\left(\frac{\partial H}{\partial c_{вых}} Q_ж + Z_д + 1\right) e^{j\omega\tau^*} - Q_ж. \qquad (1.89)$$

APPROVED FOR RELEASE: 2007/02/08: CIA-RDP82-00850R000200090053-2

APPROVED FOR RELEASE: 2007/02/08: CIA-RDP82-00850R000200090053-2

Thus, considering the cavitation, the pump is an active resistance and reactance, and it changes the frequency characteristics of the system. Let us consider the dynamic characteristics of the system (delivery main plus the pump) (Fig 1.18).

The relations between the deviations of the pressures and the flow velocities at the entrance to the tube $p_1=p(\ell)$; $v_1=v(\ell)$ and the exit from the tube $p_2=p(0)$; $v_2 \neq v(0)$ during the vibrations are defined by the equations

$$\begin{aligned} c_2 &= c_1 ch k + p_1 \frac{1}{\rho a_0} sh k; \\ p_2 &= \rho a_0 c_1 sh k + p_1 ch k, \end{aligned} \tag{1.90}$$

where $k=\frac{j\omega l}{a_0}$; $a_0=\frac{a}{\sqrt{1+\frac{2\rho a^2 r}{E\delta}}}$;

a_0 is the speed of sound in the liquid; E is the modulus of elasticity of the tube material; δ, r are the wall thickness and tube radius.

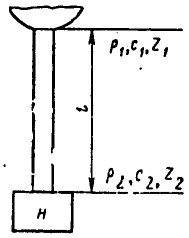

Figure 1.18. Line diagram

The boundary conditions at the entrance to the tube (x=ℓ)

$$p_1 = -Z_{\text{(1)}} c_1, \tag{1.91}$$

Key: 1. tank

where $Z_{tank}=Z_1$ is the boundary impedance at the entrance to the tube.

If the main ends in the tank open-ended, then it can be considered acoustically open, and in this case $Z_{tank}=0$. If bellows or hydraulic drags in the form of gratings or flow plates which change the flow velocity are installed in the tank, then $Z_{tank}=a+bj\omega$, that is, the impedance includes both the resistance and reactance.

The boundary condition at the exit from the line (x=0) is defined by the properties of the pump

$$p_2 = Z_{\text{н}} c_2, \tag{1.92}$$

APPROVED FOR RELEASE: 2007/02/08: CIA-RDP82-00850R000200090053-2

APPROVED FOR RELEASE: 2007/02/08: CIA-RDP82-00850R000200090053-2

where $Z_{H}=Z_2$ is the pump impedance defined by the expression (1.89).

Substituting expressions (1.91, 1.92) in equation (1.90), we obtain the characteristic equations of the system

$$\varphi=e^{2k}=\varphi_1\varphi_2, \tag{1.93}$$

where

$$\varphi_1=\frac{Z_6-Z_0}{Z_6+Z_0};\quad \varphi_2=\frac{Z_H-Z_0}{Z_H+Z_0};\quad Z_0=\varrho a_0.$$

Using the exponential form of the complex number, let us write the value of ϕ in the form

$$\varphi=r_6r_H e^{j(\theta_1+\theta_2)}, \tag{1.94}$$

where

$$r_6=\sqrt{\frac{[P(Z_6)-Z_0]^2+[Q(Z_6)]^2}{[p(Z_6)+Z_0]^2+[Q(Z_6)]^2}};$$
$$r_H=\sqrt{\frac{[P(Z_H)-Z_0]^2+[Q(Z_H)]^2}{[P(Z_H)+Z_0]^2+[Q(Z_H)]^2}}.$$

The phase θ_1 and θ_2 of the complex number ϕ is defined as follows:

$$Q_l=\operatorname{arctg}\frac{Q(Z_l)}{P(Z_l)},$$

where P(Z) and Q(Z) are the real and imaginary parts. If equation (1.93) is written in trigonometric form considering (1.94) and we equate the real and imaginary parts to 0 separately, then we obtain the known formulas for the damping coefficient and the frequency of the natural vibrations

$$\xi=\frac{a_0}{2l}\ln r_1r_2;$$
$$\omega=\frac{a_0}{2l}(\theta_1+\theta_2+2\pi n),\ n=\overline{0,\ N}. \tag{1.95}$$

If the main is open on both ends, then $Z_{\text{tank}}=Z_{\text{pump}}=0$,

$$\varphi=1 \text{ and } \xi=0,\ \omega=\frac{\pi n a_0}{l}.$$

If the main is connected to the pump in which cavitation occurs, and the entrance is acoustically open ($Z_{\text{tank}}=0$), then

$$Z_{H}=A\cos\omega\tau^*+jA\sin\omega\tau^*. \tag{1.96}$$
(1)

Key: 1. pump

FOR OFFICIAL USE ONLY

APPROVED FOR RELEASE: 2007/02/08: CIA-RDP82-00850R000200090053-2

APPROVED FOR RELEASE: 2007/02/08: CIA-RDP82-00850R000200090053-2

From the equations (1.94-1.96) it follows that the pump in which the cavitation exists can both reduce and increase the frequencies of the natural vibrations of the main. Thus, if $\pi<\omega\tau^*\leqslant 2\pi$, then the pump lowers the natural vibration frequency of the main ω; if $0<\omega\tau^*<\pi$, then it increases it. If $P(Z_{pump})<0$, then $Z_{pump}<1$. In this case $r_1 r_2$ can be greater than 1 and $\xi>0$, that is, the vibrations of the main become stable.

1.6. Turbine

The turbine torque and power are related by the expression

$$M_т=\frac{30}{\pi}\frac{N_т}{n}$$

and they depend on the regime parameters of the turbine-pump assembly and the gas generator.

The turbine power

$$N_т=\dot{m}_т L_a \eta_т, \tag{1.97}$$

where $\dot{m}_T$ is the gas flow rate through the turbine.

The adiabatic work of expansion of the gas in the turbine

$$L_a=\frac{\varkappa}{\varkappa-1}RT_т\left[1-\left(\frac{p_{2т}}{p_{гг}}\right)^{\frac{\varkappa-1}{\varkappa}}\right], \tag{1.98}$$

where p_{2T} is the gas pressure after the turbine; RT_T is the fitness of the gases at the input to the turbine guide vane, which depends on the ratio fuel components in the gas generator K'. The turbine efficiency depends on its characteristics and basically on u/c_a [10]:

$$\eta_т=b_2\left(\frac{u}{c_a}\right)^2+b_1\left(\frac{u}{c_a}\right)+b_0, \tag{1.99}$$

where u is the angular velocity of the rotor; c_a is the adiabatic escape velocity

$$c_a=\sqrt{RT_т\left[1-\left(\frac{p_{2т}}{p_{гг}}\right)^{\frac{\varkappa-1}{\varkappa}}\right]} \tag{1.100}$$

or

$$c_a=\sqrt{2L_a}.$$

APPROVED FOR RELEASE: 2007/02/08: CIA-RDP82-00850R000200090053-2

APPROVED FOR RELEASE: 2007/02/08: CIA-RDP82-00850R000200090053-2

The mass flow rate through the turbine in the general case depends on the gradient on the turbine, that is,

$$\dot{m}_т = f\left(\frac{p_{1т}}{p_{2т}}\right).$$

From the presented expressions it follows that the turbine torque depends on the following parameters

$$M_т = M(p_{гг},\ p_{1т},\ p_{2т},\ n,\ K').$$

Active Turbine

The supercritical escape regime is characteristic for an active turbine; consequently

$$p_{1т} = p_{2т};\quad \frac{p_{1т}}{p_{гг}} = \left(\frac{2}{\varkappa+1}\right)^{\frac{\varkappa}{\varkappa-1}}$$

and

$$M_т = M(p_{гг},\ K',\ n). \tag{1.101}$$

Let us consider the single-stage active turbine.

The torque

$$M_т = P_u \frac{d_т}{2}, \tag{1.102}$$

where d_T is the average diameter of the turbine rotor; P_u is the circumferential force created by the gases. In accordance with the theorem of the variation of momentum of the gases in the channel between blades, the circumferential force is defined by

$$P_u = \dot{m}_т(c_1 \cos\alpha_1 + c_2 \cos\alpha_2).$$

From the velocity triangle

$$c_2 \cos\alpha_2 = w_2 \cos\beta_2 - u;\quad w_2 = \psi w_1;$$
$$w_1 = \frac{c_1 \cos\alpha_1 - u}{\cos\beta_1},$$
ψ -- the relative velocity loss coefficient,
$$u = \frac{\pi d_т n}{60}.$$

Considering these expressions, the circumferential force of the gases

$$P_u = \varphi_т \dot{m}_т \left\{\left[1 + \psi\frac{\cos\beta_2}{\cos\beta_1}\right] c_1 \cos\alpha_1 - \left[1 + \psi\frac{\cos\beta_2}{\cos\beta_1}\right]\frac{\pi d_т}{60} n\right\}, \tag{1.103}$$

FOR OFFICIAL USE ONLY

APPROVED FOR RELEASE: 2007/02/08: CIA-RDP82-00850R000200090053-2

APPROVED FOR RELEASE: 2007/02/08: CIA-RDP82-00850R000200090053-2

where ϕ_T is the energy loss coefficient of the gas flow in the flow section of the turbine, ϕ_T=0.85-0.95. Since for an active turbine $\frac{p_{1T}}{p_{TT}}=\frac{\bar{p}_{1T}}{\bar{p}_{TT}}$, then the flow rate of the working medium $\dot{m}_T$ and the velocity c_1 are defined by the expression

$$\dot{m}_T=\frac{\bar{m}_T\sqrt{\overline{RT}_T}}{\bar{p}_{TT}}\frac{p_{TT}}{\sqrt{RT_T}};\quad c_1=\frac{\bar{c}_1}{\sqrt{\overline{RT}_T}}\sqrt{RT_T}. \tag{1.104}$$

Substituting (1.103-1.104) in (1.102), we finally obtain

$$M_T=p_{TT}\left(r_1-\frac{r_2}{\sqrt{RT}}n\right),$$
$$N_T=p_{TT}n\left(m_1-\frac{m_2}{\sqrt{RT}}n\right), \tag{1.105}$$

where

$$r_1=\frac{\varphi_T d_T\bar{m}_T\bar{c}_1\cos\alpha_1}{2\bar{p}_{TT}}\left(1+\psi\frac{\cos\beta_2}{\cos\beta_1}\right);$$
$$r_2=\frac{\varphi_T\pi d_1^2\bar{m}_T\sqrt{\overline{RT}_T}}{120\bar{p}_{TT}}\left(1+\psi\frac{\cos\beta_2}{\cos\beta_1}\right);$$
$$m_1=\frac{\varphi_T\pi d_1\bar{c}_1\bar{m}_T\cos\alpha_1}{60\bar{p}_{TT}}\left(1+\psi\frac{\cos\beta_2}{\cos\beta_1}\right);$$
$$m_2=\frac{\varphi_T\pi^2 d_1^2\bar{m}_T\sqrt{\overline{RT}_T}}{3600\bar{p}_{TT}}\left(1+\psi\frac{\cos\beta_2}{\cos\beta_1}\right);$$
$$RT=f(K'(t-\tau_{mp}).$$

For a two-stage turbine

$$M_T=\varphi_T p_{TT}\left(a_{T_1}\sqrt{RT_T}-a_{T_2}n+a_{1_3}\dot{m}_T-a_{T_4}\frac{\dot{m}_T n}{n+a_{T_5}\dot{m}_T}\right). \tag{1.106}$$

Jet Turbine

In engines with afterburning of the generator gas, jet turbines are used with subcritical escape regime.

The initial relations for determining the moment of the turbine are the equation of moment of the turbine (1.97), the power, the adiabatic work (1.98) and the efficiency (1.89).

For the jet turbine $p_{1T}\neq p_{2T}$ and the pressure gradient on the turbine depends on the degree of reactivity

$$\left(\frac{p_{1T}}{p_{TT}}\right)^{\frac{k-1}{k}}=Q+(1-Q)\left(\frac{p_{2T}}{p_{TT}}\right)^{\frac{k}{k-1}}, \tag{1.107}$$

APPROVED FOR RELEASE: 2007/02/08: CIA-RDP82-00850R000200090053-2

APPROVED FOR RELEASE: 2007/02/08: CIA-RDP82-00850R000200090053-2

FOR OFFICIAL USE ONLY

where ρ is the degree of reactivity of the turbine. For the subcritical escape regime the flow rate through the turbine is defined by the function

$$\dot{m}_т = \sqrt{\frac{2\varkappa}{\varkappa-1}\frac{p_{гг}^2}{RT_т}\left[\left(\frac{p_{1т}}{p_{гг}}\right)^{\frac{2}{\varkappa}} - \left(\frac{p_{1т}}{p_{гг}}\right)^{\frac{\varkappa+1}{\varkappa}}\right]}. \tag{1.108}$$

From the functions (1.105-1.108) it follows that

$$M_т = M(p_{гг},\ p_{2т},\ p_{1т},\ n,\ K').$$

After linearization of the equations (1.97-1.98; 1.107-1.108) we obtain

$$\begin{aligned}
&\delta M_т = \delta N_т - \delta n;\\
&\delta N_т = \delta \dot{m}_т + \delta L_a + \delta \eta_т;\\
&\delta L_a = 2\delta c_a = \delta RT_т + a_L \delta p_{гг} - a_L \delta p_{2т};\\
&\delta \dot{m}_т = \delta p_{гг} - 0{,}5\delta RT_т + a_{\dot{m}} \delta p_{1т} - a_{\dot{m}} \delta p_{гг};\\
&\delta \eta_т = a_\eta (\delta n - \delta c_a);\\
&\delta p_{1т} = a_{p_{2т}} \delta p_{2т} - a_{p_{гг}} \delta p_{гг},
\end{aligned} \tag{1.109}$$

where

$$a_L = \frac{(\varkappa-1)\pi_т^{\frac{\varkappa-1}{\varkappa}}}{2\varkappa\left[1-\pi_т^{\frac{\varkappa-1}{\varkappa}}\right]};\quad \pi_т = \frac{p_{2т}}{p_{гг}};$$

$$a_{\dot{m}} = \frac{2\pi_c^{\frac{2}{\varkappa}} - (\varkappa+1)\pi_c^{\frac{\varkappa+1}{\varkappa}}}{2\varkappa\left(\pi_c^{\frac{2}{\varkappa}} - \pi_c^{\frac{\varkappa+1}{\varkappa}}\right)};\quad \pi_c = \frac{p_{1т}}{p_{гг}};$$

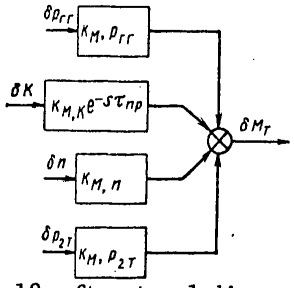

$$a_\eta = \frac{\bar{u}}{\bar{c}_a}\left(\frac{2a_2\frac{\bar{u}}{\bar{c}_a} + a_1}{\bar{\eta}_т}\right);$$

$$a_{p_{2т}}^{\text{ву}} = (1-Q)\frac{\pi_т^{\frac{\varkappa-1}{\varkappa}}}{\pi_c^{\frac{\varkappa-1}{\varkappa}}};\quad a_{p_{гг}} = Q\pi_c^{-\frac{1}{\varkappa}}.$$

Figure 1.19. Structural diagram of the turbine moment

Solving equations (1.109) jointly, we obtain the linear equation of the turbine moment

$$\begin{aligned}
\delta M_т(s) = K_{M_т,\ p_{гг}}\delta p_{гг}(s) + K_{M_т,\ p_{2т}}\delta p_{2т}(s) + K_{M_т,n}\delta n(s) +\\
+ K_{M_т,K}e^{-s\tau_{пр}}\delta K(s),
\end{aligned} \tag{1.110}$$

FOR OFFICIAL USE ONLY

APPROVED FOR RELEASE: 2007/02/08: CIA-RDP82-00850R000200090053-2

APPROVED FOR RELEASE: 2007/02/08: CIA-RDP82-00850R000200090053-2

where

$$K_{M_T,\rho_{T\Gamma}}=1+a_m(a_{\rho_{T\Gamma}}-1)+a_L(1-0{,}5a_\eta);$$
$$K_{M_T,\rho_{2T}}=a_m a_{\rho_{2T}}-a_L(1-0{,}5a_\eta);$$
$$K_{M_{T1}K'}=0{,}5(1-a_\eta)\frac{\bar{K}}{R\bar{T}_T};\quad K_{M_{T1}\eta}=a_\eta-1.$$

The structural diagram of the turbine moment is shown in Fig 1.19.

1.7. Turbine Pump Assembly (TNA)

1.7.1. TNA [Turbine Pump Assembly] Impeller Equation

In order to investigate the dynamics of the turbine pump assembly, a study is made of the movement of the impeller made up of a shaft, the turbine rotor and the pump impeller. The derivative of the angular momentum of the TNA impeller with respect to the stationary axis is equal to the moment of the external forces applied to the impeller.

The angular moment with respect to the impeller axis is

$$K=J\frac{\pi n}{30}, \tag{1.11}$$

where J is the moment of inertia.

The moment of inertia with respect to the axis of rotation is defined in general form

$$J=\iiint_{V_p}\rho_p(x^2+y^2)\,dx\,dy\,dz+\iiint_{V_ж}\rho_ж(x^2+y^2)\,dx\,dy\,dz.$$

The first integral is the moment of inertia of the impeller material, and the second integral, the moment of inertia of the liquid filling the flow section of the pumps. The Z-axis is directed along the axis of rotation. The moment of inertia of the impeller material is found by the configuration of the impeller by numerical integration, and it does not depend on the time

$$J_p=\iiint_{V_p} r^2dm,$$

where r is the distance of the elements of mass dm from the axis of rotation. It is possible to represent the complex configuration of the rotor and the impeller by a solid disc of radius R and width b with material density ρ. Then for the i-th impeller

APPROVED FOR RELEASE: 2007/02/08: CIA-RDP82-00850R000200090053-2

APPROVED FOR RELEASE: 2007/02/08: CIA-RDP82-00850R000200090053-2

$$dm=2\pi r\varrho b dr$$

and

$$J_p=2\pi b\varrho\int_0^{R_1} r^3 dr=\frac{\pi b\varrho R^4}{2}. \tag{1.112}$$

The moment of inertia of the liquid depends on the time, therefore the derivative of the angular momentum has two terms

$$\frac{dK}{dt}=(J_p+J_ж)\frac{\pi}{30}\frac{dn}{dt}+\frac{\pi}{30}n\frac{dJ_ж}{dt}. \tag{1.113}$$

Since dJ_{liquid}/dt differs from zero only during the period of filling of the cavities with the fuel components (during the startup or shutdown process), for the steady-state operating conditions it is possible, without making a large error, to set $dJ/_{liquid}/dt=0$.

The moment of the external forces is the difference between the moments of the turbine and the pumps

$$M=M_т-\sum_1^k M_{нi}, \tag{1.114}$$

where k is the number of pumps.

The final equation of the TNA impeller is written in the form

$$J_{THA}\frac{\pi}{30}\frac{dn(t)}{dt}-M_т(t)+\sum_1^k M_{нi}(t)=0, \tag{1.115}$$

Key: 1. TNA

where

$$J_{THA}=J_p+J_ж;$$

Key: 1. TNA

$M_T(t)$ and $M_{Hi}(t)$ are defined by the equations (1.79) and (1.105).

1.7.2. Linear Equation and Characteristics of the Turbine-Pump Assembly

As a result of linearization of equation (1.115), the linear equation of the TNA [turbine-pump assembly] is obtained

$$J_{THA}\frac{\pi}{30}\bar{n}\frac{d\Delta n(t)}{dt}=\bar{p}_{тг}\left(\frac{\partial M_т}{\partial p_{тг}}\right)\delta p_{тг}(t)+\left(\frac{\partial M_т}{\partial K'}\right)\bar{K}'\delta K'(t-\tau'_{пр})+$$
$$+\bar{n}\left(\frac{\partial M_т}{\partial n}\right)\delta n(t)-\sum_1^k\left(\frac{\partial M_{нi}}{\partial n}\right)\bar{n}\delta n(t)-\sum_1^k\left(\frac{\partial M_{нi}}{\partial \dot{m}}\right)\bar{\dot{m}}_i\delta\dot{m}_i(t)$$

or in operator form

$$(T_{THA}s+1)\delta n=K_{n,p_{тг}}\delta p_{тг}+K_{n,\dot{m}_i}\delta\dot{m}_i+K_{n,K'}e^{-s\tau'_{пр}}\delta K, \tag{1.116}$$

APPROVED FOR RELEASE: 2007/02/08: CIA-RDP82-00850R000200090053-2

APPROVED FOR RELEASE: 2007/02/08: CIA-RDP82-00850R000200090053-2

where $T_{TNA} = (\pi/30)(J_{TNA}/a_{TNA})$ is the time constant, a_{TNA} is the self-regulation coefficient;

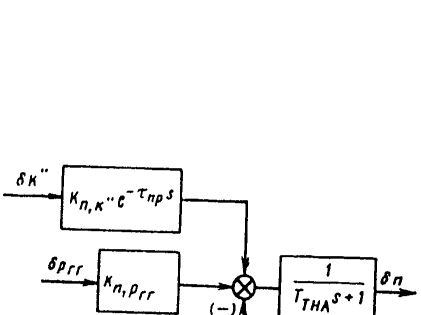

Figure 1.20. Structural diagram of the TNA

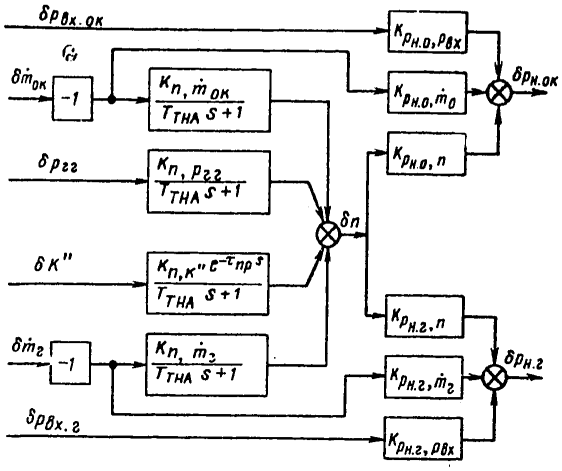

Figure 1.21. Structural diagram of the turbine-pump assembly.

$$a_{THA} = \sum_{1}^{k} \frac{\partial M_{в\,i}}{\partial n} - \frac{\partial M_т}{\partial n}; \; K_{n,x} \text{ are the boost factors.}$$

$$K_{n,x} = \frac{\bar{x}}{\bar{n} a_{THA}} \left(\frac{\partial M}{\partial x}\right),$$

where $x = \overline{p_{гг},\ K',\ \dot{m}_i}$.

Substituting the partial derivatives in a_{TNA} and $K_{n,x}$, we obtain

$$a_{THA} = \sum a_i \bar{\dot{m}}_i + \frac{\bar{p}_{гг} r_2}{\sqrt{\bar{R}\bar{T}_т}}; \quad K_{n,p_{гг}} = \frac{\bar{M}_т}{\bar{n} a_{THA}};$$

$$K_{n,K'} = \frac{\bar{K}'}{\bar{n} a_{THA}} \left(\frac{\partial M_т}{\partial RT_т}\right)\left(\frac{\partial RT_т}{\partial K'}\right);$$

$$K_{n,\dot{m}_i} = \frac{\bar{M}_{в\,i} - a_2 \bar{\dot{m}}_i^2}{\bar{n} a_{THA}},$$

In Figure 1.20 we have the structural diagram of the TNA for the case where δn is taken as the output signal.

APPROVED FOR RELEASE: 2007/02/08: CIA-RDP82-00850R000200090053-2

APPROVED FOR RELEASE: 2007/02/08: CIA-RDP82-00850R000200090053-2

For analysis of the dynamic characteristics of the engine it is expedient to take the pressures after the pumps $\delta p_{\text{pump.ox}}$ and $\delta p_{\text{pump, fuel}}$ as the output signals, and the parameters of the gas generator δp_{gg} and $\delta K'$, the intake lines $\delta p_{\text{inp.i}}$ and $\delta \dot{m}_i$ as the input parameters. If we exclude the internal variable δn in the pump and turbine equations, then two equations are obtained which describe the dynamics of the turbine-pump assembly.

$$\begin{aligned}(T_{\text{THA}}s+1)\delta p_{\text{н.ок}} &= K_{p_{\text{н.ок}},p_{\text{ГГ}}}\delta p_{\text{ГГ}}^{(2)} + K_{p_{\text{н.ок}},K'}^{(1)} e^{-s\tau'_{\text{пр}}}\delta K' - \\ &- \tilde{K}_{p_{\text{н.ок}},\dot{m}_{\text{ок}}}(1+sT_{\text{н.ок}})\delta \dot{m}_{\text{г.к}} + K_{p_{\text{н.ок}},\dot{m}_{\text{г}}}\delta \dot{m}_{\text{г}} + \\ &+ K_{p_{\text{н.ок}},p_{\text{вх.ок}}}^{(3)}(1+T_{\text{THA}}s)\delta p_{\text{вх.ок}};\end{aligned} \tag{1.118}$$

$$\begin{aligned}(T_{\text{THA}}s+1)\delta p_{\text{н.г}} &= K_{p_{\text{н.г}},p_{\text{ГГ}}}^{(4)}\delta p_{\text{ГГ}} + K_{p_{\text{н.г}},K'} e^{-s\tau'_{\text{пр}}}\delta K' + \\ &+ K_{p_{\text{н.г}},\dot{m}_{\text{г.к}}}\delta \dot{m}_{\text{г.к}} + \tilde{K}_{p_{\text{н.г}},\dot{m}_{\text{г}}}(1+T_{\text{н.г}}s)\delta \dot{m}_{\text{г}} + \\ &+ K_{p_{\text{н.г}},p_{\text{вх.г}}}(1+T_{\text{THA}}s)\delta p_{\text{вх.г}},\end{aligned}$$

Key: 1. pump,ox; 2. gg = gas generator; 3. inp ox; 4. pump, fuel; 5. TNA = turbine-pump assembly

where

$$K_{p_{\text{н}l},p_{\text{ГГ}}} = K_{p_{\text{н}l},n}K_{n,p_{\text{ГГ}}};\quad K_{p_{\text{н}l},K'} = K_{p_{\text{н}l},n}K_{n,K'};$$

$$\tilde{K}_{p_{\text{н}l},\dot{m}_l} = K_{p_{\text{н}l},\dot{m}_l} + K_{p_{\text{н}l},n}K_{n,\dot{m}_l},$$

$$T_{\text{н}l} = \frac{T_{\text{THA}}K_{p_{\text{н}l},\dot{m}_l}}{\tilde{K}_{p_{\text{н}l},\dot{m}_l}}.$$

Thus, the TNA is a set of aperiodic, forcing and delaying elements.

The structural diagram of the TNA is illustrated in Fig 1.21.

The dynamic properties of the TNA are defined by the structure and the magnitude of the time constant and the boost factors.

According to the relation (1.116) the characteristic equation of the TNA, $T_{\text{TNA}}s+1=0$ has a single root $s=-1/T_{\text{TNA}}$. The degree of structural stability will depend on the magnitude and sign of the time constant. If $T_{\text{TNA}}>0$, then TNA is stable; if $T_{\text{TNA}}<0$, then it is unstable.

The signs of the time constant are determined by the sign of the self-regulation coefficient (1.117). The larger the value of a_{TNA}, the smaller T_{TNA}, the larger $|s|$ and the higher the degree of stability of the TNA. For $s=0$, TNA will be found at the stability boundary, and for $s>0$ it will become an unstable region.

APPROVED FOR RELEASE: 2007/02/08: CIA-RDP82-00850R000200090053-2

APPROVED FOR RELEASE: 2007/02/08: CIA-RDP82-00850R000200090053-2

The self-regulation coefficient a_{TNA} is determined by the moment characteristics of the turbine and the pumps, $a_{THA}=\sum\frac{\partial M_{nl}}{\partial n}-\frac{\partial M_T}{\partial n}$.

The TNA is stable if $a_{TNA}>0$ and, consequently, the stability condition is the inequality

$$\sum_1^k\left(\frac{\partial M_{nl}}{\partial n}\right)>\frac{\partial M_T}{\partial n}.$$

Fig 1.22 shows the torques of the pumps and the turbine as a function of the rpm. From Fig 1.22 it follows that the self-regulation coefficient is equal to the difference of the tangents of the slope angles of the tangents to the curves M(n) at the investigated point

$$a_{THA}=\operatorname{tg}\alpha_n+\operatorname{tg}\alpha_T'.$$

In Fig 1.22 the point A corresponds to the stable operating conditions. Thus, whereas at this point corresponding to the rated operating conditions, $n=\bar{n}$, as a result of the disturbances, the rpm $n>\bar{n}$ varies, then $M_T>M_{pump}$ i and the rpm decreases to $\bar{n}$ as a result of the formation of excess moment of the turbine. The reverse phenomenon takes place for $n<\bar{n}$.

Instead of the tangents of the slope of the tangents to the moment characteristics it is possible to consider the value of $\varepsilon_{TNA}=\alpha_{pump}+\alpha_T'$, which characterizes the self-regulation coefficient.

Thus, the time constant and the boost factors of the TNA depend on the self-regulation coefficient and the moment of inertia of the TNA impeller.

Effect of the Rated rpm on the Dynamic Characteristics of the TNA

The rpm $\bar{n}$ is selected in the design phase from the condition of insuring the required heads of the pumps and cavitation-free operation. The variation of $\bar{n}$ leads to variation of the overall dimensions of the pump and turbine impellers and, consequently, to variation of the self-regulation coefficient and moment of inertia.

Let us consider the effect of the rpm on the self-regulation coefficient, the time constant and the boost coefficients of the TNA. Here the output characteristics of the TNA remain constant:

$$p_{nl}=\dot{p}_{nl};\ \dot{m}_l=\bar{\dot{m}}_l,\ \dot{m}_T=\bar{\dot{m}}_T,\ M_T=\sum_1^k M_{nl}.$$

APPROVED FOR RELEASE: 2007/02/08: CIA-RDP82-00850R000200090053-2

APPROVED FOR RELEASE: 2007/02/08: CIA-RDP82-00850R000200090053-2

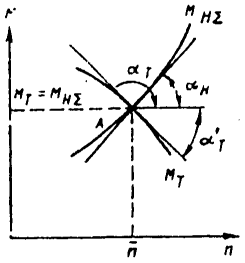

Figure 1.22. Torque of the TNA as a function of rpm

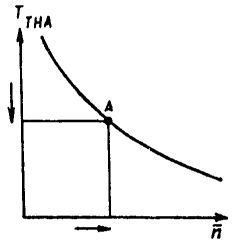

Figure 1.23. Time constant of the TNA as a function of rpm
Key:
1. TNA

Transforming the equation (1.117), we have

$$a_{\text{THA}}=\sum_{1}^{k}\frac{\pi}{30}(r_2^2-r_1^2)\dot{m}_l+\frac{\varphi_T\pi d_T^2\dot{m}_T}{120}\left(1+\psi\frac{\cos\beta_2}{\cos\beta_1}\right). \qquad (1.119)$$

Key: 1. TNA

For the given flow rates $\bar{\dot{m}}_i$ and $\bar{\dot{m}}_T$, the radii of the pump impellers and the turbine diameter are inversely proportional to the rpm, that is, $r_2=c_1/n^2$; $d_T=c_2/n^2$, where c_i are the similarity constants.

Then from the equation (1.119) it follows that $a_{\text{TNA}}=c_3/n^2$. Since on variation of the radial dimensions of the pumps, the variation in width of the impellers takes place while maintaining the given output capacity, $b=c_4/R$, and therefore from the equation (1.112), it follows that

$$J_{\text{THA}}=\frac{c_5}{n^3}.$$

Substituting the relations obtained in the expression for T_{TNA}, we have

$$T_{\text{THA}}=\frac{c_6}{n}.$$

Thus, increasing the rpm leads to a decrease in the time constant of the TNA (Fig 1.23) and an increase in the stability margin.

The boost factors $K_{n,\,p_{\Gamma\Gamma}}=\frac{M_T}{na_{\text{THA}}}$; $K_{n,\dot{m}_l}=\frac{M_{Hl}-a_2\dot{m}_l}{na_{\text{THA}}}$.

If we substitute the similarity expressions obtained above in these expressions and consider that $M_T=c_7/n$, we obtain $K_{n,\,p_{gg}}$ which does not depend on the rpm, and $K_{n,\,\dot{m}_l}=c_8/n$.

APPROVED FOR RELEASE: 2007/02/08: CIA-RDP82-00850R000200090053-2

APPROVED FOR RELEASE: 2007/02/08: CIA-RDP82-00850R000200090053-2

Effect of Operating Conditions on the Time Constant

For the specific TNA, the geometric dimensions are given, that is, J_{TNA}=const. On variation of the operating conditions, the rpm and the flow rates of the fuel components change.

From the equation of similarity of the pumps it follows that $\dot{m}_i/n$=const. If we propose that $\eta_{Hi}=\eta_H$ and on choking the motor $n_{choke}<n$, $\dot{m}_{T.choke}<\dot{m}_T$, on forcing the engine $n_\phi>n$, $\dot{m}_{T.\phi}>\dot{m}_T$, from equation (1.119) it follows that

$$(a_{THA})_{ap} < \bar{a}_{THA} < (a_{THA})_\phi;$$
$$(T_{THA})_{ap} > \bar{T}_{THA} > (T_{THA})_\phi.$$

Key: 1. choke; 2. force

Thus, when forcing the engine the stability margin of the TNA increases, and on choking, it decreases.

1.8. Elements of the Engine Control System

The joint operation in the given sequence of all of the engine assemblies, that is, execution of the given operating cyclo gram is insured by the control system. The control system is made up of devices which provide for startup and shutdown, warning and blocking, preventing an emergency situation with the engine. The elements of the control system include the automatic devices (valves and relays) which operate by the open cycle and are called automation or automata. The automata receive the operating signal which is the control signal; as a result, the output signal changes which acts on one engine unit or another; the given control program is executed at the same time.

The basic elements of the control system are the start and cutoff valves. The force required for opening or closing the valves can be created using compressed gas, liquid, an electromagnet or pyrocharge.

Depending on the type of energy providing for response of the valve, they are divided into the following groups:

Pneumatic valves;

Electromagnetic valves;

Pyrovalves.

All of the valves of the enumerated groups are being used at the present time. Let us consider one type of each group.

APPROVED FOR RELEASE: 2007/02/08: CIA-RDP82-00850R000200090053-2

APPROVED FOR RELEASE: 2007/02/08: CIA-RDP82-00850R000200090053-2

The response time of the valve is the basic characteristic for it determines the duration and stability of starting, the shutdown time and the magnitude of the aftereffect pulse, the possibility of the occurrence of hydraulic hammer, and so on.

1.8.1. Pneumohydraulic Valves

As an example let us consider the pneumohydraulic valve shown in Fig 1.24.

The flow rate through the valve is determined by the characteristics of the elastic system, the magnitude of the control pressure which established the plate position at each point in time. In order to determine the position of the valve plate at different points in time it is necessary to write the equations of motion of the sliding valve system.

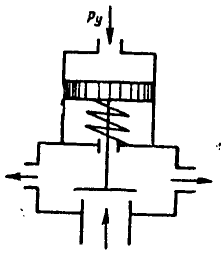

Figure 1.24. Diagram of the pneumohydraulic valve

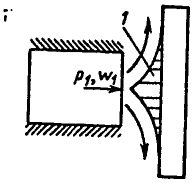

Figure 1.25. Diagram of flow around the plate:
1 -- stagnant zone

Equation of Motion of the Plate

In general form the equation of motion of the valve is written in the form

$$R_j = \sum R_i, \tag{1.120}$$

where $R_j = md^2x/dt^2$ is the force of the inertia movement of the part; m is the mass of the moving part; x is the plate displacement; R are the forces acting on the moving parts of the valve.

The following forces act on the valve:

The force of the pressure of the component on the valve plate, R_{liquid};

The force of the pressure of the controlling gas on the piston R_y;

The force of the spring $R_п$;

The frictional force R_f.

APPROVED FOR RELEASE: 2007/02/08: CIA-RDP82-00850R000200090053-2

APPROVED FOR RELEASE: 2007/02/08: CIA-RDP82-00850R000200090053-2

The force of the liquid pressure on the plate (Fig 1.25) is determined by the static and dynamic effects of the flow on the plate; on flow around it $R_{liquid}=R_d+R_{st}$. If we assume that the pressure between the plate and the valve housing is equal to the pressure after the valve, the static pressure is defined by the function

$$R_{cr}=p_1F_1-p_2F_2, \tag{1.121}$$

where

$$F_1=\frac{\pi d_c^2}{4};\ F_2=\frac{\pi}{4}(d_c^2-d_n^2).$$

For high liquid flow velocities, which occurs on closing the valve, a hydrodynamic force acts on the valve plate.

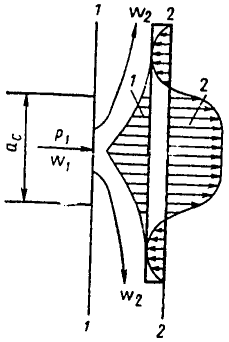

Figure 1.26. Forces acting on the plate:
1 -- stagnant zone; 2 -- pressure diagram

At the present time there are no reliable data on the hydrodynamic force as a function of various factors. It is possible to determine the hydrodynamic force approximately with the following simplifications (Fig 1.26):

The pressure and velocity are distributed uniformly in specific cross sections 1-1, 2-2, adjacent to the pipe;

The inertial forces and mass of the liquid are negligibly small;

The rarefaction zones between the nozzle and the plate are not formed.

In this case the equation of the Euler pulse theorem is in the form

$$\int_F p d\vec{F}=\int w d\vec{m}, \tag{1.122}$$

where $\int \vec{pdF}$ is the principal vector of the force (pressure force) surface considering the reaction of the plate to the liquids; $\int \vec{wdm}$ is the principal vector of the momentum.

APPROVED FOR RELEASE: 2007/02/08: CIA-RDP82-00850R000200090053-2

APPROVED FOR RELEASE: 2007/02/08: CIA-RDP82-00850R000200090053-2

Considering the assumptions made, the Euler pulse theorem (1.122) can be written in the following form:

$$(\varrho Q\vec{w}+Fp)_2-(\varrho Q\vec{w}+Fp)_1=\vec{R}. \tag{1.123}$$

Projecting the force of the reaction on the x axis and assuming that $p_2=0$, we obtain

$$R_x=-\varrho w_1^2 F_c\cos\alpha-p_c F_c\cos\alpha. \tag{1.124}$$

Assuming that there is no warping of the plate ($\alpha=0$), and considering that the force reaction to the plate R_d has a direction opposite to the force reaction from the plate on the liquid, from equation (1.124) we have

$$R_x=p_c F_c+\varrho F_c w_1^2, \tag{1.125}$$

where p_c, w_1, F_c are the liquid characteristics in the 1-1 cross section. The pressure p_c can be expressed in terms of the pressure p_1, by the Bernoulli equation

$$p_c=p_1-\frac{w_1^2\varrho}{2}. \tag{1.126}$$

Replacing the velocity by the flow rate $w=\dot{m}/\rho F$ and considering (1.126), from equation (1.125) we obtain

$$R_x=p_1F_c+\frac{\dot{m}^2}{2\varrho F_c^2}. \tag{1.127}$$

In reference [21] from the theory of jet flow of an incombustible liquid around sharp edges, a relation is obtained for the hydrodynamic force

$$R_x=C_x\frac{\varrho w_1^2}{2}L\delta, \tag{1.128}$$

where L is the width of the working opening; δ is the radial clearance; c_D is the coefficient of hydrodynamic force;

$$c_x=2\mu\varepsilon\sqrt{\left(\frac{h_c}{\delta}\right)^2+1}\left[\cos\alpha-\mu\frac{\delta}{d}\sqrt{\left(\frac{h_c}{\delta}\right)^2+1}\right].$$

ε is the experimental pressure loss coefficient; h_c is the maximum length of the opening.

The force of the pressure of the controlling gas on the piston

$$R_y=-(p_y-p_n)F_y, \tag{1.129}$$

APPROVED FOR RELEASE: 2007/02/08: CIA-RDP82-00850R000200090053-2

APPROVED FOR RELEASE: 2007/02/08: CIA-RDP82-00850R000200090053-2

where p_y, p_H are the pressure of the controlling gas and the environment, respectively; F_y is the piston area.

The force of the spring

$$R_n = \pm R_{no} - cx, \tag{1.130}$$

where c is the spring tension

$$c = \frac{Ed^4}{8iD_{cp}},$$

Key: medium

E is the modulus of shear; i is the number of turns; $R_{\pi 0}$ is the force of the initial compression of the spring.

The frictional force

$$R_f = R_1 + R_2 + R_3, \tag{1.131}$$

where R_1 is the frictional force at rest which determines the delay in opening and closing the valve; R_2 is the force of dry friction determined by the speed of movement of the contact pairs, and it depends on the magnitude of the normal force and the friction coefficient f, which depends on the sliding rate.

The friction coefficient is defined by the function

$$f = (f_1 + f_2 dx) e^{-f_3 \dot{x}} + f_4,$$

where f_1, f_2, f_3, f_4 are constants which depend on the nature and conditions of the friction of the bodies.

The frictional coefficient is approximately represented by the function

$$f = c_f \dot{x}. \tag{1.132}$$

Thus, the force of dry friction can be determined by the function

$$R_2 = f_y \overset{(1)}{[R_y} + S_y (p_y - p_n)] + f_m \overset{(2)}{[(R_m} + S_m (p_2 - p_n)],$$

Key: 1. piston; 2. rod

where R_y, R_{rod} are the tension forces of the piston and rod sleeves; S_y, S_{rod} are the contact areas of the sleeves with the cylinder and the rod. If we take the friction coefficients of the sleeves with the cylinder and the rod to be identical, then

$$R_2 = c_f w (p_y S_y + p_2 S_m + R_0 - R_a), \tag{1.133}$$

APPROVED FOR RELEASE: 2007/02/08: CIA-RDP82-00850R000200090053-2

APPROVED FOR RELEASE: 2007/02/08: CIA-RDP82-00850R000200090053-2

FOR OFFICIAL USE ONLY

where $R_0=R_y+R_ш$; $R_a=p_н(S_y+S_ш)$.

R_3 -- the viscous friction -- is defined by the function

$$R_3=\eta\frac{S_б}{\delta}\dot{x}, \tag{1.134}$$

where η is the coefficient of dynamic viscosity; S_b is the area of the lateral surface; δ is the clearance between the working surface.

Thus, the frictional force of the moving parts is determined by the equation

$$R_j=\pm\left[c_f(p_yS_y+p_2S_ш+R_0-R_a)+\eta\frac{S_б}{\delta}\right]\frac{dx}{dt}. \tag{1.135}$$

Substituting the forces defined by the functions (1.128-1.135) in the initial (1.120), we obtain the equation of motion of the moving valve system

$$m\frac{d^2x}{dt^2}\pm\left[c_f(R_a-R_0-p_yS_y-p_2S_ш)+\eta\frac{S_б}{\delta}\right]\frac{dx}{dt}+$$
$$+cx=p_1F_1-p_2F_2-(p_y-p_н)F_y\pm R_{по}. \tag{1.136}$$

Equation (1.136) includes the pressures p_1 (in front of the plate) and p_2 (after the plate) which are related by the Bernoulli equation

$$p_1=p_2+\xi(x)\varrho\frac{w_1^2}{2}, \tag{1.137}$$

where ξ is the coefficient of hydraulic losses on the valve plate [10].

$$\xi(x)=0{,}55+\frac{2d_к-1{,}2d_c}{d_c}+0{,}15\frac{d_c}{x}.$$

The magnitude of the controlling pressure is determined by the energy balance of the gas in the position in front of the piston (Fig 1.27). The equation of the first law of thermodynamics for such a system is written in the form

$$dU=dQ+i_sdm_s-(dL+idm), \tag{1.138}$$

where i_Sdm_S is the quantity of energy entering into the cavity with the incoming gas; idm is the quantity of energy removed with the outgoing gases; dQ is the quantity of heat supplied to the gas; dU is the variation in internal energy of the gas; dL is the work of expansion of the gas.

If we make the obvious substitution $dm=\dot{m}dt$ in the equation (1.138), it assumes the form

$$dQ+(i_s\dot{m}_s-i\dot{m})dt=dU+dL$$

or

$$\frac{dU}{dt}=i_s\dot{m}_s-i\dot{m}+\frac{dQ}{dt}-\frac{dL}{dt}. \tag{1.139}$$

FOR OFFICIAL USE ONLY

APPROVED FOR RELEASE: 2007/02/08: CIA-RDP82-00850R000200090053-2

APPROVED FOR RELEASE: 2007/02/08: CIA-RDP82-00850R000200090053-2

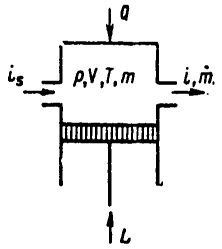

Figure 1.27. Diagram of the valve cavity

Using the equations of thermodynamics

$$dU=c_v m dT;\quad pV=mRT;$$
$$dL=pdV;\quad c_v=\frac{R}{\varkappa-1},$$

equation (1.139) is reduced to the form

$$\frac{dp}{dt}=\frac{\varkappa-1}{V}\left(i_s\dot{m}_s-i\dot{m}-\frac{\varkappa}{\varkappa-1}\,p\,\frac{dV}{dt}+\frac{dQ}{dt}\right). \tag{1.140}$$

Thus, the valve dynamics are described by the equations (1.136), (1,137), (1.140).

Process of Opening the Pneumatic Valve

The flow rate of the component through the valve is determined by the position of the plate at each point in time. In order to determine the position of the plate it is necessary to integrate the equations (1.137) and (1.140) which for the case of opening the valve have the form

$$\begin{aligned} m\frac{d^2x}{dt^2}\pm\left[c_f(R_a-R_0-p_yS_y-p_2S_ш)+\eta\frac{S_б}{\delta}\right]\frac{dx}{dt}+\\ +cx=p_1F_1-p_2F_2-(p_y-p_ш)F_y\pm R_{по};\\ \frac{dp_y}{dt}=\frac{\varkappa-1}{V}\left(-i\dot{m}-\frac{\varkappa}{\varkappa-1}\cdot p_y\cdot\frac{dV}{dt}+\frac{dQ}{dt}\right). \end{aligned} \tag{1.141}$$

In the general case these equations can be solved with respect to x(t) using a digital computer. For an approximate solution let us make the following assumptions:

The forces of inertia and friction are small by comparison with the other forces;

The pressure after the plate p_2 is constant and equal to the ambient pressure;

The heat exchange of the gas with the environment is absent.

APPROVED FOR RELEASE: 2007/02/08: CIA-RDP82-00850R000200090053-2

APPROVED FOR RELEASE: 2007/02/08: CIA-RDP82-00850R000200090053-2

On the basis of the indicated assumptions the system (1.141) assumes the form

$$p_y = p_{y_1} - b_1 x;$$
$$\frac{dp_y}{dt} = -b_2 \frac{p_y}{V} - \frac{\varkappa}{V} p_y \frac{dV}{dt}, \tag{1.142}$$

where

$$p_{y_1} = \frac{F_1}{F_y} p_1 + \left(1 - \frac{F_2}{F_y}\right) p_н \pm \frac{R_{по}}{F_y};$$
$$b_1 = \frac{c}{F_y}; \quad b_2 = \varkappa \sqrt{RT_0} A \mu F_{кр}.$$

The volume of the gas cavity under the valve piston

$$V = V_0 - F_y x, \tag{1.143}$$

where V_0 is the volume with the valve closed.

Since

$$\frac{dV}{dt} = \frac{dV}{dx} \frac{dx}{dt},$$

then

$$\frac{dV}{dt} = -F_y \frac{dx}{dt}. \tag{1.144}$$

Let us differentiate the first equation (1.142) considering the functions (1.143), (1.144); we obtain the equation of motion of the valve plate

$$\left[F_y + \frac{b_1 (V_0 - F_y x)}{p_{y_1} - b_1 x}\right] dx = b_2 dt. \tag{1.145}$$

Integrating the last equation within the limits of 0-x and 0-t, we obtain

$$t = (\varkappa + 1) \frac{F_y}{b_2} x + \frac{p_{y_1} F_y - V_0 b_1}{b_1 b_2} \ln\left(1 - \frac{b_1}{p_{y_1}} x\right). \tag{1.146}$$

If we substitute x=h in the last equation (h is the stroke of the plate), then we obtain the valve opening time

$$t_{от} = (\varkappa + 1) \frac{F_y}{b_2} h + \frac{[F_y p_1 + p_н (F_y - F_2) + R_{по} - V_0 c]}{b_1 b_2} \ln\left(1 - \frac{b_1}{p_{y_1}} h\right). \tag{1.147}$$

Process of Closing the Valve

Under the assumptions which are made for the process of opening the valve, the equations of dynamics of the valve assume the form

$$p_y = p_{y_2} - b_1 x; \tag{1.148}$$

APPROVED FOR RELEASE: 2007/02/08: CIA-RDP82-00850R000200090053-2

APPROVED FOR RELEASE: 2007/02/08: CIA-RDP82-00850R000200090053-2

$$\frac{dp_y}{dt}=\frac{\varkappa-1}{V}\left(i_s\dot{m}_s-\frac{\varkappa}{\varkappa-1}p_y\frac{dV}{dt}\right), \tag{1.149}$$

where

$$p_{y_s}=\frac{F_1}{F_y}p_1-\frac{F_2}{F_y}p_2\pm\frac{R_{no}}{F_y};$$
$$V=V_0-F_y(h-x);$$
$$\frac{dV}{dt}=F_y\frac{dx}{dt}. \tag{1.150}$$

Under the assumption of constancy of the gas parameters after the transformations analogous to the opening process, x(5) is obtained in the following form

$$x(t)=b_3\pm\sqrt{b_3^2-2hb_3+h^2+2b_4t}, \tag{1.151}$$

where

$$b_3=\frac{\varkappa(F_1p_1-F_2p_2+p_nF_y\pm R_{no})-b_1V_0}{(\varkappa+1)c};$$
$$b_4=\frac{(\varkappa-1)i_s\dot{m}_s}{c(\varkappa+1)}.$$

The time for closing the valve will be determined if we set x=0 in equation (1.151)

$$t_3=\frac{h(2b_3-h)}{2b_4}. \tag{1.152}$$

The variation in time of the flow rate of the fuel components when starting up and shutting down can be determined by using the functions (1.137), (1.146) or (1.151).

The velocity is related to the mass flow rate by the continuity equation

$$w_1=\frac{\dot{m}}{F_1\varrho\mu},$$

where μ is the flow rate coefficient of the gas for the entrance cross section of the valve.

Substituting the last function in equation (1.137), we obtain

$$\dot{m}(x)=\mu F_1\sqrt{2\varrho\frac{p_1-p_2}{0{,}55+\frac{2d_\kappa-1{,}2d_c}{d_c}+0{,}15\frac{d_c}{x}}}. \tag{1.153}$$

Solving equations (1.153) and (1.146) or (1.151) jointly, it is possible to obtain the flow rate as a function of the plate displacement $\dot{m}(x)$ or time $\dot{m}(t)$ on opening or closing the valve.

APPROVED FOR RELEASE: 2007/02/08: CIA-RDP82-00850R000200090053-2

APPROVED FOR RELEASE: 2007/02/08: CIA-RDP82-00850R000200090053-2

1.8.2. Electropneumatic Valve

The electropneumatic valves are used to control the operation of pneumo-hydraulic valves and also for direct control of the fuel component feed to the low-thrust engine.

As an example a study is made of the dynamics of the direct-action electro-pneumatic valve (Fig 1.28).

The law of variation of the current strength in the circuit of the electro-magnet is defined by the function

$$I=I_0e^{-\frac{R}{L}t}+\frac{E}{R}\left(1-e^{-\frac{R}{L}t}\right), \tag{1.154}$$

where I_0 is the current strength at the initial point in time; on closure of the circuit of the electromagnet, $I_0=0$; E is the electromotive force; L is the inductance of the electromagnet coil; R is the resistance.

The tractive force of the electromagnet

$$R_{\text{эм}}=\frac{B^2F_{\text{я}}^{(2)}}{8\pi\sin\alpha}\cdot 10^7, \tag{1.155}$$
(1)

Key: 1. em; 2. armature

where B is the magnetic inductance; F_{armature} is the area of the armature; α is half the apex angle of the electromagnet cone.

Since the magnetic induction is defined as [21]

$$B\sim\frac{Ii(1-\varepsilon)}{h},$$

where i is the number of turns of the winding; ε is the scattering coefficient of the magnetic force; h is the gap between the armature and the yoke, then

$$R_{\text{эм}}=6{,}4\cdot 10^{-4}\frac{F_{\text{я}}(1-\varepsilon)^2I^2i^2}{h^2\sin\alpha}. \tag{1.156}$$

The delay time of opening of the electropneumatic valve is determined from the closure time of the electric circuit to the beginning of the movement of the plate.

At the opening time, the following conditions must be observed

$$R_{\text{эм.о}}=(p_1-p_{\text{в}})F_{\text{с}}. \tag{1.157}$$
(1)

Key: 1. em.o

APPROVED FOR RELEASE: 2007/02/08: CIA-RDP82-00850R000200090053-2

APPROVED FOR RELEASE: 2007/02/08: CIA-RDP82-00850R000200090053-2

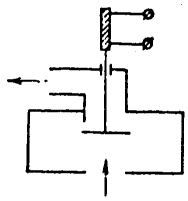

Figure 1.28. Diagram of the electropneumatic valve

Solving equations (1.156) and (1.157) with respect to I, we obtain the current strength at the time of opening of the valve

$$I_{от}=40\frac{h}{(1-\varepsilon)l}\sqrt{\frac{(p_1-p_н)F_c\sin\alpha}{F_э}}. \qquad (1.158)$$

Key: 1. open

Substituting equation (1.158) in equation (1.154), we obtain the delay time in opening the electropneumatic valve

$$t_{от}=\frac{L}{R}\ln\left(\frac{E}{E-I_{от}R}\right). \qquad (1.159)$$

In order to determine the delay time of the closure of the valve it is necessary to use the conditions (the beginning of movement of the plate)

$$R_з=(p_1-p_2)F_c$$

Key: 1. closure

and then considering equation (1.156) it is possible to obtain the magnitude of the current required to close the valve

$$I_з=40\frac{h}{(1-\varepsilon)l}\sqrt{\frac{(p_1-p_2)F_c\sin\alpha}{F_э}}.$$

Key: closure

Substituting the last function in equation (1.154), we obtain the delay time for closure of the electropneumatic valve

$$t_з=\frac{L}{R}\ln\frac{I_0}{I_з}. \qquad (1.160)$$

1.9. Hydraulic Hammer

When shutting the engine down and sometimes when starting it up, with short response time of the valve hydraulic hammers can occur which are dangerous especially for long and three-dimensionally curved lines.

APPROVED FOR RELEASE: 2007/02/08: CIA-RDP82-00850R000200090053-2

APPROVED FOR RELEASE: 2007/02/08: CIA-RDP82-00850R000200090053-2

Without considering the viscous friction and the movement of the liquid in the direction perpendicular to the tube axis, the phenomenon of hydraulic hammer can be described by the wave equation

$$\frac{1}{a_0^2}\frac{\partial^2 p}{\partial t^2}-\frac{\partial^2 p}{\partial x^2}=0, \tag{1.161}$$

where p is the excess pressure; a_0 is the effective speed of the liquid which is determined by the Zhukovskiy formula

$$a_0^2=\frac{a^2}{1+\frac{Qa^2d}{E\delta}}.$$

The solution of the equation (1.161) can be obtained in the form of a traveling wave [16]

$$p(x, t)=p_1(x-a_0t)+p_2(x+a_0t), \tag{1.162}$$

where p_1 and p_2 are defined by the boundary conditions at the ends of the tube.

Depending on the time required to close the main $t_{closure}$, direct and indirect hammer can occur.

If $t_{closure}<2\ell/a_0$, that is, the time of closure is less than the time of double the path of pressure wave through the line, there is a direct impact, and the maximum pressure in the main is defined by the formula of N. Ye. Zhukovskiy

$$p_{max}=Qv_0a_0, \tag{1.163}$$

where v_0 is the velocity of the liquid before the beginning of covering of the tube. If $t_{closure}>t_0=2\ell/a_0$, the wave reflected from the tank insures that the end cross section will be reached before the pressure increases to a value of (1.163), then indirect impact occurs.

In the case where the liquid is braked in accordance with a linear law, the pressure on impact is defined by Mish's formula [16]

$$p_{max}=Qv_0a_0\frac{t_0}{t_3}. \tag{1.164}$$

Substituting $t_0=2\ell/a_0$ and $v_0=Q/F$, we obtain

$$p_{max}=Q\frac{Q}{F}\frac{2l}{t_3}.$$

This case is close to the process which occurs on switching off the engine.

In the general case for an arbitrary law of braking of the liquid on closing the valves the pressure in the line is determined by the sum of the direct and reflected waves [16]

FOR OFFICIAL USE ONLY

APPROVED FOR RELEASE: 2007/02/08: CIA-RDP82-00850R000200090053-2

APPROVED FOR RELEASE: 2007/02/08: CIA-RDP82-00850R000200090053-2

$$p(t)=\varrho a_0 \sum_{q_0}^{q_m}(-1)^q\{[v_0-v(t-qt_0)]-[v_0-v(t-qt_0+\tau)]\}, \qquad (1.165)$$

where q=0, 1,..., q_m, q_m is the integral part of the number $a_0t/2\ell$ for q=0, $v(t-t_0q)=0$.

In order to reduce the pressure of the hydraulic hammer it is necessary, as follows from (1.164) to satisfy the condition $t_{closure}>t_0$, to apply inserts with reduced elasticity (the decrease in the effective velocity a_0) and accumulators.

In order to calculate the indirect hydraulic hammer when using a reservoir, equation (1.161) is used. The schematic of the process is as follows. At the time t=0 the liquid with constant volumetric flow rate Q_0 moves from the valve (x=ℓ) to the tank (x=0). When t>0 the flow rate in the cross section x=0 begins to decrease according to the law Q=Q(t). The reservoir is connected in the vicinity of x=0.

In order to solve the equation (1.161) the initial conditions for t=0 are

$$p(x, 0)=0;\ \frac{\partial p(x, 0)}{\partial t}=0.$$

For x=ℓ

$$p(x, l)=0.$$

The magnitude of the velocity at the end of the tube where the reservoir is installed is defined by the equation

$$v(0, t)=\frac{Q_0-Q(t)-Q_a(t)}{F_0}, \qquad (1.165,a)$$

where $Q_a(t)$ is the liquid flow rate to the accumulator which can be determined from the reservoir characteristics.

Let us propose that the reservoir is an elastic tank with the characteristics:

F is the area of the piston (bellows); m is the mass of the moving part; c_a is the rigidity of the elastic element reduced to a unit area; h is the deviation of the elastic system from equilibrium.

The equation of motion of the piston of the reservoir is

$$m\frac{d^2h}{dt^2}+Fc_ah=F_1p(0, t).$$

The initial conditions are: t=0; h=0, $\dot{h}$=0. The solution of the equation (1.165)

APPROVED FOR RELEASE: 2007/02/08: CIA-RDP82-00850R000200090053-2

APPROVED FOR RELEASE: 2007/02/08: CIA-RDP82-00850R000200090053-2

$$h(t)=\frac{F_1}{m\omega}\int_0^t p(t)\sin\omega(t-\tau)\,dt,$$
$$\omega=\sqrt{\frac{F_1 c}{m}}. \tag{1.166}$$

The liquid flow rate to the reservoir is

$$Q_a(t)=F_1\frac{dh}{dt}. \tag{1.167}$$

The solution of equation (1.161) is represented in the form of traveling direct and reflected waves

$$p(x,\ t)=p_1\left(t-\frac{x}{a_0}\right)+p_2\left(t+\frac{x}{a_0}\right); \tag{1.168}$$
$$v(0,\ t)=\frac{p_1(0,\ t)-p_2(0,\ t)}{\varrho a_0}.$$

Then from the conditions (1.165, a) using the functions (1.166) and (1.167) we have

$$\frac{p_1(0,\ t)-p_2(0,t)}{\varrho a_0}=\frac{Q_0-Q(t)}{F_0}-\frac{F_1^2}{F_0 m}\int_0^t[p_1(0,\ t)+$$
$$+p_2(0,\ t)]\cos\omega(t-\tau)\,dt. \tag{1.169}$$

Here, from equation (1.168) we obtain

$$p_2(t)=p_1\left(t-\frac{2l}{a_0}\right),$$

Substituting the last function in (1.169), for $p_1(0,t)$ we have

$$\frac{p_1(t)+p_1\left(t-\frac{2l}{a_0}\right)}{\varrho a_0}=\frac{Q_0-Q_0(t)}{F_0}-$$
$$-\frac{F_1^2}{F_0 m}\int_0^t\left[p(t)-p_1\left(t-\frac{2l}{a_0}\right)\right]\cos\omega(t-\tau)\,dt. \tag{1.170}$$

The integral in the last equation is nonzero only for $\tau=t$, for $\cos\omega(t-\tau)\to 0$. Therefore it is possible approximately to represent this integral by the series

$$\int_0^t f(t)\cos(t-\tau)\,dt=f'(t)\frac{1}{\omega^2}-f''(t)\frac{1}{\omega^4}+\ldots \tag{1.171}$$

Considering (1.171) the equation at the boundary x=0 assumes the form

$$\frac{p_1(t)+p_1\left(t-\frac{2l}{a_0}\right)}{\varrho a_0}=\frac{Q_0-Q(t)}{F_0}-\frac{F_1^2}{F_0 m}\left[p_1'(t)-p_1'\left(t-\frac{2l}{a_0}\right)+\right. \tag{1.172}$$
$$\left.+\frac{m}{F_0 c_a}\left[p_1''(t)-p_1''\left(t-\frac{2l}{a_0}\right)\right]\right.$$

or

$$p_1(t)=\sum_{q=0}^{\infty}p_q\left(t-\frac{2l}{a_0}q\right).$$

APPROVED FOR RELEASE: 2007/02/08: CIA-RDP82-00850R000200090053-2

APPROVED FOR RELEASE: 2007/02/08: CIA-RDP82-00850R000200090053-2

If we neglect the mass of the moving parts (m=0), then from (1.172) the recurrent formulas are obtained

$$p_0(t)=\varrho a_0 e^{-nt}\int_0^t e^{nt} n\,\frac{Q_0-Q(t)}{F_0}\,dt; \tag{1.173}$$

where

$$p_q(t)=e^{-nt}\int_0^t e^{nt}\left[p'_{q-1}(t)-np_{q-1}(t)\right]dt,$$

$$n=\frac{F_0 c_a}{F\varrho a_0}.$$

In order to calculate the reservoir we assume that the liquid flow rate varies according to a step law, with a step height at, that is, $Q(t)=Q_0-at_1$; here $t_1\leqslant t_{closure}$ and $t_1<t_0$. Then from the equations (1.173) for the direct wave we have

$$p_0(t)=\varrho a_0\,\frac{at_1}{F_0}(1-e^{-nt})$$

and the reflected wave

$$p_{01}(t)=-\varrho a_0\,\frac{at_1}{F_0}\left(1-e^{-n\left(t-\frac{2l}{a_0}\right)}\right),$$

and

$$p(t)=p_0(t)+p_{01}(t).$$

Since the variation of the flow rate takes place in steps after t_1, then the total pressure at the time $t>t_{closure}$

$$p(t)=\varrho a_0\,\frac{at_1}{F_0}\,\frac{(1-e^{-nt_0})(1-e^{-nt})}{1-e^{-nt_1}}.$$

If we let t_1 approach zero, then from the last equation we obtain

$$p(t)=\varrho a_0\,\frac{a}{F_0 n}(1-e^{-nt_0})(1-e^{-nt}). \tag{1.174}$$

For the actual conditions $nt_0=(F_0c_a/F_1\rho a_0)t_0\ll 1$, and in this case equation (1.174) is simplified significantly, and the calculation formula will have the form

$$p_{max}=\frac{c_a}{a_0}\,\frac{Q_0}{F_1}2l. \tag{1.175}$$

The formula can be used for approximate calculation of the reservoir.

For the given characteristics of the main ℓ, F_0, ρ, a_0, v_0 and $t_{closure}$, p_{max} is defined by the formula (1.164). If p_{max} exceeds the admissible

APPROVED FOR RELEASE: 2007/02/08: CIA-RDP82-00850R000200090053-2

APPROVED FOR RELEASE: 2007/02/08: CIA-RDP82-00850R000200090053-2

value, then $p_{max,d}$ is given, and the characteristics of the reservoir are defined

$$c_a = \frac{a_0 p_{max,1}}{2lv_0}$$

and the volume is defined

$$V_a = \frac{p_{max,1} F_0}{c_a}.$$

1.10. Frequency Characteristics of the Assemblies

As a result of the interconnection of the engine and the elastic rocket, vibrational processes occur in the engine assemblies which are determined by the dynamic properties of the assemblies such as the natural frequency of the vibrations, the damping and so on.

In the vibrations which occur in the rocket, the role of the engine can be different. If pressure fluctuations occur in the combustion chamber, then the engine serves as a source of forced vibrations of the rocket. In turn, the rocket vibrations can be intensified by the engine as a result of the forced vibrations of the arrival of the fuel in the chamber which lead to fluctuations of the pressure in the chamber and the thrust. There are many causes for the occurrence of vibrations. The basic ones of them are the following: startup and shutdown of the engine, operation of the regulation system, separation of the stages, longitudinal vibrations of the rocket, and so on.

The startup of the engine begins with sharp opening of the startup valve which up to the time of startup separates the components in the tank and the line from the engine cavity. With sharp opening of the valve the liquid rushes from the tank downward; a rarefaction is formed in the upper layers. The rarefaction wave is propagated with the speed of sound along the line to the tank and, on being replaced from it, in the form of a wave of increased pressure it returns to the flow line. The line and the liquid have elasticity, and on variation of the pressure they form a vibrational system.

On the occurrence of engine thrust, there is dynamic loading of the hull of the rocket, and longitudinal vibrations of the hull and the fuel system occur. The analogous process also occurs when the engine is shut down. In the active part of the trajectory the engine is affected by different disturbances which have a periodic nature. The frequencies of the forced vibrations can coincide with the frequencies of the natural vibrations of the assemblies. Here resonance phenomena occur. Thus, it is desirable to know the frequency properties of the engine assemblies which are characterized by the frequency characteristics.

The frequency characteristics of the assembly are uniquely defined by the complex transfer function.

APPROVED FOR RELEASE: 2007/02/08: CIA-RDP82-00850R000200090053-2

APPROVED FOR RELEASE: 2007/02/08: CIA-RDP82-00850R000200090053-2

In order to determine the complex transfer function it is proposed that a harmonic effect $x=x_1 \cos \omega t$ is fed to the input of the unit, where x_1 is the amplitude, and ω is the angular frequency of the effect.

At the output of the linear system in the steady-state mode, a harmonic function will also be obtained with the same frequency, but in the general case shifted with respect to the phase ϕ and with a different amplitude

$$y = y_1 \cos(\omega t + \varphi).$$

The amplitude y_1 and the phase ϕ are determined by the properties of the system and the frequency of forcedvibrations ω.

If from the harmonic signal we proceed to the complex form by substitution of $\cos \omega t = e^{j\omega t}$, then

$$x = x_1 e^{j\omega t}, \quad y = y_1 e^{j(\omega t + \varphi)}.$$

The complex transfer function is the ratio of the complex form of the output signal to the input signal

$$W(j\omega) = \frac{y}{x} = \frac{y_1 e^{j(\omega t + \varphi)}}{x_1 e^{j\omega t}} = A(\omega) e^{j\varphi(\omega)},$$

where $A(\omega)=y_1/x_1$ is the modulus of the complex transfer function, $A(\omega)=\text{mod } W(j\omega)$; $\phi(\omega)$ is the phase shift of the output signal with respect to the input signal; $\phi(\omega)=\arg W(j\omega)$.

The complex transfer function is obtained from the operator function if we replace the operator s in it by $j\omega$

$$W(j\omega) = W(s)|_{s=j\omega}.$$

The transfer function of any order can be represented by the sum of the real and imaginary parts

$$W(j\omega) = P(\omega) + jQ(\omega).$$

In this case the modulus (amplitude) is defined as

$$A(\omega) = \sqrt{P^2(\omega) + Q^2(\omega)},$$

and the phase

$$\varphi(\omega) = \operatorname{arctg} \frac{Q(\omega)}{P(\omega)}.$$

The function $A(\omega)$ is called the frequency-amplitude characteristic and it defines the capacity of the element to amplify the input signal at different frequencies; that is, it characterizes the pass band of the input signal.

APPROVED FOR RELEASE: 2007/02/08: CIA-RDP82-00850R000200090053-2

APPROVED FOR RELEASE: 2007/02/08: CIA-RDP82-00850R000200090053-2

The function $\phi(\omega)$ is called the frequency-phase characteristic; it defines the phase shifts introduced by the element on different frequencies.

The hodograph of the vector $W(j\omega)$ on variation of the frequency from 0 to ∞ is called the phase-amplitude frequency characteristic. As follows from the preceding items, the engine assemblies in linear dynamics are the booster (pumps), inertial (the mains, the reservoirs, the turbine-pump assembly), inertial with delay (the combustion chambers and the gas generator) and passive integrating elements.

Let us consider the standard frequency characteristics of the enumerated assemblies (see Fig 1.29).

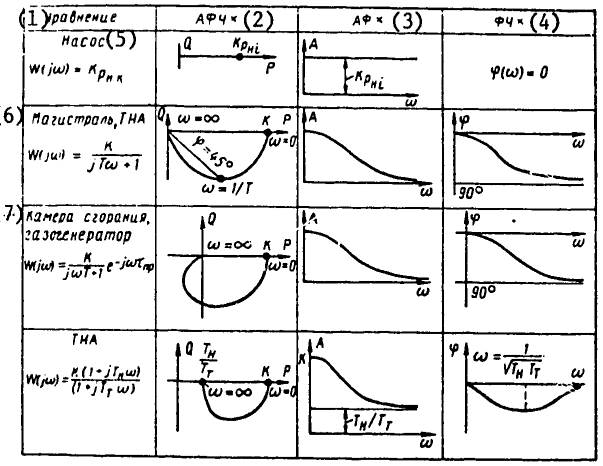

Figure 1.29. Characteristics of the Elements

Key:

1. Equation
2. Phase-amplitude frequency characteristic
3. Phase-amplitude characteristic
4. Frequency-phase characteristic
5. Pump
6. Main, turbine-pump assembly
7. Combustion chamber, gas generator

a) Pumps

The pump equation

$$\delta p_{\text{н}}(s) = K_{p_{\text{н}}.n}\delta n(s) - K_{p_{\text{н}}m}\delta \dot{m}(s) + K_{p_{\text{н}},p_{\text{вх}}}\delta p_{\text{вх}}(s).$$

The complex transfer function $W(j\omega) = K_{p_{\text{н}},x}$,

FOR OFFICIAL USE ONLY

APPROVED FOR RELEASE: 2007/02/08: CIA-RDP82-00850R000200090053-2

APPROVED FOR RELEASE: 2007/02/08: CIA-RDP82-00850R000200090053-2

Thus, the pump transmits the input vibrations, amplifies their amplitude and does not change the phase.

b) Mains, Turbine-Pump Assembly

The transfer function of the main and the turbine-pump assembly have the form

$$W(s)=\frac{K_{y.x}}{T_y s+1}.$$

The complex transfer function

$$W(j\omega)=\frac{K_{y.x}}{jT_y\omega+1}=P(\omega)+jQ(\omega);$$

$$P(\omega)=\frac{K_{y.x}}{1+T_y^2\omega^2};\quad Q(\omega)=-\frac{K_{y.x}T_y\omega}{1+T_y^2\omega^2};$$

$$A(\omega)=\frac{K_{y.x}}{\sqrt{1+T_y^2\omega^2}};$$

$$\varphi(\omega)=-\operatorname{arctg}\omega T_y.$$

In order to construct the frequency characteristic, A(ω), ϕ(ω), W(jω) are calculated for different frequencies from 0 to ∞.

In order to calculate the phase ϕ(ω) it is convenient to use the table of ϕ=ϕ(ωt) (Table 1.2).

Table 1.2

ωT	0	0,05	0,1	0,2	0,5	1	2	5	10	20	∞
φ, град (1)	0	2°50′	5°40′	11°20′	26°50′	45°	63°30′	78°40′	84°20′	87°10′	90°

Key:
1. ϕ, degrees

As follows from analysis of the functions and the graphs (see Fig 1.29) the inertial element on low frequencies amplifies the input signal and changes the phase little. For high frequencies ω>1/T vibrations occur with sharp attenuation, that is, they are poorly transmitted. The smaller the time constant T, the wider the frequency pass band.

c) Combustion Chamber and Gas Generator

The transfer function of the combustion chamber and the gas generator has the form

$$W(s)=\frac{Ke^{-s\tau_{np}}}{T\cdot s+1}.$$

APPROVED FOR RELEASE: 2007/02/08: CIA-RDP82-00850R000200090053-2

APPROVED FOR RELEASE: 2007/02/08: CIA-RDP82-00850R000200090053-2

It is possible to represent the transfer function in the form of the derivative of the transfer functions of the inertial and delay moments

$$W(j\omega)=\frac{K}{jT\omega+1}e^{-j\omega\tau_{пр}};$$

$$A(\omega)=\frac{K}{\sqrt{1+T^2\omega^2}};\ \varphi(\omega)=-\operatorname{arctg}\omega T-\omega\tau_{пр}.$$

The delay is an additional phase shift by the angle $\omega t_{пр}$

d) Pump in the TNA System

The equation for the pressure at the pump included in the TNA, depending on the flow rate of the component has the form

$$(T_{THA}s+1)\delta p_{н}(s)=-\tilde{K}_{p_{н},\dot{m}}(1+T_{н}s)\delta\dot{m}(s).$$

The transfer function

$$W(j\omega)=\tilde{K}_{p_{н},\dot{m}}\frac{(1+jT_{н}\omega)}{1+jT_{THA}\omega}.$$

The amplitude and phase characteristics

$$A(\omega)=\frac{\tilde{K}_{p_{н},\dot{m}}\sqrt{1+T_{н}^2\omega^2}}{\sqrt{1+T_{THA}^2\omega^2}};$$

$$\varphi(\omega)=-\operatorname{arctg}\frac{\omega(T_{н}+T_{THA})}{1+\omega^2T_{н}T_{THA}}.$$

The amplitude characteristic demonstrates that the element transmits low frequencies with amplification coefficient close to $\tilde{K}_{pH,\dot{m}}$. The high frequencies are suppressed. For the middle frequencies $=1/\sqrt{T_{H}T_{TNA}}$, a negative phase shift occurs.

APPROVED FOR RELEASE: 2007/02/08: CIA-RDP82-00850R000200090053-2

APPROVED FOR RELEASE: 2007/02/08: CIA-RDP82-00850R000200090053-2

CHAPTER 2. DYNAMIC ENGINE CHARACTERISTICS

2.1. Model and Structural Diagrams

The characteristics of an engine as a dynamic system and the object of control are uniquely defined by a system of linearized equations, the units describing the transient processes in the vicinity of the steady-state regime. However, the system of equations does not permit establishment of the qualitative relations between the individual units, which is necessary in the preliminary design phase.

The qualitative dynamic analysis and synthesis of an engine are conveniently realized using structural diagrams.

The structural diagram of the engine is the system depicting the interrelation of the dynamic elements described by the operator equations.

The structural diagram depends on the pyro(pneumo) hydraulic system of the engine, but it differs from it with respect to content, for it depicts not the units, but the dynamic elements and the relations between them.

The schematic diagram is a unique diagram for the given engine. The structural diagram for the same engine can be somewhat dependent on the method of breakdown of the engine into elements and the system of variables. Thus, the structural diagram depicts not only the schematic diagram of the engine, but the specific peculiarities of the processes in the units which are taken into account in the mathematical model of the engine.

The initial data for constructing the structural diagrams are the engine diagram and its mathematical model presented in operator form.

The symbolic notation for the operations on the variables closing the individual elements are taken for the construction of the structural diagrams (see Fig 2.1).

APPROVED FOR RELEASE: 2007/02/08: CIA-RDP82-00850R000200090053-2

APPROVED FOR RELEASE: 2007/02/08: CIA-RDP82-00850R000200090053-2

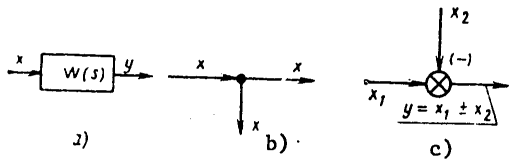

Figure 2.1. Symbols of the structural diagrams: a -- element; b -- junction; c -- adder

2.1.1. Structural Diagram of the Engine with Pressurized Feed System

The engine equations represented in operator form are presented below.

The thrust chamber equation

$$\delta p_{\kappa}(s)=W_{p_{\kappa},\dot{m}_{o\kappa}}(s)\,e^{-s\tau_{\text{пр}}}\delta\dot{m}_{o\kappa}(s)+W_{p_{\kappa},\dot{m}_{r}}e^{-s\tau_{\text{пр}}}\delta\dot{m}_{r}(s).$$

The equation of the lines from the tanks to the chamber

$$\begin{aligned}\delta\dot{m}_{o\kappa}(s)&=W_{\dot{m}_{o\kappa}\cdot p_{\delta.o\kappa}}(s)\,\delta p_{\delta.o\kappa}(s)-W_{\dot{m}_{o\kappa},p_{\kappa}}(s)\,\delta p_{\kappa}(s)-\\&\quad-W_{\dot{m}_{o\kappa},\xi_{o\kappa}}(s)\,\delta\xi_{o\kappa}(s);\\ \delta\dot{m}_{r}(s)&=W_{\dot{m}_{r},p_{\delta.r}}(s)\,\delta p_{\delta.r}(s)-W_{\dot{m}_{r},p_{\kappa}}\delta p_{\kappa}(s)-W_{\dot{m}_{r},\xi_{r}}\delta\xi_{r}(s).\end{aligned}\qquad(2.1)$$

The transfer functions are defined by the time constants and the boost factors

$$\begin{aligned}W_{p_{\kappa}\cdot\dot{m}_{l}}(s)&=\frac{K_{p_{\kappa},\dot{m}_{l}}}{T_{\kappa}s+1};\quad W_{\dot{m}_{l},p_{\kappa}}=\frac{K_{\dot{m}_{l}\cdot p_{\kappa}}}{T_{Ml}s+1};\\ W_{\dot{m}_{l},p_{\delta l}}(s)&=\frac{K_{\dot{m}_{l},p_{\delta l}}}{T_{Ml}s+1};\quad W_{\dot{m}_{l},\xi_{l}}(s)=\frac{K_{\dot{m}_{l},\xi_{l}}}{T_{Ml}s+1}.\end{aligned}\qquad(2.2)$$

In accordance with the system (2.1) the structural diagram of the engine has the form shown in Fig 2.2.

FOR OFFICIAL USE ONLY

APPROVED FOR RELEASE: 2007/02/08: CIA-RDP82-00850R000200090053-2

APPROVED FOR RELEASE: 2007/02/08: CIA-RDP82-00850R000200090053-2

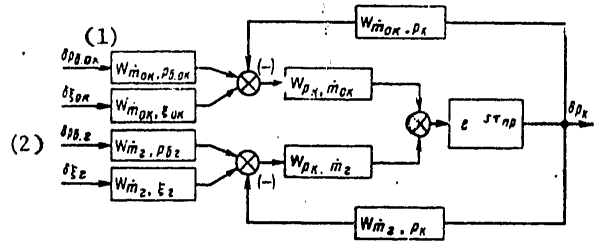

Figure 2.2. Structural diagram of the engine with pressurized feed system

Key:
1. tank, oxidizing agent
2. tank, fuel

As follows from the structural diagram, the output signals of the engine are the pressures in the tanks ($p_{\text{tank } i}$) and the hydraulic drag coefficients of the lines of the thrust chamber (ξ_i), which can be taken as the control inputs (the regulating parameters).

Positive feedback exists between the lines and the chamber, that is, the pressure in the chamber depends on the flow rate of the oxidizing agent and the combustible fuel component, and there is negative feedback -- the flow rates of the components depend on the pressure in the thrust chamber. The latter relations are realized by the transfer functions of the lines $W_{\dot{m}_i, p_k}$.

2.1.2. Structural Diagram of the Engine with Two-Component Gas Generator

The mathematical model

$$\delta p_к(s) = W_{p_к, \dot{m}'_{c.x}}(s)\, e^{-s\tau'_{пр}} \delta \dot{m}'_{ок}(s) + W_{p_к, \dot{m}'_г}(s)\, e^{-s\tau'_{пр}} \delta \dot{m}'_г(s);$$

$$\delta p_{гг}(s) = W_{p_{гг}, \dot{m}''_{ок}}(s) e^{-s\tau''_{пр}} \delta \dot{m}''_{ок}(s) + W_{p_{гг}, \dot{m}''_г} e^{-s\tau'_{пр}} \delta \dot{m}''_г(s) +$$

$$+ W_{p_{гг}, K''}(s)\, e^{-s\tau''_{пр}} \delta K''(s); \qquad (2.3)$$

APPROVED FOR RELEASE: 2007/02/08: CIA-RDP82-00850R000200090053-2

APPROVED FOR RELEASE: 2007/02/08: CIA-RDP82-00850R000200090053-2

$$\delta K''(s)=\delta\dot{m}''_{\text{ок}}(s)-\delta\dot{m}''_{\text{г}}(s);$$

$$\delta\dot{m}'_l=W_{\dot{m}''_l,\,p_{\text{н}l}}(s)\,\delta p_{\text{н}l}(s)-W_{\dot{m}'_l,\,p_{\text{к}}}(s)\,\delta p_{\text{к}}(s)-W_{\dot{m}'_l,\,\xi'_l}(s)\,\delta\xi'_l.$$

$$\delta\dot{m}''_l=W_{\dot{m}''_l,\,p_{\text{н}l}}(s)\,\delta p_{\text{н}l}(s)-W_{\dot{m}''_l,\,p_{\text{гг}}}(s)\,\delta p_{\text{гг}}(s)-W_{\dot{m}''_l,\,\xi''_l}(s)\,\delta\xi''_l;$$

$$\delta\dot{m}_l=K_{\dot{m}_l,\,\dot{m}'_l}\delta\dot{m}'_l(s)+K_{\dot{m}_l,\,\dot{m}''_l}\delta\dot{m}''_l(s);$$

$$\begin{aligned}\delta p_{\text{н.ок}}(s)=&W_{p_{\text{н.о}},\,p_{\text{гг}}}\delta p_{\text{гг}}(s)+W_{p_{\text{н.ок}},K''}(s)\,\delta K''(s)-\\&-W_{p_{\text{н.ок}},\dot{m}_{\text{ок}}}(s)\,\delta\dot{m}_{\text{ок}}(s)+W_{p_{\text{н.ок}},\dot{m}_{\text{г}}}(s)\,\delta\dot{m}_{\text{г}}(s)+\\&+W_{p_{\text{н.ок}},\,p_{\text{вх.ок}}}(s)\,\delta p_{\text{вх.ок}}(s);\end{aligned}$$

$$\begin{aligned}\delta p_{\text{н.г}}(s)=&W_{p_{\text{н.г}},\,p_{\text{гг}}}\delta p_{\text{гг}}(s)+W_{p_{\text{н.г}},\dot{m}_{\text{ок}}}(s)\,\delta\dot{m}_{\text{ок}}(s)-\\&-W_{p_{\text{н.г}},\dot{m}_{\text{г}}}(s)\,\delta\dot{m}_{\text{г}}(s)+W_{p_{\text{н.г}},K'}(s)\,\delta K'(s)+W_{p_{\text{н.г}},\,p_{\text{вх.г}}}(s)\,\delta p_{\text{вх.г}}(s).\end{aligned}\qquad(2.3)$$

The structural diagram of the engine is presented in Fig 2.3. As follows from the diagram, the input signals are the pressures of the input to the pumps and the hydraulic drag coefficients of the lines to the chamber (ξ_i') and the gas generator (ξ_i''). When analyzing the structural diagram, attention is given to the presence of two groups of circuits, inside which basically all of the feedbacks are closed; these are the "GG-TNA-GG lines" and "thrust chamber-thrust chamber lines" circuits.

Complex interaction takes place between the elements of the engine by means of the cross positive and negative feedbacks. The flow rates of the fuel components depend on the pressure after the pumps (the impeller rpm of the TNA) and the pressure in the combustion chamber (the gas generator). In turn, the magnitudes of the flow rates in each of the lines influence the pressure created by the pump which depends on the pressure in the gas generator. All of the feedbacks are closed on the turbine-pump assembly and act on the thrust chamber only by changing the TNA impeller rpm.

Therefore, the turbine-pump assembly has defining influence on the engine dynamics. The turbine-pump assembly is an inertial element with relatively large time constant by comparison with the other elements. Consequently, for sufficiently large frequencies of the disturbances and the useful signals coming from the gas generator, its rpm cannot vary, which means that the operating conditions of the thrust chamber also cannot change. At low oscillation frequencies of the input signals the turbine-pump unit can change rpm and transmit signals to the thrust chamber. Thus, in the engine the turbine-pump assembly is the filtering element.

FOR OFFICIAL USE ONLY

APPROVED FOR RELEASE: 2007/02/08: CIA-RDP82-00850R000200090053-2

APPROVED FOR RELEASE: 2007/02/08: CIA-RDP82-00850R000200090053-2

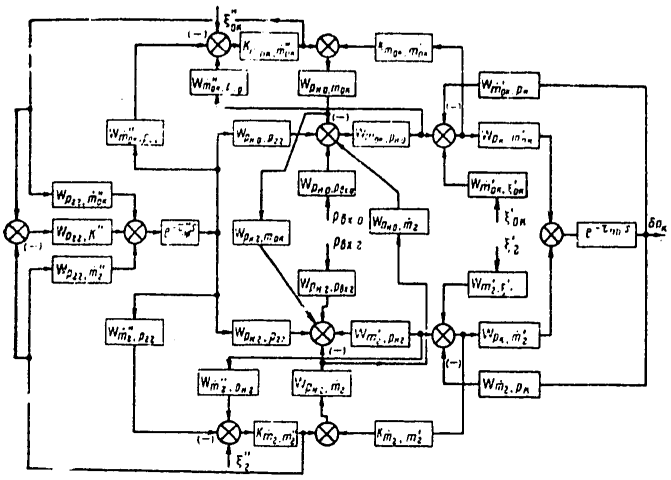

Figure 2.3. Structural diagram of the engine with the pump feed system

The structural diagram with afterburning of the generator gas differs insignificantly from the structural diagram of the engine without afterburning. Instead of feeding the liquid component to the combustion chamber without afterburning, a gasified component is fed through the gas line with the afterburning system. This peculiarity is theoretical and essentially has no effect on the engine dynamics. Whereas the flow rate of the liquid component reaching the thrust chamber depends only on the TNA impeller rpm and the pressure in the chamber, the gas parameters in the gas line basically depend on the gas pressure and temperature in the gas generator and depend only slightly on the TNA impeller rpm.

Consequently, in the system with afterburning there is a direct (positive) relation between the gas generator and the combustion chamber through the gas line not having filtering properties similar to the properties of the TNA. Therefore in such engines the operating conditions of the thrust chamber are sensitive to the disturbances coming from the gas generator.

2.2. Engine Transfer Functions

For analysis of the stability and determination of the regulating inputs (regulating parameters) it is necessary to know the engine transfer functions.

The transfer function reflects the mathematical relation between the input and output signals and is the ratio of the Laplace transforms of the output signal to the input

APPROVED FOR RELEASE: 2007/02/08: CIA-RDP82-00850R000200090053-2

APPROVED FOR RELEASE: 2007/02/08: CIA-RDP82-00850R000200090053-2

$$W_{y,x}(s)=\frac{y_i(s)}{x(s)}.$$

Knowing the transfer function, it is possible to write the equation for the relation

$$y(s)=W_{y,x}(s)x(s). \tag{2.4}$$

Since the transfer functions are ratios of polynomials

$$W(s)=\frac{b_m s^m+b_{m-1}s^{m-1}+..+b_1 s+b_0}{a_n s^n+a_{n-1}s^{n-1}+...+a_1 s+a_0},$$

the equation of this relation can be rewritten in the form

$$\begin{aligned}&(a_n s^n+a_{n-1}s^{n-1}+\ldots+a_1 s+a_0)y(s)=\\&=(b_m s^m+b_{m-1}s^{m-1}+\ldots+b_1 s+b_0)x(s).\end{aligned} \tag{2.5}$$

Using the Laplace expressions $y(s)=\int_{-\infty}^{\infty} e^{-st}y(t)\,dt$ or for the derivatives $s^n \div \frac{d^n y(t)}{dt^n}$ from equation (2.5) it is possible to proceed to the differential equation

$$\begin{aligned}&a_n\frac{d^n y(t)}{dt^n}+a_{n-1}\frac{d^{n-1}y(t)}{dt^{n-1}}+\ldots+a_1\frac{dy(t)}{dt}+a_0 y(t)=\\&=b_m\frac{d^m x(t)}{dx^m}+b_{m-1}\frac{d^{m-1}x(t)}{dt^{m-1}}+\ldots+b_1\frac{dx(t)}{dt}+b_0 x(t).\end{aligned}$$

The last equation permits determination of the reaction of the engine, that is, the change in the output parameter with time y(t) for the given disturbance x(t).

The transfer function permits a very important characteristic of the engine to be obtained simply -- the boost factor

$$K_A=\lim_{s\to 0}W(s)=\frac{b_0}{a_0}.$$

The analytical expression for the transfer function can be determined by transformation of the structural diagrams, by the method of determinants and the matrix method.

2.2.1. Method of Transformation of Structural Diagrams

In automatic control theory [5] a structural analysis method has been developed which permits as complex a structural diagram as one might like

APPROVED FOR RELEASE: 2007/02/08: CIA-RDP82-00850R000200090053-2

APPROVED FOR RELEASE: 2007/02/08: CIA-RDP82-00850R000200090053-2

to be converted to one equivalent element with the transfer function

$$W(s)=F[W_{j,i}(s)].$$

In order to determine the transfer function, the branched structural diagram is rearranged into a single-loop diagram by transformations of it according to defined rules of combining elements into one equivalent element and carrying the elements through the adders and angles [sic].

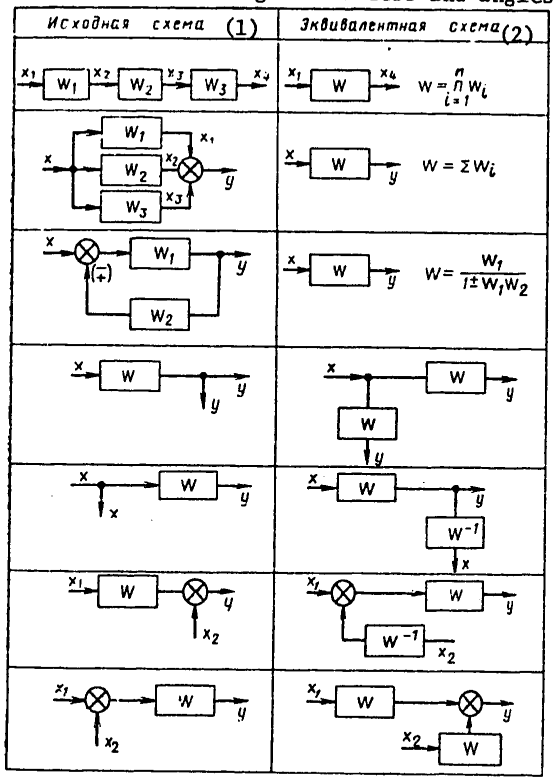

Figure 2.4. Transformations of structural diagrams

Key:
1. Initial diagram
2. Equivalent diagram

The rules of transformation of structural diagrams are shown in Fig 2.4.

In the example of the structural diagram in Fig 2.2 let us demonstrate how we obtained the transfer function of the pressure in the chamber with respect to any disturbance $\delta p_{\text{tank i}}$, $\delta \xi_i$.

APPROVED FOR RELEASE: 2007/02/08: CIA-RDP82-00850R000200090053-2

APPROVED FOR RELEASE: 2007/02/08: CIA-RDP82-00850R000200090053-2

The transfer function is determined successively for each disturbance. Others are assumed equal to zero in this case.

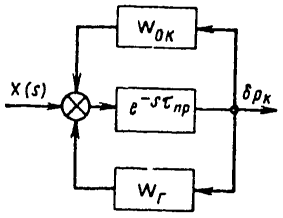

Figure 2.5. Intermediate structural diagram

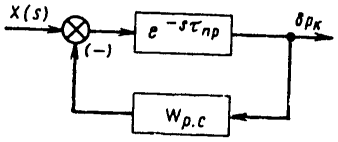

Figure 2.6. Structural diagram of the engine

The structural diagram in Fig 2.2 is converted to the diagram with one adder before the delay element; as a result, we obtain the diagram in Fig 2.5, where

$$\left.\begin{aligned} W_{ок}(s)&=W_{\dot m_{ок},\, p_к} W_{p_к,\, \dot m_{ок}};\\ W_{г}(s)&=W_{\dot m_{г},\, p_к} W_{p_к,\, \dot m_{г}}. \end{aligned}\right\} \qquad (2.6)$$

X(S) is the generalized disturbance:

$$X(s)=W_{\dot m_{ок},\, p_{б.ок}} W_{p_к,\, \dot m_{ок}} \delta p_{б.ок}(s)+W_{\dot m_{ок},\, \xi_{ок}} W_{p_к,\, \dot m_{ок}} \delta \xi_{ок}(s)+$$
$$+W_{\dot m_{г},\, p_{б.г}} W_{p_к,\, \dot m_{г}} \delta p_{б.г}(s)+W_{\dot m_{г},\, \xi_{г}} W_{p_к,\, \dot m_{г}} \delta \xi_{г}(s).$$

The structural diagram in Fig 2.5 is finally transformed into the diagram with feedback, Fig 2.6,

where $$W_{p.c}(s)=W_{ок}(s)+W_{г}(s). \qquad (2.7)$$

$W_{p.c}$ is the transfer function of the open system without considering τ_{conv} and with consideration of $W'_{p.c}(s)=e^{-\tau_{np}s} W_{p.c}(s)$.

The transfer function of the closed system

$$\Phi(s)=\frac{e^{-s\tau_{np}}}{1+W'_{p.c}(s)}. \qquad (2.8)$$

The equation of the relation between any input signal and the output signal has the form

$$\delta p_к(s)=\Phi(s)X(s), \qquad (2.9)$$

where X(S) is the input signal.

APPROVED FOR RELEASE: 2007/02/08: CIA-RDP82-00850R000200090053-2

APPROVED FOR RELEASE: 2007/02/08: CIA-RDP82-00850R000200090053-2

As an example, let us define the transfer functions for the pressure in the combustion chamber with respect to $\delta p_{\text{tank, ox}}$ and $\delta\xi_{ox}$ and the boost factors.

The initial transfer functions will be expressed in terms of the time constants and the boost factors

$$W'_{p.c}(s)=\frac{K_{\dot m_{ок},\,p_к}K_{p_к,\,\dot m_{ок}}(T_{мг}s+1)+K_{\dot m_г,\,p_к}K_{p_к,\,\dot m_г}(T_{мок}s+1)}{(T_{мок}s+1)(T_{мг}s+1)(T_к s+1)}. \qquad (2.10)$$

The boost factor of the open system is

$$K_{p.c}=\lim_{s\to 0}W_{p.c}=K_{\dot m_{ок},\,p_к}K_{p_к,\,\dot m_{ок}}+K_{\dot m_г,\,p_к}K_{p_к,\,\dot m_г}. \qquad (2.11)$$

The transfer functions with respect to the input effects

$$W_{p_к,\,p_{б.ок}}(s)=\Phi(s)X_{p_{б.ок}}(s)=\frac{e^{-s\tau_{пр}}W_{\dot m_{ок},\,p_{б.к}}W_{p_к,\,\dot m_{ок}}}{1+e^{-s\tau_{пр}}W_{p.c}(s)};$$
$$W_{p_к,\,\xi_{ок}}(s)=\Phi(s)X_{\xi_{ок}}(s).$$

The boost factor

$$K_{p_к,\,p_{б.ок}}=\frac{K_{\dot m_{ок},\,p_{б.ок}}K_{p_к,\,\dot m_{ок}}}{1+K_{p.c}};$$
$$K_{p_к,\,\xi_{ок}}=\frac{K_{\dot m_{ок},\,\xi_{ок}}K_{p_к,\,\dot m_{ок}}}{1+K_{p.c}}.$$

In some cases, for example, when analyzing the transmission of the signal in the engine system it is more convenient to use not the structural diagram, but a graph.

The set of vertices and lines is called a graph. Each line corresponds to two vertices -- the beginning and end of the line. The transfer functions can be compared to the vertex and line.

The basic properties of the graphs of the signal transmission are as follows. The vertex noted on the graph by a point corresponds to some variable (signal) of the investigated system. The line of the graph depicted by the line with an arrow indicating the direction of transmission of the signal, has a vertex -- the beginning (the input variable) and a vertex -- the end (the output variable). The output variable of the line is obtained as a result of conversion of the input variable by the corresponding operator. If several lines approach one vertex, then the

APPROVED FOR RELEASE: 2007/02/08: CIA-RDP82-00850R000200090053-2

APPROVED FOR RELEASE: 2007/02/08: CIA-RDP82-00850R000200090053-2

value corresponding to this vertex is obtained by algebraic summation of the output values of these lines.

A direct comparison exists between the structural diagram and signal transmission graph: a rectangle (element) of the structural diagram corresponds to a line, and a signal transmission line corresponds to a vertex on the graph.

In Fig 2.7, the diagram and the graph of the transmission of the signal of the pressure in the tank to the thrust chamber are depicted simultaneously for comparison.

The graph conversion rules are similar to the structural diagram conversion rule (see Fig 2.8).

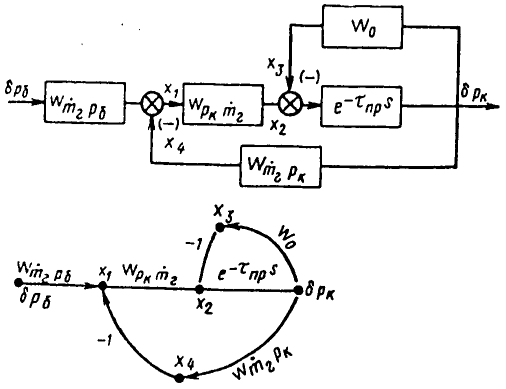

Figure 2.7. Structural diagram and its graph

2.2.2. Method of Determinants

The method of determinants is based on the known rules for the solution of a system of linear algebraic equations. The system of equations of the engine is written so that in the lefthand side will be terms with unknown parameters, and in the righthand side, terms only with the input signals and disturbances

$$\{a_{y_i y_j} \delta y_{jl}\} = \{b_{y_{ji} i} \delta x_i\}. \tag{2.12}$$

Then the transfer function $W_{y_j x_i}$ is defined as follows:

$$W_{y_j x_l}(s) = \frac{\Delta_{y_j x_l}}{\Delta}, \tag{2.13}$$

FOR OFFICIAL USE ONLY

APPROVED FOR RELEASE: 2007/02/08: CIA-RDP82-00850R000200090053-2

APPROVED FOR RELEASE: 2007/02/08: CIA-RDP82-00850R000200090053-2

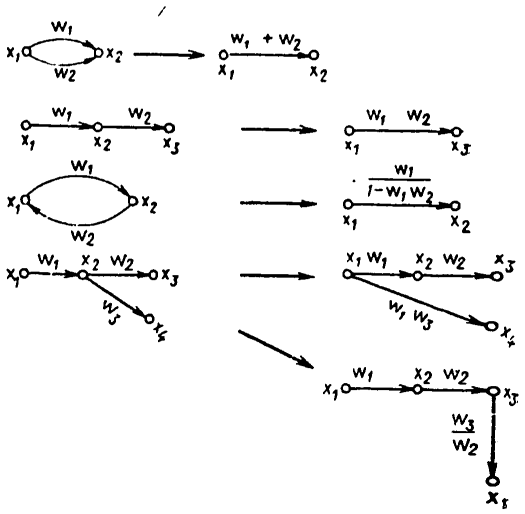

Figure 2.8. Graph conversion rule

where Δ is the principal determinant of the system made up of the coefficients on δy; $\Delta_{y_j x_i}$ is the auxiliary determinant Δ in which the column of coefficients on y_i is replaced by the column of coefficients on x_i from the righthand side of the system of equations.

As an example let us determine $W_{p_k, p_{tank,\ ox}}$ from the system 2.1 which is written in the form

$$\delta p_к(s) - W_{p_к, \dot{m}_{ок}}(s)\delta\dot{m}_{ок}(s) - W_{p_к, \dot{m}_г}(s)\delta\dot{m}_г(s) = 0;$$

$$W_{\dot{m}_{ок}, p_к}(s)\delta p_к(s) + \delta\dot{m}_{ок}(s) = W_{\dot{m}_{ок}, p_{б.ок}}\delta p_{б.ок}(s) - W_{\dot{m}_{ок}, \xi_{ок}}\delta\xi_{ок}(s);$$

$$W_{\dot{m}_г, p_к}(s)\delta p_к(s) + \delta\dot{m}_г(s) = W_{\dot{m}_г, p_{б.г}}\delta p_{б.г}(s) - W_{\dot{m}_г, \xi_г}\delta\xi_г(s).$$

The principal determinant of the system

$$\Delta = \begin{vmatrix} 1 & -W_{p_к, \dot{m}_{ок}} & -W_{p_к, \dot{m}_г} \\ W_{\dot{m}_{ок}, p_к} & 1 & 0 \\ W_{\dot{m}_г, p_к} & 0 & 1 \end{vmatrix}$$

The auxiliary determinant

APPROVED FOR RELEASE: 2007/02/08: CIA-RDP82-00850R000200090053-2

APPROVED FOR RELEASE: 2007/02/08: CIA-RDP82-00850R000200090053-2

$$\Delta_{p_к,\ p_{б.ок}}=\begin{vmatrix} 0 & -W_{p_к,\ \dot{m}_{ок}} & -W_{p_к,\ \dot{m}_г} \\ W_{\dot{m}_{ок},\ p_{б.ок}} & 1 & 0 \\ 0 & 0 & 1 \end{vmatrix}$$

The transfer function of the engine

$$W_{p_к,\ p_{б.ок}}(s)=\frac{\Delta_{p_к,\ p_{б.ок}}}{\Delta}.$$

2.2.3. Matrix Method

The engine is a multiloop (multidimensional) system containing an arbitrary number n of output variables P, p_k, K... and ℓ input effects (p_{tank}, ξ_i and so on). The relation between the output variables and the input effect can be described by nℓ transfer functions

$$y_к=\sum_{i=1}^{l}\Phi_{кi}(s)x_i, \qquad (2.14)$$

where y_k are the output variables; x_i are the input effects; Φ_{ki} is the transfer function of the closed system determining the dependence of the k-th output variable y_k on the x_i effect. It is convenient to represent the system of equations (2.14) in vector form:

$$Y=\Phi(s)X, \qquad (2.15)$$

where

$Y=\begin{Vmatrix} P \\ I_y \\ p_к \\ \vdots \\ y_n \end{Vmatrix}$ is the column matrix (n-dimensional vector) of the output variables;

$X=\begin{Vmatrix} p_{б1} \\ \xi_i \\ \vdots \\ x_l \end{Vmatrix}$ is the column matrix (ℓ-dimensional vector) of the effects

$\Phi(s)=\begin{Vmatrix} \Phi_{11}(s) & \Phi_{12}(s) & \dots & \Phi_{1l}(s) \\ \Phi_{21}(s) & \Phi_{22}(s) & \dots & \Phi_{2l}(s) \\ \dots & \dots & \dots & \dots \\ \Phi_{n1}(s) & \Phi_{n2}(s) & \dots & \Phi_{nl}(s) \end{Vmatrix}$ is a matrix of the type of nXℓ transfer functions Φ_{ki} of the closed system.

FOR OFFICIAL USE ONLY

APPROVED FOR RELEASE: 2007/02/08: CIA-RDP82-00850R000200090053-2

APPROVED FOR RELEASE: 2007/02/08: CIA-RDP82-00850R000200090053-2

The matrix transfer function of the closed system $\Phi(s)$ is defined by formulas analogous to the formulas presented above or with respect to structural diagram except for the difference that instead of the transfer functions the matrices are used in the given case.

In particular, analogously to formula (2.8) for the one-dimensional system

$$\Phi(s)=[E_m+W(s)]^{-1}W_{y,x}(s), \tag{2.16}$$

where

$$W(s)=\begin{Vmatrix} W_{11}(s) & W_{12}(s) & \dots & W_{1n}(s) \\ W_{21}(s) & W_{22}(s) & \dots & W_{2n}(s) \\ \dots & \dots & \dots & \dots \\ W_{n1}(s) & W_{n2}(s) & \dots & W_{nn}(s) \end{Vmatrix}$$

The matrix is of the type of nXn transfer function W_{ki}. $W_{y,x}(s)$ is the matrix transfer function of the open system.

$$W_{y,x}(s)=\begin{Vmatrix} W_{y_1x_1}(s) & W_{y_1x_2}(s) & \dots & W_{y_1x_l}(s) \\ W_{y_2x_1}(s) & W_{y_2x_2}(s) & \dots & W_{y_2x_l}(s) \\ \dots & \dots & \dots & \dots \\ W_{y_nx_1}(s) & W_{y_nx_2}(s) & \dots & W_{y_nx_l}(s) \end{Vmatrix}$$

$W_{y,x}(s)$ is the matrix of the type of nXℓ transfer functions of the unit; E is a unit matrix of the type of nXn (the elements of its principal diagonal are equal to one, and the rest are equal to zero); $[E+W(s)]^{-1}$ is the inverse matrix.

2.3. Frequency Characteristics of the Engine

For analysis of the stability and the reaction of the engine to the input disturbances, complex transfer functions or phase-amplitude frequency characteristics are used.

The phase-amplitude characteristics are obtained from the operator transfer functions by substitution in place of $s=j\omega$, where $j=\sqrt{-1}$, and ω is the angular frequency

$$W(j\omega)=W(s)|_{s=j\omega}=P(\omega)+jQ(\omega)=|W(j\omega)|\,e^{j\varphi(\omega)}, \tag{2.17}$$

where $P(\omega)$ is the real part of the phase-amplitude characteristic; $Q(\omega)$ is the imaginary part

$$|W(j\omega)|=\sqrt{P^2(\omega)+Q^2(\omega)},$$

$$\varphi(\omega)=\operatorname{arctg}\frac{Q(\omega)}{P(\omega)}-\text{phase}.$$

APPROVED FOR RELEASE: 2007/02/08: CIA-RDP82-00850R000200090053-2

APPROVED FOR RELEASE: 2007/02/08: CIA-RDP82-00850R000200090053-2

Thus, for example, for the engine with a pressurized feed system

$$W_{p_к\, p_{б.ок}}(j\omega)=\frac{e^{-j\omega\tau_{пр}}W_{\dot m_{ок},\, p_{б.ок}}(j\omega)\,W_{p_к,\, \dot m_{ок}}(j\omega)}{1+W_{р.с}(j\omega)\,e^{-j\omega\tau_{пр}}}.$$

Let us substitute the expressions for the transfer functions in the last equation, setting $\tau_{пр}=0$ (the consideration of $\tau_{пр}$ is presented in subsequent items)

$$W_{p_к,\, p_{б.ок}}(j\omega)=-\frac{jb_1\omega+b_0}{a_3(j\omega)^3+a_2(j\omega)^2+a_1(j\omega)+a_0}, \qquad (2.18)$$

where

$$b_1=T_{мг}K_{\dot m_{ок},\, p_{б.ок}}K_{p_к,\, \dot m_{ок}};$$
$$b_0=K_{\dot m_{ок},\, p_{б.ок}}K_{p_к,\, \dot m_{ок}};$$
$$a_3=T_кT_{мок}T_{мг};$$
$$a_2=T_кT_{мок}+T_кT_{мг}+T_{мок}T_{мг};$$
$$a_1=T_к+T_{мок}(1+K_{p_к,\, \dot m_г}K_{\dot m_г,\, p_к})+T_{мг}(1+K_{p_к,\, \dot m_{ок}}K_{\dot m_{ок},\, p_к});$$
$$a_0=1+K_{р.с};$$
$$P(\omega)=\frac{b_0(a_0-a_2\omega^2)-b_1\omega(a_3\omega^3-a_1\omega)}{(a_0-a_2\omega^2)^2+(a_3\omega^3-a_1\omega)^2};$$
$$Q(\omega)=\frac{[b_1\omega(a_0-a_2\omega^2)^2+b_0(a_3\omega^3-a_1\omega)}{(a_0-a_2\omega^2)^2+(a_3\omega^3-a_1\omega)^2}.$$

Varying the frequency ω from 0 to ∞, let us construct $W(j\omega)$ in the plane of the compiex variables.

Fig 2.9 shows the phase-amplitude characteristic $W_{pkPtank}$ in the engine with a pressurized feed system.

Figures 2.10 and 2.11 show the amplitude characteristics of the engine with a pump feed system without afterburning of the generator gas.

The phase-amplitude characteristics make it possible to establish the relation between the units and their role in the dynamic processes.

The interrelation of the phase-amplitude characteristic of the units in the engine is determined under other equal conditions by the location of the unit with respect to the turbine-pump assembly.

On variation of the hydraulic drag of the gas generator lines, the amplitude of the pressure oscillations in the gas generator (the gas generator is located before the TNA) varies insignificantly, in practice in the entire frequency range, that is, there is a wide frequency transmission band. The amplitude of the oscillations of the parameters of the units located after the TNA depends only on the frequency. With an increase in

FOR OFFICIAL USE ONLY

APPROVED FOR RELEASE: 2007/02/08: CIA-RDP82-00850R000200090053-2

APPROVED FOR RELEASE: 2007/02/08: CIA-RDP82-00850R000200090053-2

frequency, the amplitude of the oscillation decreases. This is explained by the fact that the turbine-pump assembly has filtering properties and does not transmit disturbances with high frequencies.

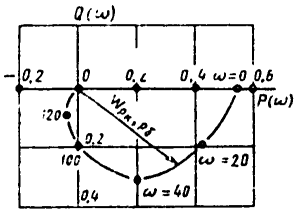

Figure 2.9. Phase-amplitude characteristic of the engine with pressurized feed system

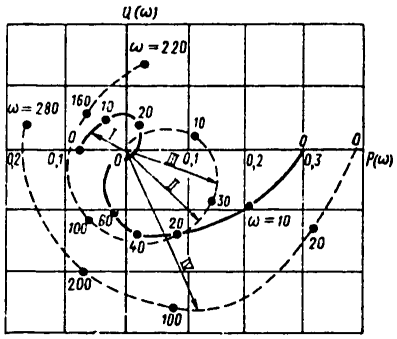

Figure 2.10. Phase-amplitude characteristic of an engine without afterburning of the generator gas:

$I - W_{\rho_к, \xi^*_{ок}}$; $II - W_{\rho_к, \xi^*_г}$; $III - W_{\rho_{гг}, \xi^*_{ок}}$;

$IV - W_{\rho_{гг}, \xi^*_г}$

On variation of the hydraulic drag of the thrust chamber lines (see Fig 2.11) the turbine-pump assembly has no significant effect on the frequency characteristics of the parameters although a natural decrease in amplitude of the pressure fluctuations in the gas chamber with an increase in frequency is observed.

The phase-amplitude characteristics indicate that the variation of the hydraulic drag coefficient of the fuel line for the combustible component has the strongest effect on the engine parameters. In this case, the largest static boost factors are obtained W(0)=K. Therefore it is expedient to install the regulating element for adjusting the operating conditions in the fuel line for the combustible component.

In Fig 2.12 we see the phase-amplitude characteristics of the engine with afterburning of the generator gas which differ significantly from the phase-amplitude characteristics of the engine without afterburning. In engines with afterburning of the generator gas, the gas generator and the turbine are connected to the chamber by the gas line. This explains the absence of a clearly expressed filtering property of the turbine-pump assembly. Between the chamber and the gas generator there is no difference in frequency characteristics. The pass bands of the frequencies are approximately the same. The disturbances occurring in the gas generator are in practice transmitted to the thrust chamber without change.

APPROVED FOR RELEASE: 2007/02/08: CIA-RDP82-00850R000200090053-2

APPROVED FOR RELEASE: 2007/02/08: CIA-RDP82-00850R000200090053-2

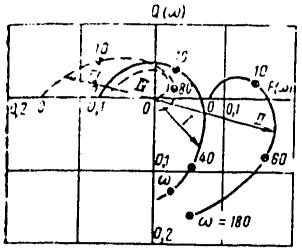

Figure 2.11. Phase-amplitude characteristic of the engine without afterburning of the generator gas: $I - W_{p_к, \xi'_{ок}}$; $II - W_{p_к, \xi'_г}$; $III - W_{p_{гг}, \xi'_{ок}}$; $IV - W_{p_{гг}, \xi'_г}$

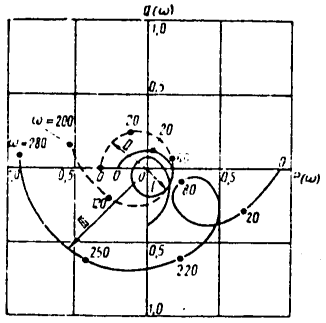

Figure 2.12. Phase-amplitude characteristic of the engine with afterburning of the generator gas:

$I - W_{p_{гг}, \xi^*_{ок}}$; $II - W_{p_к, \xi^*_{ок}}$; $III - W_{p_{гг}, \xi'_г}$

2.4. Stability

2.4.1. General Stability Characteristic

Various disturbances of an external and internal nature influence the engine. In the case of unfavorable combinations of dynamic properties of the units these disturbances can lead to unstable operating conditions of the engine. The process of the development and the operation and maintenance of the engines indicates that the causes of loss of stability are varied, but all of them are connected with various types of oscillatory processes in the engine systems.

The unstable operating conditions are characterized by fluctuations of the parameters of the operating process with different amplitude and frequency and they are the basic causes of the occurrence of engine emergencies.

The oscillations of the parameters of the operating process cause vibrations of the structural elements, which leads to breakage of the parts and units, separation of the lines, rupture of the shells and other failures. The resonance vibrations are especially dangerous, which occur on coincidence of the natural frequencies of the mechanical vibrations of the structural elements with the oscillation frequency of the parameters of the operating process.

APPROVED FOR RELEASE: 2007/02/08: CIA-RDP82-00850R000200090053-2

APPROVED FOR RELEASE: 2007/02/08: CIA-RDP82-00850R000200090053-2

BY

APPROVED FOR RELEASE: 2007/02/08: CIA-RDP82-00850R000200090053-2

APPROVED FOR RELEASE: 2007/02/08: CIA-RDP82-00850R000200090053-2

The oscillations of the engine parameters are classified by various attributes. The classification of the oscillations by frequency has become widespread.

With respect to frequency range, the vibrations are provisionally broken down into three groups [10]:

The low-frequency, all-engine vibrations with a frequency of ω=1-50 hertz;

The low-frequency vibrations in the individual units with a frequency ω=50-300 hertz;

The high-frequency vibrations in the chamber or the gas generator of the engine with a frequency above 300 hertz.

The high-frequency vibrations are the acoustic vibrations of longitudinal and transverse type. For investigation of them the nonlinear dynamics must be used considering the acoustic effects in the gas reservoirs and channels, the complex physical-chemical processes of combustion and other factors.

In view of the fact that in the given book the linear dynamic model is used which in general is not acceptable for high-frequency vibrations, hereafter the problems of stability will be investigated as applied to the low-frequency vibrations.

The low-frequency vibrations of the first type (the all-engine type) are caused by various things, the main ones of which are cavitation in the pumps, vibrations in the regulation and control system circuits and vibrations in the system made up of the rocket hull and engine.

In modern engines, volute centrifugal pumps are used to feed the fuel components from the tanks to the chamber and the gas generator. In the volutecentrifugal pump, the minimum pressure region is the flow section of the screw; therefore, as experience has shown, cavitation always exists in practice in the screws, which causes vibration in the system.

The vibrations occur because the cavitation cavity enlarges the space between the blades of the screw and, in turn, causes a decrease in pressure in the entrance section of the screw. On the other hand, the magnitude of the cavitation cavity is determined by the speed of the liquid which depends on the pressure.

Thus, positive feedback is created which leads to the occurrence of vibrations.

The results of the theoretical and experimental studies have demonstrated that the frequency and amplitude cavitation vibrations depend on the pump impeller rpm and the pressure at the entrance to the pump, Fig 2.13.

APPROVED FOR RELEASE: 2007/02/08: CIA-RDP82-00850R000200090053-2

APPROVED FOR RELEASE: 2007/02/08: CIA-RDP82-00850R000200090053-2

The rocket hull is an elastic system in which under defined conditions vibrations can occur [17, 31]. The vibrations of the rocket hull cause vibrations of the liquid in the tank, the lines and the entrance to the pumps, and the latter, pressure fluctuations in the chamber (thrust).

The thrust fluctuations in turn cause vibrations of the elastic hull.

Thus, feedback exists between the hull vibrations and the engine thrust. Both the rocket hull and the liquid in the line have a natural vibration frequency. The natural frequency of vibration of the rocket hull varies with time.

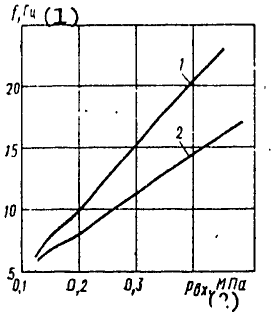

Figure 2.13. Frequency of the cavitation vibrations as a function of the pump impeller rpm and the pressure at the entrance to the pump:
1 -- n=13000 rpm; 2 -- n=1800 rpm
Key:
1. f, hertz
2. p_{inp}, MPa

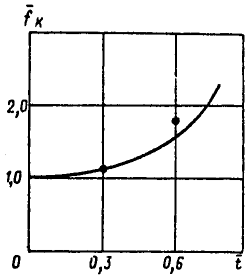

Figure 2.14. Frequency of the natural vibrations of the hull as a function of time

Fig 2.14 shows the relative natural frequency of the vibrations of the rocket hull as a function of the relative time. In the case of coincidence of the natural frequency of the rocket hull vibrations with natural frequency of the liquid vibration in the line, resonance occurs which causes an increase in the amplitude of the pressure fluctuations in front of the pumps, the thrust and the longitudinal vibrations of the hull.

The vibrations can occur in the engine even in the absence of an external effect (cavitation, vibrations of the elastic hull). Such vibrations are formed in the chamber and the gas generator of the engine as a result of the interaction of the processes of mixture formation and combustion with the pressure fluctuations in the gas reservoir.

In any autooscillatory system the following elements exist: the oscillatory element, the energy source and feedback.

APPROVED FOR RELEASE: 2007/02/08: CIA-RDP82-00850R000200090053-2

APPROVED FOR RELEASE: 2007/02/08: CIA-RDP82-00850R000200090053-2

In order for vibrations to occur, energy is required which is fed by the feedback to the oscillatory element in the required phase; this compensates for the loss of energy of the vibrations by dissipation.

Depending on the type of feedback, two mechanisms of the occurrence of vibrations can exist.

The first mechanism consists in the fact that the energy required for the vibrations is released in the fuel combustion process. The feedback producing the energy makeup is realized as a result of the dependence on the amount of incoming fuel to the chamber on the gas pressure in the chamber [20].

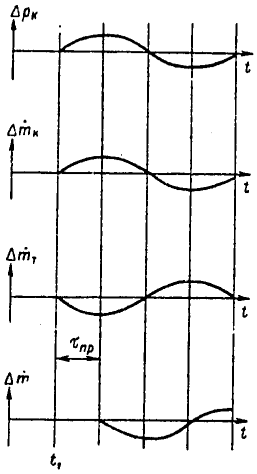

Figure 2.15. Variation of the thrust chamber parameters in the presence of low-frequency vibrations

The fuel combustion process in the combustion chamber is characterized by a burn-up curve which is determined by the complex burn-up processes including a series of physical-chemical transformations: atomizing, feeding and evaporation, diffusion and mixing of the vapors, thermochemical reactions, and so on. It is quite difficult to describe all of these processes analytically.

Accordingly, for analysis of the low-frequency vibrations we replace the actual burn-up curve with a step function (see Fig 1.1), that is, it is considered that every portion of liquid fuel coming into the chamber does not burn for the time τ_{conv} but then is instantaneously converted to the combustion products.

Using this approximation of the combustion process the problem is simplified inasmuch as the only value characterizing the combustion process in time is τ_{conv} which is called the conversion time or the delay time.

APPROVED FOR RELEASE: 2007/02/08: CIA-RDP82-00850R000200090053-2

APPROVED FOR RELEASE: 2007/02/08: CIA-RDP82-00850R000200090053-2

For low-frequency vibrations the pressure in the entire volume of the chamber at each point in time is in practice identical, for the length of the chamber and the acoustic wave length.

The model of the occurrence of the low-frequency vibrations is represented schematically as follows.

In the steady-state mode the mass flow rates of the working medium in all cross sections of the combustion chamber are identical. Let at any point in time t_1 a random increase in pressure occur in the chamber by the amount Δp_k (Fig 2.15), which corresponds to the creation of excess gas in the chamber by comparison with the gas in the steady-state regime. This causes an increase in the gas flow rate through the nozzle $\dot{m}_k$ and a reduction in the inflow of fuel into the chamber $\dot{m}_T$ as a result of a decrease in the pressure gradient in the injectors.

In view of the fact that the liquid fuel combustion takes place with a delay τ_{conv}, the decrease in the arrival of fuel causes the corresponding decrease in gas formation $\dot{m}$ not immediately, but after the time τ_{conv}. At the given time combustion of the fuel coming into the chamber earlier by τ_{conv} takes place until the pressure has risen. At the same time the gas flow rate increases by the amount $\Delta\dot{m}_k$, which with invariant gas formation ($\Delta\dot{m}=0$) leads to a pressure drop in the chamber which assumes the steady-state value.

At this time the inflow and the consumption of the fuel becomes equal, and burn-up of the portion of the fuel which come into the chamber with increased pressure in it takes place. Therefore the mass inflow of gas decreases (by comparison with the steady-state value), which causes a further decrease in the pressure. In turn, the decrease in p_k below the steady-state value leads to the corresponding reduction in the gas flow rate $\dot{m}_k$ and an increase in the flow of fuel through the jets $\dot{m}_T$. Accordingly, p_k, reaching some minimum value, again begins to increase. The further sequence of the process will be repeated.

Consequently, in the presence of a delay in the gas formation τ_{conv} leads to the appearance of positive feedback between the variation of p_k and the gas formation on combustion of the fuel. The indicated feedback causes maintenance of the oscillatory process in the chamber with random pressure variation.

The second mechanism of low-frequency vibrations is explained by the presence of the feedback between the pressure in the chamber and the conversion time.

L. Krokko proposed the relation

$$\tau_{\underset{(1)}{np}} = \frac{A}{p_k^n}, \qquad (2.19)$$

Key: 1. conv

FOR OFFICIAL USE ONLY

APPROVED FOR RELEASE: 2007/02/08: CIA-RDP82-00850R000200090053-2

APPROVED FOR RELEASE: 2007/02/08: CIA-RDP82-00850R000200090053-2

where ν is the interaction coefficient; A is a constant defined by the properties of the fuel and equality of the mix formation. For the existence of a given relation the vibrations in the chamber can also occur in the absence of feedback between the pressure and the inflow of fuel, that is, with constant flow rate of the fuel component as a result of the effect of fluctuations of the physical parameters (p_k and T) on the combustion rate.

Usually $\nu>0$; therefore an increase in p_k leads to a decrease in τ_{conv}, that is, stabilization of the system.

2.4.2. Methods of Stability Analysis

Stability is the property of an engine to return to the initial steady-state regime or a regime close to it after any departure from it as a result of any disturbance.

Fig 2.16 shows the standard curves for the transient processes in an unstable system (Fig 2.16, a) and a stable system (Fig 2.16, b).

If the system is unstable, then a disturbance as small as one might like in it is sufficient for the diverging process of departure from the initial state to begin.

In a stable system, the transient process caused by any disturbance damps with time, and the system again returns to the steady-state condition. Under actual conditions an engine operates under continuously changing effect, for example, as a result of the effect of the speed controls and emptying of the tanks when the steady-state conditions are in general absent.

Considering the indicated operating conditions it is possible to present the following, more general definition of engine stability. An engine is stable if the output variable remains limited under the conditions of the effect on it of disturbances of limited magnitude.

For analysis of the stability, the transfer functions of the engine are used.

The output parameter of the engine is related to any input parameter by the function

$$y=\Phi(s)\cdot x. \tag{2.20}$$

The transfer function $\Phi(s)$ is reduced to a fraction of the type

$$\Phi(s)=\frac{D(s)}{M(s)}, \tag{2.21}$$

where M(s) is an n-degree polynomial. Substituting (2.21) in (2.20), we obtain

$$M(s)y=D(s)x. \tag{2.22}$$

APPROVED FOR RELEASE: 2007/02/08: CIA-RDP82-00850R000200090053-2

APPROVED FOR RELEASE: 2007/02/08: CIA-RDP82-00850R000200090053-2

The solution of this linear nonuniform equation in the general case has the form

$$y(t)=\underset{(1)}{y_{\text{ч}}(t)}+\underset{(2)}{y_{\text{п}}(t)}, \tag{2.23}$$

Key: 1. partial; 2. transient

where $y_{partial}(t)$ is the partial solution of the nonuniform equation with righthand side describing the forced engine regime; $y_{transient}(t)$ is the general solution of the uniform equation $M(s)y=0$ describing the transient process caused by the disturbance x.

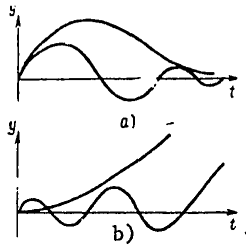

Figure 2.16. Transient process curves:
a -- stable system; b -- unstable system

From the definition of stability it follows that a system is stable if the transient process $y_{transient}(t)$ is damping, that is, for $t\to\infty$ $y_{transient}(t)\to 0$.

As is known, the solution to the uniform differential equation is

$$y_{\text{п}}(t)=\sum_{i=1}^{n} C_i e^{s_i t}, \tag{2.24}$$

where C_i is the integration constant determined by the initial conditions and the disturbances; s_i are the roots of the characteristic equation $M(s)=0$.

Thus, the transient process $y_{transient}(t)$ is the sum of the components, the number of which is equal to the number of roots s_i of the characteristic equation $M(s)$. In the general case the roots of the characteristic equation s_i are complex and conjugate

$$s_{i,i+1}=\alpha_i \pm j\beta_i,$$

where $j=\sqrt{-1}$.

FOR OFFICIAL USE ONLY

APPROVED FOR RELEASE: 2007/02/08: CIA-RDP82-00850R000200090053-2

APPROVED FOR RELEASE: 2007/02/08: CIA-RDP82-00850R000200090053-2

Each pair of such roots gives a component of the transient process in equation (2.24)

$$y_{nl}(t)=C_1e^{\alpha_i t}(\sin\beta_i t+\varphi_i).$$

This time is a sine curve with amplitude that varies in time exponentially.

If $\alpha_i<0$, then the component of the transient process will damp, and for $\alpha_i>0$ there are diverging oscillations.

If $\alpha_i=0$, then nondamping oscillations will occur. In the special case where $\beta_i=0$ (the real root) the component will damp when $\alpha_i<0$ or it increases for $\alpha_i>0$.

Thus, in the general case the transient process in the system is made up of oscillatory and aperiodic components. The general condition of the damping of all of the components, that is, the condition of stability of the system is negativeness of the real parts of all the roots of the characteristic equation, that is, all of the ones (and the zeros in the denominator) of the transfer function of the closed system.

If at least one root has a positive real part, it gives the diverging component of the transient process, and the system will be unstable. The presence of a pair of purely imaginary roots $s_{i,\ i+1}=\pm j\beta_i$ will give a harmonic nondamping component of the transient process -- the system will be at the stability limit.

The determination of the roots of the characteristic equation, especially for high-order systems is a complex process. Therefore in control theory indirect attributes have been developed (stability criteria), which permit determination of the stability without determining the roots of the characteristic equation. There are algebraic and frequency stability criteria.

The algebraic criteria which determine the stability conditions from the ratios of the coefficients of the characteristic equation, for high-order systems containing transcendental terms with factors of the type e^{st} (characteristic for engines) are not used.

The frequency criteria of Mikhaylov and Nyquist have become widespread. Omitting the proofs of these criteria which can be found in the literature on automatic control, let us only describe their practical use.

Mikhaylov Criterion

The stability of a system according to the Mikhaylov criterion is determined by the behavior of the hodograph of the polynomial M(s) -- the denominator of the transfer function of the closed system.

APPROVED FOR RELEASE: 2007/02/08: CIA-RDP82-00850R000200090053-2

APPROVED FOR RELEASE: 2007/02/08: CIA-RDP82-00850R000200090053-2

The imaginary variable jω is substituted in place of s in the polynomial M(s).

As a result, we obtain the complex function

$$M(j\omega)=P_M(\omega)+jQ_M(\omega),$$

where $P_M(\omega)$ is the real part obtained from the terms of M(jω) containing even powers of s; $Q_M(j\omega)$ is the imaginary part obtained from the terms of M(jω) with odd powers of s.

Varying the frequency ω from 0 to ∞, the hodograph of M(ω) in the plane of the complex variables is constructed, and the crosshatching is done on the right side of the hodograph with encirclement of it on variation of the frequency from 0 to ∞ (Fig 2.17). If the origin of the coordinates falls in the crosshatched region, the system is unstable. If M(ω)=0, that is, for any frequency it passes through the origin of the coordinates, the system is at the stability limit. If the hodograph M(ω) does not encompass the origin of the coordinates, then the system is stabie.

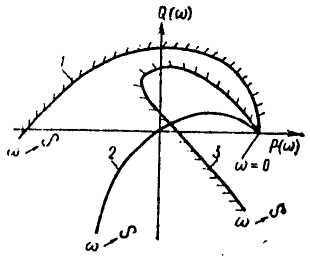

Figure 2.17. Illustration of the Mikhaylov criterion:
1 -- stable system; 2 -- stability limit; 3 -- unstable system

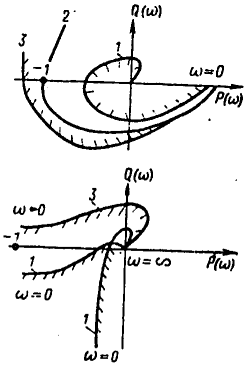

Figure 2.18. Illustration of the Nyquist criterion:
1 -- stable system; 2 -- stability boundary; 3 -- unstable system

Nyquist Criterion

The Nyquist stability criterion makes it possible to determine the stability of the closed system by the phase-amplitude frequency characteristic W(jω) of the open system.

The hodograph $W(j\omega)=P_W(\omega)+jQ_W(\omega)$ is constructed in the plane of the complex variables (Fig 2.18). If the phase-amplitude characteristic of the open system W(jω) on variation of the frequency from 0 to ∞ does not encompass

FOR OFFICIAL USE ONLY

APPROVED FOR RELEASE: 2007/02/08: CIA-RDP82-00850R000200090053-2

APPROVED FOR RELEASE: 2007/02/08: CIA-RDP82-00850R000200090053-2

the point (-1, 0) (this point does not fall into the crosshatched region), then the system is stable. If the phase-amplitude characteristic passes (-1, 0), then the system is at the stability limit.

The dynamic model of the engine even considering the delay is correct only for a natural frequency band. The stability of the engine containing any delays for limited frequency range can be characterized by the criterion proposed in reference [8].

In the complex plane a region is isolated which is bounded by the frequencies $\omega=0$ and $\omega=\Omega$ (Fig 2.19). The system is stable if all of the roots of the characteristic equation are located in the crosshatched region.

In order to determine the stability, the hodograph M(s) is constructed; instead of the operator s the complex number $s=c+j\omega$ is substituted. The parameter s varies as follows: a) $c=0$, ω varies from 0 to Ω, that is, along the imaginary axis; b) for $\omega=\Omega$ c varies from 0 to ∞, that is, along the straight line parallel to the c axis.

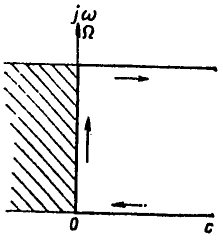

Figure 2.19. Illustration of the stability criterion

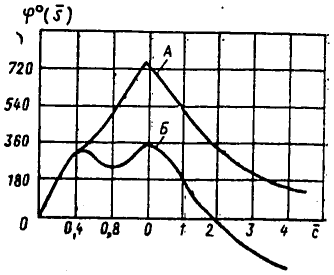

Figure 2.20. Illustration of the application of the stability criterion

The stability conditions are as follows:

$$\left.\begin{array}{l}\Delta\arg M(j\omega)|_{0<\omega<\Omega}=-\arg M(c+j\Omega)|_{0<c<\infty}\\ M(c)\neq 0\\ M(c+j\Omega)\neq 0\end{array}\right\}\ \text{for } 0\leqslant c\leqslant\infty \qquad (2.25)$$
$$M(j\omega)\neq 0 \text{ for } 0\leqslant\omega\leqslant\Omega.$$

Thus, for a stable system it is necessary that the total angle of rotation of the vector $M(c+j\omega)$ with variation of s along the straight line $0\leq\omega\leq\Omega$ for $c=0$ and $0<c<\infty$ for $\omega=\Omega$ is equal to zero, and the hodograph curve does not pass through the origin of the coordinates.

In Fig 2.20 we have an illustration of the application of the criterion for the system with several delays. The angle of rotation of the vector M(s)

APPROVED FOR RELEASE: 2007/02/08: CIA-RDP82-00850R000200090053-2

APPROVED FOR RELEASE: 2007/02/08: CIA-RDP82-00850R000200090053-2

is plotted on the y-axis; the real and imaginary parts of the complex variable s represented in dimensionless form are plotted on the x-axis:

$$\bar{s}=\bar{c}+j\bar{\omega},$$

where

$$\bar{c}=\frac{c}{\Omega};\ \bar{\omega}=\frac{\omega}{\Omega}.$$

Curve A corresponds to a stable system, and B, an unstable system.

The investigated stability curves determine the fact of stability of a specific system for which all of the parameters are given. The most interesting problem is analysis of the effect of the system parameters on its stability or determination of the required variations of the characteristics of the individual elements in order to make the system stable.

The indicated problem is solved by constructing the regions of stability, that is, determining the combinations of parameters for which the system is at the stability limit. The construction of the regions of stability using the Mikhaylov criterion is called the D-breakdown method.

By the Mikhaylov criterion, the system is at the stability limit if the hodograph $M(\omega)=P_M(\omega)+jQ_M(\omega)$ on variation of ω from 0 to ∞ passes through the origin of the coordinates. Let two parameters A, B enter into $M(\omega)$ linearly, in the plane of which the stability limit is constructed. Then according to the Mikhaylov criterion the equations of the stability limit in the space of the parameters A and B have the form

$$\left.\begin{aligned} P_M(\omega, A, B)&=0,\\ Q_M(\omega, A, B)&=0. \end{aligned}\right\} \qquad (2.26)$$

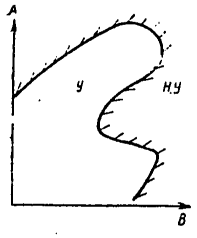

Figure 2.21. Stability limits

Varying ω from 0 to ∞, from equations (2.26), the values of A and B at the stability limit are determined (see Fig 2.21). Each point of the curve A=F(B) (D-breakdown) corresponds to a define frequency ω. Consequently, by the D-breakdown curves it is possible to establish not only the fact of loss of stability, but also to determine the frequency of the vibrations that occur.

FOR OFFICIAL USE ONLY

APPROVED FOR RELEASE: 2007/02/08: CIA-RDP82-00850R000200090053-2

APPROVED FOR RELEASE: 2007/02/08: CIA-RDP82-00850R000200090053-2

The determination of the region of stability is realized as follows.

The determinant

$$\Delta=\begin{vmatrix} \frac{\partial P_M}{\partial A} & \frac{\partial P_M}{\partial B} \\ \frac{\partial Q_M}{\partial A} & \frac{\partial Q_M}{\partial B} \end{vmatrix} \tag{2.27}$$

is compiled. If the determinant $\Delta>0$, then the curve for movement along it from $\omega=0$ to $\omega\to\infty$ crosshatched on the left; if $\Delta<0$, to the right. The region of stability is the region free of crosshatching.

In the case of applying the Nyquist criterion, the equation of the breakdown curve has the form

$$\begin{aligned} P_W(\omega, A, B)&=-1; \\ Q_W(\omega, A, B)&=0. \end{aligned} \tag{2.28}$$

Equation (2.28) is equivalent to the condition 2.26 of the Mikhaylov criterion.

2.4.3. Region of Stability of the Combustion Chamber

The linear dynamics of the thrust chamber with a constant ratio of the fuel components is described by the equation

$$T_к\frac{d\delta p_к}{dt}+\delta p_к-\delta\dot{m}_т(t-\tau_{пр})=0. \tag{2.29}$$

The arrival of fuel in the chamber is determined by the pressure gradient on the jets

$$\dot{m}_т=a\sqrt{p_ф-p_к},$$

where a is the coefficient defined by the hydraulic characteristics of the head and the density of the components. Since the oscillations with respect to the steady-state regime are being considered, the function can be represented in the form of the series

$$\dot{m}_т=a[1+0{,}5(p_ф-p_к)].$$

After linearization of the last equation considering the delay effect we obtain

$$\delta\dot{m}_т(t-\tau_{пр})=-\frac{\delta p_к(t-\tau_{пр})}{\Delta\bar{p}_ф}, \tag{2.30}$$

where

$$\Delta\bar{p}_ф=\frac{2(\bar{p}_ф-\bar{p}_к)}{\bar{p}_к}.$$

APPROVED FOR RELEASE: 2007/02/08: CIA-RDP82-00850R000200090053-2

APPROVED FOR RELEASE: 2007/02/08: CIA-RDP82-00850R000200090053-2

Let us substitute expression 2.30 in equation 2.29 and let us proceed to the operator form; finally we obtain

$$\left(T_к s+1+\frac{1}{\Delta\bar{p}_ф}e^{-s\tau_{пр}}\right)\delta p_к(s)=0.$$

The characteristic equation

$$M(s)=T_к s+\frac{1}{\Delta\bar{p}_ф}e^{-s\tau_{пр}}+1=0. \tag{2.31}$$

This equation is transcendental with respect to the operator s and has a finite number of roots. The defining stability parameters are T_k, Δp_ϕ and τ_{conv}, the values of which determine the location of the roots of the characteristic equation, that is, the stability of the thrust chamber. If in place of the operator s we substitute the complex frequency $j\omega$ in 2.31, we obtain the equation of the stability limit

$$jT_к\omega+\frac{1}{\Delta\bar{p}_ф}e^{-j\omega\tau_{пр}}+1=0. \tag{2.32}$$

Let us represent the exponential function in the form of the Euler function $e^{-j\omega\tau_{conv}}=\cos\omega\tau_{conv}-j\sin\omega\tau_{conv}$ and, finally, we obtain

$$\Delta\bar{p}_ф+\cos\omega\tau_{пр}+j(T_к\Delta\bar{p}_ф\omega-\sin\omega\tau_{пр})=0$$

or

$$P(\omega)=\Delta\bar{p}_ф+\cos\omega\tau_{пр}=0;$$
$$Q(\omega)=T_к\Delta\bar{p}_ф\omega-\sin\omega\tau_{пр}=0. \tag{2.33}$$

By the equations of 2.33, it is possible to construct the stability limit in the plane of any two parameters: Δp_ϕ-τ_{conv}; Δp_ϕ-T_k; T_k-τ_{conv}. However, the time constant of the chamber T_k numerically equal to the time the gases stay in the chamber in practice does not depend on the operating conditions, but is determined by the volume of the chamber and the fitness of the field RT_k. Therefore the time constant is taken to be constant, T_k=const, and we construct the stability limit in the plane of the parameters Δp_ϕ-τ_{conv}.

In order to facilitate the calculations in equations 2.33 let us separate the parameters of interest to us and represent them in the form

$$\Delta p_ф=\frac{1}{\sqrt{1+T_к^2\omega^2}}; \tag{2.34}$$

$$\tau_{пр}=\frac{1}{\omega}(k\pi-\operatorname{arctg}\omega T_к),$$

where k=0, 1, 2, 3, 4.

Each value of k corresponds to its own stability limit. Let us limit ourselves to the investigation of case k=1, k=0 is excluded, for when k=0 negative valuses of τ_{conv} are obtained, which contradicts reality.

FOR OFFICIAL USE ONLY

APPROVED FOR RELEASE: 2007/02/08: CIA-RDP82-00850R000200090053-2

APPROVED FOR RELEASE: 2007/02/08: CIA-RDP82-00850R000200090053-2

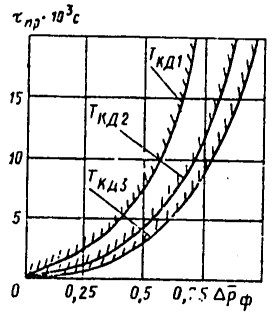

Figure 2.22. Stability limit of the thrust chamber

Thus, in the plane $\Delta p_\phi - \tau_{conv}$, being given ω from 0 to ∞, the stability limit is constructed which splits the plane into two parts. In one part the combinations of Δp_ϕ and τ_{conv} insure a stable process, and in the other part, an unstable process.

In Fig 2.22 we have the stability limits $\Delta p_\phi - \tau_{conv}$ for different values of T_k.

In order to determine the location of the stability and instability regions it is possible to use the crosshatching method which is discussed in the preceding item

$$\frac{\partial P}{\partial p_\phi} = 1; \quad \frac{\partial P}{\partial \tau_{пр}} = -\omega \sin \omega\tau_{пр};$$
$$\frac{\partial Q}{\partial \Delta p_\phi} = T_к\omega; \quad \frac{\partial Q}{\partial \tau_{пр}} = -\omega \cos \omega\tau_{пр}.$$

Let us solve the determinant

$$\Delta = \begin{vmatrix} 1 & -\omega \sin \omega\tau_{пр} \\ T_к\omega & -\omega \cos \omega\tau_{пр} \end{vmatrix} = \omega \cos \omega\tau_{пр} [T_к\omega \operatorname{tg} \omega\tau_{пр} - 1].$$

$\Delta > 0$ on variation of the frequency from zero to infinity. Consequently, by the crosshatching rule the region of stability is located to the right of the stability limit curves.

This is easy to see without using the crosshatching rule. Since the stability condition is negativeness of the real parts of the roots of the characteristic equation, let us take a point on the axis Δp_ϕ* under the stability limit curve for which $\tau_{conv} = 0$, and from equation (2.31) we determine the root

$$s = -\frac{1 + \Delta p_\phi}{T_к \Delta p_\phi}.$$

APPROVED FOR RELEASE: 2007/02/08: CIA-RDP82-00850R000200090053-2

APPROVED FOR RELEASE: 2007/02/08: CIA-RDP82-00850R000200090053-2

Since $\Delta p_\phi > 0$ and $T_k > 0$, the root s is negative and Δp_ϕ^* belongs to the region of stable operation.

A defined role in the development of the low-frequency oscillations is played by the pressure gradient on the jets, the conversion time and the time constant of the chamber. The pressure gradient on the jets Δp_ϕ determines the relation between the pressure fluctuations in the chamber and the fluctuations of the flow rate. Increasing Δp_ϕ stabilizes the combustion process, for the indicated relation decreases.

With an increase in Δp_ϕ the process of mixture formation improves, and the conversion time τ_{conv} decreases, which in turn promotes stabilization of the combustion process.

From Fig 2.22 it follows that for $\Delta p_\phi > 1$ the engine is absolutely stable for any values of τ_{conv}. The condition of absolute stability is written as follows: $\Delta p_\phi > p_k/2$.

A decrease in the conversion time promotes an increase in stability. Consequently, it is desirable to use all of the factors leading to a decrease in conversion time. In particular, this can be achieved by finer atomizing of the fuel component, uniform distribution of the component ratio with respect to chamber cross section, the application of more active fuel components in physical-chemical respects. The latter confirms the known fact from the practice of engine building. The self-igniting fuels have shorter conversion time, and the thrust chambers operating on such fuels are less inclined toward the occurrence of low-frequency vibrations.

The time constant of the chamber numerically determined by the time the gas stays in the chamber also influences the stability. Increasing T_k (an increase in the chamber volume) stabilizes the combustion process, which is explained by the fact that in large volumes the time required for the response reaction of the pressure to a change in flow rate turns out to be too large to observe the phase relations required for development of vibrations. In addition, for the same fluctuations of the flow rate of the fuel components as the volume increases (the time constant increases) the pressure oscillation amplitude decreases which, in turn, stabilizes the combustion process.

As was pointed out above, when considering the Krokko interaction ($\tau_{conv} = f(p_k)$) the chamber can lose stability even with constant component flow rate. Let us consider the effect of the interaction index ν on the stability limit of the chamber.

Considering the interaction index, the equation of the chamber is presented in the form

$$T_к \frac{dp_к}{dt} + (1-\nu)\delta p_к + \left(\nu + \frac{1}{\Delta p_\Phi}\right)\delta p_к (t - \tau_{пр}) = 0. \qquad (2.35)$$

FOR OFFICIAL USE ONLY

APPROVED FOR RELEASE: 2007/02/08: CIA-RDP82-00850R000200090053-2

APPROVED FOR RELEASE: 2007/02/08: CIA-RDP82-00850R000200090053-2

Proceeding to the operator notation, we obtain the characteristic equation

$$M(s)=T_к s+(1-\nu)+\left(\nu+\frac{1}{\Delta p_\phi}\right)e^{-s\tau_{пр}}.$$

Making the substitution s=jω as usual and equating the real and imaginary parts to zero, we obtain two equations for the construction of the stability limit

$$\frac{(1-\nu)\Delta p_\phi}{\nu\Delta p_\phi+1}=\sqrt{\frac{1}{1+\left(\frac{T_к\omega}{1-\nu}\right)^2}}; \qquad (2.36)$$

$$\operatorname{tg}\omega\tau_{пр}=\frac{T_к\omega}{1-\nu}.$$

The equations 2.36 coincide with equations 2.34 for ν=0.

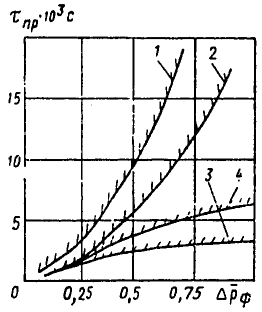

Figure 2.23. Stability limit of the thrust chamber considering the interaction index:
1 -- ν=0; 2 -- ν=0.2; 3 -- ν=0.5; 4 -- ν=10

Fig 2.23 shows the stability limits constructed by equations 2.36 for different ν and constant $T_k=5\cdot10^{-3}$ sec. For ν<0.5 the nature of the stability limits is similar to the curves for the stability limits without considering the interaction coefficient. For small values of ν the curves have the asymptote $\Delta p_\phi=1$; with an increase in ν the region of stability decreases.

For ν>0.5 there is no region of absolute stability. This means that ν>0.5 for any values of Δp_ϕ, including for $\Delta p_\phi>1$, the occurrence of oscillatory conditions is possible.

2.2.4. Limits of Stability of the Engine Systems

Let us consider the system made up of the "chamber and fuel lines" or "chamber and tanks" for an engine with pressurized feed system. For this system the structural diagram (Fig 2.6), the transfer function of the

APPROVED FOR RELEASE: 2007/02/08: CIA-RDP82-00850R000200090053-2

APPROVED FOR RELEASE: 2007/02/08: CIA-RDP82-00850R000200090053-2

open system (2.8) and the closed system (2.12) are constructed. The transfer function of the open system without considering delay $\tau_{conv}=0$ has the form

$$W'_{p.c}(s)=\frac{K_{p_к,\dot{m}_{ок}}K_{\dot{m}_{ок},p_к}}{(T_к s+1)(T_{мок}s+1)}+\frac{K_{p_к,\dot{m}_г}K_{\dot{m}_г,p_к}}{(T_к s+1)(T_{мг}s+1)}. \qquad (2.37)$$

The boost factor of the open system

$$K_p=W'_{p.c}(s)|_{s=0}=K_{p_к,\dot{m}_{ок}}K_{\dot{m}_{ок},p_к}+K_{p_к\dot{m}_г}K_{\dot{m}_г,p_к}. \qquad (2.38)$$

In order to consider the effect of the time constants of the lines let us introduce the reduced time constant of the fuel lines

$$T=\frac{1}{K_p}(K_{p_к,\dot{m}_{ок}}K_{\dot{m}_{ок},p_к}T_{мг}+K_{p_к,\dot{m}_г}K_{\dot{m}_г,p_к}T_{мок}). \qquad (2.39)$$
(1) (2)

Key: 1. line, combustible component of the fuel; 2. line, oxidant

The following relations are obvious

$$T_{мок}<T<T_{мг};\ T_{мг}<T<T_{мок};\ T=T_{мок}=T_{мг}.$$

After substitution of (2.38) and (2.39) in (2.37), we obtain

$$W'_{p.c}(s)=\frac{K_p(Ts+1)}{(T_к s+1)(T_{мок}s+1)(T_{мг}s+1)}. \qquad (2.40)$$

The open system is stable, for its characteristic equation (the denominator of the transfer function) has negative real roots.

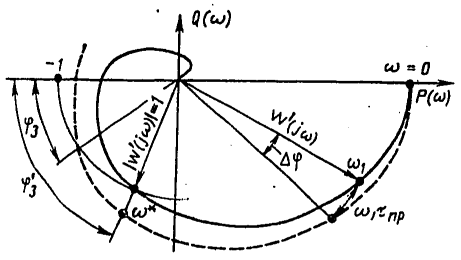

Figure 2.24. Hodograph of the engine W(jω)

The stability of the system can be defined by the Nyquist criterion. For this purpose in equations 2.40 it is necessary to make the substitution s=jω, and as a result we obtain the equation of the phase-amplitude characteristic $W'_{p.c}(j\omega)=P_{W'}(\omega)+jQ_{W'}(\omega)$.

FOR OFFICIAL USE ONLY

APPROVED FOR RELEASE: 2007/02/08: CIA-RDP82-00850R000200090053-2

APPROVED FOR RELEASE: 2007/02/08: CIA-RDP82-00850R000200090053-2

In Fig 2.24 we have the hodograph $W'_{p.c}(j\omega)$ for variation of the frequency from 0 to ∞. The hodograph $W'(j\omega)$ does not encompass the point (-1, 0); therefore the system is stable. This derivation is confirmed by the frequency characteristic shown in Fig 2.9-2.12.

The phase instability margin is defined from Fig 2.24 and is

$$\varphi'_з = \pi - |\varphi'_p(\omega_*)|, \tag{2.41}$$

where ω_* is the frequency for which $|W_{p.c}(j\omega)| = 1$;

$\phi'_p(\omega_*)$ is the phase $W'_{p.c}(j\omega)$:

$$\varphi'_p(\omega_*) = \operatorname{arctg} \frac{Q_{W'}(\omega)}{P_{W'}(\omega)}.$$

Considering the conversion time $\tau_{conv} \neq 0$ the transfer function of the open system has the form

$$W_p(j\omega) = W'_{p.c}(j\omega)\, e^{-j\omega\tau_{пр}},$$

or

$$W_p(j\omega) = |W'_{p.c}(j\omega)|\, e^{j\varphi(\omega)}, \tag{2.42}$$

where $$\varphi(\omega) = \varphi'_p(\omega) - \omega\tau_{пр}.$$

From equation (2.42) we have the effect of τ_{conv} on the phase-amplitude characteristic.

The presence of τ_{conv} deforms the phase-amplitude characteristic $W'_{p.c}$. For each fixed frequency ω the vector $W'_{p.c}(j\omega)$ is rotated by the angle $\omega\tau_{conv}$. As a result of the deformation the hodograph of the vector $W_p(j\omega)$ (Fig 2.24) turns out to be closer to the point (-1, 0) defined by the stability limit than the vector $W'_{p.c}(j\omega)$, that is, the phase stability reserve decreases

$$\varphi_з = \varphi'_з - \omega_*\tau_{пр}. \tag{2.43}$$

For $\tau^*_{пр} = \underset{(1)}{\tau_{пр.г.у}} = \frac{\varphi'_з}{\omega'_*}$ the engine is at the stability limit.

Key: 1. stability limit

Since $\varphi'_{closure}$ and ω_* are defined by the engine characteristics $(K_p, T_к, T_{мом}, T_{мг})$, by the equation $\tau'_{пр} = \frac{\varphi'_з}{\omega_*}$ corresponding to the

APPROVED FOR RELEASE: 2007/02/08: CIA-RDP82-00850R000200090053-2

APPROVED FOR RELEASE: 2007/02/08: CIA-RDP82-00850R000200090053-2

stability limit ($\phi_{closure}=0$) it is possible to determine the state of the engine parameters, the defined regions of stable and unstable operations.

The equation of the stability limit

$$\tau_{пр}^{*}=\frac{\varphi_3'(\omega)}{\omega_*}. \qquad (2.44)$$

For construction of the stability limits by equation 2.44 it is necessary to determine the presence of the analytical function of the type $\phi'_{closure}=f_1(T_i, K_p)$ and $\omega_*=f_2(T_i, K_p)$.

For simplification of the indicated functions let us set $T=T_{line, ox}$ or $T=T_{line}$, combustible component of the fuel. The described equalities are not always satisfied, but they have no effect on the correctness of the qualitative conclusions.

Then

$$W'_{p.c}(s)=\frac{K_p}{(T_к s+1)(T_м s+1)},$$

where

$T_M=T_{мг}$ for $T=T_{мок}$;

$T_M=T_{мок}$ for $T=T_{мг}$.

In this case the phase-amplitude characteristic of the open system has the form

$$W'_{p.c}(j\omega)=|W'_p(j\omega)|\,e^{j\varphi'(\omega)}=P(\omega)+jQ(\omega),$$

where

$$P(\omega)=\frac{K_p(1-T_к T_M\omega^2)}{(1-T_к T_M\omega^2)^2+(T_к+T_M)^2\omega^2};$$

$$Q(\omega)=\frac{-K_p(T_к+T_M)\omega}{(1-T_к T_M\omega^2)^2+(T_к+T_M)^2\omega^2}.$$

$$|W'_{p.c}(j\omega)|=\sqrt{\frac{K_p^2}{(1-T_к T_M\omega^2)^2+(T_к+T_M)^2\omega^2}}. \qquad (2.45)$$

$$\varphi'(\omega)=-k\pi+\operatorname{arctg}\frac{(T_к+T_M)\omega}{T_к T_M\omega^2-1}, \qquad (2.46)$$

where k=0.1, k=0 for $\omega\leq\omega'$, k=1 for $\omega>\omega'$; $\omega'=1/\sqrt{T_k T_m}$.

The frequency characterizing the stability limit ω_* is determined from the expression

$$|W'_{p.c}(j\omega)|=1.$$

APPROVED FOR RELEASE: 2007/02/08: CIA-RDP82-00850R000200090053-2

APPROVED FOR RELEASE: 2007/02/08: CIA-RDP82-00850R000200090053-2

Equating equation (2.45) to one, we obtain

$$\omega_*=\frac{1}{T_к T_M \sqrt{2}}\sqrt{\sqrt{(T_к^2+T_M^2)^2+4T_к^2T_M^2(K_p-1)}-(T_к^2+T_M^2)}. \qquad (2.47)$$

From equation 2.47 it follows that for

$$\omega_*=\omega'=\frac{1}{\sqrt{T_к T_M}};\quad K_p=\frac{T_к+T_M}{\sqrt{T_к T_M}}.$$

On the basis of equation (2.47) and $\phi'(\omega)<0$ we obtain

$$\varphi'(\omega)=(1-k)\pi+\operatorname{arctg}\frac{(T_к+T_M)\omega_*}{T_к T_M\omega^2-1}. \qquad (2.48)$$

Thus, the equation of the stability limit 2.44 based on the relation 2.47 and 2.48 assumes the form

$$\tau^*_{пр}=\frac{1}{\omega_*}\left[(1-k)\pi+\operatorname{arctg}\frac{(T_к+T_M)\omega_*}{T_к T_M\omega^2-1}\right]. \qquad (2.49)$$

Let us construct the graph of the stability limit in the plane of the parameters τ_{conv}-k_p for fixed values of T_M and T_k (Fig 2.25). For establishment of the region of stability it is necessary to check the satisfaction of the condition $\tau_{conv}<\tau^*_{conv}$ for K_p=const. Consequently, the region of stability is located to the left and below the curves. All of the stability limits are bounded by the value of K_p=1. For $K_p<1$ the engine is stable for any values of τ_{conv}.

Substituting the expressions for K_i in equation for K_p, we obtain

$$K_p=\frac{1}{2(1+K)}\left(\frac{K}{\frac{p_{н.ок}(2)}{p_к(1)}-1}+\frac{1}{\frac{p_{н.г}(3)}{p_к}-1}\right). \qquad (2.50)$$

Key: 1. Chamber 2. pump, ox; 3. pump, fuel

If set $p_{pump,\ ox}=p_{pump,\ fuel}=p_{pump}$, then from (2.49) for K_p=1 we have the condition of absolute stability $p_{pump}-p_{chamber}\geq 0.5p_{chamber}$, which is obtained when analyzing the intrachamber stability.

The location of the stability limit τ_{conv}-Kp depends on the values of the time constants of the thrust chamber and the lines. With an increase in T_k and T_M the region of stability expands. This is explained by the fact that the inertia of the lines in the chamber have a stabilizing influence on the engine with respect to the low-frequency vibrations.

APPROVED FOR RELEASE: 2007/02/08: CIA-RDP82-00850R000200090053-2

APPROVED FOR RELEASE: 2007/02/08: CIA-RDP82-00850R000200090053-2

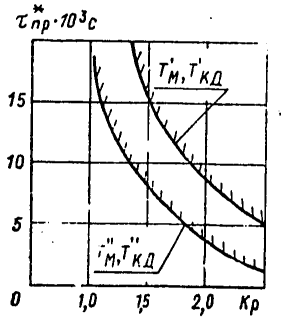

Figure 2.25. Stability limits of the engine:

$T'_к > T''_к$; $T'_M > T''_M$

2.4.5. Stability of the "Engine-Regulator" System

The introduction of a parameter regulation system for the operating process into the engine deforms the limits of stability, and for unfavorable combination of frequency characteristics of the regulator and the engine, vibrations and unstable operating conditions can occur in the engine. The stability limits of the engine together with the regulator can be constructed using the above-enumerated methods, by the transfer functions of the closed or open system.

For engineering analysis the most convenient is the construction of the stability limits using the frequency characteristics of the engine.

The equation of the relation of the adjusted parameter and the adjusting effect has the form

$$\delta y = W_{y.x} \delta x_i, \tag{2.51}$$

where δy is the variation of the adjusted parameter, for example, δp_k, δK; δx_i is the variation of the adjusting effect, for example, the coefficient of hydraulic drag of the line ξ_i.

The frequency transfer function is represented in the form

$$W_{y.x}(j\omega) = P_y(\omega) + jQ_y(\omega), \tag{2.52}$$

by which the phase-amplitude characteristics are constructed for different combinations of y and x presented in Figures 2.9-2.12. Controllable chokes with elastic elements are used as the engine regulators, the equation of which has the form

$$(T_2^2 s^2 + T_1 s + 1)\delta\xi_i = K_p \delta y, \tag{2.53}$$

FOR OFFICIAL USE ONLY

APPROVED FOR RELEASE: 2007/02/08: CIA-RDP82-00850R000200090053-2

APPROVED FOR RELEASE: 2007/02/08: CIA-RDP82-00850R000200090053-2

where T_2 is the time constant which is determined by the mass and rigidity of the moving parts; T_1 is the time constant which characterizes the damping properties of the regulator; K_p is the boost factor of the regulator. The phase-amplitude characteristic of the regulator is obtained on making the substitution s=jω

$$(1-\omega^2T_2^2+j\omega T_1)\delta\xi_l=K_p\delta y, \tag{2.54}$$

or

$$\delta\xi_l=W_p(j\omega)\delta y.$$

From equations 2.52 and 2.54 we obtain the structural diagram of the engine-regulator system (Fig 2.26).

The transfer function of the closed system

$$\Phi(j\omega)=\frac{W(j\omega)}{1+W(j\omega)W_p(j\omega)}=\frac{W_{y,x}(j\omega)(1-\omega^2T_2^2+j\omega T_1)}{1-\omega^2T_2^2+j\omega T_1+P_y(\omega)K_p+jQ_y(\omega)K_p}. \tag{2.55}$$

The characteristic equation of the closed system

$$M(j\omega)=1-\omega^2T_2^2+K_pP_y(\omega)+j(\omega T_1+K_pQ_y(\omega)).$$

The stability boundary conditions according to the Mikhaylov criterion has the form

$$P(\omega)=1-\omega^2T_2^2+K_pP_y(\omega)=0;$$
$$Q(\omega)=\omega T_1+K_pQ_y(\omega)=0. \tag{2.56}$$

It is possible to construct the stability limit in the plane of the parameters: K_p-T_1, or K_p-T_2, or T_2=T_1. The stability boundary in the plane K_p-T_1 is of the greatest interest, for these parameters basically determine the accuracy of the operation of the regulation system.

From equations 2.56 the values of K_p and T_1 corresponding to the stability limit are determined

$$K_p=\frac{1-T_2^2\omega^2}{P_y(\omega)};$$
$$T_1=\frac{(1-T_2^2\omega^2)}{P_y(\omega)\omega}Q_y(\omega). \tag{2.57}$$

Being given the frequency, from the graphs in Figures 2.9-2.12 we determine the values of $P_y(\omega)$ and $Q_y(\omega)$; the stability limit constructed for the given T_2.

APPROVED FOR RELEASE: 2007/02/08: CIA-RDP82-00850R000200090053-2

APPROVED FOR RELEASE: 2007/02/08: CIA-RDP82-00850R000200090053-2

Fig 2.27 shows the stability limit when installing the regulator P_k in the main for the combustible component or the oxidizing agent of the engine gas generator without afterburning of the generator gas.

The region of stability is determined by the sign of the determinant

$$\Delta = \begin{vmatrix} P_y(\omega) & 0 \\ Q_y(\omega) & \omega \end{vmatrix} = P_y(\omega)\omega.$$

For $\omega>0$ and $P_y(\omega)>0$, $\Delta>0$ the line corresponding to the stability limit is hatchured on the right, and for $P_y(\omega)<0$, $\Delta<0$, it is hatchured on the left.

The relations for the stability limit 2.57 permit qualitative analysis of the effect of the regulator parameters on the engine stability.

For a regulator with small mass of the moving parts ($T_2=0$) the stability limit is in the region $K_p>0$, $T_1>0$ for $P_y(\omega)>0$ and $Q_y(\omega)>0$.

This is explained by the fact that for the excitation of the oscillation it is necessary to amplify the signal on transmission of it through the closed loop of the system and realize a 180° phase shift. For $T_2=0$ the regulator is described by the aperiodic element which creates a phase shift of no more than 90°.

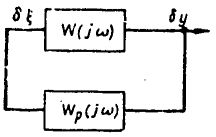

Figure 2.26. Diagram of the regulation system

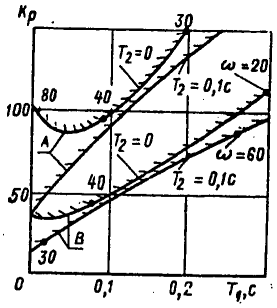

Figure 2.27. Stability limits of the engine with regulator: A -- regulator installed in the oxidant line; B -- regulator installed in the line for the combustible component from the gas generator

The mass of the regulator (the increase in T_2) greatly deforms the stability limits if $\omega^2T_2^2>1$. For this frequency range the stability region corresponds to $P_y(\omega)>0$ and $Q_y(\omega)<0$, for the regulator provides a phase shift of more than 90°.

FOR OFFICIAL USE ONLY

APPROVED FOR RELEASE: 2007/02/08: CIA-RDP82-00850R000200090053-2

APPROVED FOR RELEASE: 2007/02/08: CIA-RDP82-00850R000200090053-2

Increasing the mass of the moving parts of the regulator ($T_2>0$) has a significant influence on the region of stability only for small values of the regulator time constant.

From Fig 2.27 it follows that the region of stability is limited by the boost factor of the regulator.

The admissible boost factor of the regulator installed in the gas generator fuel line is appreciably less than in the regulator installed in the oxidant line. Consequently, in dynamic respects it is more efficient to install the regulator p_k in the oxidant line of the gas generator.

The regulation system changes the structure of the engine and its dynamic characteristics. This is explained by the fact that some of the couplings between the units are broken in order to install the regulating elements, and new couplings introduced by the regulator arise.

The analysis of the effect of the regulators on the dynamic characteristics of the engine can be made by the frequency characteristics considering the disturbances introduced by operation of the regulating system. Such an analysis is also performed and presented in reference [10].

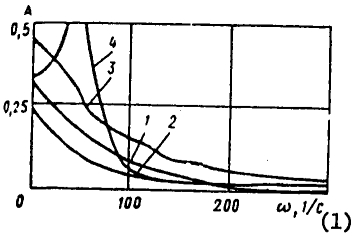

Figure 2.28. Frequency-amplitude characteristics of the engine without afterburning of the generator gas:
1 -- frequency-amplitude characteristic of the engine without the regulator; 2 -- frequency-amplitude characteristic of the engine with regulator K"; 3 -- frequency-amplitude characteristic of the engine with regulator $\dot{m}''_{fuel}$; 4 -- frequency-amplitude characteristic of the engine with regulator p_k
Key:
1. ω,1/sec

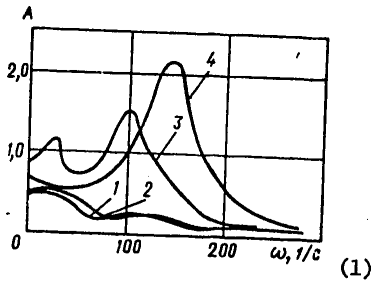

Figure 2.29. Frequency-amplitude characteristic of the engine with afterburning of the generator gas:
1 -- frequency-amplitude characteristic of the engine without the regulator; 2 -- frequency-amplitude characteristic of the engine with regulator K"; 3 -- frequency-amplitude characteristic with regulator p_k; 4 -- frequency-amplitude characteristic with regulator $\dot{m}''_{fuel}$
Key:
1. ω, 1/sec

APPROVED FOR RELEASE: 2007/02/08: CIA-RDP82-00850R000200090053-2

APPROVED FOR RELEASE: 2007/02/08: CIA-RDP82-00850R000200090053-2

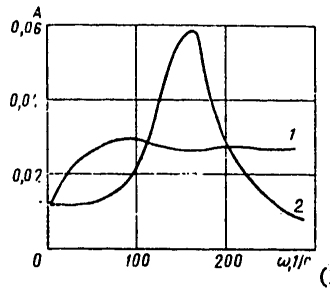

Figure 2.30 Frequency-amplitude characteristic $W_{P_k P_{tank,\ ox}}$

1 -- engine without afterburning of the generator gas; 2 -- engine with afterburning of the generator gas

Key:
1. ω, 1/sec

Let us only present the basic results. Fig 2.28 shows the frequency-amplitude characteristic with different regulation systems for the engine without afterburning of the generator gas.

The analysis of the frequency-amplitude characteristic indicates that the pressure regulator has a significant influence on the dynamic characteristics of the engine.

The analysis of the frequency-amplitude characteristics shows that the pressure regulator has a significant effect on the dynamic characteristics of the engine. Resonance can appear on defined frequencies which indicates that the combination of parameters is close to the stability limit.

Fig 2.29 shows the characteristics for the engine with afterburning of the generator gas and different regulation systems.

The longitudinal stability is significantly influenced by the transfer function $W_{P_k,\ P_{inp,\ ox}}$, that is the effect connected with the pressure variation at the entrance to the pump.

Fig 2.30 shows $W_{P_k,\ P_{inp,\ ox}}$ for two types of engines.

For the engine with afterburning of the generator gas under the corresponding conditions, resonance can occur which must be considered when analyzing the longitudinal stability.

FOR OFFICIAL USE ONLY

APPROVED FOR RELEASE: 2007/02/08: CIA-RDP82-00850R000200090053-2

APPROVED FOR RELEASE: 2007/02/08: CIA-RDP82-00850R000200090053-2

CHAPTER 3. WAVE PROCESSES IN THE LIQUID-FUEL ROCKET ENGINE LINES

3.1. Differential Equations for Uniform Movements and Their Integrals

The transient processes in the hydraulic lines of the liquid-fuel rocket engines are mathematically described by the partial differential equations. For a uniform nonsteady flow of compressible ideal liquid (gas) in the absence of external mass forces the following equations are basic:

Continuity (conservation of mass)

$$\frac{\partial \varrho}{\partial t}+\frac{\partial}{\partial x}(\varrho c)=0; \tag{3.1}$$

Momentum

$$\varrho \frac{\partial c}{\partial t}+\varrho c \frac{\partial c}{\partial x}+\frac{\partial p}{\partial x}=0; \tag{3.2}$$

State

$$p=A+B\varrho^n, \tag{3.3}$$

where ρ, p, c are the liquid (gas) density, pressure and velocity respectively.

Expressions (3.1), (3.2) are written in the Euler coordinate system.

In the equation of state (3.3) depicting the relation between the pressure and density, the parameters A, B and n are constants. This is valid in the case where the dynamic processes in the liquid (gas) are not accompanied by significant variation of the entropy, which occurs in the pressure range to several hundreds of bars [2]. Here the constants A and B are expressed in terms of the speed of sound and density, respectively:

$$B=\frac{a_0^2}{n\varrho_0^{n-1}}; \quad A=p_0-\frac{\varrho_0 a_0^2}{n}, \tag{3.4}$$

where a_0 is the speed of sound in the liquid (gas) with density and pressure ρ_0, p_0.

APPROVED FOR RELEASE: 2007/02/08: CIA-RDP82-00850R000200090053-2

APPROVED FOR RELEASE: 2007/02/08: CIA-RDP82-00850R000200090053-2

For the ideal gas A=0, and for a liquid with constant speed of sound n=1. In particular, for water in the pressure range to 30000 bars n=7.15 [2] and A=-3045 bars, B=3045 bars-cm^3/g^n, where the density ρ_0=1 g/cm^3. For water in the pressure range appreciably less than 3045 bars when the density deformation is small so that $|\Delta\rho|<<\rho$, from the expression (3.4) after transformations, a linear relation is obtained between the density and the pressure $p=p_0+3045\ n\rho/\rho_0$, which simultaneously indicates constancy of the speed of sound with liquid deformation.

The expressions for the constants (3.4) are obtained from (3.3) in accordance with the determination of the speed of sound so that the equation of state (3.3) in implicit form contains the relation between the pressure, the density and the speed of sound.

The initial equations (3.1) and (3.2) are valid for the liquid flow in a nondeformable tube of constant cross section. The consideration of the deformation of the tube walls will be made below.

If we consider the liquid as incompressible, then from the continuity equation we have constancy of the flow velocity along the length of the tube ($\partial\rho/\partial t=0, \partial\rho/\partial x=0$, $\partial c/\partial x=0$), and the integral of the equation of momentum (3.2) determines the relation between the pressure and the acceleration of the liquid column. This integral along the trajectory of displacement of the liquid particles is known in the literature as the Cauchy-Bernoulli integral. In cases where the time integral of the transient process in the line is appreciably greater than the travel time of the acoustic wave in the investigated length of line, for analysis of the transient processes it is possible to use this integral.

For a compressible liquid (gas) in the general case a parameter distribution along the tube length occurs; therefore along the trajectory of motion of the particles of liquid, it is impossible to obtain the integrals of the equations (3.1), (3.2). However, there are families of such curves in the plane of the coordinates x, t along which the integrals of the equations (3.1), (3.2) are found. For this purpose let us convert equations (3.1), (3.2) to the following form:

$$\frac{\partial p}{\partial t}+c\cdot\frac{\partial p}{\partial x}+\varrho\cdot a^2\cdot\frac{\partial c}{\partial x}=0; \tag{3.5}$$

$$\varrho\cdot a\left(\frac{\partial c}{\partial t}+c\cdot\frac{\partial c}{\partial x}\right)+a\cdot\frac{\partial p}{\partial x}=0, \tag{3.6}$$

where under the conditions of constancy of entropy the following expressions are valid:

$$\frac{\partial\varrho}{\partial t}=\frac{\partial\varrho}{\partial p}\cdot\frac{\partial p}{\partial t}=\frac{1}{a^2}\cdot\frac{\partial p}{\partial t},\quad \frac{\partial\varrho}{\partial x}=\frac{\partial\varrho}{\partial p}\cdot\frac{\partial p}{\partial x}=\frac{1}{a^2}\cdot\frac{\partial p}{\partial x}.$$

FOR OFFICIAL USE ONLY

APPROVED FOR RELEASE: 2007/02/08: CIA-RDP82-00850R000200090053-2

APPROVED FOR RELEASE: 2007/02/08: CIA-RDP82-00850R000200090053-2

The equations (3.5) and (3.6) will be reduced by term by term addition and subtraction to the following form respectively

$$\frac{\partial p}{\partial t}+(c+a)\cdot\frac{\partial p}{\partial x}+a\cdot\varrho\cdot\left[\frac{\partial c}{\partial t}+(c+a)\cdot\frac{\partial c}{\partial x}\right]=0; \tag{3.7}$$

$$\frac{\partial p}{\partial t}+(c-a)\cdot\frac{\partial p}{\partial x}-a\cdot\varrho\cdot\left[\frac{\partial c}{\partial t}+(c-a)\cdot\frac{\partial c}{\partial x}\right]=0. \tag{3.8}$$

In the relations obtained (3.7) and (3.8), the velocity and pressure are expressed by the full differentials on the curves $dx/dt=c\pm a$ and, consequently, on these curves such integral relations are valid:

$$\int\frac{dp}{a\varrho}+c=J_{1,2}=\text{const.} \tag{3.9}$$

Considering the equation of state (3.3) after integration (3.9) we find

$$\frac{2a}{n-1}\pm c=J_{1,2}. \tag{3.10}$$

The integrals (3.10) are called the Riemann invariants, and the curves on which they are valid are called the characteristics. Inasmuch as the form of the characteristics depends on the flow velocity and the speed of sound, the values of which vary from point to point, through the Riemann invariants the values of the liquid (gas) parameters in the general case at the investigated point in time and at the investigated point are found numerically. For essentially subsonic flows the characteristics can be considered as straight lines $dx/dt=\pm a$, where the speed of sound is constant. For this case the density is related to the pressure linearly, and the integrals (3.10) have the following form

$$p/a\cdot\varrho\pm c=J_{1,2}. \tag{3.11}$$

The presented solutions have an entirely defined physical meaning: namely, the traveling wave in the positive direction with respect to the stationary observer with absolute velocity c+a carries the linear combination of the speed of sound and the flow velocity J_1 from point to point without change; here, both the flow velocity and the speed of sound in the general case are variable on the path of the wave. In the opposite direction the traveling wave is propagated with absolute velocity c-a with respect to the same observer and carries over the other linear combination of velocities J_2 without change. This means if the corresponding velocities are known on the inside boundaries of the tube, inside the tubes the flow velocity and the speed of sound (and other parameters) are defined in terms of the Riemann invariants in the following way:

$$a=\frac{n-1}{4}(J_1+J_2),\quad c=\frac{J_1-J_2}{2}, \tag{3.12}$$

APPROVED FOR RELEASE: 2007/02/08: CIA-RDP82-00850R000200090053-2

APPROVED FOR RELEASE: 2007/02/08: CIA-RDP82-00850R000200090053-2

where

$$J_1=\frac{2a_1}{n-1}+c_1,\quad J_2=\frac{2a_2}{n-1}-c_2,$$

a_1, c_1 are the parameters of the liquid (gas) on the left boundary of the tube; a_2, c_2 are the parameters of the liquid (gas) on the right boundary of the tube.

For essentially subsonic flows from (3.11) we have

$$p=\frac{1}{2}\cdot a\cdot\varrho(J_1+J_2),\quad c=\frac{1}{2}(J_1-J_2), \tag{3.13}$$

where

$$J_1=p_1/a\cdot\varrho+c_1,\quad J_2=p_2/a\cdot\varrho-c_2.$$

Inasmuch as in this case the flow velocity is appreciably less than the speed of sound, the characteristics of the direct and inverse directions have the following form, respectively:

$$\left.\begin{aligned}x&=x_1+a(t-t_1);\\ x&=x_2-a(t-t_2),\end{aligned}\right\} \tag{3.14}$$

where x_1, x_2 are the coordinates of the left and right boundaries of the tube, correspondingly; t_1, t_2 are the times on the corresponding boundaries for which the liquid parameters and, consequently, the corresponding Riemann invariants are known.

In particular, $x_1=0$ can be taken as the coordinate of the lefthand boundary, and $x_2=\ell$, the righthand boundary, where ℓ is the tube length, and the liquid flow takes place in the direction from the left boundary to the right boundary.

The characteristics (3.14) under the given boundary conditions intersect at the time t at an internal point of the tube with the coordinate x which are determined from:

$$t=\frac{1}{2}\left(t_1+t_2+\frac{x_2-x_1}{a}\right),\quad x=\frac{1}{2}(x_1+x_2+at_2-at_1).$$

Beginning with the above-presented physical interpretation of the values obtained for essentially subsonic flows, the Riemann invariants can be represented in the following form:

$$J_1=\frac{p(x,t)}{a\varrho}+c(x,t)=\frac{p\left(x_1,\,t-\frac{x-x_1}{a}\right)}{a\varrho}+c\left(x_1,t-\frac{x-x_1}{a}\right);$$

$$J_2=\frac{p(x,t)}{a\varrho}-c(x,t)=\frac{p\left(x_2,\,t-\frac{x_2-x}{a}\right)}{a\varrho}-c\left(x_2,t-\frac{x_2-x}{a}\right).$$

APPROVED FOR RELEASE: 2007/02/08: CIA-RDP82-00850R000200090053-2

APPROVED FOR RELEASE: 2007/02/08: CIA-RDP82-00850R000200090053-2

Let us set $x_1=0$, $x_2=\ell$, and in the Riemann invariants the expressions for the corresponding parameters will be represented by expansions in the series limited to the linear approximation:

$$p\left(0, t-\frac{x}{a}\right)\cong p(0,t)-\frac{x}{a}\frac{\partial p}{\partial t}\Big|_{x=0};\quad c\left(0, t-\frac{x}{a}\right)\cong c(0,t)-\frac{x}{a}\frac{\partial c}{\partial t}\Big|_{x=0};$$
$$p\left(l, t-\frac{l-x}{a}\right)\cong p(l,t)-\frac{l-x}{a}\frac{\partial p}{\partial t}\Big|_{x=l};\quad c\left(l, t-\frac{l-x}{a}\right)\cong c(l,t)-$$
$$-\frac{l-x}{a}\frac{\partial c}{\partial t}\Big|_{x=l}.$$

Substituting these expansions in (3.13), after transformations we obtain such expressions for the velocity and pressure:

$$c(x,t)=\frac{p(0,t)-p(l,t)}{2a\varrho}+\frac{l-x}{2\varrho a^2}\frac{\partial p}{\partial t}\Big|_{x=l}-\frac{x}{2\varrho a^2}\frac{\partial p}{\partial t}\Big|_{x=0}-$$
$$-\frac{c(0,t)+c(l,t)}{2}-\frac{x}{2a}\frac{\partial c}{\partial t}\Big|_{x=0}-\frac{l-x}{2a}\frac{\partial c}{\partial t}\Big|_{x=l};$$
$$p(x,t)=\frac{p(0,t)+p(l,t)}{2}-\frac{x}{2a}\frac{\partial p}{\partial t}\Big|_{x=0}-\frac{l-x}{a}\frac{\partial p}{\partial t}\Big|_{x=l}+$$
$$+\frac{\varrho a}{2}[c(0,t)-c(l,t)]+\frac{\varrho(l-x)}{2}\frac{\partial c}{\partial t}\Big|_{x=l}-\frac{\varrho x}{2}\frac{\partial c}{\partial t}\Big|_{x=0}.$$

Then, considering the linear expansion for the velocity $c(\ell,t)\cong$ $\cong c(0,t)+l\cdot\frac{\partial c}{\partial x}\Big|_{x=0}$ and $\frac{\partial c}{\partial x}\sim\frac{1}{\varrho a^2}\frac{\partial p}{\partial t}$ as follows from (3.5), at the limit for an incompressible liquid ($a\to\infty$) we find the Cauchy-Bernoulli integral

$$p(x,t)=\frac{p(0,t)+p(l,t)}{2}+\frac{l-2x}{2}\varrho\frac{dc}{dt}.$$

Along with the Riemann invariants, among the characteristics there are invariants of another dimensionality. After transformations the equations (3.7), (3.8) are reduced to such differential expressions:

$$\varrho^2\cdot a^2dc^2+dp^2\pm 2a\cdot\varrho\cdot d(p\cdot c)=0,$$
$$\frac{dx}{dt}=c\pm a.$$

For a liquid with constant speed of sound when the flow rate is essentially subsonic, the integrals of these expressions are invariants

$$a\left(\frac{p^2}{2\varrho a^2}+\frac{\varrho c^2}{2}\right)\pm p\cdot c=N_{1,2}.$$

APPROVED FOR RELEASE: 2007/02/08: CIA-RDP82-00850R000200090053-2

APPROVED FOR RELEASE: 2007/02/08: CIA-RDP82-00850R000200090053-2

These invariants with the dimensionality of power reduced to a unit area of cross section of the tube are related to the Riemann invariants by the following formula:

$$a\varrho I_{1,2}^2 = 2N_{1,2}.$$

The invariants $N_{1,2}$ have the following physical meaning: the power of the surface forces of pressure $p \cdot c$ is equal to the variation of the flow of kinetic $\rho c^2/2$ and elastic energy of deformation of the liquid $p^2/2\rho a^2$ transported by the wave in the corresponding direction.

The above-presented solutions are common for the initial differential equations: they represent the fact that waves of opposite directions are propagated in the tube, and the liquid (gas) parameters under the effect of the waves are defined in terms of the linear combinations of the corresponding invariants. These solutions describe the developed nonsteady-state nature.

Let us consider another case of the nonsteady flow of a liquid (gas), when a wave is propagated in the tube in one direction, so that the wave front borders with the region of the steady-state flow. This process is also described by the system of equations (3.1)-(3.3). In a simple wave the liquid velocity and the speed of sound (pressure) are related uniquely to each other so that the following representations of the derivatives are valid:

$$\frac{\partial c}{\partial t} = \frac{\partial c}{\partial p}\frac{\partial p}{\partial t}; \quad \frac{\partial c}{\partial x} = \frac{\partial c}{\partial p}\frac{\partial p}{\partial x}.$$

Taking this into account, after transformations the equations (3.1), (3.2) reduce to the following form

$$\frac{\partial p}{\partial t} + \left[c + \varrho a^2 \frac{\partial c}{\partial p}\right]\frac{\partial p}{\partial x} = 0, \tag{3.15}$$

$$\varrho \frac{\partial c}{\partial p}\frac{\partial p}{\partial t} + \left(1 + \varrho c \frac{\partial c}{\partial p}\right)\frac{\partial p}{\partial x} = 0. \tag{3.16}$$

If the system of equations (3.15), (3.16) is solved with respect to the derivatives of the pressure with respect to time and the spatial coordinate in order to obtain the nontrival solution (when the parameters are constant) it is necessary to require that the main determinant of the system vanish, that is, the following must occur:

$$\det \begin{vmatrix} 1 & c + \varrho a^2 \frac{\partial c}{\partial p} \\ \varrho \frac{\partial c}{\partial p} & 1 + \varrho c \frac{\partial c}{\partial p} \end{vmatrix} = 0.$$

FOR OFFICIAL USE ONLY

APPROVED FOR RELEASE: 2007/02/08: CIA-RDP82-00850R000200090053-2

APPROVED FOR RELEASE: 2007/02/08: CIA-RDP82-00850R000200090053-2

After uncovering the determinant and transformations, we find that the differential expressions for the simple wave:

$$a\rho\partial c \mp \partial p=0.$$

Let us find the characteristic line, along which transport of the liquid (gas) parameters occurs, that is, dp/dt=0; dc/dt=0; da/dt=0, and so on. In this case equation (3.15) must be the expression of the total derivative with respect to time along the characteristic, and the equation of this characteristic is defined by the term of the expression (3.15):

$$\frac{\partial x}{dt}=c+\rho a^2\frac{\partial c}{\partial p}.$$

Substituting the expressions $\rho a\partial c=\pm\partial p$, we obtain the equations for the characteristics in the already known form $dx/dt=c\pm a$. However, in contrast to the general solutions, on the characteristic of the forward direction the invariant J_2 is valid, and on the characteristic of the return direction, the invariant J_1, that is

$$\frac{2a}{n-1}\mp c=J_{2,1}, \text{ for } \frac{dx}{dt}=c\pm a.$$

For a liquid with constant speed of sound the following exists, respectively:

$$p/\rho a\mp c=J_{2,1} \text{ for } \frac{dx}{dt}=c\pm a.$$

Inasmuch as along the characteristics in the simple wave the liquid (gas) parameters remain constant, the characteristics themselves are straight lines:

$$x(t, t_1)=x_1(t_1)+(c+a)_{t_1}(t-t_1),$$
$$x(t, t_2)=x_2(t_2)+(c-a)_{t_2}(t-t_2),$$

where the speed of the liquid is expressed in terms of the speed of sound at the corresponding boundary:

$$c(t_1)=c_0+\frac{2}{n-1}[a(t_1)-a_0],\quad c(t_2)=c_0-\frac{2}{n-1}[a(t_2)-a_0], \qquad (3.17)$$

where c_0, a_0 are the undisturbed parameters.

For a liquid with constant speed of sound the corresponding expressions have the form

$$c(t_1)=c_0+\frac{p(t_1)-p_0}{a\rho};\quad c(t_2)=c_0-\frac{p(t_2)-p_0}{a\rho}. \qquad (3.18)$$

Thus, if the pressure perturbation on one of the inside ends of the tube is known, then the disturbed values of all other parameters of the liquid (gas) become known.

APPROVED FOR RELEASE: 2007/02/08: CIA-RDP82-00850R000200090053-2

APPROVED FOR RELEASE: 2007/02/08: CIA-RDP82-00850R000200090053-2

The simple waves in the tubes occur during the initial period of the opening or closing of the valve, variations in the pressure take place on one of the ends of the displacement of the regulator piston, and so on. On disturbance of the uniformity of the propagation conditions of the simple wave, for example, on varying the cross section of the tube, the physical characteristics of the liquid (gas) reflection of the wave takes place, and in this case the region of interaction of the reflected incident waves is described by general solutions, in contrast to the solutions for simple waves, called special [29].

3.2. Rarefaction Waves on Variation of the External Pressure and Cross Section at the End of the Tube

The rarefaction waves occur in the tube on opening the force main with a decrease in the external pressure; the region which the waves reflected from the other end do not succeed in reaching is the region of propagation of the simple wave, the characteristics of which are straight lines. Each of them has its own slope in the plane x, t. If the tube is opened instantaneously or the external pressure drops instantaneously, aligned rarefaction waves are propagated in the tube inasmuch as all of the characteristics converge at one point lying on the axis of the tube at its open end (see Fig 3.1).

Let us consider the problem of calculating the basic parameters separately for a drop liquid with constant speed of sound and for an ideal gas.

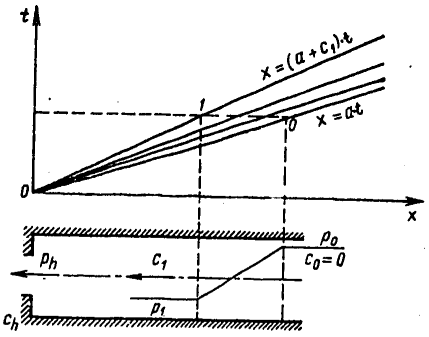

Figure 3.1. Penetration of an aligned rarefaction wave into the tube on instantaneous opening of it

For a liquid if the tube is opened completely, the external pressure enters the tube and the escape of the liquid takes place in the direction opposite to the wave propagation. On propagation of an aligned wave the following regions exist in the tube: the region with the pressure p_0 where the liquid is quiet and where the main wave front has not arrived yet; this

APPROVED FOR RELEASE: 2007/02/08: CIA-RDP82-00850R000200090053-2

APPROVED FOR RELEASE: 2007/02/08: CIA-RDP82-00850R000200090053-2

region lies below the boundary characteristic x=at; the region of nonstationary parameters in which the pressure varies within the limits of $p_h \leq p \leq p_0$, and the speed of the liquid is correspondingly within the limits of $0 \leq |c| \leq |c_h|$; for a fixed point in time this region "0-1"; the region of stationary disturbed parameters for $p=p_h$, $c=c_h$; this region is above the other boundary characteristic $x=(a+c_h)t$.

In accordance with (3.18) the stationary value of the velocity is defined

$$c_h = \frac{p_h - p_0}{a\varrho}. \tag{3.19}$$

The velocity and pressure distribution in the region of nonstationary parameters is defined by the equation of the characteristics, and in the investigated case it is necessary to set $t_1=0$, $x_1(t_1)=0$ and

$$c = \frac{x}{t} - a, \quad p = p_0 - \varrho a^2 + \varrho a \frac{x}{t}.$$

If the tube is incompletely opened and the cross section of the open end of the tube instantaneously acquires a value of s_h, in order to obtain the disturbed stationary values of the parameters it is necessary also to use the Bernoulli and flow equations in the vicinity of the open end of the tube:

$$p_h + (1+\varepsilon)\frac{1}{2}\varrho c_h^2 = p_1 + \frac{1}{2}\varrho c_1^2, \tag{3.20}$$

$$c_h s_h = c_1 s, \tag{3.21}$$

where s is the tube cross section; ε is the coefficient of local losses reduced to the escape velocity c_h.

To the system of equations (3.20), (3.21) let us add the equation relating the velocity and pressure in a simple wave (3.19), where the subscript "h" is replaced by 1.

After transformations we find the expressions for the velocity and pressure in the tube and the escape velocity of the liquid from the tube if the external pressure p_h is kept constant

$$p_1 = p_0 + \frac{\varrho a^2}{\mu} - \frac{\varrho a^2}{\mu}\sqrt{1 + \frac{2\mu}{\varrho a^2}(p_0 - p_h)},$$

$$c_1 = \frac{a}{\mu} - \frac{a}{\mu}\sqrt{1 + \frac{2\mu}{\varrho a^2}(p_0 - p_h)}, \quad \mu = (1+\varepsilon)\left[\left(\frac{s}{s_h}\right)^2 - 1\right].$$

In this case where simultaneously with variation of the area of the output cross section of the tube, the external pressure decreases instantaneously from a value of $\tilde{p}_h$ to a value of p_h, the calculated system of equations has the form:

APPROVED FOR RELEASE: 2007/02/08: CIA-RDP82-00850R000200090053-2

APPROVED FOR RELEASE: 2007/02/08: CIA-RDP82-00850R000200090053-2

$$\tilde{p}_1=\tilde{p}_h+\frac{1}{2}\tilde{\mu}\tilde{\varrho}\tilde{c}_1^2;\quad \tilde{c}_1 s=\tilde{c}_h\tilde{s}_h; \qquad (3.22)$$
$$p_1=p_h+\frac{1}{2}\mu\varrho c_1^2;\quad c_1 s=c_h s_h,$$

where the parameters with a wavy line at the top indicate their undisturbed steady-state values.

To the system of equations (3.22) let us add the equation for the simple wave considering the fact that the undisturbed value of the velocity in the tube is nonzero:

$$c_1=\tilde{c}_1+\frac{p_1-\tilde{p}_1}{a\varrho}.$$

After a number of transformations from (3.22) we find the values of the disturbed stationary parameters:

$$c_1=\frac{a}{\mu}-\frac{a}{\mu}\sqrt{1+\frac{2\mu(\tilde{p}_1-p_h)}{\varrho a^2}-\frac{2\mu c_1^2}{a}}, \qquad (3.23)$$
$$p_1=\tilde{p}_1-a\varrho\tilde{c}_1+\frac{\varrho a^2}{\mu}-a\varrho\sqrt{\left(\frac{a}{\mu}-\tilde{c}\right)^2+\left(\frac{\tilde{\mu}}{\mu}-1\right)\tilde{c}^2+\frac{2(\tilde{p}_h-p_h)}{\varrho\mu}}.$$

In the case where only the external pressure varies in the formulas it is necessary to set $\tilde{\mu}=\mu$, and if only the output cross section changes, then it is necessary to consider $\tilde{p}_h=p_h$.

In the table the results are presented from the numerical calculations for the case where the external pressure is equal to zero, and the tube opens instantaneously to values of the area of the output cross section indicated in the tables. For a liquid, $a=10^3$ m/sec, $\rho=10^3$ kg/m^3 are used.

Table 3.1

$p_0=10$ bars

s/s_h	1	5	10	30	50	100
c_1/a	10^{-3}	$0{,}99\cdot10^{-3}$	$0{,}93\cdot10^{-3}$	$0{,}745\cdot10^{-3}$	$0{,}575\cdot10^{-3}$	$0{,}358\cdot10^{-3}$
p_1/p_0	0	0,001	0,050	0,253	0,422	0,643

From the results of the numerical calculations it follows that the flow velocity of the liquid and the pressure in the region of disturbed stationarity in practice do not depend on the ratio of the cross sectional areas s/s_h under the condition: $2\mu(p_0-p_h)\ll\rho a^2$. In cases where the tube opens gradually or the external pressure decreases gradually, all of the presented calculation ratios remain valid except that the variable

FOR OFFICIAL USE ONLY

APPROVED FOR RELEASE: 2007/02/08: CIA-RDP82-00850R000200090053-2

APPROVED FOR RELEASE: 2007/02/08: CIA-RDP82-00850R000200090053-2

parameters entering into them are a time function. On propagation of the wave, the region of nonsteady-state disturbed values of the parameters widens with an increase in the distance (Fig 3.2).

Table 3.2

p_0=100 bars

s/s_k	1	5	10	30	50	100
c_1/a	10^{-2}	$0{,}897\cdot10^{-2}$	$0{,}727\cdot10^{-2}$	$0{,}372\cdot10^{-2}$	$0{,}245\cdot10^{-2}$	$0{,}135\cdot10^{-2}$
p_1/p_0	0	0,100	0,270	0,628	0,754	0,869

The widening calculations are presented below with gradual opening of the tube. Two approaches are possible here.

1. The parameter distribution is found with respect to the x coordinate for a fixed time t. The time $t_k \geq t_{0\,max}=t_0^*$ is selected where t_0^* is the time of completion of the opening of the tube, and for the given point in time $0 \leq t_0 \leq t_0^*$, the values of the parameters $\mu(t_0)$, $c_1(t_0)$ are found, and the characteristics given by the equation $x(t_k, t_0)=[a+c_1(t_0)](t_k-t_0)$ are constructed, where t_0 is the parameter. These characteristics are intersected by the straight line t=const. Then the graphs $c_1(t_k,x)$, $p_1(t_k,x)$ are constructed. The analogous thing is repeated for another point in time $t_{k+1}<t_k$.

2. For the fixed point x, the values of the parameters are found as a function of time. For the given value of x_k, depending on the time t_0, the velocity and pressure are found, and then the point in time is determined which corresponds to the coordinate x_k by the formula for the characteristic

$$t=t_0+\frac{x_k}{a+c_1(t_0)}.$$

For $t_0>t_{0\,max}$, $t>t_k$ we have the region of undisturbed parameters. Then we are given the point in time $t_0^{(2)}<t_0^{(1)}$; for it we find the values of the velocity, the pressure and t_2 (Fig 3.3). From the constructed graphs it is possible to trace the deformation of the profile of the corresponding parameter in space with respect to the initial profile on the open end of the tube. The calculation relations have the form:

$$\frac{c_1(t_0)}{a}=\frac{1}{\mu(t_0)}\left[1-\sqrt{1+\frac{2\mu(t_0)p_0}{\varrho a^2}}\right];$$

$$\frac{c_k(t_0)}{a}=\frac{c_1(t_0)}{a}\frac{s}{s_k(t_0)};\quad \frac{p_1(t_0)}{p_0}=1+\frac{\varrho a^2}{p_0}\frac{c_1(t_0)}{a},$$

APPROVED FOR RELEASE: 2007/02/08: CIA-RDP82-00850R000200090053-2

APPROVED FOR RELEASE: 2007/02/08: CIA-RDP82-00850R000200090053-2

FOR OFFICIAL USE ONLY

where the external pressure p_h is equal to zero.

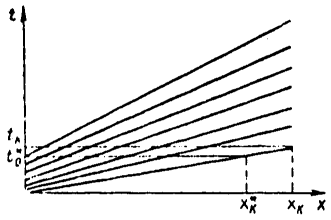

Figure 3.2. Penetration of the rarefaction wave into the tube on gradual opening of it. The field of the characteristics of the simple wave for determining the distribution of the liquid parameters inside the tube for a fixed point in time.

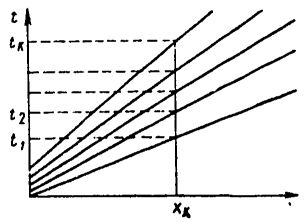

Figure 3.3. Field of the characteristics of the simple wave for determining the liquid parameters in the fixed cross section of the tube

For the points in time t we have the expression

$$\frac{t}{t_{0\max}}=\frac{t_0}{t_{0\max}}+\frac{x_k}{[a+c_1(t_0)]\,t_{0\max}},$$
$$x_k=[a+c_1(t_{0\max})]\,[t_k-t_{0\max}].$$

From what has been presented above it follows that the speed of the liquid at the opening (x=0) $c_1(t_0, 0)$ coincides with the speed of the liquid at the point x at the point in time $t=t_0+x/(a+c_1(t_0, 0))$, that is, $c_1(t_0, 0)\to c_1(t,x)$.

For the graphical constructions it is convenient to introduce the real time for each point, the beginning of which (zero) coincides with the time when the leading (forward) edge of the wave approaches this point. The natural time t_c is related to the coordinate x and the time y of the open end of the tube t_0 by the expression:

$$t_c=t-\frac{x}{a}=t_0+\frac{x}{a+c_1(t_0)}\,\frac{|c_1(t_0)|}{a}.$$

The natural point in time when the trailing edge of the wave approaches the point x, that is, the boundary between the region of the disturbed nonsteady state and the disturbed steady state, will be denoted by t_c^*. It is calculated by the formula

$$\frac{t_c^*}{t_0^*}=1-\frac{x}{[a+c_1(t_0^*)]}\,\frac{c_1(t_0^*)}{t_0^* a}.$$

The relative broadening of the time interval of the nonsteady-state process at the point x is defined as follows:

FOR OFFICIAL USE ONLY

APPROVED FOR RELEASE: 2007/02/08: CIA-RDP82-00850R000200090053-2

APPROVED FOR RELEASE: 2007/02/08: CIA-RDP82-00850R000200090053-2

$$\frac{\Delta t}{t_0^*}=\frac{t_c^*-t_0^*}{t_0^*}=-\frac{x}{at_0^*}\,\frac{c_1(t_0^*)}{a+c_1(t_0^*)}.$$

In Table 3.3 the results are presented from the numerical calculations for the law of opening of the tube $s_h(t_0)=s\sqrt{\frac{t_0}{t_0^*}}$, $t_0^*=10^{-2}$ sec, $\rho=10^3$ kg/m^3, $a=10^3$ m/sec, $\varepsilon=0$, $p_0=100$ bars, $x=10$ meters, $t_c^*=1.01\cdot10^{-2}$ sec.

Table 3.3

t_0/t_0^*	0	0,2	0,4	0,6	0,8	1,0
$c_1(t_0)/a$	0	$0{,}897\cdot10^{-2}$	$0{,}9\cdot10^{-2}$	$0{,}98\cdot10^{-2}$	10^{-2}	10^{-2}
t/t_0	1,0	1,191	1,391	1,6	1,8	2
$\mu(t_0)$	∞	4	1,5	0,67	0,25	0
$p_1(t_0, 0)/p_0$	1	0,103	0,1	0,02	0	0
t_c/t_0^*	0	0,191	0,391	0,60	0,8	1,0
x=100 м, t_c/t_0^*	0	0,290	0,490	0,7	0,09	1,1

From the numerical calculations it is obvious that on going away from the open end of the tube the time interval of the nonsteady-state process increases. The same thing occurs also with an increase in the undisturbed pressure in the tube p_0.

In order to obtain the picture of the distribution of the liquid parameters on transmission of a rarefaction wave in it along the coordinate x it is convenient to introduce the dimensionless coordinates:

$$\frac{x}{x_{max}}=\frac{x}{at}=\left(1-\frac{t_0}{t}\right)\left[1+\frac{c_1(t_0,0)}{a}\right],$$

where $x_{max}=at$ is the coordinate of the leading edge of the wave.

The coordinate of the trailing edge of the wave is defined as follows:

$$x_{min}=[a+c_1(t_0^*, 0)](t-t_0^*).$$

APPROVED FOR RELEASE: 2007/02/08: CIA-RDP82-00850R000200090053-2

APPROVED FOR RELEASE: 2007/02/08: CIA-RDP82-00850R000200090053-2

The investigated values of the coordinate x are found within the limits

$$x_{min} \leqslant x \leqslant x_{max}.$$

The relative broadening of the wave is

$$\frac{\Delta x}{x_{max}} = \frac{x_{max} - x_{min}}{x_{max}} = \frac{t_0^*}{t} - \left(1 - \frac{t_0^*}{t}\right) \frac{c_1(t_0^*, 0)}{a}.$$

Hence, it follows that the maximum broadening occurs for $t=t_0^*=1$, and minimum for $t=t_0^*$ and it is equal to $-c_1(t_0^*, 0)/a$. For calculation of the parameters in the simple wave propagated in an ideal gas, at the boundary of the open end of the tube with external medium we have the system of equations:

$$\begin{aligned} &\frac{n}{n-1} p_h/\rho_h + \frac{1}{2} c_h^2 = \frac{n}{n-1} p_1/\rho_1 + \frac{1}{2} c_1^2; \\ &c_h \rho_h s_h = c_1 \rho_1 s; \\ &c_1 = \frac{2}{n-1}(a_1 - a_0). \end{aligned} \tag{3.24}$$

It is necessary to add the equation of state (3.3) to this system, where A=0.

Expressing the density of the gas in terms of the pressure and also the speed of sound in terms of the pressure, we have the relation between the gas velocity and the pressure in front of the open end of the tube:

$$c_1 = \frac{2a_0}{n-1}\left[(p_1/p_0)^{\frac{n-1}{2n}} - 1\right]. \tag{3.25}$$

Taking this into account, the system of equations (3.24) is converted to one equation where the external pressure p_h and the gas pressure in front of the opening p_1 are related as follows:

$$(p_h/p_0)^{\frac{n-1}{n}} - (p_1/p_0)^{\frac{n-1}{n}} = \frac{2}{n-1}\left[(p_1/p_0)^{\frac{n-1}{2n}} - 1\right]^2\left[1 - \frac{s^2}{s_h^2}\left(\frac{p_1}{p_h}\right)^{\frac{2}{n}}\right]. \tag{3.26}$$

In Table 3.4 we have the results of the numerical calculations of the pressure as a function of the ratio of the cross section for different indexes n, and under the condition that the escape of the gas is subsonic, and the external pressure is kept constant $p_h=0.6p_0$.

In order to determine the conditions where the escape from the tube becomes critical, it is necessary to set $c_h=-a_h$, for the escape takes place in the direction opposite to the propagation of the wave front.

In addition, the Bernoulli equation is conveniently represented in the form

$$\frac{2a_h^2}{n-1} + c_h^2 = \frac{2a_1^2}{n-1} + c_1^2.$$

APPROVED FOR RELEASE: 2007/02/08: CIA-RDP82-00850R000200090053-2

APPROVED FOR RELEASE: 2007/02/08: CIA-RDP82-00850R000200090053-2

Table 3.4

s/s_h	p_1/p_0				
	0,6	0,7	0,8	0,9	1
$n=1,1$	1	6,8	9,2	14,2	∞
$n=1,5$	1	2,54	4,4	9,4	∞
$n=3$	1	2,85	5,8	13,85	∞

In this case instead of (3.26) after transformations we have

$$a_h^2-a_1^2=\frac{2}{n-1}(a_1-a_0)^2\left[1-\left(\frac{s_1}{s_h}\right)^2\left(\frac{a_1}{a_h}\right)^{\frac{4}{n-1}}\right], \qquad (3.27)$$

where a_h is the speed of sound of the gas in the exit from the tube.

From the equations (3.24), (3.27) under the condition $c_{hcr}=-a_{hcr}$ we find

$$a_{h\kappa p}=\frac{2(a_0-a_{1\kappa p})}{n-1}\left(\frac{a_{1\kappa p}}{a_{h\kappa p}}\right)^{\frac{2}{n-1}}\frac{s}{s_h}, \qquad (3.28)$$

where $a_{h\ cr}$, $a_{1\ cr}$ are the values of the speed of sound at the exit from the tube and before the exit from the tube, respectively when the critical escape regime occurs.

From the joint investigation of (3.28) and (3.27) after transformation we find the relation between the speed of sound in the gas in front of the opening and at the cross section of the opening:

$$\left(\frac{2}{n-1}\right)^{\frac{2(n-1)}{n+1}}\left(\frac{s}{s_h}\right)^{\frac{2(n-1)}{n+1}}\left(\frac{a_{1\kappa p}}{a_0}\right)^{\frac{4}{n+1}}\left(1-\frac{a_{1\kappa p}}{a_0}\right)^{\frac{2(n-1)}{n+1}}=$$
$$=\frac{2}{n+1}\left(\frac{a_{1\kappa p}}{a_0}\right)^2+\frac{4}{n^2-1}\left(\frac{a_{1\kappa p}}{a_0}-1\right)^2.$$

In particular, for n=3 we have the following functions:

APPROVED FOR RELEASE: 2007/02/08: CIA-RDP82-00850R000200090053-2

APPROVED FOR RELEASE: 2007/02/08: CIA-RDP82-00850R000200090053-2

$$\frac{a_{1\text{кр}}^{(1)}}{a_0}=\frac{1}{2}\left(1+\sqrt{\frac{s-s_h}{s+s_h}}\right);\quad \frac{a_{h\text{кр}}}{a_0}=\frac{1}{2}\sqrt{\frac{s}{s+s_h}};\quad \frac{p_{h\text{кр}}}{p_0}=\left[\frac{s}{2(s+s_h)}\right]^{3/2};$$

$$\frac{p_{1\text{кр}}}{p_0}=\frac{1}{8}\left(1+\sqrt{\frac{s-s_h}{s+s_h}}\right)^3;\quad \frac{c_{1\text{кр}}}{a_0}=\frac{1}{2}\left[\sqrt{\frac{s-s_h}{s+s_h}}-1\right];$$

$$\frac{c_{1\text{кр}}}{a_{1\text{кр}}^{(1)}}=\frac{\sqrt{\frac{s-s_h}{s+s_h}}-1}{\sqrt{\frac{s-s_h}{s+s_h}}+1}.$$

Key: 1. cr

In Tables 3.5, 3.6 the results are presented from numerical calculations of the critical parameters of the gas for various n when an aligned rarefaction wave enters into the tube.

Table 3.5

$n=1,1$					
s/s_h	1	1,1	1,5	2,9	∞
$a_{1\text{кр}}^{(1)}/a_0$	0,9525	0,96	0,98	0,99	1,0
$a_{h\text{кр}}/a_0$	0,9525	0,94	0,945	0,96	0,975
$p_{h\text{кр}}/p_0$	0,354	0,251	0,275	0,4	0,588

Table 3.6

$n=1,5$					
s/s_h	1	1,23	1,85	13,1	∞
$a_{1\text{кр}}^{(1)}/a_0$	0,8	0,9	0,95	0,99	1,0
$a_{h\text{кр}}/a_0$	0,8	0,801	0,79	0,89	0,895
$p_{h\text{кр}}/p_0$	0,41	0,41	0,4	0,505	0,51

Key:
1. cr

APPROVED FOR RELEASE: 2007/02/08: CIA-RDP82-00850R000200090053-2

APPROVED FOR RELEASE: 2007/02/08: CIA-RDP82-00850R000200090053-2

In the limiting case when the ratio of the tube cross section to the hole cross section is significant, that is, $s/s_h \to \infty$, we have $a_{1\ cr} \to a_0$. Here we obtain the following asymptotic expressions:

$$s/s_h \to \frac{n-1}{2(1-a_{1кр}/a_0)}\left(\frac{2}{n+1}\right)^{\frac{n+1}{2(n-1)}};\quad a_h/a_0 \to \sqrt{\frac{2}{n+1}};$$
$$p_{hкр}/p_0 \to \left(\frac{2}{n+1}\right)^{\frac{n}{n-1}}(a_{1кр}/a_0)^{\frac{4n}{n^2-1}}.$$

Hence, in particular, it is necessary that for $s/s_h \to \infty$ the critical pressure gradient for the nonsteady-state escape approaches the value of the critical gradient for the steady-state escape. In addition, the critical speed of sound in the case of the nonsteady-state escape is less than the critical speed of sound for the steady state escape, for $2/(n+1)<$ and, consequently

$$\underset{(1)}{a_{кр.нестац}} = \frac{2}{n+1}a_0 < a_0\sqrt{\frac{2}{n+1}} = \underset{(2)}{a_{кр.стац}}.$$

Key: 1. cr. nonsteady; 2. cr. steady

For complete and instantaneous opening of the tube in a vacuum, the critical escape regime is set up on the open end of the tube, and the corresponding characteristic in this cross section is directed along the t axis, that is, $x=(c_{cr}+a_{cr})t=0$. The solution of this problem is presented in references [2, 15].

3.3. Compression Waves on Variation of the External Pressure and Cross Section of the End of the Tube

The compression waves occur in a tube on closure of it and on increasing the external pressure. The characteristics of such simple compression waves are straight lines that intersect at some distance or the other. In the region where the intersection of the characteristics does not occur, all of the expressions are valid which have already been obtained earlier for the rarefaction waves.

It is of interest to investigate the problem of the condition of the intersection of all the characteristics of a simple wave at one point (Fig 3.4) At this point the parameters of the liquid (gas) undergo variations from their undisturbed values to maximum disturbed values, that is, this point is the coordinate of the compression shock (shock wave) that occurs. If $x(t, t_0)$ is the equation of the characteristic, then the condition of intersection of the characteristics is independent of the coordinate of the point of intersection with respect to the point in time t_0 corresponding to variation of the external pressure, or the cross section of the open end of the tube, that is

$$\left.\frac{\partial x(t, t_0)}{\partial t_0}\right|_{t=t^*} = 0,$$

where t* is the time of intersection of the characteristics.

APPROVED FOR RELEASE: 2007/02/08: CIA-RDP82-00850R000200090053-2

APPROVED FOR RELEASE: 2007/02/08: CIA-RDP82-00850R000200090053-2

For a drop liquid with constant speed of sound this condition is equivalent to the following

$$t^*=t_0+[a+c_1(t_0)]:\frac{dc_1(t_0)}{dt_0}. \tag{3.29}$$

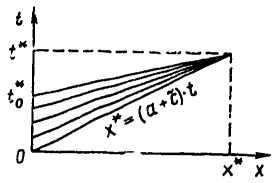

Figure 3.4. Field of the characteristics converging at one point on propagation of the compression wave in a tube

Then, since the point in time t* is identical for all characteristics, after integration of (3.29) we obtain the speed of the liquid at the open end of the tube which corresponds to the conditions of the stated problem:

$$c_1(t_0)=\frac{at_0+\tilde{c}t^*}{t^*-t_0}=\frac{\tilde{c}x^*+at_0(a+\tilde{c})}{x^*-t_0(a+\tilde{c})},$$

where c̃ is the undisturbed speed of the liquid in the tube; x* is the coordinate of the point of intersection of the characteristics determined from the general equation of the characteristics by substituting the expression for the disturbed speed of the liquid there

$$x^*(t^*)=(a+\tilde{c})t^*,\ x(t,\ t_0)=t^*(a+\tilde{c})\frac{t-t}{t^*-t_0}.$$

The pressure of the liquid in front of the opening can vary according to the law

$$p_1(t_0)=\tilde{p}+a\varrho[c_1(t_0)-\tilde{c}]=\tilde{p}+\frac{a\varrho(a+\tilde{c})t_0}{t^*-t_0}=\tilde{p}+\frac{a\varrho t_0(a+\tilde{c})^2}{x^*-t_0(a+\tilde{c})}. \tag{3.30}$$

The external pressure of the medium where escape takes place must vary in this case according to the following law:

$$p_h(t_0)=\tilde{p}+\frac{a\varrho t_0(a+\tilde{c})^2}{x^*-t_0(a+\tilde{c})}-\frac{1}{2}\varrho\mu\left[\frac{\tilde{c}x^*+at_0(a+\tilde{c})}{x^*-t_0(a+\tilde{c})}\right]^2.$$

Obviously, a point in time t_0^* exists where the liquid flow is completely braked, that is, $c_1(t_0^*)=0$. This occurs for the time $t_0^*=-t^*\cdot\tilde{c}/a$, and from (3.30) for this case we have the formula of the total hydraulic hammer at the investigated distance from the open end of the tube. For example, for $t^*=10^{-2}$ sec, $\tilde{c}=-10$ m/sec, $a=10^3$ m/sec, $t_0^*=10^{-4}$ sec and the discontinuity occurs at the distance x*=10 m.

APPROVED FOR RELEASE: 2007/02/08: CIA-RDP82-00850R000200090053-2

APPROVED FOR RELEASE: 2007/02/08: CIA-RDP82-00850R000200090053-2

In Table 3.7 the results are presented from the numerical calculations by the above-presented formulas for the case $p_h=0$, $\tilde{p}=100$ bars, $\tilde{c}=-14.1$ m/sec, $\mu=100$, $\rho=10^3$ kg/m^3, $a=10^3$ m/sec, $x^*=10$ m, $t^*=1.0141\cdot10^{-2}$ sec, $t_0^*=1.41\cdot10^{-4}$ sec.

Table 3.7

t_0/t_0^*	0	0,292	0,646	0,857	1,0
$p_h(t_0)/p$	0	0,91	1,785	2,19	2,41
$p_1(t_0)/p$	1	1,41	1,91	2,21	2,41
$c_1(t_0)/\tilde{c}$	1	0,71	0,355	0,142	0

In the case where the braking of the liquid is realized by closing the tube, that is, decreasing the area of the exit opening, all of the presented expressions remain valid, and for the cross sections the law of its closure will be defined as follows:

$$\mu(t_0)=\frac{2[p_1(t_0)-p_h]}{\rho c_1^2(t_0)},\quad s_h(t_0)=\frac{s}{\sqrt{1+\mu(t_0)}}.$$

For essentially subsonic flows of the liquid where $|\tilde{c}|<<a$, for the parameter $\mu(t_0)$ we have the expression:

$$\frac{\mu(t_0)}{\tilde{\mu}}=\frac{1-\frac{a\rho\tilde{c}}{\tilde{p}}\frac{t_0}{t_0^*}-\frac{p_h}{\tilde{p}}}{\left(1-\frac{t_0}{t_0^*}\right)^2(1-p_h/\tilde{p})},$$

where $\tilde{\mu}$ is the steady-state value of this parameter.

In Table 3.8 the results are presented from the numerical calculations for the law of closure of the tube for $p_h=0$, $\tilde{c}=-14.1$ m/sec, $\tilde{p}=100$ bars, $\rho=10^3$ kg/m^3, $a=10^3$ m/sec, $\tilde{\mu}=100$.

Table 3.8

t_0/t_0^*	0	0,1	0,2	0,3
$\mu(t_0)/\tilde{\mu}$	1	1,41	2,0	2,91
$s_h(t_0)/s$	0,1	$8,5\cdot10^{-2}$	$7,06\cdot10^{-2}$	$5,86\cdot10^{-2}$

APPROVED FOR RELEASE: 2007/02/08: CIA-RDP82-00850R000200090053-2

APPROVED FOR RELEASE: 2007/02/08: CIA-RDP82-00850R000200090053-2

Table 3, continued

t_0/t_0^*	0,5	0,7	0,8	0,9	1,0
$\mu(t_0)/\tilde{\mu}$	6,8	22,2	52,75	227	∞
$s_h(t_0)/s$	$3{,}83\cdot10^{-2}$	$2{,}13\cdot10^{-2}$	$1{,}38\cdot10^{-2}$	$6{,}63\cdot10^{-3}$	0

In the case where the tube length is less than $(a+\tilde{c})t^*$, the discontinuity does not occur inside it. This corresponds to the point in time of completion of the closure of the tube $t_0^* \geqslant -\tilde{c}/a \cdot l/a + \tilde{c} = -\frac{\tilde{c}l}{a^2}$, l is the tube length. For example, for $l=10$ meters, $a=10^3$ m/sec, $\tilde{c}=-10$ m/sec, $t_0^*=10^{-4}$ sec the discontinuity does not occur if the tube is closed for the time greater than 10^{-4} sec. For the compression waves, a decrease in the time of nonsteady-state nature is characteristic on going away from the open end of the tube, and for a faster increase in the external pressure or faster closure of the tube the point of formation of the discontinuity shifts in the direction of the open end. An increase in the parameter μ, that is, a decrease in the hole cross section, for the given magnitude of the steady-state pressure $\tilde{p}$ leads to a decrease in the modulus of the velocity of the undisturbed flow $\tilde{c}$ and the required external pressure for the formation of the discontinuity and vice versa. For the given magnitude of the parameter μ an increase in the pressure $\tilde{p}$ leads to an analogous consequence. The speed of the liquid and the pressure in the tube in front of the open cross section expressed in terms of the dimensionless time t_0/t_0^* does not depend on the coordinates of the formation of the discontinuity x^*, and for subsonic flows the nature of the dependence of the indicated parameters on time t_0/t_0^* is linear, and for external pressure, quadratic. This follows from the fact that the speed of the liquid in the compression wave is expressed by the following

$$\frac{c_1(t_0)}{\tilde{c}} = \frac{at_0 - \tilde{c}t^*}{\tilde{c}(t^* - t_0)} = \frac{1 - t_0/t_0^*}{1 + \frac{\tilde{c}}{a}\frac{t_0}{t_0^*}} \cong 1 - \frac{t_0}{t_0^*} \text{ for } |\tilde{c}| \ll a.$$

We have the analogous expression for the pressures:

$$\frac{p_1(t_0)}{\tilde{p}} = 1 - \frac{a\varrho\tilde{c}}{\tilde{p}}\frac{t_0}{t_0^*}; \quad \frac{p_h(t_0)}{\tilde{p}} = 1 - \frac{a\varrho\tilde{c}}{\tilde{p}}\frac{t_0}{t_0^*} - \left(1 - \frac{t_0}{t_0^*}\right)^2.$$

For a gas on propagation of a simple compression wave in it when the characteristics converge at one point the following equations are valid:

APPROVED FOR RELEASE: 2007/02/08: CIA-RDP82-00850R000200090053-2

APPROVED FOR RELEASE: 2007/02/08: CIA-RDP82-00850R000200090053-2

$$c_1(t_0)=\tilde{c}+\frac{2}{n-1}\left[a_1(t_0)-\tilde{a}\right],\ a_1(t_0)+c_1(t)=\tilde{a}-\frac{n-1}{2}\tilde{c}+\frac{n+1}{2}c_1(t_0),$$
$$x(t,\ t_0)=[a(t_0)+c(t_0)](t-t_0)=\left[\tilde{a}-\frac{n-1}{2}\tilde{c}+\frac{n+1}{2}c_1(t_0)\right](t-t_0). \qquad (3.31)$$

From the condition of intersection of the characteristics after transformations (3.31) we obtain the law for variation of the velocity at the opening in the tube:

$$c_1(t_0)=\frac{2\tilde{a}t_0+\tilde{c}[t^*(n+1)-t_0(n-1)]}{(n+1)(t^*-t_0)}.$$

Expressing the pressure in terms of the speed of sound, according to the equation of state, and the speed of sound in terms of the flow velocity, we find that the pressure inside the tube at the opening is related to the velocity by the formula

$$p_1(t_0)=\tilde{p}\left[1+\frac{n-1}{2\tilde{a}}(c_1(t_0)-\tilde{c})\right]^{\frac{2n}{n-1}}. \qquad (3.32)$$

The corresponding external pressure is found from equation (3.26) by substitution of the expression (3.32) in it instead of the pressure p_1. If the braking of the gas is realized by closing the opening and the external pressure remains unchanged, then from (3.26) the law is found for variation of the exit cross section of the tube; here p_h=const. .

The total braking of the gas at the opening takes place at the time t_0* defined as follows:

$$t_0^*=-\frac{\tilde{c}t^*(n+1)}{2\tilde{a}-\tilde{c}(n-1)}.$$

The pressure corresponding to this case is determined from (3.32) where it is necessary to set $c_1(t_0^*)=0$.

In particular, for $n\to 1$ $p_1(t_0^*)\to p\exp\left(-\frac{\tilde{c}}{\tilde{a}}\right)$, for n=3 $p_1(t_0^*)=\tilde{p}(1-\tilde{c}/\tilde{a})^3$, so that on braking of the sonic flow, when $\tilde{c}=-\tilde{a}$, $p_1(t_0^*)=8\tilde{p}$.

Let us consider how valid it is to use the Riemann invariants for simple waves on formation of the discontinuity. In the dense media to pressures of several hundreds of bars the entropy variation is small and the propagation of the discontinuity can be considered in the acoustic approximation (1.4). In this case the variation of the entropy S in the medium is related to the variation of the basic parameters of the liquid (gas) by the formula (1):

$$S_1-S=\frac{(p_1-\tilde{p})^3}{12\tilde{T}}\left(\frac{\partial^2 V}{\partial p^2}\right)_S=\frac{(\varrho_1-\tilde{\varrho})^3}{12\tilde{T}\varrho_1^3\tilde{\varrho}^3}\left(\frac{\partial^2 p}{\partial V^2}\right)_{S,V=\tilde{V}},$$

where V is the specific volume; T is the temperature.

APPROVED FOR RELEASE: 2007/02/08: CIA-RDP82-00850R000200090053-2

APPROVED FOR RELEASE: 2007/02/08: CIA-RDP82-00850R000200090053-2

The disturbed parameters are indicated by the index "1," and the undisturbed parameters, by the wavy line at the top.

Let us carry out the required transformations for solution of the stated problem. Considering the following expressions:

$$\frac{\partial^2 p}{\partial V^2}=2\varrho^3\frac{\partial p}{\partial \varrho}+\varrho^4\frac{\partial^2 p}{\partial \varrho^2},\ \text{and also}\ \varrho_1-\tilde{\varrho}=\frac{p_1-\tilde{p}}{a^2},\ \text{we have:}$$

$$\frac{\partial^2 p}{\partial V^2}\cong 2\tilde{\varrho}^3\tilde{a}^2\left[1+\frac{\tilde{\varrho}}{\tilde{a}}\frac{\partial a}{\partial \varrho}\right]_{\varrho=\tilde{\varrho}};$$

$$S_1-S=\frac{(p_1-\tilde{p})^3}{6\varrho^3\tilde{a}^4\tilde{T}}\left[1+\frac{\tilde{\varrho}}{\tilde{a}}\frac{\partial a}{\partial \varrho}\right]_{\varrho=\tilde{\varrho}}.$$

The derivative of the speed of sound with respect to density is found within the limits

$$\left|\frac{\partial a}{\partial \varrho}\right|_{\max}\cong\frac{a_1}{\varrho_1-\tilde{\varrho}}=\frac{a^3}{p_1-\tilde{p}},\quad \left|\frac{\partial a}{\partial \varrho}\right|_{\min}=0,$$

so that the entropy variation is within such limits:

$$\frac{(p_1-\tilde{p})^3}{6\tilde{\varrho}^3\tilde{a}^4\tilde{T}}\leqslant|S_1-S|\leqslant\frac{(p_1-\tilde{p})^2}{6\tilde{\varrho}^2\tilde{a}^2\tilde{T}}.$$

Considering the variation of the entropy the expressions based on the characteristics have the form [4]

$$d\left[c\mp\frac{2a}{n-1}\right]=\pm\frac{adS}{n(n-1)c_v},\quad \frac{dx}{dt}=c\pm a,$$

where c_V is the specific heat capacity for constant volume.

Let us denote by J_m the integral based on the characteristic considering the variation of the entropy $J_m=J+\int\frac{adS}{n(n-1)c_v}$, where J is the Riemann invariant under the assumption of constancy of entropy. For the compression $a_1>\tilde{a}$, so that the relative difference between J_m and J is defined:

$$\frac{|J_m-J|}{J}=\frac{|\Delta J|}{J}\leqslant\frac{a_1\Delta S}{n(n-1)c_vJ}.$$

Substituting in this relation the expressions for the Riemann invariant and $\Delta S=S_1-S$ after transformations we obtain

$$\frac{(p_1-\tilde{p})^3}{12\varrho^3c_vT}\leqslant\frac{|\Delta J|}{J}\leqslant\frac{(p_1-\tilde{p})^2}{12\varrho^2-a^2c_vT}.$$

APPROVED FOR RELEASE: 2007/02/08: CIA-RDP82-00850R000200090053-2

APPROVED FOR RELEASE: 2007/02/08: CIA-RDP82-00850R000200090053-2

In particular, for $p_1-\tilde{p}=100$ bars, $\rho=10^3$ kg/m^3, $a=10^3$ m/sec, T=100 K, $c_v=4\cdot10^3$ joules/kg-gK, $|\Delta J|/J<2\cdot10^5$. For a gas we have the analogous relation

$$\frac{n-1}{12n^2}<\frac{|\Delta J|}{J}<\frac{n-1}{12n}.$$

In particular, for n=1.4, $|\Delta J|/J<0.02$.

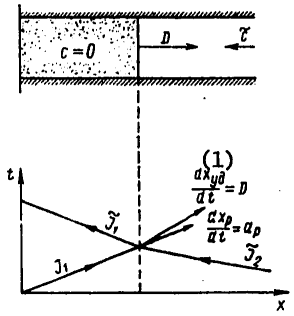

Figure 3.5. Direction of the characteristic and velocity of the shock wave front with instantaneous braking of the flow: x_{shock} is the position of the shock wave front according to shock wave theory; x_p is the position of the front determined by the Riemann expression

Key:
1. shock

The presented results offer the possibility of confirming that if the shock waves approach the compression front, then new values of the parameters go with the compression shock defined in terms of the Riemann invariants. This is valid for the near-sonic flows of gas and liquid. With significantly supersonic flows this statement is invariant. Accordingly, the problem of instantaneous complete braking of the stationary gas and liquid flow is of interest under the assumption that a shock wave occurs, the front of which is propagated opposite to the flow with a velocity D (Fig 3.5), and in the region between the initially open end of the tube and the shock wave front the gas (liquid) is quiet. For comparison, the basic calculation relations and numerical data are presented for the braking parameters based on the use of the Riemann invariants.

The basic initial expressions for shock wave are the equation of:

Continuity $\rho(c-D)=\tilde{\rho}(\tilde{c}-D)$;

Momentum $\rho a^2+n\rho(c-D^2)=\tilde{\rho}\tilde{a}^2+n\tilde{\rho}(\tilde{c}-D)^2$;

Energy $2a^2+(n-1)(c-D)^2=2\tilde{a}^2+(n-1)(\tilde{c}-D)^2$.

APPROVED FOR RELEASE: 2007/02/08: CIA-RDP82-00850R000200090053-2

APPROVED FOR RELEASE: 2007/02/08: CIA-RDP82-00850R000200090053-2

For a completely braked flow c=0 and after transformations we find the expression for the basic parameters of the braked gas expressed in terms of the parameters in the stationary undisturbed flow:

$$D=\frac{3-n}{4}\tilde{c}+a_0\sqrt{1+\left(\frac{3-n}{4}\frac{\tilde{c}}{a_0}\right)^2};$$
$$a=\sqrt{a_0^2-(n-1)\tilde{c}D},\quad \varrho=\tilde{\varrho}\left(1-\frac{\tilde{c}}{D}\right); \tag{3.33}$$
$$p=\tilde{p}\frac{\varrho a^2}{\tilde{\varrho}\tilde{a}^2}=\tilde{p}\left(1-\frac{\tilde{c}}{D}\right)\frac{a_0^2-(n-1)\tilde{c}D}{\tilde{a}^2},$$

where a_0 is the speed of sound from the entropic adiabatic braked flow defined in terms of the parameters of the undisturbed stationary flow as

$$a_0^2=\tilde{a}^2+\frac{n-1}{2}\tilde{c}^2.$$

If the braking parameters are calculated by the Riemann invariant, then in the investigated problem the invariant based on the characteristic of the opposite direction dx/dt=č-ã is constant, from which it follows that the speed of sound of the braked flow is defined as

$$a=\tilde{a}-\frac{n-1}{2}\tilde{c}=\sqrt{a_0^2-\frac{n-1}{2}\tilde{c}^2}-\frac{n-1}{2}\tilde{c}. \tag{3.34}$$

The pressure of the braked flow in this case is defined according to (3.32), where $c_1(t_0)=0$.

In Table 3.9 we have the results of the numerical calculations for the parameters of the braked flow calculated by the formulas for the shock wave (3.33) and by the formulas based on the Riemann invariants (3.34), (3.32). In the table the index "p" at the bottom indicates that the calculation is performed by these formulas, and the index "shock" at the bottom means that the calculation is performed by formulas (3.33). The calculations were performed for different values of the velocity of the stationary undisturbed flow and n=1.5. From the table data and also by the results of the calculations for n=1.1 and n=3 which are not presented here we have the conclusion that for subsonic flows of a steady-state flow up to the Mach number equal to one ($\tilde{M}$=-č/ã), the relative error according to Riemann and by the shock wave formulas will be 2.7% for the speed of sound of the braked flow for n=1.5 and 8.7% for n=3, and for n=1.1 the results in practice coincide.

For supersonic flows of a steady-state flow to Mach numbers $\tilde{M}$=5 the relative error in determining the speed of sound of the braked flow will be 20% for n=1.1, 34% for n=1.5 and 31% for n-3 respectively. In this region the Riemann calculations give low values for the speed of sound, and for the density high values with respect to the results obtained by the shock wave formulas.

FOR OFFICIAL USE ONLY

APPROVED FOR RELEASE: 2007/02/08: CIA-RDP82-00850R000200090053-2

APPROVED FOR RELEASE: 2007/02/08: CIA-RDP82-00850R000200090053-2

For the subsonic flows of a steady-state flow up to $\tilde{M}$=1 the relative error in determining the pressure of the braked flow according to Riemann will be 4% for n=1.1; 2.4% for n=1.5 and 1.85% for n=3.

For the supersonic flows the Riemann error is significant, and for $\tilde{M}$=5 it is 340% for n=1.1; 125% for n=1.5 and 100% for n=3. The values of the pressure according to Riemann are larger than the corresponding value obtained by the formulas (3.33). Thus, the braking parameters of the gas for subsonic and nearsonic flows can be calculated with high accuracy by the formulas used in the Riemann invariants.

3.4. Propagation of Waves Through the Boundary of Nonuniform Media

The disturbances propagated in the tube with the liquid gas in the general case experience reflections caused either by variation of the configuration of the tube or by disturbance of the uniformity of the liquid. Thus, on filling of the hydraulic line with liquid fuel between the liquid front and the open end of the tube a gas cavity is formed. At the liquid-gas interface the waves are reflected with one amplitude or another. When the wave reaches the free surface of the tank, reflection of it also occurs.

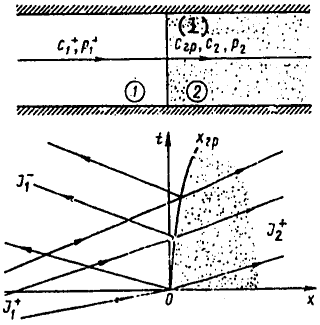

Figure 3.6. The field of characteristics at the boundary of two nonuniform media on propagation of the simple wave from medium 1 to medium 2; $x_{boundary}$ is the position of the medium interface

The interface of nonuniform media on transmission of disturbance waves through it changes the speed of movement and generates the characteristics of disturbed motion of both media (Fig 3.6).

If the disturbance passes from medium 1 to medium 2, then characteristics of the positive direction pass through medium 2, and reflected characteristics of the opposite direction into medium 1. The corresponding Riemann invariants, the values of which must be determined, are valid on these characteristics.

APPROVED FOR RELEASE: 2007/02/08: CIA-RDP82-00850R000200090053-2

APPROVED FOR RELEASE: 2007/02/08: CIA-RDP82-00850R000200090053-2

For solution of this problem we assume that the disturbance occurs in medium 1 in the form of a simple wave, and the parameters for this wave have already been given and denoted by the "+" sign at the top.

At the point of intersection of the positive characteristic of medium 1, along which the incident wave is propagated, with the interface, the Riemann invariant remains valid, but the parameters of the liquid (gas) vary on this characteristic. Thus, for the incident wave the Riemann invariant is:

$$J_1^+ = c_1^+ + \frac{2a_1^+}{n_1 - 1} = c_1 + \frac{2a_1}{n_1 - 1},$$

where c_1 is the interface velocity at the time of arrival of the disturbance with the parameters c_1^+, a_1^+, a_1 is the speed of sound in the medium 1 at the interface which is established at the time of transmission of the wave.

Table 3.9

$-\tilde{c}/\tilde{a}$	0	0,1	0,2	0,5	0,7	1	2	5
$\tilde{a}/a_0$	1	0,997	0,996	0,97	0,942	0,894	0,707	0,371
$(a/\tilde{a})_p$	1	1,025	1,05	1,125	1,17	1,25	1,5	2,25
$(a/\tilde{a})_{уд}$	1	1,02	1,049	1,125	1,19	1,285	1,68	3,27
D/a	1	0,9625	0,933	0,862	0,828	0,8	0,852	1,41
$(\varrho/\tilde{\varrho})_p$	1	1,1	1,21	1,6	1,85	2,44	5,06	25,6
$(\varrho/\tilde{\varrho})_{уд}$	1	1,104	1,24	1,58	1,845	2,25	3,35	4,54
$(p/\tilde{p})_p$	1	1,155	1,33	2,02	2,53	3,8	11,4	128
$(p/p)_{уд}$	1	1,15	1,36	2,01	2,61	3,71	9,45	48,5

For a simple wave from the condition of constancy of the Riemann invariant on the inverse characteristic the speed of the liquid is expressed as follows:

$$c_1^+ = \tilde{c}_1 + \frac{2(a_1^+ - \tilde{a}_1)}{n_1 - 1},$$

APPROVED FOR RELEASE: 2007/02/08: CIA-RDP82-00850R000200090053-2

APPROVED FOR RELEASE: 2007/02/08: CIA-RDP82-00850R000200090053-2

where $\tilde{c}_1$ is the undisturbed speed of the flow and the boundary correspondingly.

From these expressions we find the values of the invariant J_1^+ in the form

$$J_1^+=\frac{2\tilde{a}_1}{n_1-1}+2c_1^+-\tilde{c}_1.$$

Comparing both expressions for J_1^+, we find the expression for the desired speed of sound:

$$a_1=\tilde{a}_1+(n_1-1)c_1^+-\frac{n_1-1}{2}\tilde{c}_1-\frac{n_1-1}{2}\cdot c_1. \tag{3.35}$$

For medium 2 from the condition J_2^-=const we find the expression for the speed of sound at the interface:

$$a_2=\tilde{a}_2+\frac{n_2-1}{2}(c_1-\tilde{c}_1);\ c_1=c_2. \tag{3.36}$$

At the interface the pressure from the direction of medium 1 and medium 2 is identical $p_1=p_2$. Expressing the pressure according to (3.3) in terms of the speed of sound

$$p_{1,2}=A_{1,2}+(\tilde{p}_{1,2}-A_{1,2})(a_{1,2}/\tilde{a}_{1,2})^{\frac{2n_{1,2}}{n_{1,2}-1}},$$

expressions (3.35),(3.36), after a number of transformations, lead to the equation where the velocity of the interface is related to the velocity in the incident wave:

$$\frac{c_1^+}{\tilde{a}_1}=\frac{1}{n_1-1}\left\{\frac{K_2}{K_1}\frac{n_1}{n_2}\left(1+\frac{n_2-1}{2}\frac{c_1}{\tilde{a}_2}\right)^{\frac{2n_2}{n_2-1}}+1-\frac{K_2}{K_1}\frac{n_1}{n_2}\right]^{\frac{n_1-1}{2n_1}}-1+\frac{n_1-1}{2}\frac{c_1}{\tilde{a}_1}\Bigg\}, \tag{3.37}$$

where

$$K_1=\tilde{\varrho}_1\tilde{a}_1^2,\quad K_2=\tilde{\varrho}_2\tilde{a}_2^2.$$

Knowing the value of the disturbed velocity of the interface, from (3.35) and (3.36) we find the disturbed values of the speeds of sound and other parameters.

If both media are an ideal gas, then it is necessary to set

$$K_2\cdot n_1=K_1\cdot n_2.$$

The disturbed pressure at the interface is defined as follows:

$$p_1=\tilde{p}_1-\frac{\tilde{\varrho}_1\tilde{a}_1^2}{n_1}+\frac{\tilde{\varrho}_1\tilde{a}_1^2}{n_1}\left[1-\frac{(n_1-1)}{2}\cdot\frac{c_1^+}{\tilde{a}_1}-\frac{n_1-1}{2}\frac{\tilde{c}_1+c_1}{\tilde{a}_1}\right]^{\frac{2n_1}{n_1-1}}. \tag{3.38}$$

APPROVED FOR RELEASE: 2007/02/08: CIA-RDP82-00850R000200090053-2

APPROVED FOR RELEASE: 2007/02/08: CIA-RDP82-00850R000200090053-2

If the disturbance is propagated from a drop liquid to a gas, then $K_1 \gg K_2$, and formula (3.37) is transformed to the form

$$\frac{c_1^+}{\tilde{a}_1} = \frac{1}{2}\frac{c_1}{\tilde{a}_1} + \frac{K_2}{2n_2K_1}\left[\left(1+\frac{n_2-1}{2}\frac{c_1}{\tilde{a}_2}\right)^{\frac{2n_2}{n_2-1}} - 1\right]. \qquad (3.39)$$

If the disturbance is propagated from the gas to the drop liquid, then $K_2 \gg K_1$, and formula (3.31) is correspondingly transformed:

$$\frac{c_1^+}{\tilde{a}_1} = \frac{1}{2}\frac{c_1}{\tilde{a}_1} + \frac{1}{n_1-1}\left[\left(1+\frac{n_1K_2}{K_1}\frac{c_1}{\tilde{a}_2}\right)^{\frac{n_1-1}{2n_1}} - 1\right].$$

In the case where the speed of the interface is essentially subsonic, from (3.37) and (3.38) for this case we find the expressions:

$$c_1 \cong \frac{2c_1^+\tilde{\rho}_1\tilde{a}_1 + \tilde{c}(\tilde{\rho}_2\tilde{a}_2 - \tilde{\rho}_2\tilde{a}_1)}{\tilde{\rho}_1\tilde{a}_1 + \tilde{\rho}_1\tilde{a}_2};$$

$$p_1 = \tilde{p}_1 + \frac{2\tilde{\rho}_1\tilde{\rho}_2\tilde{a}_1\tilde{a}_2(c_1^+ - \tilde{c}_1)}{\tilde{\rho}_1\tilde{a}_1 + \tilde{\rho}_2\tilde{a}_2}. \qquad (3.40)$$

In Table 3.10 the results are presented from numerical calculations by the formulas (3.39), (3.38) and (3.40), from which it follows that the linear approximation in a number of cases does not justify itself. The calculations are performed for the compression wave propagated from a drop liquid in a gas with $n_2=1.5$. The undisturbed pressure in both media is $\tilde{p}=100$ bars, $\tilde{c}_1=\tilde{c}_2=0$, $\tilde{\rho}_1=10^3$ kg/m^3, $\tilde{a}_1=10^3$ m/sec.

Table 3.10

$c_1/\tilde{a}_1$	0,1	0,2	0,3	0,4	0,5	0,6	0,7	0,8	0,9
$c_1^+/\tilde{a}_1$	0,05168	0,1038	0,1565	0,2099	0,2638	0,3191	0,375	0,4325	0,4916
$(c_1^+/\tilde{a}_1)_{\text{лин}}$ (1)	0,0515	0,103	0,1545	0,206	0,257	0,309	0,36	0,412	0,4625
$p_1/\tilde{p}_1$	1,33	1,76	2,3	3	3,8	4,84	6,2	7,6	9,4
$(p_1/\tilde{p}_1)_{\text{лин}}$ (1)	1,3	1,6	1,9	2,2	2,5	2,8	3,1	3,4	3,7

Key: 1. lin

In the table we have the results of the calculations by formula (3.40) marked by the subscript (lin). The results must be interpreted as follows: what value the initial disturbance must have (velocity in the liquid) so that the interface of the two media will begin to move at the velocity indicated in the upper row of the table. By the results of the calculations it is obvious that in the velocity range of the interface

FOR OFFICIAL USE ONLY

APPROVED FOR RELEASE: 2007/02/08: CIA-RDP82-00850R000200090053-2

APPROVED FOR RELEASE: 2007/02/08: CIA-RDP82-00850R000200090053-2

$c_1/\tilde{a}_1$=0.1 to 0.9 the required value of the velocity with respect to linear theory is 99.5-94%, respectively, of the velocity by formulas (3.39), and the pressures are 97.7-39.3%, that is, the error in the linear approximation is large.

In Table 3.11 the results are presented from the numerical calculations for propagation of the rarefaction wave from the drop liquid to the gas under the same conditions. The relative error with respect to linear theory for the velocity $c_1^+/\tilde{a}_1$ will be 0.5 to 1.65% for $-c_1/\tilde{a}_1$=0.1 to 0.9, and the pressures according to linear theory will be 94.5-75.5% of the pressures calculated by (3.48) in the velocity range of $-c_1/\tilde{a}_1$=0.1 to 0.3 respectively. For large rarefactions by the formulas of the linear approximation when $-c_1/a_1<0.3$ the calculated values of the pressure are negative, and the error is large.

Table 3.11

$-c_1/\tilde{a}_1$	0,1	0,2	0,3	0,4	0,5	0,7	0,8	0,9
$-c_1^+/\tilde{a}_1$	0,05125	0,1023	0,153	0,2037	0,254	0,355	0,4077	0,455
$p_1/\tilde{p}_1$	0,74	0,53	0,374	0,26	0,178	0,076	0,047	0,0278
$(p_1/\tilde{p}_1)_{\text{лин}}$ (1)	0,7	0,4	0,1	−0,5	—	—	—	—

Key:
1. lin

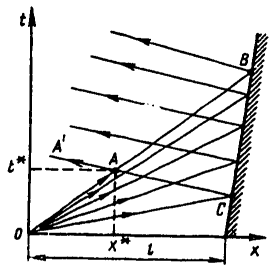

Figure 3.7. Field of the characteristics on reflection of the aligned rarefaction wave from a moving piston

Let us consider the problem of the reflection of an aligned rarefaction wave from a moving piston moving with constant velocity $\tilde{c}$. The solution

APPROVED FOR RELEASE: 2007/02/08: CIA-RDP82-00850R000200090053-2

APPROVED FOR RELEASE: 2007/02/08: CIA-RDP82-00850R000200090053-2

of this problem for the stationary piston is presented in reference [17]. Let us propose that the piston parameters are such that $\rho_2\tilde{a}_2^2 \gg \rho_1\tilde{a}_1^2$, and the medium 1 is an ideal gas.

On reflection of the aligned wave (Fig 3.7) the following regions are formed in the medium 1: ABC -- the region of general solutions of the equations of the nonsteady flow in which the incident and reflected waves interact; ACO -- the region of nonstationarity for a simple wave; OAA' -- the region of disturbed stationarity.

Let us find the boundary of the region of general solutions, that is, the coordinate of the point A, calculating that in the time of incidence of the aligned wave the piston will not move a significant distance, which occurs for significantly subsonic rate of its displacement, that is, $\tilde{c}_1 \ll a_1$.

Let us first find the equation of the boundary characteristic AC. The parameters of the simple wave on the characteristic OA will be noted by the superscript "+"

$$c^+ = \tilde{c} + \frac{2}{n-1}(a^+ - \tilde{a}) = \tilde{c}\frac{n-1}{n+1} - \frac{2}{n+1}\tilde{a} + \frac{2x}{(n+1)t};$$
$$a^+ = \frac{2}{n+1}\tilde{a} + \frac{n-1}{n+1}\frac{x}{t} - \frac{n-1}{n+1}\tilde{c}.$$

Inasmuch as the speed of the piston $\tilde{c}$ is given, the parameters in the incident wave are known, the speed of sound for the reflected wave at the wall of the piston is known and equal to $a_1 = \tilde{a} + \frac{1}{2}(n-1)(2c^+ - \tilde{c})$.

Considering these expressions, we obtain the equation for the characteristic OA:

$$\frac{dx^-}{dt} = c - a = 2\tilde{c}\frac{n-1}{n+1} - \frac{4}{n+1}\cdot\tilde{a} + \frac{3-n}{n+1}\cdot\frac{x^-}{t}.$$

After integration we obtain

$$x^- = \left(\tilde{c} - \frac{2}{n-1}\cdot\tilde{a}\right)t + \frac{n+1}{n-1}\tilde{a}t_0\left(\frac{t}{t_0}\right)^{\frac{3-n}{n+1}},\quad t_0 = \frac{l}{\tilde{a}+\tilde{c}},$$

where l is the distance from the center of the aligned wave to the piston.

The equation for the characteristic OA is:

$$x^+ = \left(\tilde{a} + \frac{n+1}{2}c^* - \frac{n-1}{2}\tilde{c}\right)t,$$

where c* is the speed of the gas at the point A.

APPROVED FOR RELEASE: 2007/02/08: CIA-RDP82-00850R000200090053-2

APPROVED FOR RELEASE: 2007/02/08: CIA-RDP82-00850R000200090053-2

Equating the coordinates of the characteristics OA and AC to each other, after transformations we find

$$t^*=t_0\left[1+\frac{n-1}{2}(M^*-\tilde{M})\right]^{-\frac{n+1}{2(n-1)}};$$

$$x^*=\tilde{a}t_0\frac{1+\frac{n+1}{2}M^*-\frac{n-1}{2}\tilde{M}}{\left[1+\frac{n-1}{2}(M^*-\tilde{M})\right]^{\frac{n+1}{2(n-1)}}},$$

where

$$M^*=\frac{c^*}{\tilde{a}};\quad \tilde{M}=\frac{\tilde{c}}{\tilde{a}}.$$

In particular, x*=0 for M*=n-1/n+1 $\tilde{M}$ -2/n+1. If the aligned rarefaction wave passes through the liquid with constant speed of sound, then the position of the point A will be defined as follows:

$$x^*=(a+\tilde{c})t-2at\ln t/t_0,\ t^*=t_0\exp-\frac{M^*-\tilde{M}}{2}.$$

In particular, for significant subsonic flow conditions of the liquid in front of the piston and $\tilde{M}$=0 we find $x^*\cong at^*(1+M^*)=at_0(1+0.5M^*)$, so that the width of the region of interaction of the waves will be defined as $\Delta x=\ell-x^*=0.5\ M^*$.

The solution in the region ABC will be constructed as follows. The speed of sound is defined in the incident wave from the condition of constancy of the invariant on the characteristic of the undisturbed medium, that is, $a^+=\tilde{a}+(c^+-\tilde{c})(n-1)/2$. Then we construct the invariant J_1^+ for the disturbed region $J_1^+=c_1^+-\frac{2a_1^+}{n-1}=2c^+-\tilde{c}+\frac{2\tilde{a}}{n-1}=c+\frac{2a}{n-1}$ -- the parameters of medium 1 on the line BC. Hence we determine the speed of sound on the line BC $a=\tilde{a}+\frac{n-1}{2}(2c^+-\tilde{c}-c)$ and we construct the invariant $J^-=c-\frac{2a}{n-1}=$

$$=2c+\tilde{c}-2c^+-\frac{2\tilde{a}}{n-1}.$$

Let us denote by J_i^+ the invariant on the forward characteristic $dx_i/dt=c_i+a_i$, J_j^-, the invariant on the return characteristic $dx_j/dt=c_j-a_j$. For determination of the gas parameters at the point of intersection of the characteristics of a different family we have the equation

$$J_i^+=\frac{2}{n-1}\tilde{a}-\tilde{c}+2c_i^+=c_{ij}+\frac{2a_{ij}}{n-1};$$

$$J_j^-=2c_j+\tilde{c}-2c_j^+-\frac{2\tilde{a}}{n-1}=c_{ji}-\frac{2a_{ji}}{n-1}.$$

APPROVED FOR RELEASE: 2007/02/08: CIA-RDP82-00850R000200090053-2

APPROVED FOR RELEASE: 2007/02/08: CIA-RDP82-00850R000200090053-2

Hence, we find the disturbed parameters

$$c_{ij}=\frac{J_i^+ + J_j^-}{2}=c_j+c_i^+-c_j^-;$$
$$a_{ij}=\frac{n-1}{4}(J_i^+ - J_j^-)=\tilde{a}+\frac{n+1}{2}(c_i^+ + c_j^+ - \tilde{c} - c_j),$$

where $c_j=\tilde{c}$; c_j^+ is the value of the velocity on the characteristic in the forward direction in a simple wave which has a common point with the characteristic in the return direction on the line BC.

In conclusion, let us consider the problem of the decay of the discontinuity, by the terminology of [37], in the liquid-gas medium when at the initial point in time the liquid is separated in the tube from the gas by a diaphragm. The initial pressure in the liquid is $\tilde{p}_1$, and in the gas $\tilde{p}_2$. The diaphragm is removed instantaneously; at the point of contact of the media, the pressure is established as identical. In the acoustic approximation where the speed of the interface of the media remains essentially subsonic on propagation of the wave to the liquid, the invariant on the forward characteristic $\tilde{J}_1=\tilde{p}_1/\rho_1 a_1$ remains constant, and in the gas the invariant on the return characteristic $\tilde{J}_2=-\tilde{p}_2/\rho_2 a_2$ remains constant. In this case, for determination of the interface parameters we have the equations

$$c^*-\frac{p^*}{\varrho_2 a_2}=-\frac{\tilde{p}_2}{\varrho_2 a_2};\quad c^*+\frac{p^*}{\varrho_1 a_1}=\frac{\tilde{p}_1}{\varrho_1 a_1}.$$

Hence, the speed of the interface c* and the pressure on both sides of it are:

$$c^*=\frac{\tilde{p}_1-\tilde{p}_2}{\varrho_1 a_1+\varrho_2 a_2};\quad p^*=\frac{a_1\varrho_1\tilde{p}_2+a_2\varrho_2\tilde{p}_1}{\varrho_1 a_1+\varrho_2 a_2}.$$

Knowing how the parameters are expressed at the interface for each of the media, let us construct the invariant J_1^- for the liquid on the characteristic of the return direction and the invariant J_2^+ for the gas on the characteristic of the forward direction:

$$J_1^-=c^*-p^*/\varrho_1 a_1,\quad J_2^+=c^*+p^*/\varrho_2 a_2.$$

Let us consider another important case of developed nonstationarity where the characteristics arrive at the interface of two nonuniform media on which the invariants of the general solutions are valid, for the speed of the interface of the media varies at all times, the invariants on the corresponding characteristics also vary, and their variation is determined by the boundary conditions on both ends of the tube. In this case, on the boundary we have the following:

APPROVED FOR RELEASE: 2007/02/08: CIA-RDP82-00850R000200090053-2

APPROVED FOR RELEASE: 2007/02/08: CIA-RDP82-00850R000200090053-2

$$J_1^+ = c_1 + \frac{2a_1}{n-1}; \quad J_2^- = c_1 - \frac{2a_2}{n_2-1}, \tag{3.41}$$

where J_1^+, J_2^- are the invariants on the characteristics running correspondingly from the left end of the tube and the right end.

These invariants are known. In addition to them we have the condition of equality of the pressures on both sides of the interface in the form

$$A_1 + (\tilde{p}_1 - A_1)\left(\frac{a_1}{\tilde{a}_1}\right)^{\frac{2n_1}{n_1-1}} = A_2 + (\tilde{p}_2 - A_2)\left(\frac{a_2}{\tilde{a}_2}\right)^{\frac{2n_2}{n_2-1}}.$$

The desired parameters of the system (3.41) are the speed of the interface c_1 and the speed of sound a_1, a_2. For essentially subsonic velocities of the boundary where it is possible to present

$a \cong \tilde{a}(1-\delta)$, $|\delta| \ll 1$, we have $(a/\tilde{a})^{\frac{2n}{n-1}} \cong \frac{2n}{n-1}\frac{a}{\tilde{a}} - \frac{n+1}{n-1}$, so that the condition of equality of the pressures after the transformations assumes the form:

$$\frac{2a_2}{n_2-1} = \frac{2\tilde{a}_2}{n_2-1} - \frac{2\tilde{a}_2}{n_1-1}\cdot\frac{\tilde{\varrho}_1\tilde{a}_1^2}{\tilde{\varrho}_2\tilde{a}_2^2} + \frac{2a_1}{n_1-1}\frac{\tilde{\varrho}_1\tilde{a}_1}{\tilde{\varrho}_2\tilde{a}_2}.$$

In this case from (3.41), we find the expressions for the speed of sound at the interface:

$$a_1 = \frac{J_1^+ - J_2^- - \frac{2\tilde{a}_2}{n_2-1}\left(1 - \frac{n_2-1}{n_1-1}\frac{\tilde{\varrho}_1\tilde{a}_1^2}{\tilde{\varrho}_2\tilde{a}_2^2}\right)}{\frac{2}{n_1-1}\left(1 + \frac{\tilde{\varrho}_1\tilde{a}_1}{\tilde{\varrho}_2\tilde{a}_2}\right)}.$$

The pressure on the interface is defined correspondingly

$$p_1 = p_2 = \tilde{p}_1 - \frac{2}{n_1-1}\tilde{\varrho}_1\tilde{a}_1^2 + \frac{\tilde{\varrho}_1\tilde{a}_1^2}{n_1-1}\frac{2a_2}{\tilde{a}_1}.$$

When both media are drop liquids, in the linear approximation the speed of the boundary and the pressure on it are defined

$$c_1 = \frac{\varrho_1 a_1 J_1^+ + \varrho_2 a_2 J_2^-}{\varrho_1 a_1 + \varrho_2 a_2}, \quad p_1 = p_2 = \frac{a_1 a_2 \varrho_1 \varrho_2 (J_1^+ - J_2^-)}{\varrho_1 a_1 + \varrho_2 a_2}.$$

When the medium 1 is a drop liquid, and medium 2 is a gas, we have, respectively:

APPROVED FOR RELEASE: 2007/02/08: CIA-RDP82-00850R000200090053-2

APPROVED FOR RELEASE: 2007/02/08: CIA-RDP82-00850R000200090053-2

$$c_1=\frac{\tilde{a}_2\tilde{\varrho}_2 J_2^- + a_1\varrho_1 J_1^+ + \frac{n_2+1}{n_2-1}\,\frac{\tilde{\varrho}_2\tilde{a}_2^2}{n_2}}{\varrho_1 a_1+\varrho_2 a_2};$$

$$p=\frac{a_1\tilde{a}_2\varrho_1\tilde{\varrho}_2\left(J_1^+ - J_2^- - \frac{\tilde{a}_2}{n_2}\,\frac{n_2+1}{n_2-1}\right)}{\varrho_1 a_1+\varrho_2 a_2}.$$

3.5. Propagation of Waves Through Discontinuities of the Tube Cross Section

A study is made of the transmission of a simple wave in a liquid with constant speed of sound when the tube cross section changes abruptly. In the case where the motion of the waves passes along the positive direction of the x-axis, after the cross section discontinuity a simple wave will be propagated, and before the discontinuity, a reflected wave occurs which interacts with the incident wave. Thus, for known values of the parameters of the incident wave it is necessary to determine the parameters of the liquid on both sides of the discontinuity of the tube cross section at the time of transmission of the wave.

Let us consider that on the left end of the tube the disturbed value of the pressure is given as p_1^+, and that it and the corresponding disturbed value of the velocity c_1^+ are related to each other by the condition of constancy of the Riemann invariant for a steady-state flow

$$a_1\varrho c_1^+ = a_1\varrho\tilde{c}_1 + p_1^+ - \tilde{p}_1.$$

Hence, the invariant for a simple wave on the characteristic in the positive direction is

$$J_1^+ = c_1^+ + \frac{p_1^+}{a_1\varrho} = \tilde{c}_1 + \frac{2p_1^+ - \tilde{p}_1}{a_1\varrho}.$$

Then, since on reflection of the wave from the cross section discontinuity J_1^+ remains constant (the region of general solutions), before the cross section discontinuity the pressure p_1 and the velocity c_1 of the liquid are related to each other as follows:

$$p_1 = 2p_1^+ - \tilde{p}_1 + a_1\varrho(\tilde{c}_1 - c_1) = \tilde{p}_1 + 2a_1\varrho c_1^+ - a_1\varrho c_1 - a_1\varrho\tilde{c}_1.$$

The pressure and the velocity of the liquid after discontinuity are related by the condition of constancy of the invariant on the return characteristic of the undisturbed flow:

$$p_2 = \tilde{p}_2 + a_2\varrho(c_2 - \tilde{c}_2).$$

APPROVED FOR RELEASE: 2007/02/08: CIA-RDP82-00850R000200090053-2

APPROVED FOR RELEASE: 2007/02/08: CIA-RDP82-00850R000200090053-2

In the vicinity of the cross section discontinuity the liquid parameters are related to each other by the Bernoulli equation:

$$p_1+\frac{\varrho c_1^2}{2}=p_2+\frac{1}{2}\varrho(1+\varepsilon)c_2^2,$$

where ε is the coefficient of local losses.

From the joint investigation of the above-presented equations after transformations we find the velocity c_1 from the continuity equations c_2, then the pressures p_1 and p_2

$$c_1=-\frac{a_1+a_2s_1/s_2}{\mu}\times$$
$$\times\left\{1-\sqrt{1+\mu\frac{2\frac{(\tilde{p}_1-\tilde{p}_2)}{\varrho}+4a_1c_1^+-2\tilde{c}_1(a_1-a_2s_1/s_2)}{(a_1+a_2s_1/s_2)^2}}\right\},$$

where $$\mu=(1+\varepsilon)\frac{s_1^2}{s_2^2}-1;\quad \tilde{c}_1^2=\frac{2(\tilde{p}_1-\tilde{p}_2)}{\varrho\mu}.$$

In the linear approximation where the expression under the sign of the radical is close to one, we obtain

$$c_1\cong\frac{2c_1^*}{1+k}-\tilde{c}_1\frac{1-k}{1+k};\quad p_1\cong\tilde{p}_1+\frac{2a_1\varrho k}{1+k}(c_1^+-\tilde{c}_1),$$
$$k=\frac{a_2}{a_1}\frac{s_1}{s_2},\quad p_2=\tilde{p}_2+\frac{2a_1\varrho k}{1+k}\left(c_1^+-\tilde{c}_1\frac{1-k}{2}\right). \qquad (3.42)$$

When a simple wave is propagated in a stationary liquid $\tilde{c}_1=\tilde{c}_2=0$, from these expressions it follows that the excess pressures on both sides of the tube cross section discontinuity on transmission of the wave are identical, that is, $\Delta p_1=p_1-\tilde{p}_1=\Delta p_2=p_2-\tilde{p}_2$. This result coincides with the formulas of linear acoustics [6].

Knowledge of the parameters on the cross section discontinuity of the tube offers the possibility of constructing the invariants for the tube with the cross section s_1 on the return (reflected) characteristics, and for the tube s_2 on the forward characteristics:

$$J_1^-=c_1-\frac{p_1}{a_1\varrho},\quad J_2^+=c_2+\frac{p_2}{a_2\varrho}.$$

When on the left end of the tube the pressure disturbance reaches a value of $p_1^+=0.5(\tilde{p}_1+\tilde{p}_2)-0.5(1+k)a_1\tilde{c}_1\rho$, on passing through the tube cross section discontinuity the liquid stops, that is, $c_1=c_2=0$ and $p_1=p_2$ of which we are convinced by substitution of the expression p_1^+ in (3.42).

From analysis of the formulas of the linear approximation (3.42) obtained by representation of the radical in terms of the Newton binomial by the

APPROVED FOR RELEASE: 2007/02/08: CIA-RDP82-00850R000200090053-2

APPROVED FOR RELEASE: 2007/02/08: CIA-RDP82-00850R000200090053-2

first two terms it follows that in the first approximation the hydraulic drag in the wave process has an insignificant effect on the numerical values of the desired parameters.

If waves approach the discontinuity of the tube cross section simultaneously from opposite ends of the tube, on the characteristics of which the invariants $J_1^+ = c_1^+ + \frac{p_1^+}{a_1\rho}$, $J_2^- = c_2^+ - \frac{p_2^+}{a_2\rho}$, are valid, for determination of the liquid parameters in the vicinity of the discontinuity instead of (3.42) we have:

$$p_1 = (J_1^+ - c_1)\, a_1\rho; \quad p_2 = (c_2 - J_2^-)\, a_2\rho.$$

The Bernoulli equation and the continuity equation are added to these equations. After transformations we find the desired values of the parameters:

$$c_1 = -\frac{a_1(1+k)}{\mu} + \sqrt{\frac{a_1^2(1+k)^2}{\mu^2} + \frac{2}{\mu}(J_2^- a_2 + J_1^+ a_1)}. \qquad (3.43)$$

Then we determine the velocity c_2 and the pressure p_1, p_2; then we construct the invariants for the tube of cross section s_2 on the forward characteristics $J_2^+ = c_2 + p_2/a_2\rho$, for a tube with cross section s_1 on the return characteristic $J_1^- = c_1 - p_1/a_1\rho$. The invariants obtained on the reflected characteristics are related to the invariants of the incident waves by the expressions:

$$J_1^+ + J_1^- = 2c_1, \quad J_2^+ + J_2^- = 2c_2.$$

In the linear approximation where $2\mu(J_2^- a_2 + J_1^+ a_1) \ll a_1^2(1+k)^2$, is valid, from (3.43) we find

$$c_1 \cong \frac{a_2 J_2^- + a_1 J_1^+}{a_1 + a_2 s_1/s_2} = \frac{a_1 c_1^+ \rho + a_2 c_2^+ \rho + p_1^+ - p_2^+}{a_1\rho(1+k)},$$

$$p_1 \cong p_2 \cong a_2\rho\, \frac{J_1^+ s_1/s_2 - J_2^-}{1+k}.$$

The expressions obtained above are applicable to the problem of nonstationary escape of a liquid from a tank on opening the valve in the bottom of the tank. It is proposed that the flow in the tank is uniform so that the tank-tube system is considered as a string of pipe with a cross section discontinuity. Let us consider the case of instantaneous opening of the hole in the bottom of the tank (Fig 3.8) where the external pressure penetrates in the tank like an aligned rarefaction wave reflected on the free surface of the tank. In the region of intersection of the characteristics of a different family $a_1b_1c_1$ the characteristics are distorted, and the liquid parameters in this region are calculated by the formulas from

FOR OFFICIAL USE ONLY

APPROVED FOR RELEASE: 2007/02/08: CIA-RDP82-00850R000200090053-2

APPROVED FOR RELEASE: 2007/02/08: CIA-RDP82-00850R000200090053-2

the general solutions. The relative width of this region where the wave front is included is on the order of $\Delta x/\ell \sim c/a$, where ℓ is the height of the column of liquid in the tank. This eroded front approaches the bottom of the tank, it is reflected, creating a region of interaction of incident reflected waves $a_2b_2c_2$, and so on. If the total number of reflections of the waves from the free surface of the tank and from the bottom of the tank is "n," then the total relative width of the wave front will be $\Delta xn/\ell \sim cn/a$, and for a value appreciably less than one the erosion of the front will be neglected.

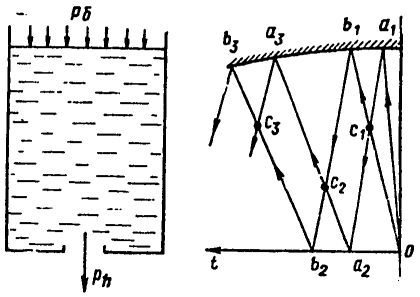

Figure 3.8. The field of characteristics for nonsteady-state escape of a liquid from a tank a_1, b_1, a_3, b_3 -- position of the free surface of the liquid in the tank

At the initial point in time of opening of the tank for the selected positive direction of the x-axis the rate of escape, according to (3.23) is defined as follows:

$$c^{(1)}=\sqrt{\frac{a^2}{\mu^2}+\frac{2(p_б-p_h)}{Q\mu}}-\frac{a}{\mu},$$

where p_{tank} is the blowing pressure of the tank.

At the bottom of the tank in this case the following pressure is established: $p^{(1)}=p_{tank}-a\rho c^{(1)}$. These expressions are valid for the time interval $2\ell/a \geq t \geq 0$, that is, up to the time of approach to the bottom of the wave reflected from the free surface.

On the free surface of the tank, a velocity of $c^{(2)}$ and a pressure according to (3.40) are established in the linear approximation:

$$c^{(2)}=\frac{2c^{(1)}}{1+k_б},\quad p^{(2)}=p_б-\tilde{a}_б\tilde{Q}_б c^{(2)},\quad k_б=\frac{\tilde{a}_б\tilde{Q}_б}{aQ},$$

Key: 1. tank

a_{tank}, ρ_{tank} are the speed of sound and gas density above the free surface of the tank.

APPROVED FOR RELEASE: 2007/02/08: CIA-RDP82-00850R000200090053-2

APPROVED FOR RELEASE: 2007/02/08: CIA-RDP82-00850R000200090053-2

In practice for the investigated type of problems $a\rho >> a_{tank}\rho_{tank}$; therefore it is possible to consider that when the wave reaches the free surface the speed of the liquid doubles, and the pressure does not change.

The wave reflected from the free surface of the tank approaches the bottom, is reflected from it and the velocity $c^{(3)}$ and the pressure $p^{(3)}$ are established in front of the hole:

$$c^{(3)} = -\frac{a(1+k)}{\mu} \times$$

$$\times\left[1-\sqrt{1+\frac{\mu}{a^2(1+k)^2}\left[\frac{2(p^{(1)}-p_h)}{\varrho}+4ac^{(2)}+2ac^{(1)}(k-1)\right]}\right],$$

$$p^{(3)} = p^{(1)}+2a\varrho c^{(2)}-a\varrho c^{(3)}-a\varrho c^{(1)} = 2p_6-p^{(1)}+a\varrho\left(c^{(1)}-c^{(3)}\right),$$

$$k=\frac{a_0 s}{a s_0},$$

s, s_0 are the cross sections of the tank and the hole, respectively.

On the next reflection of the wave from the free surface of the tank, the velocity of the liquid on it is defined as follows:

$$c^{(4)} = \frac{2c^{(3)}+(k_6-1)c^{(2)}}{1+k_6} = 2c^{(3)}-c^{(2)} = 2\left(c^{(3)}-c^{(1)}\right).$$

For subsequent reflection of the wave from the bottom the velocity and pressure in front of the opening are defined as follows:

$$c^{(5)} = -\frac{a(1+k)}{\mu} \times$$

$$\times\left[1-\sqrt{1+\frac{\mu}{a^2(1+k)^2}\left[\frac{2(p^{(3)}-p_h)}{\varrho}+4ac^{(4)}+2ac^{(3)}(k-1)\right]}\right],$$

$$p^{(5)} = 2p_6-p^{(3)}+a\varrho\left(c^{(3)}-c^{(5)}\right) \text{ и т. д.}$$

In Table 3.12 the results are presented from numerical calculations for p_h=1 bar, p_{tank}=10 bars, $\rho=10^3$ kg/m^3, a=10 m/sec, s=100 s_0, k=20, $\mu=2\cdot10^4$, ε=1. The calculations were performed until the steady-state conditions were established.

Let us consider the problem of the nonsteady flow of a liquid in a tube when the tube is partially filled with liquid. On instantaneous response of a diaphragm the liquid begins to fill the line (Fig 3.9). The length of the segment of tubes between the forward edge of the liquid in the bottom of the tank is small so that in this section the wave can be reflected a multiple number of times from the leading edge of the liquid and from the hole out of the tank, before the reflected wave arrives from the free surface of the tank. Under this condition the invariant on the positive characteristic of the tank remains unchanged.

FOR OFFICIAL USE ONLY

APPROVED FOR RELEASE: 2007/02/08: CIA-RDP82-00850R000200090053-2

APPROVED FOR RELEASE: 2007/02/08: CIA-RDP82-00850R000200090053-2

Table 3.12

(1) Номер отражения	(2) $c^{(i)}$, м/с	$p^{(i)}$	(1) Номер отражения	(2) $c^{(i)}$, м/с	$p^{(i)}$	(1) Номер отражения	(2) $c^{(i)}$, м/с	$p^{(i)}$
1	0,14	8,6	9	0,221	8,87	21	0,274	9,26
2	0,28		10	0,334		23	0,28	10,68
3	0,173	11,07	11	0,242	10,925	25	0,2788	9,332
4	0,066		12	0,149		29	0,283	9,384
5	0,189	8,77	13	0,247	9,02	33	0,286	9,434
6	0,312		15	0,2625	10,825	37	0,287	9,484
7	0,21	11,02	17	0,263	9,17	41	0,289	9,504
8	0,108		19	0,273	10,73	43	0,289	10,496

Key:
1. No of the reflection
2. $c^{(1)}$, m/sec

On the leading front of the liquid in contact with the gas in the tube, the expressions for decay of the discontinuity are valid; let us denote by p_1, c_1 the values of the pressure and the velocity in the tank before the hole, p_2, c_2, the values of the pressure and the velocity of the liquid in the tube. Here, at the tank-tube interface these parameters have an even superscript, and at the liquid-gas interface (the leading edge), an odd superscript (the interface of medium 2, 3).

Thus, for the tank-tube interface on the i-th reflection of the wave from it running from the leading edge of the liquid along the return characteristic, we have the system of equations:

$$p_2^{(i+1)}=a_{2Q}\left[c_2^{(i+1)}-J_2^{(i)}\right],\quad J_2^{(i)}=c_3^{(i)}-\frac{p_3^{(i)}}{a_{2Q}},$$
$$p_1^{(i+1)}=\tilde{p}_1-a_{1Q}c_1^{(i+1)}. \tag{3.44}$$

Considering the equations of the flow rate and the Bernoulli equation from joint investigation of (3.44) after transformation we obtain:

$$c_1^{(i+1)}=-\frac{a_1(1+k_2)}{\mu}+\sqrt{\frac{a_1^2(1+k_2)^2}{\mu^2}+\frac{2\tilde{p}_1}{Q\mu}+\frac{2a_2J_2^{(i)}}{\mu}}, \tag{3.45}$$

where $k_2=s_1a_2/s_2a_1$, s_1, s_2 are the tank and tube cross sections, respectively; i=1, 3, 5, 7,....

APPROVED FOR RELEASE: 2007/02/08: CIA-RDP82-00850R000200090053-2

APPROVED FOR RELEASE: 2007/02/08: CIA-RDP82-00850R000200090053-2

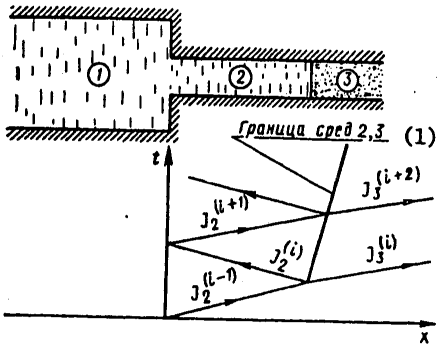

Figure 3.9. Field of the characteristic of the tube when it is filled with liquid in the tank

Key:

1. Interface of media 2, 3

Knowing the value of the velocity $c_1^{(i+1)}$, we find the velocity of the liquid at the entrance to the tube $c_2^{(i+1)}=c_1^{(i+1)}s_1/s_2$, the pressures on both sides of the cross section discontinuity, that is, at the opening on the side of the tank p_1^{i+1} and the tube $p_2^{(i+1)}$ according to (3.44)

Then let us construct the invariant on the forward characteristic of the tube, along which the wave is propagated from the tank to the leading edge of the liquid:

$$J_2^{(i+1)}=c_2^{(i+1)}+\frac{p_2^{(i+1)}}{a_2\varrho}=c_3^{(i+2)}+\frac{p_3^{(i+2)}}{a_2\varrho}.$$

The pressure on the interface of media 2, 3 is defined from the condition of constancy of the invariant of the return characteristic in the gas

$$p_3^{(i+2)}=\tilde{p}_3+a_3\varrho_3c_3^{(i+2)}.$$

From the obvious condition $p_3^{(i+2)}=p_2^{(i+2)}$, $c_3^{(i+2)}=c_2^{(i+2)}$ after transformations from these expressions the velocity pressure and the interface of the media 2, 3 will be defined

$$c_2^{(i+2)}=\frac{J_2^{(i+1)}}{1+k_3}-\frac{\tilde{p}_3}{a_2\varrho(1+k_3)},\quad p_2^{(i+2)}=\frac{\tilde{p}_3+a_3\varrho_3J_2^{(i+1)}}{1+k_3},$$

where $k_3=a_3\rho_3/a_2\rho_2$, ρ_3, a_3 are the density and speed of sound in medium 3.

Then let us construct the invariant J_2^- for the reflections from the interface 2, 3 of the wave and so on so that we have the recurrent formulas for the invariants

$$J_2^{(i)}=c_3^{(i)}-\frac{p_3^{(i)}}{a_1\varrho},\quad J_2^{(i+1)}=c_2^{(i+1)}+\frac{p_2^{(i+1)}}{a_2\varrho}.$$

FOR OFFICIAL USE ONLY

APPROVED FOR RELEASE: 2007/02/08: CIA-RDP82-00850R000200090053-2

APPROVED FOR RELEASE: 2007/02/08: CIA-RDP82-00850R000200090053-2

For numerical calculations where multiple reflections of the waves from the cross section discontinuity takes place (the medium 1, 2), in order to obtain the steady-state value of the pressure gradient at the discontinuity (p_1p_2~μc_1^2) it is impossible to use the linear approximation. With a sufficiently high degree of accuracy it is possible instead of (3.45) to use the formula taking into account the nonlinearity by the third term of the expansion of the binomial in a series

$$c_1^{(l+1)} \cong \frac{\tilde{p}_1 + a_2\varrho J_2^{(l)}}{a_1\varrho(1+k_2)} - \frac{(\tilde{p}_1 + a_2\varrho J_2^{(l)})^2}{2a_1^3\varrho^2(1+k_2)^3}\,\mu,$$

so that the pressure gradient at the cross section discontinuity

$$p_1^{(l+1)} - p_2^{(l+1)} \cong \frac{(\tilde{p}_1 + a_2\varrho J_2^{(l)})^2}{2a_1^2\varrho(1+k_2)^2},$$

where the expression of the first term is the value of the velocity c_1^{i+1} in the linear approximation.

In Table 3.13 the results are presented from numerical calculations for the case where $s_1=100s_2$, $p_3=1$ bar, $\tilde{p}_1=\tilde{p}_2=10$ bars, $a_1=a_2=10^3$ m/sec, $\rho_1=10^3$ kg/m^3, $\rho_3=1$ kg/m^3, $a_3=300$ m/sec, $k_3=3\cdot10^{-4}$, $k_2=100$, $\varepsilon=1$, $\mu=2\cdot10^4$. The calculation was performed until the time when the invariants on the positive characteristic coincided, which means the occurrence of the steady-state conditions of filling the line.

3.6. Propagation of Disturbances Through an Intermediate Reservoir in the Tube

The relations obtained for calculating the parameters of the drop liquid at the tube discontinuity on propagation of the wave will be used for the case where the wave passes through the segment of the tube which is a reservoir of constant cross section. In the general case the tubes connected to this reservoir have different cross sections, and the speed of sound of the liquid in the tubes and the reservoir is different (Fig 3.10). Let us introduce the notation a_1, a_2, a_3 -- the speed of sound in the tube to the left of the reservoir (region 1), in the intermediate reservoir and in the tube to the right of the reservoir (region 3), respectively. Let us introduce the dimensionless time $t=ta_2/\ell$, ℓ is the length of the reservoir, the dimensionless coordinate $x=x/\ell$. In the plane x, t the equation of the characteristics for essentially subsonic flows have the form $dx=\pm dt$. For convenience of calculations, the time interval $\Delta t=2$ is broken down into n small intervals so that the elementary time step is $\Delta t_n=2/n$, where n is assumed to be even. In this case in the time interval $0\leq t\leq 2$, $r_{max}=n+1$ characteristics of one family are found, where r is the characteristic number. Then let us denote by k=1 the cross section discontinuity at the interface of the regions 1, 2 and k=2, the discontinuity of the cross sections at the interface of the regions 2, 3, respectively.

APPROVED FOR RELEASE: 2007/02/08: CIA-RDP82-00850R000200090053-2

APPROVED FOR RELEASE: 2007/02/08: CIA-RDP82-00850R000200090053-2

Table 3.13

Номер отражения (1)	c_1, м/с (2)	c_2, м/с (3)	p_1, бар (4)	p_2, бар (5)	J_2^+, м/с (6)	J_2^-, м/с (7)
1	0	0,9	10	1	—	0,8
2	0,0178	1,78	9,82	9,79	2,76	—
3	0,0178	2,66	9,82	1,008	—	2,56
4	0,0352	3,52	9,64	9,522	4,47	—
5	0,0352	4,367	9,64	1,01	—	4,266
6	0,0522	5,22	9,478	9,208	6,14	—
25	—	18,2092	—	1,0546	—	18,1037
26	0,1865	18,65	8,135	4,645	19,1145	—
41	—	22,6132	—	1,0677	—	22,5064
42	0,228	22,8	7,72	2,52	23,052	—
51	—	23,9628	—	1,0717	—	23,8556
52	0,241	24,1	7,59	1,79	24,279	—
61	—	24,6416	—	1,0739	—	24,5342
62	0,247	24,7	7,53	1,41	24,846	—
71	—	25,0373	—	1,0747	—	24,9298
72	0,2508	25,08	7,492	1,202	25,2	—
83	—	25,3783	—	1,0762	—	25,27
84	0,254	25,4	7,46	1,01	25,5	—
85	—	25,393	—	1,0762	—	25,2857
86	0,25393	25,393	7,46	1,07	25,5	—

Key:
1. Reflection No
2. c_1, m/sec
3. c_2, m/sec
4. p_1, bar
5. p_2, bar
6. J_2^+, m/sec
7. J_2^-, m/sec

At the interface k=1 or 4=1 (first series of characteristics of the positive direction in the reservoir) we have such initial expressions:

$$2\bar{p}_1+\bar{c}_1^2=2\bar{p}_2+\bar{c}_2^2,\quad \bar{J}_1=\bar{c}_1+\bar{p}_1/w_1,$$
$$\bar{J}_2=\bar{c}_2-\bar{p}_2,\quad \bar{c}_1=\bar{c}_2\bar{s}_2, \tag{3.46}$$

where the bar at the top means that the investigated parameter is dimensionless: namely,

$$\bar{J}_1=J_1/a_2;\quad \bar{J}_2=J_2/a_2;\quad \bar{J}_3=J_3/a_3;\quad \bar{p}_1=p_1/a_{2Q}^2;$$
$$\bar{p}_2=p_2/a_{2Q}^2;\quad \bar{p}_3=p_3/a_{2Q}^2;\quad \bar{c}_1=c_1/a_2;\quad \bar{c}_2=c_2/a_2;$$
$$\bar{s}_2=s_2/s_1;\quad w_1=a_1/a_2.$$

FOR OFFICIAL USE ONLY

APPROVED FOR RELEASE: 2007/02/08: CIA-RDP82-00850R000200090053-2

APPROVED FOR RELEASE: 2007/02/08: CIA-RDP82-00850R000200090053-2

After the transformations from (3.46) we find the values of the velocity in the reservoir for the cross section k=1 for an arbitrary series of characteristics r.

$$\bar{c}_{r,1}^{(2)}=\frac{1+w_1\bar{s}_2}{1-\bar{s}_2^2}\left\{\sqrt{1+\frac{2(1-\bar{s}_2^2)}{(1+w_1\bar{s}_2)}(\bar{J}_{r-1,2}^{(2)}+w_1J_{r,0}^{(1)})}-1\right\}, \tag{3.47}$$

where the superscript in the braces denotes the number of the region to which the value of the corresponding parameter belongs, the lower first index indicates the number of the series of characteristics, the lower second index denotes the number of the tube cross section in it. In particular, the index "0" pertains to the cross section of the tube 1 at its input on the left.

Knowing the speed in the reservoir, from (3.46) we find the speed in the tube 1 and the corresponding pressures:

$$\bar{c}_{r,1}^{(1)}=\bar{c}_{r,1}^{(2)}\bar{s}_2;$$
$$\bar{p}_{r,1}^{(1)}=w_1(\bar{J}_{r,0}^{(1)}-\bar{c}_{r,1}^{(1)});$$
$$\bar{p}_{r,1}^{(2)}=\bar{c}_{r,1}^{(2)}-\bar{J}_{r-1,2}^{(2)},$$

where the invariants are known

$$\bar{J}_{r-1,2}^{(2)}=\bar{c}_{r-1,2}^{(2)}-\bar{p}_{r-1,2}^{(2)};$$
$$\bar{J}_{r,0}^{(1)}=\bar{c}_{r,0}^{(1)}+\bar{p}_{r,0}^{(1)}/w_1.$$

Here it is proposed that the disturbance is propagated from left to right that is, from tube 1 to reservoir 2 and then to tube 3; therefore the speed and the pressure in tube 1 are related to each other according to the formulas for the simple waves $\bar{c}_{r,0}^{(1)}=\frac{\bar{p}^+-\bar{p}_0}{w_1}$, $\bar{p}_{r,0}^{(1)}=\bar{p}^+$, where $\bar{p}^+$ is the disturbed value of the pressure on the left end of tube 1, $\bar{p}_0$ is the undisturbed pressure in the tube.

After determination of the parameters in the circles of cross section k=1 let us construct the invariant $\bar{J}^{(2)}_{r,1}$ carried along the forward characteristic in the reservoir from the cross section k=1 to the cross section k=2:

$$\bar{J}_{r,1}^{(2)}=\bar{c}_{r,1}^{(2)}+\bar{p}_{r,1}^{(2)}.$$

In the vicinities of the cross section k=2 we have the following initial relations:

$$2\bar{p}_2+\bar{c}_2^{(2)}=2\bar{p}_3+\bar{c}_3^2;\quad \bar{J}_2=\bar{c}_2+\bar{p}_2;$$
$$\bar{J}_3=\bar{c}_3-\bar{p}_3/w_3;\quad \bar{c}_2=\bar{c}_3\bar{s}_3,$$

APPROVED FOR RELEASE: 2007/02/08: CIA-RDP82-00850R000200090053-2

APPROVED FOR RELEASE: 2007/02/08: CIA-RDP82-00850R000200090053-2

where $w_3 = a_3/a_2;\ \bar{s}_3 = s_3/s_2.$

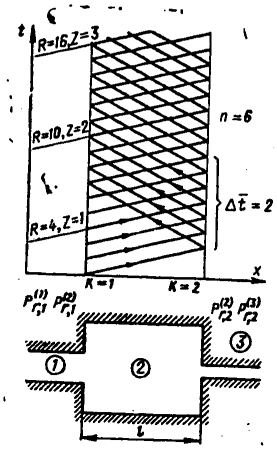

Figure 3.10. Propagation of the simple waves through an intermediate reservoir in the tube. The field of the characteristics inside the reservoir.

After the transformations we find the speed in the tube 3 for an arbitrary series of characteristics r:

$$\bar{c}^{(3)}_{r,2} = \frac{w_3 + \bar{s}_3}{1 - \bar{s}_3^2}\left\{\sqrt{1 + \frac{2(1-\bar{s}_3^2)}{(w_3+\bar{s}_3)^2}(w_3 - \bar{J}^{(3)}_{r-1,3} + \bar{J}^{(2)}_{r,1})} - 1\right\}, \qquad (3.48)$$

where the invariant $\bar{J}^{(2)}_{r,1}$ is known (in particular, for the initial conditions), and the invariant $\bar{J}^{(3)}_{r-1,3}$ has the form:

$$\bar{J}^{(3)}_{r-1,3} = \bar{c}^{(3)}_{r-1,3} - \bar{p}^{(3)}_{r-1,3}/w_3.$$

Knowing the speed in the tube 3, we find the values of the other parameters in the vicinities of the cross section k=2:

$$\bar{c}^{(2)}_{r,2} = c^{(3)}_{r,2}\bar{s}_3;$$
$$\bar{p}^{(2)}_{r,2} = \bar{J}^{(2)}_{r,1} - \bar{c}^{(2)}_{r,2};\quad \bar{p}^{(3)}_{r,2} = w_3(\bar{c}^{(3)}_{r,2} - \bar{J}^{(3)}_{r-1,3}).$$

Then let us construct the invariant for the reservoir on the characteristic of the return direction:

$$\bar{J}^{(2)}_{r,2} = \bar{c}^{(2)}_{r,2} - \bar{p}^{(2)}_{r,2}.$$

APPROVED FOR RELEASE: 2007/02/08: CIA-RDP82-00850R000200090053-2

APPROVED FOR RELEASE: 2007/02/08: CIA-RDP82-00850R000200090053-2

In the linear approximation from (3.47), (3.48) we obtain the following expressions:

$$\bar{c}^{(2)}_{r,1}\cong\frac{\bar{J}^{(2)}_{r-1,2}+w_1\bar{J}^{(1)}_{r,0}}{1+w_1\bar{s}_2};\quad \bar{c}^{(3)}_{r,2}\cong\frac{w_3\bar{J}^{(3)}_{r-1,3}+\bar{J}^{(2)}_{r,1}}{w_3+\bar{s}_3};$$
$$\bar{p}^{(1)}_{r,1}\cong\bar{p}^{(2)}_{r,1};\quad \bar{p}^{(2)}_{r,2}\cong\bar{p}^{(3)}_{r,2}.$$

The above-presented expressions are valid for the case where on the characteristic of one family on both sides of it (bottom and top) the Riemann invariants are different, which corresponds to the propagation of the shock through the intermediate reservoir. For disturbance of arbitrary shape when there are n small intervals in the time interval $\Delta t=2$, in relations (3.47), (3.48) and others, it is necessary to write the following invariants in this form: instead of $\bar{J}^{(2)}_{r-1}$, (3.47), (3.48) we have

$$\bar{J}^{(2)}_{r-n,2}=\bar{c}^{(2)}_{r-n,2}-\bar{p}^{(2)}_{r-n,2},\qquad \text{and also } w_1\bar{J}^{(1)}_{r,0}=2\bar{p}^{(1)}_{r,0}-\bar{p}_0;\ \bar{J}^{(2)}_{r-n,2}=-\bar{p}_0.$$

Under these conditions the formulas of the linear approximations are converted to the form:

$$\bar{c}^{(2)}_{r,1}=\frac{2(\bar{p}^{(1)}_{r,0}-\bar{p}_0)}{1+w_1\bar{s}_2},\quad \bar{p}^{(1)}_{r,1}=\bar{p}^{(2)}_{r,1}=\bar{p}_0+\frac{2(\bar{p}^{(1)}_{r,0}-\bar{p}_0)}{1+w_1\bar{s}_2}.$$

Correspondingly, for the cross section k=2 we have the formulas of the linear approximation:

$$\bar{J}^{(2)}_{r,1}=\bar{p}_0+\frac{4(\bar{p}^{(1)}_{r,0}-\bar{p}_0)}{1+w_1\bar{s}_2},\quad \bar{J}^{(3)}_{r-1,3}=-\bar{p}_0/w_3,$$
$$\bar{c}^{(3)}_{r,2}=\frac{4(\bar{p}^{(1)}_{r,0}-\bar{p}_0)}{(1+w_1\bar{s}_2)(w_3+\bar{s}_3)};$$
$$\bar{p}^{(3)}_{r,2}=\bar{p}^{(2)}_{r,2}=\bar{p}_0+\frac{4w_3(\bar{p}^{(1)}_{r,0}-\bar{p}_0)}{(1+w_1\bar{s}_2)(w_3+\bar{s}_3)}.$$

The above-presented expressions are valid for $r\geq n+1$, and for $r<n+1$ it is necessary to set $\bar{J}^{(2)}_{r-n}=-p_0=\text{const}$.

Let us consider the case where the wave reflected from the boundary k=2 approaches the boundary k=1. Here the corresponding invariants and velocities will be expressed in terms of the pressure at the interface k=1, $\bar{p}^{(1)}_{r,0}$. For this we shall exclude the corresponding invariants from the investigation, and the desired parameters will be defined in terms of the limiting pressure. Let us introduce the notation:

$$\Psi_1=1+w_1s_2,\ \Psi_3=w_3+\bar{s}_3,\ \Psi^*_3=\bar{s}_3-w_3.$$

APPROVED FOR RELEASE: 2007/02/08: CIA-RDP82-00850R000200090053-2

APPROVED FOR RELEASE: 2007/02/08: CIA-RDP82-00850R000200090053-2

Then we shall denote by z the number of the reflection at the boundary k=1. For example, z=1 means that the wave from tube 1 has approached the cross section discontinuity k=1.

Let us denote by R the number of the series for the time interval $\bar{t} \subset [0,2]$ or $R \subset [1, n]$.

In order to obtain the recurrent expressions let us use the recursion method.

For the boundary k=1 from (3.55) considering the expressions for the invariants $\bar{J}^{(2)}_{r-n,2}$ we have:

$$\bar{c}^{(2)}_{R+(z-1)n,1} = \frac{\bar{J}^{(2)}_{R+(z-2)n,2} + 2\bar{p}^{(1)}_{R+(z-1)n,0} - \bar{p}_0}{\Psi_1}.$$

$\bar{J}^{(2)}_{R-n,2} = -\bar{p}_0$, $\bar{p}^{(1)}_{R,0} = \bar{p}_0$ -- if there is no pressure discontinuities z=1, 2, 3,... Then we find the pressure

$$\bar{p}^{(2)}_{R+(z-1)n,1} = \bar{p}^{(1)}_{R+(z-1)n,1} = \frac{2\bar{p}_{R+(z-1)n,0} - \bar{p}_0}{\Psi_1} + \left(\frac{1}{\Psi_1} - 1\right)\bar{J}^{(2)}_{R+(z-2)n,2}.$$

By using these formulas we construct the invariant on the forward characteristic running from the cross section k=1 to the cross section k=2:

$$\bar{J}^{(2)}_{R+(z-1)n,1} = \frac{2}{\Psi_1}\left(2\bar{p}^{(1)}_{R+(z-1)n,1} - \bar{p}_0\right) + \left(\frac{2}{\Psi_1} - 1\right)\bar{J}^{(2)}_{R+(z-2)n,2}.$$

At the interface k=2 in the linear approximation we have the expressions for the velocity and pressure:

$$\bar{c}^{(3)}_{R+(z-1)n,2} = \frac{\bar{J}^{(2)}_{R+(z-1)n,1} - \bar{p}_0}{\Psi_3};$$

$$\bar{p}^{(2)}_{R+(z-1)n,2} = \bar{p}^{(3)}_{R+(z-1)n,2} = \bar{p}_0\left(1 - \frac{\varpi_3}{\Psi_3}\right) + \frac{\varpi_3}{\Psi_3}\bar{J}^{(2)}_{R+(z-1)n,1}.$$

Then we construct the invariant for the characteristic of the return direction running from the cross section k=2 to the cross section k=1:

$$\bar{J}^{(2)}_{R+(z-1)n,2} = \frac{\Psi^*_3}{\Psi_3}\bar{J}^{(2)}_{R+(z-1)n,1} - \left(1 + \frac{\Psi^*_3}{\Psi_3}\right)\bar{p}_0 \text{ and so on.}$$

After transformations for the cross section k=1 we have the recurrent expressions for the basic parameters of the liquid:

$$\bar{p}^{(2)}_{R+(z-1)n,1} = \bar{p}_0 + \frac{2\left(\bar{p}^{(1)}_{R+(z-1)n,0} - \bar{p}_0\right)}{\Psi_1} +$$

$$+ \frac{4\Psi^*_3}{\Psi_1\Psi_3}\left(\frac{1}{\Psi_1} - 1\right)\sum_{m=2}^{z}\Psi^{z-m}\left(p^{(1)}_{R+(m-2)n,0} - \bar{p}_0\right); \qquad (3.49)$$

APPROVED FOR RELEASE: 2007/02/08: CIA-RDP82-00850R000200090053-2

APPROVED FOR RELEASE: 2007/02/08: CIA-RDP82-00850R000200090053-2

$$\bar{c}^{(2)}_{R+(z-1)n,1}=\frac{2\left(\bar{p}^{(1)}_{R+(z-1)n,0}-\bar{p}_0\right)}{\Psi_1}+\frac{4\Psi^*_3}{\Psi_1^2\Psi_3}\sum_{m=2}^{z}\Psi^{z-m}\left(\bar{p}^{(1)}_{R+(m-2)n,0}-\bar{p}_0\right);$$

$$\bar{c}^{(1)}_{R+(z-1)n,1}=\bar{c}^{(2)}_{R+(z-1)n,1}\bar{s}_2,\quad \Psi=\frac{\Psi^*_3}{\Psi_3}\left(\frac{2}{\Psi_1}-1\right).$$

Correspondingly, for the interface k=2 we have:

$$\begin{aligned}
&\bar{p}^{(2)}_{R+(z-1)n,2}=\bar{p}_0+\frac{4w_3}{\Psi_1\Psi_3}\sum_{m=1}^{z}\Psi^{z-m}\left(\bar{p}^{(1)}_{R+(m-1)n,0}-\bar{p}_0\right);\\
&\bar{c}^{(3)}_{R+(z-1)n,2}=\frac{4}{\Psi_1\Psi_3}\sum_{m=1}^{z}\Psi^{z-m}\left(\bar{p}^{(1)}_{R+(m-1)n,0}-\bar{p}_0\right);\\
&\bar{c}^{(2)}_{R+(z-1)n,2}=\bar{c}^{(3)}_{R+(z-1)n,2}\bar{s}_3.
\end{aligned}\qquad (3.50)$$

The transition from the notation z, R to r and time is performed by the formula

$$r=R+(z-1)n,\quad \bar{t}=\frac{2(R-1)}{n}+2\cdot(z-1).$$

In the above-presented formula the terms in the lower indexes (z=1)n or (m-1)n, (m-2)n are multiples for the time interval t=2 with the factor (z=1), (m-1), (m-2), and so on.

In the special case where the pressure discontinuity enters into the intermediate reservoir in the form of a step so that $\bar{p}^{(1)}_{R+(m-2)n,0}=\bar{p}^{+}$, $\bar{p}^{(1)}_{R+(m-1)n,0}=\bar{p}^{+}$, where $\bar{p}^{+}$ is the disturbed pressure on the left end of the tube 1, the expressions (3.49) and (3.50) are transformed to the form:

$$\begin{aligned}
&\bar{p}^{(2)}_1-\bar{p}_0=\frac{2(\bar{p}^{+}-\bar{p}_0)}{\Psi_1}+\frac{4\Psi^*_3(\bar{p}^{+}-\bar{p}_0)}{\Psi_1\Psi_3}\left(\frac{1}{\Psi_1}-1\right)\frac{\Psi^{z-2}-1}{\Psi-1};\\
&\bar{p}^{(2)}_2-\bar{p}_0=\frac{4w_3}{\Psi_1\Psi_3}(\bar{p}^{+}-\bar{p}_0)\frac{\Psi^{z-1}-1}{\Psi-1};\\
&\bar{c}^{(2)}_1=\frac{2(\bar{p}^{+}-\bar{p}_0)}{\Psi_1}+\frac{4\Psi^*_3(\bar{p}^{+}-\bar{p}_0)}{\Psi_1^2\Psi_3}\frac{\Psi^{z-2}-1}{\Psi-1};\\
&\bar{c}^{(3)}_2=\frac{4(\bar{p}^{+}-\bar{p}_0)}{\Psi_1\Psi_3}\frac{\Psi^{z-1}-1}{\Psi-1}.
\end{aligned}$$

When establishing the steady-state flow in the intermediate reservoir where the pressure "goes down" as a result of numerous reflections from the cross sections k=1,2, the values of the parameters are calculated by the above-presented formulas in which it is necessary to set $z=\infty$. In this case we obtain

APPROVED FOR RELEASE: 2007/02/08: CIA-RDP82-00850R000200090053-2

APPROVED FOR RELEASE: 2007/02/08: CIA-RDP82-00850R000200090053-2

$$\Delta\bar{p}_{1\infty}^{(2)}=\bar{p}_1^{(2)}-\bar{p}_0=\Delta\bar{p}_{2\infty}^{(2)}=\bar{p}_2^{(2)}-\bar{p}_0=\frac{2w_3(\bar{p}^+-\bar{p}_0)}{w_3+w_1s_2s_3}.$$

From analysis of this formula it follows that the magnitude of the excess pressure in the intermediate reservoir does not depend on the elastic properties of the reservoir, but is determined by the characteristics of the tubes 1, 3. On going from the dimensionless parameters to the dimensional parameters, we obtain:

$$\Delta p_{1\infty}^{(2)}=\Delta p_{2\infty}^{(2)}=\frac{2(p^+-p_0)}{1+\frac{a_1s_3}{a_3s_1}}.$$

For limiting values of the velocities, corresponding, we obtain (for z=∞):

$$\bar{c}_{1\infty}^{(2)}=\frac{2\bar{s}_3(\bar{p}^+-\bar{p}_0)}{w_3+w_1\bar{s}_2\bar{s}_3};\quad \bar{c}_{1\infty}^{(1)}=\frac{2\bar{s}_2\bar{s}_3(\bar{p}^+-\bar{p}_0)}{w_3+w_1\bar{s}_2\bar{s}_3};$$
$$\bar{c}_{2\infty}^{(3)}=\frac{2(\bar{p}^+-\bar{p}_0)}{w_3+w_1\bar{s}_2\bar{s}_3};\quad \bar{c}_{2\infty}^{(2)}=\frac{2\bar{s}_3(\bar{p}^+-\bar{p}_0)}{w_3+w_1\bar{s}_2\bar{s}_3}.$$

From the investigation of these formulas it follows that in the limiting case, just as should be expected, in the intermediate reservoir and on both boundaries of it an identical liquid flow rate is established.

In Table 3.14 the results are presented from numerical calculations of the transmission of the rarefaction shock from the tube 1 to the intermediate reservoir of the same cross section and then to the tube 3 under the condition: $\bar{p}^+=0$,

$$\bar{p}_0=10^{-2},\ \bar{s}_2=\bar{s}_3=1,\ w_1=w_3=3,\ \bar{J}_{r,0}^{(1)}w_1+\bar{p}_0=0,$$
$$\bar{J}_{r-1,3}^{(3)}w_3+\bar{p}_0=0,\ \bar{J}_{0,2}^{(2)}+p_0=0,\ \bar{J}_{0,3}^{(3)}w_3+\bar{p}_0=0.$$

The results presented in the table must be multiplifed by 10^{-2}.

In Table 3.15 the results are presented from the numerical calculations for the passage of the compression shock $\bar{p}^+=10^{-2}$, $p_0=0$ through the intermediate reservoir and for the remaining conditions as for Table 14. Here

$$\bar{J}_{r,0}^{(1)}=\frac{2}{3},\ \bar{J}_{0,3}^{(3)}=\bar{J}_{0,2}^{(2)}=0.$$

In the intermediate reservoir the cross section of which is identical with the cross sections of tubes 1, 3, the speed of the liquid at z=∞ approaches the value which occurs in the simple wave of the initial disturbance propagated in tube 1 and determined in accordance with the formulas for the simple wave $\bar{c}_{1,0}^{(1)}=\frac{\bar{p}^+-\bar{p}_0}{w_1}=0{,}333\cdot10^{-2}$.

APPROVED FOR RELEASE: 2007/02/08: CIA-RDP82-00850R000200090053-2

APPROVED FOR RELEASE: 2007/02/08: CIA-RDP82-00850R000200090053-2

Table 3.14

r	$\bar{c}^{(2)}_{r,1}=\bar{c}^{(1)}_{r,1}$	$\bar{p}^{(1)}_{r,1}=\bar{p}^{(2)}_{r,1}$	$\bar{c}^{(2)}_{r,2}=\bar{c}^{(3)}_{r,2}$	$\bar{p}^{(3)}_{r,2}=\bar{p}^{(2)}_{r,2}$	$\bar{J}^{(2)}_{r,1}$	$\bar{J}^{(2)}_{r,2}$
1	−0,5	0,5	−0,25	0,25	0	−0,5
2	−0,375	0,125	−0,3125	0,0625	−0,25	−0,375
3	−0,344	0,031	−0,328	0,015	−0,313	−0,343
4	−0,336	0,007	−0,332	0,003	−0,329	−0,335
5	−0,3335	0,0015	−0,333	0,001	−0,332	−0,334
6	−0,3335	0,0005	−0,3335	0,0005	−0,333	−0,334

Table 3.15

r	$\bar{c}^{(2)}_{r,1}=\bar{c}^{(1)}_{r,1}$	$\bar{p}^{(1)}_{r,1}=\bar{p}^{(2)}_{r,1}$	$\bar{c}^{(2)}_{r,2}=\bar{c}^{(3)}_{r,2}$	$\bar{p}^{(3)}_{r,2}=\bar{p}^{(2)}_{r,2}$	$\bar{J}^{(2)}_{r,1}$	$\bar{J}^{(2)}_{r,2}$
1	0,5	0,5	0,25	0,75	1	−0,5
2	0,375	0,875	0,3125	0,9375	1,25	−0,625
3	0,343	0,968	0,327	0,984	1,311	−0,657
4	0,336	0,993	0,332	0,997	1,329	−0,665

In the conclusion of this item, a study is made of the problems of the propagation at the leading edge of the pressure (velocity) discontinuity in the liquid filling the intermediate reservoir of complex configuration and made up of a number of successive reservoirs, each of which have constant cross section (see Fig 3.11), and the other properties of the reservoirs are identical, that is, $a_1=a_2=a_3=\ldots a_{n+2}$, where n is the total number of intermediate cross sections (reservoirs) between the tube 1 (s_1) and the tube n+2 (s_{n+2}). If the number n=1, then the total number of regions is equal to 3 as occurs in the above-presented cases. In Fig 3.11 the total number of intermediate cross sections (reservoirs) is equal to 2.

Let us denote by $\Delta p^+=p^+-p_0$ the pressure gradient at the shock front in the tube 1, $\Delta p_{n+2}=p_{n+2}-p_0$, the pressure gradient at the shock front. At the output from the finite intermediate reservoir, and according to (3.49) we have the relation between them

$$\Delta p_{n+2}=2^{n+1}\Delta p^+\prod_{l=1}^{n}s_l:\left[\prod_{l=1}^{n}(1+\bar{s}_l)\left(K+\prod_{l=1}^{n}\bar{s}_l\right)\right], \qquad (3.51)$$

where $\bar{s}_l=\frac{s_{l+1}}{s_l}$, $K=\frac{s_{n+2}}{s_1}$ is the total gradient of the cross sections between the right and left tubes.

APPROVED FOR RELEASE: 2007/02/08: CIA-RDP82-00850R000200090053-2

APPROVED FOR RELEASE: 2007/02/08: CIA-RDP82-00850R000200090053-2

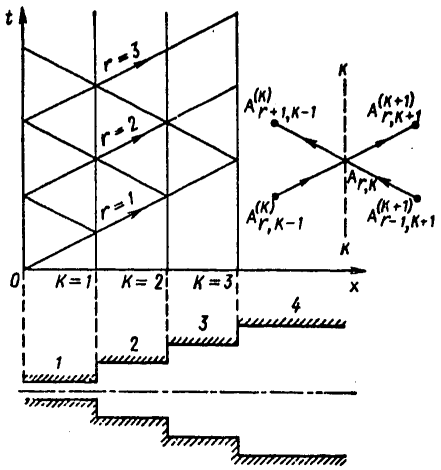

Figure 3.11. Propagation of simple waves through a series of series-connected reservoirs. The field of the characteristics for the cross section k are converging at the point $A_{r,k}$

The maximum value of the pressure gradient at the exit occurs when the ratio of the cross sections of the corresponding intermediate reservoirs is defined as follows: $\bar{s}_i = \sqrt[n+1]{K}$.

In this case from (3.51) we find:

$$(\Delta p_{n+2})_{max} = 2^{n+1}\Delta p^+ : (1+\sqrt[n+1]{K})^{n+1}. \qquad (3.52)$$

At the limit when the number of intermediate reservoirs is very large and n>>1, so that $\sqrt[n+1]{K} = 1+\delta$ and $|\delta|<<$, we have $\sqrt[n+1]{K} \cong 1+\frac{\ln K}{n+1}$ and $(1+\sqrt[n+1]{K})^{n+1} \cong \left(2+\frac{\ln K}{n+1}\right)^{n+1} \cong 2^{n+1}\left(1+\frac{\ln \sqrt{K}}{n+1}\right)^{n+1}$.

After transformations for n=∞ we find:

$$(\Delta p_{n+2})_{max,\, n\to\infty} = \Delta p^+/\sqrt{K}.$$

The ratio of the pressure gradient for the case of n intermediate cross sections to the pressure gradient for the case of n=0 for different K is presented in Table 3.16.

The presence of intermediate reservoirs is felt to a greater degree when their number is large and the cross section gradient of the tubes K is significant.

FOR OFFICIAL USE ONLY

APPROVED FOR RELEASE: 2007/02/08: CIA-RDP82-00850R000200090053-2

APPROVED FOR RELEASE: 2007/02/08: CIA-RDP82-00850R000200090053-2

Table 3.16

K	n					
	0	1	2	3	4	∞
2	1	1,035	1,036	1,044	1,048	1,062
4	1	1,11	1,155	1,185	1,186	1,25
10	1	1,272	1,4	1,48	1,53	1,74
100	1	1,67	2,25	2,7	3,05	5,04

Any deviation of the ratio of the cross sections $\bar{s}_i$ from the optimal value leads to a decrease in the pressure amplitude in the leading edge of the shock.

The problem of the propagation of a disturbance through a series of intermediate reservoirs can be generalized to the case of the propagation of a disturbance through the tube of variable cross section. For this purpose the tube of variable cross section is considered as a complex string of pipe made up of individual short sections of tubing of constant cross section, that is, the continuous nature of the variation of the tube cross section is replaced by discontinuous. In each section of tubing of constant cross section the corresponding Riemann invariants are valid, and the calculation of the liquid parameters on going from one tube to another is realized in accordance with the presented formulas for the tube cross section discontinuity.

If the segment of tubing of variable cross section is broken down into "n" segments of tubing of constant cross section (see Fig 3.11), the total number of investigated regions is n+1. Let us denote by $A_{r,k}$ the coordinate of the point lying at the intersection of the forward characteristic r and the discontinuity cross section of the tubing k. To the left of this cross section is the region with the index "k," that is, the section of tubing of constant cross section s_k, and to the right of this cross section is the region with the index "k+1," that is, the segment with tubing of constant cross section s_{k+1}. The index of the region with the corresponding parameter is located at the top in parentheses, and the index of the cross section is at the bottom. In order to determine the liquid parameters on both sides of the cross section "k" it is necessary to know the value of the invariant on the characteristic of the inverse direction, running from the cross section "k+1" from the characteristic of the forward direction along below and also the value of the invariant of the light characteristic, but running from the cross section "k-1" (see Fig 3.11).

The initial system of equations for the point $A_{r,k}$ has the form:

APPROVED FOR RELEASE: 2007/02/08: CIA-RDP82-00850R000200090053-2

APPROVED FOR RELEASE: 2007/02/08: CIA-RDP82-00850R000200090053-2

$$\bar{p}_{r,k}^{(k)}=\bar{J}_{r,k-1}^{(k)}-\bar{c}_{r,k}^{(k)};\quad 2\bar{p}_{r,k}^{(k)}+\bar{c}_{r,k}^{(k)^2}=2\bar{p}_{r,k}^{(k+1)}+\bar{c}_{r,k}^{(k+1)^2};\qquad (3.52,a)$$

$$\bar{p}_{r,k}^{(k+1)}=\bar{c}_{r,k}^{(k+1)}-\bar{J}_{r-1,k+1}^{(k+1)};\quad s^{(k+1)}=\frac{s_{k+1}}{s_k};$$

$$\bar{c}_{r,k}^{(k)}=\bar{c}_{r,k}^{(k+1)}s^{(k+1)},$$

where the invariants $\bar{J}_{r,k-1}^{(k)}$, $\bar{J}_{r-1,k+1}^{(k+1)}$ are found from the preceding calculations:

$$\bar{J}_{r,k-1}^{(k)}=\bar{c}_{r,k-1}^{(k)}+\bar{p}_{r,k-1}^{(k)};\quad \bar{J}_{r-1,k+1}^{(k+1)}=\bar{c}_{r-1,k+1}^{(k+1)}-\bar{p}_{r-1,k+1}^{(k+1)}.$$

After the transformations (3.52, a) we find the expression for determining the velocity:

$$\bar{c}_{r,k}^{(k+1)}=\frac{1}{1+s^{(k+1)}}\left\{\sqrt{1+\frac{2(1-s^{(k+1)})}{1+s^{(k+1)}}\left(\bar{J}_{r,k-1}^{(k)}+\bar{J}_{r-1,k+1}^{(k+1)}\right)}-1\right\}.$$

Then from (3.52,a) we find the values of all other parameters of the liquid and construct the invariants:

$$\bar{J}_{r,k}^{(k+1)}=\bar{c}_{r,k}^{(k+1)}+\bar{p}_{r,k}^{(k+1)};\quad \bar{J}_{r,k}^{(k)}=\bar{c}_{r,k}^{(k)}-\bar{p}_{r,k}^{(k)}.$$

If at the initial point in time the liquid in the tube has become quiet, then the initial conditions for the problem are the following:

$\bar{J}_{0,k+1}^{(k+1)}+\bar{p}_0=0$. and $\bar{p}_0$ is the initial pressure. Otherwise $\bar{J}_{0,k+1}^{(k+1)}=\bar{c}_{0,k+1}^{(k+1)}-\bar{p}_{0,k+1}^{(k+1)}$, where the initial parameters are given for the undisturbed flow of liquid.

When the pressure discontinuity p^+ enters into the tube in the form of a rectangular step, so that the reflections at the cross sections k=0 and k=n+1 are absent, the boundary conditions are written in the following form:

$$\bar{J}_{r,0}^{(1)}=2\bar{p}^+-\bar{p}_0;\quad \bar{J}_{r,n+2}^{(n+2)}+\bar{p}_0=0. \qquad (3.53)$$

When at the boundary k=0 the pressure is given $\bar{p}_{r,0}^{(0)}=\bar{p}_{r,0}^{+}$ the boundary condition in this cross section is written as follows:

$$\bar{J}_{r,0}^{(1)}=2\bar{p}_{r,0}^{(0)}+\bar{J}_{r-1,1}^{(1)},\quad \bar{J}_{0,1}^{(1)}+\bar{p}_0=0.$$

The time is related to the parameters r, k by the expression

$$\bar{t}_{r,k}^{(k)}=\bar{t}_{r,k}^{(k+1)}=\frac{2(r-1)}{n+1}+\frac{k}{n+1},$$

APPROVED FOR RELEASE: 2007/02/08: CIA-RDP82-00850R000200090053-2

APPROVED FOR RELEASE: 2007/02/08: CIA-RDP82-00850R000200090053-2

where $\bar{t}=ta/\ell$, ℓ is the total length of the segment of tubing of variable cross sections; a is the speed of sound in the liquid.

In Table 3.17 the results of the calculations are presented with respect to propagation of the rarefaction shock to the tube of variable cross section when $s_{n+1}=9s_1$, $s^{(k+1)}=1.73$; $\bar{p}^+=0$, $\bar{p}_0=10^{-2}$ under the boundary conditions (3.62) and n=4. The table values of the parameters must be multiplied by 10^{-2}.

Table 3.17

r	$-\bar{c}^{(1)}_{r,1}$	$-\bar{c}^{(3)}_{r,3}$	$-\bar{c}^{(5)}_{r,4}$	$\bar{p}^{(1)}_{r,1}$	$\bar{p}^{(3)}_{r,3}$	$\bar{p}^{(5)}_{r,4}$
1	1,267	0,682	0,288	0,267	0,6085	0,7125
2	1,515	0,715	0,226	0,515	0,796	0,774
3	1,73	0,608	0,1975	0,73	0,813	0,802
4	1,89	0,578	0,1925	0,895	0,809	0,8075
5	1,81	0,598	0,202	0,81	0,794	0,798
6	1,783	0,606	0,215	0,783	0,796	0,797
7	1,79	0,603	0,2015	0,79	0,799	0,798
8	1,8	0,602	0,201	0,8	0,799	0,799
9	1,8	0,602	0,201	0,8	0,8	0,8

The analysis of the results of the numerical calculations indicates that in a channel of variable cross section the appearance of both large pressure amplitudes and small significantly exceeding the amplitude of the initial disturbance with respect to magnitude is possible. Thus, on propagation of the rarefaction shock to the converging channel, the calculated values of the pressures reach negative values, which indicates the possibility of the appearance of cavitational phenomena. In particular, for the constricting channel the maximum surge of negative pressures occurs on the characteristic of the first series in which the parameters of the liquid are determined to (3.51). If we denote by p_s the saturated vapor pressure in the liquid, then the minimum value of the pressure at the entrance to the tube for which the pressure at the exit reaches the value of p_s for $n=\infty$ will be defined by the formula (3.51) after the corresponding transformation:

$$(p^*_{\min}-p_0)=-\frac{1}{\bar{s}}(p_0-p_s),\quad \bar{s}=s_{\text{вход}}/s_{\text{выход}}$$

(1) (2)

Key: 1. input 2. output

In particular, for $\bar{s}=100$, $p_s=0$, $\bar{p}_0=10^{-2}$, $\bar{p}^+_{\min}=0.9\cdot10^{-2}$. This means that for $\bar{p}^+<p^+_{\min}$ the pressure at the exit is expected to be less than p_s.

3.7. Propagation of Disturbances Through the Joints of Complex Tubing

A study is made of the case of the propagation of a disturbance through the joints of complex tubing in which a drop liquid moves with constant

APPROVED FOR RELEASE: 2007/02/08: CIA-RDP82-00850R000200090053-2

APPROVED FOR RELEASE: 2007/02/08: CIA-RDP82-00850R000200090053-2

speed of sound (n=1). At the joint several simple pipes converge where the basic main line has a cross section s_0. The disturbance is propagated from the main line through the joint to the other tubes (see Fig 3.12). The solution of the problem for this case is generalized to another where the disturbance approaches the joint made up of tube with cross section s_i.

The initial system of equations has the form

$$p_i=\tilde{p}_i+a_i\varrho(c_i-\tilde{c}_i);\ p_0=\tilde{p}_0+a_0\varrho(2c_0^+-\tilde{c}_0-c_0);$$
$$2p_0+\varrho c_0^2=2p_i+(1+\varepsilon_i)\varrho c_i^2; \qquad (3.54)$$
$$c_0s_0=\sum_{i=1}^{m}c_is_i,$$

where m is the number of tubes running from the joint; ε_i is the coefficient of local losses reduced to the velocity c_i; p_i, p_0, c_i, c_0 are the values of the corresponding parameters in the vicinity of the joint which are established at the time of transmission of the disturbance.

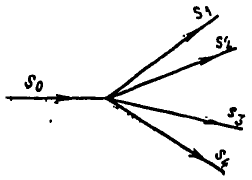

Figure 3.12. Schematic of the complex tubing with joint

In the case where two pipes run from the junction, in particular, one to the gas generator and the other to the combustion chamber, the system of equations (3.54) is resolved in radicals with independence of the coefficients ε_i with respect to the velocity. After transformations, for m=2 we have:

$$c_0^4a_4+c_0^3a_3+c_0^2a_2+c_0a_1+a_0=0, \qquad (3.55)$$

where the following notation is introduced:

$$a_4=B^2-D;\ a_3=4B(A+\varepsilon)+4a_0D;$$
$$a_2=4(A+\varepsilon)^2+2B(A^2-k_1^2Q_1-k_2^2Q_2)-4a_0^2D-\frac{4k_1^2k_2^2}{1+\varepsilon_1}Q_2-\frac{4k_1^2k_2^2Q_1}{1+\varepsilon^2};$$
$$a_1=4(A+\varepsilon)(A^2-k_1^2Q_1-k_2^2Q_2)+8a_0k_1^2k_2^2\left(\frac{Q_1}{1+\varepsilon_2}+\frac{Q_2}{1+\varepsilon_1}\right);$$
$$a_0=(A^2-k_1^2Q_1-k_2^2Q_2)^2-4k_1^2k_2^2Q_1Q_2;$$
$$A=\frac{a_1k_1}{1+\varepsilon_1}+\frac{a_2k_2}{1+\varepsilon_2};\ B=1-\frac{k_1^2}{1+\varepsilon_1}-\frac{k_2^2}{1+\varepsilon_2};$$
$$D=\frac{4k_1^2k_2^2}{(1+\varepsilon_1)(1+\varepsilon_2)};$$

FOR OFFICIAL USE ONLY

APPROVED FOR RELEASE: 2007/02/08: CIA-RDP82-00850R000200090053-2

APPROVED FOR RELEASE: 2007/02/08: CIA-RDP82-00850R000200090053-2

$$\varepsilon=\frac{a_0k_1^2}{1+\varepsilon_1}+\frac{a_0k_2^2}{1+\varepsilon_2};\quad Q_1=\frac{a_1^2}{(1+\varepsilon_1)^2}+\frac{2\Delta F_1}{1+\varepsilon_1};$$

$$Q_2=\frac{a_2^2}{(1+\varepsilon_2)^2}+\frac{2\Delta F_2}{1+\varepsilon_2};$$

$$\Delta F_1=\frac{F_0-F_1}{Q};\quad \Delta F_2=\frac{F_0-F_2}{Q};\quad F_0=\tilde{p}_0+a_0Q(2c_0^+-\tilde{c}_0);$$
$$F_1=\tilde{p}_1-a_1Q\tilde{c}_1;\quad F_2=\tilde{p}_2-a_2Q\tilde{c}_2;\quad k_1=s_1/s_0;$$
$$k_2=s_2/s_0.$$

The roots of the equation (3.55) coincide with the roots of two quadratic equations.

$$c_0^2+\left(\frac{\alpha_3}{\alpha_4}+\beta\right)\frac{1}{2}c_0+\left(y+\frac{\alpha_3y}{\alpha_4\beta}-\frac{\alpha_1}{\alpha_4\beta}\right)=0,$$

where y is the real root of the cubic equation of the type

$$8y^3-4\frac{\alpha_2}{\alpha_4}y^2+\left(\frac{2\alpha_1\alpha_3}{\alpha_4^2}-\frac{8\alpha_0}{\alpha_4}\right)y+\frac{\alpha_0}{\alpha_4}\left(\frac{4\alpha_2}{\alpha_4}-\frac{\alpha_3^2}{\alpha_4^2}\right)-\frac{\alpha_1^2}{\alpha_4^2}=0.$$

In turn, the parameter β is defined:

$$\beta=\pm\sqrt{8y+\left(\frac{\alpha_3}{\alpha_4}\right)^2-4\frac{\alpha_2}{\alpha_4}}.$$

The disturbed values of the velocities in the tubes 1, 2 are defined, respectively, as follows:

$$c_{1,2}=-\frac{a_{1,2}}{1+\varepsilon_{1,2}}+\sqrt{\frac{a_{1,2}^2}{(1+\varepsilon_{1,2})^2}+\frac{2\left(\Delta F_{1,2}-a_0c_0+\frac{1}{2}c_0^2\right)}{1+\varepsilon_{1,2}}}.$$

The disturbed values of the pressures are determined according to (3.54).

For essentially subsonic flows of liquid where the following inequalities are valid

$$|2(1+\varepsilon_i)(\Delta F_i-a_0c_0+0{,}5c_0^2)|\ll a_i^2,$$

APPROVED FOR RELEASE: 2007/02/08: CIA-RDP82-00850R000200090053-2

APPROVED FOR RELEASE: 2007/02/08: CIA-RDP82-00850R000200090053-2

the disturbed value of the velocity in the tube s_0 in the vicinity of the junction for arbitrary m with accuracy to the linear terms of the expansion is defined

$$c_0 \cong \frac{\sum_{l=1}^{m} \frac{k_l}{a_l}\left(\frac{\tilde{p}_0 - \tilde{p}_l}{\varrho} + 2a_0 c_0^+ - a_0\tilde{c}_0 + a_l\tilde{c}_l\right)}{1 + a_0\sum_{l=1}^{m}\frac{k_l}{a_l}}.$$

The disturbed values of the velocities in the other tubes in this case are defined

$$c_l \cong \frac{\Delta F_l - a_0 c_0}{a_l}.$$

In the case where the disturbances approach the junction simultaneously along all of the tubes, on the corresponding characteristics of which the invariants J_0^+, J_i^- are given, in the initial system of equations instead of (3.54) it is necessary to write the following:

$$p_l = a_l\varrho(v_l - J_l^-);\ p_0 = a_0\varrho(J_0^+ - c_0);\ J_0^+ = c_0^+ + \frac{p_0^+}{a_0\varrho};$$

$$J_l^+ = c_l^+ - \frac{p_l^+}{a_l\varrho}.$$

In the linear approximation in this case the expressions for the velocities are valid:

$$c_0 \cong \sum_{l=1}^{m}\frac{k_l}{a_l}(a_0 J_0^+ + a_l J_l^-) : \left(1 + a_0\sum_{l=1}^{m}\frac{k_l}{a_l}\right);$$

$$c_l \cong J_l^- + \frac{a_0}{a_l}(J_0^+ - c_0).$$

3.8. Propagation of Simple Waves Through the Gas Line Cross Section Discontinuity

It is of interest to consider the problem of the propagation of the simple compression or rarefaction wave through the cross section discontinuity of a tube filled with an ideal gas that is moving or is at rest, for in this case the subsonic nonsteady flow of gas in the simple wave can become a sonic flow on observation of defined conditions.

For determinacy we assume that the simple wave is propagated from left to right, and through the cross section discontinuity of the tubes it goes from the tube with cross section s_1 to the tube with cross section s_2. In this case in the cross section discontinuity the simple wave experiences a reflection to the internal region of the tube s_1 (to the left of the cross section discontinuity) and passes as a simple wave with altered values of the parameters into the tube s_2.

FOR OFFICIAL USE ONLY

APPROVED FOR RELEASE: 2007/02/08: CIA-RDP82-00850R000200090053-2

APPROVED FOR RELEASE: 2007/02/08: CIA-RDP82-00850R000200090053-2

The initial system of equations for calculating the parameters of the gas on transmission of the wave includes the equations:

of mass flow rate

$$\rho_1 c_1 s_1 = \rho_2 c_2 s_2; \tag{3.56}$$

energy

$$2a_1^2 + (n-1)c_1^2 = 2a_2^2 + (n-1)c_2^2; \tag{3.57}$$

the adiabatic curve in altered form

$$a_{2\rho_1}^{2\,n-1} = a_{1\rho_2}^{2\,n-1};$$

the equation of constancy of the Riemann invariant on the positive characteristic at the time of reflection

$$J_1^+ = \frac{2a_1^+}{n-1} + c_1^+ = \frac{2a_1}{n-1} + c_1;$$

the equation of constancy of the Riemann invariant on the positive characteristic for a simple wave

$$J_2^- = \frac{2a_2}{n-1} - c_2.$$

The parameters with the subscript "1" pertain to the gas in the tube s_1, and with the subscript "2" to the tube s_2. In the investigated problem the invariants J_1^+, J_2^- are given. Therefore it is expedient to express the desired values of the velocities c_1 and c_2 in terms of them. After transformations instead of (3.58) and (3.59) we have the system of equations:

$$a_2^2 - \frac{2a_2 J_2^- (n-1)}{n+1} = a_1^2 - \frac{2a_1 J_1^+ (n-1)}{n+1} + (J_1^+ - J_2^-)\frac{(n-1)^2}{2(n+1)}; \tag{3.58}$$

$$\left(J_1^+ - \frac{2a_1}{n-1}\right) s_1 = \left(\frac{2a_2}{n-1} - J_2^-\right)\left(\frac{a_2}{a_1}\right)^{\frac{2}{n-1}} s_2. \tag{3.59}$$

In order to obtain the numerical results, let us be given a number of values of the speed of sound a_1 in the tube s_1 for the given disturbance propagated in the tube s_1; then from (3.58) we find the corresponding values of the speed of sound a_2 which occur on disturbance of the gas in the tube s_2. Then from (3.59) we find the values of the cross section ratios s_1/s_2 which correspond to the given values of a_1. The results of the numerical calculations for the case $\tilde{c}_1 = \tilde{c}_2 = 0$, $\tilde{a}_1 = \tilde{a}_2 = 300$ m/sec, $n = 1.4$, $a_1^+ = 330$ m/sec, $c_1^+ = 150$ m/sec, $J_1^+ = 1800$ m/sec, $J_2^- = 1800$ m/sec are presented in Table 3.18. Obviously, the cases of subsonic or sonic gas flows are of practical interest.

APPROVED FOR RELEASE: 2007/02/08: CIA-RDP82-00850R000200090053-2

APPROVED FOR RELEASE: 2007/02/08: CIA-RDP82-00850R000200090053-2

Table 3.18

a_1	0	200	220	230	290	300	310	330	340	360
a_2	559	375	359	352	324	300	324	330	337	345
c_1	1800	800	700	650	350	300	250	150	100	0
c_2	1295	373	295	262	120	120	120	150	183	224
M_1	∞	4	3,18	2,82	1,2	1	0,805	0,455	0,284	0
M_2	2,32	0,995	0,823	0,745	0,37	0,37	0,37	0,455	0,54	0,65
s_1/s_2	∞	10,8	4,88	3,36	0,6	0,585	0,597	1	1,77	∞

By the results of the numerical calculation we have the conclusion that the critical flow conditions in the tube s_1 come for defined magnitude of the disturbance (in the given cases compression). Here the speed of sound in the tube s_2 reaches the minimum value just as the cross section ratio of the tubes s_1/s_2. Hence it follows that the following condition must be satisfied:

$$\frac{\partial}{\partial a_1}\left(\frac{s_1}{s_2}\right)=0.$$

In expanded form this condition has the form

$$\frac{\partial a_2}{\partial a_1}\frac{a_2+c_2}{a_2c_2}+\frac{c_1-a_1}{a_1c_1}=0,$$

which is valid on observation of the identities:

$$c_1=a_1,\ \partial a_2/\partial a_1=0.$$

From the equations (3.58), (3.59) considering these identities after the transformation we find that on transmission of the compression wave in the tube s_1, the sonic conditions of the flow are established for the dependence of the ratio of the tube cross sections on the initial disturbance expressed in terms of the invariant J_1^+:

$$s=s_1/s_2=\frac{\sqrt{\frac{2}{n-1}(J^2-1)}}{J}\left(\frac{1+\sqrt{\frac{n-1}{2}(J^2-1)}}{J}\right)^{\frac{2}{n-1}}, \qquad (3.60)$$

where we have denoted $J=J_1^+/J_2^-$.

FOR OFFICIAL USE ONLY

APPROVED FOR RELEASE: 2007/02/08: CIA-RDP82-00850R000200090053-2

APPROVED FOR RELEASE: 2007/02/08: CIA-RDP82-00850R000200090053-2

From physical arguments it follows that the criticial (sonic) flow conditions are established for the given magnitude of the ratio of the tube cross sections for the interval of dimensionless invariant

$$\sqrt{\frac{2}{n+1}} \leqslant J \leqslant \frac{n+1}{3-n}.$$

In Table 3.19 the results are presented from the numerical calculations for n=1.4.

Table 3.19

J	1,094	1,1	1,2	1,3	1,4	1,5
s	0	0,03	0,59	0,86	0,97	1

The expression (3.60) denotes that if for a given value of the cross section ratio s the disturbance is larger than J (defined by Table 3.19 as an example for n=1.4), sonic conditions are established, and vice versa. The other is also valid: for the given disturbance J the sonic conditions are established for a value of the cross section ratios less than defined by formula (3.60).

In the tube s_2 the sonic conditions of the flow on transmission of the compression wave are established under the condition $c_2=a_2$ so that the cross section ratio is related to the disturbance by the expression

$$\frac{s_2}{s_1}=\frac{1}{s}=\left(J_n-\sqrt{\frac{2}{n-1}(1-J_n^2)}\right)\cdot\left(J_n+\sqrt{\frac{n-1}{2}(1-J_n^2)}\right)^{\frac{2}{n-1}} \qquad (3.61)$$

where

$$J_n=J\frac{3-n}{n+1}=\frac{J_1^+}{J_2^-}\frac{3-n}{n-1}.$$

The dimensionless invariant J_n is found from the physical arguments in such limits:

$$\sqrt{\frac{2}{n+1}} \leqslant J_n \leqslant 1.$$

The results of the numerical calculations for n=1.4 by formula (3.61) are presented in Table 3.20.

APPROVED FOR RELEASE: 2007/02/08: CIA-RDP82-00850R000200090053-2

APPROVED FOR RELEASE: 2007/02/08: CIA-RDP82-00850R000200090053-2

Table 3.20

J	1,5	1,47	1,4	1,37
s	1	1,3	48	∞

Let us consider the cases of the establishment of sonic flows on transmission of the rarefaction disturbance from tube s_1 to tube s_2. If the sonic flow is established in tube s_1, then it is necessary to assume that considering the direction of propagation of the wave and the direction of the disturbed velocity opposite to it,

$$c_1=-a_1=-\frac{n-1}{3-n}J_1^+.$$

Taking this into account after the transformations (3.59), (3.58), we obtain the relation between the ratio of the cross sections and the disturbance:

$$s=\frac{1}{J}\left(\frac{3-n}{n+1}-\sqrt{\frac{2}{n-1}J^2-\left(\frac{3-n}{n+1}\right)^2}\right)\times$$
$$\times\left(\frac{1}{J}\left[\frac{3-n}{n+1}+\sqrt{\frac{n-1}{2}\left(J^2-\left(\frac{3-n}{n+1}\right)^2\right)}\right]\right)^{\frac{2}{n-1}}. \qquad (3.62)$$

In Table 3.21 the results are presented from the numerical calculations for n=1.4 by formula (3.62).

Table 3.21

J	0,666	0,68	0,69	0,7	0,71	0,72	0,73
s	1	0,73	0,555	0,393	0,257	0,119	0

Here the dimensionless invariant J is within the limits:

$$\frac{3-n}{n+1}\leqslant J\leqslant\frac{3-n}{\sqrt{2(n+1)}}.$$

The sonic flow is established in tube s_2 on propagation of the rarefaction wave under the condition

$$c_2=-a_2=-\frac{n-1}{n+1}J_2^-.$$

Here the cross section ratio is defined

$$\frac{s_2}{s_1}=\frac{1}{s}=\left(\sqrt{\frac{2}{n-1}(1-J^2)}-J\right)\left(J+\sqrt{\frac{n-1}{2}(1-J^2)}\right)^{\frac{2}{n-1}}, \qquad (3.63)$$

APPROVED FOR RELEASE: 2007/02/08: CIA-RDP82-00850R000200090053-2

APPROVED FOR RELEASE: 2007/02/08: CIA-RDP82-00850R000200090053-2

where the dimensionless invariant is within the limits

$$\frac{3-n}{n+1} \leqslant J \leqslant \sqrt{\frac{2}{n+1}}.$$

In Table 3.22 the results are presented from numerical calculations for n=1.4 by formula (3.63).

Table 3.22

J	0,675	0,7	0,75	0,8	0,85	0,9	0,912
s	1	1,035	1,086	1,33	1,99	8,5	∞

APPROVED FOR RELEASE: 2007/02/08: CIA-RDP82-00850R000200090053-2

APPROVED FOR RELEASE: 2007/02/08: CIA-RDP82-00850R000200090053-2

FOR OFFICIAL USE ONLY

CHAPTER 4. RANDOM PROCESSES IN ENGINES

4.1. Sensitivity of Dynamic Characteristics to the Disturbances

Previously, a study was made of the engine characteristics under the assumption that the values of the parameters of the working process coincide with the values adopted for planning and design.

At the same time as a result of a number of causes (the effect of the internal and external disturbing factors) the real values of the parameters always differ from the calculated ones.

It is natural that this leads to variation of the dynamic characteristics and deformation of the stability limits of the engine.

The analysis of the effect of the variation of the parameters on the dynamic characteristics of the engine can be made using the sensitivity functions.

The sensitivity functions are the partial derivatives of the j coordinate of the system with respect to the variation of the i-th parameter $\mu_{ji}=\partial x_j/\partial\sigma_i$ -- the frequency derivatives calculated for the rated values of the parameters.

Initially let us consider the application of the sensitivity functions in general form. Let the transfer function depend on the parameter α_i, that is, $\Phi(s, \alpha_i)$; then $\mu_{\alpha_l}(s)=\frac{\partial\Phi(s,\alpha_l)}{\partial\alpha_l}$, which determines the additional transfer function equal to

$$\Delta\Phi_l(s,\alpha_l)=\tilde{\Phi}(s,\alpha_l)-\Phi(s,\alpha_l)=\mu_{\alpha_l}(s)\,\Delta\alpha_l. \tag{4.1}$$

Since the initial transfer function can be represented in the form of the ratio of two polynomials, the additional transfer function is defined as follows:

$$\Delta\Phi_l(s,\alpha_l)=\frac{\partial}{\partial\alpha_l}\frac{R(s,\alpha_l)}{D(s,\alpha_l)}\Delta\alpha_l=\frac{1}{D(s,\alpha_l)}[\Delta R(s)-\Phi(s,\alpha_l)\,\Delta D(s)], \tag{4.2}$$

FOR OFFICIAL USE ONLY

APPROVED FOR RELEASE: 2007/02/08: CIA-RDP82-00850R000200090053-2

APPROVED FOR RELEASE: 2007/02/08: CIA-RDP82-00850R000200090053-2

where $\Delta R(s)$ and $\Delta D(s)$ are the versions of the polynomials in the numerator and denominator of the transfer function. Formula (4.2) makes it possible to construct the structural diagram of the sensitivity (Fig 4.1), which can be used to calculate the errors on a computer.

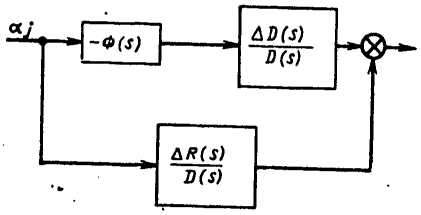

Figure 4.1. Structural sensitivity diagram

For analysis of the dynamic characteristics, in particular, the frequency characteristics, it is expedient to consider the variation of the amplitude and phase frequency characteristics as a result of deviations of the engine parameters.

Let the transfer function of the engine parameter have the following form without considering the transformation time:

$$W(s)=\frac{K_{p_K,\dot{m}}}{T_K s+1}. \tag{4.3}$$

The amplitude and phase characteristics

$$H(\omega)=\frac{K_{p_K,\dot{m}}}{\sqrt{1+T_K^2\omega^2}};\quad \varphi(\omega)=-\operatorname{arctg}\omega T_K. \tag{4.4}$$

Let us assume that K_{p_k}, $\dot{m}$ and T_k are calculated values, ΔK_{p_k}, $\dot{m}$, ΔT_K are their deviations from the calculated values.

In this case in the linear approximation the amplitude and phase characteristic has the form

$$\begin{aligned} H(\omega,\Delta K,\Delta T)&=H(\omega)+\mu_{H,K}\Delta K+\mu_{H,T}\Delta T,\\ \varphi(\omega,\Delta K,\Delta T)&=\varphi(\omega)+\mu_{\varphi,K}\Delta K+\mu_{\varphi,T}\Delta T, \end{aligned} \tag{4.5}$$

where μ_{ij} are the first-order sensitivity functions

$$\Delta T=\Delta T_K,\ \Delta K=\Delta K_{p_K,\dot{m}}.$$

APPROVED FOR RELEASE: 2007/02/08: CIA-RDP82-00850R000200090053-2

APPROVED FOR RELEASE: 2007/02/08: CIA-RDP82-00850R000200090053-2

The sensitivity functions μ_{ji} are defined by expansion of the initial function in a Taylor series in the vicinity of the calculated values of the parameters and dropping the terms of the series above first order.

Thus, from expression 4.4 the sensitivity functions are defined as follows

$$\mu_{H,K}=\frac{\partial H}{\partial K_{\rho_K,m}}=\frac{1}{\sqrt{1+T_K^2\omega^2}};\quad \mu_{H,T}=-\frac{K\omega^2T_K}{(1+T_K^2\omega^2)^{3/2}};$$

$$\mu_{\varphi,K}=0;\quad \mu_{\varphi,T}=-\frac{\omega}{1+T_K^2\omega^2}.$$

Considering the sensitivity functions, the phase-amplitude frequency characteristics (4.4) will have the form

$$H(\omega)=\frac{K_{\rho_K,m}+\Delta K}{\sqrt{1+T_K^2\omega^2}}-\frac{K_{\rho_K,m}\omega^2T_K-\Delta T}{(1+T_K^2\omega^2)^{3/2}};$$

$$\varphi(\omega)=-\operatorname{arctg}\omega T_K-\frac{\omega\Delta T}{1+T_K^2\omega^2}.$$

In the general case the transfer function of the engine has the form

$$W(s)=\frac{b_0s^m+b_1s^{m-1}+\ldots+b_{m-1}s+b_m}{a_0s^n+a_1s^{n-1}+\ldots+a_{n-1}s+a_n}. \tag{4.6}$$

The coefficients of the transfer function depend on the parameters α_i, that is, $b_k=b(\alpha_i)$; $a_\ell=a(\alpha_i)$, k=0, 1,2,..., m, ℓ=0, 1,2,3,...,n. If we make the substitution s=jω in the equation (4.6) and after making the corresponding transformations, we obtain

$$H(\omega)=\sqrt{\frac{A^2(\omega)+B^2(\omega)}{C^2(\omega)+D^2(\omega)}};$$

$$\varphi(\omega)=\operatorname{arctg}\frac{B(\omega)C(\omega)-A(\omega)D(\omega)}{A(\omega)C(\omega)+B(\omega)D(\omega)}. \tag{4.7}$$

$$\begin{aligned}A(\omega)&=P[b(j\omega)]=b_m-b_{m-2}\omega^2+b_{m-4}\omega^4+\ldots\\ B(\omega)&=Q[b(j\omega)]=b_{m-1}\omega-b_{m-3}\omega^3+\ldots\\ C(\omega)&=P[a(j\omega)]=a_n-a_{n-2}\omega^2+a_{m-4}\omega^4+\ldots\\ D(\omega)&=Q[a(j\omega)]=a_{n-1}\omega-a_{n-3}\omega^3+a_{n-5}\omega^5+\ldots\end{aligned} \tag{4.8}$$

P[·] is the real part, Q[·] is the imaginary part of the polynomials.

Since the coefficients b_k and a_ℓ depend on α_i, then

$$\begin{aligned}H(\omega)&=H[\omega; a_0(\alpha_i);\ldots a_n(\alpha_i);\ b_0(\alpha_i),\ldots b_m(\alpha_i)]\\ \varphi(\omega)&=\varphi[\omega; a_0(\alpha_i);\ldots a_n(\alpha_i);\ b_0(\alpha_i);\ldots b_m(\alpha_i)]\end{aligned} \tag{4.9}$$

FOR OFFICIAL USE ONLY

APPROVED FOR RELEASE: 2007/02/08: CIA-RDP82-00850R000200090053-2

APPROVED FOR RELEASE: 2007/02/08: CIA-RDP82-00850R000200090053-2

and the sensitivity functions are defined as follows:

$$\frac{\partial H}{\partial \alpha_l}=\sum_{k=0}^{n}\frac{\partial H}{\partial a_k}\frac{\partial a_k}{\partial \alpha_l}+\sum_{k=0}^{m}\frac{\partial H}{\partial b_k}\frac{\partial b_k}{\partial \alpha_l}; \tag{4.10}$$

$$\frac{\partial \varphi}{\partial \alpha_l}=\sum_{k=0}^{n}\frac{\partial \varphi}{\partial a_k}\frac{\partial a_k}{\partial \alpha_l}+\sum_{k=0}^{m}\frac{\partial \gamma}{\partial b_k}\frac{\partial b_k}{\partial \alpha_l}. \tag{4.11}$$

The factors $\frac{\partial H}{\partial a_k}; \frac{\partial H}{\partial b_k}; \frac{\partial \gamma}{\partial a_\kappa}; \frac{\partial \varphi}{\partial b_k}$ are defined only by the structure of the transfer function (the values of m and n) and the values of the coefficients a_k and b_k.

In accordance with the equations 4.7 the cofactors in the equations 4.10 and 4.11 are determined by the equations of the type

$$\frac{\partial H}{\partial a_k}=\begin{cases}(-1)^{\frac{k+2}{2}}\omega^k C(\omega)H^3(\omega)|b(j\omega)|^{-2}, & \text{if k is even,}\\ (-1)^{\frac{k+1}{2}}\omega^k D(\omega)H^3(\omega)|b(j\omega)|^{-2}, & \text{if k is odd.}\end{cases}$$

$$\frac{\partial H}{\partial b_k}=\begin{cases}(-1)^{\frac{k}{2}}\omega^k A(\omega)H(\omega)|b(j\omega)|^{-2}, & \text{if k is even,}\\ (-1)^{\frac{k-1}{2}}\omega^k B(\omega)H(\omega)|b(j\omega)|^{-2}, & \text{if k is odd.}\end{cases}$$

$$\frac{\partial \varphi}{\partial a_k}=\begin{cases}(-1)^{\frac{k}{2}}\omega^k H^2(\omega)D(\omega)|b(j\omega)|^{-2}, & \text{if k is even,}\\ (-1)^{\frac{k+1}{2}}\omega^k C(\omega)H^2(\omega)|b(j\omega)|^{-2}, & \text{if k is odd.}\end{cases}$$

$$\frac{\partial \varphi}{\partial b_k}=\begin{cases}(-1)^{\frac{k+2}{2}}\omega^k B(\omega)|b(j\omega)|^{-2}, & \text{if k is even,}\\ (-1)^{\frac{k-1}{2}}\omega^k A(\omega)|b(j\omega)|^{-2}, & \text{if k is odd.}\end{cases}$$

The factors $\partial a_k/\partial \alpha_i$ and $\partial b_k/\partial \alpha_i$ are defined by the coefficients of the transfer function as a function of the parameters α_i.

The sensitivity functions make it possible to estimate the effect of the deviation of the engine parameters on the dynamic characteristics. Let us use the expressions

APPROVED FOR RELEASE: 2007/02/08: CIA-RDP82-00850R000200090053-2

APPROVED FOR RELEASE: 2007/02/08: CIA-RDP82-00850R000200090053-2

$$H(\omega)=H[\omega, \alpha_1+\Delta\alpha_1; \alpha_2+\Delta\alpha_2; \ldots \alpha_m+\Delta\alpha_m]=$$
$$=H(\omega, \alpha_1, \alpha_2, \ldots \alpha_m)+\sum_{i=1}^{m}\mu_{H,\alpha_i}\Delta\alpha_i; \qquad (4.12)$$
$$\varphi(\omega)=\varphi[\omega, \alpha_1+\Delta\alpha_1; \alpha_2+\Delta\alpha_2; \ldots \alpha_m+\Delta\alpha_m)=$$
$$=\varphi(\omega, \alpha_1, \alpha_2 \ldots, \alpha_m)+\sum_{i=1}^{m}\mu_{\varphi,\alpha_i}\Delta\alpha_i,$$

From the equations (4.12) it is possible to determine the dispersion and the mean square deviation of the dynamic characteristics.

In particular, in the absence of a correlation between the random parameters α_i we obtain

$$D_H=\sum_{i=1}^{m}\mu_{H,\alpha_i}^2 D_{\alpha_i};$$
$$D_\varphi=\sum_{i=1}^{n}\mu_{\varphi,\alpha_i}^2 D_{\alpha_i}, \qquad (4.13)$$

where D_H is the dispersion of the frequency amplitude characteristic; D_ϕ is the dispersion of the phase characteristics; D_{α_i} is the dispersion of the engine parameters. In the case of normal distribution of the values of α_i the probability that $H(\omega)$ or $\phi(\omega)$ will be within admissible limits H_1 and H_2; ϕ_1 and ϕ_2 will be defined by the equation

$$P(H_1<H<H_2)=0{,}5\left[\Phi\left(\frac{H_2-m_H}{\sqrt{2D_H}}\right)-\Phi\left(\frac{H_1-m_H}{\sqrt{2D_H}}\right)\right],$$
$$P(\varphi_1<\varphi<\varphi_2)=0{,}5\left[\Phi\left(\frac{\varphi_2-m_\varphi}{\sqrt{2D_\varphi}}\right)-\Phi\left(\frac{\varphi_1-m_\varphi}{\sqrt{2D_\varphi}}\right)\right], \qquad (4.14)$$

where $\Phi[\cdot]$ is the Laplace table function. The sensitivity functions also permit determination of the probability of stable operation of the engine.

As an example, let us consider the stability limit (Fig 2.27). The parameters of the regulator K_p, T_1 in the plane of which the stability limit is constructed are the random variables, and they are defined:

$$K_p=K_p[\omega, T_2, P_y(\omega)];$$
$$T_1=T_1[\omega, T_2, Q_y(\omega)].$$

In turn, $P_y(\omega)$ and $Q_y(\omega)$ depend on the engine characteristics. Using the functions (4.13), the dispersions D_{T_1} and D_{k_p} are determined.

As a result of the scattering of K_p and T_1 the stability limit also will have scattering. In order to estimate the probability of stable operation considering the scattering of the engine and regulator parameters it is expedient to use the reliability method "fitness conditions," "load-strength" [7].

FOR OFFICIAL USE ONLY

APPROVED FOR RELEASE: 2007/02/08: CIA-RDP82-00850R000200090053-2

APPROVED FOR RELEASE: 2007/02/08: CIA-RDP82-00850R000200090053-2

In the given case, by load we mean the values of K_{pp} and T_{1p} considering the random scattering, and by strength, their values at the stability limit $K_{p\Gamma}$, $T_{1\Gamma}$.

Since the boost factor and the time constant of the regulator can be considered statistically independent, the probability of stable operation is defined as

$$P=P_{K_p}P_{T_1}, \tag{4.15}$$

where P_{k_p} is the probability of satisfaction of the condition $K_{p\Gamma}-K_{pp}>0$; P_{T_1} is the probability of satisfaction of the condition $T_{1\Gamma}-T_{1p}>0$. For normal distribution, according to [7], the probability of stable operation will be defined by the function

$$\begin{aligned} P_{K_p}&=\Phi\left(\frac{K_{\Gamma\Gamma}-K_{pp}}{\sqrt{\sigma^2_{K_{pr}}+\sigma^2_{K_{pp}}}}\right)\\ P_{T_1}&=\Phi\left(\frac{T_{1\Gamma}-T_{1p}}{\sqrt{\sigma^2_{T_{1r}}+\sigma^2_{T_{1p}}}}\right), \end{aligned} \tag{4.16}$$

where $\Phi[\cdot]$ are the Laplace table functions.

The equations (4.16) make it possible to determine the required values of the boost factor and the time constant insuring the given probability of stable operations.

Being given $\overline{P}_{k_p}$ and $\overline{P}_{T_1}$ from equations (4.16) we determine

$$Z_{kp}=\frac{K_{pr}-K_{pp}}{\sqrt{\sigma^2_{K_{pr}}+\sigma^2_{K_{pp}}}} \text{ и } Z_{T_1}=\frac{T_{1r}-T_{1p}}{\sqrt{\sigma^2_{T_{1r}}+\sigma^2_{T_{1p}}}}.$$

From the tables for $\Phi(Z)$ of [27] for $\overline{P}_i=0.995$ we find $Z_i=2.58$, $\overline{P}_i=0.99$, $Z_i=2.33$. Thus, for example, if $\overline{P}_i=0.995$ is given, then the stability margins

$$\begin{aligned} \Delta K_p&=K_{pr}-K_{pp}=2{,}58\sqrt{\sigma^2_{K_{pr}}+\sigma^2_{K_{pp}}};\\ \Delta T_1&=T_{1r}-T_{1p}=2{,}58\sqrt{\sigma^2_{T_{\Gamma\Gamma}}+\sigma^2_{T_{1r}}}, \end{aligned}$$

which insures stable operation of the engine under operating conditions with the probability $P=P_{k_p}P_{T_1}=0.995\text{x}0.995=0.99$.

APPROVED FOR RELEASE: 2007/02/08: CIA-RDP82-00850R000200090053-2

APPROVED FOR RELEASE: 2007/02/08: CIA-RDP82-00850R000200090053-2

4.2. General Characteristics of Random Processes

During the operation of the engine under operating conditions all of the parameters are random, for they are realized as a result of the combined effect of various random processes occurring in the individual assemblies and external disturbances.

The basic causes determining the random process are the following:

Turbulence of the flow of fuel and gas components in the lines and reservoirs;

The presence in the liquid and gas flows of bodies that are poorly streamlined (valves, chokes, jets, turns, and so on), which cause turbulization and eddy formation;

Internal sources of disturbances in the form of the flashing of the blades of the pumps and turbines, pulsation of the fuel combustion, and so on;

Cavitation phenomena in the pumps;

Variation of the parameters of the operating process as a result of functioning of the control systems, and so on.

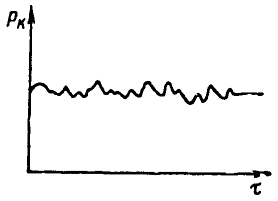

Figure 4.2. Form of the oscillogram $p_k(t)$

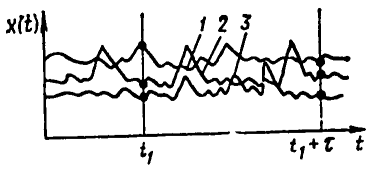

Figure 4.3. Realization of the random process x(t)

As a result of the enumerated and other random processes the parameters of the operating process in the set of engines are formed as random time functions.

As an example, let us consider the variation of the pressure in the thrust chamber in the steady-state mode. The recording of the pressure on the oscillogram for a specific engine will have approximately the form shown in Fig 4.2.

The pressure in the second engine of the same structural design and simply operating in the same mode will vary differently than in the first engine. In general the recordings of the variation of the pressure of the different engines in time are not at all similar.

FOR OFFICIAL USE ONLY

APPROVED FOR RELEASE: 2007/02/08: CIA-RDP82-00850R000200090053-2

APPROVED FOR RELEASE: 2007/02/08: CIA-RDP82-00850R000200090053-2

The time function describing the random phenomenon is called a realization; in our example, $p_1(t)$, $p_2(t)$ and $p_k(t)$ are realizations. The set of all realizations which can be obtained when recording the given random phenomenon is called a random process.

Stationary and nonstationary random processes are distinguished. In turn, the stationary random processes can be ergodic and nonergodic. The concept of stationarity and ergodicity is defining for the construction of the mathematical model of the process and its calculation.

Let the random process have n realizations (Fig 4.3). Then the mean value (the first moment of the distribution) of the random process at the time t_1 will be defined as

$$m_x(t)=\lim_{n\to\infty}\frac{1}{n}\sum_{i=1}^{n}x_i(t), \tag{4.17}$$

where $x_i(t)$ is the realization of the random process. Analogously, the correlation between the values of the random process at two different points in time (mixed time) called the autocorrelation function, is defined by averaging the products of the instantaneous values of the process at the times t_1 and $t_1+\tau$ over the realizations:

$$R_x(t_1; t_1+\tau)=\lim_{n\to\infty}\frac{1}{n}\sum_{i}^{n}x_i(t_1)x_i(t_1+\tau). \tag{4.18}$$

Here it is proposed that the appearance of all of the realizations is equiprobable.

The functions which have static properties that are uniform in time, that is, for the stationary random process the correlation moment $R_x(t_1, t_2)=Rx(t)$ (depends on one argument $\tau=t_2-t_1$) and the mathematical expectation does not depend on time are considered stationary random functions; otherwise, the process is nonstationary. The checking of the stationarity of the random process is done by static processing of the results.

However, in some cases the stationarity of the process can be determined from analysis of the physical nature of the phenomenon to which the realization belongs.

If the basic physical factors defining the processes do not depend explicitly on time, then it is possible without further investigation to propose the random process to be stationary.

Let us consider, for example, the random process of the pressure variation in the chamber during operation of the engine.

In the steady-state mode the pressure in the chamber will be defined by the function

APPROVED FOR RELEASE: 2007/02/08: CIA-RDP82-00850R000200090053-2

APPROVED FOR RELEASE: 2007/02/08: CIA-RDP82-00850R000200090053-2

$$p_к = \frac{\dot{m}\sqrt{RT_к}}{b(\varkappa)F_{кр}}.$$

If a program variation of the mass flow rate (the thrust relation) does not take place, then all of the values defined by p_k are random, not depending on the operating time, and they vary as a result of the effect of the external and internal disturbing factors. Consequently, the process of variation of $p_k(t)$ in the steady-state mode can be considered stationary.

During the process of the testing and the application of the engine, it is not the set that is obtained, but one realization of the random function of the operating process. Therefore, it is necessary by this realization to characterize the properties of the random process. This can be done only in the case where the process is stationary and has the property of ergodicity.

Thus, if the random stationary process has the property of ergodicity, the observation of one realization in a sufficiently large time interval t=T in the sense of the volume of obtained information turns out to be equivalent to the observation of several realizations.

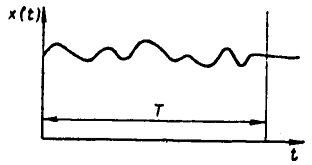

Figure 4.4. Realization of the ergodic process

For such random functions the mean with respect to the set of realizations is equal to the mean with respect to time of one realization in an infinite interval T (Fig 4.4)

$$m_x = \lim_{T\to\infty}\frac{1}{T}\int_0^T x(t)\,dt;$$

$$R_x(\tau) = \lim_{T\to\infty}\frac{1}{T}\int_0^T [x(t)-m_x][x(t+\tau)-m_x]\,dx. \qquad (4.19)$$

The mathematical apparatus has been quite completely developed for random processes having the property of stationarity and ergodicity.

FOR OFFICIAL USE ONLY

APPROVED FOR RELEASE: 2007/02/08: CIA-RDP82-00850R000200090053-2

APPROVED FOR RELEASE: 2007/02/08: CIA-RDP82-00850R000200090053-2

4.3. Statistical Characteristics of Random Processes

4.3.1. Characteristics of Random Processes

The random process is fully characterized by the correlation function $R_X(t)$ and the spectral density $S(\omega)$. Having the indicated characteristics, it is possible also to define others, for example, the mathematical expectation and dispersion (the mean square deviation). The correlation function is defined by the equations (4.18) and (4.19). The value of $R_X(\tau)$ is always a real, even function with maximum at the point $\tau=0$; it can be both positive and negative, that is, $R_X(-\tau)=R_X(\tau)$. The mathematical expectation, dispersion and mean square deviation of the random function with the correlation function are related by the functions [4]

$$\begin{aligned} m_x &= \sqrt{R_x(\infty)}; \\ D_x &= R(0)-R(\infty); \\ \sigma_x &= \sqrt{R(0)-R(\infty)}. \end{aligned} \tag{4.20}$$

Fig 4.5 shows the correlation function of the pressure in the thrust chamber and the pressure after the fuel pump of one of the engines without afterburning of the generator gas.

For the overwhelming majority of random functions of the operating process the analytical approximation of the correlation function has the form

$$R_x(\tau) = D_x e^{-\alpha|\tau|}, \tag{4.21}$$

where D_X is the dispersion of the random function; α is the damping parameter defined by the static properties of the engine.

The analysis of the relations between the different random functions which are characterized by mutual correlation functions is of practical interest.

Let the realization of two random functions x(t) and y(t) occur (see Fig 4.6). The statistical interrelation between the functions x(t) and y(t) will be defined by the mutual correlation function

$$R_{xy}(\tau) = \lim_{T\to\infty} \frac{1}{2T} \int_{-T}^{T} x(t)\,y(t+\tau)\,dt. \tag{4.22}$$

$R_{XY}(\tau)$ is always a real function which can be both positive and negative. In addition, the function $R_{XY}(\tau)$ does not necessarily have a maximum at the point $\tau=0$, and it is not necessarily even.

In the case where $R_{XY}(\tau)=0$, the functions x(t) and y(t) are statistically independent, that is, uncorrelated. If x(t) and y(t) are interdependent, then always $R_{XY}(\tau) \gtrless 0$.

APPROVED FOR RELEASE: 2007/02/08: CIA-RDP82-00850R000200090053-2

APPROVED FOR RELEASE: 2007/02/08: CIA-RDP82-00850R000200090053-2

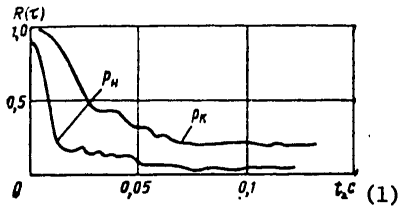

Figure 4.5. Correlation functions R_{p_k} and $R_{p_{pump}}$

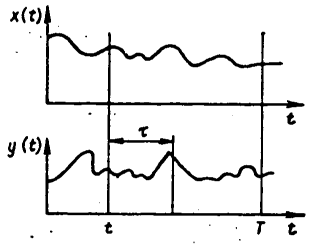

Figure 4.6. Realization of two random processes

Key:
1. t, sec

Since $R_{xy}(\tau)$ is an odd function, its value must be calculated for $\tau>0$ and $\tau<0$

$$R_{xy}(\tau)=\begin{cases}\lim\limits_{T\to\infty}\dfrac{1}{T-\tau}\displaystyle\int_0^{T-\tau}x(t)\,y(t+\tau)\,dt \text{ for } \tau>0,\\ \lim\limits_{T\to\infty}\dfrac{1}{T+\tau}\displaystyle\int_0^{T+\tau}x(t-\tau)\,y(t)\,dt \text{ for } \tau<0.\end{cases}\qquad(4.23)$$

Fig 4.7 shows the mutual correlation function for the pressure in the thrust chamber and the flow rate of the combustible component of the fuel to the gas generator, and Fig 4.8 for the flow rate of the combustible component to the gas generator and the flow rate of the combustible component to the transfer mains of the regulator in the engine with afterburning of the generator gas. As follows from the presented figures the engine parameters are correlated.

Another important characteristic of the random process is the spectral density $S_x(\omega)$.

The spectral density characterizes the energy distribution of the random function investigated in the form of an infinite superposition of harmonic oscillations with random amplitudes and phases with respect to frequencies.

Thus, the spectral density characterizes the dynamic load taken by the engine from the effect of the random process.

$$S_x(\omega)=\lim_{T\to\infty}\frac{1}{2T}|F_x(j\omega)|^2,\qquad(4.24)$$

where $F_x(j\omega)$ is the Fourier expansion of the random function $x(t)$.

FOR OFFICIAL USE ONLY

APPROVED FOR RELEASE: 2007/02/08: CIA-RDP82-00850R000200090053-2

APPROVED FOR RELEASE: 2007/02/08: CIA-RDP82-00850R000200090053-2

The spectral density is related to the correlation function by the Fourier transformation

$$S_x(\omega) = \int_{-\infty}^{\infty} R_x(\tau) e^{-j\omega t}\, dt. \tag{4.25}$$

Since the spectral density and the correlation functions are even real functions, the formula (4.25) is represented in the form

$$S_x(\omega) = 2\int_0^{\infty} R_x(\tau)\cos\omega t\, dt;$$
$$R_x(\tau) = \frac{1}{\pi}\int_0^{\infty} S_x(\omega)\cos\omega t\, dt. \tag{4.26}$$

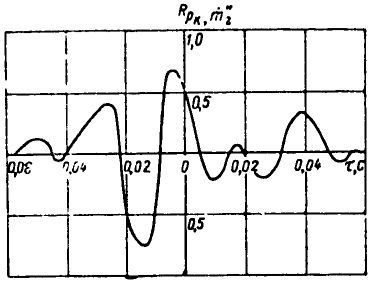

Figure 4.7. Mutual correlation function $R_{p_k,\ \dot{m}''_{fuel}}(\tau)$

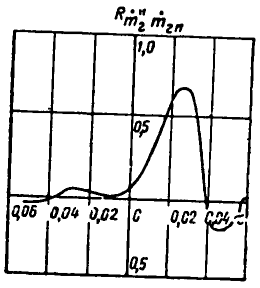

Figure 4.8. Mutual correlation function $R_{\dot{m}_{fuel},\ \dot{m}_{gn}}(\tau)$

The spectral density uniquely determines the dispersion of the random variables

$$D_x = \frac{1}{\pi}\int_0^{\infty} S_x(\omega)\, d\omega. \tag{4.27}$$

If as the argument we use the frequency $f=\omega/2\pi$ and replace the integration limits, we obtain

$$S_x(f) = 4\int_0^{T} R_x(\tau)\cos 2\pi f\tau\, dt. \tag{4.28}$$

Fig 4.9 shows the spectral density of the pressure in the thrust chamber; Fig 4.10 shows the pressures in the gas generator, and Fig 4.11 gives the pressures after the engine fuel pump with afterburning of the generator gas.

APPROVED FOR RELEASE: 2007/02/08: CIA-RDP82-00850R000200090053-2

APPROVED FOR RELEASE: 2007/02/08: CIA-RDP82-00850R000200090053-2

Under real conditions it is possible to represent the random function as the sum of the nonrandom component and the elementary random components imposed on it

$$x(t) = m_x + \sum V_\nu x_\nu(t), \tag{4.29}$$

where m_x is the mathematical expectation; V_ν is the random mutually correlated coefficients with zero mathematical expectations; $x_\nu(t)$ are the elementary random components.

The representation of the random functions in the form of (4.29) is called the canonical expansion. There are various methods for finding the canonical expansion of the random functions [36].

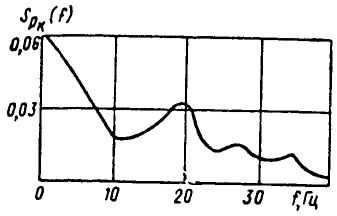

Figure 4.9. Spectral density $S_{p_k}(f)$

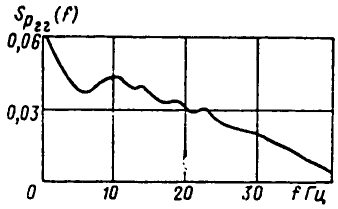

Figure 4.10. Spectral density $S_{p_{gg}}(f)$

When using the canonical expansion, the execution of the operations on the random functions is simplified.

From (4.29) the correlation function is defined as follows:

$$R_x(t, t_1) = m_x^2 + \sum D_\nu x_\nu(t) x_\nu(t_1), \tag{4.30}$$

where D_ν is the dispersion of coefficients of the canonical expansion. For the stationary random function given in the interval $-T<t<T$ the difference $\tau=t_1-t$ varies in the interval $-2T<\tau<2T_H$, the expansion of the correlation function can be written in the form of a Fourier series

$$R(\tau) = m_x^2 + \sum_{\nu=1}^{\infty} 2D_\nu \cos \omega_\nu \tau, \tag{4.31}$$

where

$$\omega_\nu = \frac{\pi\nu}{2T}; \quad \nu = \overline{1, n}.$$

FOR OFFICIAL USE ONLY

APPROVED FOR RELEASE: 2007/02/08: CIA-RDP82-00850R000200090053-2

APPROVED FOR RELEASE: 2007/02/08: CIA-RDP82-00850R000200090053-2

APPROVED FOR RELEASE: 2007/02/08: CIA-RDP82-00850R000200090053-2

APPROVED FOR RELEASE: 2007/02/08: CIA-RDP82-00850R000200090053-2

This correlation function corresponds to the canonical expansion of the random function itself

$$x(t)=m_x+\sum_{\nu=0}^{\infty}(X_\nu\cos\omega_\nu t+Y_\nu\sin\omega_\nu t), \tag{4.32}$$

where X_ν, Y_ν are the mutually uncorrelated random variables with $m_\nu=0$ and with identical dispersions $0.5D_\nu$.

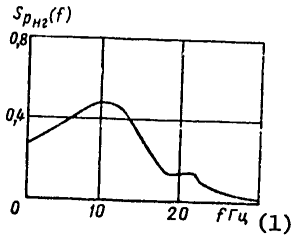

Figure 4.11. Spectral density $S_{p_{\text{pump, fuel}}}(f)$

Key:
1. f, hertz

In the case where the difference between the two adjacent harmonics $\Delta\omega=\omega_\nu-\omega_{\nu+1}=\pi/2T$ approaches zero, which corresponds to $T\to\infty$, the spectral density of the process

$$S(\omega)=\lim_{T\to\infty}4TD_\nu. \tag{4.33}$$

The mutual spectral density is defined analogously to the mutual correlation function. Just as the spectral density of one realization of the process is the Fourier transformation of the correlation function, so also the mutual spectral density of the two realizations is the Fourier transform of the mutual-correlation function

$$S_{xy}(\omega)=\int_{-\infty}^{\infty}R_{xy}(\tau)e^{-j\omega t}dt. \tag{4.34}$$

Inasmuch as the mutual correlation function does not have the property of evenness, the spectral density is a complex variable.

As the argument let us take the frequency $f=2\pi/\omega$; then [4]

$$\begin{aligned}S_{xy}(f)&=2[S_P(f)+jS_Q(f)];\\ S_P(f)&=\int_{-\infty}^{\infty}R_{xy}\cos 2\pi ftdt;\\ S_Q(f)&=-\int_{-\infty}^{\infty}R_{xy}(\tau)\sin 2\pi ftdt,\end{aligned} \tag{4.35}$$

APPROVED FOR RELEASE: 2007/02/08: CIA-RDP82-00850R000200090053-2

APPROVED FOR RELEASE: 2007/02/08: CIA-RDP82-00850R000200090053-2

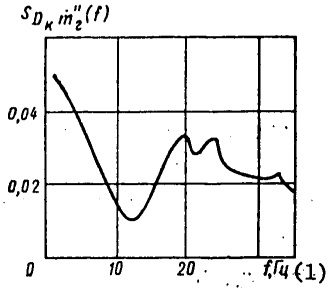

Figure 4.12. Mutual spectral density $S_{D_K \dot{m}_r''}(f)$

Key:
1. hertz

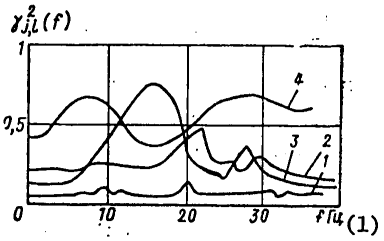

Figure 4.13. Coherence coefficient: $1-\gamma^2_{D_K, \dot{m}_r''}$; $2-\gamma^2_{p_K, \xi_{OK}''}$; $3-\gamma^2_{p_K, \xi_r'}$; $4-\gamma^2_{p_K, \xi_{OK}'}$

Key:
1. hertz

where $S_Q(f)$ is the real component, and $S_Q(f)$ is the imaginary component. In exponential form the mutual spectral density is written in the form

$$S_{xy}(f) = |S_{xy}(f)| e^{-j\theta_{xy}(f)}, \tag{4.36}$$

where the modulus $|S_{xy}|$ and the argument θ_{xy} are defined by the formulas

$$|S_{xy}(f)| = \sqrt{S_P^2(f) + S_Q^2(f)}; \qquad \theta_{xy} = \operatorname{arctg} \frac{S_Q(f)}{S_P(f)}. \tag{4.37}$$

Fig 4.12 shows the mutual spectral density between the chamber diameter and the flow rate of the fuel into the gas generator.

In order to estimate the degree of the mutual effect of the random functions, the coherence factor is used [4]

$$\gamma^2_{xy}(f) = \frac{|S_{xy}(f)|^2}{S_x(f) S_y(f)}. \tag{4.38}$$

If for some value of the frequency $\nu_{xy}(f)=0$, the functions x(t) and y(t) on the given frequency are independent, if $\gamma^2_{xy}(f)=1$, the functions are dependent on all frequencies. Thus, the coherence factor characterizes the dynamic relation between the parameters of the operating process.

FOR OFFICIAL USE ONLY

APPROVED FOR RELEASE: 2007/02/08: CIA-RDP82-00850R000200090053-2

APPROVED FOR RELEASE: 2007/02/08: CIA-RDP82-00850R000200090053-2

Fig 4.13 shows $\gamma^2_{xy}(f)$ for different combinations of parameters of the operating process and disturbances for the engines without afterburning of the generator gas.

For each combination of parameters the form of $\gamma^2_{xy}(f)$ is entirely defined and is characteristic only of the given combination.

This property of the coherence factor can be used for diagnosing the state of the engine, and $\gamma^2_{xy}(f)$ can be taken as the diagnostic attributes.

4.3.2. Determination of the Statistical Characteristics of the Properties of the Random Process

The determination of the correlation functions and the spectral densities of the random variables of the parameters of the operating processes is an independent problem going beyond the framework of this monograph. Here we shall only indicate the general events in the solution of the problem.

In the most general form it is possible to isolate five steps in the determination of these statistical characteristics:

a) Gathering

b) Recording and transmission of data;

c) Preparation;

d) Estimation of the basic properties;

e) Analysis.

The first step of gathering the data provides for the conversion of the investigated physical variable using the special conversion devices.

The converter converts the physical variable (pressure, temperature, flow rate, rpm and so on) to another one, as a rule, the electric one -- the voltage.

In the ideal case the transformation must be made without any distortions of the measured variable as a time function. In other words, if the realization of the input process is $x(t)$, and the output process $y(t)$, then in the case of the ideal converter the relation between them has the form $y(t)=cx(t)$, where c is the calibration constant. Unfortunately, this situation in practice is unattainable. For operation of the converters, as a rule, variation of the amplitudes and phases takes place, which leads to errors in the gathering and processing of the data.

The data is recorded for various methods; the basic ones are oscillographic recording on magnetic tape and radio telemetry. The preparation of the

APPROVED FOR RELEASE: 2007/02/08: CIA-RDP82-00850R000200090053-2

APPROVED FOR RELEASE: 2007/02/08: CIA-RDP82-00850R000200090053-2

data for analysis depends on the method of processing. In the case of processing the data in analog form, scaling is carried out. If the analysis is performed in digital form, then it is necessary to convert the analog signal to a digital signal, that is, carry out digitalization.

The digitalization is the process of determining the points in time in which the samples can be taken. In addition to the digitalization, quantization is carried out, that is, conversion of the readings taken at the corresponding points in time to digital form.

Let at the output of the recorder a continuous random function be obtained (see Fig 4.14). It is necessary to select the magnitude of the digitalization interval $\Delta t=h$, T is the realization time. On the one hand, for small values of h the number of points will be large, and correlated data can be obtained.

On the other hand, when selecting large h it is possible to confuse the low and high-frequency components of the process and skip the characteristic components.

For selection of h the following function is recommended [4]

$$h=\frac{1}{2f_c}, \tag{4.39}$$

where f_c is the maximum expected frequency in the spectrum of the process.

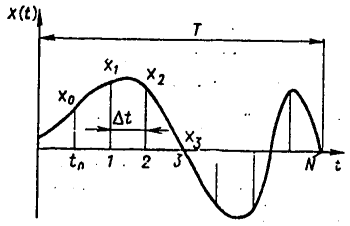

Figure 4.14. Digitalization of the process

The estimation of the basic indexes of the properties is made at the present time by two methods: analog and digital. In the analog method the calculation of the correlation functions and the spectral density is made by direct processing of the electric signals which are realizations of the process with continuous time.

In the digital method the required calculations are made by operations on the numbers which represent the analyzed process in digital form.

FOR OFFICIAL USE ONLY

APPROVED FOR RELEASE: 2007/02/08: CIA-RDP82-00850R000200090053-2

APPROVED FOR RELEASE: 2007/02/08: CIA-RDP82-00850R000200090053-2

For determination of the correlation function $R_x(\tau)$ by the experimental realization of the random function, the following operation is used

$$R_x(\tau)=\frac{1}{T}\int_0^T x(t)\,x(t+\tau)\,dt.$$

Replacing the integral $R_x(\tau)$ by the sum, the correlation function is calculated. In order to calculate the correlation function, the oscillogram of the random process is represented in the form of segments of the y-axes at a distance $h=\Delta t$ from each other (see Fig 4.14). Then the individual points of the correlation function as the mean value of the paired products of the y-axes of the realization curve separated by the interval ih (i=0, n) can be calculated using the equations

$$\begin{aligned} R(0)&=\frac{1}{n}(x_1^2+x_2^2+\ldots+x_n^2);\\ R(\Delta\tau)&=\frac{1}{n}(x_1x_2+x_2x_3+\ldots+x_nx_{n-1});\\ &\cdots\cdots\cdots\cdots\\ R(N\Delta\tau)&=\frac{1}{n}(x_1x_{n+1}+x_2x_{n+2}+\ldots+x_nx_{n+N}). \end{aligned} \qquad (4.40)$$

The correlation function is measured using correlators, the block diagram of which appears in Fig 4.15.

The correlator contains a multiplier (2), an element with adjustable delay (1), and a smoothing circuit (3). The output variable from the multiplier $x(t)x(t-\tau)$ goes to the smoother, which transmits the constant component and the slowly varying components of the signal $x(t)x(t-\tau)$.

The digital computers insure higher accuracy. They determine $R_x(\tau)$ by the equations (4.40). Magnetic correlographs have become widespread. On such correlographs the graph of the investigated process is recorded immediately on two tracks of the magnetic tape with constant time shift τ. Then by variation of the position of one roll of the tape drive mechanism by the amount $\tau/2$, a shift τ in time is established between the magnetic recordings read by the heads. The signal from the heads processed in a special computer is output to an electronic potentiometer which records the correlogram.

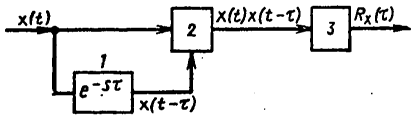

Figure 4.15. Schematic of the correlator

It is possible to check the stationarity of the random process by the criterion [27]

APPROVED FOR RELEASE: 2007/02/08: CIA-RDP82-00850R000200090053-2

APPROVED FOR RELEASE: 2007/02/08: CIA-RDP82-00850R000200090053-2

FOR OFFICIAL USE ONLY

$$J=\frac{1}{h(N-1)}\sum_{k=1}^{N}\frac{1}{N-k}\sum_{t=1}^{N}\sum_{t=0}^{T}[R_k(t,t')-R_t(t,t')]^2, \qquad (4.41)$$

where N is the number of digitalization steps; n is the digitalization step; T is time. If J=0, then the function is stationary. The analysis of the calculation data indicates that all of the random functions of the parameters of the liquid-fuel jet engines are stationary.

The condition of ergodicity of the process is $\int_0^\infty |R_x(\tau)|\,dt<\infty$,

that is, with an increase in τ, $R(\tau)$ approaches zero.

The graph of the correlation function $R_x(\tau)$ obtained as a result of the calculation is approximated by the mathematical function. The correlation functions of the parameters of the liquid-fuel jet engines in the majority have the form

$$R_x(\tau)=D_x e^{-\alpha|\tau|}, \qquad (4.42)$$

where α is a parameter which characterizes the rate of decrease of the curve. In the specialized literature [30] it is demonstrated that any correlation function can be approximated by the series

$$R(\tau)=\sum c_k e^{-\alpha_k|\tau|}.$$

It is possible to define the spectral density by different methods [27] -- by direct calculation with respect to correlation functions, expansion of x(t) in the Fourier series and using the analog spectrometers. The digital analog of the theoretical functions (4.28) is the estimate of the spectral density for arbitrary values of f in the range $0<f<f_c$.

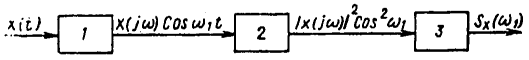

Figure 4.16. Diagram of the calculation of the spectral density

$$S_x(f)=2h\left(R_0+2\sum_{r=1}^{m-1}R_r\cos\frac{\pi rf}{f_c}+R_m\cos\frac{\pi mf}{f_c}\right), \qquad (4.43)$$

where f_c is the cutoff frequency (4.39); h is the digitalization interval; R_i is the estimate of the correlation function for the step r, m is the maximum number of steps, $m=T_{max}/n$.

FOR OFFICIAL USE ONLY

APPROVED FOR RELEASE: 2007/02/08: CIA-RDP82-00850R000200090053-2

APPROVED FOR RELEASE: 2007/02/08: CIA-RDP82-00850R000200090053-2

The estimate of the spectral density by equation (4.43) cannot be mixed with the two-way theoretical spectral density which is defined both for positive and for negative frequencies.

In addition to the described method, wide use has been made of the determination of the spectral density using the analyzer which makes use of the Fourier expansion (4.24). The random function x(t) is fed to the harmonic analyzer 1 (Fig 4.16) which is a narrow-band filter with fixed frequency ω_1. At the output of the analyzer the harmonic with ω_1 is generated. The output signal from the filter is squared using the squarer (2), and it is fed to the measuring device 3, which averages the signal in the interval 2T. At the output a spectral density is obtained with a frequency $\omega=\omega_1$. By varying the adjustment of the analyzer to other frequencies, the series $S_x(\omega_i)$ is defined, and the graph $S_x(\omega)$ is constructed.

For the majority of random processes the spectral density is approximated by the function

$$S_x(\omega)=\frac{\tilde{C}\alpha}{\alpha^2+\omega^2}. \tag{4.44}$$

4.4. Transmission of Random Signal

The engine of the dynamic system can be represented by the equation

$$y(t)=\Phi(s)x(t),$$

where x(t) is the input coordinate; y(t) is the output coordinate; $\Phi(s)$ is the transfer function. If the spectral density of the input signal $S_x(\omega)$ is known, then the spectral density of the output signal is defined by the function [30]

$$S_y(\omega)=|\Phi(j\omega)|^2 S_x(\omega). \tag{4.45}$$

Thus, the spectral density of the output variable is obtained by multiplying the spectral density of the input variable by the square of the modulus of the partial transfer function.

A dispersion with respect to the nonspectral density is defined as follows:

$$\sigma_y^2=D_y=\frac{1}{2\pi}\int_{-\infty}^{\infty}|\Phi(j\omega)|^2 S_x(\omega)\,d\omega. \tag{4.46}$$

If there are several input variables and they are independent and their spectral densities are known S_{x_1}, S_{x_2} and S_{x_n}, then

$$D_y=D_{yx_1}+D_{yx_2}+\ldots+D_{yx_n}. \tag{4.47}$$

APPROVED FOR RELEASE: 2007/02/08: CIA-RDP82-00850R000200090053-2

APPROVED FOR RELEASE: 2007/02/08: CIA-RDP82-00850R000200090053-2

The transfer function of the engine and the spectral density are rational expressions

$$\Phi(j\omega)=\frac{b(j\omega)}{a(j\omega)}; \quad S(\omega)=\frac{c(\omega)}{d(\omega)},$$

where a, b, c, d are polynomials of the argument jω.

The square of the modulus of the frequency transmission function

$$|\Phi(j\omega)|^2=\Phi(j\omega)\,\Phi(-j\omega)=\frac{b(j\omega)\overline{b(j\omega)}}{a(j\omega)\overline{a(j\omega)}},$$

where $\overline{b(j\omega)}$ and $\overline{a(j\omega)}$ are complex conjugate variables. The denominator and the numerator of the spectral density can also be expanded in the complex conjugate factors

$$c(\omega)=c(j\omega)\overline{c(j\omega)}; \quad d(j\omega)=d(j\omega)\overline{d(j\omega)}.$$

Considering the presented expressions, we have

$$|\Phi(j\omega)|S_x(\omega)=\frac{b(j\omega)\overline{b(j\omega)}\,c(j\omega)\overline{c(j\omega)}}{d(j\omega)\,d(j\omega)\overline{a(j\omega)}\,\overline{d(j\omega)}}. \tag{4.48}$$

Let us denote

$$B(j\omega)=b(j\omega)\,c(j\omega),$$
$$A(j\omega)=a(j\omega)\,d(j\omega).$$

From (4.46) we obtain

$$D_y=\frac{1}{2\pi}\int_{-\infty}^{\infty}\frac{B(j\omega)\overline{B(j\omega)}}{A(j\omega)\overline{A(j\omega)}}\,d\omega. \tag{4.49}$$

In formula (4.49) we proceed to the variable s=jω, we obtain

$$D_y=J_n=\frac{1}{j^{2\pi}}\int_{-j\infty}^{j\infty}\frac{B(s)\overline{B(s)}}{A(s)\overline{A(s)}}\,ds, \tag{4.50}$$

where

$$B(s)=\sum_{k=0}^{n-1}c_k s^k; \quad A(s)=\sum_{k=0}^{n}d_k s^k.$$

The integral (4.50) is resolvable; let us present the final values of J_n for n from 1 to 4 expressed in explicit form [5] for the coefficients c_k and d_k

FOR OFFICIAL USE ONLY

APPROVED FOR RELEASE: 2007/02/08: CIA-RDP82-00850R000200090053-2

APPROVED FOR RELEASE: 2007/02/08: CIA-RDP82-00850R000200090053-2

$$J_1=\frac{c_0^2}{2d_0d_1};$$
$$J_2=\frac{c_1^2d_0^2+c_0^2d_2}{2d_0d_1d_2};$$
$$J_3=\frac{c_2^2d_0d_1+d_0d_3(c_1^2-2c_0c_2)+c_0^2d_2d_3}{2d_0d_3(d_1d_2-d_0d_3)};\qquad(4.51)$$
$$J_4=\frac{e_0+e_1}{e_2},$$

where

$$e_0=c_3^2(d_0d_1d_2-d_0^2d_3)+(c_2^2-2c_1c_2)d_0d_1d_4+(c_1^2-2c_0c_2)d_0d_3d_4;$$
$$e_1=c_0(d_2d_3-d_1d_4)d_4;$$
$$e_2=2d_0d_4(d_1d_2d_3-d_0d_3^2-d_1^2d_4).$$

As an example let us consider the transmission of the random signal from the pump to the thrust chamber (see Fig 2.2).

Let the spectral density of the pressure after the pump

$$S_{p_H}(\omega)=\frac{D_{p_H}\alpha}{\alpha^2+\omega^2}.$$

The transfer function of the engine

$$\Phi(s)=\frac{b_1s+b_0}{a_3s^3+a_2s^2+a_1s+a_0},$$

where b_i, $a_i=f(K_p, T_k, T_M)$. Let us represent the spectral density in the form

$$S_{p_H}(\omega)=\frac{\sigma_{p_H}\sqrt{\alpha}}{\alpha+s}\;\frac{\sigma_{p_H}\sqrt{\alpha}}{\alpha-s},$$

where $\sigma_{p_H}=\sqrt{D_{p_H}}$.

Following the discussed procedure, we determine

$$B(s)=\sigma_{p_H}\sqrt{\alpha}(b_1s+b_0);$$
$$A(s)=(a_3s^3+a_2s^2+a_1s+a_0)(s+\alpha).$$

The coefficients of the integral c_k and d_k

$$c_0=b_0\sigma_{p_H}\sqrt{\alpha};\ c_1=b_1\sigma_{p_H}\sqrt{\alpha};$$
$$d_0=\alpha a_0;\ d_1=\alpha+a_0;\ d_2=\alpha a_2+a_1;$$
$$d_3=\alpha a_3+a_2,\ d_4=a_3$$
$$D_y=J_4=\frac{e_0+e_1}{e_2}.\qquad(4.52)$$

APPROVED FOR RELEASE: 2007/02/08: CIA-RDP82-00850R000200090053-2

APPROVED FOR RELEASE: 2007/02/08: CIA-RDP82-00850R000200090053-2

Substituting the expression for the coefficients in equation (4.52), we obtain the pressure dispersion in the combustion chamber as a function of the pressure dispersion after the pump and the values of the time constant and the boost factors

$$D_{p_k} = D_{p_H} \frac{\alpha b_1^2 a_0 (\alpha a_3 + a_2) + b_0^2 [(\alpha a_2 + a_1)(\alpha a_3 + a_2) - a_3 (\alpha + a_0)]}{2a_0 [(\alpha + a_1)(\alpha a_2 + a_3)(\alpha a_3 + a_2) - a_3 (\alpha + a_0)^2 - \alpha^3 a_0 a_3^2]}.$$

APPROVED FOR RELEASE: 2007/02/08: CIA-RDP82-00850R000200090053-2

APPROVED FOR RELEASE: 2007/02/08: CIA-RDP82-00850R000200090053-2

CHAPTER 5. STARTING UP THE ENGINE

5.1. General Start-Up Characteristic

5.1.1. Components of the Start-Up Process

The engine start-up is a nonsteady-state operating condition, during which the parameters of the operating process vary with time from their initial values to the values of the rated regime.

During the start-up process large parameter gradients exist. Thus, for modern engines the gradient of the pressure variation in the gas cavities is $(200\text{-}1000)\cdot 10^5$ Pa/sec; the gas velocity gradient is 200-3500 m/sec^2, and the temperature gradient 4000 K/sec.

As a result of the large gradients in the variation of the parameters in the start-up process, the engine and the aircraft are under the effect of significant mechanical and thermal loads capable of leading to destruction of the structure. In addition, as a result of the high rate of occurrence of the processes the start-up mode is uncontrollable. All of this taken together gives rise to great complexity of the organization and development of the start-up process and isolates it from all of the operating conditions.

The presence of the specific processes which includes the following is a distinguishing factor of the start-up conditions from others:

Filling of the hydraulic lines and reservoirs with fuel components;

Winding up the TNA impeller, during which the pumps receive the necessary power providing for feeding the fuel components to the thrust chamber and the gas generator;

Ignition and combustion of the fuel components;

Emergence of the engine in the rated regime, that is, achievement of the rated values by the parameters of the operating process.

APPROVED FOR RELEASE: 2007/02/08: CIA-RDP82-00850R000200090053-2

APPROVED FOR RELEASE: 2007/02/08: CIA-RDP82-00850R000200090053-2

During the start-up process replacement of the indicated phenomena takes place in a defined sequence, but there are inverse interrelations among them. Thus, for example, the characteristics of the process of filling the gas generator and thrust chamber reservoirs with the fuel components determine the conditions of ignition and combustion of the fuel, and this, in turn, influences the winding up of the TNA impeller and movement of the fuel components through the lines.

In the engine with a pump feed system the sequence of replacement of the phenomena in the start-up process is the following. On sending the instructions to start up, the start-up valves installed in the input lines of the pump open. The fuel components, under the effect of the pressure from blowing the tanks and the hydrostatic head, fill the hydraulic channels (the lines, pump cavities), and they approach the injectors of the gas generator and the thrust chamber. At a defined point in time the command is sent to ignite the pyrostarter (in the case of starter start-up), the powder gases of the pyrostarter go to the vanes of the TNA impeller. Accordingly, the rpm increases, the pressure after the pump rises, and forced pumping of the fuel components into the gas generator and the gas chamber is realized. In the gas generator the fuel components ignite, combustion takes place and a further increase in pressure after the pumps.

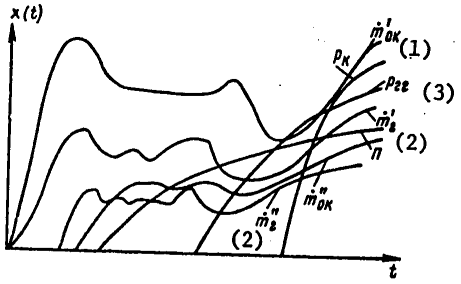

Figure 5.1. Nature of the variation of the parameters of the operating process during start-up

Key:
1. oxidizing agent
2. combustible component of the fuel
3. gas generator

At some point in time, the filling of the chamber reservoirs ends, ignition and combustion of the fuel takes place in it. At this time the turbine has sufficient power to insure the required flow rate of the fuel components to the chamber and forced emergence at the rated regime.

The qualitative variation of the parameters during the start-up process is illustrated in Fig 5.1. At t_0 -- the time of opening of the start-up valves, the fuel components, under the blowing pressure $p_{tank,\ ox}$ and

APPROVED FOR RELEASE: 2007/02/08: CIA-RDP82-00850R000200090053-2

APPROVED FOR RELEASE: 2007/02/08: CIA-RDP82-00850R000200090053-2

and $p_{tank,\ fuel}$ fill the free volumes of the fuel lines and approach the injector head. The flow rates initially increase, and then as the lines are filled and the hydraulic drags increase, they decrease.

At the time t_3, the ignition of the pyrostarter takes place, and windup of the TNA impeller and an increase in the flow rates begin.

When the jets are filled, the flow rates slowly decrease as a result of the hydraulic drags.

At the time t_4, the fuel components are injected into the gas generator, and the gas generator goes into operation with further windup of the TNA impeller.

At the time t_5, the filling of the injector head of the thrust chamber ends, and ignition and combustion of the fuel (t_4) take place in the latter. The engine reaches the rated regime.

The nature of variation of the parameters during the start-up process is determined by the structural diagram and the cyclogram of the start up and for a specific engine will differ from that shown in Fig 5.1.

5.1.2. Classification of Types of Start-Up

It is possible to classify start-ups by various attributes.

Depending on the method of initial windup of the TNA impeller, there can be two types of start-ups: starter and starterless. In the case of starter starting, special starters are included in the engine (pyrostarters or pneumatic starters, feed starter systems, and so on).

The pyrostarters are pyrotechnical caps installed in front of the guide vanes of the turbine.

The pneumatic starters are compressed gas reservoirs located on board the aircraft.

The powder gases (pyrostarters) or compressed gas go through special or working nozzles to the turbine vanes and create excess pressure capable of providing for the initial turnover of the TNA impeller.

The pyrostarters are capable of creating significant thermal gradients in the turbine with insignificant gas flow rates. However, the pyrostarters starting have a significant deficiency. As a rule, the pyrogases contain excessive combustible fuel components and are capable of afterburning in the oxidizing medium of the generator gas on the turbine vanes during joint operation of the gas generator and the starter, as a result of which a dangerous rise in temperature and burning of the vanes can take place.

APPROVED FOR RELEASE: 2007/02/08: CIA-RDP82-00850R000200090053-2

APPROVED FOR RELEASE: 2007/02/08: CIA-RDP82-00850R000200090053-2

Therefore in the case of an oxidizing gas generator the pyrostarter is installed on an auxiliary starting tubine.

Pyrostarter starting is used in the engines without afterburning of the generator gas with active turbines. In the engines with afterburning of the generator gas with jet turbines, the required pressure gradient on the turbine providing for the required excess power can be created without the application of the pyrostarter.

In this case the initial feed of the fuel components to the gas generator is realized from the fuel tanks under the force of the blowing pressure and the hydraulic pressure of the fuel column.

Fig 5.2 shows the nature of variation of the turbine rotor rpm during the starter and starterless start-up.

Curve (1) corresponds to the starter start-up, t_c is the operating time of the pyrostarter. Curve (2) is characteristic of starterless start-up. The time for turning over the TNA impeller in the starterless starting is greater than for the starter starting.

With respect to nature of variation of the pressure in the thrust chamber in time, starting can be: slow, fast and "full-flow" (Fig 5.3).

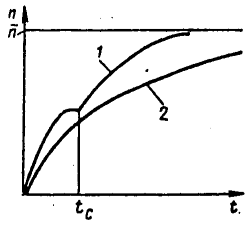

Figure 5.2. Variation of the rpm during starter and starterless starting

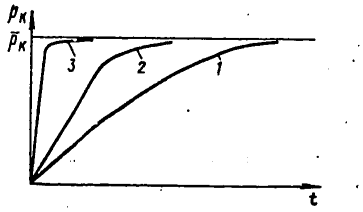

Figure 5.3. Types of start-ups

In the case of slow starting (curve 1) the pressure in the thrust chamber varies smoothly, and the rate of variation of the pressure is variable $dp_k/dt=var$. The pressure build-up time in the chamber with this form of starting can reach 2 seconds. Fast start-up (curve 2) is characterized by a constant rate of pressure variation $dp_k/dt=const$; the pressure build-up time will be approximately 1 second.

The full-flow starting (see curve 3) is characterized by constant and large magnitude of the pressure build-up rate $dp_k/dt \to \infty$; the pressure build-up time will be tenths and even hundredths of a second.

APPROVED FOR RELEASE: 2007/02/08: CIA-RDP82-00850R000200090053-2

APPROVED FOR RELEASE: 2007/02/08: CIA-RDP82-00850R000200090053-2

Slow starting is used for engines which have large thrust, for in this case the dynamic load on the structure of the flight vehicle decreases.

Fast starting is used for medium thrust engines, and full-flow for low-thrust engines and the engine for which the time (the upper bound) for reaching the operating conditions is limited.

In addition to the investigated types, start-ups can be single-stage and double-stage. The double-stage start-ups are used in high-thrust engines and engines inclined to high frequency vibrations.

In this case the double-stage fuel valves are used. When starting, the valves are first opened to the preliminary stage, and the fuel is fed with small flow rates to the thrust chamber which begins to operate. The pressure in the chamber is set at (0.4 to 0.6)p_k (Fig 5.4), the delay of t=0.5-2 seconds is realized for $p_k \sim p_{k.conv}$ for monitoring the fitness of the engine and then the valves are opened to the main stage and the engine reaches the rated operating conditions.

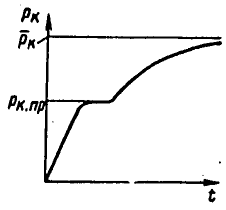

Figure 5.4. Diagram of the two-stage start-up

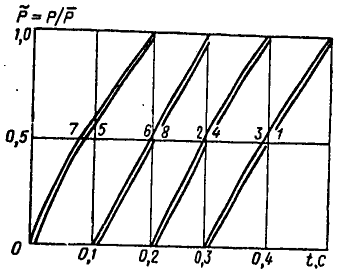

Figure 5.5. Diagram of the multi-chamber engine start-up

In the engines with afterburning of the generator gas, the two-stage start-up can be realized by separation of the operation of the thrust chamber and the gas generator in time.

Initially the gas generator is started, and it reaches the steady-state operating conditions (the preliminary stage); then the thrust chamber is switched on, and the engine reaches the rated operating conditions.

The propulsion devices of the booster rocket having large thrusts have several engines.

If all of the engines are started simultaneously, then as a result of the large total thrust, large dynamic loads and vibrations are possible which can lead to destruction of the structural elements. Therefore such propulsion devices are started by individual chambers (blocks) after short, strictly fixed time intervals. In order to exclude the appearance of

APPROVED FOR RELEASE: 2007/02/08: CIA-RDP82-00850R000200090053-2

APPROVED FOR RELEASE: 2007/02/08: CIA-RDP82-00850R000200090053-2

moments with respect to the rocket axis, simultaneous start-up of two chambers arranged symmetrically with respect to the rocket axis is used.

Fig 5.5 shows the cyclogram of the starting up of the engines of the first stage in the Saturn booster rocket. As is obvious from Fig 5.5, the engines are started in pairs every 0.1 second; here the force causing vibrations is no more than 0.2 of the maximum total thrust.

5.1.3. Forcing the Start-Up Process

In order to reduce the prestart consumption circuit, decrease the effect of the gases on the starting devices and the time for separation of the stages, it is desirable to organize the starting process so that there will be minimum time of developing thrust from the time of sending the start-up command.

In the general case the start-up time can be provisionally divided into the following components:

$$t = \underset{(1)}{t_a} + \underset{(2)}{t_{agr}} + \underset{(3)}{t_{tr}} + \underset{(4)}{t_k}$$

Key: 1. automation; 2. agr = assembly; 3. tr = lines; 4. chamber

Let us consider the indicated components:

1) t_a is the response time of the automation which includes the time of transmission of the instructions to open the start valves and the time for opening the valves.

In order to decrease the start-up time it is expedient to use high-speed fuel valves, which include the starting pyrovalves and the separating pyrodiaphragm assemblies.

It is possible to approximately define the time for opening of the start-up valve as follows.

The required gas pressure in the cavity V_0 required for shearing the diaphragm of the thickness Δ is determined from the equality

$$p_n \frac{\pi d_0^2}{4} = \pi d_0 \sigma_c \Delta, \qquad (5.1)$$

where σ_c is the admissible shearing tension. The maximum gas pressure in the cavity V_0 on combustion of the pyrocharge in the pyrocartridge is determined from the equation of state

$$p_{max} = \frac{\chi\omega}{V_0 - \alpha\omega}, \qquad (5.2)$$

where χ is the strength of the pyrocharge; α is the covalue taking into account the volume of liquid and solid residues in the combustion products of the pyrocompound.

FOR OFFICIAL USE ONLY

APPROVED FOR RELEASE: 2007/02/08: CIA-RDP82-00850R000200090053-2

APPROVED FOR RELEASE: 2007/02/08: CIA-RDP82-00850R000200090053-2

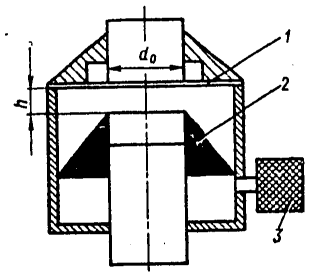

Figure 5.6. Schematic of the start-up pyrovalve:
1 -- diaphragm; 2 -- piston-knife; 3 -- pyrocharge

For smoke powder $\chi=(3\text{-}3.4)10^6$ joules/kg; $\alpha=0.5\cdot10^{-3}$ m^3/kg; for the pyrocomposition $\chi=2.1\cdot10^6$ joules/kg, $\alpha=0.3\cdot10^{-3}$ m^3/kg; ω is the mass of the charge.

For reliable cutting of the diaphragm between p_{max} and $p_п$ the following expressions must be observed:

$$p_{max}\approx 2p_п. \tag{5.3}$$

Solving equations (5.1)-(5.3) jointly we obtain the required charge mass

$$\omega=\frac{V_0}{d_0\chi/8\sigma_c\Delta+\alpha}. \tag{5.4}$$

After response of the pyrocartridge, the piston knife moves upward and cuts the diaphragm. The speed of the piston knife is determined by the magnitude of the work of the products of combustion on the path of movement of the knife. The work of the products of combustion is calculated approximately by the function

$$A=\varphi p_{max}hF_п, \tag{5.5}$$

where ϕ is the filling factor of the pressure diaphragm, $\phi=0.6$ to 0.7; $F_п$ is the area of the piston knife. If we do not consider the losses to friction, the kinetic energy of movement of the knife at the diaphragm cutting time is determined from the equality

$$\frac{mv_к^2}{2}=\varphi p_{max}hF_п. \tag{5.6}$$

Taking the average speed of movement of the knife $v_{ave}=v_k/2$, we obtain the relation for determining the response time of the start-up valve

$$t_к=\frac{h}{\sqrt{\frac{\varphi\chi\omega_0-V_0}{m(V_0-\alpha\omega)}}}, \tag{5.7}$$

APPROVED FOR RELEASE: 2007/02/08: CIA-RDP82-00850R000200090053-2

APPROVED FOR RELEASE: 2007/02/08: CIA-RDP82-00850R000200090053-2

2) $t_{assembly}$ is the time for the engine assemblies to reach the rated regime.

When analyzing the dynamic characteristics of the assemblies, it was demonstrated that out of all of the engine assemblies, the turbine-pump assembly has the greatest inertia.

The inertia of the turbine-pump assembly is characterized by the time constant

$$T_{\text{THA}}=\frac{J\frac{\pi}{30}}{a_{\text{THA}}}.$$

Key: 1. TNA = turbin-pump assembly

The time for turning over the impeller of the turbine-pump assembly is approximately estimated by the value

$$t_{\tau}\simeq 3T_{\text{THA}}.$$

Consequently, in order to reduce the time for the TNA to reach the rated regime it is necessary to decrease the moment of inertia of the rotating parts and increase the self-equalization factor a_{TNA} which is determined from the excess power of the turbine.

In turn, in order to decrease the excess power of the turbine it is expedient, if the engine diagram permits, to apply pyrostarter starting.

3) t_{line} is the time for the fuel components to fill the reservoirs and lines.

The movement of the component through the lines is described by the function

$$R\frac{d\dot{m}}{dt}+\frac{\xi}{\varrho}\dot{m}^2=p_1(t)-p_2(t), \qquad (5.8)$$

where $p_1(t)$ is the pressure at the entrance to the main; $p_2(t)$ is the pressure at the exit from the main. During the process of filling of the mains after the start valves are open the pressure at the entrance to the main is determined by the pressure in front of the start valve, and it can be taken as constant.

The pressure at the exit from the main is correspondingly equal to the pressure of the medium which also is constant to the time of arrival of the component at the reservoir.

APPROVED FOR RELEASE: 2007/02/08: CIA-RDP82-00850R000200090053-2

APPROVED FOR RELEASE: 2007/02/08: CIA-RDP82-00850R000200090053-2

Assuming that during the process of filling the mains the coefficients R and ξ are constants (the indicated assumption will be discussed further), the equation (5.8) reduces to the form

$$\frac{d\dot{m}}{dt}=a-b\dot{m}^2, \tag{5.9}$$

where

$$a=\frac{p_1-p_2}{R};\quad b=\frac{\xi}{\varrho R}.$$

After integration of equation (5.9), we obtain the filling time of the main

$$t_м=\frac{1}{2\sqrt{\frac{\xi(p_1-p_2)}{R^2\varrho}}}\ln\frac{\dot{m}-\sqrt{p_1-p_2}}{\dot{m}+\sqrt{p_1-p_2}}. \tag{5.10}$$

From analysis of the function (5.10) it follows that in order to decrease the filling time of the mains it is necessary to increase the pressure gradient on the main during the starting period and decrease the hydraulic drag coefficient, that is, decrease the length of the lines and the local resistances.

5.1.4. Requirements Imposed on the Starting Process

When designing and developing the engines, the interrelation and sequence for putting the assemblies into operation which insures that the following requirements can be satisfied are established.

1. The elimination of the possibility of accumulating a quantity of fuel mix in the thrust chamber and the gas generator at the time of ignition which can lead to explosion or inadmissible rises in the pressure.

2. The creation of the powerful initial flame in the thrust chamber and the gas generator capable of igniting the fuel components moving with high velocity.

3. Insurance of the required starting cyclogram.

4. Elimination of the possibility of the occurrence of low-frequency and high-frequency pressure fluctuations in the starting process.

5. Insurance of reliable start-up under vacuum and weightlessness conditions.

APPROVED FOR RELEASE: 2007/02/08: CIA-RDP82-00850R000200090053-2

APPROVED FOR RELEASE: 2007/02/08: CIA-RDP82-00850R000200090053-2

5.2. Conditions of Emergency-Free Starting

5.2.1. Ignition of the Components

At the end of the process of filling the lines, the fuel components arrive with quite high velocity through the injectors and the working cavity of the gas generator and the thrust chamber where they are ignited and burned.

The process of ignition and burning of the fuel in the thrust chamber is a complicated set of physical and chemical phenomena which are discussed in specialized literature. Here the basic principles are considered which pertain only to the starting process without giving details about its various components.

In order to insure reliable ignition, it is necessary to create a powerful heat source, for the ignition temperature of the nonself-igniting fuel components exceeds 570 K. In the case of application of nonself-igniting fuel components to create thermal conditions of reliable ignition, special thermal igniters are used: pyrotechnical and electrical.

Pyrotechnical ignition is realized by creation of a powerful heat source in the chamber on combustion of a special pyrotechnical compound. The dimensions of the cartridge igniter are selected so that the thermal energy of the powder gases will be sufficient for reliable ignition of the fuel components.

Electric ignition is realized both for the internal combustion engines, electrical discharge created by specialized electric sparkplugs.

For ignition of certain fuels (for example, hydrogen peroxide), catalytic surfaces are used which promote the occurrence of chemical reactions.

The self-igniting fuel components do not require special igniters, for they react on contact of the liquid phases under ordinary thermal conditions.

The organization of reliable ignition is only one of the problems of insuring emergency-free starting. After ignition it is necessary to insure continuous combustion and variation of the parameters of the operating process with respect to the given law.

The basic characteristic of ignition and combustion is ignition delay. The ignition delay is the time which passes from the injection time to the beginning of combustion.

The accumulation of a mixture of fuel and oxidizing agent in the combustion chamber which is an explosive mixture inclined toward knock is a consequence of the presence of ignition delay time. The amount of accumulated mix depends on the flow rates of the fuel component and the ignition delay time: $M_{mix}=\dot{m}_{T}\tau_{delay}$. On ignition of this mixture, a sharp build-up of pressure of the gases formed is possible (see Fig 5.7, a), as a result of

APPROVED FOR RELEASE: 2007/02/08: CIA-RDP82-00850R000200090053-2

APPROVED FOR RELEASE: 2007/02/08: CIA-RDP82-00850R000200090053-2

which rupture of the structure can take place as a result of peak thermal and dynamic loads. In addition, as a result of presence of feedback between the pressure in the combustion chamber and the arrival of fuel, unstable combustion occurs (Fig 4.7, b). The ignition delay time depends on the physical-chemical properties of the fuel, the quality of injection and mix formation, the power of the igniter, the pressure and the temperature.

Under equal conditions the amount of accumulated fuel in the combustion chamber depends on the mixture burnup rate.

It has been established that the maximum combustion rate (the minimum burnup time) occurs for the stoichiometric ratio of the fuel components).

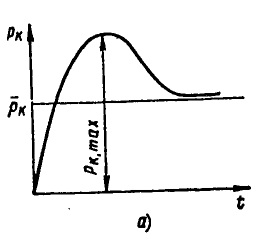

Figure 5.7. Relation of p_k for start-up

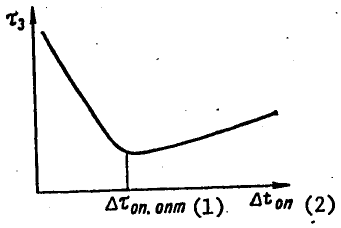

Figure 5.8. Ignition delay time as a function of the lead time
Key:
1. optimal lead
2. lead

Consequently, in order to decrease the combustion rate, that is, exclude the explosion of the accumulated mix, it is required that during starting the first lots of fuel be fed to the combustion chamber for the ratios $K \gtrless K_{st}$, that is, a lead of the component by the amount Δt_{lead}=0.03-0.2 sec must be insured. The fuel feed to the chamber with lead of one of the components leads to ballasting of the mix and excludes the knock; in addition, as the experiments show, ballasting of the hot mix by one of the components leads to a decrease in the ignition delay time, Fig 5.8.

5.2.2. Starting Overload of the Chamber

The starting overload is the ratio of the maximum gas pressure in the chamber during the starting process to the rated pressure (see Fig 5.7, a), that is,

APPROVED FOR RELEASE: 2007/02/08: CIA-RDP82-00850R000200090053-2

APPROVED FOR RELEASE: 2007/02/08: CIA-RDP82-00850R000200090053-2

$$n_{\pi}=\frac{p_{\kappa max}}{p_{\kappa}}. \tag{5.11}$$

The magnitude of the starting overload must not exceed the admissible value of $n_{\pi_{,d}}$ which is designated considering the dynamic strength of the structure and the limits of stable operation engine. For a well-organized start-up process $n_{\pi}=1$. For approximate estimation of the expected magnitude of the starting overload, the assumption of instantaneous burnup of the fuel is used, that is, the actual burnup curve is replaced by the step curve.

The equation of this burnup curve has the form

$$\phi(t)=\begin{cases} 0 \text{ for } t\leqslant\tau_{\text{пр}}; \\ 1 \text{ for } t>\tau_{\text{пр}}, \end{cases} \tag{1}$$

Key: 1. conv

where τ_{conv} is the conversion time of the fuel to the combustion products. Then the maximum pressure in the combustion chamber is defined by the equation of state

$$p_{\kappa max}=\frac{M_{\text{т}}(RT)_{\text{з}}}{V_{\kappa}}, \tag{5.12}$$

where M_T is the mass of accumulated fuel in the chamber. The mass of accumulated fuel is

$$M_{\text{т}}=(\dot{m}_{\text{з.ок}}+\dot{m}_{\text{з.г}})\tau_{\text{пр}}, \tag{5.13}$$
(1) (2) (3)

Key: 1. start, ox; 2. start, combustible fuel component; 3. conv

where $\dot{m}_{start\ i}$ are the arrivals per second of the fuel components in the chamber on start-up

$$\dot{m}_{\text{з}i}=a_{\text{з}i}\sqrt{\varrho_i\Delta p_{\text{ф.з}i}} \tag{5.14}$$
(1)

Key: 1. injector, start i

where $a_{start\ i}$ is the coefficient which depends on the geometric characteristics and the flow rate factor of the injector; $\Delta p_{injector,\ start\ i}$ is the pressure gradient in the injectors during the start-up process. Considering the expression $K_{\text{з}}=\frac{\dot{m}_{\text{ок.з}}}{\dot{m}_{\text{г.з}}}$, and after substitution of (5.14), (5.13) in (5.12), we obtain

$$p_{\kappa max}=\frac{(K_{\text{з}}+1)a_{\text{з.г}}\sqrt{\varrho_{\text{г}}\Delta p_{\text{ф.з.г}}}\tau_{\text{пр}}(RT)_{\text{з}}}{V_{\kappa}}. \tag{5.15}$$

FOR OFFICIAL USE ONLY

APPROVED FOR RELEASE: 2007/02/08: CIA-RDP82-00850R000200090053-2

APPROVED FOR RELEASE: 2007/02/08: CIA-RDP82-00850R000200090053-2

Under steady state operating conditions the pressure in the chamber is determined from the flow rate equation

$$\bar{p}_к = \frac{\beta}{F_{кр}} \dot{\bar{m}}_т. \qquad (5.16)$$
(1)

Key: 1. cr

Since $\dot{\bar{m}}_т = (K+1)\bar{a}_г \sqrt{\varrho_г \Delta p_{ф.г}}$, then after substitution of equations (5.15) and (5.16) in the function (5.11) we finally obtain

$$n_д = \frac{(k_э + 1)\, z \bar{v}_{пр}}{(\bar{K}+1) l_{пр}} \sqrt{\frac{\Delta p_{ф.э.г}}{\Delta \bar{p}_{ф.г}}}, \qquad (5.17)$$

where $z = \frac{a_{эг}}{\bar{a}_г} \frac{\sqrt{(RT)_э}}{\beta}$; $l_{пр} = \frac{V_к}{F_{кр}}$.

Thus, the coefficient of the starting overload is determined by the pressure gradient on the injectors, the reduced length of the chamber and the conversion time of the fuel to the combustion products.

The primary factors influencing the start-up overload coefficient which can be controlled during the start-up process are the pressure gradient on the injectors and the ratio of the fuel components.

5.3. Power Engineering Starting Capabilities

In order to realize the start-up process the engine must have defined power engineering capabilities insuring an increase in time of all of the parameters of the operating process. In the engines with a turbine-pump feed system the power engineering capabilities of the starting are characterized by excess power of the turbine insuring an increase in the rpm and an increase in the flow rates of the fuel components coming into the thrust chamber and the gas generator (see Fig 5.9)

$$\Delta N_{изб} = N_т - \sum N_{нj}.$$
(1)

Key: 1. excess

The excess power of the turbine determines the magnitude and the rate of variation of the rpm

$$J\left(\frac{\pi}{30}\right)^2 n(t) \frac{dn(t)}{dt} = \Delta N_т(t). \qquad (5.18)$$

In order to increase the rpm (the turnover of the TNA impeller) dn(t)/dt>, the condition $\Delta N_Т > 0$ must be satisfied.

APPROVED FOR RELEASE: 2007/02/08: CIA-RDP82-00850R000200090053-2

APPROVED FOR RELEASE: 2007/02/08: CIA-RDP82-00850R000200090053-2

The required value of ΔN_{excess} in order to insure start-up is 15-20% of the rated value of the turbine power.

As the rpm increases from 0 to n_p, the fuel component flow rate to the gas chamber increases, and the pressure in the gas generator rises. With an increase in flow rate, the available power of the turbine N_T and the intake power of the pumps increase. Depending on the turbine and pump characteristics the relation between $\partial N_T/\partial n$ and $\partial N_H/\partial n$ can be different, and the case is possible where for the same value of n $N<\Sigma N_{Hi}$ (Fig 5.10), that is, negative excess turbine power is obtained. In this case, in order to turn over the TNA impeller $dn/dt>0$ it is necessary to use an additional source of power in the form of a starter, for example, a pyrostarter.

The starting device is designed from the condition providing for turning over the impeller ("winding up") of the TNA for the conditions with rpm $n=(1.1-1.2)\ n_{min}$.

The run-up time of the TNA impeller is defined by the relation

$$t_n=\int_0^n \frac{J\frac{\pi}{30}n}{N_n-\sum N_{nl}}\,dn. \qquad (5.19)$$

In region A (see Fig 5.10) the excess power is created by the pyrostarter. The greater the starter energy, the greater N_π and the shorter the run-up time of the TNA impeller.

In region B the excess power is obtained as a result of operation of the gas generator on the basic fuel components.

The power engineering realizability of starterless starting is determined by the characteristics of the mains, the turbine-pump assembly and the gas generator. The excess turbine power depends on the flow rate of the fuel components to the gas generator and work capacity of the combustion products which in turn are determined by the pressures in the tanks and the ratio of the fuel components.

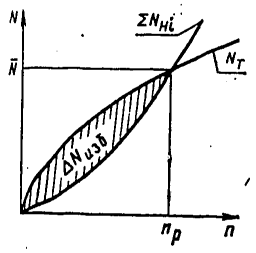

Figure 5.9. Diagram of the formation of the excess power

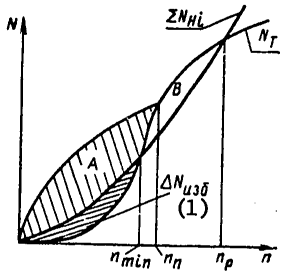

Figure 5.10. Excess power as a function of the rpm
Key: 1. excess

FOR OFFICIAL USE ONLY

APPROVED FOR RELEASE: 2007/02/08: CIA-RDP82-00850R000200090053-2

APPROVED FOR RELEASE: 2007/02/08: CIA-RDP82-00850R000200090053-2

The flow rates of the fuel components going to the gas generator after filling the lines and the pump housing can be defined by the following relations

$$\left.\begin{aligned}\dot{m}_{ок}&=a_{10}(p_{б.ок}-p_{гг});\\ \dot{m}_{т}&=a_{1т}(p_{б.т}-p_{гг}),\end{aligned}\right\} \qquad (5.20)$$

where a_{1i} are the hydraulic drag coefficients.

The equation (5.20) is written under the assumption that the movement of the fuel components through the hydraulic channels is laminar. For turbulent motion, the function (5.20) becomes quadratic, but this has no influence on the qualitative analysis.

The initial pressure in the gas generator is defined by the flow rate equation

$$p_{гг}=\frac{\beta}{F_c}\dot{m}_{т}, \qquad (5.21)$$

where $\dot{m}_T$ is the gas flow rate to the turbine. Solving the equations (5.20) and (5.21) jointly considering $K=\dot{m}_{ox}/\dot{m}_{\text{combustible fuel component}}$, $\dot{m}_T=\dot{m}_{ox}+\dot{m}_{\text{combustible fuel component}}$, we obtain

$$\left.\begin{aligned}\dot{m}_{т}&=b_0\left(\frac{K+1}{K}\right)p_{б.ок};\ (1)\\ \dot{m}_{т}&=b_{т}(K+1)\,p_{б.т};\ (2)\end{aligned}\right\} \qquad (5.22)$$

Key: 1. tank, ox; 2. tank, combustible component of the fuel

By equations (5.22) for the specific engine design (given values of b_0, $b_{\text{combustible component}}$) the nomogram of $\dot{m}_T+M(p_{\text{tank, ox}}, p_{\text{tank, combustible component of the fuel}}, K)$ of Fig 5.11) is constructed.

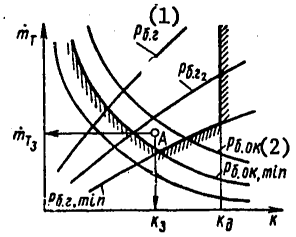

Figure 5.11. Start-up region

Key:
1. tank, combustible fuel component
2. tank, ox

APPROVED FOR RELEASE: 2007/02/08: CIA-RDP82-00850R000200090053-2

APPROVED FOR RELEASE: 2007/02/08: CIA-RDP82-00850R000200090053-2

On the nomogram the hatchures denote the maximum values of $P_{tank, i\ min}$ (from the conditions of cavitationless operation of the pumps) and K_d (from the condition of thermal stability of the operating vanes of the turbine).

Being given the value of the excess turbine power, $N_{excess}=(0.25-0.2)\overline{N}_T$, the required flow rate of the working medium is defined

$$\dot{m}_{T.3}=\frac{(0,15-0,2)\overline{N}_T}{N_{уд}(1)},$$

Key: 1. spec

where N_{spec} is the specific power of the turbine determined for the given ratio of the fuel components and minimum (start-up) pressure gradient on the turbine. With respect to the values of $\dot{m}_{T.3}$ and K_3 from the graph in Fig 5.11 the pressures are determined in the tanks and by the equations (5.22) the coefficients b_0 and b_g for which starterless starting is possible (the point A).

5.4. Characteristic Features of Starting Engines in a Vacuum under Weightlessness Conditions

5.4.1. Starting in a Vacuum

At altitudes of more than 40 km, the ambient pressure in practice is absent and there is a vacuum. The vacuum imposes additional requirements on the conditions of emergency for a starting of the engines. Under vacuum conditions there is no counterpressure in the combustion chamber, and this leads to the following:

An increase in the ignition delay time and the time of conversion of the fuel to the combustion products;

An increase in the flow rates of the fuel components entering the combustion chamber and the gas generator;

Worsening of the quality of the atomizing and the mixing of the fuel components;

Loss by some of the self-igniting components of the fuel of the capacity for self-ignition.

All of this taken together leads to accumulation of a mass of fuel in the reservoirs of the chamber and the gas generator at the time of ignition, a drop in pressure on ignition (an increase in the starting overload), and explosion or nonstarting of the engine.

For reliable starting of the engines in a vacuum, the following measures are taken:

APPROVED FOR RELEASE: 2007/02/08: CIA-RDP82-00850R000200090053-2

APPROVED FOR RELEASE: 2007/02/08: CIA-RDP82-00850R000200090053-2

Installation of sealing blind flanges in the vicinity of the critical cross section of the nozzle which are knocked out by the pressure of the combustion products;

Preliminary purging of the cavities in the combustion chamber or the gas generator with gas before starting up the engine.

The engines operating on low-boiling fuel components do not require special purging of the chamber with gas.

In this case, sublimation (evaporation) of the components takes place in the chamber during starting, as a result of which the pressure in the reservoir rises, and favorable starting conditions are created.

5.4.2. Starting Under Weightlessness Conditions

The state of weightlessness occurs on disappearance of the g-loads acting on the medium. In the state of weightlessness the liquid components and the gases in the tanks do not have flat interfaces, and the liquid and gas equilibrium is insured only by the effect of the capillary forces, which are small. Therefore for nonwettable liquids the gas is located around the periphery of the tank, and the liquid coagulates in the volumes inside the tank (Fig 5.12, a) and vice versa for wetting liquids (Fig 5.12, b).

The condition of conversion to a state of weightlessness is approximately defined by the Bond criterion:

$$B_0 = \frac{9{,}81 n (\rho_{ж}^{(1)} - \rho_{г}^{(2)}) l^2}{\sigma},$$

Key: 1. liquid; 2. gas

where n is the load factor; ρ_{liquid}, ρ_{gas} are the densities of the liquid and gas, respectively; l is the characteristic dimension (diameter) of the tank; σ is the coefficient of the surface tension of the liquid. For $B_0<1$, the condition of weightlessness sets in. Under the conditions of weightlessness, the gas or gas-fuel mix enters the fuel lines, and this leads either to unstable starting or to the fact that the engine in general cannot be started. Accordingly, for start-up under weightlessness conditions, the necessity arises for developing special fuel collectors or the taking of other measures to insure continuity of the flow of the liquid, separation of the liquid and gas phase and reliable starting.

All of the systems providing for continuity of flow of the liquid and separation of phases are divided into active and passive systems.

The passive systems do not require expenditures of additional energies; they include the separating, accumulating and capillary devices. The separating devices include those in which the gas is separated from the liquid by nonpermeable partitions (diaphragms, elastic bags, bellows,

APPROVED FOR RELEASE: 2007/02/08: CIA-RDP82-00850R000200090053-2

APPROVED FOR RELEASE: 2007/02/08: CIA-RDP82-00850R000200090053-2

and so on). Such devices are also called compensators, for in addition to separation they also provide for compensation of the thermal expansion of the fuel in the tanks.

Fig 5.13 shows the bellows distributing device and an elastic bag.

When starting the engine the gas for purging the tank is fed to the compensator, which, increasing in volume, forces the liquid components of the fuel out of the tank into the main. After starting and the occurrence of g-loads when the weightlessness conditions are eliminated, the purging of the tank will be realized by the usual method.

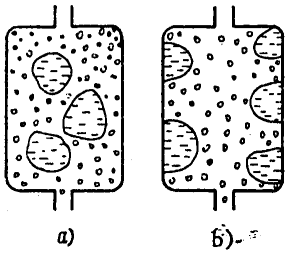

Figure 5.12. Location of the liquid and gas in the tanks

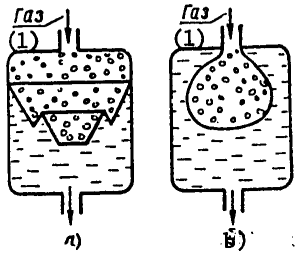

Figure 5.13. System of separators: a -- bellows; b -- elastic bag
Key:
1. Gas

The deficiencies of the compensators include the following:

An increase in mass of the feed system;

Significant remains of fuel components in the tank;

Not all of the materials of the compensators are compatible with the fuel; some have permeability with respect to liquid and gases.

The latter deficiency limits the application of the compensators and the engines of the space systems with prolonged time of existence. The accumulators are special reservoirs in which a defined amount of fuel used for subsequent starting is accumulated (see Fig 5.14). On accelerated movement of the flight vehicle the fuel component fills the accumulating reservoir, and a reserve of the component is formed for repeated starting. For repeated starting from the accumulating reservoir, the components go to the feed system, and the engine starts.

An effective method of separating the liquid from the gas is the capillary devices (screens) in which the phase interface is formed on the screen as a result of capillary forces (Fig 5.15). The liquid film formed on the

FOR OFFICIAL USE ONLY

APPROVED FOR RELEASE: 2007/02/08: CIA-RDP82-00850R000200090053-2

APPROVED FOR RELEASE: 2007/02/08: CIA-RDP82-00850R000200090053-2

mesh of the screen prevents penetration of the gas under the screen. During starting, when the G-load appears, the interface (of the film) is broken, and the fuel component goes into the feed system.

The height of the column of the liquid on which the capillary forces act can be determined by the approximate relation

$$h=\frac{0{,}29\sigma\cos\theta}{n\rho\delta},$$

where θ is the wetting angle of the liquid; δ is the capillary size.

The active phase separate systems require expenditures of additional energy to create a gravitational field. The active systems are separated into two groups: the systems creating the initial G-loads and the separation systems.

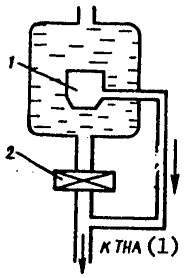

Figure 5.14. Diagram of the accumulating device:
1 -- storage element; 2 -- separating valve
Key:
1. to the TNA [turbine-pump assembly]

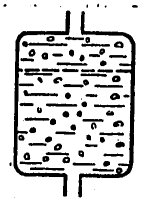

Figure 5.15. Capillary separator

The initial g-load required for starting is created by various methods:

a) Starting the engines of the upper stages with the engines of the lower stages operating;

b) The application of solid-fuel engines to create g-loads;

c) The rotation of the tank or the spacecraft as a whole, as a result of which the g-loads are created from the effect of the centrifugal forces.

The required g-load created by the enumerated systems is defined by the Bond criterion

APPROVED FOR RELEASE: 2007/02/08: CIA-RDP82-00850R000200090053-2

APPROVED FOR RELEASE: 2007/02/08: CIA-RDP82-00850R000200090053-2

As a result of creating the g-loads (artificial gravity) the gas bubbles in the mass of the fuel components float to the surface in 10 to 20 seconds.

The operating principle of the separation systems is based on the difference in gas and liquid densities, as a result of which the gas from the liquid is separated by an active flow.

5.5. Theoretical Calculation of the Starting Process

5.5.1. Peculiarities of Calculating Start-Up

Experimental methods still prevail in developing the start-up process. During the experimental development, the cyclogram of the operation of the automation and assemblies, the parameters of the starters are determined, as a result of which the program is established for the functioning of the systems and the interrelation of the parameters which insure emergency-free starting and a given law of pressure variation in the thrust chamber.

This method of start-up is not optimal, for it requires significant expenditures of material means and time. Therefore, along with the experimental methods of developing the starting process, the theoretical methods of calculation are being developed and are finding practical application.

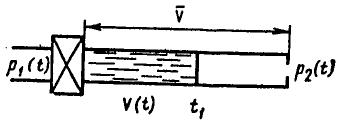

Figure 5.16. Schematic of filling of the line

The theoretical calculation of the starting process is based on solving a system of differential and algebraic equations describing the nonstationary processes in the engine assemblies.

The initial data for calculating start-up are as follows:

The engine diagram;

The system of equations, that is, the mathematical model of the start-up process.

The system of equations includes the equations of the thrust chamber, the gas generators, the pumps, the turbines, the intake and delivery lines, valves and regulators, and all of the enumerated equations are presented in Chapter 1.

However, when compiling the mathematical model of the starting process it is necessary to consider the specific peculiarities of starting. First of all, these peculiarities include the dynamics of the filling of the

APPROVED FOR RELEASE: 2007/02/08: CIA-RDP82-00850R000200090053-2

APPROVED FOR RELEASE: 2007/02/08: CIA-RDP82-00850R000200090053-2

free volumes of the assemblies (pumps, heads, chambers) and the lines with the fuel components.

During start-up after opening of the starting valves, successive filling of the subsequent sections of the lines with the fuel components takes place (see Fig 5.16).

The equation of motion of the liquid for an entirely filled line has the form

$$R\frac{d\dot{m}(t)}{dt}+\frac{\xi}{\varrho}\dot{m}^2(t)=p_1(t)-p_2(t). \tag{5.23}$$

During the process of filling of the lines the form of the equation (5.23) is maintained, but the coefficients of inertia R and hydraulic drag ξ will be variable, and they depend on the filled volume V(t).

The functions R(V) and ξ(V) are determined by the geometric and hydraulic characteristics of the lines, and they can be calculated or determined experimentally.

The approximately indicated functions are approximated by polynomials of the type

$$\begin{aligned} R(V)&=aV^2(t)+bV(t)+c,\\ \xi(V)&=a'V^2(t)+b'V(t)+c', \end{aligned} \tag{5.24}$$

where a,b,c are the approximation coefficients.

Thus, the consideration of the process of filling the line is carried out by introduction of the new variable V(t) into the equation (5.23) which can be determined from the equation

$$\varrho V(t)=\int_{t_0}^{t}\dot{m}(t)dt, \tag{5.25}$$

where t is the current time; t_0 is the time of beginning of filling.

From equation (5.25) it is easy to obtain the relation

$$\frac{dV(t)}{dt}-\frac{\dot{m}(t)}{\varrho}=0. \tag{5.26}$$

Thus, the process of filling the lines with the fuel components is described by the equations (5.23) and (5.26). On filling of the lines with low-boiling fuel components as a result of heat exchange in the liquid with the walls, gasification can take place. For the gas-saturated liquid the equation of gas and liquid balance has the form:

$$\dot{m}_{\text{ж}}(t)=[1-\varphi(t)]\dot{m}(t), \tag{5.27}$$

APPROVED FOR RELEASE: 2007/02/08: CIA-RDP82-00850R000200090053-2

APPROVED FOR RELEASE: 2007/02/08: CIA-RDP82-00850R000200090053-2

where $\dot{m}(t)$ is the total flow rate of the component; $\dot{m}_{liquid}(t)$ is the liquid phase flow rate;

$$\varphi(t)=\frac{\dot{m}_{\text{газ}}^{(1)}(t)}{\dot{m}_{ж}^{(2)}(t)}.$$

Key: 1. gas; 2. liquid

If it is assumed that the gaseous phase is in the volume $[\overline{V}-V(t)]$ between the moving liquid front and the final boundary of the line, for the given case equation (5.26) assumes the form

$$\frac{dV(t)}{dt}-\frac{[1-\varphi(t)]\dot{m}(t)}{\varrho}=0. \tag{5.28}$$

5.5.2. Mathematical Model of the Starting Process

The system of equations which are presented in Table 5.1 is compiled for the specific engine layout.

Depending on the layout of the engine, the number of equations can reach 100 to 200.

Table 5.1

Order No	Equation	Formula No
1	Thrust chamber	1.12
2	Gas Generators	1.21
3	Pump	1.73
4	Turbine	1.106
5	Automation and regulators	1.136; 1.141
6	All sections of mains	1.32; 1.33
7	Filling of the mains	5.23; 5.24; 5.26
8	Filling of the pump cavities	5.23; 5.24; 5.26

For convenience of calculation and compilation of the program, all of the equations are written in relative variables $\tilde{x}=x/\overline{x}$. As the base value of x, the rated values of the parameters are selected.

For example, the equation (5.27) in relative values assumes the form

$$R\overline{\dot{m}}\frac{d\tilde{\dot{m}}(t)}{dt}+\frac{\xi}{\varrho}\overline{\dot{m}}^2\tilde{\dot{m}}^2(t)=\overline{p}_1\tilde{p}_1(t)-\overline{p}_2\tilde{p}_2(t).$$

In addition to the system of equations, the initial and boundary conditions are given.

The initial conditions are values of the parameters

APPROVED FOR RELEASE: 2007/02/08: CIA-RDP82-00850R000200090053-2

APPROVED FOR RELEASE: 2007/02/08: CIA-RDP82-00850R000200090053-2

at the time of sending instructions to the start valves t=0

$$\tilde{p}_к(0)=\tilde{p}_{гг}(0)=\tilde{n}(0)=\tilde{m}(0)=\tilde{V}_j(0)=\ldots=0$$

and at the time of completion of the starting process $t=t_{start}$

$$\bar{p}_к(t)=1;\ \tilde{m}(t)=1 \text{ and so on.}$$

The boundary conditions of the operating conditions of the automation, for example, conditions of the type

$$0\leqslant h_o(t)\leqslant\tilde{h}_o;\ 0<h_г<\tilde{h}_г \text{ and so on}$$

where $\tilde{h}_O$, $\tilde{h}_g$ are the maximum possible displacements of the moving parts of the start valves, the regulators, and so on.

Since the starting process is a change in an entire series of phenomena and events, the onset of which is realized only after satisfaction of defined conditions, it is expedient to formulate these conditions in advance and denote the times of their appearance on the time axis.

The peculiarities of such conditions are determined by the engine layout and the starting cyclogram.

Such conditions and times are the following:

opening of the start valve

$$[0]\longrightarrow t_0;$$

filling of the lines from the valves to the pumps

$$[\tilde{V}_{1_{(1)}}=1]\rightarrow t_1;\ [\tilde{V}_{1_{(2)}}=1]\rightarrow t_2;$$

Key: 1. ox; 2. combustible component of the fuel

filling of the pump cavity

$$[\tilde{V}_{н.ок}=1]\rightarrow t_3;\ [\tilde{V}_{н.г}=1]\rightarrow t_4;$$

filling of the lines from the pumps to the gas generators

$$[\tilde{V}'_{ок}=1]\rightarrow t_5;\ [\tilde{V}'_{г}=1]\rightarrow t_6;$$

. . . . . .

$$[\tilde{p}_к=1]-t_з.$$

The conditions [j] and the times t_j separate the starting process into a number of characteristic steps, and every t_j informs about the completion of a defined step.

APPROVED FOR RELEASE: 2007/02/08: CIA-RDP82-00850R000200090053-2

APPROVED FOR RELEASE: 2007/02/08: CIA-RDP82-00850R000200090053-2

The indicated unique relation between the condition [j] and the time t_j makes it possible during the calculation process to select the subsystem of equations describing the transient process before the time the next condition is reached from the mathematical model.

For example, under the condition [0], the equations of the start valves and filling of the lines from the valves to the pumps are included in the calculation. At the time t_2 on satisfaction of the conditions [$\tilde{V}_{1\ ox}$=1] and [$V_{1\ fuel}$=1] the system of equations will contain the following:

The equations of the component mains to the pumps;

The equations of filling of the pump cavities, and so on.

For the designed engine the times t_j are unknown, and they are determined during the calculation process, that is, the start cyclogram is defined.

As a result of the calculation, the characteristics of the start process $p_k(t)$, $p_{gg}(t)$, n(t), and so on, similar to those indicated in Fig 5.1 are determined.

Thus, by varying the boundary conditions of the hydraulic system of the engine and the parameters of the starting devices, it is possible to determine the cyclogram and the starting characteristics satisfying the technical specifications.

Some of the special problems of the starting process can be solved without calling on the entire complex system of equations.

5.5.3. Calculation of the Starting of the Microengines

In the engines used for control of spacecraft, it is necessary to know the law of variation of pressure in the chamber and the thrust created each time the engine is switched on.

The control engines have low thrust, the simplest feed system, small lengths of lines (the start valve is located on the head of the combustion chamber). For such engines it is possible to neglect the inertia of the fuel components in the line and determine the nature of variation of $p_k(t)$, using only two equations: equation of the thrust chamber and the equation of the hydraulic drag of the injector head. Here the inertia of the valve either is not considered or it is estimated by the functions presented in Chapter 1.

Setting τ_{conv}=0, the equation of the thrust chamber is written in the form

$$\frac{V_к}{RT_к}\frac{dp_к}{dt}=\dot{m}_{ок}+\dot{m}_г-\dot{m}. \qquad (5.29)$$

FOR OFFICIAL USE ONLY

APPROVED FOR RELEASE: 2007/02/08: CIA-RDP82-00850R000200090053-2

APPROVED FOR RELEASE: 2007/02/08: CIA-RDP82-00850R000200090053-2

The gas flow rate from the chamber is

$$\dot{m}=\beta p_{\kappa}, \tag{5.30}$$

where $$\beta=\frac{\bar{\dot{m}}}{\bar{p}_{\kappa}}.$$

For the approximate calculation it is possible to assume that $RT_k=\overline{RT}_k$ and does not depend on the pressure in the combustion chamber. Under actual conditions RT_k depends very weakly on p_k and is defined by the relation of the fuel components. In the case of using a single-component engine the condition $RT_k=\overline{RT}_k$ is correct.

The inflow of fuel components to the thrust chamber is determined by the hydraulic characteristics of the injector head

$$\dot{m}_i=\mu_i F_i \sqrt{2\varrho_i (p_{\phi i}-p_{\kappa})}, \tag{5.31}$$

where $p_{\phi i}$ is the pressure in front of the injectors.

Setting $\mu F_i \sqrt{2\varrho_i}=\alpha_i$ and $p_{\phi.ok}=p_{\phi.r}=p_{\phi}$, we obtain

$$\dot{m}_{ok}+\dot{m}_r=A\sqrt{p_{\phi}-p_{\kappa}}, \tag{5.32}$$

where

$$A=\alpha_{ok}+\alpha_r=\frac{\bar{\dot{m}}}{\sqrt{\bar{p}_{\phi}-p_{\kappa}}}.$$

Substituting (5.30) and (5.32) in equation (5.31), we obtain

$$\frac{V_{\kappa}}{RT_{\kappa}}\frac{dp_{\kappa}}{dt}=A\sqrt{p_{\phi}-p_{\kappa}}-\beta p_{\kappa}.$$

or

$$t=\frac{V_{\kappa}}{dt}\int_0^{p_{\kappa}}\frac{dp_{\kappa}}{A\sqrt{p_{\phi}-p_{\kappa}}-\beta p_{\kappa}}. \tag{5.33}$$

Introducing the dimensionless variable $\tilde{p}_k=p_k/\bar{p}_k$ into the equation (5.33), after transformations we obtain

$$t=\frac{V\bar{p}_{\kappa}}{\bar{\dot{m}}RT_{\kappa}}\int_0^{\tilde{p}_{\kappa}}\frac{d\tilde{p}_{\kappa}}{a\sqrt{b-\tilde{p}_{\kappa}}-\tilde{p}_{\kappa}}, \tag{5.34}$$

where

$$a=\frac{1}{\sqrt{\frac{p_{\phi}}{p_{\kappa}}-1}};\quad b=\frac{p_{\phi}}{p_{\kappa}}.$$

If we make the substitution of variables of the type $x=\sqrt{b-\tilde{p}_k}$ in the last equation, the integral (5.34) reduces to the table integral

APPROVED FOR RELEASE: 2007/02/08: CIA-RDP82-00850R000200090053-2

APPROVED FOR RELEASE: 2007/02/08: CIA-RDP82-00850R000200090053-2

$$\int \frac{d\bar{p}_к}{a\sqrt{b-\bar{p}_к-\bar{p}_к}} = -\int \frac{2x\,dx}{x^2+ax-b} = -\ln(x^2+ax-b) + \\ + \frac{a}{\sqrt{a^2+4b}} \ln \frac{a+2x-\sqrt{a^2+4b}}{a+2x+\sqrt{a^2+4b}}.$$

Returning to the initial variables, after substitution of the integration limits 0 and $\bar{p}_k$ we obtain

$$t\frac{\dot{m}R\bar{T}_к}{V_к\bar{p}_к} = \ln \frac{\sqrt{\frac{p_ф}{p_к}}}{\sqrt{\frac{p_ф}{p_к}-\frac{p_к}{\bar{p}_к}}-\frac{p_к}{\bar{p}_к}\sqrt{\frac{p_ф}{p_к}-1}} - \frac{1}{2\frac{p_ф}{p_к}-1} \times \\ \times \ln \frac{\sqrt{\left(\frac{p_ф}{p_к}-\frac{p_к}{\bar{p}_к}\right)\left(\frac{p_ф}{p_к}-1\right)}+\frac{p_ф}{p_к}\left(1+\sqrt{\frac{p_ф}{p_к}\left(\frac{p_ф}{p_к}-1\right)}\right)-\left(\frac{p_ф}{p_к}\right)^2}{\sqrt{\left(\frac{p_ф}{p_к}-1\right)\frac{p_ф}{p_к}}+\frac{p_ф}{p_к}\left(1+\sqrt{\left(\frac{p_ф}{p_к}-1\right)\left(\frac{p_ф}{p_к}-\frac{p_к}{\bar{p}_к}\right)}\right)-\left(\frac{p_ф}{p_к}\right)^2}.$$

The left side of equation (5.36) is the dimensionless starting time, and the right side is the dimensionless pressure in the chamber and in front of the injectors.

The graph of the function (5.36) for various values of $p_ф/\bar{p}_k$ is shown in Fig 5.17; the results of the experimental determination of the starting characteristics of the micromotor with thrust of 23 N are presented which indicate the satisfactory accuracy of the calculation.

For the given rated engine parameters, the graph permits determination of $p_k(t)$ and the start-up time.

Since in equation (5.36) the second term is negligibly small in comparison with the first term, the starting time is approximately defined by the function

$$t_з = \frac{V_к\bar{p}_к}{\dot{m}R\bar{T}_к} \ln \frac{\sqrt{\frac{p_ф}{p_к}}}{\sqrt{\frac{p_ф}{\bar{p}_к}-0{,}95}-0{,}95\sqrt{\frac{p_ф}{\bar{p}_к}-1}}. \qquad (5.37)$$

APPROVED FOR RELEASE: 2007/02/08: CIA-RDP82-00850R000200090053-2

APPROVED FOR RELEASE: 2007/02/08: CIA-RDP82-00850R000200090053-2

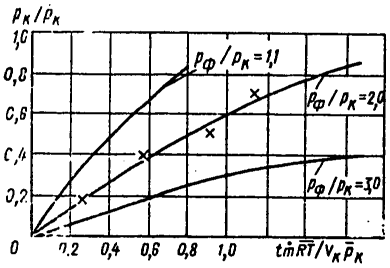

Figure 5.17. Variation of the dimensionless pressure in the chamber during starting process

APPROVED FOR RELEASE: 2007/02/08: CIA-RDP82-00850R000200090053-2

APPROVED FOR RELEASE: 2007/02/08: CIA-RDP82-00850R000200090053-2

CHAPTER 6. SHUTTING DOWN THE ENGINE

6.1. Basic Specifications of the Shutdown Process

6.1.1. Types of Shutdown

Engine shutdown is a responsible process, which determines the choice of the method of separation of stages, the separation of the pay load, dispersion of the velocity and the coordinates of the end of the active section of the trajectory.

When shutting down the engine a transient process occurs during which all of the parameters of the operating process vary with time from the rated values to zero.

The nature of variation of the parameter in time depends on the shutdown sequence which, in turn, is determined by the method of controlling the range, the purpose of the engine and the thrust and the layout of the engine itself.

The basic range control method is to shut down the engine when the rocket reaches the given velocity and the coordinates of the end of the active section of the trajectory. Consequently, in order to select the shutdown time it is necessary to determine the velocity with high accuracy. Obviously the less the thrust and acceleration of the rocket, the smaller the error will be in determining the shutdown time of the engine and the dispersion of the target points. Beginning with this requirement, the engine can be shut down in one or two stages.

In both cases the engine is shut down by closing the fuel valves. If the engine has insignificant thrust, it is shut down in one stage. In this case the command is sent to close the fuel valves, the fuel feed to the thrust chamber stops, and the thrust drops from the rated value to zero (Fig 6.1). Engines having high thrust are shut down in two stages. Initially the engine is converted to the reduced thrust mode (the final stage). The thrust then decreases to a value of $p=(0.1-0.5)\overline{P}$.

FOR OFFICIAL USE ONLY

APPROVED FOR RELEASE: 2007/02/08: CIA-RDP82-00850R000200090053-2

APPROVED FOR RELEASE: 2007/02/08: CIA-RDP82-00850R000200090053-2

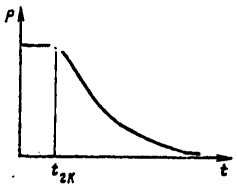

Figure 6.1. Thrust variation during engine shutdown

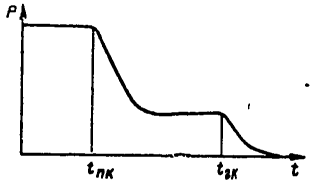

Figure 6.2. Diagram of two-stage shutdown

The magnitude of the thrust in the final stage is determined by the limiting pressure in the thrust chamber for which stable operation is insured. The operating time in the final stage (Fig 6.2) is determined by the requirements of accuracy of operation of the range control system.

When the rocket reaches the given velocity, the primary command to shut down the engine is sent; on this command the fuel valves close and the fuel feed stops.

In cases where in addition to the primary propulsion device the rocket stage has steering engines, it is shut down in two stages. On the preliminary command, the primary engines are shut down, and on the primary command, the steering engines (Fig 6.3).

6.1.2. Afterflaming Impulse of an Engine (IPD)

After shutting the fuel valves, as a result of inertia of the valves, the lines and the compression chamber the thrust does not drop instantaneously, but over some time interval. In view of the fact that the operation of the engine after closing the valves becomes uncontrollable and depends on various factors, the nature of variationof the thrust from engine to engine is not reproducible, and it has the dispersion shown in Fig 6.4. As a result of variation of the thrust with time after the valves are closed, an impulse thrust is created which influences the rocket after the engines are shut down. This impulse is called afterflaming impulse (IPD) and is denoted by I. In Fig 6.4 the area of the crosshatched region determines the magnitude of the dispersion of the afterflaming impulse.

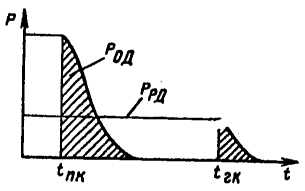

Figure 6.3. Shutdown diagram with steering engine

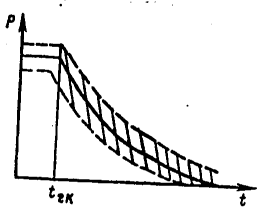

Figure 6.4. Dispersion of the engine afterflaming impulse

APPROVED FOR RELEASE: 2007/02/08: CIA-RDP82-00850R000200090053-2

APPROVED FOR RELEASE: 2007/02/08: CIA-RDP82-00850R000200090053-2

In the general case the IPD is defined by the function

$$I=\int_{t_{rk}}^{t} P dt. \tag{6.1}$$

The thrust of the engine is defined by the function

$$P=R-F_a p_n, \tag{6.2}$$

where R is the thrust in a vacuum.

Considering the last function, we obtain

$$I=\int_{t_{rk}}^{t} R dt - F_a \int_{t_{rk}}^{t} p_n dt. \tag{6.3}$$

From equation (6.3) it follows that the IPD is defined by the law of variation of the thrust in a vacuum and the ambient pressure.

Since under flight conditions the engine is shut down at high altitudes where the atmospheric pressure is low (for example, at an altitude of 25 km the atmospheric pressure does not exceed 2% of the pressure at sea level), the first term in equation (6.3) has practical significance.

The thrust in a vacuum is defined by the function

$$R=K_p F_{kp} p_k, \tag{6.4}$$

where K_p is the thrust factor, $K_p=K_p(\chi, p_a/p_k)$, which as a result of variation of the fuel component ratio during the shutdown process is a variable; for approximate calculation it is possible to assume that K_p is a constant and to determine it by the parameters of the steady-state regime

$$\overline{K}_p=\frac{\overline{R}}{\overline{p}_k F_{kp}}. \tag{6.5}$$

Fig 6.5 shows the function $K_p/\overline{K}_p=f(p_k)$ for the process of engine shutdown obtained experimentally where $\overline{K}_p$ is the thrust factor for the rated operating conditions. Substituting the relations (6.4) and (6.5) in the initial equation and taking the time of sending the instruction to shut down the engine as the origin, we obtain

$$I=\frac{\overline{R}}{\overline{p}_k}\int_0^t p_k(t)\,dt. \tag{6.6}$$

FOR OFFICIAL USE ONLY

APPROVED FOR RELEASE: 2007/02/08: CIA-RDP82-00850R000200090053-2

APPROVED FOR RELEASE: 2007/02/08: CIA-RDP82-00850R000200090053-2

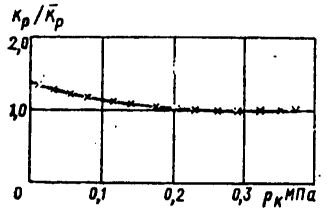

Figure 6.5. Relative thrust factor as a function of p_k
Key:
1. MPa

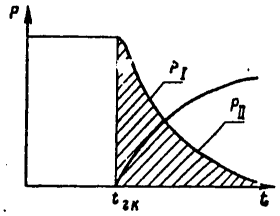

Figure 6.6. Variation of the thrust of the engines of the first and second stages

Thus, in order to calculate the IPD it is necessary to know the law of variation of the pressure in the thrust chamber after closing the fuel valves.

The afterflaming impulse of an engine depends on many factors, the basic ones of which are the following: the thrust, the response time of the automation, the volume of the cavity filled with fuel, the temperature of the fuel components, and so on.

As a result of the fact that the indicated factors are random variables, the amount of IPD is also random and varies within broad limits. For example, for an engine with a thrust of 28000 kN the mean of amount IPD is 40 kN, and the mean square deviation is 3 kN.

After sending the command to shut down the engine, the engine becomes uncontrollable because the control system ceases to operate. The afterflaming process is highly undesirable because the presence of arbitrary and uncontrolled thrust leads to a significant increase in the range dispersion or the stage separation conditions. This dispersion is determined by the dispersion of the IPD. The afterflaming impulse of an engine can also play a positive role. The engines of the upper stages should have positive acceleration to insure reliable starting. In order to create acceleration of the upper stage when starting its engine, it is possible to use the afterflaming of the lower stage. In this case the command to start the upper stage is fed simultaneously with the command to shut down the engines of the first stage (Fig 6.6). The required acceleration is created by the thrust pulse.

6.2. Components of the Afterflaming Impulse

The engine is shut down by closing the fuel valves which control the fuel feed to the thrust chamber.

After closing the fuel valves part of the fuel remains in the cavities between the chamber and the valves (Fig 6.7) and will go to the chamber, afterflame and create thrust.

APPROVED FOR RELEASE: 2007/02/08: CIA-RDP82-00850R000200090053-2

APPROVED FOR RELEASE: 2007/02/08: CIA-RDP82-00850R000200090053-2

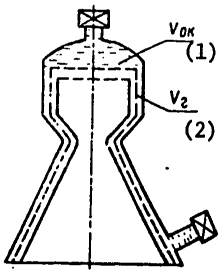

Figure 6.7. Fuel component reservoirs
Key:
1. ox
2. combustible component of the fuel

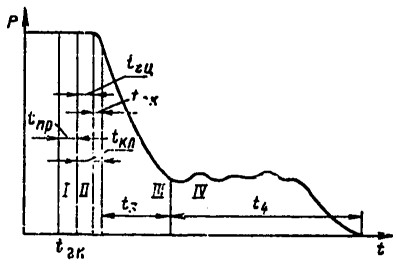

Figure 6.8. Thrust variation after sending the primary command to shut down

The standard nature of thrust or pressure variation in the thrust chamber during the shutdown process is shown in Fig 6.8.

The entire IPD (the area under the curve $p_k(t)$) can be broken down into four characteristic sections which are determined by the peculiarities of the processes occurring when the valves are closed.

The first section (I) is caused by the presence of the conversion time of the fuel fed to the combustion chamber and the products of combustion. The portion of fuel fed to the chamber at the time the instruction is sent to close the valves is converted to combustion products at the time $t=t_{conv}+t_{gk}$. During this time the engine does not react to the command; therefore the entire process is shifted to the right along the time axis. The conversion time depends on the type of fuel, the structural design of the injector head and the organizational scheme of the mix formation process. The conversion time is 0.001 to 0.1 second. In view of the fact that τ_{conv} for the given fuel and pressure in the engine chamber is a stable value, the dispersion of the **afterflaming thrust** in the first section is determined by the thrust dispersion and shutdown time.

The second segment (II) is explained by the presence of inertia in the response of the control circuits and the valves themselves. From the time of sending the command to shut the valve to the beginning of the closing process is a defined time which is caused by the inertia of the valve control system. The inertia time depends on the type of control automation the valve has. For pneumatic automation t_{2c}=0.05-0.15 seconds; for pyroautomation t_{2c}=0.001-0.015 seconds. Since in the time t_2 the valve does not move, the flow rates of the fuel components and the thrust will be constant and equal to the rated values.

From the time t_{2c} the valve closing process begins which takes place also during a finite time interval t_{2k}. By the valve closing time we mean the

APPROVED FOR RELEASE: 2007/02/08: CIA-RDP82-00850R000200090053-2

APPROVED FOR RELEASE: 2007/02/08: CIA-RDP82-00850R000200090053-2

time of the beginning of movement of the valve plate to complete closure of it. In this case the area of the through cross section of the valve changes; the law of variation of this area depends on the law of variation of the control pressure, the pipe and the structural design of the valve. During the process of closing the valve, the fuel component flow rate and thrust vary. The law of variation of the flow rate depends on the variation of the area of the through cross section of the valve F_{valve}, the flow rate factor μ and the liquid pressure before the valve p_{valve}, that is,

$$\dot{m}=m(F_{кл}, \mu, p_{кл}).$$
(1) (1)

Key: 1. valve

The pressure of the liquid in front of the valve varies as a result of a reduction in the rpm of the TNA and the g-loads in flight. The valve closing time depends on the structural design of the valve. For pneumohydraulic valve t_{2k}=0.1-3 seconds; for pyrovalves, this time is negligibly small t_{2k}<0.001 sec.

The segment (III) of sharp pressure and thrust drum is described. After complete closure of the valves, the chamber is emptied of combustion products quickly, as a result of which the pressure in the combustion chamber decreases to tenths of a bar. The time for the chamber to be emptied of combustion products depends on the volume and magnitude of the initial pressure and is thousandths of a second.

The segment (IV) of evaporation of the fuel components which is caused by the unstable process of flow of the fuel components from the reservoirs in front of the injectors to the chamber and afterburning. During the process of emptying the combustion chamber, in accordance with the pressure drop in it the pressure of the components in the reservoirs decreases. When the pressure in the reservoirs in front of the injectors drops to the saturated vapor pressure of the components with the corresponding temperature of the liquid in the head, the components begin to boil and evaporated. The vapor formed maintains the pressure in the reservoirs ahead of the injectors equal to the saturated vapor pressure. Under the effect of this pressure the components go through the injectors to the chamber and afterburn.

As a result of the pressure gradient on the injectors the vapor content increases. During the process of movement through the cooling jacket the component is warmed up by the heat taken from the wall to the boiling point. The temperature of the vapor-liquid mix decreases as a result of expansion and discharge into the chamber. This decrease in temperature is only compensated for by supplying heat from the walls. The temperature drop leads to boiling of the entire mass of liquid (combustible components) in the cooling jacket and it is emptied of the vapor-liquid mixture under the effect of the saturated vapor pressure.

APPROVED FOR RELEASE: 2007/02/08: CIA-RDP82-00850R000200090053-2

APPROVED FOR RELEASE: 2007/02/08: CIA-RDP82-00850R000200090053-2

The component (oxidizing agent) which is in the cavity from the cutoff valve to the injectors has identical temperature in the entire volume. It begins to boil when the pressure in the chamber is compared with the saturated vapor pressure. The oxidizing agent is fed to the chamber also under the effect of the saturated vapor pressure. The inflow of fuel components in the form of finely-disperse vaporizing liquid mix promotes an improvement in quality of the mix formation. If we consider that the components come into the hot chamber, then in spite of the low pressure in the chamber, the fuel components burn. However, as a result of the fact that the processes of evaporation of the combustible component and the oxidizing agent are different as a result of different saturated vapor pressures, the fuel feed to the chamber takes place with a variable ratio of the components and differing from the optimal value. This leads to unstable combustion and pressure fluctuations.

The combustion process continues until one of the components is used up. From that time only one component will enter the chamber, and it turns out to be in excess.

The engine thrust will be created by the reaction of the escape of the vapor or products of thermal decomposition. The evaporation process is the longest. Depending on the type and the quantity of fuel in the pre-injector reservoirs, the evaporation time can vary within broad limits from several seconds to several minutes.

After sending the instruction to shut off the engine, the turbine-pump assembly is not shut down immediately as a result of inertia of the gas generation system and the TNA itself. If the cutoff valves are closed before the rpm begins to drop, then the inertia of the TNA does not have any influence on the magnitude of the IPD. Otherwise, the shutdown process is greatly complicated by the necessity for considering the pressure variation of the fuel components after the pumps.

Thus, the total time of the afterflaming impulse is defined by the sum

$$t=t_1+t_{2\text{д}}+t_{2\text{к}}+t_3+t_4. \tag{6.7}$$

The total afterflaming impulse can be represented by the sum of its components

$$I=I_1+I_2+I_3+I_4. \tag{6.8}$$

The calculations and the experimental data indicate that the second and fourth components have the highest specific weight in the total IPD and, as a rule, the following expression is valid

$$I_2 + I_4 = (0.7 \text{ to } 0.85)\ I$$

6.3. Calculation of the Engine Afterflaming Impulse

In order to calculate the magnitude and the characteristics of the dispersion of the IPD, it is necessary to know the law of variation of the

APPROVED FOR RELEASE: 2007/02/08: CIA-RDP82-00850R000200090053-2

APPROVED FOR RELEASE: 2007/02/08: CIA-RDP82-00850R000200090053-2

pressure in the chamber in the engine shutdown process. For this purpose it is theoretically possible to compile a system of algebraic and differential equations describing the processes in the engine assemblies on shutdown and solve it under the given boundary conditions.

The procedure for calculating the variation of the parameters with time in the engine shutdown process and the magnitude of the afterflaming impulse was developed by V. A. Makhin [21].

In accordance with the physical processes of the formation of the engine afterflaming impulse (see Fig 6.8), it is expedient to perform the calculation by individual components of the IPD.

6.3.1. Calculation of the Components of the IPD in the First and Second Sections I_{1-2}

The engine thrust in the first section formed as a result of the presence of the conversion time of the liquid fuel to combustion products, is constant and equal to the thrust of the final stage.

In the second section during the process of closing the cutoff valve the fuel flow rate is variable, and it is determined by the variable cross sectional area between the seat and the plate of the valve. However, as a result of insignificant response time of the valve (especially if pyrovalves are used), commensurate with the time constants of the mains and chamber, without making a large error it is possible to assume that the thrust in the second section is also constant.

Then it is possible to make $P_1=P_2=\overline{P}$, where $\overline{P}$ is the thrust at the time of sending the primary command to shut down the engine.

The magnitude of the afterflaming impulse is

$$I_{1-2}=\overline{P}t_{1-2}, \tag{6.9}$$

where

$$t_{1-2}=\underset{(1)}{\tau_{\text{пр}}}+\underset{(3)}{t_{2\text{ш}}}+\underset{(2)}{t_{2\text{кл}}}.$$

Key: 1. conv; 2. valve; 3. 2c

6.3.2. Calculation of the Component I_3

In the third section a sharp decrease in pressure in the thrust chamber takes place. The pressure drop in the thrust chamber is described by the chamber equation and the equation of the line between the valve and the thrust chamber.

APPROVED FOR RELEASE: 2007/02/08: CIA-RDP82-00850R000200090053-2

APPROVED FOR RELEASE: 2007/02/08: CIA-RDP82-00850R000200090053-2

The equation of the thrust chamber (1.12) without considering the conversion time is

$$\frac{dp_к}{dt}=(\dot{m}_{\text{ок}}+\dot{m}_{\text{г}})\frac{RT_к}{V_к}-\frac{b(\varkappa)F_{\text{кр}}\sqrt{RT_к}}{V_к}p_к. \qquad (6.10)$$

(1) (2) (3) (4)

Key: 1. oxidizing; 2. combustible component of the fuel; 3. cr; 4. chamber

The equations of the mains (1.29)

$$p_i=p_к-b_{1i}\dot{m}_i^2+b_{2i}\frac{d\dot{m}_i}{dt}-p_{zi}, \qquad (6.11)$$

where p_i is the pressure after the cutoff valve; p_{2i} is the piezometric pressure of the component included between the valve and the chamber.

It is possible to determine $p_k(t)$ by the procedure of [21] if we make the following assumptions:

The cutoff valves are closed instantaneously and simultaneously;

The cutoff valves are located close to the thrust chamber; in this case it is possible to set $p_z=0$;

During the process of the decrease in pressure, the component ratio remains constant;

The quadratic dependence of the flow rate of the fuel component on the pressure gradient is replaced by a linear function

$$b_1\dot{m}^2=B\dot{m}, \qquad (6.12)$$

where

$$B=\frac{\bar{p}-\bar{p}_к}{\bar{\dot{m}}}.$$

Making the indicated assumptions and excluding p_k from the equations (6.10)-(6.12), it is possible to obtain the equation for the flow rate of the combustible component of the fuel (or the oxidant)

$$\frac{d^2\dot{m}_{\text{г}}}{dt^2}+2a_1\frac{d\dot{m}_{\text{г}}}{dt}+a_2\dot{m}_{\text{г}}=0, \qquad (6.13)$$

where

$$2a_1=\frac{KB_{\text{ок}}-B_{\text{г}}}{Kb_{2\text{ок}}-b_{2\text{г}}}.$$

The function (6.13) is a second-order differential equation with constant coefficients, the characteristic equation of which is

$$s^2+2a_1s+a_2=0.$$

APPROVED FOR RELEASE: 2007/02/08: CIA-RDP82-00850R000200090053-2

APPROVED FOR RELEASE: 2007/02/08: CIA-RDP82-00850R000200090053-2

Since for actual conditions the determinant of the characteristic equation $s=\sqrt{a_1^2-a_2}<0$, the solution of the equation (6.13) has the form

$$\dot{m}_r(t)=e^{-a_1 t}(c_1\cos st+c_2\sin st), \tag{6.14}$$

where c_1, c_2 are constants determined by the initial conditions

$$c_1=\bar{\dot{m}}_r,$$
$$c_2=\frac{\bar{\dot{m}}_r+a_1\bar{\dot{m}}_r}{s}.$$

Since K=const, then

$$\dot{m}_{ok}(t)=K\dot{m}_r(t). \tag{6.15}$$

Substitution (6.14) and (6.15) in equation (6.10), we obtain

$$\frac{dp_k}{dt}+\frac{b(x)F_{kp}\sqrt{RT_k}}{V_k}p_k-\dot{m}_r(1+K)\frac{RT_k}{V_k}\times$$
$$\times e^{-a_1 t}\left(\bar{\dot{m}}_r\cos st+\frac{\bar{\dot{m}}_r(1+a_1)}{s}\right)=0. \tag{6.16}$$

The integral of the equation (6.16) represents the function $p_k(t)$

$$p_k(t)=\bar{p}_k e^{-a_1 t}+$$
$$+\frac{[sA_{k_1}+(A_k-a_1)A_{k_2}]\sin st+[(A_k-a_1)A_{k_1}-sA_{k_2}](\cos st-1)}{e^{a_1 t}[s^2+(A_k-a_1)^2]}, \tag{6.17}$$

where

$$A_k=\frac{b(x)F_{kp}\sqrt{RT_k}}{V_k};\quad A_{k_1}=\frac{(1+\bar{K})RT_k}{V_k}\bar{\dot{m}}_r;$$
$$A_{k_2}=\frac{(1+K)RT_k\bar{\dot{m}}_r(2+a_1)}{2V_k s}.$$

The component of the IPD I_3 is determined from the equation (6.6)

$$I_3=\frac{\bar{p}}{\bar{p}_k}\left\{\frac{1-e^{-a_1 t_3}}{a_1}\left(\bar{p}_k+\frac{\delta_2}{\delta_3}\right)+\right.$$
$$\left.+\frac{e^{-a_1 t_3}(s\delta_2-a_1\delta_1)\sin st_3+(s\delta_1+a_1\delta_1)(1-e^{-a_1 t_3}\cos st_3)}{\delta_3(a_1^2+s_2)}\right\}, \tag{6.18}$$

where

$$\delta_1=sA_{k_1}+(A_k-a_1)A_{k_2};$$
$$\delta_2=(A_k-a_1)A_{k_1}-sA_{k_2};$$
$$\delta_3=s^2+(A_k-a_1)^2.$$

APPROVED FOR RELEASE: 2007/02/08: CIA-RDP82-00850R000200090053-2

APPROVED FOR RELEASE: 2007/02/08: CIA-RDP82-00850R000200090053-2

FOR OFFICIAL USE ONLY

The calculations of I_3 by equation (6.18) are awkward, and the accuracy of the determination depends on the reliability both in the initial data and the assumptions made.

For approximate analysis the component of the engine aftereffect pulse I_3 can be defined by the following method.

In the third section there is a sharp pressure drop in the process of emptying the combustion products from the thrust chamber. The initial pressure in the chamber is equal to the pressure at the time of sending the shutdown command, that is, $p_3=p_{gk}$. The pressure drop in the chamber takes place to the highest saturated vapor pressure of the components $p_k=p_{s\ max}$.

The nature of the pressure variation is illustrated in Fig 6.9.

As a result of the fact that the chamber is emptied very quickly, it is possible to assume that the composition of the gases and their temperature do not drop, that is, a nonequilibrium process takes place. In this case the law of pressure variation can be defined by the equation describing the escape of a gas from a semiclosed vessel

$$p=\frac{p_к}{\sqrt{1+\frac{\varkappa+1}{2}\frac{\dot{m}RT_к}{p_кV_к}t_3}^{\frac{\varkappa-1}{2\varkappa}}}. \tag{6.19}$$

From the last relation, setting $p=p_{s\ max}$, and $\bar{p}_k=p_k$, $\dot{\bar{m}}=m$ the emptying time is determined

$$t_3=\frac{\left(\frac{\bar{p}_к}{p_{s,max}}\right)^{\frac{2\varkappa}{\varkappa-1}}-1}{\frac{\varkappa-1}{2}\frac{\dot{\bar{m}}RT_к}{\bar{p}_кV_к}}. \tag{6.20}$$

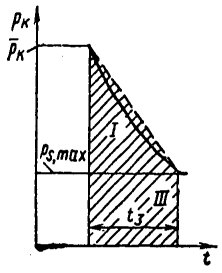

Figure 6.9. Diagram of the third shutdown section

FOR OFFICIAL USE ONLY

APPROVED FOR RELEASE: 2007/02/08: CIA-RDP82-00850R000200090053-2

APPROVED FOR RELEASE: 2007/02/08: CIA-RDP82-00850R000200090053-2

The component of the IPD in the third section

$$I_3=\frac{\bar{p}}{\bar{p}_к}\int_{t_2}^{t_3} p_к dt. \qquad (6.21)$$

As follows from Fig 6.9, the integral $\int_{t_2}^{t_3}$ can be replaced by the sum of two areas

$$\int_{t_2}^{t_3}=S_1+S_2,$$

where

$$S_1=\frac{1}{2}(\bar{p}_к-p_{s,max})t_3;\ S_2=p_{s\,max}t_3.$$

Finally,

$$I_3=\frac{\bar{P}(p_к+p_{s,max})t_3}{2\bar{p}_к}.$$

6.3.3. Calculation of the Component I_4

In the section of evaporation of the fuel components, the latter are fed to the thrust chamber under the effect of the forces created by the saturated vapor pressure in the cooling jacket and in the injector head. Since the fuel components boil in the reservoirs ahead of the injectors, a finely disperse vapor-liquid mixture reaches the thrust chamber. Therefore in order to calculate the pressure variation in the chamber with time in the fourth section it is necessary to consider not only the hydrodynamic relations, but also the equations describing the process of vapor formation and escape of the emulsion from the injectors.

The procedure for calculating the evaporation of the fuel components was developed by V. N. Makhin [21].

In order to calculate the pressure variation in the thrust chamber, systems of equations have been compiled.

The material balance equation for variable amount of emulsion

$$\frac{dm'}{dt}=-\dot{m}_ф'+\dot{m}_к', \qquad (6.22)$$

where m' is the mass of the emulsion; $\dot{m}_ф'$ is the flow rate per second of the emulsion through the injector; $\dot{m}_к'$ is the inflow per second of the emulsion as a result of boiling of the liquid. Then the following notation is introduced: y is the liquid parameter; y' is the emulsion parameter; y" are the vapor parameters. The variation of the volume of emulsion in the prechamber cavity

$$\frac{dV}{dt}=\dot{V}_ж+\dot{V}_п, \qquad (6.23)$$

APPROVED FOR RELEASE: 2007/02/08: CIA-RDP82-00850R000200090053-2

APPROVED FOR RELEASE: 2007/02/08: CIA-RDP82-00850R000200090053-2

where V is the emulsion volume, $\dot{V}_k$ is the volume of boiling liquid arriving per second; $\dot{V}_d$ is the volumetric flow rate per second. The energy equation of the emulsion, considering the supply of heat from the chamber wall and the liquid,

$$\frac{d(u'm')}{dt}=\frac{dQ}{dt}-i\dot{m}'_{\Phi}+i\dot{m}_{\Phi}-p\dot{V}_{д}, \tag{6.24}$$

where u', i' are the internal energy and enthalpy of the emulsion; p is the saturated vapor pressure; m, i are the flow rate and enthalpy of the liquid combustible fuel component. The amount of boiled component is determined, on the one hand, by the heating as a result of heat release from the walls of the thrust chamber, and on the other hand, as a result of a reduction in emulsion temperature and saturated vapor pressure

$$\dot{V}_{к}=\varepsilon v'\dot{m}_{д}+\frac{1}{K_{т}}\frac{dT}{dt}; \tag{6.25}$$

$$\dot{m}'_{к}=\varepsilon\dot{m}_{д}+\frac{Q'}{K_{т}}\frac{dT}{dt}, \tag{6.26}$$

where

$$\varepsilon=\sqrt{\frac{\dot{m}'_{д}}{\dot{m}_{д}}},$$

K_T is the coefficient defined by the results of calculating the engine cooling in the shutdown mode from the equation:

$$T=T_{\Phi}+K_{т}V;$$

V is the dynamic volume of the cooling jacet; T_ϕ is the liquid temperature at the injectors. The amount of heat supplied to the emulsion in the cooling jacket is determined by solution of the heat exchange equations

$$\frac{dQ}{dt}=K_{Q}A_{т}v\dot{m}'_{\Phi}, \tag{6.27}$$

where

$$K_{Q}=\frac{h^{1,5}T_{ср}^{2,5}F_{б.к}}{F_{ж.ср}};$$

$$\Lambda_{1}^{0,4}=\frac{20,8(\lambda)^{1,3}Q^{0,2}(Q'')^{0,06}}{r^{0,5}\sigma^{0,5}(Q'')^{0,66}(\nu)^{0,3}(c)^{0,3}}$$ is the component characteristic;

$h=\Pi/d_e$, d_e is the equivalent diameter; Π is the wet perimeter; $F_{b.k}$ is the side surface of the chamber; $F_{ж.ср}$ is the mean through area of the cooled channel; T_{cp} is the average temperature in the cooling jacket. The inflow of emulsion to the chamber through the injectors is determined by the flow of two-phase liquid in the injector

$$\dot{m}'_{\Phi}=\frac{\mu}{(1-\psi_{c})}\pi r_{c}^{2}\sqrt{2Q\Delta p_{\Phi}}, \tag{6.28}$$

FOR OFFICIAL USE ONLY

APPROVED FOR RELEASE: 2007/02/08: CIA-RDP82-00850R000200090053-2

APPROVED FOR RELEASE: 2007/02/08: CIA-RDP82-00850R000200090053-2

where μ is the flow rate coefficient; r_c is the radius of the injector nozzle; ψ_c is the vapor content of the emulsion in the injector nozzle

$$\psi_c = \frac{g(i_s - i_r) + \psi_s r_c}{r_c + \left(\frac{v_c'}{2}\right)}, \tag{6.29}$$

where g is the gravimetric proportion of the light fraction in the component; ψ_s is the vapor content in front of the injector. The mass and volumetric flow rate of the emulsion in the drainage channels

$$\dot{m}_л' = \mu_л F_л \sqrt{2\frac{\varrho(p_s - p_к)}{1 + 2b_1 \varrho F_л^2}}; \tag{6.30}$$

$$\dot{V}_л = v\dot{m}_л'.$$

The equation for the pressure in the combustion chamber

$$\frac{dp_к}{dt} = \frac{RT_к}{V_к}\left(\dot{m}_{ок}' + \dot{m}_г' - \frac{p_к}{\beta}\right), \tag{6.31}$$

where

$$\beta = \frac{\sqrt{RT_к}}{b(\varkappa) F_{кр}}.$$

It is necessary to add the equations of the physical parameters u, i, r_c, ρ of the component on the saturation line to the equations (6.22)-(6.31).

Let us present the approximate formulas for determining the physical parameters on the saturated line [21] (Table 6.1).

The following notation is introduced in all of the formulas

$$\bar{T} = \frac{T}{T_{кр}}; \quad \bar{p} = \frac{p}{p_{кр}},$$

where T_{kp} and p_{kp} are the critical temperature and pressure of the components.

APPROVED FOR RELEASE: 2007/02/08: CIA-RDP82-00850R000200090053-2

APPROVED FOR RELEASE: 2007/02/08: CIA-RDP82-00850R000200090053-2

FOR OFFICIAL USE ONLY

Table 6.1

Physical variables	Liquid	Vapor
Density, kg/m^3	$\rho=A_\rho(16.47-9\ \overline{T})$	$\rho''=1.77A_\rho\overline{T}^{10}$
Specific volume, m^3/kg	$v=A_v(0.04+0.084\ \overline{T})$	$v'=0.565A_v\overline{T}^{10}$
Heat capacity, kjoules/kg-K	$c_p=A_c(3+3.7\ \overline{T})$	
Enthalpy, kjoules	$i=A_i(3+1.85)\overline{T}^2$	
Heat of vaporization, kjoules	$r=A_r(1.85-3.27\ \overline{T})$	
Pressure, MPa	$p=a+b\overline{T}^m$	
Internal energy, kjoules	$u=i+vp_{kp}\overline{p}$	

The coefficients A_j depend on the critical parameters p_{kp}, T_{kp}, the molecular mass and the compressibility factor. The value of A_j for the propagated fuel components is presented in Table 6.2.

The equations (6.22)-(6.31) and Tables 6.1-6.2 permit by numerical integration determination of $\dot{m}_{ox}(t)$ and $\dot{m}_{fuel}(t)$, calculation of $p_k(t)$ and the engine afterflaming impulse created by evaporation of the fuel components from the preinjector reservoirs.

However, as a result of the fact that many perimeters enter into the system of equations (6.22)-(6.31), determination of which with high accuracy does not appear possible, the accuracy of calculating I4 is low.

In cases where it is not necessary to know the law of pressure variation in the combustion chamber with time, in the process of evaporation of the fuel components, the magnitude of the aftereffect pulse of the engine can be determined with a sufficient degree of accuracy by approximate relations.

In view of the fact that the saturation pressures of the components and the hydraulic characteristics of the mains differ significantly, it is possible to make the assumption of arrival of the components in the chamber at different times.

Evaporation of one component, as a rule, the combustible fuel component takes place first in the combustion chamber, then combustion of both components and, finally, evaporation of the component remaining in excess. Consequently, the component ratio in the fourth section varies within the limits of $0<K<\infty$.

In this case the fourth component can be estimated by the total energy reserve of the fuel found in the pre-injection cavities.

Taking the thrust in the fourth section equal to the mean value (Fig 6.10), it is possible to write the obvious equality for the afterflaming impulse component

$$I_4=P_4t_4=I_{y4}\dot{m}_4t_4, \qquad (6.32)$$

FOR OFFICIAL USE ONLY

APPROVED FOR RELEASE: 2007/02/08: CIA-RDP82-00850R000200090053-2

APPROVED FOR RELEASE: 2007/02/08: CIA-RDP82-00850R000200090053-2

Table 6.2

	(2)	(3)	(4)	(5)	(6)	(7)	(8)	(9)			
Компонент (1)	Газовая постоянная R, кДж/кг·К	Критическая температура $T_{кр}$, К	Критическое давление $P_{кр}$, Н/м²·10^{-5}	A_0, кг/м³	$A_v \cdot 10^2$, м³/кг	A_i, кДж/кг	A_i, кДж/кг	A_r, кДж/кг	a	b	m
(10) Вода	463	647,4	221,3	83,4	1,2	8,16	529	607	—	—	—
(11) 96%-ный эгиловый спирт	198	521,4	68,6	70,9	1,41	0,64	332	230	0	39	18,5
(12) Несимметричный диметилгидразин	139	507	49,6	70,3	1,42	0,52	263	163	—0,0034	1,46	9,8
(13) Кислород	260	155	48,4	101,5	0,98	0,35	55	71	0,064	1,35	7,14
(14) N_2O_4	90,4	431	98,1	139	0,72	0,34	146	78	0	1,58	13,12
(15) Водород	4190	33,1	12,9	9,45	1,06	7,35	244	247			
(16) Фтор	219	172	557	148	0,68	0,43	75	71			
(17) Азотная кислота	132	490	141,3	138	0,72	0,35	170	202			

Key:

1. Component
2. Gas constant R, kjoules/kg-K
3. Critical temperature T_{cr}, K
4. Critical pressure p_{cr}, N/m^2-10^{-5}
5. A_q, kg/m^3
6. $A_v \cdot 10^2$, m^3/kg
7. A_i, kjoules/kg
8. A_i, kjoules/kg
9. A_r, kjoules/kg
10. Water
11. 96% ethyl alcohol
12. Asymmetric dimethylhydrazine
13. Oxygen
14. N_2O_4
15. Hydrogen
16. Fluorine
17. Nitric acid

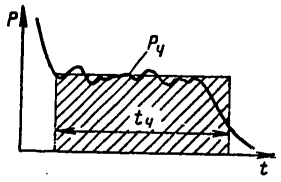

Figure 6.10. Equivalent representation of the fourth shutdown section

where I_y is the specific thrust impulse ; t_4 is the length of the fourth section in time. The relation $\dot{m}_4 t_4 = M_{ox} + M_{fuel}$ -- the mass of the fuel components in the pre-injection reservoirs -- is also obvious.

The mass of the fuel components in the pre-injection reservoirs

$$M_{ок} = V_{ок}\rho_{ок}; \quad M_г = V_г\rho_г, \tag{6.33}$$

APPROVED FOR RELEASE: 2007/02/08: CIA-RDP82-00850R000200090053-2

APPROVED FOR RELEASE: 2007/02/08: CIA-RDP82-00850R000200090053-2

where V are the volumes of the reservoirs included between the injectors and the valves (see Fig 6.7). The specific impulse is proportional to the capacity for work of the combustion products

$$I_{y4}=\bar{I}_y\sqrt{\frac{\overline{(RT_k)_4}}{\overline{RT}_k}}, \tag{6.34}$$

where $\bar{I}_y$ and $\overline{RT}_k$ are the specific thrust and the capacity for work of the combustion products at the time of sending the primary command to shut down the engine.

$$\bar{I}_y=\frac{\bar{P}}{\dot{m}}. \tag{6.35}$$

The capacity for work of the gases $(RT_k)_4$ in the fourth section in the evaporation process is defined under the assumption that only the process of evaporation of the fuel components occurs.

The capacity for work of the fuel component vapor is

$$\begin{aligned} RT_{ok}&=\frac{8320}{\mu_{ok}}T_{sok};\\ RT_r&=\frac{8320}{\mu_r}T_{sr}, \end{aligned} \tag{6.36}$$

where $T_{s\ ox}$ and $T_{s\ fuel}$ are the boiling points of the components in the pre-injector reservoirs. In accordance with the assumption of different time of arrival of the fuel components in the thrust chamber, the capacity for work of the gases can be taken as the average value

$$(RT)_4=8320\left(\frac{Z}{Z+1}\frac{T_{sok}}{\mu_{ok}}+\frac{1}{Z+1}\frac{T_{sr}}{\mu_r}\right), \tag{6.37}$$

where $Z=M_{ox}/M_{fuel}$ is the ratio of the masses of the fuel components. The value of Z varies within the limits of $0<Z<\infty$. For $Z=\infty$, evaporation of only the oxidizing agent takes place in the thrust chamber.

Substituting the functions (6.33)-(6.35) and (6.37) in the initial (6.32) considering $\sqrt{RT}/b(\chi)=\beta$, we obtain the equation for the fourth component of the engine afterflaming impulse

$$I_4=29\frac{\bar{P}}{\dot{m}}(V_{ok}\varrho_{ok}+V_r\varrho_r)N, \tag{6.38}$$

where

$$N=\sqrt{\left(\frac{Z}{Z+1}\frac{T_{sok}}{\mu_{ok}}+\frac{1}{Z+1}\frac{T_{sr}}{\mu_r}\right)\frac{1}{\beta}}.$$

APPROVED FOR RELEASE: 2007/02/08: CIA-RDP82-00850R000200090053-2

APPROVED FOR RELEASE: 2007/02/08: CIA-RDP82-00850R000200090053-2

The total engine afterflaming impulse

$$I=I_{1-2}+I_3+I_4. \tag{6.39}$$

6.4. Dispersion of the Engine Afterflaming Impulse

The dispersion of the target points of the nose cones and the conditions of separation of the stages (the dispersion of the velocity of the stage) is determined not so much by the magnitude of the engine afterflaming impulse as by the dispersion.

The magnitude of the engine afterflaming impulse is defined by the function (6.39).

A comparison of the experimental values of the engine afterflaming impulse with the calculated values indicates that the calculation by the approximate functions (6.9), (6.21) and (6.38) insures an error that does not exceed 15%.

Therefore for further analysis we shall use the approximate functions.

After substitution of the expressions (6.9), (6.21), (6.38) in equation (6.39), we obtain

$$I=\overline{P}\left(t_{1-2}+at_3+\frac{b}{\dot{m}}\right), \tag{6.40}$$

where

$$a=0{,}5\left(1+\frac{p_{s.max}}{\overline{p}_к}\right);\ b=29(V_{ок}\varrho_{ок}+V_r\varrho_r)N.$$

The engine aferflaming impulse depends on a number of regime and structural factors which vary from engine to engine and are random variables

$$I=I(p_к,\ \dot{m},\ P,\ t_l,\ V_i,\ \varrho_l).$$

Assuming the enumerated random variables to be independent, subject to a normal distribution law, it is possible to determine the dispersion of the engine afterflaming impulse

$$D_I=\sum\left(\frac{\partial I}{\partial y_j}\right)^2 D_{y_j}, \tag{6.41}$$

where D_{y_j} are the dispersions of the random parameters y. From the equation (6.40) the influence coefficients are defined

$$\frac{\partial I}{\partial P}=\frac{\overline{I}}{\overline{P}};\ \frac{\partial I}{\partial p_к}=-\frac{0{,}5\overline{P}p_{s.max}t_3}{\overline{p}_к^2};$$
$$\frac{\partial I}{\partial \dot{m}}=-\frac{\overline{P}b}{\overline{\dot{m}}^2};\ \frac{\partial I}{\partial t_{1-2}}=\overline{P}; \tag{6.42}$$

APPROVED FOR RELEASE: 2007/02/08: CIA-RDP82-00850R000200090053-2

APPROVED FOR RELEASE: 2007/02/08: CIA-RDP82-00850R000200090053-2

$$\frac{\partial I}{\partial V_l}=29\frac{\bar{P}}{\bar{m}}N\bar{Q}_l;$$

$$\frac{\partial I}{\partial Q_l}=29\frac{\bar{P}}{\bar{m}}NV_l.$$

Substituting the relations (6.42) in (6.41), we obtain

$$D_y=\bar{P}^2(d_PD_P+d_{\dot{m}}D_{\dot{m}}+d_{p_k}D_{p_k}+D_l+d_{V_l}D_{V_l}+d_{Q_l}D_{Q_l}), \tag{6.43}$$

where

$$d_P=\frac{\bar{I}^2}{\bar{P}^4};\quad d_{\dot{m}}=\frac{b^2}{\bar{m}^4};\quad d_{p_k}=\frac{0{,}25p_{s.\max}^2t_3^2}{\bar{p}_k^4};$$

$$dV_l=8320\frac{N^2Q_l^2}{\bar{m}^2};$$

$$d_{Q_{ok}}=d_{V_{ok}}\frac{V_{ok}^2}{\bar{Q}_{ok}^2};\quad d_{Q_r}=d_{V_{ok}}\frac{V_r^2}{\bar{Q}_{ok}^2}.$$

The mean square deviation of the engine afterflaming impulse

$$\sigma_I=\sqrt{D_I}. \tag{6.44}$$

The probability of obtaining the engine afterflaming impulse within the given limits of I_{max} and I_{min} is defined by the function

$$P(I_{\min}<I<I_{\max})=$$
$$=\Phi\left[\frac{I_{\max}-m_I}{\sigma_I}\right]-\Phi\left[\frac{I_{\min}-m_I}{\sigma_I}\right], \tag{6.45}$$

where $\Phi[\cdot]$ is the Laplace function; m_I is the mathematical expectation of the value.

6.5. Methods of Decreasing the Mean Value of the IPD and Its Dispersion

The mean value of the IPD and especially its dispersion influence the conditions of separation of the rocket stages and dispersion of the coordinates and velocity of the end of the active section of the trajectory. This negative influence of the IPD is paired with two groups of methods: a decrease in the IPD and its dispersion and organization of the shutdown and separation of the stages excluding the effect of the IPD.

FOR OFFICIAL USE ONLY

APPROVED FOR RELEASE: 2007/02/08: CIA-RDP82-00850R000200090053-2

APPROVED FOR RELEASE: 2007/02/08: CIA-RDP82-00850R000200090053-2

6.5.1. Decrease in Mean Value and Dispersion of the IPD

As was demonstrated above, the magnitude of the IPD and dispersion depend upon many factors, which include the engine thrust at the shutdown time, the response time of the automation, the volumes of the cavities for the combustible components of the fuel and the oxidizing agent between the valves and the injectors, and so on.

Consequently, in order to decrease the magnitude and the dispersion of the IPD, first of all it is necessary to have an effect on the enumerated factors.

1. Shutdown of the Propulsion Device with Choking of the Thrust

The thrust at the time of sending the shutdown command has a defining effect on the mean magnitude and dispersion of the IPD. The engines having high thrust are shut down in two stages. In the final stage the thrust is appreciably less than in the rated operating conditions. The thrust in the final stage will be $(0.1\text{-}0.5)\overline{P}$. As a result of the decrease in the thrust at the time of shutting down the engine, as follows from the function (6.20), the magnitude of the IPD and its dispersion decrease proportionally to it.

In the case where the propulsion device has steering chambers, shutdown also takes place in two stages. On the preliminary command, primary engines are shut down, and on the primary command, steering engines (see Fig 6.3).

The time of sending the primary command is determined by the condition $P_{o.d}=0$; otherwise the IPD of the main engines can be superposed on the steering IPD.

2. Decrease in Volume of the Pre-injector Cavities

The volume of the pre-injector cavities determines the reserve of fuel components which will evaporate and creates the forced component of the IPD. The volume of the pre-injector cavities is decreased by location of the fuel valves directly at the entrances to the propulsion chamber and also by decreasing the volume of the injector head.

3. Decreasing the Response Time of the Valve

The response time of the valves depends on their schematic diagram. The pyrovalves have the least response time. However, when using high-speed valves under certain conditions hydraulic hammer and destruction of the lines can occur. When the valve is closed, the speed of the liquid decreases, as a result of which the pressure in front of the valve increases significantly, and a characteristic wave arises which moves from the valve to the reservoir and back.

APPROVED FOR RELEASE: 2007/02/08: CIA-RDP82-00850R000200090053-2

APPROVED FOR RELEASE: 2007/02/08: CIA-RDP82-00850R000200090053-2

The magnitude of the increased pressure during hydraulic hammer can be determined by the equation (1.164)

$$p_{max} = \varrho \frac{\dot{m} 2l}{F_0 t_з}. \qquad (6.46)$$

Formula (6.46) permits determination of the geometric dimensions of the line and the time of closure of the valve for which the admissible increase in pressure is insured or the required valve closing time for which there is no increase in pressure above admissible.

$$t_з \geqslant \frac{2\varrho \dot{m} l}{F_0 p_д}. \qquad (6.47)$$

4. Scavenging and Draining Pre-injector Cavities

In order to decrease the IPD it is necessary to eliminate the process of evaporation of the fuel components from the pre-injector cavities. For this purpose it is possible to scavenge cavities and drain the component into the surrounding environment (see Fig 6.11).

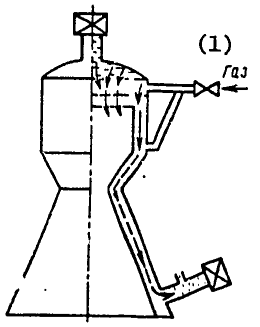

Figure 6.11. Scavenging and draining system
Key:
1. Gas

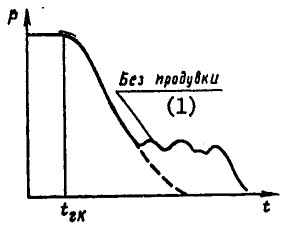

Figure 6.12. Variation of the engine thrust during shutdown with scavenging
Key:
1. Without scavenging

A compressed gas (air or nitrogen) is fed to the combustible component and oxidizing agent cavities, the components are forced into the propulsion chamber and through the valves to the outside environment. As a result of forced displacement of the fuel components, the fourth component of the IPD is eliminated (Fig 6.12), and the magnitude of the IPD is reduced by 2 or 3 times.

6.5.2. Methods Excluding the Effect of the IPD on the Stage Separation Conditions

One of the radical methods of decreasing the effect of the IPD on the stage separation conditions is creation of a counterthrust at the engine shutdown time.

APPROVED FOR RELEASE: 2007/02/08: CIA-RDP82-00850R000200090053-2

APPROVED FOR RELEASE: 2007/02/08: CIA-RDP82-00850R000200090053-2

The creation of the counterthrust is accomplished by two methods: the application of braking engines or discharge of gases from the tanks.

1. The application of braking engines.

Braking engines, as a rule, solid-fuel jet engines, the direction of the thrust of which is opposite to the thrust of the main engines, are installed in the hull of the rocket. When sending the primary command to shut down the engine, the braking engines are switched on, as a result of which the IPD of the main engines is compensated for by the thrust of the braking engines (Fig 6.13).

The parameters of the braking engines are selected from the condition

A deficiency of the given method is the increase in passive weight.

2. The use of the energy of the gases in the tanks.

In large rockets, in which tanks are scavenged by hot gases, at the end of operation of the engines, a significant gas energy reserve is created in the fuel reservoirs. In this case, counterthrust nozzles are installed

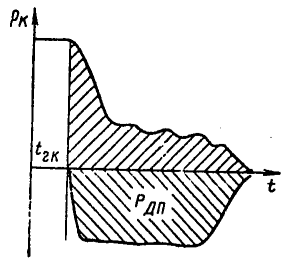

Figure 6.13. Variation of the thrust of the main and braking engines

in the tanks. When the primary command to shut down the engine is sent, the nozzles open and the gases are drained out of the tanks. Since the escape of the gases takes place into a vacuum, a significant thrust is created which is capable of compensating for the IPD.

APPROVED FOR RELEASE: 2007/02/08: CIA-RDP82-00850R000200090053-2

APPROVED FOR RELEASE: 2007/02/08: CIA-RDP82-00850R000200090053-2

SECTION II. DYNAMIC CHARACTERISTICS OF SOLID FUEL ENGINES

The dynamic processes occurring in the solid-fuel rocket engines are highly complex, and at the present time still have not been completely studied. Although the structural design of the solid-fuel rocket engine, in contrast to the liquid-fuel rocket engine, is characterized by great simplicity and, above all, limited use of mechanisms with moving and rotating elements, the combustion of the solid fuel which is the basis for the operating process in the solid-fuel rocket engines is a complex phenomenon for which a complete mathematical description has still not been found. This is explained, on the one hand, by insufficient study of the nature of this phenomenon itself; in particular, this pertains to the combustion of the mixed fuels, nonstationary combustion of two types of fuels and the ignition processes. On the other hand, the creation of a mathematical model of the combustion of solid rocket fuel which is convenient for engineering practice is complicated by the multiparametric relations characteristic of the combustion process and also the difficulties of experimental determination of the individual parameters, without numerical values for which it is impossible to use the already known relations. The indicated circumstances create significant difficulties when resolving the problems of the dynamics of solid-fuel rocket engines.

The primary problems connected with the investigated dynamic characteristic of solid-fuel rocket engines are the following:

1. Investigation of the dynamic stability of the operating conditions of the engine;

2. Study of the operation of the solid-fuel engines in the transient modes;

3. Investigation of the solid-fuel rocket engines as an object of control;

4. Study of the process of ignition of the solid-fuel rocket engine charge when starting the engine.

In order to solve the indicated roblems, a mathematical model of the solid-fuel rocket engine must be constructed which will be in the form of a set of equations describing the individual component elements of the operating process of the engine.

APPROVED FOR RELEASE: 2007/02/08: CIA-RDP82-00850R000200090053-2

APPROVED FOR RELEASE: 2007/02/08: CIA-RDP82-00850R000200090053-2

These equations will be:

1. The material balance equation of the chamber of the solid-fuel rocket engine;

2. The equation of state;

3. The equation of the energy balance of the solid-fuel rocket engine chamber (the energy equation);

4. The gas inflow equation;

5. The equation of the variation of charge configuration and combustion chamber during the combustion process;

6. The equation of heat exchange of the combustion products with the surface of the engine and the charge;

7. The equation of combustion of solid fuel.

The form of the equations is determined by the nature of the stated problem. In order to investigate the operation of solid-fuel rocket engines in the transient regimes when the operating parameters of the engine vary within broad limits, nonlinear differential equations are used. With limited variation of the parameters in the case of regulation of the solid-fuel rocket engines or when estimating the operating stability, the equations in small deviations are used. In view of this fact, the equations of the dynamics of the solid-fuel rocket engines are presented below both in nonlinear and in linearized form.

In a number of the equations of the dynamics of solid-fuel rocket engines, a special role is played by the equations of combustion of the solid fuel permitting determination of the local value of the nonsteady-state combustion rate of the fuel. Since the solution of the system of equations of fuel combustion is in essence an independent problem, the investigation of it has been confined to Chapter 8. The use of this system is mandatory in case where the fuel combustion process is explicitly nonsteady state. The determination of the nonstationarity criterion will be presented in Chapter 8. It is necessary, however, to point out that in a number of cases when solving the problems connected with studying the nonsteady state processes of solid-fuel rocket engines, the combustion process can be considered as quasistationary. Here there is no necessity for solving the system of equations of combustion of the fuel inasmuch as the combustion rate can be determined on the basis of the empirical combustion law relating it to the pressure in the engine, the speed of the gas flow along the charge and the initial fuel temperature.

When compiling the material balance equations or the equations of state and energy, we shall consider the solid-fuel rocket engine chamber as a system with lumped parameters; in other words, we shall assume the thermodynamic

APPROVED FOR RELEASE: 2007/02/08: CIA-RDP82-00850R000200090053-2

APPROVED FOR RELEASE: 2007/02/08: CIA-RDP82-00850R000200090053-2

parameters to be averaged over the entire free volume of the chamber reduced to the nozzle input conditions. This approach excludes direct consideration of the variation of the parameters along the length or over the free volume of the chamber. The consideration of the effect of the variation of the gas flow parameters along the length of the channel (for example, the erosion effect leading to variation in the combustion rate along the length of the charge) is realized using additional expressions which determine the average values of the attendant characteristics.

We shall also propose that the combustion products of the solid fuel have the properties of an ideal gas, and the deviations from these properties caused by the presence of the condensed phase will be considered by means of the reduced values of the thermodynamic constants -- the gas constant, heat capacity, and so on calculated for the two-phase system.

APPROVED FOR RELEASE: 2007/02/08: CIA-RDP82-00850R000200090053-2

APPROVED FOR RELEASE: 2007/02/08: CIA-RDP82-00850R000200090053-2

CHAPTER 7. EQUATIONS OF DYNAMICS OF THE SOLID-FUEL ROCKET ENGINE CHAMBER

7.1. Material Balance Equation of the Solid-Fuel Rocket Engine Chamber

The equation of the mass balance of the fuel combustion products in the thrust chamber is written in the form

$$\frac{dm_к}{dt}=Y(t)-\dot{m}_c(t), \tag{7.1}$$

where m_k is the mass of gas in the solid-fuel rocket engine chamber at the time t; Y(t) is the mass arriving per second from combustion of the fuel; $\dot{m}_c(t)$ is the flow rate of the gas per second through the nozzle.

The value of Y(t) in general form is expressed as

$$Y(t)=\rho_т\int_0^S u\,dS,$$

where ρ_T is the fuel density; u is the local combustion rate of the fuel, which in the general case is the variable over the combustion surface of the charge. The flow rate of the gas per second through the nozzle usually is determined by the formula for the steady-state escape

$$\dot{m}_c=\frac{\varphi_c A F_{кр}^{(1)}}{\sqrt{RT_к}_{(2)}}p_к, \tag{7.2}$$

Key: 1.cr; 2. chamber

where ϕ_c is the nozzle flow rate coefficient;

$$A=\left(\frac{2}{k+1}\right)^{\frac{1}{k-1}}\sqrt{\frac{2k}{k+1}};$$

k is the exponent of the adiabatic curve; F_{cr} is the critical cross section area; T_k, p_k are the gas temperature and pressure in the chamber.

In certain cases the righthand side of the equation (7.1) is supplemented by the term $\Delta Y(t)$ expressing the flow rate of the additional component fed to the chamber -- the cooling liquid for stopping combustion or the reagent for adjusting the thrust.

APPROVED FOR RELEASE: 2007/02/08: CIA-RDP82-00850R000200090053-2

APPROVED FOR RELEASE: 2007/02/08: CIA-RDP82-00850R000200090053-2

The second expression for dm_k/dt can be obtained by differentiating the equation of state of the gas

$$p_к = \frac{m_к RT_к}{W(t)}, \tag{7.3}$$

where W(t) is the free volume of the chamber

$$\frac{dm_к}{dt} = \frac{W}{RT_к}\frac{dp}{dt} + \frac{p_к}{RT_к}\frac{dW}{dt} - \frac{p_к W}{(RT_к)^2}\frac{d(RT_к)}{dt}. \tag{7.4}$$

Equating the righthand sides of equations &.1) and (7.4), substituting (7.2) and considering that $Y(t)=\rho_T dW/dt$, we obtain the summary equation which sometimes is called the primary equation of dynamics of the chamber

$$\frac{W}{RT_к}\frac{dp}{dt} = \frac{dW}{dt}\rho_т\left(1 - \frac{p_к}{\rho_т RT_к}\right) - \frac{\varphi_c A F_{кр}}{\sqrt{RT_к}} p_к + \frac{p_к W}{(RT_к)^2}\frac{d(RT_к)}{dt}. \tag{7.5}$$

The expression obtained can be simplified by neglecting the subtrahend in the parentheses $p_k/\rho_T RT_k$ in view of its smallness with respect to one. Linearization of the equation (7.5) leads to the expression

$$\frac{W}{RT_к}\frac{d\Delta p}{dt} = \rho_т \frac{d\Delta W}{dt} - \frac{\varphi_c A F_{кр}}{\sqrt{RT_к}}\Delta p + \frac{\varphi_c A F_{кр}}{2\sqrt{(RT_к)^3}}\Delta(RT_к) + \\ + \frac{p_к W}{(RT_к)^2} - \frac{d\Delta(RT_к)}{dt} + \frac{d(RT_к)}{dt}\left[\frac{p_к \Delta W}{(RT_к)^2} + \frac{W\Delta p_к}{(RT_к)^2} - \frac{2W p_к}{(RT_к)^3}\Delta(RT_к)\right]. \tag{7.6}$$

For the case where the combustion rate is constant over the entire surface of the charge, and the gas temperature in the chamber remains constant with time, the equation (7.6) is rewritten in the form

$$\frac{W}{RT_к}\frac{dp}{dt} = \rho S\bar{u} - \frac{\varphi_c A F_{кр}}{\sqrt{RT_к}} p_к. \tag{7.7}$$

The linearization of this equation leads to the expression

$$\frac{W}{RT_к}\frac{d\Delta p}{dt} = \rho S\Delta u - \frac{\varphi_c A F_{кр}}{\sqrt{RT_к}}\Delta p. \tag{7.8}$$

Dividing both sides of this equation by the cofactor for Δp and proceeding to the relative deviations, we obtain

$$\frac{W}{\varphi_c A F_{кр}\sqrt{RT_к}}\frac{d\delta p}{dt} = \frac{\rho S\bar{u}\sqrt{RT_к}}{\varphi_c A F_{кр} p}\delta u - \delta p.$$

For the case where a study is made of the small deviations of the pressure from its steady-state value $p=p_0$, the cofactor on δu expressing the ratio of the inflow and the flow rate of the gases approaches one. The complex on the derivative in the lefthand side, as it is easy to see, has the dimensionality of time. It is called the time constant of the chamber

APPROVED FOR RELEASE: 2007/02/08: CIA-RDP82-00850R000200090053-2

APPROVED FOR RELEASE: 2007/02/08: CIA-RDP82-00850R000200090053-2

$$\tau_к = \frac{W}{\varphi_c A F_{кр} \sqrt{RT_к}}. \tag{7.9}$$

Finally,

$$\tau_к \frac{d\delta p_к}{dt} = \delta u - \delta p_к. \tag{7.10}$$

7.2. Energy Balance Equation of the Solid-Fuel Rocket Engine Chamber

The energy balance equation of the solid-fuel rocket engine chamber is described in general form as follows:

$$\varphi_{cr} Y(t) I_T^0 = \frac{d(m_к U_к)}{dt} + \dot{m}_c E_c + \frac{dQ}{dt}. \tag{7.11}$$

Here the lefthand side expresses the inflow of energy per second as a result of combustion of the fuel; the first term in the righthand side expresses the variation per second of the total internal energy of the gas filling the free volume of the chamber; the second term is the flow rate per second of the energy released together with the gases escaping through the nozzle; the third term is the heat losses caused by the heat transfer to the engine housing, and in some cases, also other factors (for example, the entrance of cooling liquid when the thrust is cut off).

Equation (7.11) includes I_T^0 -- the total enthalpy of the fuel determined experimentally of as a result of thermodynamic calculations.

The first term of the righthand side can be written as follows:

$$\frac{d}{dt}(m_к U_к) = \frac{dm_к}{dt} U_к + m_к \frac{dU_к}{dt}$$

or, considering (7.1) (7.1)

$$\frac{d}{dt}(m_к U_к) = Y(t) U_к - \dot{m}_c U_к + m_к c_V \frac{dT}{dt},$$

where U_k is the specific internal energy of the gases for the temperature T_k equal to $c_V T_k$.

Assuming that in the temperature range from T_k to T_V, where T_V is the isochoric temperature of combustion, the composition of the combustion products and the heat capacity c_V vary little, the difference in total enthalpy of the combustion products and the specific internal energy of the gases at the temperature T_k can be represented as follows:

$$I_t^0 - U_к = \int_{T_к}^{T_V} c_V dT \approx (T_V - T_к) c_V.$$

The specific energy of the gases escaping through the nozzle can be defined as $E_c = v_{lim}^2/2$, where v_{lim} is the limiting escape velocity which is achieved on escape into a vacuum; consequently,

APPROVED FOR RELEASE: 2007/02/08: CIA-RDP82-00850R000200090053-2

APPROVED FOR RELEASE: 2007/02/08: CIA-RDP82-00850R000200090053-2

$$E_c = \frac{k}{k-1} RT_к.$$

Let us also note that $c_V = R/(k-1)$.

Considering the transformations, the initial equation is rewritten in the form

$$\frac{p_к W}{T_к} \frac{dT}{dt} = Y(t) R(T_V - T_к) - \dot{m}_c (k-1) RT_к - \frac{dQ}{dt} (k-1). \qquad (7.12)$$

In the case where the heat losses and also incompleteness of combustion of the fuel are considered by means of the heat loss coefficient reduced to the total enthalpy of a unit mass of combustion products of the fuel, the equation (7.12) assumes the form

$$\frac{pW}{T_к} \frac{dT}{dt} = Y(t) R(\chi T_V - T_к) - (k-1) \dot{m}_c RT_к. \qquad (7.13)$$

The equations (7.12) or (7.13) integrated jointly with the other equations of the system of dynamics of the solid-fuel rocket engine permit us to obtain the gas temperature variation in the solid-fuel rocket engine as a function of time.

Without resorting to the solution of the entire system of equations, from equation (7.13) it is possible to establish the limit to which the gas temperature will approach in the chamber on exit to the steady-state conditions of the engine ($p = p_{\text{steady state}}$). Setting $dT/dt = 0$, $Y(t) = \dot{m}_c$, we obtain

$$T_{к.уст} = \frac{\chi T_V}{k}.$$
(1)

Key: 1. chamber, steady state

This relation is known in the theory of solid-fuel rocket engines as the Langevin formula.

Equation &7.13) can be transformed to the form

$$\frac{pW}{(RT_к)^2} \frac{d(RT_к)}{dt} = Y(t) \left(\frac{\chi RT_V}{RT_к} - 1 \right) - (k-1) \frac{\varphi_c A F_{кр}}{\sqrt{RT_к}} p. \qquad (7.14)$$
(1)

Key: 1. critical

Substituting (7.14) in equation (7.5), we obtain the second expression of the basic equation of the dynamics of solid-state rocket engines

APPROVED FOR RELEASE: 2007/02/08: CIA-RDP82-00850R000200090053-2

APPROVED FOR RELEASE: 2007/02/08: CIA-RDP82-00850R000200090053-2

The product RT_V $$W\frac{dp}{dt}=Y(t)\chi RT_V-k\varphi_c AF_{кр}\sqrt{RT_к}p_к. \quad (7.15)$$

The product RT_V called the strength of the fuel and denoted as f_V is used as one of the basic energy characteristics of the solid rocket fuel. In addition, the reduced strength of the fuel is used which is defined as

$$f_p=\frac{f_V}{k}.$$

7.3. Equation of Gas Inflow and Variation of the Charge Configuration

The gas inflow when burning the fuel from an elementary segment of the charge is defined as $\Delta Y=\rho_T U\Delta S$. When determining the total gas inflow it is necessary to consider the possible differences in the linear combustion rate, and in some cases, the fuel density for different sections of the combustion surface.

Let us enumerate the basic causes of these differences.

1. The application of combined charges made up of the fuels of different composition and with different ballistic properties.

2. Different conditions of flow of the gases over the different sections of the combustion surface of the charge from one fuel; here, for the different sections different erosion effect of increasing the combustion rate is observed.

3. The nonuniformity of the initial temperature field of the charge. Here, if the combustion front does not coincide during its movement with the temperature field isotherms, the difference in the initial fuel temperatures in the individual sections of the combustion surface also causes a difference in the combustion rates in these sections.

4. The technological flaws of the composition and structure of the fuel: the local deviations of the ratio of the components from the norm, porosity and so on which can cause temporary deviations of the combustion rate in individual sections of the burning surface.

Therefore in the general case the equation of the gas inflow assumes the form

$$Y(t)=\int_0^S \rho_T u dS. \quad (7.16)$$

The use of the function (7.16) for the periods of nonstationary combustion of the fuel presupposes determination of the combustion rate entering into it from the system of equations of fuel combustion investigated in Chapter 8.

In cases where the solid-fuel combustion is of a stationary nature, when calculating the gas inflow, the empirical combustion law is used -- most

APPROVED FOR RELEASE: 2007/02/08: CIA-RDP82-00850R000200090053-2

APPROVED FOR RELEASE: 2007/02/08: CIA-RDP82-00850R000200090053-2

frequently, the step function $u_1 p^{\nu}$ supplemented by the empirical relations for the combustion rate as a function of the gas flow rate along the surface and the initial charge temperature.

For steady combustion of the fuel we use the function

$$u = u_{10} f(\lambda) \varphi(T_н) p_к^{\nu} = u_1 p^{\nu}, \tag{7.17}$$

where $f(\lambda) = 1 + k_\lambda (\lambda - \lambda_0)$ is the function taking into account the variation of the combustion rate as a function of the dimensionless gas flow rate λ; λ_0 is the threshold value of λ, on the feeding of which, an erosion effect appears; $\phi(T_H)$ is the relation taking into account the variationof the combustion rate as a function of the initial charge temperature T_H.

In order that the expression Y(t) introduced into the equation of dynamics of the solid-fuel rocket engine be made more compact, let us use the integral characteristic of gas formation introduced in part I of this book and defined as

$$\Gamma(\psi) = \sum^{s} \Delta S \cdot u_1 (r, Z, \varphi),$$

where $u_1(r, Z, \phi)$ is the function characterizing the variation of the unit combustion rate with respect to the cylindrical coordinates, r, Z, ϕ.

Let us specify the general expression for the gas inflow as applied to characteristic cases based on the function (7.17). In the case of a charge made up of fuels with different combustion rate

$$Y(t) = \varrho S_1 u_{11} p^{\nu} + \varrho S_{11} u_{111} p^{\nu} + \ldots + \varrho S_n u_{1n} p^{\nu}.$$

Here

$$\Gamma(\psi) = S_1(\psi) u_{11} + S_{11}(\psi) u_{111} + \ldots + S_n(\psi) u_{1n}, \tag{7.18}$$

here $S_n(\psi)$ is the current value of the combustion surface of the n-th element of the charge.

The determination of $\Gamma(\psi)$ on manifestation of the erosion effect during the initial period of operation of the solid-fuel rocket engine with high filling coefficient of the chamber cross section with fuel and with long charge length is more complex.

For this case

$$\Gamma(\psi) = u_{10}(S_б k_a + S_т), \tag{7.19}$$

where u_{10} is the unit rate of end combustion of the fuel for the given initial charge temperature; S_b is the surface of the charge channel (the lateral combustion surface for charges with two-way combustion);

APPROVED FOR RELEASE: 2007/02/08: CIA-RDP82-00850R000200090053-2

APPROVED FOR RELEASE: 2007/02/08: CIA-RDP82-00850R000200090053-2

S_T is the combustion area of the end turned toward the nozzle; k_u is the ratio of the combustion rate of the fuel averaged over the length of the channel to the rate of end combustion of the same fuel for the pressure in the prenozzle volume.

The value of k_u according to the derivations presented in Part I of this book is defined by the formula

$$k_u=\left(\frac{2}{k+1}\right)^{\frac{1}{k-1}}\frac{y(\lambda_k)[r(\lambda_k)]^{1-\nu}}{\Phi(\lambda_k)}, \tag{7.20}$$

where λ_k is the dimensionless flow rate in the output cross section of the channel; $y(\lambda_k)$, $r(\lambda_k)$ are the table gas dynamic functions.

The graphs and the relation for calculating the function $\Phi(\lambda_k)$ are presented in Part I of the book.

The value of λ_k in the combustion process varies as the charged channel is eroded in accordance with the varation of the ratio of the channel ar: and the critical cross section of the nozzle — F_k/F_{cr}. Inasmuch as $F_k=F_{k.c}(1-\varepsilon)$, where $F_{k.c}$ is the area of the transverse cross section of the combustion chamber, according to the relations investigated in Part I

$$\frac{F_{k.c}}{\varphi_c F_{kp}}(1-\varepsilon)=\frac{\sigma_c}{q(\lambda_k)\left(1+\frac{1}{k_u}\bar{S}\right)}, \tag{7.21}$$

where $\bar{S}=S_T/S_b$, σ_c is the recovery coefficient of the total pressure for the prenozzle volume defined by the formula

$$\sigma_c=1-\xi\frac{k}{k+1}\pi(\lambda_k)\lambda_{kr}^2$$

where ξ is the coefficient of hydraulic losses; $\pi(\lambda_k)$, $q(\lambda_k)$ are the gas dynamic table functions.

Let us denote the righthand side of equation (7.21) which is a function of two parameters λ_k and $\bar{S}$ in terms of $\tilde{F}(\lambda_k, \bar{S})$. As an example in Fig 7.1 we have the graph of the function $\tilde{F}(\lambda_k, \bar{S})$ constructed with the following initial data $\lambda_0=0.15$, $k_\lambda=3$, $\nu=0.3$. In the same figure the graph is presented for $k_u=f(\lambda_k, \bar{S})$ constructed for the same data. Inasmuch as the current values of ε and ψ for the charge of given shape are interrelated, it appears possible for any dynamic value of ψ, calculating the lefthand side of the equality (7.21) to enter with respect to the value of $F_{k.c}(1-\varepsilon)/\phi_c F_{cr}$ into the graph $\tilde{F}(\lambda_k, \bar{S})$ and defining λ_k, to obtain a value of k_u required to calculate $\Gamma(\psi)$ from the second graph.

The difference in value of u_1 as a result of nonuniformity of the initial temperature field of the fuel depends both on the nature of the temperature field and on the location of the combustion front determined by the shape of the charge and the entire preceding combustion process. The approach

APPROVED FOR RELEASE: 2007/02/08: CIA-RDP82-00850R000200090053-2

APPROVED FOR RELEASE: 2007/02/08: CIA-RDP82-00850R000200090053-2

to determination of the characteristic Γ for different types of charges was investigated in Part I (see Chapter 10).

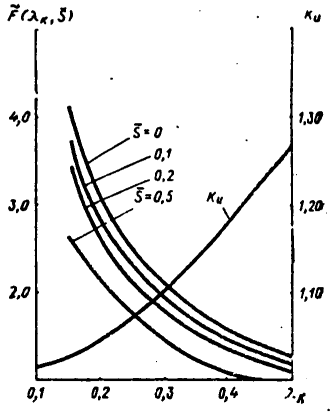

Figure 7.1. Graphs of the functions $\bar{F}(\lambda_k, \bar{S})$ and $k_u(\lambda_k)$

The calculation of the gas inflow and the characteristic defining edge is based on the functions describing the variation of the charge configuration and chamber in the combustion process.

The basic geometric characteristic of the charge expressing the variation of its surface in time is $\sigma=S/S_0$ is the ratio of the dynamic value of the combustion surface to its initial value.

For a uniform velocity field of the charge, the rupture variation of the combustion surface σ can be calculated using the elementary geometric functions as a function of ψ -- the relative proportion of the running fuel. The basis for such calculations is the law of fuel combustion in parallel layers.

In the case of a nonuniform velocity field, this approach in determining σ can be maintained for the initial operating period until the nonuniformity of burnup of the charge in the individual sections leads to significant deformation of the combustion front. However, when calculating the transient operating conditions of the solid-fuel rocket engine following the periods of prolonged operation with a nonuniform velocity field, the changes in configuration of the burning surface accumulated at this time must be taken into account (see Chapter 10 of Part I).

For erosion combustion the characteristic σ in conformity with the structure of the formula (7.19) must be determined separately for the side and end surfaces. Here the current value of the area of the end of the charge will

FOR OFFICIAL USE ONLY

APPROVED FOR RELEASE: 2007/02/08: CIA-RDP82-00850R000200090053-2

APPROVED FOR RELEASE: 2007/02/08: CIA-RDP82-00850R000200090053-2

be defined as $S_T=S_{T0}(\varepsilon/\varepsilon_0)$, where ε is the current value of the filling factor of the chamber cross section with fuels, ε_0 is the initial value.

The value ε is the second geometric characteristic of the charge and the chamber. It determines the area of the through cross section, which determines the local gas flow rate, in turn determining the erosion effect and the intensity of the heat exchange of the gases with the engine housing. The values of σ and ε for each specific version of the charge are mutually related.

For the charge with erosion combustion over the surface of the channel or over the lateral surface, formula (7.19) considering σ and ε assumes the form

$$\Gamma(\psi)=u_{1T}\left[\sigma_6(\psi)S_{60}k_u(\varepsilon)+S_{T0}\frac{\varepsilon}{\varepsilon_0}\right]. \tag{7.22}$$

When solving the problems of the dynamics of solid-fuel rocket engines it is also necessary to consider the variation in time of the free volume of the chamber W(t) described by the equation

$$\frac{dW}{dt}=\sum_{i=1}^{n}\Delta S_i u_i. \tag{7.23}$$

In the simplest case for steady-state combustion of the fuel with an exponential combustion law we obtain

$$\frac{dW}{dt}=\Gamma p^{\nu}. \tag{7.24}$$

7.4. Equations of Heat Exchange of the Combustion Products with the Surface of the Engine and the Charge

The heat exchange parameters when solving the problems of the dynamics of solid-fuel rocket engines are calculated considering the thermal losses which influence the thermodynamic parameters of the gas in the chamber, for determination of the ignition time of the individual sections of the charge surface when starting the engine and also for estimating the igniting effect on the fuel of the heated elements of the structure after extinguishing the charge.

In view of the special specific nature of the process of the interaction of the combustion products of the igniter with the charge surface, everything that is connected with this process, including the problems of heat exchange during ignition, has been put into a separate chapter.

The role of the thermal losses in the dynamic processes of solid-fuel rocket engines varies within broad limits depending on the bore and the structural design of the engine and also the nature of the process itself. The necessity for correct consideration of the heat losses increases for the period of emergence of the solid-fuel rocket engine in the stationary regime

APPROVED FOR RELEASE: 2007/02/08: CIA-RDP82-00850R000200090053-2

APPROVED FOR RELEASE: 2007/02/08: CIA-RDP82-00850R000200090053-2

where the hot gases interact with the cold surface of the engine, and it becomes less urgent for the processes occuring after operation of the solid-fuel rocket engine in the steady-state mode, with heated wall and steady-state conditions of removal of the coating. For a small-bore engine, in view of the higher ratio of the heated surface to the free volume of the chamber, the role of the heat losses will be higher than for the large-bore engine geometrically similar to it. The role of the heat losses reduces to a minimum for the engines of compact structural design with clamped charge and heat insulated housing, and it increases sharply for engines without thermal insulation, in particular, for structural designs with gas lines, gas manifolds and other intermediate reservoirs.

The general thermal losses in the chamber of the solid-fuel rocket engine per unit time are defined as

$$\frac{dQ}{dt}=\int_0^{S_к}\alpha(T_к-T_{cв})\,dS_к, \tag{7.25}$$

where α is the local heat transfer coefficient; T_{cB} is the local temperature of the chamber surface; S_k is the heat exchange surface.

The defining forms of heat exchange in the solid-fuel rocket engines are the forced convection and radiation.

When determining the parameters of the convective heat exchange in the solid-fuel rocket engines, the entire variety of versions of the gas flow can in the first approximation be reduced to the following characteristic cases:

1. Axial movement of the gas flow through the long channels of constant cross section (the free cross section of the chamber between the enclosed charge and the housing, the slit section for the slit charge, and so on).

2. The eddy movement of the gas on arrival of the flow from the narrow channel in the volume with large free cross section (the prenozzle volume, the gas manifold, the intermediate volume between sections of the sectioned charge, and so on).

3. Movement of the flow in the entrance tube of the nozzle.

For the case of axial movement of the gas through the channels of free cross section, the local value of the effective gas transfer coefficient can be determined with accuracy acceptable for the given problem from the criterial empirical function obtained for effective heat exchange in the case of gradientless flow in the tubes or along the surface of the plate having the form

$$\mathrm{Nu}=c\,\mathrm{Re}^n\,\mathrm{Pr}^m, \tag{7.26}$$

FOR OFFICIAL USE ONLY

APPROVED FOR RELEASE: 2007/02/08: CIA-RDP82-00850R000200090053-2

APPROVED FOR RELEASE: 2007/02/08: CIA-RDP82-00850R000200090053-2

where $Nu=\alpha\ell/\lambda$ is the Nusselt number; $Re=v\ell/\nu$ is the Reynolds number; $Pr=\nu c_p\rho/\lambda$ is the Prandtl number; c, n, m are the dimensionless constant; α is the heat transfer coefficient; ℓ is the defining dimension; λ,ν are the coefficients of thermal conductivity and kinematic viscosity of the gas; c_p,ρ are the specific heat capacity and density of the gas.

In Table 7.1 a summary of the basic functions of this type known from the literature is presented. In the formulas presented in the table T_{00} is the braking temperature of the gas flow, T_{cB} is the surface temperature.

The index "d" for the Nu and the Re numbers indicates that the channel diameter is taken as the defining dimension; the index "z" denotes that the defining dimension is the distance from the beginning of the channel to the investigated cross section.

When using these relations for the cross sections of complex configuration the equivalent hydraulic diameter is calculated by the formula

$$d=\frac{4F_{cB}}{\Pi}, \quad (1)$$

Key: free

where F_{free} is the area of the free cross section of the chamber; Π is the cross section perimeter.

The coefficient of convective heat transfer determined from these relations can be represented in the form

$$\alpha_к=k_\alpha\left(\frac{\dot{m}}{F_{cB}}\right)^{0,8}\frac{1}{d^{0,2}},$$

where $\dot{m}$ is the local gas flow rate.

Inasmuch as in the section of the chamber occupied by the charge $F_{free}=F_{k.c}(1-\varepsilon)$, the local flow rate of the gas $\dot{m}\approx\dot{m}_k(Z/L)$, where $\dot{m}_k$ is the flow rate in the final cross section of the charge; L is the length of the charge; the heat transfer coefficient can be expressed in the formula

$$\alpha=k_\alpha\left(\frac{\dot{m}_к}{L}\right)^{0,8}\left(\frac{\Pi}{4}\right)^{0,2}\frac{Z^{0,8}}{F_{к.c}(1-\varepsilon)} \quad (7.27)$$

or, in general form

$$\alpha_{к(1)}=f_1(\dot{m}_к, Z, \varepsilon).$$

APPROVED FOR RELEASE: 2007/02/08: CIA-RDP82-00850R000200090053-2

APPROVED FOR RELEASE: 2007/02/08: CIA-RDP82-00850R000200090053-2

Table 7.1

Номер формулы (1)	Авторы (2)	Формула (3)	Источник (4)
1	Г. Краусольд (5) М. А. Михеев (6)	$Nu_d = 0{,}023 Re_d^{0,8} Pr^{0,4}$	[3]
2	Б. С. Петухов (7) В. В. Кириллов (8)	$Nu_d = 0{,}044 \varphi\, Re_d^{0,73} Pr^{0,43} [\tau(\lambda)]^{0,33}$; $\tau(\lambda)$ — газодинамическая функция (9); $\varphi = 1{,}3 (Z/d)^{-0,12}$ при $Z/d < 10$; $\varphi = 1$ при $Z/d > 10$ (10)	[33]
3	Те же (11)	$Nu_Z = 0{,}034 Re_Z^{0,77} Pr^{0,43} [\tau(\lambda)]^{0,33} (Z/d)^{0,06}$	[33]
4	Г. Дейви (12)	$Nu_d = 0{,}036 Re_d^{0,8} Pr^{0,4} (Z/d)^{-0,2} \times (T_{00}/T_{св})^{0,18}$	[49]

Key:
1. No of the formula
2. Authors
3. Formula
4. Source
5. G. Kraussol'd
6. M. A. Mikheyev
7. B. S. Petukhov
8. V. V. Kirillov
9. $\tau(\lambda)$ -- gas dynamic function
10. for
11. The same
12. G. Davey

With significant content of condensed particles in the combustion products, the coefficient of convective heat transfer is determined by the formula [9]:

$$\alpha = c_{p_f} \frac{\dot{m}}{F_{св} Pr^{2/3}} \left[\frac{1 + 3 k_D \eta \frac{d_э}{d_ч} \frac{Q_г}{Q_ч} \frac{1}{Re_ч}}{4{,}8 + 2{,}5 \ln \frac{d_э}{2 d_ч}} \right]^2, \qquad (7.28)$$

(1) (2)

Key: particle; 2. free

where η is the mass concentration of the condensed phase; $d_{particle}$ is the average particle diameter (the Sutter diameter); $\rho_{particle}$ is the particle density,

$$Re_ч = \frac{d_ч v_a}{\nu_г},$$

v_a is the mean flow velocity; c_{p_f} is the reduced heat capacity of the two-phase medium

$$c_{p_f} = \frac{c_{p_г} + \eta c_ч}{1 + \eta}.$$

FOR OFFICIAL USE ONLY

APPROVED FOR RELEASE: 2007/02/08: CIA-RDP82-00850R000200090053-2

APPROVED FOR RELEASE: 2007/02/08: CIA-RDP82-00850R000200090053-2

Here c_{p_g}, $c_{particle}$ are the specific heat capacities of the gas and the condensate, respectively; k_D is the coefficient of resistance of the particle.

For volumes with eddy movement of the gas if we limit ourselves to determination of the heat flux averaged over the surface of the volume, when determining the coefficient of convective heat transfer it is possible to begin with the simplified heat transfer system. We shall assume that the entire volume filled with the eddy has the property of isotropy with respect to turbulence. This makes it possible by using the relations for isotropy turbulence to obtain the working formula for determining the average coefficient of convective heat transfer [9]:

$$\alpha_{cp}=c\lambda_r\left(\frac{\varrho^3 v_к^2}{\mu^3}\frac{\pi d_к^2}{8W}\right)^{1/4}. \tag{7.29}$$

where d_k is the diameter of the input channel; v_k is the gas velocity at the exit from the channel; W is the volume into which the gas flows.

If the gas flow with a flow rate of $\dot{m}_k$ goes into the free volume from the channels of the charge located above it, it is possible to give formula (7.29) the form

$$\alpha_{cp\,II}=c\lambda_r\left(\frac{\dot{m}_к}{\mu}\right)^{3/4}\frac{1}{W^{1/4}[F_{к.c}(1-\varepsilon)]^{1/2}}.$$

Thus, in this case

$$\alpha_{cp\,II}=cf_2(\dot{m}_к,\ W,\ \varepsilon).$$

The determination of the heat transfer coefficient for the entrance section of the nozzle can be made by the Bartz formula [48]

$$\alpha_{к\,III}=0{,}026c_p\mu^{0,2}\frac{\mathrm{Pr}^{-0,6}}{d^{0,2}}\left(\frac{\dot{m}}{F}\right)^{0,8}\left(\frac{d_{кр}}{r}\right)^{0,1}\sigma, \tag{7.30}$$

where r is the radius of curvature of the wall in the meridional cross section

$$\sigma=(\varrho_f/\varrho_{00})^{0,8}(\mu_f/\mu_{00})^{0,7}.$$

The parameters ρ_f, μ_f are taken for the defining temperature calculated by the formula

$$T_f=0{,}5(T_r+\overset{(1)}{T_{св}})+0{,}22\,\mathrm{Pr}^{1/3}(T_{00}-\overset{(2)}{T_r}),$$

Key: 1. free; 2. g

where T_{00} is the braking temperature, T_g is the static gas temperature.

APPROVED FOR RELEASE: 2007/02/08: CIA-RDP82-00850R000200090053-2

APPROVED FOR RELEASE: 2007/02/08: CIA-RDP82-00850R000200090053-2

On wear of the material off the wall surface in the relation for determining the coefficient of convective heat transfer a correction factor is introduced $\Psi=\alpha/\alpha_0$, where α_0 is the heat transfer coefficient in the absence of wear. For moderate wear rates of the material, the value of Ψ is determined in the first approximation [39] as

$$\psi=1-\frac{\dot{m}_S\bar{c}_p}{2\alpha_0},$$

where $\dot{m}_S$ is the mass wear rate of the material.

Defining α by the relations presented above, it is possible to find

$$\frac{dQ}{dt}=\int_0^{S_I}\alpha_{к(I)}(T_к-T_{св})\,dS+\sum^{S_{II}}\Delta S_{II}\alpha_{срII}(T_к-T_{св})+ \\ +\int_0^{S_{III}}\alpha_{кIII}(T_г-T_{св})\,dS, \tag{7.31}$$

where S_I, S_{II}, S_{III} are the surfaces of the three characteristic heat exchange zones.

For the simplest system the magnitude of the heat losses can be related to the coefficient ε by the formula

$$\frac{dQ}{dt}=\int_0^{S_I}f_1(\dot{m}_к,\ Z,\ \varepsilon)(T_к-T_{св})\,dS+ \\ +S_{II}cf_2(\dot{m}_к,\ W,\ \varepsilon)(T_к-T_{св})+\int_0^{S_{III}}\alpha_{кIII}(T_г-T_{св})\,dS.$$

For exact determination of the temperature on the heat exchange surface T_{free} it is necessary in parallel with calculating the dynamics of the solid-fuel rocket engine, to solve the problem of nonsteady thermal conductivity of the engine wall with a boundary condition of the third type including the values of the heat transfer coefficient attained from the above-presented conditions.

The simplified approach to determining T_{free} consists in the fact that initially α is averaged with time; then by these average values, using the engineering methods of calculating the temperature field of the single-layer wall, the approximate value of T_{free} is determined [39].

In the case where the heat losses are taken into account by means of the heat loss coefficient χ reduced to the total enthalpy of a unit mass of combustion products, the use of the semianalytical and empirical relations expressing the coefficient χ as a function of ψ, for example, the relation of the type [43] is possible:

$$\chi=1-\frac{B}{1+a\psi}, \tag{7.32}$$

where B and a are empirical coefficients.

APPROVED FOR RELEASE: 2007/02/08: CIA-RDP82-00850R000200090053-2

APPROVED FOR RELEASE: 2007/02/08: CIA-RDP82-00850R000200090053-2

CHAPTER 8. SYSTEM OF EQUATIONS FOR DETERMINING THE COMBUSTION RATE OF SOLID ROCKET FUEL

8.1. Model of the Combustion of Solid Rocket Fuel

The combustion of solid rocket fuel is a sequence of physical-chemical processes beginning in the solid phase and ending in the gas phase at some distance from the surface of the charge by the formation of the equilibrium composition of the combustion products.

For description of the process of combustion of the solid rocket fuels usually a mathematical model is used which generalizes the picture of the phenomenon occurring on combustion of the ballistite and mixed fuels. Before proceeding to a discussion of it, it is appropriate to consider the peculiarities of the combustion mechanism of each type of solid rocket fuel so that beginning with the basic differences between them the limits of use of the generalized model of combustion of the solid rocket fuel are established. Let us first consider the combustion of ballistite fuel (Fig 8.1).

On heating the ballistite fuel, thermal decomposition of its components takes place with the formation of a gas mixture which contains the combustible materials (formaldehyde and other complex organic compounds, carbon monoxide, hydrogen), oxidizing agents (primarily NO_2) and inert products. The actions of the gasification of the solid fuel are accompanied by the positive thermal effect $Q_{\dot{S}}$.

The temperature on the combustion surface T_S according to the data for measuring the thin thermocouple [13, 22] is, depending on the combustion conditions and the composition of the fuel, from 600 to 900 K.

The zone called the gasification zone is adjacent to the combustion surface, in which as a result of reduction of NO_2 to NO the oxidizing processes take place. These processes are accompanied by high heat release (about half the calorie content of the fuel) and an increase in the gas temperature (to 1100-1400K).

APPROVED FOR RELEASE: 2007/02/08: CIA-RDP82-00850R000200090053-2

APPROVED FOR RELEASE: 2007/02/08: CIA-RDP82-00850R000200090053-2

As the reserves of NO_2 formed during gasification of the fuel are expended, the oxidizing processes halt. A further rise in temperature stops, and the temperature remains constant, equal to T_1, within the boundaries of some region. This region is called the preparatory or preflame zone. The next step in the chemical activity is connected with the accumulation of active centers in the gas mixture which takes place with respect to the entire preparatory zone and leads to the occurrence of a bright flame on the outer boundary of this zone. In the bright flame zone afterburning of the CO and H_2 takes place as a result of reduction of NO to N_2. Here the amount of heat equal approximately to half the calorie content of the fuel is released, and the gas temperature increases to the level corresponding to the formation of the equilibrium composition of the combustion products $T_0=T_k$. For moderate pressures the width of the preparatory zone is found to be significant, which limits the effect of the bright flame on the processes proceeding on the surface of the fuel by the radiation effect. The supply of heat to the charge surface in the first approximation will be determined by the thermal conductivity of the gasification zone.

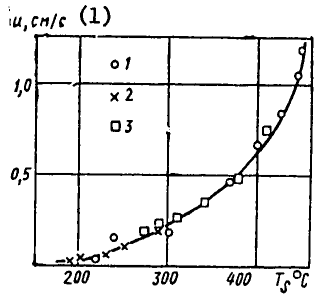

Figure 8.1. Unique dependence of the combustion rate on the surface temperature for the ballistic fuel H:
1 -- T_H=+20°C; 2 -- p=1 MPa; 3 -- p=20 MPA

Key:
1. cm/sec

The linear combustion rate of the fuel, that is, the gasification rate of the condensed phase, as the studies show, is expressed by the equation

$$u=K_u e^{-\frac{E}{2RT_s}}, \qquad (8.1)$$

where K_u is the chemical constant; E is the activation energy; R is the universal gas constant.

Special studies were performed in order to check the uniqueness of the relation between the combustion rate and the combustion surface temperature, that is, in order to establish whether the combustion rate is determined only by the surface temperature or, in addition to it, influences the pressure. In Fig 8.2 we see the results of the experiments from reference [32] in which along with determining the combustion rate using

APPROVED FOR RELEASE: 2007/02/08: CIA-RDP82-00850R000200090053-2

APPROVED FOR RELEASE: 2007/02/08: CIA-RDP82-00850R000200090053-2

microthermocouples, the temperature was determined at the combustion surface. As is obvious from the graph, the values of the combustion rate, independently of the pressure, for which they were obtained, lie on one exponential curve expressing the function (8.1). Thus, with accuracy to the experimental error it is possible to confirm that the relation between the surface temperature and the combustion rate is unique.

The basic factors taken together which determine the gasification surface temperature, and in terms of it, the fuel combustion rate are the following: the supply of heat to the charge surface from the gas phase, the release of heat as a result of chemical reactions on the surface layer of the fuel or on the combustion surface and the transfer of heat from the surface deep into the charge. The amount of heat supplied from the gas phase to the combustion surface by thermal conductivity is defined by the magnitude of the temperature gradient in the gas phase at the combustion surface which, in turn, is related to the length of the gasification zone. With an increase in pressure, the rate of the reactions occurring in the zone increases, as a result of which they are completed closer to the combustion surface. The reduction of the length of the zone with a fixed temperature level T_1 leads to an increase in the thermal flux of the gas phase to the surface. Thus, the experimental combustion laws for stationary conditions, including the most widespread exponential law among them express the effect of the pressure on the combustion rate by means of variation of combustion surface temperature. For steady-state combustion, the relation between the pressure and the surface temperature and, consequently, the combustion rate is unique. For nonsteady combustion, this uniqueness is disturbed. Thus, for example, for sharp variation of the pressure from the p_0 level to the p_1 level, the surface temperature cannot follow the pressure radiation at the same time as the combustion rate follows the temperature variation. Here, although the pressure equal to p_1 is established in the chamber, the combustion rate remains for some period close to that which corresponds to p_0. Consequently, in the general case when determining the combustion rate it is necessary to be guided by the basic relation (8.1), which is valid for any operating conditions of the engine.

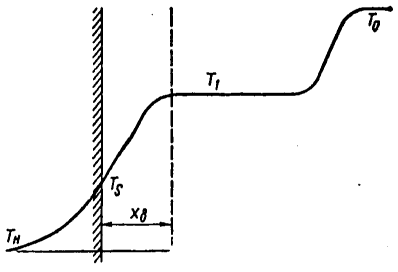

Figure 8.2. Temperature profile during combustion of ballistite fuel

APPROVED FOR RELEASE: 2007/02/08: CIA-RDP82-00850R000200090053-2

APPROVED FOR RELEASE: 2007/02/08: CIA-RDP82-00850R000200090053-2

Let us consider in general features, the peculiarities of the combustion mix fuels. When heating the surface layers of the mixed fuel, thermal decomposition of the mineral oxidizing agent and the organic combustible-binder takes place. The rate of decomposition of the two components is subject to the exponential Arrhenius function (8.1). The majority of mineral oxidizing agents has a decomposition temperature that is higher than the temperature of pyrolysis of the combustible binder. Accordingly, when burning the fuel the particles of the oxidizing agent appearing over the burned sections of the binder fall into the hotter layers of the gas over the charge surface. The processes of decomposition (pyrolysis) of the organic binder are endothermal; the decomposition of the oxidizing agent is accompanied by the release of heat. Inasmuch as the oxidizing agent is the predominant component, on the whole, the processes of gasification of the mixed fuel, just as ballistite, are exothermal.

On decomposition of the components of the mixed fuel, flows of combustible and oxidizing gases occur which are directed from the charge surface. Thus, the heterogeneous nature of the structure of the mixed fuels gives rise to nonuniformity of the gas phase above the combustion surface. The chemical interaction among the reactive gases must be preceded by mixing of them. The combustible and oxidizing gases emerging from the molten surface, arrive partially mixed. In the case of a dry combustion surface as, for example, for fuel based on ammonium perchlorate, preliminary mixing is absent.

Considering the processes occurring during combustion of a mixed fuel in the gas phase it is possible to isolate two limiting cases. At low pressure the process rate will be determined by the combustion reaction rate in the gas phase (the kinetic combustion). At high pressures when the chemical reaction rate is large and ceases to be the limiting factor, the process rate will be determined by the mixing of the gaseous components (diffusion combustion).

In the first case the model of combustion of the mixed fuels approaches the model of combustion of the ballistite fuels. Let us consider the second case (diffusion combustion). On decomposition of the particles of oxidizing agent in the gas phase, accumulations of products of decomposition are formed in the amount

$$d \approx \sqrt[3]{\frac{m_{ox}}{\varrho}}\,(1) \qquad (8.2)$$

Key: 1. ox

where m_{ox} is the mass of the oxidizing agent particle.

The time of existence of such an accumulation can be assumed to be proportional to the area of the transverse cross section of the particle and inversely proportional to the diffusion factor D which characterizes the

APPROVED FOR RELEASE: 2007/02/08: CIA-RDP82-00850R000200090053-2

APPROVED FOR RELEASE: 2007/02/08: CIA-RDP82-00850R000200090053-2

intensity of the molecular diffusion of two gaseous components, $\tau=d^2/D$. If we assume that the combustion time in the gas phase is determined only by the time for mixing of the components, the distance from the combustion surface on which the temperature of the equilibrium composition of the combustion products T_0 is established, will be defined as

$$\delta_{rA}=\frac{d^2}{D}\ u\ \frac{\rho_T}{\rho_r}, \tag{8.3}$$

where ρ_T and ρ_g are the fuel and gas density.

Substituting the value of d from expression (8.2), we obtain

$$\delta_{rA}\approx\frac{m_{ox}^{2/3}u\rho_T}{\rho_r^{5/3}D}. \tag{8.4}$$

Inasmuch $\rho_g\sim p$, $D\sim 1/p$, with an increase in pressure δ_{gd} decreases.

Just as when burning ballistite fuels, the amount of heat supplied from the gas phase to the combustion surface of the mixed fuel will be determined by the steepness of the temperature profile of the gas phase near the surface; consequently, with an increase in pressure as δ_{gd} decreases, the thermal flux to the surface increases. However, in contrast to the ballistite fuels, new factors appear and, in turn, the disperseness of the particles of the oxidant characterized by the mass of the individual particle m_{ox}.

A comparison of the combustion diagrams of ballistite and mixed fuels reveals a number of features which unite them: the exothermal nature of gasification of the solid phase, the presence of transitional reaction or reaction-diffusion zone between the combustion surface and the zone where some limiting temperature T_1 is reached as a result of the gas-phase reaction for ballistite and T_0, for mixed. This makes it possible to use the generalizing mathematical model in the first approximation to describe the combustion process of both types of fuel. Of course, such a model becomes inappropriate in cases where the heterogeneous properties of the mixed fuel begin to reach the primary level as, for example, when investigating the problems of ignition of solid rocket fuel. In such cases, for each type of solid rocket fuel it is necessary to create its own model of the process. The description of the combustion process is presented below on the basis of the generalized level of combustion of solid rocket fuel.

8.2. System of Differential Equations of the Combustion Rate

As follows from the above-investigated model of combustion in the solid rocket fuel, in order to determine the rate of its combustion it is necessary to know the temperature at the combustion surface or, more precisely, the temperature field of the heated layer of fuel. Therefore, the systems of equations for solving the given problem are equations of the nonsteady-state heat and mass exchange for the condensed phase.

APPROVED FOR RELEASE: 2007/02/08: CIA-RDP82-00850R000200090053-2

APPROVED FOR RELEASE: 2007/02/08: CIA-RDP82-00850R000200090053-2

The most correct form of notation for the thermal conductivity equation of the condensed phase in the moving coordinate system connected with the combustion surface has the form

$$\frac{\partial T}{\partial t}=\frac{1}{Q_T c_T}\frac{\partial}{\partial x}\left(\lambda_T\frac{\partial T}{\partial x}\right)+\frac{u}{Q_T c_T}\frac{\partial T}{\partial x}+\frac{Q_S}{Q_T c_T}\frac{dm}{dt}, \tag{8.5}$$

where λ_T is the coefficient thermal conductivity of the fuel; c_T is the specific heat capacity; dm/dt is the rate of the chemical reaction occurring in the condensed phase; Q_S is the thermal effect of this reaction.

The last term of equation (8.5) expresses the volumetric rate of heat release as a result of the exothermal reactions in the condensed phase.

It is proposed that the reaction of decomposition of the fuel component is a process which takes place with respect to the entire thickness of the heated layer of different intensity determined by the local temperature. Usually this reaction is assumed to be monomolecular, and its rate is expressed by the function

$$\frac{dm}{dt}=k_V Q_t (1-\beta)\, e^{-\frac{E}{RT}}, \tag{8.6}$$

where k_V is the factor in front of the exponent; β is the relative proportion of the mass of the fuel subject to chemical decomposition; E is the energy of activation for the defining reaction of the composition; T is the local fuel temperature; R is the universal gas constant.

Equation (8.6) can be rewritten in the form

$$\frac{1}{Q_T}\frac{dm}{dt}=\frac{\partial\beta}{\partial t}-u\frac{\partial\beta}{\partial x}=k_V(1-\beta)\, e^{-\frac{E}{RT}}. \tag{8.7}$$

The first boundary condition is written in the form

$$x=0\ q_{\underset{(1)}{T}}=-\lambda_T\frac{\partial T}{\partial x}\Big|_{x=0}\ T=T_S\ \beta=\beta_S,$$

Key: 1. g

where q_g is the heat flux to the surface from the gas phase; T_S and β_S are the values of the parameters T and β on the surface determined from the additional relation mathematically expressing the condition of the combustion surface. The second boundary condition is written in the form

$$x=\infty\ \frac{\partial T}{\partial x}=0\ \ \beta=0. \tag{8.8}$$

The initial condition

$$t=0\ \ T(x,t)=\overset{(1)}{T_{\text{нач}}}(x)\ \beta(x,t)=0. \tag{8.9}$$

Key: 1. init

APPROVED FOR RELEASE: 2007/02/08: CIA-RDP82-00850R000200090053-2

APPROVED FOR RELEASE: 2007/02/08: CIA-RDP82-00850R000200090053-2

The difficulties of solving the system (8.5)-(8.9) arise from the necessity of giving the additional mathematical relation for the combustion surface, the physical formulation of which does not appear to be sufficiently clear.

In practice usually the system of equations is used which is based on the simplified mathematical model. As a result of the exponential dependence of the decomposition reaction rate on the temperature, this reaction basically takes place for a temperature close to the surface temperature T_S (the concept of Ya. B. Zel'dovich and D. A. Frank-Kamenetskiy [13]). This makes it possible to assume that the reactions occurring in the solid phase are concentrated in the reaction layer adjacent to the surface, the thickness of which by comparison with the thickness of the heated layer can be neglected, that is, they are assumed to occur on the combustion surface. With this approach the condition of the burning surface is formulated by the function (8.1), which is equivalent to the condition of inertialessness of the reaction layer of the condensed phase. This simplified approach is justified in the majority of cases with the exception of a few where the inertia of the reaction layer must be taken into account (see 9.4).

Here the system of equations for determining the combustion rate of the fuel assumes the form

$$\frac{\partial T_\tau}{\partial t} = \frac{1}{\rho_\tau c_\tau}\frac{\partial}{\partial x}\left(\lambda_\tau \frac{\partial T_\tau}{\partial x}\right) + u\frac{\partial T_\tau}{\partial x}; \qquad (8.10)$$

$$u = K_u \exp\left(-\frac{E}{2RT_S}\right);$$

$$x=0 \quad T=T_S \quad -\lambda_\tau \frac{\partial T_\tau}{\partial x}\Big|_S + \rho u Q_S = -\lambda_\tau \frac{\partial T_\tau}{\partial x}\Big|_S; \qquad (8.11)$$

$$x=\infty \quad T=T_u(x, 0); \qquad (8.12)$$

$$t=0 \quad T=T_u(x, 0). \qquad (8.13)$$

The equation (8.10) is the equation of the nonsteady-state thermal conductivity of a chemically inert homogeneous material in the moving coordinate. For fuels with heterogeneous structure, the correctness of the use of this equation with substitution of the average thermophysical characteristics of the fuel in it ρ_T, c_T and λ_T will be determined by the ratio of the dimensions of the component particles and the total thickness of the heated layer.

The boundary condition (8.11) is the equation of the energy balance for the combustion surface. In the lefthand side its first term expresses the heat flux fed to the surface from the gas phase; the second term is the heat released on the surface during gasification. The righthand side expresses the heat flux in depth of the charge.

APPROVED FOR RELEASE: 2007/02/08: CIA-RDP82-00850R000200090053-2

APPROVED FOR RELEASE: 2007/02/08: CIA-RDP82-00850R000200090053-2

For determination of the heat flux fed from the gas phase to the combustion surface of the fuel it is necessary to note the temperature profile in the gas layer adjacent to the combustion surface.

In the general case the equation of nonsteady-state thermal conductivity for the gas phase near the combustion surface is written in the form

$$\frac{\partial T_r}{\partial t}=a_r\frac{\partial^2 T_r}{\partial x^2}+Ku\frac{\partial T_r}{\partial x}+q(x, T_r). \qquad (8.14)$$

Here $K=u_g/u=\rho_T/\rho_g-1$ is the ratio of the gas velocity with respect to the combustion surface to the combustion rate. The last term in the righthand side expresses the local heat influx as a result of the chemical reactions occurring in the given layer.

In accordance with the above-mentioned concept of Ya. B. Zel'dovich and D. A. Frank-Kamenetskiy, it is possible to assume that the heat released during the reactions of the gas phase is concentrated at the outside boundary of the built-up zone of the temperature which lags behind the surface of the solid fuel by a distance δ_g. On the outside boundary in the case of combustion of ballistite fuels at moderate pressures, a temperature of T_1 is reached (the temperature of the preparatory zone); in the case of combustion of mixed fuels, the temperature T_0 (the flame temperature). Let us denote it as T_δ for generality.

Under this assumption the third term in the righthand disappears, and the thermal effect of the reactions is taken into account when determining the temperature T_δ entering into the condition for the outside boundary

$$x=\delta \quad T=T_\delta.$$

The second boundary condition is the equation (8.11).

The function which closes the system of equations is the law of the fuel gasification rate.

In a number of cases it appears more convenient to give the magnitude of the heat flux from the gas phase in Newtonian form:

$$q_r=-\lambda_r\frac{\partial T_r}{\partial x}\Big|_S=\alpha(T_\delta-T_S),$$

where α is the effective heat transfer coefficient.

The studies of the inertia of the gas phase presented in reference [32] prove that when calculating the combustion rate with respect to the given dependence of the external conditions (pressure, gas flow rate) on the time the gas phase can be considered inertialless by comparison with the heated layer of the condensed phase. When determining the value of α

FOR OFFICIAL USE ONLY

APPROVED FOR RELEASE: 2007/02/08: CIA-RDP82-00850R000200090053-2

APPROVED FOR RELEASE: 2007/02/08: CIA-RDP82-00850R000200090053-2

this makes it possible to use the relation for the quasistationary thermal conductivity $\alpha=\lambda_g/\delta_g$. The depth of the zone δ_g, within the limits of which the buildup of the gas temperature takes place from T_S to T_δ is determined from the fuel of given composition by the pressure and the velocity of the gas flow, that is

$$\delta=\delta(p, v)$$

For the steady-state combustion conditions ($\partial T_T/\partial t=0$), the equation (8.10) under the assumption of independence of the thermophysical characteristics of the fuel with regard to the temperature, assumes the form

$$a_T \frac{d^2T}{dx^2} = - u \frac{dT}{dx}, \qquad (8.15)$$

where $a_T=\lambda_T/\rho_T c_T$ is the coefficient of thermal diffusivity of the fuel. The integration of 8.15 leads to the equation of the temperature profile in the fuel before the combustion front in the steady-state mode

$$T-T_н=(T_{S_0}-T_н)e^{-\frac{u_0 x}{a_T}}, \qquad (8.16)$$

where the subscript "0" refers to the steady-state regime. The temperature profile described by the equation 8.16 usually is called the Michelson profile.

Let us consider some peculiarities of the Michelson profile.

The distance from the gasification surface to the layer with temperature T is defined by the function

$$x=\frac{a_T}{u}\ln\frac{T-T_н}{T_S-T_н}.$$

If we take the isotherm corresponding to the following condition as the conditional heating boundary

$$\frac{T-T_н}{T_S-T_н}=0{,}05,$$

then the depth of heating determined from this condition will be

$$x_{пр}=3\frac{a_T}{u}.$$
(1)

Key: 1. heat

The condition $(T-T_H)/(T_S-T_H)=e$ corresponds to the depth of heating

$$x_p=\frac{a_T}{u}. \qquad (8.17)$$

APPROVED FOR RELEASE: 2007/02/08: CIA-RDP82-00850R000200090053-2

APPROVED FOR RELEASE: 2007/02/08: CIA-RDP82-00850R000200090053-2

The value of x_p is the characteristic length which corresponds to the characteristic time τ_p, the time for passage of the combustion front through a zone of depth x_p:

$$\tau_p = \frac{x_p}{u} = \frac{a_T}{u^2}.$$

This time is called the thermal relaxation time of the fuel.

For ballistite fuels when $a_T \sim 10^{-7}$ m^2/sec, $u_0 \sim 10^{-2}$ m/sec, we obtain $x_p \sim 10^{-5}$ m. Thus, the depth of heating of the fuel during steady-state combustion of it will be a very narrow region several tens of microns deep.

The temperature gradient of the gasification surface will be

$$\left(\frac{\partial T}{\partial x}\right)_S = -(T_{S_0} - T_н)\frac{u_0}{a_T}.$$

The magnitude of the heat flux released from the surface into the depth of the charge will be

$$-\lambda_T\left(\frac{\partial T}{\partial x}\right)_S = \rho_T c_T u_0 (T_{S_0} - T_н). \qquad (8.18)$$

The quantity of heat accumulated in the heated layer calculated per unit area of gasification surface is defined as

$$Q_{ак} = \int_0^\infty \rho_T c_T (T - T_н)\, dx.$$

(1)

Key: 1. acc

Considering (8.16) we obtain

$$Q_{ак} = \frac{\lambda}{u_0}(T_{S_0} - T_н).$$

In the case of the steady-state fuel combustion mode when $\partial T_g/\partial t = 0$, from solution of equation (8.14) for the indicated boundary conditions we obtain the relation for the temperature profile in the gas phase

$$T_г - T_{S_0} = \frac{T_\delta - T_{S_0}}{e^{Ku_0\delta/a_г} - 1}\left(e^{-\frac{Ku_0}{a_г}x} - 1\right). \qquad (8.19)$$

Determining the derivative $\left.\frac{\partial T_г}{\partial x}\right|_S$ from (8.19) and substituting it in (8.11) and also using the expression (8.18), we obtain the equation for determining the steady-state surface temperature T_{S_0}

$$\frac{\lambda_г K}{a_г}\frac{T_\delta - T_{S_0}}{e^{\frac{Ku_0\delta}{a_г}}} = \rho_T Q_S + \rho_T c_T (T_{S_0} - T_н). \qquad (8.20)$$

APPROVED FOR RELEASE: 2007/02/08: CIA-RDP82-00850R000200090053-2

APPROVED FOR RELEASE: 2007/02/08: CIA-RDP82-00850R000200090053-2

Equation (8.20) jointly with the function (8.1) permits analytical determination of the steady-state combustion rate of the fuel under the given conditions.

8.3. System of Linearized Equations of Solid Fuel Combustion. Estimation of the Degree of Nonstationarity

In a number of cases when studying the individual problems of the dynamics of solid fuel rocket engines it appears possible to limit ourselves to the investigation of small deviations from the steady-state combustion conditions. First of all it is necessary to establish the limits within which the nonstationarity of the process can be neglected.

Let us represent the nonsteady-state changes in temperature and combustion rate of the fuel in the form of a sum of variables corresponding to the steady-state regime and denoted by the index "0" and the disturbances

$$T=T_0(x)+\Delta T(x, t); \tag{8.21}$$

$$T_s=T_{s_0}+\Delta T_s(t); \tag{8.22}$$

$$u=u_0(T_{s_0})+\Delta u(\Delta T_s). \tag{8.23}$$

Substituting the expressions (8.21)-(8.23) in the equation (8.10) and limiting ourselves to the terms of the first-order disturbance, we obtain:

$$\frac{\partial \Delta T}{\partial t}=a_r\frac{\partial^2 \Delta T}{\partial x^2}+u_0\frac{\partial \Delta t}{\partial x}+\Delta u\frac{\partial T_0}{\partial x}. \tag{8.24}$$

For convenience of linearization it is expedient to represent the heat flux from the gas phase entering into the boundary condition (8.11) by a simplified function. The basis for this simplified function is the concept of the gas layer adjacent to the surface as a heat conducting element subject to the ordinary equation of steady-state thermal conductivity. This assumption agrees with the above-investigated condition of inertiallessness mass of the gas phase. Here

$$q_r=\alpha(T_\delta-T_s)=\frac{\bar{\lambda}_r}{\delta_{эфф}}(T_\delta-T_s), \tag{8.25}$$
(1)

Key: 1. eff

where δ_{eff} is the effective thickness of the layer; λ_g is the coefficient of thermal conductivity of the gas averaged over the thickness of the layer δ_{eff}.

APPROVED FOR RELEASE: 2007/02/08: CIA-RDP82-00850R000200090053-2

APPROVED FOR RELEASE: 2007/02/08: CIA-RDP82-00850R000200090053-2

The effective heat transfer coefficient can be defined as $\alpha=F/u$, where the complex F characterizes the dependence of α on the gas flow parameters, including the pressure. This complex can also be represented in the form of the sum of the steady-state value and the disturbance

$$F=F_0+\Delta F(t). \tag{8.26}$$

The boundary condition using the function (8.25) is written in the form

$$F(T_\text{в}-T_S)=\varrho u^2 Q_S-\lambda u\left.\frac{\partial T}{\partial x}\right|_S. \tag{8.27}$$

Linearizing (8.27), we obtain

$$\left.\frac{\partial \Delta T}{\partial x}\right|_S+\left.\frac{\partial T_0}{\partial x}\right|_S\frac{\Delta u}{u}=\frac{2\varrho Q_S\Delta u}{\lambda_\text{т}}+\frac{F_0}{\lambda_\text{т}u_0}\Delta T_S-\frac{\Delta F}{\lambda_\text{т}u_0}(T_\text{в}-T_{S_0}). \tag{8.28}$$

Logarithmizing and then differentiating the function (8.1) and proceeding to finite increments, we obtain

$$\Delta u=u_0\frac{E}{2RT_{S_0}^2}\Delta T_S. \tag{8.29}$$

Considering (8.18) and (8.29), it is possible to rewrite equation (8.28) in the form

$$\left.\frac{\partial \Delta T_S}{\partial x}\right|_S-\left[\frac{u_0E}{2RT_{S_0}^2}\left(\frac{T_{S_0}-T_\text{н}}{a_\text{т}}+\frac{2\varrho Q_S}{\lambda_\text{т}}\right)-\frac{F_0}{\lambda_\text{т}u_0}\right]\Delta T_S+ \\ +\frac{\Delta F}{\lambda_\text{т}u_0}(T_\text{в}-T_{S_0})=0. \tag{8.30}$$

Let us consider the deviations from the steady-state mode of combustion of the fuel caused by disturbances accumulated on it. Without going into the primary causes of these disturbances (the random factors, interference of the regulating elements), we shall assume that they reduce to variation of the thermodynamic parameters of the chamber and influence the fuel combustion process by changing the complex F. This, in turn, implies variation of the fuel temperature both on the surface and in depth of the heated layer, and, consequently, the combustion rate. For generality of the investigation we shall assume the variations of ΔF and, consequently, the combustion temperature and rate to be periodic:

$$\left.\begin{aligned}\Delta F&=F_1e^{i\omega t};\\ \Delta T&=f(x)e^{i\omega t};\\ \Delta T_S&=f(0)e^{i\omega t}.\end{aligned}\right\} \tag{8.31}$$

The variation in time of the combustion rate will be determined by the variation in the surface temperature. According to the simplest model of combustion, the reaction zone of the condensed phase is inertialess (see 8.2). This assumption is retained even in the given analysis for low frequencies ω. However, at high frequencies this assumption becomes

FOR OFFICIAL USE ONLY

APPROVED FOR RELEASE: 2007/02/08: CIA-RDP82-00850R000200090053-2

APPROVED FOR RELEASE: 2007/02/08: CIA-RDP82-00850R000200090053-2

incorrect, and the necessity arises for supplementing the function (8.29) by the cofactor taking into account the delay time τ_{delay}:

$$\Delta u = u_0 \frac{E}{2RT_{S_0}^2} f(0)\, e^{i\omega(t-\tau)}. \tag{8.32}$$

Substituting expressions (8.31) and their derivatives in the equation (8.24), after division of both sides by $a_T e^{i\omega t}$ we obtain:

$$f''(x) + \frac{u_0}{a_T} f'(x) - \frac{i\omega}{a_T^2} f(x) = \tilde{A} f(0)\, e^{-\frac{u_0 x}{a_T}}, \tag{8.33}$$

where

$$\tilde{A} = \left(\frac{u_0}{a_T}\right)^2 \frac{E(T_{S_0} - T_H)}{2RT_{S_0}^2} e^{-i\omega\tau}.$$

The boundary condition is converted to the form

$$f'(0) - bf(0) + D = 0, \tag{8.34}$$

where

$$b = \frac{u_0 E}{2RT_{S_0}^2}\left[\frac{T_{S_0} - T_H}{a_T} + \frac{2\varrho Q_S}{\lambda_T}\right] e^{-i\omega\tau} + \frac{F_0}{\lambda_T u_0};$$

$$D = \frac{F_1}{\lambda_T u_0}(T_\delta - T_{S_0}).$$

The characteristic equation of the differential equation (8.33) will have the form

$$z^2 + \frac{u_0}{a_T} z - i\frac{\omega}{a_T} = 0.$$

Its roots will be

$$z_{1,2} = \frac{u_0}{2a_T}\left[-1 \pm \sqrt{1 + i\frac{4\omega a_T}{u_0^2}}\right].$$

Adding the partial solution, we obtain the total solution of the equation (8.33) in the form

$$f(x) = c_1 e^{z_1 x} + c_2 e^{z_2 x} - \frac{a_T}{i\omega}\tilde{A} f(0)\, e^{-\frac{u_0 x}{a_T}}. \tag{8.35}$$

Inasmuch as the amplitude of the temperature fluctuations f(x) for $x \to \infty$ must approach zero, as a result of scattering of the heat waves in the thickness of the fuel the constant c_2 corresponding to the value of z_2 with a plus in front of the radical must equal zero. The constant c_1

APPROVED FOR RELEASE: 2007/02/08: CIA-RDP82-00850R000200090053-2

APPROVED FOR RELEASE: 2007/02/08: CIA-RDP82-00850R000200090053-2

is found from the condition x=0, f(x)=f(0). Defining c_1 and substituting in (8.35), we finally obtain:

$$f(x)=f(0)\left[\left(1+\frac{a_T}{l\omega}\tilde{A}\right)e^{z_1 x}-\frac{a_T}{l\omega}\tilde{A}e^{-\frac{u_0 x}{a_T}}\right]. \tag{8.36}$$

Here

$$f'(0)=f(0)\left[z_1\left(1+\frac{a_T}{l\omega}\tilde{A}\right)+\frac{u_0}{l\omega}\tilde{A}\right]. \tag{8.37}$$

Substituting (8.37) in the boundary condition (8.34), we obtain:

$$f(0)\left[z_1\left(1+\frac{a_T}{l\omega}\tilde{A}\right)+\frac{u_0}{l\omega}\tilde{A}-b\right]+D=0. \tag{8.38}$$

The equations (8.36) and (8.38) define the function f(x) describing the disturbances of the temperature profile of the heated layer of fuel. They can be used to investigate the disturbed combustion conditions of the solid rocket fuel for various oscillatory processes in the engine, but in the given case they are of interest to us from other points of view. When studying the dynamics of the operating process in the solid-fuel rocket engines, the problem acquires primary significance of the admissible limits of use of the steady-state combustion law significantly simplifying the solution of a number of the practical problems, in particular, the problems connected with engine regulation, with calculation of the arrival of the engine at the rated parameter conditions. The time constant of these processes can be provisionally defined as

$$\tau_{\text{дв}}=\frac{1}{4}T=\frac{\pi}{2\omega}.$$

Key: 1. engine

Obviously, the deviation of the disturbed combustion conditions of the fuel from the steady-state conditions is determined by the deviation of the functions f(0) and f(x) from the corresponding functions for the steady-state process. Let us perform this analysis, assuming in advance that $4\omega a_T/u_0^2<<1$. Here the expression for z_1 can be represented in the form

$$z_1=-\frac{u_0}{a_T}\left(1+l\frac{\omega a_T}{u_0^2}\right). \tag{8.39}$$

Substituting (8.39) in equation (8.36), after transformation we obtain

$$f(x)=f(0)\left[e^{-\frac{u_0 x}{a_T}}e^{-l\frac{\omega}{u_0}x}+\frac{a_T}{l\omega}\tilde{A}e^{-\frac{u_0 x}{a_T}}\left(1-e^{-\frac{l\omega x}{u_0}}\right)\right].$$

FOR OFFICIAL USE ONLY

APPROVED FOR RELEASE: 2007/02/08: CIA-RDP82-00850R000200090053-2

APPROVED FOR RELEASE: 2007/02/08: CIA-RDP82-00850R000200090053-2

Expanding the exponent exp $(-xi\omega/u_0)$ in a series and dropping the terms of the expansion of the second order of smallness for the first term and the third order of smallness for the second, and after a series of transformations we obtain

$$f(x)=f(0)\,e^{-\frac{u_0 x}{a_T}}\left(1-\frac{i\omega x}{u_0}\right).$$

Let us convert the second term in parentheses

$$\frac{i\omega x}{u_0}=\frac{i\omega x}{a_T/u_0}\frac{a_T}{u_0^2}=i\,\frac{\pi}{2}\,\frac{\tau_p}{\tau_{кв}}\,\frac{x}{x_p}.$$

Substituting (8.39) in (8.38), we obtain

$$f(0)=\frac{D}{b+\frac{u_0}{a_T}\left(1+\frac{i\omega}{u_0^2}\,a_T\right)}. \tag{8.40}$$

Let us convert the second term in parentheses

$$\frac{i\omega}{u_0^2}a_T=i\,\frac{\pi}{2}\,\frac{\tau_p}{\tau_{кв}}.$$

Using the expressions obtained, let us represent f(x) in the form

$$f(x)=\frac{D}{b+\frac{u_0}{a_T}\left(1+i\frac{\pi}{2}\,\frac{\tau_p}{\tau_{кв}}\right)}\,e^{-\frac{u_0 x}{a_T}}\left(1-i\,\frac{\pi}{2}\,\frac{\tau_p}{\tau_{кв}}\,\frac{x}{x_p}\right). \tag{8.41}$$

According to the relation obtained, the deviation of the disturbed profile from exponential exp $(-u_0x/a_T)$ will increase on going away from the surface as a result of the thermal inertia of the fuel. For $x=x_p$ the relative deviation will be $i(\pi/2)(\tau_p/\tau_{engine})$. On satisfaction of the inequality $|\pi\tau_p/2\tau_{engine}|<<1$, for the disturbed profile we obtain the relations

$$f(x)=f(0)\,e^{-\frac{u_0 x}{a_T}} \tag{8.42}$$

$$f(0)=\frac{F_1(T_в-T_{S_0})}{\left(b+\frac{u_0}{a_T}\right)\lambda_T u_0}. \tag{8.43}$$

The expressions (8.43) can be obtained from the boundary condition (8.27) written for the stationary process

$$F(T_в-T_{S_0})+Q_T u^2 Q_S=c_T\varrho_T u^2(T_{S_0}-T_н). \tag{8.44}$$

APPROVED FOR RELEASE: 2007/02/08: CIA-RDP82-00850R000200090053-2

APPROVED FOR RELEASE: 2007/02/08: CIA-RDP82-00850R000200090053-2

We shall assume that the variation of the gas dynamic parameters causing variation of F from F_0 to F_0+F_1 implies variation of ΔT_S and the combustion rate Δu without disturbance of the stationarity of the process, that is, the equation (8.44) is retained. Here, for the disturbed process we obtain

$$F_0\Delta T_S+F_1(T_s-T_{s_0})+2Q_S\Delta u=2c_\tau Qu(T_{s_0}-T_\infty)\Delta u+c_\tau Q_\tau u^2\Delta T_{s_0}. \quad (8.45)$$

Expressing Δu in terms of ΔT_S according to the function (8.29) and determining the variation of the combustion surface temperature ΔT_S from equation (8.45) caused by the variation of the complex F_1, we arrive at the expression identical to (8.43).

Consequently, when observing the condition $|(\pi/2)(\tau_p/\tau_{engine}|<<1$, the function f(0) expresses the temperature variation of the combustion surface and, consequently, the combustion rate without disturbance of the stationarity of the combustion process. The satisfaction of this condition for the equation (8.41) leads to the fact that the surface temperature variation implies rearrangement of the temperature profile of the heated layer also without departing from the Michelson exponential curve. Hence, the simplest condition of the use of the known relations for the steady-state combustion is obtained, including the power law of combustion on variation of the operating conditions of the solid fuel rocket engine

$$\tau_{AB}\gg\frac{\pi}{2}\tau_p.$$

Usually the time of thermal relaxation fluctuates within the limits of 0.001-0.004 sec. Here the time of the transient process permitting calculations based on the steady-state combustion conditions will be 0.005 to 0.02 seconds.

8.4. Instability of Combustion in Solid-Fuel Rocket Engines

In Part I a study was made of the problem of the static stability of the operating conditions of the solid-fuel rocket engine which will always be insured for $\nu<1$ under the assumption that the combustion rate will vary according to the stationary law $u=u_1p^\nu$.

The concept of the dynamic stability will be related to the nonstationarity of combustion occurring for random fluctuations of the pressure in the chamber. The random fluctuations of the pressure in the chamber of the solid-fuel rocket engine will lead to variation of the combustion rate, and the variation of the inflow of gases caused by this will imply pressure variation. Inasmuch as the pressure variation in the oscillatory process takes place quite rapidly, the combustion surface temperature cannot trace these variations, and the combustion process will acquire a nonsteady-state nature.

FOR OFFICIAL USE ONLY

APPROVED FOR RELEASE: 2007/02/08: CIA-RDP82-00850R000200090053-2

APPROVED FOR RELEASE: 2007/02/08: CIA-RDP82-00850R000200090053-2

The discovery of the conditions for which the dynamic instability of the combustion appears has great practical importance inasmuch as the dynamically unstable combustion process can in certain cases lead to complete extinguishing of the combustion, and in other cases, to loss of pressure threatening the stability of the engine.

At the present time two basic types of instability of combustion in solid-fuel rocket engines are distinguished.

1) Low-frequency instability for which the pressure varies with respect to the entire rocket chamber simultaneously (f<<100 hertz);

2) High-frequency instability which is connected with the propagation of acoustic waves through the chamber which amplify on reflection from the combustion surface (f>100 hertz).

8.4.1. Low-Frequency Instability of Combustion in the Solid-Fuel Rocket Engines

The study of the low-frequency instability can be performed on the basis of the linearized system of equations investigated in 8.3. In addition, it is necessary to use the equation 7.8 which relates the pressure variation in the chamber to the gas inflow and the gas flow rate to the nozzle and also the equation of the pressure fluctuations

$$\frac{\Delta p}{p_0} = pe^{i\omega t},$$

where p is the dimensionless amplitude of the pressure.

On the basis of solving the analogous system of equations B. V. Novozhilov [32] defined the conditions of occurrence of the low-frequency instability. According to these investigations the basic complex parameters determining the limits of stable combustion are the following: $\chi_\tau=\tau_k/\tau_p$ is the ratio of the time constant of the chamber to the time of thermal relaxation;

$$K=D(T_{s_0}-T_н),$$

where D is the temperature constant of the fuel (see Part I, Chapter 10).

$$r=\left(\frac{\partial T_{s_0}}{\partial T_н}\right)_{p=\text{const}}.$$

The results of the investigations of B. V. Novozhilov are presented in Fig 8.3 [32]. The regions of stability with possible extinguishing of combustion are to the right of the plotted curves.

For powder H, according to B. V. Novozhilov, in the range $T_н$=-50 to +50°C, the value of K varies from 1.2 to 2.0. Here r varies from 0.2 to 0.4.

APPROVED FOR RELEASE: 2007/02/08: CIA-RDP82-00850R000200090053-2

APPROVED FOR RELEASE: 2007/02/08: CIA-RDP82-00850R000200090053-2

These figures obtained for fuel with high temperature function in the first approximation determine the operating region of the graph for which the values of χ_τ vary within the limits from 0.3 to 1.5.

According to the graph when estimating the combustion stability the criterion χ_τ plays an important role. The importance of this criterion is confirmed by many experimental data.

In foreign literature the low-frequency instability has come to be called the L* type instability inasmuch as the limits of its appearance are connected with the reduced length of the chamber $L^*=W/F_{cr}$. In reference [19] an experimental graph is presented which defines the region of stable combustion in the coordinates L*-u (Fig 8.4). The graph is constructed by the test data for different compositions of the solid rocket fuel, with a wide range of combustion rates. The lower stability limit is defined by the equation

$$L^* = 13{,}8/u^2,$$

where L* is in liters, and u is in mm/sec.

The meaning of this relation becomes clear from the expanded expression for χ_τ:

$$\chi_\tau = \frac{\tau_к}{\tau_p} = \frac{Wu^2}{F_{кр}} \frac{1}{\varphi_c A \sqrt{\chi f_p a_\tau}},$$

from which

$$L^* u^2 = \chi_\tau \varphi_c A \sqrt{\chi f_p a_\tau}. \qquad (8.46)$$

As follows from the graphs in 8.3 and from the analysis of the function 8.46, the stability of combustion with low-frequency oscillations can be insured for a value of χ_τ essentially less than one, that is, for $\tau_k < \tau_p$. This is obviously explained by the fact that the variation of the combustion rate for low-frequency oscillations touches on variation of a small section of the temperature profile of the heated layer of the fuel and does not require rearrangement of the entire profile.

The combustion stability increases with an increase in the operating pressure inasmuch as in this case τ_k increases as a result of a decrease in the recorded area F_{cr}, and τ_p decreases as a result of an increase in the combustion rate.

The combustion stability increases also when the temperature dependence of the combustion rate decreases, that is, when the characteristic D decreases.

The low-frequency instability is characteristic of small engines inasmuch as the values of τ_k and L* decrease with a decrease in the bore. This is explained by the fact that when observing the geometric similarity,

APPROVED FOR RELEASE: 2007/02/08: CIA-RDP82-00850R000200090053-2

APPROVED FOR RELEASE: 2007/02/08: CIA-RDP82-00850R000200090053-2

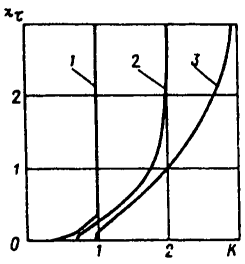

Figure 8.3. Boundaries of the low-frequency instability of combustion in a solid-fuel rocket engine in the coordinates χ_τ, K: 1 -- r=0; 2 -- r=1/3; 3 -- r=1.

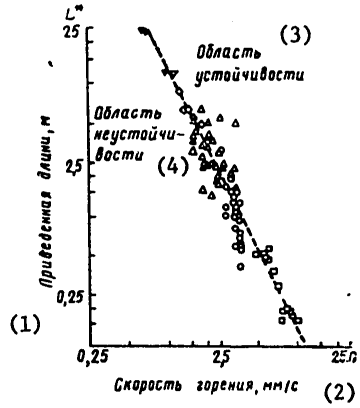

Figure 8.4. Boundaries of low-frequency instability of combustion in the solid-fuel rocket engines in the coordinates L*, u
Key:
1. Reduced length, meters
2. Combustion rate, mm/sec
3. Region of stability
4. Region of instability

the free volume varies proportionately to the tube of the bore at the same time as the area of critical cross section for the given pressure varies proportionately to the square of the bore.

The low-frequency instability of combustion can lead to discontinuous combustion and extinguishing of the charge. In order to exclude the possibility of this phenomenon it is necessary to observe the condition L* $L^*>13.8/u^2$ when designing the engine.

8.4.2. High-Frequency Instability of the Combustion in the Solid-Fuel Rocket Engine

Under certain conditions of combustion in solid-fuel rocket engines, the acoustic vibrations in the chamber cavity, interacting with the combustion surface, can be amplified. The amplification of the vibrations can lead to the occurrence of a stable oscillatory mode in which the average linear combustion rate of the fuel increases significantly by comparison with its steady-state value. The consequence is a sharp rise in pressure in the engine. This phenomenon is known in the literature as acoustic instability of combustion, vibration or resonance combustion. The outward sign of the vibration combustion is the appearance on the oscillogram of secondary pressure peaks.

APPROVED FOR RELEASE: 2007/02/08: CIA-RDP82-00850R000200090053-2

APPROVED FOR RELEASE: 2007/02/08: CIA-RDP82-00850R000200090053-2

Acoustic instability is related to the amplification of one of the modes of the acoustic vibrations of the column of gas in the inside cavity of the charge. It is possible for various shapes of charge, but caps with cylindrical channels are the most predisposed to it.

The inclination of the operation conditions of the engine to the occurrence of acoustic instability is determined by the relation of the inflow of the energy of the acoustic vibrations and its losses. The amplification of the pressure waves on reflection of them from the combustion surface can be suppressed by the damping effect of the structural elements and also condensed particles present in the products of the combustion and fuel. The operating stability criterion is the losses exceeding the energy inflow:

$$E_{ak} - E_g - E_k < 0,$$

where E_{ak} is the inflow of acoustic energy per second; E_g are the losses caused by the damping effect of the particles of the condensed phase; E_k are the losses caused by the boundaries of the gas volume including the extinguishing effect of the engine housing, the charge and the subsonic part of the nozzle and also the losses as a result of heat transfer.

APPROVED FOR RELEASE: 2007/02/08: CIA-RDP82-00850R000200090053-2

APPROVED FOR RELEASE: 2007/02/08: CIA-RDP82-00850R000200090053-2

CHAPTER 9. OPERATION OF SOLID-FUEL ROCKET ENGINES UNDER TRANSITIONAL CONDITIONS

9.1. General Characteristics of the Transitional Operating Conditions of Solid-Fuel Rocket Engines

By the transitional operating conditions of a solid-fuel rocket engine we mean the process of deep variation of its operating parameters on transition from one steady-state or quasisteady-state to another.

The basic types of transitional operating conditions of the solid-fuel rocket engines are the following:

1. Arrival of the engine at the stationary operating conditions after ignition of the charge;

2. Transitional operating conditions with step variation of the thrust;

3. Theafterflaming period of the solid-fuel rocket engine after burnup of the fuel;

4. The period of extinguishing of the charge carried out in order to kill the thrust.

It is also necessary to consider some of the processes caused by the random disturbing factors among the transitional operating conditions.

All of the indicated cases can be described by a unique system of nonlinear differential equations which on the basis of the calculations of Chapter 7 can be represented in general form as

$$1.\ \frac{W}{RT_к}\frac{dp}{dt}=\frac{dW}{dt}Q_т\left(1-\frac{p_к}{Q_тRT_к}\right)-\frac{\varphi_c AF_{кр}}{\sqrt{RT_к}}p_к+\frac{p_кW}{(RT_к)^2}\frac{d(RT_к)}{dt};$$

$$2.\ \frac{p_кW}{T_к}\frac{dT}{dt}=Y(t)R(\chi T_V-T_к)-(k-1)\varphi_c AF_{кр}p\sqrt{RT_к}-\frac{dQ}{dt}(k-1);$$

APPROVED FOR RELEASE: 2007/02/08: CIA-RDP82-00850R000200090053-2

APPROVED FOR RELEASE: 2007/02/08: CIA-RDP82-00850R000200090053-2

$$
\begin{aligned}
&3.\ p_к = \frac{m_к R T_к}{W};\\
&4.\ Y(t) = \int_0^{S_э} \varrho u dS_э;\\
&5.\ \frac{dQ}{dt} = \int_0^{S_к} \alpha (T_к - T_{сн})\, dS_к;\\
&6.\ S = S_0 \sigma(\psi)\ \varepsilon = \varepsilon_0 f(\psi).
\end{aligned}
\qquad (9.1)
$$

The solution of the system 9.1 makes it possible to determine the variation in time of the basic thermodynamic parameters averaged over the engine volume -- the pressure, density and temperature of the combustion products, and in case of necessity, calculations of the thrust parameters of the engine on the basis of their values.

The system of equations (9.1) presented in this form does not reflect the individual peculiarities of one engine or another, and in each individual case it is necessary to specify equations 4, 5, 6 in accordance with the model used and the combustion law of the fuel, the shape of the charge and the structural layout. Depending on the investigated version of the problem, the initial conditions vary under which the integration of system (9.1) is performed, and the equations themselves can be subject to certain alterations. For example, when solving the problem of extinguishing of the charge by introducing a coolant, additional terms are introduced into equations 1 and 2. In individual cases entire equations drop out.

In the general case the system of equations (9.1) can be solved only by numerical methods. The difficult of its solution is determined not by the mathematical complexity of the problem which easily can be overcome by using the computer, but by the insufficiency of digital data and the functional relations for determining a number of the input parameters.

In order to obtain approximate analytical solutions it is necessary to make a number of simplifying assumptions determined by the specific statement of the problem.

In the given chapter a discussion is presented of the solutions obtained for the basic cases of the transitional operating conditions of solid-fuel rocket engines.

FOR OFFICIAL USE ONLY

APPROVED FOR RELEASE: 2007/02/08: CIA-RDP82-00850R000200090053-2

APPROVED FOR RELEASE: 2007/02/08: CIA-RDP82-00850R000200090053-2

30 JUNE 1980 YE. B. VOLKOV, T. A. SYRITSYN AND G. YU. MAZIN 4 OF 4

BY

APPROVED FOR RELEASE: 2007/02/08: CIA-RDP82-00850R000200090053-2

APPROVED FOR RELEASE: 2007/02/08: CIA-RDP82-00850R000200090053-2

9.2. Engineering Method of Calculating the Arrival of the Solid-Fuel Rocket Engine in the Steady-State Operating Conditions

The process of starting a solid-fuel rocket engine can provisionally be divided into periods:

1) Ignition of the solid-fuel charge under the effect on its surface of the products of combustion of the igniters;

2) Arrival of the engine at the rated parameter regime.

Although a clear boundary between these periods is absent, it is expedient to consider them separately in view of the significant difference of the physical picture of the process and the mathematical model corresponding to it.

The period of arrival of the solid-fuel rocket engine at the steady-state operating conditions is characterized by a sharp increase in pressure in the combustion chamber and thrust. When organizing this process usually we are guided by the maximum admissible time for reaching the operating conditions which, depending on the engine bore, can fluctuate within very broad limits.

The approximate procedure for calculating the parameters of the solid-fuel rocket engines when reaching the rated thrust regime is based on the following assumptions:

1. The fuel combustion regime is assumed to be quasistationary. Under this condition the combustion rate of the fuel varies in strict correspondence to the pressure according to the empirical stationary combustion law (power law, linear law, Sommerfield law).

2. The thermodynamic temperature of combustion of the fuel is assume to be constant and equal to T_V/k.

3. The heat losses are considered by the heat loss coefficient χ introduced into the calculation in the form of the function of ψ or a constant mean value.

4. It is proposed that during the period of reaching the operating conditions the effect of the incompletely burned remains of the igniter is negligibly small.

The first assumption, which is entirely correct for the conditions of the given problem, exclude the system of equations describing the nonsteady-state combustion of the fuel from investigation. In the given item the power law of combustion is used in place of it.

APPROVED FOR RELEASE: 2007/02/08: CIA-RDP82-00850R000200090053-2

APPROVED FOR RELEASE: 2007/02/08: CIA-RDP82-00850R000200090053-2

FOR OFFICIAL USE ONLY

The second and third assumptions pertain to consideration of the temperature variation of the gases in the solid fuel rocket engine chamber which in the general case is described by the equation 7.12. As the numerical equation of the systems of equations similar to 9.1 indicates [43], [3], during the course of reaching the operating conditions the temperature variations of the gases in the chamber defined by equations 7.12 in the absence of heat losses to the engine housing is small. The actual value of the gas temperature in the chamber of the solid-fuel rocket engine is determined to a significant degree by the heat losses. With time the ratio T_k/T_V determined from equation 7.12 in the absence of heat losses decreases, asymptotically approaching a value of 1/k, and the coefficient χ increases, which leads to partial compensation of the effects of these factors. In the case where the law of variation of χ from ψ is determined from experience, it reflects the combined appearance of two factors.

Under the adopted assumptions, the system of equations 9.1 assumes the form

$$\begin{aligned}
&1.\ \frac{W}{\chi f_p}\frac{dp}{dt}=Y(t)-\frac{\varphi_c A F_{кр}}{\sqrt{\chi f_p}}p_к.\\
&2.\ p_к=\frac{m_к \chi f_p}{W}.\\
&3.\ Y(t)=Q_т\frac{dW}{dt}=Q_т\Gamma p^\nu.\\
&4.\ \Gamma(\psi)=u_{1т}\left[\sigma_б(\psi)S_{б_0}k_и\varepsilon+S_{т_0}\frac{\varepsilon(\psi)}{\varepsilon_0}\right].\\
&5.\ \chi=\chi(\psi)\ \text{или}\ \chi=\text{const}=\bar{\chi}.
\end{aligned}\tag{9.2}$$

The initial conditions

$$t=0;\ \psi=0;\ p=p_0;\ W=W_0.$$

Let us rewrite the first equation of system 9.2 in the form

$$\frac{W}{\chi f_p}\frac{dp}{dt}=Q_т\Gamma p^\nu-\frac{\varphi_c A F_{кр}}{\sqrt{\chi f_p}}p.\tag{9.3}$$

Let us make the substitution:

$$dt=\frac{dW}{\Gamma p^\nu}.\tag{9.4}$$

Substituting (9.4) in (9.3) and separating variables, we obtain

$$Q_т\chi f_p\frac{dW}{W}=\frac{dp}{1-\frac{\varphi_c A F_{кр}}{Q\Gamma\sqrt{\chi f_p}}p^{1-\nu}}.\tag{9.5}$$

FOR OFFICIAL USE ONLY

APPROVED FOR RELEASE: 2007/02/08: CIA-RDP82-00850R000200090053-2

APPROVED FOR RELEASE: 2007/02/08: CIA-RDP82-00850R000200090053-2

Let us proceed to the relative pressure $\pi_p = p/p_{steady\ state}$, where $p_{steady\ state}$ is the pressure in the steady state operating conditions of the solid fuel rocket engine determined from the Bohr equation:

$$p_{\underset{(1)}{уст}} = \left(\frac{\varrho_T \sqrt{\chi f_p}}{\varphi_c A F_{\underset{(2)}{кр}}}\right)^{\frac{1}{1-\nu}}. \tag{9.6}$$

Key: 1. steady state; 2. cr

The dynamic value of the free volume will be expressed as

$$W = W_0 + \frac{\omega}{\varrho_T}\psi = W_0\left(1 + \frac{\omega}{\varrho_T W_0}\psi\right),$$

where W_0 is the free volume at the beginning of the process; ψ is the relative proportion of the charge burning by the investigated point in time; ω is the mass of the charge.

Let us denote $b = \omega/\rho_T W_0$.

Here $dW = W_0 b d\psi$.

The equation (9.5) is written in new variables in the form

$$\frac{\varrho_T \chi f_p}{p_{\underset{(1)}{уст}}} \frac{b d\psi}{1 + b\psi} = \frac{d\Pi}{1 - \Pi^{1-\nu}}. \tag{9.7}$$

Key: 1. steady state

It is possible to substitute the function $\chi(\psi)$ in the equation obtained. Let us substitute it in accordance with the recommendations of Prof Ya. M. Shapiro [43] in the form

$$\chi = 1 - \frac{Б}{1 + a\psi}.$$

Integrating the lefthand side with respect to ψ within the limits from 0 to ψ and the righthand side from Π_0 to Π, we obtain

$$\ln(1 + b\psi) - \frac{Бb}{b - a}\ln\left|\frac{1 + b\psi}{1 + a\psi}\right| = \frac{p_{пр}}{\varrho_T f_p}[M(\Pi, \nu) - M(\Pi_0, \nu)], \tag{9.8}$$

where

$$M(\Pi, \nu) = \int_0^{\Pi} \frac{d\Pi}{1 - \Pi^{1-\nu}}.$$

The integration of equation (9.7) for constant average value of $\bar{\chi}$ leads to the function

APPROVED FOR RELEASE: 2007/02/08: CIA-RDP82-00850R000200090053-2

APPROVED FOR RELEASE: 2007/02/08: CIA-RDP82-00850R000200090053-2

$$\ln(1+b\psi)=\frac{p_{\text{нр}}^{(1)}}{\varrho_{\text{т}}\chi f_{\text{р}}}[M(\Pi,\nu)-M(\Pi_0,\nu)]. \qquad (9.9)$$

Key: 1. lim

The values of the function M(Π, ν) are presented in Table 9.1. According to the function (9.7)

$$\frac{d\Pi}{d\psi}=\frac{\varrho_{\text{т}}\chi f_{\text{р}}b}{p_{\text{уст}}(1+b\psi)}[1-\Pi^{1-\nu}].$$

Equating dΠ/dψ to zero, we obtain the condition of maximum: $\Pi^{1-\nu}=1$, defining the limited to which the pressure approaches in the chamber during the process of its growth: Π→1, $p\to p_{\text{lim}} \equiv p_{\text{steady state}}$. From the expression for Mx(Π, ν) it follows that for the operating condition limit Π=1 the value of the integral approaches infinity; according to the equation (9.9) in this case ψ also is equal to infinity. Consequently, the pressure in the steady state mode defined by the equality of the flow rate and the arrival of the gases is the limit to which the actual pressure approaches asymptotically. However, in practice for Π>0.95-0.97 the pressure deviations from the theoretical value become less than the deviations caused by the dispersion of the charging parameters and other random factors.

If in the charge combustion process in the investigated period a change in the charging parameters takes place, this leads to variation of the limiting pressure. It is necessary most frequently to deal with the variable value of Γ. The variation of Γ is caused primarily by variations of the erosion effect during erosion of the charge channel, and to a lesser degree by variation of the combustion surface. With variation of Γ, the limit will change to which the pressure approaches in the engine at the given point in time. In other words, the limit itself is a sliding value, which must find reflection in the procedure for calculating the curve p(t) or p(ψ).

Let us consider the sequence for calculating the curve p(t) based on the relations obtained.

A. Procedure for Constructing the Pressure Curve with a Constant Value of Γ(ψ)

By the given values of the charge parameters using formula 9.6, the limiting pressure p_{lim} and the value of $\Pi_0=p_0/p_{\text{lim}}$ corresponding to it is calculated.

2. Being given arbitrary values of ψ, let us determine the value of the function M(Π, ν) corresponding to them:

$$M(\Pi,\nu)=M(\Pi_0,\nu)+\frac{\varrho_{\text{т}}\chi f_{\text{р}}}{p_{\text{нр}}}\ln(1+b\psi)$$

FOR OFFICIAL USE ONLY

APPROVED FOR RELEASE: 2007/02/08: CIA-RDP82-00850R000200090053-2

APPROVED FOR RELEASE: 2007/02/08: CIA-RDP82-00850R000200090053-2

Table 9.1

$$M(\Pi, \nu)=\int_0^{\Pi}\frac{d\Pi}{1-\Pi^{1-\nu}}$$

Π \ ν	0,25	0,3	0,4	0,5	0,6	0,7
0,10	0,1116	0,1137	0,1193	0,1278	0,1416	0,1660
0,20	0,2435	0,2499	0,2665	0,2911	0,3298	0,3966
0,24	0,3025	0,3111	0,3336	0,3665	0,4178	0,5062
0,28	0,3654	0,3766	0,4058	0,4481	0,5139	0,6266
0,32	0,4327	0,4469	0,4835	0,5366	0,6186	0,7586
0,36	0,5048	0,5224	0,5675	0,6326	0,7327	0,9033
0,40	0,5823	0,6037	0,6584	0,7369	0,8574	1,0621
0,44	0,6601	0,6916	0,7570	0,8506	0,9939	1,2368
0,48	0,7567	0,7871	0,8644	0,9750	1,1438	1,4294
0,52	0,8554	0,8912	0,9821	1,1117	1,3091	1,6425
0,56	0,9636	1,0054	1,1116	1,2626	1,4924	1,8797
0,60	1,0829	1,1317	1,2552	1,4305	1,6968	2,1453
0,64	1,2158	1,2725	1,4158	1,6189	1,9269	2,4450
0,68	1,3654	1,4312	1,5973	1,8324	2,1885	2,7868
0,72	1,5361	1,6125	1,8052	2,0777	2,4898	3,1816
0,76	1,7344	1,8234	2,0477	2,3645	2,8431	3,6457
0,80	1,9703	2,0747	2,3374	2,7079	3,2672	4,2043
0,84	2,2608	2,3844	2,6952	3,1331	3,7936	4,8994
0,88	2,6374	2,7865	3,1608	3,6878	4,4818	5,8102
0,90	2,8770	3,0425	3,4578	4,0421	4,9222	6,3940
0,92	3,1711	3,3569	3,8229	4,4782	5,4647	7,1140
0,94	3,5513	3,7635	4,2956	5,0434	6,1686	8,0492
0,96	4,0885	4,3384	4,9646	5,8441	7,1671	9,3772
0,98	5,0094	5,3243	6,1131	7,2204	8,8849	11,6642
0,99	5,9319	6,3123	7,2650	8,6016	10,6102	13,9630

On assigning the coefficient χ the average value,

$$M(\Pi, \nu)=M(\Pi_0, \nu)+\frac{Q_T\chi f_p}{p_{np}}\left[\ln(1+b\psi)-\frac{Бb}{b-a}\ln\frac{1+b\psi}{1+a\psi}\right]$$

On assigning χ as a function of ψ.

3. In order to obtain the values of $M(\Pi, \nu)$ the values of Π are found from the tables, the value of $p=p\lim\Pi$ is calculated, and the graph of the function $p(\psi)$ is constructed.

APPROVED FOR RELEASE: 2007/02/08: CIA-RDP82-00850R000200090053-2

APPROVED FOR RELEASE: 2007/02/08: CIA-RDP82-00850R000200090053-2

4. In order to reconstruct the curve $p(\psi)$ into the curve $p(t)$, an auxiliary function is used:

$$dt = \frac{dW}{\Gamma p^{\nu}} = \frac{\omega d\psi}{\varrho_{\tau}\Gamma p^{\nu}},$$

from which

$$\Delta t = \frac{\omega}{\varrho_{\tau}\Gamma p^{\nu}}\Delta\psi.$$

B. Procedure for Constructing the Pressure Curve with a Variable Value of $\Gamma(\psi)$.

The calculation of the pressure curve is preceded by construction of the graph $\Gamma(\psi)$.

For this purpose it is necessary:

1) Being given the arbitrary values of ψ, using the geometric relations for the charge of given shape, we determine the values of $\sigma_b(\psi)$ and $\varepsilon(\psi)$ corresponding to the assumed ψ.

2) By the complex $F_{k.c}(1-\varepsilon)/\phi_c F_{cr}$, from the graph 7.1, we determine Ku for each of the adopted ψ.

3) Calculate the values of $\Gamma(\psi)$ by formula 7.22.

In the case where the function $\Gamma(\psi)$ undergoes significant changes in the time of reaching the operating conditions, the proposed interval ψ from zero to the finite value is broken down into a number of sections permitting the assumption of the value of $\Gamma(\psi)$ within the limits of each of them to be the average constant value. Here, for each of the sections the sequence for the calculations is assumed to be the following:

1. The mean values are determined

$$\bar{\Gamma}(\psi) = \frac{1}{2}[\Gamma(\psi_i) + \Gamma(\psi_{i-1})];$$

$$\bar{\chi} = \frac{1}{2}[\chi(\psi_i) + \chi(\psi_{i-1})];$$

$$p_{np\,i} = \left(\frac{\varrho_{\tau}\bar{\Gamma}(\psi)\sqrt{\bar{\chi} f_p}}{\varphi_c A F_{\kappa p}}\right)^{\frac{1}{1-\nu}}.$$

2. The values of $\Pi_{i=1} = p_{i-1}/p_{\lim\, i}$ are determined.

For $i-1=0$, $p_{i-1} = p_0$.

APPROVED FOR RELEASE: 2007/02/08: CIA-RDP82-00850R000200090053-2

APPROVED FOR RELEASE: 2007/02/08: CIA-RDP82-00850R000200090053-2

3. The value of the function is found

$$M(\Pi_i, \nu) = M(\Pi_{i-1}, \nu) + \frac{\varrho_T \bar{\chi} f_p}{p_{\text{кр}} l} \ln \frac{1 + b\psi_i}{1 + b\psi_{i-1}}.$$

4. From the tables Π_i is found, and $p_i = p_{\lim i} \Pi_i$ is calculated. The reconstruction of the curve $p(\psi)$ into $p(t)$ is realized just as in the case of Γ=const.

If the parameters of the transient regime are to be determined in the first approximation, it is possible to use the relation obtained when assuming W=const.

The integration of the equation (9.3) for $W=W_0$=const leads to the function

$$t = \frac{W_0}{\varphi_c A F_{\text{кр}} \sqrt{\bar{\chi} f_p}} \int_{\Pi_0}^{\Pi_\text{к}} \frac{d\Pi}{\Pi^\nu - \Pi}. \qquad (9.10)$$

Inasmuch as Π=1 is reached for $t \to \infty$ when estimating the time of reaching the operating conditions it is necessary to give the value of Π_k differing from one, but quite close to it. The formula (9.10) can be represented in the form

$$\frac{t}{\tau_{\text{к}0}} = N(\Pi_0, \nu),$$

where $\tau_{\text{к}0} = \frac{W_0}{\varphi_c A F_{\text{кр}} \sqrt{\bar{\chi} f_p}}$. is the time constant of the solid-fuel rocket engine chamber calculated for $W=W_0$.

In Table 9.2 the values are presented of the integral $N(\Pi_0, \nu)$ which we calculated for Π_k=0.95.

Table 9.2

$$N = \int_{\Pi_0}^{0,95} \frac{d\Pi}{\Pi^\nu - \Pi}$$

ν \ Π_0	0,1	0,2	0,25	0,30	0,35	0,40	0,50
0,3	4,4603	4,2186	4,0978	3,9739	3,8453	3,7101	3,4125
0,4	5,3452	5,0286	4,8749	4,7194	4,5595	4,3930	4,0305
0,5	6,5920	6,1667	5,9660	5,7854	5,5612	5,3505	4,8964
0,6	8,4726	7,8791	7,6065	7,3373	7,0661	6,7884	6,1962
0,7	11,6211	10,7401	10,3459	9,9611	9,5772	9,1872	8,3640

APPROVED FOR RELEASE: 2007/02/08: CIA-RDP82-00850R000200090053-2

APPROVED FOR RELEASE: 2007/02/08: CIA-RDP82-00850R000200090053-2

9.3. Transient Conditions on Step Variation of the Thrust

In rocket building the two-regime solid-state rocket engine with program step variation of the thrust during the operating process of the engine has become mostly widespread.

The reconstruction of the operating conditions of the solid-state rocket engine can be insured by different means:

By selecting the form of the charge with step variation of the surface during combustion;

By application of the combined charge from two successively burning fuels with different u_1;

By variation of the area of the critical cross section of the nozzle.

Various combinations of the indicated procedures are possible. If the variation of the combustion surface or the combustion rate combined with the variation of F_{cr} running in the same direction (a decrease or an increase), the step diagram of the thrust is insured for constant pressure in the engine without reconstruction of the chamber operating conditions. In the given case we are not interested in such conditions. Let us consider the conditions of variation of the thrust connected with variation of the operating pressure in the engine.

In the case where the pressure in the engine increases with step adjustment of the thrust, the relations obtained in Section 9.2 can be used to calculate the transient process. In this case it is necessary to remember that the calculation of ψ can begin with zero. The free volume of the chamber available at this point in time and the remaining mass of fuel are taken as the zero parameters. The coefficient b is calculated by these parameters. By the characteristics of the remaining part of the charge, the new value of $p_{lim\ 2}$ is calculated. The value of $p_{lim\ 1}$ corresponding to the preceding period is taken as p_0 for the calculation. In this case $\Pi_0=p_{lim\ 1}/p_{lim\ 2}$.

For cases where the pressure variation is caused by step variation of the combustion surface or u_1, the calculation can be performed by the procedure for the version of constant F_{cr}.

In the case of step variation of F_{cr} which is insured by shifting the central body or the moving entrance part of the nozzle [47], the kinematics of the overlap of F_{cr} can be taken into account: $\Delta F_{cr}=f(t)$. In this case the calculation is made by the procedure for the case of $\Gamma(\psi)$=var, except that $\Gamma(\psi)$ remains constant, and $p_{lim\ i}$ varies as a function of the current value of F_{cr}. Here the calculation is made in this order. For each point in time the current value of F_{cr} is determined, and by it, $p_{lim\ i}$ is calculated. The step size with respect to ψ for each next step of the calculation is defined as

APPROVED FOR RELEASE: 2007/02/08: CIA-RDP82-00850R000200090053-2

APPROVED FOR RELEASE: 2007/02/08: CIA-RDP82-00850R000200090053-2

$$\Delta\psi=\psi_i-\psi_{i-1}=\frac{\varrho_\tau\Sigma p_i^\nu}{\omega}\Delta t.$$

For the rest the calculation scheme remains as before.

Let us consider the case of step decrease in pressure in the solid-fuel rocket engine. In this case the pressure in the chamber for transient operating conditions, approaching its new limit, will approach it from the top. In this case the values of $\Pi=p/p_{lim\ 2}$ will decrease, beginning with $\Pi_1=p_{lim\ 1}/p_{lim\ 2}$, asymptotically approaching one. For the investigated case the equations investigated in Section 9.2 remain valid except for the difference that the derivative dp/dt will have a negative sign which leads to variation of the integration limits. Here the summary function assumes the form

$$\frac{\varrho_\tau\chi f_p}{p_{np2}}\ln(1+b\psi)=\int_{\Pi_1}^{\Pi}\frac{d\Pi}{\Pi^{1-\nu}-1}.$$

Let us denote

$$\tilde{M}(\Pi,\nu)=\int_{\Pi_1}^{\Pi_k}\frac{d\Pi}{\Pi^{1-\nu}-1},$$

where Π_k is the provisional integration limit differing from one, permitting the appearance of a nonsingular integral to be avoided. Then the operating function assumes the form:

$$\ln(1+b\psi)=\frac{p_{np2}}{\varrho_\tau\bar{\chi}f_p}[\tilde{M}(\Pi_1,\nu)-\tilde{M}(\Pi,\nu)]. \tag{9.11}$$

Here the calculation sequence remains the same as with a rise in pressure. The values of $\tilde{M}(\Pi,\nu)$ which we calculated for different values of ν and Π_1 are presented in Table 9.3. For the calculation, as the upper integration limit we used $\Pi_k=1.05$. In a number of cases when calculating the process of the pressure decrease it is necessary to consider the variation of the charge parameters. For example, the afterburning of the launch charge element leads to some smoothing of the surface variation step. In this case the necessity arises for considering a variable surface when calculating the transient process. Sometimes within the limits of correctness of the calculation it is necessary to consider the kinematics of the opening of the nozzle $\Delta F_{cr}=f(t)$. In this case the calculation is performed for the time intervals within the limits of which the altered parameters can be assumed constant average values. The basic operating formula for this case assumes the form

$$\tilde{M}(\Pi_i,\nu)=\tilde{M}(\Pi_{i-1},\nu)-\frac{\varrho_\tau\bar{\chi}f_p}{p_{np\,i}}\ln\frac{1+b\psi_i}{1+b\psi_{i-1}}. \tag{9.12}$$

APPROVED FOR RELEASE: 2007/02/08: CIA-RDP82-00850R000200090053-2

APPROVED FOR RELEASE: 2007/02/08: CIA-RDP82-00850R000200090053-2

In a number of cases for the transient conditions with step variation of the thrust the free volume can be assumed to be constant. Here the integration of equation (9.3 leads to the relation for the process time

$$t=\tau_к\int_{\Pi_1}^{\Pi_к}\frac{d\Pi}{\Pi-\Pi^\nu}, \qquad (9.13)$$

where Π_k is a value exceeding one, but quite close to it.

It is possible to represent the formula in the form:

$$t=\tau_к\bar{M}(\Pi_1, \nu),$$

where τ_k is the time constant of the chamber calculated for the conditions of the beginning of the transient process.

Table 9.3

$$\bar{M}(\Pi_1,\nu)=\int_{\Pi_1}^{\Pi_к}\frac{d\Pi}{\Pi^{1-\nu}-1}$$

Π_1 \ ν	0,2	0,25	0,3	0,4	0,5	0,6	0,7
5,0	5,8257	6,3119	6,8698	8,2725	10,2489	13,2298	18,2199
4,0	5,3941	5,8306	6,3309	7,5867	9,3529	12,0126	16,4592
3,0	4,80719	5,1817	5,6104	6,6848	8,1932	10,4611	14,2480
2,8	4,6582	5,0179	5,4296	6,4610	7,9085	10,0842	13,7162
2,6	4,4933	4,8370	5,2303	6,2153	7,5972	9,6738	13,1396
2,4	4,3081	4,6343	5,0075	5,9421	7,2527	9,2215	12,5068
2,2	4,0965	4,4034	4,7544	5,6330	6,8649	8,7149	11,8012
2,0	3,8491	4,1341	4,4600	5,2755	6,4186	8,1348	10,9972
1,9	3,7074	3,9801	4,2920	5,0725	6,1661	7,8080	10,5461
1,8	3,5499	3,8094	4,1060	4,8483	5,8882	7,4492	10,0523
1,7	3,3726	3,6174	3,8972	4,5973	5,5781	7,0501	9,5045
1,6	3,1693	3,3976	3,6586	4,3115	5,2260	6,5984	8,8867
1,5	2,9305	3,1399	3,3794	3,9782	4,8168	6,0753	8,1733
1,4	2,6404	2,8275	3,0414	3,5762	4,3252	5,4489	7,3222
1,3	2,2695	2,4288	2,6108	3,0661	3,7035	4,6599	6,2541
1,25	2,0358	2,1779	2,3404	2,7466	3,3154	4,1688	5,5911
1,2	1,7510	1,8725	2,0115	2,3589	2,8454	3,5752	4,7915
1,15	1,3854	1,4810	1,5903	1,8635	2,2460	2,8199	3,7763
1,10	0,8726	0,9324	1,0007	1,1716	1,4108	1,7697	2,3679

FOR OFFICIAL USE ONLY

APPROVED FOR RELEASE: 2007/02/08: CIA-RDP82-00850R000200090053-2

APPROVED FOR RELEASE: 2007/02/08: CIA-RDP82-00850R000200090053-2

Table 9.4.

$$\tilde{N} = \int_{\Pi_1}^{\Pi_k} \frac{d\Pi}{\Pi - \Pi'}$$

Π_1 \ ν	0,3	0,4	0,5	0,6	0,7
5	5,8494	6,6714	7,8262	9,5636	12,3530
4	5,5055	6,2946	7,4023	9,0678	11,8489
3,5	5,2839	6,0503	7,1257	8,7420	11,4401
3,0	5,0088	5,7454	6,7785	8,3306	10,9209
2,8	4,8774	5,5991	6,6112	8,1316	10,6683
2,6	4,7294	5,4339	6,4217	7,9053	10,3805
2,4	4,5602	5,2444	6,2037	7,6441	10,0470
2,2	4,3629	5,0229	5,9478	7,3368	9,6527
2,0	4,1271	4,7570	5,6396	6,9644	9,1739
1,9	3,9896	4,6015	5,4587	6,7454	8,8911
1,8	3,8350	4,4261	5,2543	6,4973	8,5699
1,7	3,6584	4,2254	5,0198	6,2119	8,1995
1,6	3,4530	3,9914	4,7456	5,8773	7,7640
1,5	3,2081	3,7116	4,4167	5,4748	7,2387
1,4	2,9056	3,3649	4,0081	4,9732	6,5818
1,3	2,5119	2,9121	3,4726	4,3134	5.7150
1,25	2,2604	2,6222	3,1287	3,8887	5,1554
1,20	1,9509	2,2646	2,7039	3,3629	4,4613
1,15	1,5494	1,7999	2,1507	2,6768	3,5537
1,10	0,0980	1,1394	1,3526	1,8974	2,2554

The values of $\tilde{N}(\Pi_1, \nu)$ which we calculated for $\Pi_k = 1.05$ are presented in Table 9.4.

With a sharp decrease in the pressure in the engine with step thrust regulation in some cases the danger of disturbance of the stability of the charge combustion arises. The problem of stability of combustion in the case of a pressure drop is considered in Section 9.4.

The calculation of the pressure drop in the chamber and the thrust of the solid-fuel rocket engine after burnup of the fuel is performed by the same functions which were investigated in Chapter 6 for the liquid-fuel rocket engine. However, when calculating this process for the solid-fuel rocket engine it is necessary to keep in mind that for certain forms of charges after burn-up of the basic mass of the fuel, degressive remains are formed, the afterburning of which during the afterflaming period leads to a sharp lengthening of the period. In particular, the charges with a channel of star-shaped cross section have this peculiarity.

APPROVED FOR RELEASE: 2007/02/08: CIA-RDP82-00850R000200090053-2

APPROVED FOR RELEASE: 2007/02/08: CIA-RDP82-00850R000200090053-2

The calculation of the pressure drop process in the engine during afterburning of the charge elements can be made by the regulations (.12) with breakdown of the decrease period into intervals, within the limits of which the combustion surface of the degressive residues can be considered constant.

In order to reduce the undesirable lengthening of the decreased period as a result of afterburning of the fuel residues to a minimum, part of the chamber volume is filled with inserts made of inert light material in the form of the degressive residues [23]. Fig 9.1 shows the graph of the decrease in thrust for the engine with charge in the form of a 10-ray star [23]. The curve 0 corresponds to the total burn-up of the degressive fuel residues; curve 1 corresponds to complete replacement of the degressive residues by inert inserts; the remaining curves correspond to partial replacement of the residues.

9.4. Extinguishing the Charge of the Solid-Fuel Rocket Engine with a Fast Decrease in Pressure

In the solid-fuel ballistic missiles, the cutoff of the thrust of the last stage is a means of insuring the given range and minimum dispersion of the target points. The necessity for forced extinguishing of the charge arises also when creating a multiple starting engine used for correction of the trajectory and for maneuvering the flight vehicle.

At the present time two methods of extinguishing the charge have found application in practice:

A sharp drop in pressure in the case of a discontinuous increase in F_{cr};

Introduction of the cooling agent.

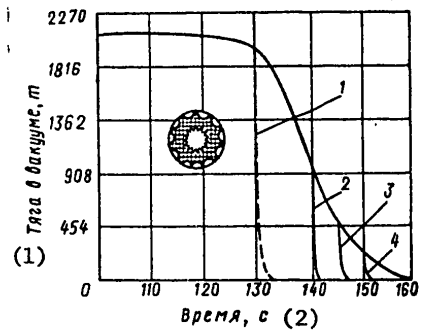

Figure 9.1. Thrust drop in time using wall inserts: 1 -- 100% insert (burn-up of the charge arch); 2 -- 20% insert; 3 -- 11% insert; 4 -- 3% insert
Key:
1. thrust in a vacuum, tons;
2. time, seconds

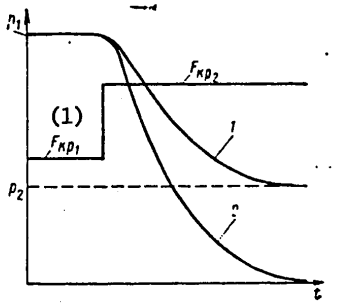

Figure 9.2. Pressure decrease in the chamber of the solid-fuel rocket engine with a sharp increase in F_{cr}
Key:
1. cr

APPROVED FOR RELEASE: 2007/02/08: CIA-RDP82-00850R000200090053-2

APPROVED FOR RELEASE: 2007/02/08: CIA-RDP82-00850R000200090053-2

Let us consider the processes of extinguishing the charge in the case of a discontinuous increase in F_{cr} which can be insured either by opening additional nozzles or by variation of the through cross section of the adjustable nozzle by the methods indicated in Section 9.3.

In the case of step variation of the area of the critical cross section of the nozzles as a function of the rate of the decrease in pressure following this, two limiting cases are possible:

1) Fuel combustion with a decrease in pressure maintains a quasisteady state nature, that is, the combustion rate varies in strict correspondence to the pressure variation by the steady-state combustion law. In this case the pressure drop stops on reaching the level $p_{lim\ 2}$ corresponding to the new steady-state conditions for $F_{cr}=F_{cr\ 2}$ (Fig 9.2, curve 1);

2) With a drop in pressure the nonsteady-state fuel combustion begins which is completed on extinguishing of it, after which free escape of the gas from the chamber takes place until equalization of the pressure in the chamber with the ambient pressure (curve 2).

The performed studies of the behavior of the fuel with a sharp increase in critical cross section of the nozzle permit us to obtain an answer to two questions:

How to insure reliable extinguishing of the charge in order to stop the operation of the engine (with realization of case 2);

How to avoid the possibility of extinguishing the charge with deep step variation of the pressure in order to regulate the thrust in the two-mode engine (realization of case 1).

Let us note that the problem of extinguishing the charge is solved independently of the pressure decrease rate if the second steady-state pressure level is below the limit of stable fuel combustion $p_2<p^*$. However, for the modern high-energy solid fuels the solid fuels the limiting pressure p^* is too small ($p^*<0.014$ MPa) for practical use of this method of extinguishing.

The initial stage of the transient conditions in the case of discontinuous increase in F_{cr} is characterized by significant nonstationarity of the gas flow in the chamber as a result of the gas dynamic wave processes. The duration of this stage is estimated as $\Delta t_1 \sim L_k/a$, where L_k is the chamber length, a is the speed of sound under chamber conditions. Then, after completion of the nonstationary wave rearrangement of the flow, the basic stage of the process begins characterized by the quasistationary escape of gas from the engine nozzles. When estimating the rate of pressure decrease usually the entire process of escape of the gases from the engine is considered as quasistationary.

APPROVED FOR RELEASE: 2007/02/08: CIA-RDP82-00850R000200090053-2

APPROVED FOR RELEASE: 2007/02/08: CIA-RDP82-00850R000200090053-2

The theoretical studies of the process of nonsteady combustion of solid fuel with a decrease in pressures still have not led to analytical relations completed by a charge extinguishing criterion which is suitable for the practice of defining solid fuel rocket engines. However, they have greatly facilitated the empirical solution of this problem, indicating the paths of performance of the experiment and the form of processing the experimental data.

Beginning with a simplified model of the nonstationary combustion of the solid rocket fuel it is possible to assume that the transmission to the unstable combustion as a result of a decrease in pressure in the engine takes place if the decrease time is less than the relaxation time of the thermal layer of the fuel, that is,

$$\frac{p_1 - p_2}{dp/dt} < \tau_p = \frac{a_\tau}{u_1 p_{(1)}^{2\nu}},$$

where the index 1 refers to the initial state and the index 2, to the final state.

Consequently, the condition of extinguishing the charge can be represented in the form

$$\text{const} < \frac{a_\tau}{u_{(1)}^2 p_1} \frac{dp}{dt} \frac{1}{1 - \frac{p_2}{p_1}}. \qquad (9.14)$$

According to function (9.14) the charge extinguishing criterion must include two dimensionless parameters:

The dimensionless pressure decrease rate

$$\dot{p} = \frac{a_\tau}{u_{(1)}^2} \frac{dp}{dt} \frac{1}{p_1}$$

and the relative final pressure for the decrease $H=p_2/p_1$.

Let us note that the expression (9.14) proposed by Ya. B. Zel'dovich is based on the assumption of absence of reactions in the condensed phase.

The role of the parameter p in the process of extinguishing the charge was confirmed by numerous experiments. Thus, K. Siplach [41], performing experiments with respect to extinguishing charges made up of mixed fuel based on ammonium perchlorate and butadiene rubber copolymer, established the existence of a critical pressure decrease rate in the engine $(dp/dt)_{cr}$ insuring final cessation of combustion. Although the temporary extinguishing of the combustion was observed with a pressure decrease rate less than critical, only for $(dp/dt) > (dp/dt)_{cr}$ is it possible to avoid renewal of combustion at decreased pressure. It was established that the magnitude of $(dp/dt)_{cr}$ depends on the operating pressure in the engine p_1, increasing with an increase in the latter. For the fuel with which K. Siplach

APPROVED FOR RELEASE: 2007/02/08: CIA-RDP82-00850R000200090053-2

APPROVED FOR RELEASE: 2007/02/08: CIA-RDP82-00850R000200090053-2

experimented, the magnitude of the critical pressure drop in the pressure range of p_1=2.8-8.5 MPa can be represented by the function

$$\left(\frac{dp}{dt}\right)_{кр} = 150p - 180.$$

The later studies of the extinguishing of the solid rocket fuel with a fast decrease in pressure performed by V. N. Marshakov and O. I. Leypupskiy [24] demonstrated that in the general case the magnitude of the complex $\dot{p}$ insuring extinguishing and, consequently, $(dp/dt)_{cr}$ varies with variation of the parameter H. Their experiments were performed on a setup made of a bomb in which the charge was burned and a receiver which was separated from the bomb by a diaphragm at the beginning of combustion of the charge. At a defined point in time forced rupture of the diaphragm took place, and the gas flowed from the bomb into the receiver. The required value of $H=p_1/p_2$ was insured by varying the ratios of the bomb and receiver volumes and also by creating a preliminary pressure in the receiver. The various rates of decrease in pressure were insured by varying the through cross section of the nozzle connecting the bomb to the receiver. The experiments were performed on charges made of nitroglycerine powder with 2% magnesium oxide additive.

The experimental results were presented in the form of graphs $H(\dot{p})$ separating the coordinate plane in two regions. In region I where the depth and rate of decrease are small, the combustion in the transient regime does not stop. Region II corresponds to complete extinguishing of the charge. The standard curve $H(\dot{p})$ for the initial pressure p_1=6 MPa is presented in Fig 9.3. Similar graphs were obtained for the pressures of 4 and 5 MPa. According to the experimental data, a characteristic decreased time τ_{dec} was determined -- the time in which the difference between the initial and final pressures decrease by e times.

All of the graphs constructed by the experimental data are made up of steep and gently sloping sections. A comparison of the characteristic pressure decreased time and relaxation time of the thermal layer of fuel demonstrated that on the steep section of the graph they are commensurate. For the gently sloping section of the graph the characteristic of decreased time turns out to be on the order of the relaxation time of the reaction layer of the compensated phase: the inertia of the chemical reaction zone becomes the defining factor in the behavior of the fuel.

On the basis of the physical prerequisites of charge extinguishing found during the experiments it is possible to approach the determination of the additional area of critical cross section required for extinguishing.

Inasmuch as the charge extinguishing is usually preceded by steady-state operating conditions, according to (9.3) at the time of discovery of the additional area F_{cr}, the condition

APPROVED FOR RELEASE: 2007/02/08: CIA-RDP82-00850R000200090053-2

APPROVED FOR RELEASE: 2007/02/08: CIA-RDP82-00850R000200090053-2

$$\frac{W}{RT}\frac{dp}{dt}=Q_T\Gamma p_1^{\nu}\left[1-\frac{\varphi_c A F_{кр_2}}{Q_T\Gamma\sqrt{RT}}p_1^{1-\nu}\right], \tag{9.15}$$

is satisfied, where $F_{cr\ 2}$ is the total area of the critical cross sections after uncovering the additional area.

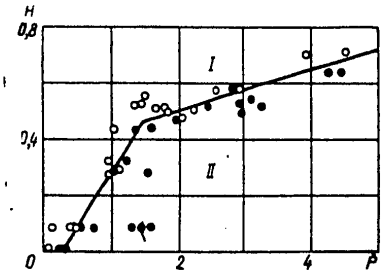

Figure 9.3. Graph of the extinguishing of ballistite fuel H:
1 -- combustion; II -- extinguishing

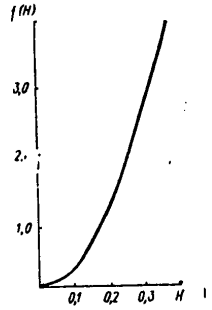

Figure 9.4. Graph of the function f(H)

Dividing and multiplying the second term by $F_{cr\ 1}$ (the initial critical cross section area), it is possible to present equation (9.15) in the form

$$\frac{1}{p_1}\frac{a_T}{u_{(1)}^2}\frac{dp}{dt}=\frac{a_T RT_к Q_T S}{Wu_{(1)}p_1}\left[1-\frac{F_{кр2}}{F_{кр1}}\right]. \tag{9.16}$$

Let us express the ratio of the critical cross sections in terms of the pressures corresponding to them in the steady-state conditions

$$\frac{F_{кр1}}{F_{кр2}}=\left(\frac{p_2}{p_1}\right)^{1-\nu}=H^{1-\nu}.$$

Here equation (9.16) can be represented in the form

$$D=\frac{\dot{p}}{1-\frac{1}{H^{1-\nu}}}, \tag{9.17}$$

where

$$D=\frac{a_T RT Q_T S}{Wu_{(1)}p_1}.$$

APPROVED FOR RELEASE: 2007/02/08: CIA-RDP82-00850R000200090053-2

APPROVED FOR RELEASE: 2007/02/08: CIA-RDP82-00850R000200090053-2

The lefthand side of the equality (9.17) is the function f(H). The right-hand side is a dimensionless complex made up of the charge parameters and the combustion rate of the fuel at a pressure of p_1.

Having an experimental function $\dot{p}(H)$ available for the used fuel or for the fuel similar with respect to composition, it is easy to construct the graph of the function f(H). As an example, in Fig 9.4 the graph is presented for this function which we constructed according to the data of [24].

Calculating the complex D for the specific engine, it is possible to enter the graph f(H) with it and determine the value of $H=p_1/p_2$ from it corresponding to the stability limit of combustion for the adopted charging parameters on dropping the pressure, and then the ratio of the areas of the critical cross sections $F_{cr\ 2}/F_{cr\ 1}$ corresponding to it.

The magnitude of the complex parameter D is defined by the type of fuel, the pressure in the steady-state mode, the ratio of the combustion surface to the free volume of the chamber and the extinguishing time. With an increase in pressure and an increase in the combustion rate, the stable combustion boundary shifts in the direction of low values of H. For geometrically similar engines with an increase in bore the charge surface increases proportionally to the square of the bore; the free volume increases proportionally to the cube of the bore. Here the parameter D will vary inversely proportionally to the engine bore. Consequently, for engines of medium and large bores the operating part of the graph f(H) is limited by the low values of H. Here the basic factors determining the extinguishing of the charge is the relaxation time of the thermal layer. Only for small bores does the region of high values of H acquire practical significance, for which the relaxation time of the chemical reaction layer becomes defining:

$$\tau_{p2}=\frac{l_{\text{реакц}}}{u_0}\overset{(1)}{=}\frac{a_\tau}{u_0^2}\frac{2RT_S}{E}=\tau_{p1}\frac{2RT_S}{E}.$$

Key: 1. reaction

In order to insure reliable extinguishing of the charge, it is necessary to use a sharper pressure drop than that which corresponds to the combustion stability limit. In other words, when determining $F_{cr\ 2}$ it is necessary to begin at the value of H which is low as opposed to that which is determined by the expression (9.17).

On the contrary, in order to insure stability of combustion of the charge in the case of application of a step pressure diagram with a decrease it is necessary to move in the direction of higher H.

APPROVED FOR RELEASE: 2007/02/08: CIA-RDP82-00850R000200090053-2

APPROVED FOR RELEASE: 2007/02/08: CIA-RDP82-00850R000200090053-2

9.5. Extinguishing of the Charge of the Solid-Fuel Rocket Engine by Introducing Coolant into the Combustion Chamber

The extinguishing of the charge by introducing the cooling component -- coolant -- into the combustion chamber has a number of advantages by comparison with the above-investigated procedure. They include the absence of additional nozzles, the gas lines, protective shields for the useful load,absence of a flame which appears on opening the additional nozzles.

The introduction of the coolant into the chamber of the solid-fuel rocket engine is accompanied by the following forms of effects on the operating process of the engine:

1. A reduction in the gas phase temperature as a result of loss of heat to evaporation of the coolant and heating of its vapor.

2. A direct effect of the coolant on the hot surface of the charge;

3. A drop in pressure in the chamber as a result of a sharp drop in temperature of the gases.

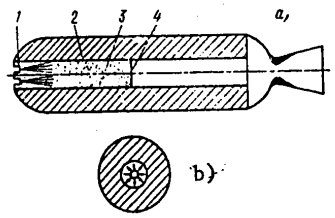

Figure 9.5. Basic version of supplying the coolant to the solid-fuel rocket engine chamber:
a -- axial; 1 -- spray jets; 2 -- charge; 3 -- cooled gas zone; 4 -- cooling front; b -- radial

The use of extinguishing systems with liquid and solid coolant is possible. Each of them has advantages and disadvantages. When using the liquid coolant it is simpler to realize multiple extinguishing of the charge in the multiple starting engine. When using a solid coolant, the structural design of the extinguishing assembly is simplified, there is no necessity for the liquid feed system with pressure storage tank, hydraulic lines, and so on.

Two versions of supplying the coolant to the chamber are possible for both types of coolants -- axial and radial. In the case of axial feed (Fig 9.5, a) the drops of liquid or particles of the solid coolant, moving along the charged channel in the hot combustion products evaporate, removing heat from them. As a result, a zone of cooled gases mixed with coolant vapor is formed on the bottom front of the engine. The next lots of coolant fed to the chamber penetrate the cooled zone, in practice not

FOR OFFICIAL USE ONLY

APPROVED FOR RELEASE: 2007/02/08: CIA-RDP82-00850R000200090053-2

APPROVED FOR RELEASE: 2007/02/08: CIA-RDP82-00850R000200090053-2

evaporating in it, and they begin to evaporate intensely on reaching the hot gas region and, thus moving the cold zone boundary in the direction of the nozzle. The pressure in the coolant evaporation zone decreases, which causes movement of the combustion products from the nozzle to the bottom front of the engine. It is proposed that the fuel is extinguished in the cooled gas zone. The extinguishing boundary moves after the gas cooling front.

In the case of radial coolant feed, it begins to arrive along the entire length of the chamber in practice simultaneously. The coolant particles penetrate the gas volume, partially evaporating in the hot combustion products and at angles close to normal, they strike against the burning surface (Fig 9.5, b).

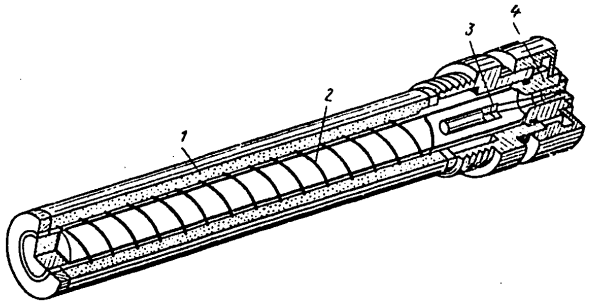

Figure 9.6. Pyroinjector for radial feed of solid coolant:
1 -- pressed coolant; 2 -- spiral explosive charge; 3 -- detonator;
4 -- ignition assembly

When using the solid coolant its radial feed can be realized by a pyro-injector placed along the axis of the charged panel. One such device is presented in Fig 9.6 [12]. In it the coolant powder is pressed on the fuse-type explosive charge. The detonation of the explosive insures dispersion of the coolant to smaller particles and communicates velocities of more than a hundred m/sec to them.

The primary advantage of radial feed is more effective use of the coolant in view of the increasing role of the direct effect on the combustion surface. The basic disadvantage is the necessity for thermal protection of the injector located in the charge channel during operation of the engine.

The process of the pressure decrease in the solid fuel rocket engine in the case of axial feed of the coolant was investigated in great detail in reference [36].

Let us consider how the pressure varies in the engine with radial feed of the coolant.

APPROVED FOR RELEASE: 2007/02/08: CIA-RDP82-00850R000200090053-2

APPROVED FOR RELEASE: 2007/02/08: CIA-RDP82-00850R000200090053-2

The material balance equation of the chamber when feeding the coolant assumes the form

$$\frac{W}{RT}\frac{dp}{dt}=Y_т(t)+Y_ж(t)-\frac{\varphi_c AF_{кр}}{\sqrt{RT}}p+\frac{pW}{(RT)^2}\frac{d(RT)}{dt}, \qquad (9.18)$$

where $Y_т(t)$ is the gas inflow per second from combustion of the fuel; $Y_ж(t)$ is the gas inflow per second from evaporation of the coolant fed to the chamber.

Let us note that the value of $Y_ж(t)$ is determined not by the flow rate of the coolant feed to the chamber, but by the evaporation rate of its disperse particles in the hot gas environment and on contact with the heated surfaces.

The energy balance equation is rewritten in the form

$$\frac{pW}{(RT)^2}\frac{d(RT)}{dt}=Y_т(t)\left(\frac{RT_V}{RT}-1\right)-(k-1)\frac{\varphi_c AF_{кр}}{\sqrt{RT}}p-$$
$$-Y_ж(t)-\frac{k-1}{RT}\frac{dQ}{dt}. \qquad (9.19)$$

Here dQ/dt is the flow rate per second of the heat filling to heat the coolant to boiling point and evaporate it. It can be represented in the form

$$\frac{dQ}{dt}=\frac{dQ}{dm_ж}\frac{dm_ж}{dt}=H_ж Y_ж(t),$$

where $H_ж$ is the reduced heat of vaporization of the coolant. Let us note that the heat going to heat the coolant vapor from the boiling point to the temperature of mixing of the gases is taken into account when deriving the equation by the third term in the righthand side.

Combining equations (9.18) and (9.19) into one, we obtain

$$\frac{W}{RT_к}\frac{dp}{dt}=Y_т(t)\frac{RT_V}{RT_к}-k\frac{\varphi_c AF_{кр}}{\sqrt{RT_к}}p-\frac{k-1}{RT_к}H_ж Y_ж(t).$$

Dividing both sides of the equality by $m_k=p_k W/RT_k$, we obtain:

$$\frac{1}{p}\frac{dp}{dt}=\frac{Y_т RT_V}{m_к}-k\frac{\varphi_c AF_{кр}\sqrt{RT_к}}{W}-\frac{k-1}{RT_к}\frac{H_ж Y_ж}{m_к}. \qquad (9.20)$$

FOR OFFICIAL USE ONLY

APPROVED FOR RELEASE: 2007/02/08: CIA-RDP82-00850R000200090053-2

APPROVED FOR RELEASE: 2007/02/08: CIA-RDP82-00850R000200090053-2

The equation obtained permits a comparative estimate of the various factors causing a pressure drop in the engine. The effect of the coolant on the combustion surface is characterized by the first term (variation of the gas inflow Y_T). The second term determines the effect of the process of escape of the gases through the nozzle. The third term characterizes the pressure drop as a result of cooling of the gases on evaporation of the coolant particles in the free volume of the chamber.

Let us consider the pressure drop as a result of the second and third terms. Let us denote the relative rate of decrease caused by the second and third terms in terms of $z_{2,3}=(1/p)(dp/dt)$. Let us linearize the equation (9.20) for $Y_T=0$. Here we shall assume that the free volume W after the time of introducing the coolant remains constant. We obtain

$$z_{2,3}=\left[\frac{(k-1)H_xY_x}{m_к(RT_к)^2}-\frac{k\varphi AF_{кр}}{2W\sqrt{RT_к}}\right]\Delta(RT_к)+\frac{(k-1)H_xY_x}{m_к^2RT_к}\Delta m_к.$$

The first term in the righthand side expresses the variation of the pressure decrease as a result of cooling the gases ($\Delta(RT_k)$ is negative). The effect provided by cooling of the gas is reduced as a result of the fact that with a decrease in RT_k, the amount of energy carried away with the gases through the nozzle decreases. The second term in the righthand side reflects the trend of the pressure toward an increase as a result of increase in the mass of the gases in the chamber on evaporation of the coolant. The choice of the coolant must be made considering that a significant excess of the first component over the second will be insured. If in the first approximation we neglect the second term in parentheses, we obtain the simplest condition of selecting the coolant in the form

$$\frac{\Delta(RT_к)}{RT_к}:\frac{\Delta m_к}{m_к}>1,$$

that is, the relative decrease in RT_k must be higher than the relative amount of coolant introduced for this.

According to the published data [12], water is the best of the liquid coolants. Among the solid coolants which have been tested in the solid-fuel rocket engines, ammonium and potassium bicarbonates, potassium bromide and aluminum sulfate crystal hydrates are noted. The best results have been obtained when using the latter. When splitting off the crystallization water and evaporation of it, 1510 kjoules (387 kcal) is absorbed per kg of material, which amounts to 66% of the heat of vaporization of 1 kg of water under the same conditions. In order to reduce the temperature of the combustion products in the solid-fuel rocket engine chamber to 500° (~by 6 times) about 3.5 kg of this material per kg of gases is required.

When selecting the required amount of coolant evaporated in the gas phase, we begin not only with the condition of fast decrease in pressure in the chamber. It is necessary to insure a temperature decrease in the chamber for which repeated ignition is excluded.

APPROVED FOR RELEASE: 2007/02/08: CIA-RDP82-00850R000200090053-2

APPROVED FOR RELEASE: 2007/02/08: CIA-RDP82-00850R000200090053-2

The effect of the coolant on the combustion surface can be different depending on the penetrating capacity of the particle which is determined by its size and speed on approaching the combustion surface. Three cases are possible:

1. The particles remain on the combustion surface in the boundary layer, acting on the temperature profile of the gas phase on evaporation near the combustion surface, at the same time changing the heat flux to the charge.

2. The particles introduced into the reaction layer of the condensed phase, varying its energy balance, that is, lowering the value of Q_s.

3. The particles are introduced into the thermal layer of the condensed phase.

The application of the fluorescent dyes demonstrated that the coolants can penetrate into the fuel to a depth of ~100 microns [12]. In the case of penetration of the particles to great depths their effect can be manifested only with respect to the escape time on the order of τ_p when they turn out to be in the temperature zone insuring gasification of them. The most effective turns out to be the effect of the particles when they penetrate to the depth of the reaction layer. The experimental data indicate that even for extinguishing the fuel with high metal content (18% Al) when using the aluminum sulfate crystal hydrate, ~0.36g/cm^2 of charge combustion surface is required [12].

9.6. Random Transient Conditions

During the operation of the solid-fuel rocket engines, random transient conditions can occur which are caused by short-term effect of different disturbing factors for which significant deviations of the pressure and the thrust from the steady-state values are possible. The solution of such problems in the general case does not permit linearization and must be carried out on the basis of the nonlinear equations.

Let us indicate the individual versions of the random transient conditions.

1. The short-term decrease in critical cross section area of the nozzle on discharge of a piece of the heat insulating coating or part of the case of the igniter from the engine [19].

2. Short-term increase in combustion surface as a result of a crack or the accumulation of pores. Duration of their effect on the operating process of the engine is determined by the burn-up time of the layer of their occurrence.

3. The delay in the dispersion of the two-position nozzles providing for operation of the two-regime engine with step variation of the thrust at constant pressure in the chamber. In this case when the launch and sustainer charges burn successively in the chamber of the solid-fuel rocket

APPROVED FOR RELEASE: 2007/02/08: CIA-RDP82-00850R000200090053-2

APPROVED FOR RELEASE: 2007/02/08: CIA-RDP82-00850R000200090053-2

engine, the delay in covering the nozzle leads to a decrease in pressure at the beginning of combustion of the sustainer charge (the charge with small surface). In the case of the transition from combustion of the charge with small surface to combustion of the charge with large surface the delay in opening the nozzle leads to a rise in pressure.

The investigated versions are characterized by significant variation of one charge parameter or another (the combustion surface, the area of the critical cross section of the nozzle, the unit combustion velocity), which implies variation of the pressure in the engine. The variable pressure in this case approaches the limit defined by new disturbed charge conditions. The degree of approach of the pressure to its new limit is determined by the duration of the period τ_{dist} during which altered charging parameters are maintained.

The time τ_{dist} is a random variable which in each individual case is determined by a set of different factors.

Let us consider the simplified approach to the solution of these problems, assuming that the charging pararmeters vary instantaneously and then remain unchanged for a period τ_{dist}. We shall also assume that the free volume of the chamber during the period τ_{dist} remains in practice constant. This assumption, in view of smallness of τ_{dist} is correct. Under these assumptions, the relation between the pressure which is reached at the end of the period and the duration of the period for the processes with a build-up in pressure is expressed by the function

$$\underset{(1)}{\tau_{возм}}=\frac{W}{\varphi_c A F_{кр}\sqrt{\underset{(2)}{\chi f_p}}}\int_{\Pi_i}^{\Pi_{i+1}}\frac{d\Pi}{\Pi^{\nu}-\Pi}$$

Key: 1. dist; 2. cr

or

$$\tau_{возм}=\tau_к[N(\Pi_i,\nu)-N(\Pi_{i+1},\nu)].$$

Here

$$\Pi_i=\frac{p_i}{p_{пр.возм}};\quad \Pi_{i+1}=\frac{p_{i+1}}{p_{пр.возм}},$$

(1)

Key: 1. lim dist

$p_{lim\ dist}$ is the limiting pressure determined by the formula (9.6) by the values of the disturbed charge parameters; p_i is the pressure at the beginning of the period; p_{i+1} is the pressure at the end of the period. Correspondingly, for processes with a decrease in pressure we obtain

$$\tau_{возм}=\tau_к[\tilde{N}(\Pi_i,\nu)-\tilde{N}(\Pi_{i+1},\nu)].$$

APPROVED FOR RELEASE: 2007/02/08: CIA-RDP82-00850R000200090053-2

APPROVED FOR RELEASE: 2007/02/08: CIA-RDP82-00850R000200090053-2

CHAPTER 10. CHARGE IGNITION PERIOD OF A SOLID-FUEL ROCKET ENGINE

10.1. Basic Types of Igniters and Ignition Models

Ignition is the initial stage of combustion of solid fuel. The organization of the processes of ignition to a significant degree determines the reliability and the ballistic perfection of the engine. In the case of a weak igniter, failures of charge ignition are possible; the arrival of the engine at the operating conditions is drawn out. In the case of a strong igniter, pressure peaks appear which threaten the strength of the structural elements.

Reliable ignition of the solid rocket fuel is determined by the interaction of many physical and chemical processes differing with respect to their nature. In the complex intertwining of the phenomena which taken together make up the ignition process, the contribution of the individual phenomenon can vary on variation of the fuel composition, the ambient parameters, the type of heating and its rate and the gas pressure. Accordingly, the ignition of the rocket fuel remains the least investigated period of the operating process of a solid-fuel rocket engine.

The process of charge ignition of a solid-fuel rocket engine usually is divided into the following stages:

1. Propagation of the front of the combustion products of the igniter with respect to the free volume of the rocket chamber.

2. Heating of the charge surface by the combustion products of the igniter until some critical ignition conditions are reached.

3. Spread of the flame, that is, the region in which the critical ignition conditions are reached, over the surface of the charge.

4. Direct combustion of the primary charge and the residue of the ignition compound until some provisional pressure level (ignition pressure) is reached, which is the initial condition of calculating the arrival of the engine at the rated parameter conditions.

FOR OFFICIAL USE ONLY

APPROVED FOR RELEASE: 2007/02/08: CIA-RDP82-00850R000200090053-2

APPROVED FOR RELEASE: 2007/02/08: CIA-RDP82-00850R000200090053-2

This division is somewhat provisional in view of the absence of clear boundaries between the indicated stages and also in view of significant differences in the ignition process caused by using various types of fuels, igniters and compounds.

These causes complicate the development of an acceptable model of the ignition process.

The great variety of ignition conditions of the solid-fuel rocket engines observed in practice exclude the possibility of constructing a unique model of ignition reflecting all of the cases deserving attention. It appears expedient to group the various combinations of defining factors into basic generalizing versions, for each of which the development of its own process model is admissible. With this approach it is possible to isolate four types of ignition:

1. Frontal ignition of the charge of ballistite fuel by the hot gas with any directional displacement of the flame front along the charge surface.

2. Center ignition of the charge of ballistite fuel under the effect of hot condensed particles on its surface.

3. Frontal ignition of the charge of mixed fuel by the hot gas.

4. Center ignition of the mixed fuel by the condensed particles.

Below, the theoretical problems are investigated as applied to the indicated versions, in the first approximation encompassing the variety of ignition conditions in the solid-fuel rocket engine.

In all cases, for ignition of the fuel it is necessary for its surface layer to be brought to the temperature condition for which the heat release as a result of thermal decomposition of the condensed phase or as a result of reaction of the gas phase near the surface will become greater than the heat losses, and the reaction of decomposition of the solid phase will begin to develop stably. In order to determine the time of ignition of the fuel in each individual section of the surface it is necessary to have at our disposal a complete description of the process of heat and mass exchange of the combustion products of the igniter with the surface, that is, a relation which determines the variation of the heat and mass fluxes of the condensed particles in time and space. The nature of this function, in turn, is determined by the type of igniter and the composition applied in it. The compositions used for ignition of the solid rocket fuel can be divided into three groups:

1. Smoking powder.

2. Pyrotechnical composition based on mineral oxidizing agents and metals.

3. Ballistite and mixed fuels.

APPROVED FOR RELEASE: 2007/02/08: CIA-RDP82-00850R000200090053-2

APPROVED FOR RELEASE: 2007/02/08: CIA-RDP82-00850R000200090053-2

Ignition compounds can be used in the form of powders, granules, tablets and blocks, according to the form of storage elements for the charges of the solid-fuel rocket engines.

Depending on the structure in which the igniting compound is placed, the following types of igniters are distinguished [37]:

1. Igniters without a housing or with destructable housing (fabric bags, boxes, housing with diaphragm).

2. Igniters with perforated, undestroyed housing.

3. Igniters of the "engine to engine" type with output of the combustion products through the nozzle devices which can be provisionally called jet igniters.

The type of igniter combined with the compound used in it determine the nature of the behavior of the combustion products of the igniter and their effect on the surface of the primary fuels.

In the first case after destruction of the case or rupture of the diaphragm, the burning granules of the ignition compound together with the combustion products are distributed over the entire free volume. The combustion rate of the igniter granules is determined by the conditions for the entire volume of the solid-fuel rocket engine and varies with insignificant limits.

In the second case the basic mass of the compound burns under the conditions of a semiclosed volume of the ignition device, and only the combustion products enter into the free volume of the engine. Here the pressure inside the igniter case can differ significantly from the pressure in the chamber of the solid-fuel rocket engine. In the case of a supercritical pressure gradient, the combustion of the igniter ceases to depend on the conditions inthe chamber, and it is entirely determined by the internal ballistics of the ignition device.

In the third case, the combustion process of the ignition compound is wholly controlled by such factors as the configuration of the elements of the total area of the critical cross sections of the nozzles. The nature of interaction of the combustion products of the igniter with the charge surface will to a significant degree be determined by the topography of the jets escaping from the nozzles, that is, the inclination of the nozzles, their number and placement on the igniter case.

The ignition device can be placed in the bottom part of the chamber, in the nozzle section, in the intermediate volume between the charge sections. Finally, the jet igniters can be placed outside the combustion chamber of the solid-fuel rocket engine on the starter, providing for ignition of the charge by a jet of hot gases blown into the chamber through the engine nozzle. Each of the indicated versions of placement of the igniter has its own specific nature, which cannot be investigated within the scope of

FOR OFFICIAL USE ONLY

APPROVED FOR RELEASE: 2007/02/08: CIA-RDP82-00850R000200090053-2

APPROVED FOR RELEASE: 2007/02/08: CIA-RDP82-00850R000200090053-2

this chapter. The processes connected with ignition of the solid rocket fuel charge are investigated as applied to the given version.

The authors of reference [46] have tried to relate the weight of the igniter to the thrust and the free volume of the solid-fuel rocket engine (Fig 10.1 and 10.2) and also to determine the region of use of one type of igniter or another on the basis of the developed models of the engines known to them. The graph presented in Fig 10.1 gives some representation of the boundaries of the use of the igniters of various types. At the same time it indicates the provisionalness of these boundaries, the absence of the established recommendations with respect to selecting the type of igniter and its weight, which to a significant degree reflects the state of the ignition theorv.

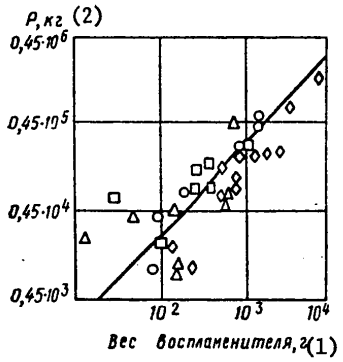

Figure 10.1. Statistical dependence of the mass of the igniter on the engine thrust according to reference [46]:
○ -- igniter made of black powder or mortar powders; Δ -- igniter based on the B+KNO_3 composition; □ -- igniter based on Al+$KClO_2$; ◇ -- jet type igniter
Key:
1. Weight of igniter, g
2. P, kg

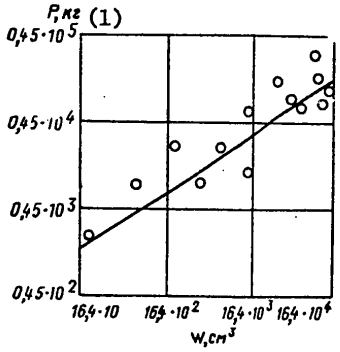

Figure 10.2. Statistical dependence of the initial free volume of the solid-fuel rocket engine chamber on the thrust according to reference [46]
Key:
1. P, kg

10.2. Heat and Mass Exchange Between the Combustion Products of the Igniter and the Charge Surface

10.2.1. Heat and Mass Exchange when Using a Jet Igniter

The behavior of the supersonic jet of combustion products of the igniter after the nozzle tip is determined by the ratio d_c/D_k, where d_c is the diameter of the output cross section of the nozzle, D_k is the diameter of the charge channel. Depending on the value of d_c/D_k, two cases are distinguished [14] (Fig 10.3).

APPROVED FOR RELEASE: 2007/02/08: CIA-RDP82-00850R000200090053-2

APPROVED FOR RELEASE: 2007/02/08: CIA-RDP82-00850R000200090053-2

In the first case where d_c/D_k is large, the jet at a relatively small distance after the nozzle tip enters into contact with the surface. Later the flow remains supersonic. The variation of the gas dynamic parameters of the jet is determined by the losses to friction when moving through a channel of constant cross section. Here the greatest intensity of the heat exchange is reached in the collision zone of the expanding jet with the channel surface. Then as the boundary layer develops along the streamlined surface the convective heat flux decreases. The value of the convective heat transfer coefficient can be determined by the well-known relations for flow over a plate.

The second case is characterized by the small ratio d_c/D_k (see Fig 10.3, b). Here the jet entering the channel decays into individual eddies without coming in contact with the channel surface.

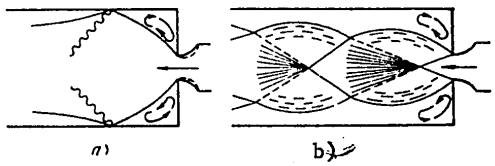

Figure 10.3. Versions of behavior of the gas jet on escape from the nozzle of the igniter:
a -- for a large ratio d_c/D_k; b -- for a small ratio d_c/D_k

Let us discuss in more detail the second case with a more complex heat exchange mechanism, which is of the greatest practical interest. As the experiment of [46], [14] shows, the distribution of the values of the heat transfer coefficient of the heat fluxes with respect to length of the channel and in time for this case is characterized by large nonuniformity. In Fig 10.4 [14] the results are presented from an experiment performed on a model device. The graph of the variation of the coefficient of convective heat transfer along the length of the channel is constructed in relative coordinates. The relative removals from the nozzle tip z/d_c is plotted along the x-axis, and the ratio of the local value of the heat transfer coefficient to its value for hydrodynamically stabilized flow is plotted along the y-axis. As follows from the graph, on the halflength of the charge turned toward the engine nozzle, the heat transfer coefficient has a value which is close to that which is determined by the functions for the heat exchange in long tubes (see Table 7.1). In the initial section of the flow, erosion is observed which exceeds the indicated value by ~3 times. In Fig 10.5 we have the experimental graph from reference [46] characterizing the variation of the heat flux when using a jet igniter in time and along the heat coordinate. According to this graph the specific heat flux in the initial section is twice its value at the end of the simulator charge channel. Here, in the initial section the heat flux after a sharp rise in the initial operation of the igniter then remains in practice constant in time. The maximum heat fluxes at a distance of one-third

APPROVED FOR RELEASE: 2007/02/08: CIA-RDP82-00850R000200090053-2

APPROVED FOR RELEASE: 2007/02/08: CIA-RDP82-00850R000200090053-2

of the charge and in the final section coincide. However, the times for the heat fluxes to reach the maximum level are relatively large.

Figure 10.4. Variation of the heat transfer coefficient along the length of the channel with a jet igniter [14]:
- - - - L/D_k=12; ——— L/D_k=8; ——·—— L/D_k=5

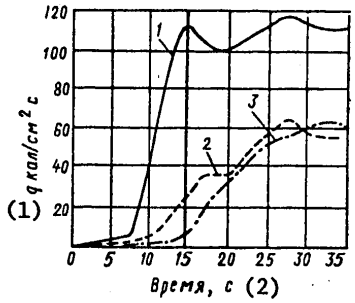

Figure 10.5. Variation of the heat flux to the surface of the charge as a function of time at various distances from the nozzle of the jet igniter:
1 -- z=76 mm; 2 -- z=405 mm; 3 -- z=1270 mm
Key: 1. q, cal/cm²-sec; 2. time, sec.

The initial section of the channel playing an important role in the process of charge ignition as a result of its location and high intensity of the heat exchange deserves special attention. The complex nature of variation of the heat transfer parameters in this section is related to rearrangement of the gas dynamic structure of the flow and the variation in this case of the structure of the turbulent eddies.

The theoretical difficulties arising even in the simplest cases when solving the problems of turbulent boundary layer increase with transition to

APPROVED FOR RELEASE: 2007/02/08: CIA-RDP82-00850R000200090053-2

APPROVED FOR RELEASE: 2007/02/08: CIA-RDP82-00850R000200090053-2

the more complex forms of movement of the gas. A simple solution for the case of interest to us can be obtained by combining the simplified model representation of the process with the individual derivations of the statistical theory of turbulence.

We shall assume that a supersonic jet decays into turbulent eddies, the direction of which ℓ_c in the first approximation is determined by the characteristic size of the jet, that is, its diameter: $\ell_c=c_d d_c$, where c_d is a constant. Then decay of the primary large-scale eddies into finer turbulent formations takes place. The process of making the scale of the eddies smaller takes place to some scale of movement ℓ_0 called the internal scale of the turbulence, beginning with which the movement of the gas acquires a viscous nature. The turbulent pulsations of the scale $\ell \sim \ell_0$ cannot be carried to smaller ones: they gradually disappear as a result of viscosity, and the kinetic energy which they have is converted to heat. The fine-scale pulsations are an element determining the intensity of the heat transfer in the viscous sublayer of the turbulent boundary layer. However, in order to determine the order of magnitude of ℓ_0, it is necessary to consider the behavior of the large-scale eddies carrying the basic part of the energy.

The simplest statistical characteristic of the turbulence is the mean energy of the pulsations equal to

$$E=\frac{\varrho}{2}(\bar{u}'^2+\bar{v}'^2+\bar{w}'^2)=\frac{\varrho V^2}{2},$$

where $\bar{u}'$, $\bar{v}'$, $\bar{w}'$ are the average pulsation velocities along the coordinates x, y, z.

Let us use the Prandtl-Dryden function for the case of degeneration of the turbulence occurring after the local resistance in the flow [34]. This function expresses the decrease in V with time. Assuming that our case is analogous to the case investigated by the Prandtl-Dryden, let us represent V in the form

$$V=\frac{c_V l_e}{T+t}, \tag{10.1}$$

where t is the time from beginning of decay of the jet, $T=c_T \ell_e/u_e$ is a time constant characterizing the decay of the large eddies, c_V, c_T are constants.

The expression (10.1) permits determination of the mean value of the energy dissipation of turbulent eddies in a unit volume of gas per unit time:

$$D=\frac{dE}{dt}=\varrho V\frac{dV}{dt}=\varrho\frac{c_V^2 l_e^2}{(T+t)^3}. \tag{10.2}$$

If in the first approximation we assume just as L. Prandtl assumes for the analogous case, the turbulence of the flow is locally isotropic, the

FOR OFFICIAL USE ONLY

APPROVED FOR RELEASE: 2007/02/08: CIA-RDP82-00850R000200090053-2

APPROVED FOR RELEASE: 2007/02/08: CIA-RDP82-00850R000200090053-2

internal scale of the turbulence can be determined in terms of the specific dissipation by the function (see reference [45]):

$$l_0=\left(\frac{\mu^3}{\varrho^2 D}\right)^{1/4},$$

where μ is the dynamic viscosity coefficient.

The coefficient of convective heat transfer is related to the characteristic l_0 by the approximate function

$$\alpha=c_* \frac{\lambda_r}{l_0}.$$

Let us relate time t to the coordinate z (the removal of the igniter from the tip of the nozzle) by the function $t=z/v_{mean}$, where v_{mean} is the mean velocity of the movement of the flow of combustion products of the igniter along the channel in the section c-z.

Thus, we obtain the chain of relations permitting representation of the variation of the coefficient of convective heat transfer α with respect to length of the charge channel for the pseudostationary process of escape of the combustion products from the nozzle of the ignition device

$$\alpha=\text{const}\,\lambda_r\left(\frac{\varrho u_c}{\mu}\right)^{3/4}\frac{1}{d_c^{1/4}}\frac{1}{\left(1+\frac{z}{d_c}\frac{u_c}{v_{cp}}\frac{1}{c_c}\right)^{3/4}}. \tag{10.3}$$

The constant in front of the entire expression in the righthand side and also the constants $c_c=c_T c_d$ must be determined experimentally. The value of v_{mean} must be determined from the gas dynamic calculation.

The second term in the parentheses of the denominator is appreciably larger than one. Thus, the heat transfer coefficient α varies after its maximum along the length of the channel somewhat less than $(z/d_c)^{-3/4}$ which agrees with the experimental data of reference [14] (see Fig 10.4).

The obtained relation can be represented in criterial form, multiplying both sides of equality (10.3) by d_c/λ_g

$$\text{Nu}_d=\text{const}\,\text{Re}_d^{0,75}\frac{1}{\left(1+\frac{z}{d_c}\frac{u_c}{v_{cp}}\frac{1}{c_c}\right)^{0,75}}, \tag{10.4}$$

where

$$\text{Nu}_d=\frac{\alpha d_c}{\lambda_r};$$

$$\text{Re}_d=\frac{u_c d_c}{\nu}$$

are the Nusselt and Reynolds numbers defined for the parameters of the nozzle tip -- d_c and u_c.

APPROVED FOR RELEASE: 2007/02/08: CIA-RDP82-00850R000200090053-2

APPROVED FOR RELEASE: 2007/02/08: CIA-RDP82-00850R000200090053-2

Another form of writing the function (10.4) is

$$\mathrm{Nu}_D = \text{const}\,\mathrm{Re}_D^{0,75}\,\mathrm{Pr}^{0,3}\,\frac{(u_c/v_{cp})^{0,75}(D_к/d_c)^{0,25}}{\left(1+\frac{z}{d_c}\frac{u_c}{v_{cp}}\frac{1}{c_c}\right)^{0,75}}, \tag{10.5}$$

where

$$\mathrm{Nu}_D = \frac{\alpha D_к}{\lambda_г}, \quad \mathrm{Re}_D = \frac{v_{cp} D_к}{\nu}$$

are determined for the flow parameters of the channel, and from the constant $\mathrm{Pr}^{0.3}$ is separated by the cofactor.

Inasmuch as the structure of the flow turbulence as a result of rearrangement and decay of the large eddies approaches that which is established for flow of a gas in long tubes, the lower boundary of the use of the function (10.3) is the values of Nu or α determined by the formulas in Table 7.1.

10.2.2. Heat and Mass Exchange of Using an Igniter with Rupturable Case

When using an igniter with rupturable case, the granules of the ignition compound burn in the free volume of the chamber of the solid-fuel rocket engine, moving along the charge chamber together with the combustion products.

The basic factors determining the intensity of the heat exchange and the variation of its parameters along the charge surface are:

1. The local inflow of gas from combustion of the grains of igniter.

2. The gas dynamic parameters of the two-phase flow of combustion products and burning trains.

3. The parameters of the secondary gas flows caused by the construction of the flow by the grains of the ignition compound.

In view of the low degree to which these factors have been studied and the complexity of their interaction, a complete analytical description of the process is difficult.

The experimental data on the heat exchange parameters for the investigated case known from the literature are few. Thus, for example, in reference [46] by using the thermocouples mounted in the surface of the charged simulator, heat fluxes were determined to the surface for the experiments with an ignition compound $B+KNO_3$ pressed into tablets. In Fig 10.6 we have the graphs of the variation of the heat fluxes with time at different distances from the igniter. Fig 10.7 shows the graph of the pressure variation of

APPROVED FOR RELEASE: 2007/02/08: CIA-RDP82-00850R000200090053-2

APPROVED FOR RELEASE: 2007/02/08: CIA-RDP82-00850R000200090053-2

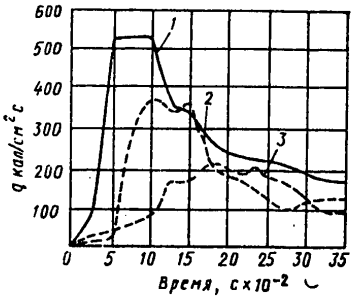

Figure 10.6. Variation of the heat flux to the charged surface as a function of time at different distances from the igniter with rupturable case ($B+KNO_3$):
1 -- z=76 mm; 2 -- z=405 mm;
3 -- z=1270 mm
Key:
1. q, cal/cm^2-sec
2. time, sec x 10^{-2}

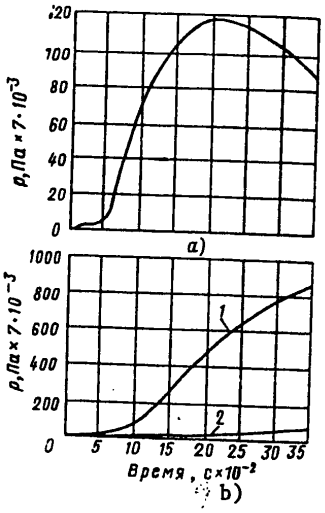

Figure 10.7. Pressure variation in the chamber of the solid-fuel rocket engine with time when using igniters:
a -- with rupturable case based on $B+KNO_3$; b -- jet type; 1 -- pressure in the igniter chamber;
2 -- pressure in the model thrust chamber
Key:
1. p, Pa x $7 \cdot 10^{-3}$
2. time, sec x 10^{-2}

the chamber obtained in the same experiment. As follows from the graphs, for each coordinate the function q(t) passes through a maximum. Here, as we go away from the igniter the maximum decreases, and the maximum itself becomes more rounded.

On the basis of the existing experimental data and in accordance with the general physical concepts of the principles of the process, the variation of the heat flux with time and the coordinate z for an igniter with rupturable case can be represented by the simulating function of the type

$$q = A_q \frac{t^m}{z^n} e^{-k\frac{t}{z}}, \qquad (10.6)$$

where A_q, m, n, k are constants determined experimentally.

APPROVED FOR RELEASE: 2007/02/08: CIA-RDP82-00850R000200090053-2

APPROVED FOR RELEASE: 2007/02/08: CIA-RDP82-00850R000200090053-2

The quantity and dimensions of the compensated particles transferred to the charge surface depends to a significant degree on the composition of the combustion products of the igniter. The distribution of the particle sizes also depends on the chemical composition of the igniter. Below, in Table 10.1 we have the size distribution of the condensed particles for two compositions from reference [52].

Table 10.1

Диапазон размеров частицы, мкм (1)	(2) Весовой %	
	$B+KNO_3$	$Mg+KNO_3$
0—4,9	84	52
5—9,9	12,5	33,5
10—14,9	1,5	7,5
15—19,9	1	5
20—24,9	0,5	1,5
25—29,9	0,1	0,33
30—34,9	—	0,33

Key:
1. Size range of the particles, microns
2. Percent by weight

In view of the similarity of the processes of heat and mass transfer for the mass flow of condensed particles to the charge surface it is possible to begin with the function analogous to (10.6)

$$\dot{m}_S = A_m \frac{t^m}{z^n} e^{-k\frac{t}{z}}. \tag{10.7}$$

10.3. Frontal Ignition of Ballistite Fuel by Hot Gas

In the investigated case the effect of the combustion products on the charge surface is manifested in uniform supply of heat insuring frontal heating of the upper layers of the fuel. This type of effect is observed with an insignificant content of the condensed phase in the combustion products of the igniter, and also for dimensions of the condensed particles below the limiting diameter of the center ignition (see (10.4).

In order to calculate the intrachamber parameters of the solid-fuel rocket engine during the ignition period it is necessary to have at our disposal:

The ignition criterion permitting determination of whether ignition of the fuel has taken place for the given parameters of the effect of the igniter;

The distribution law of the flame over the surface of the charge;

APPROVED FOR RELEASE: 2007/02/08: CIA-RDP82-00850R000200090053-2

APPROVED FOR RELEASE: 2007/02/08: CIA-RDP82-00850R000200090053-2

The law of variation of the combustion rate on the ignited charge particles.

When determining the critical ignition conditions of ballistite fuel usually the theories of ignition in the condensed phase are adhered to. The proponents of this theory begin with the fact that in the process of combustion and ignition of ballistite solid rocket fuel, a decisive role is played by exothermal reactions in the condensed phase, as a result of which the charge ignition takes place in a defined stage of their development connected, in turn, with the thermal state of the surface layer of the charge. The development of the ignition theory began with the works of Ya. B. Zel'dovich. The model of ignition in the condensed phase was formulated in the papers of Frazer and Hicks [51, 50], and at the present time it has won a large number of followers.

For calculation of the nonsteady-state temperature field of the charge during frontal ignition, the system of equations presented in 8.2 can be used.

Let us consider the approximate solution of the problem based on the provisional separation of the process in the two stages: the first stage when the release of heat from the chemical reactions in the fuel is negligibly small by comparison with the heat flux supplied to the surface from the gas phase; the second stage where the heat release in the condensed phase becomes commensurate with the supplied heat flux.

In the first stage the temperature distribution in the fuel is found from the solution of the classical problem of nonstationary thermal conductivity for a semibounded solid state with second or third type boundary conditions. In the case of a second type boundary conditions, for the average magnitude of the heat flux q in time, the temperature distribution in the charge is expressed by the formula

$$T=T_{н}+\frac{2\bar{q}}{\lambda_{т}}\sqrt{a_{т}t}\,\mathrm{ierfc}\left(\frac{x}{2\sqrt{a_{т}t}}\right), \qquad (10.8)$$

where ierfc is the integral of the Gauss error function for the argument $(x/2\sqrt{a_T t})$. When $x=0$, $T=T_S$, the duration of the first stage is determined from the formula (10.8) as

$$t_1=\frac{(T_S^*-T_{н})^2\rho_{т}c_{т}\lambda_{т}}{\bar{q}^2}, \qquad (10.9)$$

where T_S^* is the surface temperature for which intense gasification of the fuel begins.

In the first approximation on identification of the fuel ignition process with heating of an inert body to some given temperature level the function (10.9) can be considered as the formula for determining the ignition time.

APPROVED FOR RELEASE: 2007/02/08: CIA-RDP82-00850R000200090053-2

APPROVED FOR RELEASE: 2007/02/08: CIA-RDP82-00850R000200090053-2

The function (10.9) does not give an answer to the question as to what the temperature T_S* is which can be taken as the ignition point of the fuel. The temperature T_S* also cannot be established from analysis of the function $u(T_S)$ (8.1) inasmuch as it expresses the monotonic variation of u with an increase in T_S.

For this purpose let us consider the second stage. As the analysis of the results of numerical integration of the system of equations (10.8)-(10.9) shows, the temperature profile in the fuel during nonsteady-state heating with removal of mass is approximated with acceptable accuracy by the exponential curve

$$T-T_н=(T_S-T_н)e^{-hx}, \tag{10.10}$$

where h is the approximation coefficient determined for each point in time from the boundary condition (8.11) by the formula

$$h=\frac{q(t,z)+\varrho uQ_S}{\lambda_T(T_S-T_н)}. \tag{10.11}$$

Substituting (10.10) in equation (8.10), we obtain

$$\frac{\partial T}{\partial t}=(T_S-T_н)he^{-hx}a_т\left(h-\frac{u}{a_т}\right). \tag{10.12}$$

The function (10.12) establishes three possible versions of the evolution of the temperature profile of the charge after reaching a temperature of T_S* on the surface which insures a gasification rate u:

1) $h>\frac{u}{a_т}\frac{\partial T}{\partial t}>0$ -- the temperature of the surface layer of fuel continues to rise; here an increase in T_S and the gasification rate take place;

2) $h=\frac{u}{a_т}\frac{\partial T}{\partial t}=0$ -- here the steady-state combustion conditions are achieved, T_S=const; for $h=u/a_t$ the temperature profile corresponds to the Michelson profile;

3) $h<\frac{u}{a_т}\frac{\partial T}{\partial t}<0$ -- the temperature of the surface layer of the fuel decreases; the supply of heat and heat release on the surface do not compensate for the heat release in depth of the charge as a result of thermal conductivity.

For reliable ignition of the charge it is necessary that the following condition be satisfied: $\frac{\partial T}{\partial t}\geqslant 0$ $h\geqslant\frac{u}{a_т}$. The limit of the transition from the stage of inert heating of the solid state to the initial

APPROVED FOR RELEASE: 2007/02/08: CIA-RDP82-00850R000200090053-2

APPROVED FOR RELEASE: 2007/02/08: CIA-RDP82-00850R000200090053-2

combustion stage is related to the achievement of the quality of the heat inflow rates from the outside source and from the fuel gasification reaction. From the expression for h and the condition $h \geqslant u/a_T$ it follows that:

$$2q(t, z) \geqslant u(T_S - T_н)\varrho_T c_T. \tag{10.13}$$

Inasmuch as $u=f(T_S)$, expression (10.13) uniquely defines the temperature T_S^*, for which the gasification of the solid fuel becomes a stable, self-supporting process. According to the function (10.13) the value of T_S^* gives a function of the heat flux, and it increases with an increase in q.

In the first rough approximation, the exponential function in the range of possible values of T_S on ignition can be approximated by the parabola $u=B_u(T_S-T_H)^2$. Defining T_S-T_H here from the condition (10.13) and substituting in (10.9), we obtain the approximate function

$$t_в = \frac{\text{const}}{q^{1,33}} \sim \frac{\text{const}}{q}.$$

The results of the experiments with respect to igniting the solid rocket fuel by means of the hot gas generated in the shock tube confirm that in the high thermal flux range (400 to 4000 kilojoules/m^2-sec) the ignition delay time varies inversely proportionally to the average heat flux to the charge surface [25].

Determining T_S-T_H from the condition (10.13) and substituting in (10.9) it is also possible to obtain the function $t_B=4a_T/a^2\sim 4\tau_p$, which itself does not determine the ignition conditions, but indicates the relation of the ignition time to the thermal relaxation time for the steady-state combustionconditions achieved during ignition at q=const.

Thus, the functions (10.9) and (10.13) for a known average value of $\bar{q}(t)$ for the given section of the surface make it possible to determine the beginning of intensive gasification of the fuel and its rate for this section.

In the case of discrete determination of the heating conditions for separate strips of charge, the local flame propagation rate in the direction z is defined as

$$v = \frac{z_2 - z_1}{t_{в_2} - t_{в_1}},$$

where z_1, z_2 are the strip coordinates; t_{B1}, t_{B_2} are the ignition times corresponding to them.

If the magnitude of the eat flux averaged in time can be given as a continuous function of z, the local propagation rate of the flame is defined as

APPROVED FOR RELEASE: 2007/02/08: CIA-RDP82-00850R000200090053-2

APPROVED FOR RELEASE: 2007/02/08: CIA-RDP82-00850R000200090053-2

$$v = \frac{1}{\frac{dt_s}{d\bar{q}} \frac{d\bar{q}(z)}{dz}}.$$

10.4. Center Ignition of a Charge of Ballistite Fuel under the Effect on Its Surface of Hot Condensed Particles

The condensed particles formed on combustion of the pyrotechnical compositions and smoke powder, hitting the charged surface and being introduced into the solid fuel monolith form the ignition centers scattered over the surface. On contact with the particle having high temperature with the surface, heating of the contact microlayer takes place to the gasification point. Here a gas interlayer is formed between the particles and the fuel, the thermal conductivity of which later limits the heat transfer from the particle to the charge.

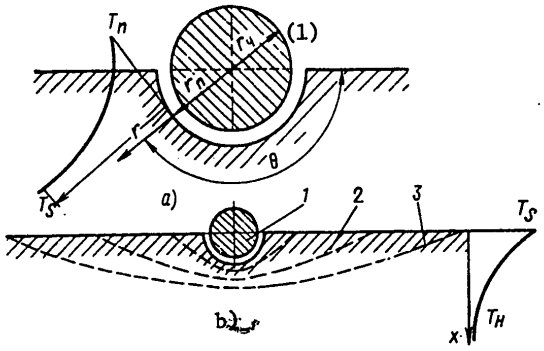

Figure 10.8. Diagram of the center ignition of the fuel: a -- occurrence of the ignition center; b -- evolution of the center in time: 1 -- condensed particle; 2 -- fuel; 3 -- fuel gasificaton front

Key:
1. particle

In order to estimate the igniting capacity of a condensed particle settling on the surface, let us consider the relations which determine the temperature variation of the fuel in its vicinity (Fig 10.8). We shall assume that the particle is a sphere with the radius $r_{particle}$, that it is completely submerged in the fuel, and the heat exchange between the particle and the fuel follows the Newtonian function.

Considering the process of thermal conductivity in the spherical coordinate system, we obtain the system of equations:

FOR OFFICIAL USE ONLY

APPROVED FOR RELEASE: 2007/02/08: CIA-RDP82-00850R000200090053-2

APPROVED FOR RELEASE: 2007/02/08: CIA-RDP82-00850R000200090053-2

a) For a particle

$$\frac{\partial T_ч}{\partial t} = \underset{(1)}{a_ч}\left(\frac{\partial^2 T_ч}{\partial r^2} + \frac{2}{r}\frac{\partial T_ч}{\partial r}\right). \tag{10.14}$$

Key: 1. particle

The initial condition

$$t=0 \quad T_ч(r, 0) = \text{const} = T_{ч0}. \tag{10.15}$$

The boundary condition

$$r=r_ч \quad \alpha(T_{чп} - T_п) = -\lambda_ч \frac{\partial T_ч}{\partial r}\Big|_{r=r_ч}. \tag{10.16}$$

b) For the fuel

$$\frac{\partial T_т}{\partial t} = a_т\left[\frac{\partial^2 T_т}{\partial r^2} + \frac{2}{r}\frac{\partial T_т}{\partial r} + \frac{1}{r^2 \sin\theta}\frac{\partial}{\partial\theta}\left(\sin\theta\frac{\partial T_т}{\partial\theta}\right)\right]. \tag{10.17}$$

The initial condition

$$t=0 \quad T_т = T_т(x, 0), \tag{10.18}$$

where x=r sin θ.

The boundary condition

$$\begin{gathered} r=r_п \quad \alpha(T_{чп} - T_п)\frac{r_ч^2}{r_п^2} = -\lambda_т \frac{\partial T}{\partial r}\Big|_{r=r_п} \\ r=\infty \quad T_т = T(r\sin\theta, 0). \end{gathered} \tag{10.19}$$

In the above-presented relation the index "particle" pertains to the particle parameters, and the index "T" to the fuel.

The initial condition for the fuel expresses the temperature distribution in the surface layer of the charge developing under the effect of heat flux fed to the given section of the surface before the particle is incident on it. The boundary condition for r=∞ corresponds to the initial temperature distribution. This recording of the boundary condition presupposes the absence of thermal interaction between the adjacent ignition centers.

The boundary conditions for $r=r_{particle}$ (particle radius) and for $r=r_т$ (the radius of a sphere burned in the fuel) express the law of heat exchange between the particle and the fuel. Here the heat fluxes to the fuel will be variable with respect to the coordinate θ, that is, the

APPROVED FOR RELEASE: 2007/02/08: CIA-RDP82-00850R000200090053-2

APPROVED FOR RELEASE: 2007/02/08: CIA-RDP82-00850R000200090053-2

heating of the fuel will be asymmetric in view of the initial nonuniformity of the temperature field of the surface layer of the charge.

The heat transfer process to the gas interlayer between the particle and the fuel is characterized by the heat transfer coefficient which, according to the experimental data of reference [52] is assumed to be independent of the temperature gradient and the particle size.

By computer solution of the above-presented system of equations, numerical results can be obtained which characterize the ignition capacity of the particles of different size and with different initial temperature $T_{particle\ 0}$.

In view of the fact that the solution of the system of equations (10.14)-(10.19) appears to be awkward, let us also consider the approximate method of estimating the igniting capacity of the condensed particles. Inasmuch as we are interested in the limiting ignition characteristic connected with using small size particles, in the first approximation we can set the temperature field of the fuel at depth equal to the particle radius provisionally uniform with the mean temperature equal to the surface temperature of the charge T_S. Here the problem becomes symmetric, and the equation of thermal conductivity of the fuel can be written in the form

$$\frac{\partial T_т}{\partial t}=a_т\left(\frac{\partial^2 T_т}{\partial r^2}+\frac{2}{r}\frac{\partial T_т}{\partial r}\right). \tag{10.20}$$

Let us be given the nature of the temperature profile analogously to how this was done in 10.3:

$$T-T_S=(T_п-T_S)e^{-h(r-r_п)}, \tag{10.21}$$

where h is the matching coefficient determined for each point in time from the boundary condition

$$r=r_п\quad \frac{\partial T_т}{\partial r}=\frac{\alpha}{\lambda}(T_ч-T_п)=(T_п-T_S)h,$$

from which

$$h=\frac{\alpha}{\lambda}\frac{T_ч-T_п}{T_п-T_S}. \tag{10.22}$$

Substituting (10.21) in (10.20), we obtain

$$\frac{\partial T_т}{\partial t}=a_т(T_п-T_S)\left(h^2-\frac{2}{r}h\right)e^{-h(r-r_п)}. \tag{10.23}$$

The limiting condition of local fuel ignition by the solid particle includes two requirements:

The temperature of the contact surface $T_п$ must reach the level $T_п^*$ corresponding to the beginning of the steep section of the Arrhenius curve;

APPROVED FOR RELEASE: 2007/02/08: CIA-RDP82-00850R000200090053-2

APPROVED FOR RELEASE: 2007/02/08: CIA-RDP82-00850R000200090053-2

At this level the heating of the deep layer of fuel must continue, that is, it is necessary that $\partial T/\partial t>0$.

Considering the limiting ignition condition, we can neglect the heat released during gasification of the fuel on the contact surface making up a small portion of the heat delivered by the particle. At the limit for $\partial T_T/\partial t$ 0 from (10.23) we obtain the expression for the minimum particle radius for which the local fuel ignition becomes impossible

$$r_{np}=2\frac{\lambda_T(T_n-T_S)}{\alpha(T_q-T_n)}. \qquad (10.24)$$

Setting $T_п-T_S$=200 K, $T_{particle}-T_п$=2500 K, $\lambda_T=16\cdot10^{-2}$ watts/m^2, α=2 kilowatts/m^2, we obtain $r_{lim}=1.3\cdot10^{-5}$ m=13 microns. With an increase in surface and particle temperature, the limiting radius increases.

In reference [52] the process of igniting the solid rocket fuel by condensed particles was simulated using wires made of nickel and chromium alloy, which were heated by the current, and then were introduced into samples of the fuel to a depth equal to the wire radius. The presence of ignition was recorded on the basis of recording the thermocouple signals. According to the results of processing the experimental data obtained, the average heat exchange coefficient α is equal to 2 kilowatts/m^2 and it depends relatively weakly on the wire temperature. It was also established that ignition of the solid rocket fuel is insured by particles 10-15 microns in diameter.

The number of particles capable of forming centers of ignition per unit area per unit time will be defined as

$$n_ц=\dot{m}\int_{r_{np}}^{r_{max}}\varphi(r)\,dr,$$

where $\dot{m}$ is the specific flow of mass of solid particles to the surface; $\phi(r)$ is the distribution function representing the number of particles with the size r+dr per unit mass of condensed phase; r_{max} is the maximum radius of the particles.

After contact ignition of the fuel, the gasification surface radius begins to increase, and the effect of the particle as a source of heat decreases rapidly. The erosion of the fuel in the vicinity of the particles will be nonuniform on the basis of nonuniformity of the temperature field of the charge. With time as the depth of erosion approaches the thickness of the layer heated by the external heat flux (frontal burning), the nonuniformity of the erosion will be intensified. Here the process of flame propagation over the surface will depend less and less on the initial configuration of the center, and everything will in a higher degree be determined by the temperature of the heated surface of the charge.

APPROVED FOR RELEASE: 2007/02/08: CIA-RDP82-00850R000200090053-2

APPROVED FOR RELEASE: 2007/02/08: CIA-RDP82-00850R000200090053-2

Let us consider the dynamics of the center charge ignition, with assumptions and simplifications that are avoidable when describing such a complex phenomenon.

Let us make the following assumptions:

1. Each particle with radius $r \geq r_{lim}$, incident on an unignited section of the surface, forms an ignition center.

2. The flow of igniting solid particles aimed at the surface is a given function of the coordinate and time

$$n_s = \dot{m}(z, t) \int_{r_{np}}^{r_{max}} \varphi(r)\, dr. \qquad (10.25)$$

3. The propagation rate of the flame over the surface is an exponential function of the surface temperature T_{SH} reached as a result of heating by the heat fluxes from the gas phase

$$v = k_v e^{D(T_{SH} - c)}. \qquad (10.26)$$

4. The surface temperature T_{SH} represents a known value determined from the condition of nonsteady-state heating of the fuel as an inert material for the given local value of the heat flux from the given section q(z,t).

The number of centers appearing per unit time per unit area of the charge surface will depend not only on the specific flow of particles n_B to the surface, but also on the probability that these particles will be incident on unexcited sections. We shall assume that the distribution of the particles incident on the surface within the limits of a small section of the surface, follows the law of equal probability. Then the probability of incidence of a particle on the unexcited section will be defined as

$$P_i = 1 - \bar{S}_B,$$

where $\bar{S}_B$ is the relative area occupied at the point in time by the ignition centers. The mathematical expectation of formation of the new centers in the time interval Δt will be

$$N = n_s (1 - \bar{S}_B) \Delta t.$$

The ignition centers will be represented in the form of circles. At an arbitrary point in time t the area of such a circle will be

$$S_i = \pi \left(r_0 + \int_{\tau_i}^{t} v\, dt \right)^2,$$

APPROVED FOR RELEASE: 2007/02/08: CIA-RDP82-00850R000200090053-2

APPROVED FOR RELEASE: 2007/02/08: CIA-RDP82-00850R000200090053-2

or, substituting the value of v:

$$S_i=\pi\left(r_0+\int_{\tau_i}^{t}k_v e^{D(T_{S_H}-c)}dt\right)^2,$$

where τ_i is the time of formation of the given center, r_0 is its initial radius.

If the time t from the beginning of the ignition process is divided into three identical small intervals Δt, then the relative area of the ignited surface at the given point in time, if we neglect the term πr_0^2, will be expressed as

$$S_B=\pi\Delta t n_{B1}\left(\int_0^t v\,dt\right)^2+\pi\Delta t n_{B2}\left[1-n_{B1}\pi\left(\int_0^{\Delta t}v\,dt\right)^2\right]\left(\int_{\Delta t_1}^{t}v\,dt\right)^2+$$
$$+\pi\Delta t n_{B3}\left\{1-\Delta t n_{B1}\left(\int_0^{2\Delta t}v\,dt\right)^2+\Delta t n_{B2}\left[1-n_{B1}\left(\int_0^{2\Delta t}v\,dt\right)^2\right]+\right.$$
$$\left.+\Delta t n_{B2}\left[1-n_{B1}\left(\int_0^{2\Delta t}v\,dt\right)^2\right]\left(\int_{\Delta t}^{2\Delta t}v\,dt\right)^2\right\}\left(\int_{2\Delta t}^{t}v\,dt\right)^2+\ldots\ldots \qquad (10.27)$$

It must be noted that this approach to the determination of the area of the ignited surface will be used under the condition that each ignition center increases independently of the increase in the adjacent centers, and does not reflect the final stage -- the effect of the centers.

However, in view of the fast speed of the concluding stage, the time of formation of the solid combustion front can be estimated by the time of reaching $\bar{S}_B$=0.65-0.70.

10.5. Frontal Ignition of Mixed Fuel by a Hot Gas Flow

The difference in the combustion models of ballistite and mixed fuel gives rise to different models of their ignition. When heating the mixed fuel, gasification of its components takes place, the decomposition products of which enter into the exothermal reaction at some distance from the charge surface. For the occurrence of a reaction it is necessary that some critical temperature and defined concentration of the reagents be reached. The heat released as a result of the reaction promotes an increase in the heat fluxes directed at the charge surface. The intensification of the heating of the surface of the fuel components is accompanied by intensification of their gasification, which promotes intensification of the reaction in the gas phase. Occurring in more heated gas layers remote from the surface, the reaction front shifts as the exothermal oxidizing processes develop toward the fuel surface until stabilization of it takes place at a distance corresponding to the steady-state fuel combustion.

APPROVED FOR RELEASE: 2007/02/08: CIA-RDP82-00850R000200090053-2

APPROVED FOR RELEASE: 2007/02/08: CIA-RDP82-00850R000200090053-2

Thus, the model of ignition of the mixed fuel by a hot gas includes three basic stages:

1. Heating of the charge surface ending in intense gasification of both fuel components.

2. Formation of a reactive mixture of the products of decomposition of the fuel in the gas phase near the charge surface.

3. Development of an exothermal reaction in the gas phase ending in establishment of a stable combustion front near the charge surface.

Let us consider these stages separately.

10.5.1. Heating of the Surface of the Mixed Fuel During Ignition

A significant difference in the thermophysical and physical-chemical properties of the basic components of the mixed fuel causes a difference in their behavior when heating by the products of combustion of the igniter. In Table 10.2 we have the basic characteristics of the R-13 fuel and ammonium perchlorate [39].

Table 10.2

Компоненты (1)	ρ, кг/м³ (2)	c, кДж/кг·К (3)	λ, Вт/кг·К (4)	a, м²/с (5)	Q_S, кДж/кг (6)	K_m, м/с (7)	E/2R, К (8)
(9) Перхлорат аммония	1950	1,26	0,46	$1{,}86 \cdot 10^{-7}$	1050	46	10000
(10) Нитрат аммония	1720	1,09	0,67	$2{,}72 \cdot 10^{-7}$	810	120	3550
(11) Горючее-связка Р-13	1210	1,67	0,167	$0{,}83 \cdot 10^{-7}$	—100	0,18	5400

Key:
1. Components
2. ρ, kg/m^3
3. c, kjoules/kg-K
4. λ, watts/kg-K
5. a, m^2/sec
6. Q_S, kjoules/kg
7. K_m, m/sec
8. E/2R, K
9. Ammonium perchlorate
10. Ammonium nitrate
11. R-13 fuel-binder

Inasmuch as the thermal diffusivity of the fuel-binder is several times lower than for the oxidizing agent, under identical conditions of supplying heat in the case of nonsteady heating, the temperature of the surface of the combustible component of the fuel increases more rapidly than on the surface of the oxidizing agent. Here, the temperature difference in the surface of the oxidant crystals and sections of the combustible component

APPROVED FOR RELEASE: 2007/02/08: CIA-RDP82-00850R000200090053-2

APPROVED FOR RELEASE: 2007/02/08: CIA-RDP82-00850R000200090053-2

can be several hundreds of degrees. Inasmuch as the rate of thermal decomposition of the components of the mixed fuel follows an exponential function of the heating temperature, a significant discontinuity in time appears between the beginning of the intensity composition of the binder and the oxidant.

Therefore after a short inert heating of the surface layers of the combustible component and the oxidant, a quite long period begins during which only the combustible components -- the products of pyrolysis of the binder -- come from the charge surface to the flow of gases washing over it, and at the beginning of decomposition of the oxidant adjacent to the charge surface the region can be assumed solidly filled with gaseous combustible components.

The system of equations describing the nonsteady-state heating of the components is made up of the equations of thermal conductivity for the basic fuel components with the boundary conditions:

a) For the fuel-binder

$$\frac{\partial T_{rc}}{\partial t} = a_{rc} \frac{\partial^2 T_{rc}}{\partial x^2} \tag{10.28}$$

for x=0

$$-\lambda_r \frac{\partial T_r}{\partial x}\Big|_S = -\lambda_{rc} \frac{\partial T_{rc}}{\partial x}\Big|_S + \Delta H_{rc} \varrho_{rc} K_{m_{ro}} \exp\left(-\frac{E_{rc}}{2RT_{S_{rc}}}\right);$$

b) For the oxidant

$$\frac{\partial T_{ok}}{\partial t} = a_{ok} \frac{\partial^2 T_{ok}}{\partial x^2} \tag{10.29}$$

for x=0

$$-\lambda_r \frac{\partial T_r}{\partial x}\Big|_S = -\lambda_{ok} \frac{\partial T_{ok}}{\partial x}\Big|_S + \Delta H_{ok} \varrho_{ok} K_{m_{ok}} \exp\left(-\frac{E_{ok}}{2RT_{S_{ok}}}\right); \tag{10.30}$$

for t=0, $T=T_H=const.$

The arrival of the gasified components from a unit area of the charged surface will be defined by the equations

a) For the combustible component-binder

$$Y_{rc} = \varrho_r \bar{S}_{rc} K_{m_{rc}} \exp\left(-\frac{E_{rc}}{2RT_{S\,rc}}\right); \tag{10.31}$$

APPROVED FOR RELEASE: 2007/02/08: CIA-RDP82-00850R000200090053-2

APPROVED FOR RELEASE: 2007/02/08: CIA-RDP82-00850R000200090053-2

b) For the oxidant

$$Y_{(1)ок}=\varrho_{ок}(1-\bar{S}_{rc})K_{m_{ок}}\exp\left(-\frac{E_{ок}}{2RT_{Sок}}\right), \qquad (10.32)$$

Key: 1. fuel-binder

where $\bar{S}_{\text{fuel-binder}}$ is the relative proportion of the charged surface occupied by the binder.

The control equation expresses the achievement of the ratio of inflows of $Y_{\text{fuel-binder}}$ and Y_{ox} determining the beginning of intense inflow of the products of decomposition of the oxidant.

$$n=\frac{Y_{ок}}{Y_{rc}},$$

where the value of n is provisional level taken as the beginning of the second stage at the ignition process. The ratio $\bar{S}_{\text{fuel-binder}}/(1-\bar{S}_{\text{fuel-binder}})$ in the first approximation will be defined as $(\dot{m}_{\text{fuel-binder}}/m_{ox})$ $(\rho_{ox}/\rho_{\text{fuel-binder}})$, where $m_{\text{fuel-binder}}/m_{ox}$ is the mass ratio of the combustible component and the oxidant in the fuel. It is necessary to consider that in the process of aging of the mixed fuel, enrichment of the surface layer by the combustible component takes place, in view of which the relation $\bar{S}_{\text{fuel-binder}}/(1-\bar{S}_{\text{fuel-binder}})$ increases, and the second ignition stage comes later, which is confirmed in practice: the old charges made up of the mixed fuel are ignited worse than the new ones [25].

10.5.2. Formation of a Reactive Mixture of the Products of Composition of the Fuel in the Gas Phase and Its Ignition

For purposes of simplifying the solution of the problem usually the mass transfer of the products of decomposition of the oxidant and the combustible component are investigated in a stationary gas medium in which there is no convective transfer of mass and heat. This approach appears to be acceptable if we assume that for the actual picture of the gas flow over the charged surface a viscous sublayer is formed near it with predominance of the molecular mechanism of mass-heat transfer. We shall also assume that the gas density of the transfer characteristics do not depend on the local temperature, and the reactions occurring in the gas phase can be reduced to one resultant second-order reaction.

The complete system of equations includes, along with the equations (10.28), (10.29), also their boundary conditions, the equations of thermal conductivity of the diffusion of the products of decomposition of the basic components in the gas phase

$$\frac{\partial C_{rc}}{\partial t}=D\frac{\partial^2 C_{rc}}{\partial x^2}+C_{rc}C_{ок}K_f e^{-\frac{E_f}{RT}}; \qquad (10.33)$$

APPROVED FOR RELEASE: 2007/02/08: CIA-RDP82-00850R000200090053-2

APPROVED FOR RELEASE: 2007/02/08: CIA-RDP82-00850R000200090053-2

$$\frac{\partial C_{ок}}{\partial t} = D\frac{\partial^2 C_{ок}}{\partial x^2} + nC_{rc}C_{ок}K_f e^{-\frac{E_f}{RT}}; \tag{10.34}$$

$$\frac{\partial T_r}{\partial t} = a_r\frac{\partial^2 T_r}{\partial x^2} + \frac{Q_f}{c_p}C_{rc}C_{ок}K_f e^{-\frac{E_f}{RT}}. \tag{10.35}$$

The boundary conditions

$$x=0$$

a) For the oxidant

$$C_{ок}\dot{m}_{ок} = -D\varrho\left(\frac{\partial C_{ок}}{\partial x}\right)_S; \tag{10.36}$$

$$\dot{m}_{ок} = (1-\bar{S}_{rc})\varrho_{ок}K_{m_{ок}}\exp(-E_{ок}/2RT_{S\,ок}); \tag{10.37}$$

$$T = T_{S\,ок};$$

$$-\lambda_r\frac{\partial T_r}{\partial x}\Big|_S = -\lambda_{ок}\frac{\partial T_{ок}}{\partial x}\Big|_S + \frac{\Delta H_{ок}\dot{m}_{ок}}{1-\bar{S}_{rc}}; \tag{10.38}$$

b) For the combustible component-binder

$$C_{rc}\dot{m}_{rc} = -D\varrho\left(\frac{\partial C_{rc}}{\partial x}\right)_S; \tag{10.39}$$

$$\dot{m}_{rc} = \bar{S}_{rc}\varrho_{rc}K_{m_{rc}}\exp(-E_{rc}/2RT_{S\,rc}); \tag{10.40}$$

$$T = T_{S\,rc};$$

$$-\lambda_r\frac{\partial T_r}{\partial x}\Big|_S = -\lambda_{rc}\frac{\partial T_{rc}}{\partial x}\Big|_S + \frac{\Delta H_{rc}}{\bar{S}_{rc}}\dot{m}_{rc}; \tag{10.41}$$

$$x=\infty$$

$$C_{ок}=0$$

$$C_{rc}=1$$

$$T=T_\infty$$

$$t=0;\ C_{rc}=1;\ C_{ок}=0;\ T_{S\,ок}=T_{S_{ок.нач}}$$

$$T_{S_{rc}}=T_{S_{rc.нач}}.$$

Here D is the diffusion coefficient of the products of decomposition of the combustible component of the fuel and the oxidant in the gas phase, which in the first approximation is assumed for all decomposition products to be identical; $C_{\text{fuel binder}}$, C_{ox} are the relative concentrations of the products of decomposition of the combustible component and the oxidants; K_f, E_f, Q_f are the factors in front of the exponent, the energy of activation and the heat for the resultant reaction in the gas phase; n is the stoichiometric coefficient in the reaction equation in the presence of the oxidizing component.

APPROVED FOR RELEASE: 2007/02/08: CIA-RDP82-00850R000200090053-2

APPROVED FOR RELEASE: 2007/02/08: CIA-RDP82-00850R000200090053-2

The solution of the above-presented system of equations makes it possible to determine the nonsteady-state concentration and temperature fields near the charge surface during ignition. It is proposed that the distribution of the products of gasification of the fuel-binder in the first stage of the process encompass the zone exceeding the zone of chemical reactions in the second stage, which makes it possible to resort to a simplifying expression of the boundary condition, assuming for $x=\infty$, $C_{\text{fuel-binder}}=1$.

According to the equation (10.35) at each point of the investigated space the variation in time of the local gas temperature is determined by the relation of two factors: the heat release as a result of the chemical interaction of the products of gasification of the combustible component and the oxidant, and the heat transfer. The terms in the righthand side of equation (10.35) expressing the effect of these factors explicitly depend on the pressure inasmuch as $a_{\text{fuel}}\sim 1/p$, $\rho_{\text{fuel}}\sim p$. Thus, the pressure level will determine the degree of predominance of the second term over the first. For sufficiently low pressure the heat transfer can turn out to be greater than the heat released during the chemical reaction and ignition will not occur.

In the presence of oxygen in the gaseous environment, the second term of equation (10.35) can be predominant before this takes place as a result of the inflow of the products of decomposition of the oxidizing agent. Thus, the relation noted by many researchers for the ignition time of the mixed fuel as a function of the oxygen concentration in the igniting gas becomes understandable.

The equation (10.35) permits establishment of the ignition time for which the condition $\partial T/\partial t \geq 0$ is satisfied, that is,

$$a_r \frac{\partial^2 T_r}{\partial x^2} = \frac{Q_f}{c_p} C_{re} C_{ok} K_f e^{-\frac{E_f}{RT}}. \qquad (10.42)$$

In order to obtain from condition (10.42) the criterion determining the ignition time, it is necessary to substitute the functional relations for the composition and temperature as a function of time and the coordinate x in it.

10.6. Center Ignition of Mixed Fuel

For center ignition of mixed fuel, the initiating effect of the igniter particles and the condensed products of its combustion is manifested both in the surface layer of the fuel and in the gas phase near the charged surfaces.

On introduction of large particles of igniter into the surface layer of the fuel, just as in the case investigated in 10.4, an interlayer is formed around the particles filled with the products of gasification of the fuel components. If the dimensions of the igniter particle essentially exceed

APPROVED FOR RELEASE: 2007/02/08: CIA-RDP82-00850R000200090053-2

APPROVED FOR RELEASE: 2007/02/08: CIA-RDP82-00850R000200090053-2

the dimensions of the grains of fuel oxidant, the products of decomposition of both the oxidant and the combustible component will reach the gas interlayer. On moving with streamlining of the settled particle and under the effect of its hot surface, they begin to react chemically with the generation of a significant quantity of heat. Consequently, when large particles hit the fuel surface in the formation and development of the ignition center an obvious role is played by the factor of the heterogeneous structure of the fuel.

When fine particles hit the surface, the heterogeneous nature of the structure will be manifested more weakly, and the ignition mechanism will approach that which was investigated in 10.4.

In the gas phase near the combustion surface around the condensed particles as sources of high temperature, centers of ignition of the gas mixture can occur which are formed during frontal heating of the charge surface. The occurrence of such centers can take place for lower temperature of the mixture than that which determines its self-ignition according to equation 10.34.

In view of the fact that the phenomena forming the basis for the fourth ignition model have been little studied, it appears to be difficult to formulate critical ignition conditions for it.

10.7. System of Equations for Determining the Thermodynamic Parameters of Solid Fuel Rocket Engines During the Ignition Period and Joint Combustion of the Igniter and the Charge

Let us consider the united system of equations which in general form describes the variation of the basic thermogas-dynamic parameters in the chamber of the solid-fuel rocket engine during the ignition period. This system follows from the previously presented system 9.1 and includes the additions determined by the above-investigated models of ignition of the solid rocket fuel:

$$\begin{cases} 1)\ \dfrac{W}{(RT)_c}\dfrac{dp}{dt} = Y_т(t) + Y_в(t) - \dot{m}_c(t) + \dfrac{pW}{(RT)_c}\dfrac{d(RT)_c}{dt}; \\ 2)\ \dfrac{pW}{T_c}\dfrac{dT_c}{dt} = Y_т(t)\dfrac{k_c-1}{k_т-1}R_т(T_{V_т}-T_c) + \\ \quad + Y_в(t)\dfrac{k_c-1}{k_в-1}R_в(T_{V_в}-T_c) - (k_c-1)\varphi_c A_c F_{кр} p\sqrt{(RT)_c} - \dfrac{dQ}{dt}(k_c-1); \\ 3)\ \dot{m}_c = \dfrac{\varphi_c A F_{кр} p}{\sqrt{(RT)_c}}; \\ 4)\ p = \dfrac{m_c(RT)_c}{W}; \\ 5)\ Y_т(t) = \varrho_т \int_0^{S_в} u\,dS; \end{cases} \tag{10.43}$$

APPROVED FOR RELEASE: 2007/02/08: CIA-RDP82-00850R000200090053-2

APPROVED FOR RELEASE: 2007/02/08: CIA-RDP82-00850R000200090053-2

$$\left|\begin{array}{l} 6)\ Y_{\text{в}}(t)=\varrho_{\text{в}}S_{\text{в}}\mu_{1\text{в}}p^{\nu_{\text{в}}}- \qquad \text{-- for an igniter with rupturable case} \\ Y_{\text{в}}(t)=\varrho_{\text{в}}S_{\text{в}}\mu_{1\text{в}}p_{\text{в}}^{\nu_{\text{в}}}=\dfrac{\varphi_{\text{св}}A_{\text{в}}F_{\text{кр.в}}}{\sqrt{(RT)_{\text{в}}}}p_{\text{ц}}- \qquad \text{-- for a jet type igniter} \\ 7)\ \dfrac{dQ}{dt}=\int\limits_0^{S_{\text{к}}}\alpha(T_{\text{с}}-T_{\text{с.в}})\,dS_{\text{к}}. \end{array}\right.$$

Here the index "T" pertains to the products of combustion of the fuel, the index "B" pertains to the products of combustion of the igniter, and the index "c" to the mixture of these products.

Equations (1) and (2) differ from the corresponding equations of system 8.1 in that they take into account the inflow of heterogeneous products into the chamber: the products of combustion of the igniter, the products of combustion of the fuel and also the presence of a mixture of these products.

In order to determine the thermophysical characteristics of the mixture, additional relations are used:

$$R_{\text{с}}=nR_{\text{т}}+(1-n)R_{\text{в}};$$
$$c_{v_{\text{с}}}=nc_{v_{\text{т}}}+(1-n)c_{v_{\text{в}}};$$
$$c_{p_{\text{с}}}=nc_{p_{\text{т}}}+(1-n)c_{p_{\text{в}}};$$
$$k_{\text{с}}=\frac{c_{p_{\text{с}}}}{c_{v_{\text{с}}}},$$

where $n=m_T/m_k$ is the ratio of the mass of the products of combustion of the fuel m_T to the total mass of the combustion products in the chamber

$$m_{\text{к}}=m_{\text{т}}+m_{\text{в}}.$$

The variation in time of the mass fraction n is defined by the equation

$$m_{\text{к}}\frac{dn}{dt}=Y_{\text{т}}(t)(1-n)-Y_{\text{в}}(t)n.$$

For the period of ignition, the charge configuration can be assumed invariant. Here, from the system of equations the equations are dropped which describe the variation in time of the combustion surface and the through cross section of the charge. Instead of this, the equations appear which describe the variation in time of the igniter combustion surface.

The equations of the arrival of the products of combustion of the igniter assume different forms depending on the type of ignition device. For an igniter with rupturable case, the inflow of the combustion products is

FOR OFFICIAL USE ONLY

APPROVED FOR RELEASE: 2007/02/08: CIA-RDP82-00850R000200090053-2

APPROVED FOR RELEASE: 2007/02/08: CIA-RDP82-00850R000200090053-2

determined by the pressure in the chamber of the solid fuel rocket engine. For the igniter with unrupturable case with supercritical pressure gradient between the igniter chamber and the engine volume, the inflow of the combustion products is determined by the pressure set up in the igniter chamber p_B.

Equation (5) expressing the gas inflow from the ignited sections of the charge presents a primary difficulty in the mathematical description of the ignition process. Above, we investigated the basic models of the ignition determining the approach to the formulation of this equation for various situations. In all cases for correct solution of the problem equation (5) runs into the system of equations describing the nonsteady-state heating and combustion of the fuel.

The simplified approach to the solution of the problem consists in introducing the critical ignition conditions based on a number of simplifying assumptions as was illustrated in Sections 10.3, 10.4, 10.5. Then it is proposed that in the ignited sections combustion follows a stationary law. Here

$$Y_T(t) = \varrho_T u_1 \overline{S}_B S_0 p^\nu.$$

For frontal ignition by a hot gas

$$\overline{S}_B = \frac{l_B}{L_3} \quad l_B = \int_{\tau_3}^{t} v dt;$$

$$v = \frac{1}{\frac{dt_B}{d\bar{q}} \frac{d\tilde{q}(z)}{dz}},$$

where ℓ_B is the length of the ignited section; v is the propagation rate of the flame along the length of the charge; τ_3 is the time of appearance of the first flame.

In the case of center ignition the determination of $\overline{S}_B$ becomes more complicated, and it is determined by formula (10.27).

Further simplification of the system of equations consists in the fact that instead of the energy equations (2) the relation is introduced which determines the equilibrium value of $(RT)_c = (RT)_k$ as

where

$$(RT)_k = \frac{(1-n) R_B T V_B + n R_T T V_T}{k_c},$$

$$k_c = (1-n) k_B + n k_T.$$

APPROVED FOR RELEASE: 2007/02/08: CIA-RDP82-00850R000200090053-2

APPROVED FOR RELEASE: 2007/02/08: CIA-RDP82-00850R000200090053-2

The solution of the system (10.43) is bound to the time of complete burn-up of the igniter. The thermogas-dynamic parameters determined for this time are initial conditions for calculating the arrival of the solid-fuel rocket engine at the rated parameter regime investigated in Chapter 9.

APPROVED FOR RELEASE: 2007/02/08: CIA-RDP82-00850R000200090053-2

APPROVED FOR RELEASE: 2007/02/08: CIA-RDP82-00850R000200090053-2

CHAPTER 11. DYNAMICS OF THE SOLID-FUEL ROCKET ENGINE CHAMBERS AS OBJECTS OF AUTOMATED CONTROL SYSTEMS

11.1. Peculiarities and Possible Methods of Regulating the Thrust of Solid-Fuel Rocket Engines

The regions and conditions of application of solid-fuel rocket engines are basically analogous to the regions and conditions of the use of liquid-fuel rocket engines, which determines the similarity of the problems of regulating these types of rocket engines.

These problems, in particular, include the variation of the thrust of the rocket or spacecraft engine in order to obtain optimal flow characteristics. As is known, as applied to liquid-fuel rocket engines such regulation has been mastered and is used quite frequently. For solid-fuel engines, in spite of the fact that these engines are appreciably simpler with respect to design than the liquid-fuel engines, the regulation of the magnitude of the thrust is realized with significantly greater difficulty and is rarely used. However, the gain in a number of the most important characteristics of the rockets and spacecraft when introducing engine regulation is so obvious and noteworthy that interest in the problem of regulating solid-fuel rocket engines has not waned, which is indicated by the numerous publications in the field.

A number of solid-fuel engine regulation systems have been proposed. Some of them have been brought to practical implementation. However, the investigation of these regulation systems and devices for solid-fuel rocket engines is beyond the scope of the given book and therefore only an analysis of some of its dynamic characteristics of solid-fuel rocket engine chambers as objects of automatic control are presented below.

Usually the engine thrust or the pressure in its chamber are considered as the controllable parameters for solid-fuel engines, just as for liquid-fuel rocket engines. As for the regulating factors, that is, the factors by means of which the required effect on the regulatable parameters is obtained, there can be several of them. Let us consider the possible method of influencing the thrust of the solid-fuel rocket engine.

APPROVED FOR RELEASE: 2007/02/08: CIA-RDP82-00850R000200090053-2

APPROVED FOR RELEASE: 2007/02/08: CIA-RDP82-00850R000200090053-2

The force of the rocket engine thrust is determined by the flow rate of the combustion products of the fuel and the specific momentum of the force of the thrust

$$P=\dot{m}I_y.$$

In any case it is necessary to maintain the specific thrust at its highest value in connection with which the alteration of the flux through I_y is meaningless. The regulation of the thrust of the solid-fuel rocket engine is possible in practice only by varying the flow rate of the combustion products (gases) through the nozzle.

Fig 11.1 shows a schematic of a solid-fuel rocket engine, the chamber of which has an additional component introduced into it (liquid or gas). If we denote the gas flow rate through the nozzle as $\dot{m}_p$, the gas formation of the charge $\dot{m}_T$, the flow rate of the additional mass $\dot{m}_D$, then in the steady-state regime

$$\dot{m}_p=\dot{m}_т+\dot{m}_д=\dot{m}.$$

Let us assume the law of the charge combustion rate in the form $u=u_1p_k^{\nu}$. Then, considering the equation of gas formation of the charge $\dot{m}_T=Su\rho T$ and the expression for the flow rate through the nozzle $\dot{m}_p=\frac{\varphi_c A p_k F_{кр}}{\sqrt{RT_к}}$ and assuming that in the process of variation of the output conditions of the engine the gas composition does not change (RT_k=const), we find that

$$\dot{m}^{\nu}=\frac{1}{u_1 S\rho_т}\left(\frac{\varphi_c A F_{кр}}{\sqrt{RT_к}}\right)^{\nu}(\dot{m}-\dot{m}_д).$$

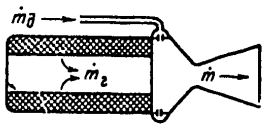

Figure 11.1. Schematic of the solid-fuel rocket engine with introduction of an additional component

Figure 11.2. Schematic of a solid-fuel rocket engine with thrust adjustment by varying the vibrational characteristics of the chamber
Key:
1. ultrasonic generator

In the case of the usual design of the solid-fuel rocket engine, that is, for $\dot{m}_д=0$

$$\dot{m}=(u_1 S\rho_т)^{\frac{1}{1-\nu}}\left(\frac{\sqrt{RT_к}}{\varphi_c A F_{кр}}\right)^{\frac{\nu}{1-\nu}}.$$

FOR OFFICIAL USE ONLY

APPROVED FOR RELEASE: 2007/02/08: CIA-RDP82-00850R000200090053-2

APPROVED FOR RELEASE: 2007/02/08: CIA-RDP82-00850R000200090053-2

Linearizing the presented relations in the vicinity of the rated operating conditions, the flow rates at which $\bar{\dot{m}}_T$ and $\bar{\dot{m}}_D$ are compiled, we obtain

$$\left(\frac{\bar{\dot{m}}}{\bar{\dot{m}}-\bar{\dot{m}}_д}-\nu\right)\delta\dot{m}=\frac{\bar{\dot{m}}_д}{\bar{\dot{m}}-\bar{\dot{m}}_д}\delta\dot{m}_д-\nu\delta F_{кр}+\delta u_1+\delta S \qquad (11.1)$$

and for $\dot{m}_D=0$

$$(1-\nu)\delta\dot{m}=\delta u_1+\delta S-\nu\delta F_{кр}, \qquad (11.2)$$

where $\delta\dot{m}$, δu_1... denote the relative variations of the parameters.

From (11.1) it follows that the methods of varying the gas flow rates through the nozzle of a solid-fuel rocket engine (and its thrust) are:

Variation of the critical cross section of the nozzle. An increase in F_{cr} leads to a decrease in the flow rate and the thrust. The intensity of the effect depends on the magnitude of the exponent ν; for $\nu=0$ the method is impossible;

By varying the combustion surface S. Increasing S leads to an increase in the flow rate. The method is less effective, the smaller ν, but it is possible even when $\nu=0$;

By variation of the coefficient u_1 in the law of the fuel combustion rate. The effect is analogous to the effect of varying the combustion surface;

By variation of the amount of additional mass introduced into the chamber. Under the adopted assumptions, increasing $\dot{m}_D$ leads to an increase in the thrust. Increasing ν increases the effectiveness of the methods;

By simultaneous variation of several of the noted factors.

From the enumerated methods of influencing the thrust of the solid-fuel rocket engine in practice only the method of variation of the charge combustion surface in the operating process of the engine is unrealizable. All the remaining methods are possible for practical use (theoretically).

The variation of the critical cross section of the nozzle for thrust regulation is possible by mechanical or gas dynamic methods.

The first of the indicated methods can be realized, for example, by movement of the central body in the axial direction in the vicinity of the critical cross section of the nozzle, which together with the basic nozzle forms the critical cross section.

The gas dynamic method is based on introduction of gas from the gas generator or from the main thrust chamber into the nozzle obviously so that the variation of the feed realized by any regulator will lead to variation of the flow rate of the main flow.

APPROVED FOR RELEASE: 2007/02/08: CIA-RDP82-00850R000200090053-2

APPROVED FOR RELEASE: 2007/02/08: CIA-RDP82-00850R000200090053-2

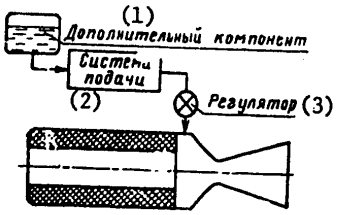

Figure 11.3. Schematic of the solid-fuel rocket engine with adjustment of the thrust by varying the feed of the additional liquid component
Key:
1. additional component
2. feed system
3. regulator

Figure 11.4. Schematic of the solid-fuel rocket engine with thrust regulation by variation of the feed of the initial gaseous component

The adjustment of the solid-fuel rocket engine by direct effect during their operating process on the combustion rate (variation of the coefficient u_1) still appears to be problematic. As an example of a possible scheme for such regulation, the schematic of the solid-fuel rocket engine is considered (Fig 11.2), in the chamber of which vibrations of the gas column are artificially excited.

If the fuel combustion rate depends on the parameters of the vibration process, then, by regulating the thrust of the vibrations (the ultrasonic generator), it is possible to influence the flow rate of the fuel and, consequently, the thrust of the engine.

As the additional mass introduced into the chamber of the solid-fuel rocket engine, for adjustment of its thrust, liquid or gaseous material can be used. The application of a liquid for these purposes requires the presence of a tank in the engine system (Fig 11.3) for storage of it and devices for feeding liquid to the chamber, including the flow rate regulator. The solid fuel engine becomes in essence a hybrid rocket engine. In order to feed the liquid and regulate its flow rate, the corresponding devices of the liquid fuel rocket engine can be used.

If it is proposed that gas be introduced into its chamber to regulate the engine, then the required storage for this gas must be created on board the flight vehicle. Even with relatively small flow rates of the gas to the chamber, its storage in compressed form leads to inadmissible increase in weight of the structure. Therefore the schematic of the solid-fuel rocket engine with thrust adjustment by the introduction of gas into the chamber is the most realistic in the case where this gas is generated during combustion of the solid-fuel in the gas generator (additional chamber).

FOR OFFICIAL USE ONLY

APPROVED FOR RELEASE: 2007/02/08: CIA-RDP82-00850R000200090053-2

APPROVED FOR RELEASE: 2007/02/08: CIA-RDP82-00850R000200090053-2

One of the possible schematics of the solid-fuel rocket engine with the given control system is presented in Fig 11.4.

11.2. Equation of the Chamber with Adjustable Critical Cross Section of the Nozzle

Above (7.1), the equation of the material balance of the solid-fuel rocket engine chamber is obtained in the form

$$\frac{W}{RT_к}\frac{dp_к}{dt}=Q_т Su-\frac{\varphi_c AF_{кр}}{\sqrt{RT_к}}p_к,$$

where W is the free volume of the chamber.

Let us assume a power law of the combustion rate of the fuel

$$u=u_1 p_к^{\nu}.$$

Proceeding to the small deviations $\delta p_к=\frac{\Delta p_к}{\bar{p}_к}$; $\delta F_{кр}=\frac{\Delta F_{кр}}{\bar{F}_{кр}}\ldots$, where $\Delta p_к=$ $=p_к-\bar{p}_к$; $\Delta F_{кр}=F_{кр}-\bar{F}_{кр}\ldots$, we find the linearized equation of the solid-fuel rocket engine chamber with adjustable or critical cross section of the nozzle:

$$\bar{y}\delta\dot{p}_к+\bar{\dot{m}}(1-\nu)\delta p_к\pm\bar{\dot{m}}\delta F_{кр}=0.$$

Here $\bar{y}=\frac{\bar{p}_к\bar{W}}{RT_к}$; $\bar{\dot{m}}=\bar{\dot{m}}_т=\bar{\dot{m}}_р=\delta u_1 Q_т\bar{p}_к^{\nu}=\frac{\varphi\bar{A}\bar{p}_к\bar{F}_{кр}}{\sqrt{RT_к}}-$ are the rated values of the amount of gas in the chamber and its flow rate through the nozzle (or the gas formation of the charge); in addition, we denote

$$\delta\dot{p}_к=\frac{d(\Delta p_к)}{dt}.$$

Finally, the chamber equation is written in the form

$$T\delta\dot{p}_к+\delta p_к=K_{p_к}^{F_{кр}}\delta F_{кр}, \tag{11.3}$$

where the time constant of the solid-fuel rocket engine chamber

$$T=\frac{\bar{y}}{\bar{\dot{m}}(1-\nu)}. \tag{11.4}$$

The boost factor (transmission factor) is

$$K_{p_{кр}}^{F_{кр}}=\frac{1}{\nu-1}. \tag{11.5}$$

APPROVED FOR RELEASE: 2007/02/08: CIA-RDP82-00850R000200090053-2

APPROVED FOR RELEASE: 2007/02/08: CIA-RDP82-00850R000200090053-2

The equation of the solid-fuel rocket engine (11.3) corresponds to the equation of the aperiodic first-order length. The operator-transfer function of the solid-fuel rocket engine chamber, as an element of t engine pressure control system has the form

$$W(p)_{p_к} = \frac{K^{F_{кр}}_{p_к}}{T_p + 1}. \tag{11.6}$$

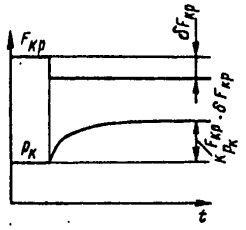

Figure 11.5. Change in chracteristics of the solid-fuel rocket engine with adjustment of the critical cross section of the nozzle with respect to pressure

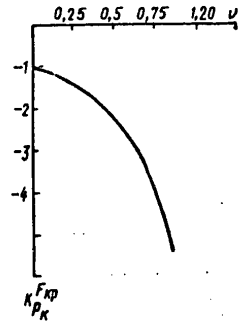

Figure 11.6. Boost factor with respect to pressure as a function of the exponent ν

The transient characteristic of the process of the pressure variation in the chamber with step variation of the area of the critical cross section of the nozzle by $\delta F_{cr}=1$ is described by the equation

$$\delta p_к = K^{F_{кр}}_{p_к}\left(1 - e^{-\frac{t}{T}}\right). \tag{11.7}$$

For

$$\delta F_{кр} \neq 1$$

$$\delta p_к = K^{F_{кр}}_{p_к}\delta F_{кр}\left(1 - e^{-\frac{t}{T}}\right). \tag{11.8}$$

At the end of the process ($t=\infty$)

$$\delta p_к = K^{F_{кр}}_{p_к}\delta F_{кр};$$

$$p_к = \bar{p}_к\left(1 + K^{F_{кр}}_{p_к}\delta F_{кр}\right).$$

FOR OFFICIAL USE ONLY

APPROVED FOR RELEASE: 2007/02/08: CIA-RDP82-00850R000200090053-2

APPROVED FOR RELEASE: 2007/02/08: CIA-RDP82-00850R000200090053-2

The form of the transient characteristic is presented in Fig 11.5.

The boost factor $K^{F_{cr}}_{p_k}$ in the given case is uniquely determined by the magnitude of the exponent ν in the combustion rate law (Fig 11.6). With an increase in the exponent ν the boost factor increases, that is, the control of the engine becomes more effective.

For $\nu=1$ and $K^{F_{cr=\infty}}_{p_k}$, that is, the process becomes unstable.

The time constant T is determined not only by the exponent ν (the greater this exponent, the greater the time constant), but also the ratio of the amount of gas in the chamber through the flow rate per second of it through the nozzle. Inasmuch as in the operating process of the solid-fuel rocket engine the free volume of the chamber varies, the time constant also varies. Let us estimate the order of magnitude of the constant T. For this purpose, on the basis of the data presented in the literature let us take the following parameters of a hypothetical engine:

Thrust	4.5 kN
Pressure in the chamber	4.0 mPa
Initial free volume	0.2 m^3

Let us assume approximately that for this engine the specific thrust I_y=225 sec and RT_k=100000 kg-m/kg. Then the flow rate per second of the gas will be m=20 kg/sec, and the initial amount of gas in the free volume of the chamber y_0=0.8 kg. Consequently, at the initial point in time $y_0/\dot{m}$=0.04 sec.

With time of operation of the engine and for ρ_T=1600 kg/m^2 the free volume of the chamber varies according to the law

$$W = W_0 + \frac{\dot{m}t}{\rho_T}$$

or $W=[0.2+0.012t]m^3$, where [t], sec.

Taking this into account

$$\frac{y}{\dot{m}} = 0{,}04 + 0{,}0024t \;\&.\; T = \frac{0{,}04 + 0{,}0024t}{1-\nu}.$$

In Fig 11.7 we have the graph of the constant T as a function of the operating time of the investigated engine for various values of the exponent ν. From the graph it is possible to conclude that for standard values of ν=0.3 to 0.6 and operating time of the engine to t=50 sec the time constant lies within the limits of T=(0.06-0.4) sec, that is, it is on the order of 0.1 sec.

APPROVED FOR RELEASE: 2007/02/08: CIA-RDP82-00850R000200090053-2

APPROVED FOR RELEASE: 2007/02/08: CIA-RDP82-00850R000200090053-2

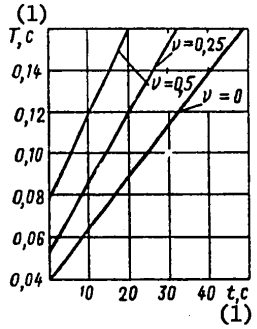

Figure 11.7. Time constant as a function of the operating time of the engine and the exponent ν

Key:
1. sec

Let us note that this value is appreciably larger than the time constant of the liquid-fuel rocket engine chamber.

Let us consider the properties of the solid-fuel rocket engine chamber with altered critical cross section of the nozzle as the engine thrust adjustment element.

The thrust of the rocket engine

$$P = K_\tau^\infty p_к F_{кр} - F_a p_н,$$

where $K_\tau^\infty = f\left(\frac{p_к}{p_a}\right)$ — is the thrust factor in a vacuum, F_a is the area of the exit cross section of the nozzle, p_H is the outside pressure, p_a is the gas pressure at the nozzle tip.

During the adjustment process $F_a p_H$=const and

$$\delta P = \delta K_\tau^\infty + \delta p_к + \delta F_{кр}.$$

The adjustment of the solid-fuel rocket engine is accompanied by variation of F_{cr}/F_a and, consequently, by variation of the ratio p_k/p_a, which in turn causes variation of the thrust in a vacuum. However, this variation is very small. Thus, for K=1.25 and p_k/p_a=150, $dK_T^\infty/d(p_k/p_a) \approx 0.0005$. Accordingly, δK^∞_t is one or two orders less than δp_k and δF_{cr}. Neglecting the effect of the variation of the coefficient K_t^∞ on the thrust during its adjustment process, we obtain

$$\delta P = \delta F_{кр} + \delta p_к.$$

FOR OFFICIAL USE ONLY

APPROVED FOR RELEASE: 2007/02/08: CIA-RDP82-00850R000200090053-2

APPROVED FOR RELEASE: 2007/02/08: CIA-RDP82-00850R000200090053-2

Taking this into account, the linearized equation of the solid-fuel rocket engine chamber describing the process of the thrust variation on regulation of the critical cross section of the nozzle described in the form

$$T\delta\dot{P}+\delta P=\left(1+K_{p_к}^{F_{кр}}\right)\delta F_{кр}+T\delta\dot{F}_{кр}.$$

Denoting the thrust boost factor

$$K_p^{F_{кр}}=1+K_{p_к}^{F_{кр}};\qquad K_p^{F_{кр}}=\frac{\nu}{1-\nu}, \tag{11.9}$$

we obtain

$$T\delta\dot{P}+\delta P=K_p^{F_{кр}}\delta F_{кр}+T\delta\dot{F}_{кр}. \tag{11.10}$$

Equation (11.10) corresponds to the equation of the forcing element of the first order for which the operator transfer function has the form

$$W(p)_p=\frac{Tp+K_p^{F_{кр}}}{Tp+1}=1+W(p)_{p_к}. \tag{11.11}$$

The transient process of the chamber with step variation of the area of the critical cross section by δF_{cr} is described by the function

$$\delta P=\delta F_{кр}\left[1+K_{p_к}^{F_{кр}}\left(1-e^{-\frac{t}{T}}\right)\right] \tag{11.12}$$

or

$$\delta P=\delta F_{кр}\left[K_p^{F_{кр}}+\left(1-K_p^{F_{кр}}\right)e^{-\frac{t}{T}}\right]. \tag{11.13}$$

At the end of the process ($t=\infty$)

$$\delta P=K_p^{F_{кр}}\delta F_{кр}=\frac{\nu}{1-\nu}\delta F_{кр}.$$

Since always $\nu<1$, the variation of the thrust with respect to sign is opposite to the variation of the critical cross section of the nozzle. In Fig 11.8 we have the relation for $K_p^{F_{cr}}$ as a function of ν.

For $\nu=0$, $K_p^{F_{cr}}=0$, and the adjustment of the engine thrust is impossible. Returning to the pressure variation, from (11.5), we find that for the case $K^{F_{cr}}=-1$ and, consequently, $\delta p_k=-\delta F_{cr}$, as a result of which

p_k

$$\delta P_{\nu=0}=0.$$

In the case where the fuel combustion rate does not depend on the pressure, the relative elongation p_k is equal to the relative decrease in critical

APPROVED FOR RELEASE: 2007/02/08: CIA-RDP82-00850R000200090053-2

APPROVED FOR RELEASE: 2007/02/08: CIA-RDP82-00850R000200090053-2

cross section of the nozzle, which makes thrust adjustment as a result of input to F_{cr} impossible.

For $\nu=0.5$ $K_{p_k}^{F_{cr}}=-1$ and $\delta P=-\delta F_{cr}$.

The time constant for thrust adjustment is equal to the time constant obtained for the case of pressure adjustment, that is,

$$T=\frac{\bar{w}}{\dot{m}(1-\nu)}.$$

The transient characteristic of the process is depicted in Fig 11.9. Let us pay attention to the fact that at the time of variation of the critical cross section by δF_{cr} the thrust also varies discontinuously (in the same direction) by the amount $\delta P=\delta F_{cr}$, which follows from (11.3) for the case $t=0$.

Only after expiration of the time τ_1 does the thrust again reach the initial value and begin to vary in the required direction.

The time τ_1 is found from (11.12) for the case $\delta P=0$

$$\tau_1=-T\ln\left(1+\frac{1}{K\frac{F_{кр}}{p_к}}\right)$$

or

$$\tau_1=-T\ln\nu. \tag{11.14}$$

Consequently, for the investigated case, at the beginning of the process the thrust varies not in the required direction, but in the opposite direction.

Let us determine the force of the thrust from the beginning of the transient processes to the time τ_1, calling this pulse the "counteraction pulse."

$$I_{пр}=\int_0^{\tau_1}\Delta P\,dt;$$

$$I_{пр}=\frac{\bar{P}T\delta F_{кр}}{1-\nu}(1-\nu+\nu\ln\nu). \tag{11.15}$$

Fig 11.10 shows the dependence on the value of ν of the dimensionless ratio τ_1/T and $I_{1im}/\bar{P}T\delta F_{cr}$.

FOR OFFICIAL USE ONLY

APPROVED FOR RELEASE: 2007/02/08: CIA-RDP82-00850R000200090053-2

APPROVED FOR RELEASE: 2007/02/08: CIA-RDP82-00850R000200090053-2

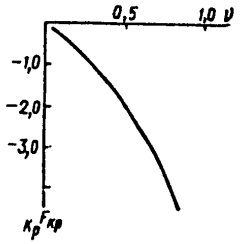

Figure 11.8 Boost factor with respect to thrust as a function of the index ν.

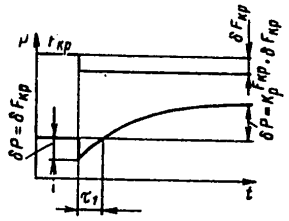

Figure 11.9 Transient characteristic of a solid-fuel rocket engine with regulation of the critical cross-section of the nozzle with respect to thrust.

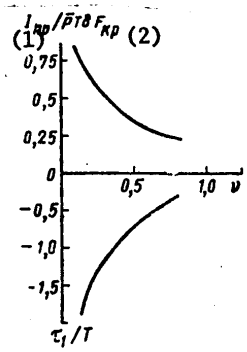

Figure 11.10. The relations determining the exponents of the "countereffect" period when adjusting the solid-fuel rocket engine

Key:
1. lim
2. cr

If we assume, in addition, for the condition of the preceding example, that ν=0.25, T=0.2 sec and δF_{cr}=0.2, the time τ_1 and the countereffect pulse are τ_1=0.25 sec, $I_{lim} \approx 100$ kN-sec.

The initial thrust variation ΔP=0.200 kN.

APPROVED FOR RELEASE: 2007/02/08: CIA-RDP82-00850R000200090053-2

APPROVED FOR RELEASE: 2007/02/08: CIA-RDP82-00850R000200090053-2

If the engine has several nozzles, of which not all are adjustable, then

$$\left.\begin{aligned} K_{p_к}^{F_{кр}} &= \frac{\bar{\dot{m}}_{per}}{\bar{\dot{m}}_т(\nu-1)}; \\ K_p^{F_{кр}} &= \frac{\bar{\dot{m}}_{per}\nu}{\bar{\dot{m}}_т(\nu-1)}; \end{aligned}\right\} \qquad (11.16)$$

Key: 1. adj

where $\bar{\dot{m}}_T$ is the total rated gas flow rate (the gas formation of the charge); $\bar{\dot{m}}_{adj}$ is the gas consumption through the adjustable nozzles.

Let us estimate the effect of the pressure variations (dynamics) during the process of regulation of the critical cross section of the nozzle on the fuel combustion rate. As is obvious, for significant pressure gradients dp_k/dt, the variations of the nature of the fuel combustion are possible, which makes ordinary laws of fuel combustion rate inapplicable for the conditions.

The largest pressure gradient (see Fig 11.15) is characteristic for the initial time of the transient process. At this point in time

$$\left[\frac{d(\delta p_к)}{dt}\right]_{t=0} = \frac{K_{p_к}^{F_{кр}}\delta F_{кр}}{T}; \quad \left[\frac{d(\Delta p_к)}{dt}\right]_{t=0} = \frac{K_{p_к}^{F_{кр}}\delta F_{кр}\bar{p}_к}{T}.$$

For the above-investigated example

$$\left[\frac{d(\Delta p_к)}{dt}\right]_{t=0} = 53 \text{ kg/cm}^2\text{-sec}.$$

The total pressure variation will be Δp_k=1.1 MPa/cm^2. As is known, for the aperiodic element in the time Δt=3T, 0.95 of the total increment of the regulatable value is achieved. Consequently, the average pressure gradient in the time interval 3T=0.6 sec is equal to $\Delta p_k/\Delta t$=0.95·11/0.6= 17.5 MPa/cm^2-sec.

As was noted earlier, the dynamics of the process must be taken into account when determining the combustion rate only in the case where

$$\frac{dp}{dt} > 1{,}50 \text{ MPa/cm}^2\text{-sec}.$$

Consequently even in the ideal statement of the calculation (instantaneous variation of δF_{cr}), which was assumed, the stability limits of the process will not be disturbed. In reality, of course, as a result of unavoidable inertia of the system of regulating elements, the variation of the critical cross section will not take place instantaneously, which leads to the corresponding decrease in the pressure variation gradients, that is, to a large increase in the stability margin (in the investigated sense).

FOR OFFICIAL USE ONLY

APPROVED FOR RELEASE: 2007/02/08: CIA-RDP82-00850R000200090053-2

APPROVED FOR RELEASE: 2007/02/08: CIA-RDP82-00850R000200090053-2

In addition, it must be noted that the combustion stability can be disturbed in the adjustment process as a result of another factor influencing the nature of this combustion and, namely, as a result of the reduction in pressure to the values for which combustion is realized incompletely or stops altogether.[1] According to the data of the foreign press, a controllable multiple starting engine can be built on this basis.

11.3. Equation of the Chamber with Charge Gas Formation Control

Let us consider the case where the gas formation of the charge is regulated by the effect on its combustion rate.

Let us denote the parameter, with variation of which the fuel combustion rate varies (for example, the amplitude, frequency, type of pulse for the case of adjustment by varying the vibration characteristics of the gases in the chamber) by L. For calculating the transient characteristics of the adjustment process, the combustion rate must be known as a function of this parameter. Let us take the combustion rate law in the form

$$u=u_L p_k^{\nu},$$

where $u_L(y)$ is a known function.

The gas formation of the charge

$$\dot{m}_r = S_{Q_r} u_L p_k^{\nu}. \tag{11.17}$$

The equation of the solid-fuel rocket chamber for determining the pressure variation in small deviations

$$T\delta\dot{p}_k+\delta p_k=K^L_{p_k}\delta L, \tag{11.18}$$

where the time constant and the boost factor

$$T=\frac{\bar{g}}{\bar{\dot{m}}_r(1-\nu)};$$

$$K^L_{p_k}=\frac{\bar{L}}{\bar{u}_L}\frac{\partial u_L}{\partial L}. \tag{11.19}$$

Thus, the equation of the solid-fuel rocket engine chamber for the given control system corresponds to the equation of the aperiodic first-order element.

[1] In the above-investigated example Δp_k=1.1 MPa/cm^2 and if the nozzle cross section was enlarged in the adjustment process, the new value of pressure will be p_k=4.0-1.1=2.9 MPa/cm^2, which for the fine fuel composition can turn out to be close to the value for which the combustion is disturbed.

APPROVED FOR RELEASE: 2007/02/08: CIA-RDP82-00850R000200090053-2

APPROVED FOR RELEASE: 2007/02/08: CIA-RDP82-00850R000200090053-2

The transient process in the chamber with respect to pressure for step variation of the regulating control input L is described by the equation

$$p_к = \bar{p}_к \left[1 + K^L_{p_к} \delta L \, (1 - e^{-t/T})\right].$$

At the end of the process

$$p_к = \bar{p}_к \left[1 + K^L_{p_к} \delta L\right].$$

In the expression for the thrust $P = K^{\infty}_{т} p_к F_{кр} - p_н F_а$ for regulation only the pressure in the chamber is varied, and therefore in the transient process

$$P = \bar{P} + \bar{p}_к F_{кр} K^L_{p_к} K^{\infty}_{т} (1 - e^{-t/T}).$$

The new steady-state value of the thrust will be

$$P = p_к F_{кр} K^{\infty}_{т} (1 + K^L_{p_к}) - F_а p_н.$$

Let us consider the transient process in the chamber for variation of the charge combustion surface. Adjustment of the thrust by an arbitrary law by varying the combustion surface S is in practice impossible. However, cases where the transient process caused by variation of the S occurs are possible. This pertains to engines having a charge with variable combustion surface or to cases where the charge has certain defects (cracks, delamination of the armor, and so on).

The equation of the chamber with respect to pressure has the following form for this case

$$T \delta \dot{p}_к + \delta p_к = K^S_{p_к} \delta S, \qquad (11.20)$$

The transient processes with respect to pressure and thrust in the case of step variation of the combustion surface will also be analogous to the ones investigated above.

11.4. Equations of Chambers with Thrust Adjustment by Varying the Feed of the Additional Component

The introduction of an additional mass of material into the solid-fuel rocket engine chamber to regulate its parameters can be realized (Fig 11.11) either through the head or into the space in front of the nozzle or simultaneously to both of these parts of the chamber. Depending on which of these versions of introducing the additional material is selected, the adjustment will be realized differently. If the additional component is introduced into the free nozzle space, that is, after the solid-state charge, then the introduction of it influences the combustion rate of the charge only through increasing the pressure in the chamber as a result of

FOR OFFICIAL USE ONLY

APPROVED FOR RELEASE: 2007/02/08: CIA-RDP82-00850R000200090053-2

APPROVED FOR RELEASE: 2007/02/08: CIA-RDP82-00850R000200090053-2

increasing the gas flow rate from the nozzle. If the combustion rate does not depend on the pressure ($\nu=0$), then the introduction of the additional component in this case in general will not be felt in the gas formation of the charge. If the additional component is introduced through the head of the chamber and then passes through the charge channel, the gas formation of the charge can increase not only as a result of an increase in pressure, but also as a result of increase in the flow velocity in the channel. In the theory of hybrid rocket engines, most frequently it is assumed that the gas formation rate of the solid fuel in such cases is proportional to $(\rho v)^{\beta}=(\dot{m}/F_k)^{\beta}$, where $\dot{m}$, ρ, v is the flow rate, density and velocity of the flow, F_k is the channel crosshatching, β is the coefficient. It is obvious that in the case of introducing an additional component through the head to the charged channel, it is possible to obtain a more effective effect on the engine parameters than in the case of feeding it to the free nozzle space of the chamber.

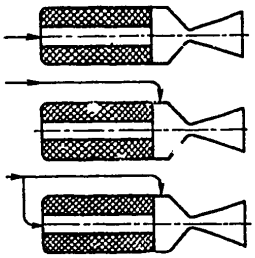

Figure 11.11. Diagrams of the solid-fuel rocket engine chambers with different versions of introducing the additional material

Analyzing the processes of adjusting the engine with introduction of an additional component [9], it is possible to see that the systems with introduction of the component only through the chamber head or only into the prenozzle space of the chamber in the general case have the deficiency that in the adjustment process the ratio of the fuel and the additional component flow rates changes, which can be felt unfavorably in the energy and weight characteristics of the engine.

It is possible to avoid this deficiency by using a system with simultaneous introduction of the component both in the charge itself and after the charge. If simultaneously with variation of the total flow rate of the additional component in a defined way, its distributions between the two points of entry also varies, then in some adjustment range it is possible to maintain the ratio of the flow rates constant.

APPROVED FOR RELEASE: 2007/02/08: CIA-RDP82-00850R000200090053-2

APPROVED FOR RELEASE: 2007/02/08: CIA-RDP82-00850R000200090053-2

In the theory of liquid-fuel rocket engines when analyzing the dynamic processes of the chambers, consideration is given to the interaction time of the two fuel components, by which we mean the time from the time of arrival of the liquid component in the chamber to the time of completion of combustion in the vapor with other components. Accordingly, the chamber of the liquid-fuel rocket engine is a delay element in the control system. The consideration of the conversion time has practical meaning in the case where it is of the same order as the chamber time constant.

For modern liquid-fuel rocket engines characterized by high pressures in the chambers and small volumes, this ratio of the delay time in the transformation of the component and the time constant is characteristic. For solid-fuel engines with the investigated control systems, there are no data on the conversion time of the additional component, but it is possible quite certainly to propose that this time will have (for efficient organization of the introduction of the component into the chamber) the same order as the corresponding time for the liquid-fuel rocket engines. This proposition is based on the fact that the additional component will be introduced in liquid or gas form in the flow of gases having high temperature and speed, which creates favorable conditions for its conversion and mixing with the basic flow. At the same time the time constant of the solid-fuel rocket engine is appreciably larger than the time constant of the liquid-fuel rocket engines. Therefore it is necessary to expect that between the conversion time of the additional component and the chamber time constant there will be a difference by at least one or two orders. Accordingly, later the delay in conversion of the additional components when analyzing the chamber dynamics will not be considered.

For analysis of the control systems with solid-fuel rocket engines with the introduction of an additional component, the estimation and the selection of this component have special significance. For its selection the requirement is natural that the energy characteristic of the engine not be lowered during adjustment, that is, that its specific pulse remain at some given level. This means that during the adjustment process noticeable changes in capacity for work of the gases escaping from the nozzle must not be permitted.

Accordingly, hereafter when analyzing the chamber characteristic it is assumed that during the process of regulation RT_k=const, and, finally (also as was done previously), which was stipulated at the beginning of Chapter 7), the solid-fuel rocket engine chamber will be considered as a system with lumped parameters, that is, with gas parameters averaged over the entire free volume of the chamber and reduced to the nozzle input conditions. Consideration of the effect of the variation of the parameters of the gas flow in the channel when feeding the component to this channel on the gasification rate will be realized by introducing the additional expressions.

FOR OFFICIAL USE ONLY

APPROVED FOR RELEASE: 2007/02/08: CIA-RDP82-00850R000200090053-2

APPROVED FOR RELEASE: 2007/02/08: CIA-RDP82-00850R000200090053-2

Equation of the Chamber with Introduction of an Additional Component to the Charged Channel

The schematic of the chamber is presented in Fig 11.12. Let us assume that the gas formation rate of the charge is

$$u = u_1 \left(\frac{\dot{m}}{F_{кр}}\right)^{\beta} p_к^{\nu}. \tag{11.21}$$

In the case where the charge has one cylindrical channel of length L and diameter d, the total gas formation of it, considering the variation of the gasification rate with respect to length, can be determined [9] by the function

$$\dot{m}_т = \left[4^{\beta}\pi^{1-\beta}(1-\beta)\,u_1 Q_т L d^{1-2\beta} p_к^{\nu} + \dot{m}_в^{1-\beta}\right]^{\frac{1}{1-\beta}} - \dot{m}_в, \tag{11.22}$$

where $\dot{m}_в$ is the flow rate of the additional component. Let us denote the ratio of the flow rates as $K = \frac{\dot{m}_в}{\dot{m}_т}$.

The equation of the material balance of the gas in the chamber

$$\frac{dy}{dt} = \dot{m}_{кр} - \dot{m}_р,$$

where the inflow of the mass

$$\dot{m}_к = \dot{m}_т + \dot{m}_в.$$

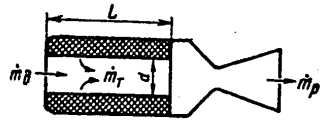

Figure 11.12. Schematic of the solid-fuel rocket engine with introduction of an additional component into the chamber head

From the equation of material balance and considering the fact that

$$\frac{dW}{dt} = \frac{\dot{m}_т}{Q_т}$$

we obtain

$$\frac{W}{RT_к}\frac{dp_к}{dt} + \frac{\varphi A p_к}{\sqrt{RT_к}} F_{кр} = \dot{m}_т\left(1 - \frac{p_к}{RT_к Q_т}\right) + \dot{m}_в.$$

APPROVED FOR RELEASE: 2007/02/08: CIA-RDP82-00850R000200090053-2

APPROVED FOR RELEASE: 2007/02/08: CIA-RDP82-00850R000200090053-2

Just as for the ordinary solid-fuel rocket engine $p_k/RT_k\rho_T<<1$. Neglecting the value of $p_k/RT_k\rho T$ and using the function (11.22), we find that

$$\theta_k \frac{dp_k}{dt} + p_k = Q\left(Bp_k^{\nu} + \dot{m}_k^{1-\beta}\right)^{\frac{1}{1-\beta}};$$

where

$$\theta_k = \frac{\bar{\psi}}{\dot{m}_{kp}}; \quad Q = \frac{\sqrt{RT_k}}{\varphi_c \bar{A} F_{kp}};$$

$$B = 4^{\beta}\pi^{1-\beta}(1-\beta)\,a_1 Q_T L d^{1-2\beta}.$$

On proceeding to small relative deviations on the parameters, we obtain the equation of the chamber of the solid-fuel rocket engine of the given system in the form

$$T\delta\dot{p}_k + \delta p_k = K^{\dot{m}_k}_{p_k}\delta\dot{m}_k. \tag{11.23}$$

Here T and $K^{\dot{m}_D}_{p_k}$ is the time constant of the chamber and the boost factor with respect to flow rate of the additional component

$$T = \frac{\theta_k}{1-\frac{\nu}{1-\beta}\left[1-\left(\frac{\bar{K}}{1+\bar{K}}\right)^{1-\beta}\right]}; \tag{11.24}$$

$$K^{\dot{m}_k}_{p_k} = \frac{\left(\frac{\bar{K}}{1+\bar{K}}\right)^{1-\beta}}{1-\frac{\nu}{1-\beta}\left[1-\left(\frac{\bar{K}}{1+K}\right)^{1-\beta}\right]}. \tag{11.25}$$

For step variation of the flow rate of the additional component, the pressure variation in the chamber is defined by the expression

$$\delta p_k(t) = K^{\dot{m}_k}_{p_k}\delta\dot{m}_k\left(1-e^{-\frac{t}{T}}\right). \tag{11.26}$$

Just as for the previously investigated cases the solid-fuel rocket engine chamber of the given system is an aperiodic link.

Under the adopted sections (RT_k=const) the gas flow rate through the nozzle varies exactly as the pressure in the chamber varies. It is only by variation of the pressure that the thrust adjustment law is defined.

As follows from (11.24) the time constant of the chamber depends on its geometric dimensions, the characteristics of the operating process, and the peculiarities of the gas formation of the charge, and it increases during the operating process of the engine.

APPROVED FOR RELEASE: 2007/02/08: CIA-RDP82-00850R000200090053-2

APPROVED FOR RELEASE: 2007/02/08: CIA-RDP82-00850R000200090053-2

For the approximate estimation of the order of magnitude of the time constant and the nature of the effect on it of various factors let us take the law of variation of the ratio of the quantity of gas in the chamber to the flow rate per second of the gases through the nozzles in the form obtained for the example investigated in 11.2, that is, in the form

$$\frac{y}{\dot{m}_{кр}} = [0{,}04 + 0{,}0024t]_{сек},$$

where t is the operating time of the engine.

In accordance with (11.24)

$$T = \frac{y}{\dot{m}_{кр}\left\{1 - \frac{\nu}{1-\beta}\left[1 - \left(\frac{\bar{K}}{1+\bar{K}}\right)^{1-\beta}\right]\right\}}.$$

Fig 11.13 shows the results of calculations of the time constant of the chamber for various values of the parameters determining it. As is obvious from the data presented in Fig 11.13, the variation of the amount of gas in the free volume of the chamber during the charge combustion process has primary influence on the magnitude of the time constant. For the investigated example, for 50 seconds of operation of the engine the time constant increases by fourfold.

With an increase in the coefficient of gas ratio of the flow rates, the time constant decreases. The effect of the gas formation coefficient β on the time constant is insignificant; its increase from 0.25 to 0.75, that is, by threefold, causes an increase in T by less than 10%.

The coefficient ν has somewhat greater effect on the magnitude of the time constant -- a twofold increase in ν (from 0.25 to 0.5) causes approximately a 20% increase in T.

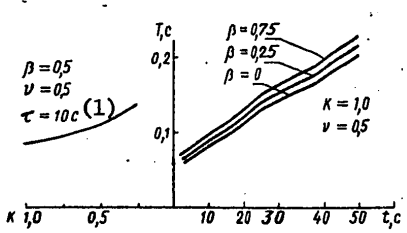

Figure 11.13. Time constant as a function of the process characteristics in the chamber with introduction of an additional component into the head

Key:
1. sec

APPROVED FOR RELEASE: 2007/02/08: CIA-RDP82-00850R000200090053-2

APPROVED FOR RELEASE: 2007/02/08: CIA-RDP82-00850R000200090053-2

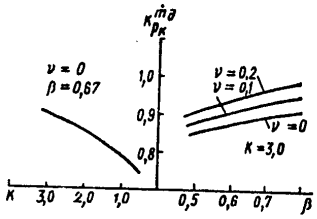

Figure 11.14. Boost factor as a function of the process characteristics in the chamber

On the whole the order of magnitude of the time constant for the solid-fuel rocket engine with the given control system is the same as for the solid-fuel rocket engine with regulation of the critical cross section of the nozzle; this order is equal to hundredths to tenths of a second.

Fig 11.14 shows the graph that illustrates the dependence on various factors of the boost coefficient in accordance with expression (11.25).

Just as should be expected, the boost factor depends noticeably on the relation of the flow rates of the additional component and the charge combustion products. For the values of this expression in the vicinity of 0.5 to 1.0 and for the remaining values of the parameters used in the calculation, the boost factor will be $K_{p_K}^{m_3}$=0.7 to 0.8, that is, in the case of necessity of variation of the thrust within the limits, for example, 5%, it is necessary to change the flow rate of the additional component by approximately 6 to 8%.

Chamber Equation with Introduction of the Additional Component in the Prenozzle Space

The material balance equation for the chamber of this type is analogous to the corresponding equation of the chamber with introduction of the component into the charged channel. Accordingly, the chamber equation describing the transient process on variation of the liquid feed can be written in the form (11.23), that is, as

$$T\dot{\delta p}_K + \delta p_K = K_{p_K}^{\dot{m}_3}\delta \dot{m}_3.$$

The expression for the time constant T and the boost factor $K_{p_k}^{\dot{m}_D}$ can be obtained from (11.24) and (11.25) considering that in the given case β=0, for the additional component does not pass through the charged channel, and therefore the variation of its flow rate as no direct effect on the gas formation rate.

FOR OFFICIAL USE ONLY

APPROVED FOR RELEASE: 2007/02/08: CIA-RDP82-00850R000200090053-2

APPROVED FOR RELEASE: 2007/02/08: CIA-RDP82-00850R000200090053-2

Let us also consider that

$$\dot{m}_{\text{к}}+\dot{m}_{\text{т}}=\dot{m}_{\text{кр}}$$

$$1+K=\frac{\dot{m}_{\text{кр}}}{\dot{m}_{\text{т}}}.$$

Here

$$T=\frac{\bar{y}}{\bar{\dot{m}}_{\text{кр}}\left(1-\nu\frac{\bar{\dot{m}}_{\text{т}}}{\bar{\dot{m}}_{\text{кр}}}\right)}; \tag{11.27}$$

$$K\frac{\dot{m}_{\text{к}}}{\rho_{\text{к}}}=\frac{\bar{\dot{m}}_{\text{к}}}{\bar{\dot{m}}_{\text{кр}}\left(1-\nu\frac{\bar{\dot{m}}_{\text{т}}}{\bar{\dot{m}}_{\text{кр}}}\right)}. \tag{11.28}$$

Let us note that for $\dot{m}_{\text{т}}=\dot{m}_{\text{cr}}$ (no introduction of the additional component)

$$T=\frac{\bar{y}}{\bar{\dot{m}}_{\text{т}}(1-\nu)}.$$

This expression for the time constant was obtained previously for a chamber with adjustment of the nozzle critical cross section (11.4). In Fig 11.15 the results are presented from calculating T as a function of ν and $\dot{m}_{\text{т}}/\dot{m}_{\text{cr}}$ under the conditions of the previously investigated example (for 10 seconds of operation of the engine, that is, for $y/\dot{m}_{\text{cr}}=0.064$).

From the results of the calculations it follows that the time constant chamber with given adjustment system, just as for the chambers of other, previously investigated systems, is on the order of hundredths to tenths of a second.

Equation of the Chamber with Introduction of the Additional Components Simultaneously in the Chamber Head and into the Prenozzle Space

A schematic of the chamber and the notation for the distribution of the flow rate of the additional component are presented in Fig 11.16.

The material balance equation for the chamber of the given type is as follows:

$$\frac{dy_{\text{г}}}{dt}=\dot{m}_{\text{к}}+\dot{m}_{\text{хг}}+\dot{m}_{\text{дс}}-\dot{m}_{\text{р}},$$

where $\dot{m}_{\text{хг}}$ is the flow rate of the additional component to the charge channel (through the chamber head): $\dot{m}_{\text{дс}}$ is the flow rate of the additional component to the prenozzle space.

APPROVED FOR RELEASE: 2007/02/08: CIA-RDP82-00850R000200090053-2

APPROVED FOR RELEASE: 2007/02/08: CIA-RDP82-00850R000200090053-2

In order to consider the distribution of the additional component between the two points of its entrance into the chamber, the following coefficient is introduced:

$$\varphi=\frac{\dot{m}_{\text{дс}}}{\dot{m}_{\text{д}}},$$

where $\dot{m}_{\text{д}}=\dot{m}_{\text{дг}}+\dot{m}_{\text{дс}}$ is the total flow rate of the additional component. In the given case, by the coefficient on the expression for the flow rate we mean

$$K=\frac{\dot{m}_{\text{д}}}{\dot{m}_{\text{т}}}.$$

The equation of the chamber, just as for other, previously investigated chamber schematics with introduction of the additional component, is written in the form (11.23), that is, it corresponds to the equation of the aperiodic element in the control system.

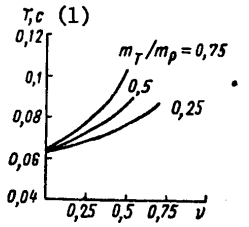

Figure 11.15. Time constant of the chamber with introduction of the additional component to the prenozzle space
Key:
1. sec

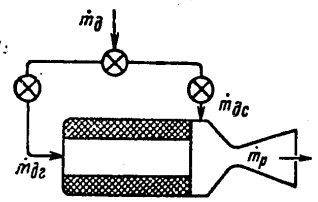

Figure 11.16. Schematic of a solid-fuel rocket engine with simultaneous input of an additional component to the head and to the prenozzle space

The time constant and the boost factor for the chamber in the given system have the form

$$T=\frac{\theta}{1-\frac{\nu}{1-\beta}\frac{1+\bar{\varphi}\bar{K}}{1+\bar{K}}\left[1-\left(\frac{\bar{\varphi}\bar{K}}{1+\bar{\varphi}\bar{K}}\right)^{1-\beta}\right]}; \qquad (11.29)$$

$$K_{\rho_{\text{к}}}^{\dot{m}_{\text{д}}}=\frac{1-\frac{1+\bar{\varphi}\bar{K}}{1+\bar{K}}\left[1-\left(\frac{\bar{\varphi}\bar{K}}{1+\bar{\varphi}\bar{K}}\right)^{1-\beta}\right]}{1-\frac{\nu}{1-\beta}\frac{1+\bar{\varphi}\bar{K}}{1+\bar{K}}\left[1-\left(\frac{\bar{\varphi}\bar{K}}{1+\bar{\varphi}\bar{K}}\right)^{1-\beta}\right]}. \qquad (11.30)$$

FOR OFFICIAL USE ONLY

APPROVED FOR RELEASE: 2007/02/08: CIA-RDP82-00850R000200090053-2

APPROVED FOR RELEASE: 2007/02/08: CIA-RDP82-00850R000200090053-2

It is easy to see that for $\bar{\phi}=1$, that is, for $\dot{m}_{ж}=\dot{m}_{д}$, which corresponds to the case of feeding the additional component only to the head, expressions (11.29) and (11.30) acquire the form (11.24) and (11.25). The chamber with introduction of the additional component into the head and the prenozzle space is the general case for the previously investigated systems.

BIBLIOGRAPHY

1. Aranovich, G. V.; Kartvelishvili, N. A.; Lyubimtsev, Ya. K. GIDRAVLICHESKIY UDAR I URAVNITEL'NYYE REZERVUARY [Hydraulic Hammer and Equalizing Reservoirs], Moscow, Nauka, 1968, 120 pp.

2. Baum, F. A., et al. FIZIKA VZRYVA [Explosion Physics], Moscow, Nauka, 1975, 321 pp.

3. Barrer. RAKETNYYE DVIGATELI [Rocket Engines], Moscow, Oborongiz, 1962, 800 pp.

4. Bendat, J., Pirsol, A. IZMERENIYA I ANALIZ SLUCHAYNYKH PROTSESSOV [Measurement and Analysis of Random Processes], Moscow, Mir, 1974, 464 pp.

5. Besekerskiy, V. A.; Popov, Ye. P. TEORIYA SISTEM AVTOMATICHESKOGO REGULIROVANIYA [Theory of Automatic Control Systems], Moscow, Nauka, 1975, 756 pp.

6. Volkov, Ye. B.; Golovkov, L. G.; Syritsyn, T. A. ZHIDKOSTNYYE RAKETNYYE DVIGATELI [Liquid-Fuel Rocket Engines], Moscow, Voyenizdat, 1971, 590 pp.

7. Vokov, Ye. B; Sudakov, R. S.; Syritsyn, T. A. OSNOVNYYE TEORII NADEZHNOSTI RAKETNYKH DVIGATELEY [Basic Reliability Theory of Rocket Engines], Moscow, Mashinostroyeniye, 1974, 400 pp.

8. Volkov, V. Ya.; Kupriyanov, N. S. "Stability Criterion of Linear Systems with Many Delays," IZVESTIYA AN SSSR. TEKHNICHESKAYA KIBERNETIKA [News of the USSR Academy of Sciences. Technical Cybernetics], No 5, 1968, pp 170-175.

9. Volkov, Ye. B.; Mazing, G. Yu.; Shishkin, Yu. N. RAKETNYYE DVIGATELI NA KOMBINIROVANNOM TOPLIVE [Combined Fuel Rocket Engines], Moscow, Mashinostroyeniye, 1973, 184 pp.

10. Glikman, B. F. AVTOMATICHESKOYE REGULIROVANIYE ZHIDKOSTNYKH RAKETNYKH DVIGATELEY [Automatic Control of Liquid-Fuel Rocket Engines], Moscow, Mashinostroyeniye, 1974, 396 pp.

APPROVED FOR RELEASE: 2007/02/08: CIA-RDP82-00850R000200090053-2

APPROVED FOR RELEASE: 2007/02/08: CIA-RDP82-00850R000200090053-2

11. Dobrovol'skiy, M. V. ZHIDKOSTNYYE RAKETNYYE DVIGATELI [Liquid-Fuel Rocket Engines], Moscow, Mashinostroyeniye, 1968, 396 pp.

12. Dey, Ye. Ye.; Beyli, A. G. "Development of Solid-Fuel Rocket Engines with Thrust Control Systems," VOPROSY RAKETNOY TEKHNIKI [Problems of Rocket Engineering], No 6, 1972, pp 49-56.

13. Zel'dovich, Ya. B.; Leypunskiy, O. I.; Librovich, V. B. TEORIYA NESTATSIONARNOGO GORENIYA POROKHA [Theory of Nonsteady-State Combustion of Powder], Moscow, Nauka, 1975, 180 pp.

14. Karlson, L. V.; Sider, Ya. D. "Heat Exchange on Ignition of Solid Fuel," RAKETNAYA TEKHNIKA I KOSMONAVTIKA [Rocket Engineering and Cosmonautics], No 5, Vol 7, 1967, pp 29-32.

15. Kochin, N. Ye.; Kibel', I. A.; Roze, N. V. TEORETICHESKAYA MEKHANIKA Theoretical Mechanics], OGIZ, GITL, 1948, 683 pp.

16. Kolesnikov, K. S.; Samoylov, Ye. A.; Rybak, S. A. DINAMIKA TOPLIVNYKH SISTEM ZHRD [Fuel System Dynamics for Liquid-Fuel Rocket Engines], Moscow, Mashinostroyeniye, 1975, 172 pp.

17. Kolesnikov, K. S. PRODOL'NYYE KOLEBANIYA RAKETY S ZHIDKOSTNYM RAKETNYM DVIGATELEM [Longitudinal Vibrations of a Rocket with Liquid-Fuel Rocket Engines], Moscow, Mashinostroyeniye, 1971, 260 pp.

18. KOSMONAVTIKA. MALEN'KAYA ENTSIKLOPEDIYA [Cosmonautics. Small Encyclopedia], Chief editor, Academician V. P. Glushko, 2d edition, Moscow, Sovetskaya entsiklopediya, 1970,592 pp.

19. Kouts, R. L.; Korton, M. D. "Analysis of the Stability of the Operating Process when Designing Solid-Fuel Rocket Engines," VOPROSY RAKETNOY TEKHNIKI, No 7, 1969, pp 14-28.

20. Krokko, L.; Chzhen'-Sin', I. TEORIYA NEUSTOYCHIVOGO GORENIYA V ZHIDKOSTNYKH RAKETNYKH DVIGATELYAKH [Theory of Stable Combustion in Liquid-Fuel Rocket Engines], Moscow, IL, 1958, 352 pp.

21. Makhin, V. A.; Prisnyakov, V. F.; Belik, N. P. DINAMIKA ZHIDKOSTNYKH RAKETNYKH DVIGATELEY [Dynamics of Liquid-Fuel Rocket Engines], Moscow, Mashinostroyeniye, 1969, 384 pp.

22. Makhin, V. A.; Milenko, N. P.; Pron', L. V. TEORETICHESKIYE OSNOVY EKSPERIMENTAL'NOY OTRABOTKI ZHRD [Theoretical Principles of Experimental Development of Liquid-Fuel Rocket Engines], Moscow, Mashinostroyeniye, 1973, 282 pp.

23. Mayoros, Yu.; Sarlat, I. M. "Control of the Afterflaming Impulse of Solid-Fuel Rocket Engines," VOPROSY RAKETNOY TEKHNIKI, No 6, 1967, pp 15-21.

FOR OFFICIAL USE ONLY

APPROVED FOR RELEASE: 2007/02/08: CIA-RDP82-00850R000200090053-2

APPROVED FOR RELEASE: 2007/02/08: CIA-RDP82-00850R000200090053-2

24. Marshakov, V. N.; Leypunskiy, O. I. "Combustion and Extinguishing of Powder with a Fast Pressure Drop," FIZIKA GORENIYA I VZRYVA [Physics of Combustion and Explosion], No 5, 1967, pp 11-22.

25. Mak-Alevi, R. F.; Kauan, P. L.; Sammerfild, M. "Mechanism of the Ignition of Mixed Solid Fuels by Hot Gas," ISSLEDOVANIYA RAKETNYKH DVIGATELEY NA TVERDOM TOPLIVE [Investigation of Solid-Fuel Rocket Engines], Moscow, IL, 1963.

26. "Minuteman Intercontinental Ballistic Missile," VOPROSY RAKETNOY TEKHNIKI, No 6, 1963, pp 27-33.

27. Mitropol'skiy, A. K. TEKHNIKA STATISTICHESKIKH VYCHISLENIY [Statistical Calculation Techniques and Equipment], Moscow, Mashinostroyeniye, 1971, 576 pp.

28. Moshkin, Ye. K. NESTATSIONARNYYE REZHIMY RABOTY ZHRD [Nonsteady-State Operating Conditions of Liquid-Fuel Rocket Engines], Moscow, Mashinostroyeniye, 1970, 336 pp.

29. Mizes, R. MATEMATICHESKAYA TEORIYA TECHENIYA SZHIMAYEMOY ZHIDKOSTI [Mathematical Theory of the Flow of a Compressible Liquid], Moscow, IL, 1961, 318 pp.

30. Natanzon, M. S., et al. "Experimental Studies of Cavitation Vibrations of a Centrifugal Pump," IZVESTIYA AN SSSR. ENERGETIKA I TRANSPORT [News of the USSR Academy of Sciences, Power Engineering and Transportation], No 2, 1973, pp 151-157.

31. Natanzon, M. S. "Longitudinal Autovibrations of the Hull of a Rocket Accompanied by Discontinuous Vibrations of the Liquid in the Lines," IZVESTIYA AN SSSR. ENERGETIKA I TRANSPORT, No 2, 1971, pp 154-159.

32. Novozhilov, B. V. NESTATSIONARNOYE GORENIYE TVERDYKH RAKETNYKH TOPLIV [Nonsteady-State Combustion of Solid Rocket Fuels], Moscow, Nauka, 1973, 176 pp.

33. Petukhov, B. S.; Kirillov, V. V. "Heat Exchange During Turbulent Flow of a Compressible Gas in Tubes in M Range to 4," TEPLOENERGETIKA [Thermal Power Engineering], No 5, 1960, pp 24-41.

34. Prandtl, L.. GIDROAEROMEKHANIKA [Hydroaeromechanics], Moscow, IL, 1951, 576 pp.

35. Pugachev, V. S.; Kazakov, I. Ye.; Yelanov, L. G. OSNOVY STATISTICHESKOY TEORII AVTOMATICHESKIKH SISTEM [Fundamentals of the Statistical Theory of Automated Systems], Moscow, Mashinostroyeniye, 1974, 400 pp.

APPROVED FOR RELEASE: 2007/02/08: CIA-RDP82-00850R000200090053-2

APPROVED FOR RELEASE: 2007/02/08: CIA-RDP82-00850R000200090053-2

36. Rayzberg, B. A.; Yerokhin, B. T.; Samsonov, K. P. OSNOVY TEORII RABOCHIKH PROTSESSOV V RAKETNYKH SISTEMAKH NA TVERDOM TOPLIVE [Fundamentals of the Theory of Operating Processes in Solid-Fuel Rocket Systems], Moscow, Mashinostroyeniye, 1972, 384 pp.

37. Robertson, V. Ye. "Solid-Fuel Rocket Engine Igniters," VOPROSY RAKETNOY TEKHNIKI, No 9, 1975, pp 67-81.

38. Ovsyannikov, B. V.; Borovskiy, B. I. TEORIYA I RASCHET AGREGATOV PITANIYA ZHIDKOSTNYKH RAKETNYKH DVIGATELEY [Theory and Calculation of the Feed Assemblies of Liquid-Fuel Rocket Engines], Moscow, Mashinostroyeniye, 1971, 540 pp.

39. Orlov, B. V.; Mazing, G. Yu. TERMODINAMICHESKIYE I BALLISTICHESKIYE OSNOVY PROYEKTIROVANIYA RAKETNYKH DVIGATELEY NA TVERDOM TOPLIVE [Thermodynamic and Ballistic Principles of Designing Solid-Fuel Rocket Engines], Moscow, Mashinostroyeniye, 1968, 536 pp.

40. Sorkin, R. Ye. GAZOTERMODINAMIKA RAKETNYKH DVIGATELEY NA TVERDOM TOPLIVE [Gas Thermodynamics of Solid-Fuel Rocket Engines], Moscow, Nauka, 1967, 368 pp.

41. Siplach, S. "Effect of Fast Decrease in the Pressure of a Solid Fuel," VOPROSY RAKETNOY TEKHNIKI, No 11, 1961, pp 21-29.

42. Chaki, F. SOVREMENNAYA TEORIYA UPRAVLENIYA [Modern Control Theory], Moscow, Mir, 1975, 424 pp.

43. Shapiro, Ya. M.; Mazing, G. Yu.; Prudnikov, N. Ye. TEORIYA RAKETNOGO DVIGATELYA NA TVERDOM TOPLIVE [Solid-Fuel Rocket Engine Theory], Moscow, Voyenizdat, 1966, 256 pp.

44. Sharakshane, A. S.; Zheleznov, I. G. ISPYTANIYA SLOZHNYKH SISTEM [Testing Complex Systems], Moscow, Vyyeshaya shkola, 1974, 184 pp.

45. Khintse. TURBULENTNOST' [Turbulence], Moscow, Fizmatgiz, 1963, 556 pp.

46. Ellen, D. S.; Bastres, Ye. K.; Smit, K. A. "Heat Transfer Processes During Ignition of the Solid-Fuel Rocket Engine Charge," RAKETNAYA TEKHNIKA I KOSMONAVTIKA [Rocket Engineering and Cosmonautics], Vol 5, No 7, 1967, pp 78-86.

47. Ellis, R. A. "Designing the Nozzles of Solid-Fuel Rocket Engines," VOPROSY RAKETNOY TEKHNIKI, No 3, 1974, pp 29-35.

48. Bartz, D. R. "A Simple Equation for Rapid Estimation of Rocket Nozzle Convective Heat Transfer Coefficients," JET PROPULSION, No 21, 1957.

FOR OFFICIAL USE ONLY

APPROVED FOR RELEASE: 2007/02/08: CIA-RDP82-00850R000200090053-2

APPROVED FOR RELEASE: 2007/02/08: CIA-RDP82-00850R000200090053-2

49. Davey, T. "Entrance Region Heat Transfer Coefficients," HEAT TRANSFER, No 59, 1963.

50. Frazer, J. H.; Hicks, B. L. PHYS. A COLLOID CHEM, No 50, 1956.

51. Hiks, B. L. CHEM. PHYS, No 22, 1954.

52. Siddiqui, K. M.; Smith, I. E. "The Ignition of Double-Base Propellants by Hot Particles Arising in the Igniter Products," AIAA PAP, No 1087, 1974.

COPYRIGHT: Izdatel'stvo "Mashinostroyeniye," 1978

10845
CSO: 8144/1115

- END -

APPROVED FOR RELEASE: 2007/02/08: CIA-RDP82-00850R000200090053-2